

RADIOLOGICAL PERFORMANCE ASSESSMENT FOR THE E-AREA VAULTS DISPOSAL FACILITY

by

James R. Cook

**Westinghouse Savannah River Company
Savannah River Site
Aiken, South Carolina 29808**

Paul D. Hunt

DOE Contract No. DE-AC09-89SR16036

This paper was prepared in connection with work done under the above contract number with the U. S. Department of Energy. By acceptance of this paper, the publisher and/or recipient acknowledges the U. S. Government's right to retain a nonexclusive, royalty-free license in and to any copyright covering this paper, along with the right to reproduce and to authorize others to reproduce all or part of the copyrighted paper.

DISCLAIMER

This report was prepared as an account of work sponsored by an agency of the United States Government. Neither the United States Government nor any agency thereof, nor any of their employees, makes any warranty, express or implied, or assumes any legal liability or responsibility for the accuracy, completeness, or usefulness of any information, apparatus, product, or process disclosed, or represents that its use would not infringe privately owned rights. Reference herein to any specific commercial product, process, or service by trade name, trademark, manufacturer, or otherwise does not necessarily constitute or imply its endorsement, recommendation, or favoring by the United States Government or any agency thereof. The views and opinions of authors expressed herein do not necessarily state or reflect those of the United States Government or any agency thereof.

This report has been reproduced directly from the best available copy.

Available to DOE and DOE contractors from the Office of Scientific and Technical Information, P. O. Box 62, Oak Ridge, TN 37831; prices available from (615) 576-8401.

Available to the public from the National Technical Information Service, U. S. Department of Commerce, 5285 Port Royal Rd., Springfield, VA 22161

RADIOLOGICAL PERFORMANCE ASSESSMENT FOR THE E-AREA VAULTS DISPOSAL FACILITY (U)

Prepared for the
WESTINGHOUSE SAVANNAH RIVER COMPANY
Aiken, South Carolina

by

**MARTIN MARIETTA ENERGY SYSTEMS, INC.
EG&G IDAHO, INC.
WESTINGHOUSE SAVANNAH RIVER COMPANY**

April 15, 1994

Rev. 0

*Authenticated
Mary Mullis
5/16/94*

CONTENTS

FIGURES	xi
TABLES	xix
ACRONYMS AND ABBREVIATIONS	xxv
EXECUTIVE SUMMARY	xxix
 1. INTRODUCTION	 1-1
1.1 PURPOSE AND SCOPE	1-3
1.2 PERFORMANCE OBJECTIVES	1-5
1.2.1 Time for Compliance with Performance Objectives	1-6
1.2.2 Performance Objective for Groundwater Protection	1-7
1.2.3 Radon	1-11
2. DISPOSAL FACILITY DESCRIPTION	2-1
2.1 REGIONAL CHARACTERISTICS	2-1
2.1.1 Geography of the Region	2-2
2.1.2 Demography	2-5
2.1.3 Meteorology	2-7
2.1.4 Hydrogeology	2-7
2.1.5 Seismicity	2-13
2.1.6 Surface Water Hydrology	2-16
2.1.7 Water Quality and Usage	2-17
2.1.8 Soils	2-18
2.1.9 Ecology	2-20
2.1.10 Existing Radiological Environment	2-21
2.2 E-AREA SITE DESCRIPTION	2-26
2.2.1 E-Area Location, Description, and Land Use	2-26
2.2.2 Hydrogeology of E-Area	2-28
2.2.3 Surface Water in the Vicinity of E-Area	2-34

2.2.4	Water Quality and Usage in the E-Area Vicinity	2-35
2.2.5	Existing Radiation and Chemical Environment at E-Area	2-38
2.3	DESCRIPTION OF E-AREA OPERATIONS, FACILITIES, AND FEED STREAMS	2-44
2.3.1	Description of the Waste Types at E-Area	2-44
2.4	E-AREA VAULTS WASTE COMPOSITION	2-44
2.4.1	Physical Characteristics of Waste Types	2-44
2.4.2	Waste Packaging	2-46
2.4.3	Radioactive Inventory of Waste Types	2-48
2.5	DESCRIPTION OF THE E-AREA VAULTS DISPOSAL SITE	2-49
2.5.1	Site Layout and Capacity	2-49
2.5.2	Vault Descriptions	2-51
2.6	PROPOSED TRENCHES FOR DISPOSAL OF SUSPECT SOIL	2-56
2.7	PROPOSED NAVAL REACTOR COMPONENT DISPOSAL	2-56
2.8	HAZARDOUS WASTE/MIXED WASTE DISPOSAL FACILITY	2-58
2.9	E-AREA CLOSURE CONCEPT	2-64
2.9.1	Physical Description of the EAVs Closure Concept	2-64
2.9.2	Functional Description of the E-Area Closure Concept	2-67
2.9.3	Post Closure Groundwater Monitoring	2-68
3.	ANALYSIS OF PERFORMANCE	3-1
3.1	SOURCE TERM	3-3
3.1.1	Radionuclides of Interest	3-3
3.1.2	Release Mechanisms	3-4
3.1.3	Engineered Barriers Degradation and Failure	3-5
3.2	PATHWAYS AND SCENARIOS	3-10
3.2.1	Time Periods of Concern	3-10
3.2.2	Transport Pathways	3-11
3.2.3	Exposures of Off-Site Members of the Public and Protection of Groundwater	3-19
3.2.4	Exposure Scenarios for Inadvertent Intruders	3-39

3.3	MODELS AND ASSUMPTIONS	3-54
3.3.1	Near-Field Model	3-55
3.3.2	Groundwater Transport Model	3-74
3.3.3	Models for Dose Estimation	3-80
3.4	PERFORMANCE ANALYSIS METHODOLOGY	3-83
3.4.1	Near-Field Model Analysis	3-83
3.4.2	Groundwater Flow and Mass Transport	3-89
3.4.3	Methods for Dose Analysis	3-98
3.5	QUALITY ASSURANCE	3-99
4.	RESULTS OF ANALYSIS	4-1
4.1	ANALYSIS RESULTS	4-1
4.1.1	Screening Results for the Groundwater Pathway	4-2
4.1.2	Near-Field Model Results	4-2
4.1.3	Groundwater Concentrations	4-17
4.1.4	Dose Analysis for Off-Site Releases of Radionuclides	4-28
4.1.5	Dose Analysis for Inadvertent Intruders	4-34
4.2	SENSITIVITY AND UNCERTAINTY ANALYSES	4-81
4.2.1	Analysis of Near-Field and Groundwater Transport	4-81
4.2.2	Analysis of Dose Model from Off-Site Releases	4-85
4.2.3	Analysis of Dose Models for Inadvertent Intruders	4-86
4.3	INTERPRETATION OF RESULTS	4-90
4.3.1	Off-Site Doses and Groundwater Protection	4-91
4.3.2	Inadvertent Intruders	4-92
4.3.3	Disposal Limits for Waste at E-Area	4-93
5.	PERFORMANCE EVALUATION	5-1
5.1	COMPARISON TO PERFORMANCE OBJECTIVES	5-1
5.2	DESIGN CHANGES REQUIRED TO MEET PERFORMANCE OBJECTIVES	5-2
5.3	DATA AND RESEARCH NEEDS	5-2
6.	PREPARERS	6-1
7.	REFERENCES	7-1

APPENDIX A DETAILS OF MODELS AND ASSUMPTIONS

A.1 NEAR-FIELD MODEL	A-1
A.1.1 Infiltration	A-1
A.1.2 Flow and Mass Transport Through Vaults	A-5
A.2 GROUNDWATER FLOW AND MASS TRANSPORT MODEL	
 AND SIMULATIONS	A-14
A.2.1 Conceptual Saturated Flow and Transport Model	A-14
A.2.2 Saturated Flow and Transport Simulations	A-22
A.3 ANALYSIS OF ATMOSPHERIC EFFLUENT	A-22
A.3.1 Dose Analysis of Tritium Crucibles in the ILT Vaults	A-23
A.3.2 Dose Analysis of ^3H in JCW in the ILT Vaults	A-26
A.3.3 Dose Analysis of ^3H in JCW in the ILNT Vaults	A-29
A.3.4 Dose Analysis of ^{14}C in the ILNT Vaults	A-30
A.3.5 Dose Analysis of ^3H in JCW in the LAW Vaults	A-32
A.3.6 Dose Analysis of ^{14}C in the LAW Vaults	A-33
A.3.7 Analysis of Radon Flux	A-34
A.4 DOSE ANALYSIS FOR OFF-SITE INDIVIDUALS AND	
 INADVERTENT INTRUDERS	A-39
A.4.1 Introduction	A-39
A.4.2 Radionuclides of Importance for Dose Analyses	A-40
A.4.3 Assumed Exposure Scenarios and Exposure Pathways	A-45
A.4.4 Dose Conversion Factors for Internal and External	
Exposure	A-50
A.4.5 Models and Parameter Values for Exposure Pathways	A-62
A.4.6 Summary	A-97
APPENDIX A REFERENCES	A-100

APPENDIX B COMPUTER CODES

B.1 CODE SELECTION CRITERIA AND CONSIDERATIONS	B-1
B.2 GEOCHEMICAL COMPUTER CODE	B-3

B.3 VAULT DEGRADATION COMPUTER CODE	B-7
B.4 SATURATED/UNSATURATED FLOW AND TRANSPORT CODE	B-15
APPENDIX B REFERENCES	B-28

APPENDIX C DATA TABULATION

C.1 RADIONUCLIDE SCREENING AND TRIGGER LEVEL RESULTS	C-1
C.2 E-AREA STREAM FLOW DATA	C-71
C.3 RADIONUCLIDE SCREENING RESULTS FOR SUSPECT SOIL	C-74
C.4 NEAR-FIELD RESULTS	C-97
C.5 GROUNDWATER RESULTS	C-110
C.6 ATMOSPHERIC TRANSPORT	C-142

APPENDIX D GEOCHEMICAL INTERACTIONS

D.1 INTRODUCTION	D-1
D.2 RADIONUCLIDES CONSIDERED	D-2
D.3 VAULT WATER COMPOSITION	D-2
D.4 RADIONUCLIDE SORPTION BEHAVIOR	D-2
D.5 TRITIUM RELEASE MECHANISMS	D-30
D.6 SORPTION IN SOILS	D-36
APPENDIX D REFERENCES	D-38

APPENDIX E HYDROGEOLOGY OF THE SRS

E.1 GEOLOGY	E-1
E.1.1 Late Cretaceous Lumbee Group	E-1
E.1.2 Paleocene-Eocene Black Mingo Group	E-3
E.1.3 Middle Eocene Orangeburg Group	E-4
E.1.4 Late Eocene Barnwell Group	E-6
E.1.5 "Upland Unit"	E-7
E.1.6 Quaternary Deposits	E-7

E.2 GROUNDWATER HYDROLOGY	E-7
E.2.1 Aquifer System I	E-8
E.2.2 Confining System I-II	E-8
E.2.3 Aquifer System II	E-8
E.2.4 Hydrologic Characteristics of the Unsaturated Zone	E-17
APPENDIX E REFERENCES	E-23

APPENDIX F SOFTWARE QA PLANS

APPENDIX G COMPLETENESS REVIEW GUIDE

APPENDIX H PERFORMANCE ASSESSMENT PEER REVIEW PANEL RECOMMENDATIONS

APPENDIX I SUSPECT SOIL PERFORMANCE ANALYSIS

I.1 DESCRIPTION OF SUSPECT SOIL TRENCHES	I-1
I.1.1 Physical Characteristics of Suspect Soil	I-1
I.1.2 Layout and Capacity of the Trenches	I-1
I.1.3 Radioactive Inventory of Suspect Soil	I-3
I.1.4 Closure Concept	I-3
I.2 ANALYSIS OF PERFORMANCE OF SUSPECT SOIL	I-3
I.2.1 Source Term	I-4
I.2.2 Pathways and Scenarios	I-4
I.2.3 Models and Assumptions	I-8
I.2.4 Performance Analysis Methodology	I-17
I.2.5 Quality Assurance	I-19
I.3 RESULTS OF SUSPECT SOIL ANALYSIS	I-19
I.3.1 Analysis Results	I-20
I.3.2 Interpretation of Results	I-39

I.4 PERFORMANCE EVALUATION	I-39
I.4.1 Comparison to Performance Objectives	I-39
I.4.2 Design Required to Meet Performance Objectives	I-42
I.4.3 Data and Research Needs	I-42
I.5 PORFLOW INPUT FILES	I-43
APPENDIX I REFERENCES	I-60

APPENDIX J SENSITIVITY/UNCERTAINTY ANALYSIS

J.1 INTRODUCTION	J-1
J.2 PRELIMINARY SAMPLE	J-2
J.3 SENSITIVITY ANALYSIS	J-3
J.4 UNCERTAINTY ANALYSIS	J-5
J.5 SUMMARY	J-6
J.6 RESPONSE PLOTS AND CUMULATIVE PROBABILITY DISTRIBUTION	J-6
APPENDIX J REFERENCES	J-18

APPENDIX K E-AREA VAULTS VAULT DEGRADATION STUDY

APPENDIX L DESCRIPTION OF NAVAL REACTOR WASTE DISPOSAL

L.1 DESCRIPTION OF NAVAL REACTOR (NR) WASTE DISPOSAL	L-1
L.1.1 Description of NR Waste Forms	L-1
L.1.2 Layout and Capacity of NR Waste Disposal Site	L-1
L.1.3 Radioactive Inventory of NR Waste	L-4
L.1.4 Closure Concept	L-4
L.2 ANALYSIS OF PERFORMANCE OF NR WASTE	L-4
L.2.1 Source Term	L-6
L.2.2 Pathways and Scenarios	L-7
L.2.3 Models and Assumptions	L-10
L.2.4 Performance Analysis Methodology	L-20
L.2.5 Quality Assurance	L-22

L3 RESULTS OF NR WASTE ANALYSIS	L-22
L3.1 Analysis Results	L-22
L3.2 Interpretation of Results	L-39
L4 PERFORMANCE EVALUATION	L-41
L4.1 Comparison to Performance Objectives	L-41
L4.2 Design Changes Required to Meet Performance Objectives	L-41
L4.3 Data and Research Needs	L-42
L5 PORFLOW INPUT FILES	L-43
APPENDIX L REFERENCES	L-51

APPENDIX M PORFLOW INPUT FILES

M.1 PORFLOW INPUT FILES - NEARFIELD:	M-1
M.2 PORFLOW INPUT FILES - GROUNDWATER	M-18

FIGURES

1.1-1.	Location map of the Savannah River Site	1-2
2.1-1.	SRS regional location map	2-3
2.1-2.	Facility location map of the SRS, showing surface drainage	2-4
2.1-3.	Population distribution within an 80-km radius of the central SRS	2-6
2.1-4.	Average rainfall at SRS: 1952 - 1992	2-8
2.1-5.	Hydrologic and stratigraphic units underlying the SRS.	2-10
2.1-6.	Location of the Bowman and Charleston-Summerville seismic zones, and the Dunbarton Basin on the SRS	2-14
2.1-7.	The total average effective dose equivalent from various sources in the Central Savannah River Area.	2-23
2.2-1.	Topographic map in the vicinity of E-Area	2-27
2.2-2.	Location of groundwater wells at E-Area.	2-29
2.2-3.	Lithologic cross section, D-D ¹ , in the vicinity of E-Area	2-30
2.2-4.	Lithologic cross section, E-E ¹ , in the vicinity of E-Area	2-31
2.2-5.	Location of E-Area monitoring wells used to assess the groundwater quality and radionuclide activities	2-43
2.5-1.	Projected vault layout in the EAVDF	2-50
2.5-2.	General arrangement of the ILNT and ILT vaults	2-53
2.5-3.	Typical section through LAWV cell	2-55
2.6-1.	Conceptual drawing of proposed suspect soil trenches	2-57
2.7-1.	Conceptual layout of 100 NR waste disposal containers	2-59
2.7-2.	Typical NR waste disposal container	2-60
2.8-1.	Location map for HW/MWDF	2-63
2.9.1.	Vault closure concept (2 cm/year infiltration)	2-65
2.9.2.	Vault closure concept (40 cm/year infiltration)	2-66
3.0-1.	Overall conceptual model for the Radiological Performance Assessment of the E-Area Vaults Disposal Facility	3-2

3.2-1.	Potential pathways to human exposure for undisturbed buried LLW	3-13
3.3-1.	Flow path through near-field vadose zone.	3-56
3.3-2.	Conceptual model for the cover	3-58
3.3-3.	Conceptual model for the ILNT and ILT vaults	3-59
3.3-4.	Conceptual model for the LAW vault	3-60
3.3-5.	Fitted moisture characteristic curve for the backfill soil	3-65
3.3-6.	Fitted moisture characteristic curve for the gravel soil	3-66
3.4-1.	Integration of computational methods for the Radiological Performance Assessment of EAVs	3-84
3.4-2.	Model domain for PORFLOW simulations of groundwater at E-Area.	3-91
3.4-3.	Actual potentiometric surface for Aquifer Unit IIB, Zone 2 (water table), and simulated surface for Aquifer Unit IIB, Zone 2.	3-92
3.4-4.	Actual potentiometric surface for Aquifer Unit IIB, Zone 1 (Barnwell/McBean), and simulated surface for Aquifer Unit IIB, Zone 1..	3-94
3.4-5.	Actual potentiometric surface for Aquifer Unit IIA (Congaree) and simulated surface for Aquifer Unit IIA	3-95
3.4-6.	Locations of stream-gaging stations in creeks near E-Area..	3-96
3.4-7.	Illustration of EAV source area in PORFLOW grid..	3-97
3.4-8.	Locations of stream-gauging stations in creeks near E-Area.	3-94
4.1-1.	Engineered barrier steady-state saturation	4-6
4.1-2.	Vertical fluxes beneath the engineered barrier	4-7
4.1-3.	Steady state saturation for the Intact period for the ILNT (a), and LAW (b) vaults	4-11
4.1-4.	Steady-state saturation for the Cracked period for the ILNT (a), and LAW (b) vaults	4-12
4.1-5.	Steady state saturation for the Failed period for the ILNT (a), and LAW (b) vaults	4-13
4.1-6.	Contaminant plume overlap for the LAW and ILNT vaults at E-Area	4-18

4.1-7.	Illustrated results of preliminary numerical simulations of Tc-99 transport in groundwater in E-Area vicinity	4-34
4.2-1.	Cumulative distribution function for peak groundwater concentration of ⁹⁹ Tc, based on ranges of parameters specified in Appendix J	4-83
6.0-1.	E-Area PA organizational chart	6-14
A.1-1.	Idealized cross-section for the SRS vadose zone.	A-2
A.1-2.	Domain of the cover simulation	A-4
A.2-1.	Model domain for PORFLOW simulation of groundwater in E-Area vicinity	A-15
A.2-2.	Location of E-Area groundwater wells	A-16
A.3-1.	PORFLOW input file for radon calculations	A-37
C.2-1.	Locations of stream-gaging stations in creeks near E-Area	C-73
C.4-1.	Fractional flux to the water table from the ILNT vaults	C-98
C.4-2.	Fractional flux to the water table from the ILNT vaults	C-99
C.4-3.	Fractional flux to the water table from the ILNT vaults	C-100
C.4-4.	Fractional flux to the water table from the ILNT vaults	C-101
C.4-5.	Fractional flux to the water table from the ILNT vaults	C-102
C.4-6.	Fractional flux to the water table from the ILNT vaults	C-103
C.4-7.	Fractional flux to the water table from the LAW vaults	C-104
C.4-8.	Fractional flux to the water table from the LAW vaults	C-105
C.4-9.	Fractional flux to the water table from the LAW vaults	C-106
C.4-10.	Fractional flux to the water table from the LAW vaults	C-107
C.4-11.	Fractional flux to the water table from the LAW vaults	C-108
C.4-12.	Fractional flux to the water table from the LAW vaults	C-109
C.5-1.	Predicted groundwater concentration of H-3 as a function of time	C-111
C.5-2.	Predicted groundwater concentration of C-14 as a function of time	C-112
C.5-3.	Predicted groundwater concentration of Ni-59 as a function of time	C-113
C.5-4.	Predicted groundwater concentration of Se-79 as a function of time	C-114
C.5-5.	Predicted groundwater concentration of Sr-90 as a function of time	C-115

C.5-6.	Predicted groundwater concentration of Te-99 as a function of time	C-116
C.5-7.	Predicted groundwater concentration of Sn-126 as a function of time	C-117
C.5-8.	Predicted groundwater concentration of I-129 as a function of time	C-118
C.5-9.	Predicted groundwater concentration of Cs-135 as a function of time	C-119
C.5-10.	Predicted groundwater concentration of Th-232 as a function of time	C-120
C.5-11.	Predicted groundwater concentration of U-233 as a function of time	C-121
C.5-12.	Predicted groundwater concentration of U-234 as a function of time	C-122
C.5-13.	Predicted groundwater concentration of U-235 as a function of time	C-123
C.5-14.	Predicted groundwater concentration of U-236 as a function of time	C-124
C.5-15.	Predicted groundwater concentration of U-238 as a function of time	C-125
C.5-16.	Predicted groundwater concentration of Np-237 as a function of time	C-126
C.5-17.	Predicted groundwater concentration of Am-241 as a function of time	C-127
C.5-18.	Predicted groundwater concentration of Am-243 as a function of time	C-128
C.5-19.	Predicted groundwater concentration of Pu-238 as a function of time	C-129
C.5-20.	Predicted groundwater concentration of Pu-239 as a function of time	C-130
C.5-21.	Predicted groundwater concentration of Pu-240 as a function of time	C-131
C.5-22.	Predicted groundwater concentration of Pu-242 as a function of time	C-132
C.5-23.	Predicted groundwater concentration of Pu-244 as a function of time	C-133
C.5-24.	Predicted groundwater concentration of Cm-244 as a function of time	C-134
C.5-25.	Predicted groundwater concentration of Cm-245 as a function of time	C-135
C.5-26.	Predicted groundwater concentration of Cm-246 as a function of time	C-136
C.5-27.	Predicted groundwater concentration of Cm-247 as a function of time	C-137
C.5-28.	Predicted groundwater concentration of Cm-248 as a function of time	C-138
C.5-29.	Predicted groundwater concentration of Bk-247 as a function of time	C-139
C.5-30.	Predicted groundwater concentration of Cf-249 as a function of time	C-140
C.5-31.	Predicted groundwater concentration of Cf-251 as a function of time	C-141
D.4-1.	Adsorption of Pu on goethite as a function of pH at two plutonium concentrations (from Sanchez et al. 1985)	D-6

- D.4-2.** The effect of carbonate alkalinity on the adsorption of Pu(IV) on goethite (from Sanchez et al. 1985). Alkalinity in the vault will be approximately 60 meg/L D-8
- D.4-3.** Adsorption of uranyl on a 1 g/L goethite suspension as a function of pH in a 0.1 M NaNO₃ solution (from Hsi and Langmuir 1985). a) uranyl at 10⁻⁵ M, b) dissolved uranium at 10⁻⁵ M and varying total carbonate, c) effect of changes in total carbonate on the adsorption of uranyl D-10
- D.4-4.** Adsorption of Sr²⁺ on goethite as a function of pH in a 1.0 M NaNO₃ solution (from Dzombak and Morel 1990). a) 6.9 g goethite/L, b) 8.9 g goethite/L, c) 8.9 g goethite/L, d) 8.9 g goethite/L, e) 8.9 g goethite/L, f) 8.9 g goethite/L, g) 8.9 g goethite/L, h) 1.8 g goethite/L, i) 4.4 g goethite/L, j) 8.9 g goethite/L, k) 17.8 g goethite/L D-12
- D.4-5.** Adsorption of nickel on goethite as a function of pH in a 0.1 M NaNO₃ solution (from Dzombak and Morel 1990) D-19
- D.4-6.** Adsorption of selenite on goethite as a function of pH in a 0.5 M NH₄NO₃ solution (from Dzombak and Morel 1990) D-21
- D.4-7.** Adsorption of barium on goethite as a function of pH as an analog for radium (from Dzombak and Morel 1990). a) 0.05 g goethite/L, b) 0.05 g goethite/L, c) 0.01 g goethite/L, d) 0.06 g goethite/L, e) 0.2 g goethite/L D-22
- D.4-8.** Adsorption of thorium on goethite as function of pH in 0.422 mol/Kg NaCl electrolyte at different thorium/oxide ratios (Hunter et al. 1988). Triangles: 9 micromol/L Th, 8.6 g/L goethite; Circles: 9 micromol/L Th, 0.54 g/L goethite; Squares: 45 micromol/L Th, 0.54 g/L goethite D-27
- D.4-9.** Adsorption of neptunium on goethite as function of pH (Girvin et al. 1988). Triangles: 0.3 g/L goethite; Circles: 0.9 g/L goethite; Squares: 0.09 g/L goethite . D-28
- D.4-10.** Adsorption of mercury on goethite as function of pH as an analog for tin (from Dzombak and Morel 1990). a) 0.05 g/L goethite, b) 0.05 g/L goethite D-29
- D.4-11.** Adsorption of chromium III on goethite as function of pH as an analog for americium (from Dzombak and Morel 1990) D-31

D.5-1.	Estimated Pu(IV) solubility under E-Area conditions	D-33
D.5-2.	Estimated total uranium solubility under E-Area conditions	D-35
D.5-3.	Comparison of uranium solubilities under E-Area conditions	D-37
E.1-1.	Hydrologic and stratigraphic units underlying the SRS	E-2
E.2-1.	Surface drainage map of the SRS	E-11
E.2-2.	Potentiometric surface of Aquifer Unit IIA at E-Area	E-12
E.2-3.	Regional potentiometric surface of Aquifer Unit IIA (Christensen and Gordon 1983)	E-13
E.2-4.	Potentiometric surface of Aquifer Unit IIB, Zone 1, at E-Area	E-15
E.2-5.	Potentiometric surface for Aquifer Unit IIB, Zone 2, at E-Area	E-18
E.2-6.	Soil water content-pressure relationships for undisturbed soils at SRS burial grounds (Gruber 1980)	E-19
E.2-7.	Unsaturated hydraulic conductivity as a function of moisture content at SRS burial grounds (Gruber 1980)	E-20
E.2-8.	Soil water content-pressure relationships for undisturbed soils in Z-Area (Quisenberry 1985)	E-21
E.2-9.	Unsaturated hydraulic conductivity as a function of moisture content at Z-Area (Quisenberry 1985)	E-22
I.1-1.	Conceptual drawing of proposed suspect soil trenches	I-2
I.2-1.	Simulation domain for the suspect soil trenches in the vadose zone	I-10
I.5-1.	PORFLOW input file - flow in the vadose zone	I-43
I.5-2.	Example PORFLOW input file - mass transport in vadose zone	I-52
I.5-3.	Example PORFLOW input file - mass transport in groundwater	I-55
L.1.1.	Naval reactor waste disposal container	L-2
L.1.2.	Proposed layout of Naval Reactor Waste Disposal Area in the EAV facility	L-3
L.2-1.	Near-field simulation domain for NR waste	L-11
L.5-1.	PORFLOW input file - flow in the vadose zone for NR waste analysis	L-43
L.5-2.	Example PORFLOW input file - mass transport of NR waste radionuclides in vadose zone	L-45

L.5-3.	Example PORFLOW input file - mass transport of NR waste radionuclides in groundwater	L-48
M.1-1.	PORFLOW Input File - File simulation through intact ILNT vault	M-1
M.1-2.	PORFLOW Input File - File simulation through cracked ILNT vault	M-4
M.1-3.	PORFLOW Input File - Flow simulation through failed ILNT vault	M-7
M.1-4.	PORFLOW Input File - Mass transport simulation for intact ILNT vault	M-10
M.1-5.	PORFLOW Input File - Mass transport simulation for intact ILNT vault, solubility-limited source	M-14
M.2-1.	PORFLOW-3D input files for the groundwater flow field	M-18
M.2-2.	PORFLOW-3D input file for the groundwater mass transport of C-14 and Tc-99 ..	M-23

TABLES

2.1-1.	Water quality of the Savannah River above SRS (Cummins et al. 1990)	2-19
2.1-2.	Comparison of natural radiation doses near SRS with U.S. averages	2-24
2.2.1.	Summary of hydraulic conductivities reported for Aquifer System II	2-33
2.2-2.	Concentration of dissolved elements in groundwater in Aquifer Unit IIA and Units IIB1 and IIB2 near E-Area (Cummins et al. 1990)	2-36
2.2-3.	Water quality of UTR Creek at Road A (Cummins et al. 1990)	2-37
2.2-4.	Maximum constituent results exceeding applicable standards for wells at the EAVDF (Arnett et al. 1991)	2-39
2.2-5.	Groundwater monitoring results for the EAVDF (Cummins et al. 1990)	2-40
2.2-6.	Monitoring well results of radionuclides in groundwater for the EAVDF (Cummins et al. 1990)	2-42
2.7-1.	NR waste radioactive inventory	2-61
2.9.1	Values for hydraulic properties of vault closure design	2-67
3.2-1.	Maximum contaminant limits for radionuclides in groundwater corresponding to different options for groundwater protection requirement	3-24
3.3-1.	Summary of hydraulic and van Genuchten fitting parameters	3-62
3.3-2.	Partition coefficients used in PORFLOW near-field simulations, mL/g	3-69
3.3-3.	LAW vault parameters	3-71
3.3-4.	ILNT vault parameters	3-72
3.3-5.	Degradation times for vaults, years	3-73
3.3-6.	Hydraulic conductivities for saturated zone simulations	3-79
3.3-7.	Aquifer matrix-specific mass transport parameters	3-80
3.5-1.	Implementation of NQA-1 by ORNL for the EAVDF RPA	3-100
3.5-2.	Implementation of NQA-1 by INEL for the EAVDF RPA	3-102
4.1-1.	Trigger values for radionuclides selected for detailed groundwater analyses	4-3
4.1-2.	Simulation time for each state of the vault	4-10

4.1-3.	Peak fractional flux release to the aquifer for EAV radionuclides except isotopes of U and Pu	4-15
4.1-4.	Solubility limit and peak flux to the aquifer for isotopes of U and Pu	4-16
4.1-5.	Predicted groundwater compliance concentration for the ILNT vaults	4-19
4.1-6.	Predicted groundwater compliance concentration for the LAW vaults	4-21
4.1-7.	Annual EDEs from drinking water pathway per unit concentration of radionuclides in groundwater	4-30
4.1-8.	Comparison of MCLs and allowable groundwater concentrations based on the 25 mrem per year performance objective for off-site individuals	4-31
4.1-9.	Calculated allowable inventories based on the groundwater pathway (for off-site doses up to 10,000 years after disposal)	4-33
4.1-10.	SDCFs for agriculture scenario for inadvertent intruders	4-36
4.1-11.	SDCFs for resident scenario for inadvertent intruders	4-37
4.1-12.	SDCFs for post-drilling scenario for inadvertent intruders	4-38
4.1-13.	Geometrical reduction factors (G) used in dose analyses for inadvertent intruders	4-39
4.1-14.	Results of dose analysis for intruder agriculture scenario for ILNT vaults	4-46
4.1-15.	Results of dose analysis for intruder agriculture scenario for LAW vaults	4-52
4.1-16.	Results of dose analysis for intruder agriculture scenario for ILT vaults	4-56
4.1-17.	Results of worst-case dose analysis for resident scenario for ILNT vaults at 100 years after disposal	4-60
4.1-18.	Results of dose analysis for resident scenario for ILNT vaults at 10,000 years after disposal	4-62
4.1-19.	Results of dose analysis for resident scenario for LAW vaults at 100 years after disposal	4-64
4.1-20.	Results of worst-case dose analysis for resident scenario for ILT vaults at 100 years after disposal	4-66
4.1-21.	Results of dose analysis for resident scenario for ILT vaults at 10,000 years after disposal	4-67
4.1-22.	Results of dose analysis for post-drilling scenario for LAW vaults	4-70

4.1-23.	Disposal limits of radionuclides for ILNT and ILT vaults based on analyses of exposure scenarios for inadvertent intruders	4-74
4.1-24.	Concentration limits of radionuclides for Class-C waste specified in NRC's 10 CFR Part 61	4-76
4.1-25.	Disposal limits of radionuclides for LAW vaults based on analyses of exposure scenarios for inadvertent intruders	4-77
4.1-26.	Disposal limits of radionuclides for ILT vaults based on analyses of exposure scenarios for inadvertent intruders	4-80
4.3-1.	E-Area Vault Disposal Facility performance-based inventory limits (Ci/vault) and limiting performance objectives	4-94
4.3-2.	Comparison of LAW vault calculated disposal limits with estimated inventory	4-95
4.3-3.	Comparison of ILNT and ILT vault calculated disposal limits with estimated inventory	4-96
6.0-1.	E-Area PA organizational chart	6-14
A.1-1.	Longitudinal and transverse dispersivities used in the PORFLOW near-field model	A-7
A.2-1.	Measured and assumed hydraulic conductivities for saturated hydraulic units	A-20
A.2-2.	Total porosities - E-Area	A-21
A.4-1.	Radionuclides considered in dose analyses for off-site individuals or inadvertent intruders	A-41
A.4-2.	Internal dose conversion factors for ingestion of radionuclides	A-51
A.4-3.	Internal dose conversion factors for inhalation of radionuclides	A-53
A.4-4.	External dose-rate conversion factors for radionuclides uniformly distributed in 15 cm of surface soil	A-57
A.4-5.	External dose-rate conversion factors for radionuclides uniformly distributed in infinite thickness of soil-equivalent material	A-58
A.4-6.	Annual EDEs from drinking water pathway per unit concentration of radionuclides in water	A-65
A.4-7.	Elemental plant-to-soil concentration ratios in vegetables	A-69

A.4-8.	Annual EDEs from vegetable pathway per unit concentration of radionuclides in exhumed waste for agriculture scenario	A-71
A.4-9.	Annual EDEs from soil ingestion pathway per unit concentration of radionuclides in exhumed waste for agriculture scenario	A-74
A.4-10.	Annual EDEs from external exposure in vegetable garden per unit concentration of radionuclides in exhumed waste for agriculture scenario	A-77
A.4-11.	Annual EDEs from external exposure in home per unit concentration of radionuclides in disposal units for agriculture scenario	A-79
A.4-12.	Annual EDEs from inhalation exposure in vegetable garden per unit concentration of radionuclides in exhumed waste for agriculture scenario	A-82
A.4-13.	Annual EDEs from inhalation exposure in home per unit concentration of radionuclides in disposal units for agriculture scenario	A-84
A.4-14.	Annual EDEs per unit concentration of radionuclides in disposal units from all exposure pathways for agriculture scenario	A-89
A.4-15.	Annual EDEs per unit concentration of radionuclides in disposal units for resident scenario	A-93
A.4-16.	Annual EDEs per unit concentration of radionuclides in exhumed waste for post-drilling scenario	A-95
A.4-17.	Summary of radionuclide-independent parameter values used in dose analyses for off-site individuals and inadvertent intruders	A-99
B.4-1.	Evaluation of identified alternative subsurface flow and transport codes	B-20
C.1-1.	Screening calculations and trigger levels for the ILT vaults	C-2
C.1-2.	Screening calculations and trigger levels for the ILNT vaults	C-24
C.1-3.	Screening calculations and trigger levels for the LAW vaults	C-46
C.1-4.	Weighted dose conversion factors for radionuclides with multiple daughters	C-68
C.2-1.	Steam gaging results for SRS creeks in the vicinity of E-Area	C-72
C.3-1.	Screening calculations and trigger values for the suspect soil trenches	C-75
C.6-1.	AIRDOS-PC data for the volatile radionuclide pathway	C-143

D.4-1.	Summary of distribution coefficients for selected radionuclides on goethite	D-4
D.4-2.	Adsorption of Pu(IV) on goethite as a function of ionic strength	D-7
D.4-3.	Adsorption data for strontium used to estimate K_d	D-18
D.4-4.	Adsorption data for barium used to estimate radium K_d	D-25
D.5-1.	Plutonium reactions considered	D-34
D.5-2.	Uranium reactions considered	D-36
I.2-1.	Radionuclides considered in the detailed groundwater analysis for suspect soil trenches	I-6
I.2-2.	Distribution coefficients assumed for elements in suspect soil trenches	I-12
I.3-1.	Peak flux to the water table from suspect soil trenches	I-21
I.3-2.	Predicted groundwater compliance concentration for the suspect soil trenches	I-24
I.3-3.	Comparison of MCLs and allowable groundwater concentrations based on the 25 mrem per year performance objective for off-site individuals	I-28
I.3-4.	Groundwater-based disposal limits for the suspect soil trenches	I-30
I.3-5.	Suspect soil disposal limits based on the air pathway	I-33
I.3-6.	Results of dose analysis for intruder agriculture scenario for suspect soil trenches ..	I-34
I.3-7.	Summary of disposal limits for the suspect soil trenches	I-40
J.1-1.	Factor specification for Latin Hypercube Sample generation	J-2
J.3-1.	Variable definitions for multiple regression model	J-4
J.3-2.	Important variable combinations	J-4
J.4-1.	Confidence intervals for mean	J-5
J.4-2.	Tolerance limits on response distribution	J-5
L.1-1.	Radioactive inventory for 41 NR disposal casks to be shipped to E-Area	L-5
L.2-2.	Distribution coefficients assumed for subsurface transport simulations for radionuclides in NR waste	L-14
L.3-1.	Peak flux to the water table from NR waste	L-23
L.3-2.	Predicted groundwater compliance concentration for the NR waste	L-25
L.3-3.	Groundwater-based disposal limits for the NR waste	L-26
L.3-4.	Disposal limits for NR waste based on the air pathway	L-28
L.3-5.	Groundwater-based disposal limits versus expected inventory for the NR waste ..	L-40

ACRONYMS AND ABBREVIATIONS

ACRI	Analytic and Computational Research, Inc.
ALARA	as low as reasonably achievable
ANSI	American National Standards Institute
ARARs	applicable or relevant and appropriate requirements
ASL	above sea level
ASME	American Society of Mechanical Engineers
CCF	concentration/consumption factor
CERCLA	Comprehensive Environmental Resource, Compensation, and Liability Act
cm	centimeters
cpu	central processor unit
CRDMS	control rod drive mechanisms
CSRA	Central Savannah River Area
CTT	contaminant travel time
D&D	decommissioning and decontamination
DCF	dose conversion factor
DOE	Department of Energy
DWPF	Defense Waste Processing Facility
DWS	drinking water standards
EAVs	E-Area vaults
EAVDF	E-Area Vault Disposal Facility
EDE	effective dose equivalent
EH	Environment, Safety, and Health
EM	Environmental Restoration and Waste Management
EPA	Environmental Protection Agency
ER	environmental restoration

FM	Facilities Management
GSA	General Separations Area
h	hour(s)
HAD	Hazard Assessment Document
HFO	hydrous ferric oxide
HLW	high-level waste
HW/MWDF	Hazardous Waste/Mixed Waste Disposal Facility
IAW	Intermediate Activity Waste
ILTV	Intermediate Level Tritium Vaults
ILNTV	Intermediate Level Non-Tritium Vaults
in.	inches
INEL	Idaho National Engineering Laboratory
kg	kilograms
L	liter(s)
LAW	Low Activity Waste
LAWV	Low Activity Waste Vault
LLW	low-level waste
LLWSB	long-lived waste storage building
m	meters
MCLs	maximum contaminant levels
mg	milligrams
mm	millimeters
MMI	Modified Mercalli Intensity
mol	mole(s)
MPC	maximum permissible concentration
MSL	mean sea level
MW	mixed waste
NCRP	National Council on Radiation Protection and Measurements

Rev. 0

NESHAPs	National Emissions Standards for Hazardous Air Pollutants
NPL	National Priority List
NQA	Nuclear Quality Assurance
NR	naval reactor
NRC	Nuclear Regulatory Commission
ORNL	Oak Ridge National Laboratory
OSRs	Operational Safety Requirements
PA	performance assessment
PC	personal computer
PDWS	primary drinking water standards
ppm	parts per million
QA	Quality Assurance
RCRA	Resource Conservation and Recovery Act
RPA	Radiological Performance Assessment
s	second(s)
SAR	Safety Analysis Report
SCDHEC	South Carolina Department of Health and Environmental Control
SDCFs	scenario dose conversion factors
SDF	Saltstone Disposal Facility
Sect.	Section
SMSA	Standard Metropolitan Statistical Area
SRS	Savannah River Site
SWDF	Solid Waste Disposal Facility
TRU	transuranic waste
TV	trigger value
UTR	Upper Three Runs (Creek)

WAC	waste acceptance criteria
WCR	water to cement ratio
WITS	Waste Information Tracking System
WSRC	Westinghouse Savannah River Company

Rev. 0

xxviii

EXECUTIVE SUMMARY

This radiological performance assessment (RPA) for the Savannah River Site (SRS) E-Area Vaults (EAVs) Disposal Facility was prepared to meet the requirements of Chapter III of the U.S. Department of Energy Order 5820.2A. The Order specifies that an RPA should provide reasonable assurance that a low-level waste (LLW) disposal facility will comply with the performance objectives of the Order. The performance objectives require that:

- 1) exposures of the general public to radioactivity in the waste or released from the waste will not result in an effective dose equivalent of 25 mrem per year;
- 2) releases to the atmosphere will meet the requirements of 40 CFR 61;
- 3) inadvertent intruders will not be committed to an excess of an effective dose equivalent of 100 mrem per year from chronic exposures, or 500 mrem from a single acute exposure; and
- 4) groundwater resources will be protected in accordance with Federal, State, and local requirements.

The EAVs, located on a 200-acre site immediately north of the current LLW burial site, will provide a new disposal and storage site for solid, low-level, non-hazardous radioactive waste. As presently planned, the EAV Disposal Facility will contain several large concrete vaults divided into cells. The EAVs consist of three types of structures to house four designated waste types. One type of structure is partitioned into two segments [the Intermediate Level Tritium Vaults (ILTV) and Intermediate Level Non-Tritium Vaults (ILNTV)] and receives two categories of waste. The ILNTV receives waste radiating ≥ 200 mR/h at 5 cm from the exterior of the outer disposal container. The ILTV receives waste which is contaminated with more than incidental quantities of tritium. Administratively, the lower limit for the ILTV is 10 Ci of tritium per package. These two vaults share a similar design, are adjacently located, share waste handling equipment, and will be closed as one facility. The second type of structure is designated as the Low Activity Waste Vaults (LAWV). The LAWV is designed to receive waste radiating < 200 mR/h at 5 cm from the exterior of the outer disposal container and containing < 10 Ci of tritium per package. The third facility is the Long Lived Waste Storage Building (LLWSB). The LLWSB is designed to provide covered, long term storage for waste containing long lived isotopes which exceeds

performance criteria for disposal. This waste would eventually be removed to a suitable disposal facility. In addition to the disposal activities described previously, two additional types of disposal are proposed: 1) trench disposal of suspect soil, and 2) naval reactor component disposal. Five below grade trenches will be constructed to contain suspect soil, which is soil from regulated areas and designated as potentially contaminated. An area of approximately 1700 m² is planned to receive several containers of naval reactor (NR) components. These components can include control rods, control rod drive mechanisms, resin vessels, adapter flanges, and similar equipment.

The long-term performance of the vaults is key to the prediction of the transport of radionuclides into the environment at E-Area. A special study was conducted by an independent engineering firm to study the degradation mechanisms and their effects on the integrity of the vault systems. The results of this study predicted the time required for cracking of the vaults and collapse of the roof structures.

To evaluate the long-term performance of the EAVs, site-specific conceptual models were developed to consider: 1) exposure pathways and scenarios of potential importance; 2) potential releases from the facility to the environment; 3) effects of degradation of engineered features; 4) transport in the environment; and 5) doses potentially received from releases determined from unit concentrations of the radionuclides of interest in each vault type. Initial radionuclide inventories were not assumed in this performance assessment. The EAV performance assessment was used as a means to determine the allowable radionuclide concentrations and inventories in each type of disposal unit. This methodology provides reasonable assurance that the performance objectives will be met if these inventories are used to establish limits in the waste acceptance criteria.

When compared to a reasonable estimate of the amount of waste that could be received at the E-Area Vault Disposal Facility, the performance-based maximum radionuclide inventory limits in this report will allow disposal of all waste types expected at SRS, with the exception of the NR components. These components will be received as planned, but will be stored. It is expected that additional wasteform information will be received to enable revision of the performance assessment for this type of waste, to show acceptable performance.

1. INTRODUCTION

The Savannah River Site (SRS) was acquired by the U.S. Government in 1950. Since that time, the U. S. Government has contracted for the design, development, construction, and operation of various facilities at the SRS to support national defense and space exploration. Because of these activities at the site, low-level, solid, non-hazardous radioactive wastes will continue to be generated. In addition, environmental restoration (ER) and decommissioning and decontamination (D & D) activities will generate increasing quantities of low-level radioactive wastes.

The policies and guidelines of the Department of Energy (DOE) and other regulatory agencies require that radioactive waste be managed, treated, stored, and disposed in a manner that protects public health and safety, the environment, and groundwater resources. These practices must be done in accordance with standards specified in federal, state, and local regulations. The level of radioactivity in any effluent released to the environment should be maintained "as low as reasonably achievable (ALARA)", known as the "ALARA" principle within the DOE complex.

DOE Order 5820.2A, issued in 1988 (U.S.DOE 1988a), established policies, guidelines, and minimum requirements for the management of radioactive waste, mixed waste (MW), and contaminated facilities at the DOE sites. This Order addresses the storage, treatment, and disposal of high-level waste (HLW), MW, low-level waste (LLW), transuranic waste (TRU), and naturally occurring and accelerator-produced radioactive materials that are generated by the DOE operations. Chapter III of the Order requires the DOE field sites to prepare and maintain a site-specific radiological performance assessment (RPA) for any LLW disposal facility located at DOE field sites. An RPA must provide reasonable assurance that the facility design and method of disposal will comply with the performance objectives of the Order (Dodge et al. 1991).

The E-Area Vaults Disposal Facility (EAVDF) (Fig. 1.1-1) is one of several new facilities at SRS that will incorporate radioactive solid waste generated at the SRS for near-surface disposal.

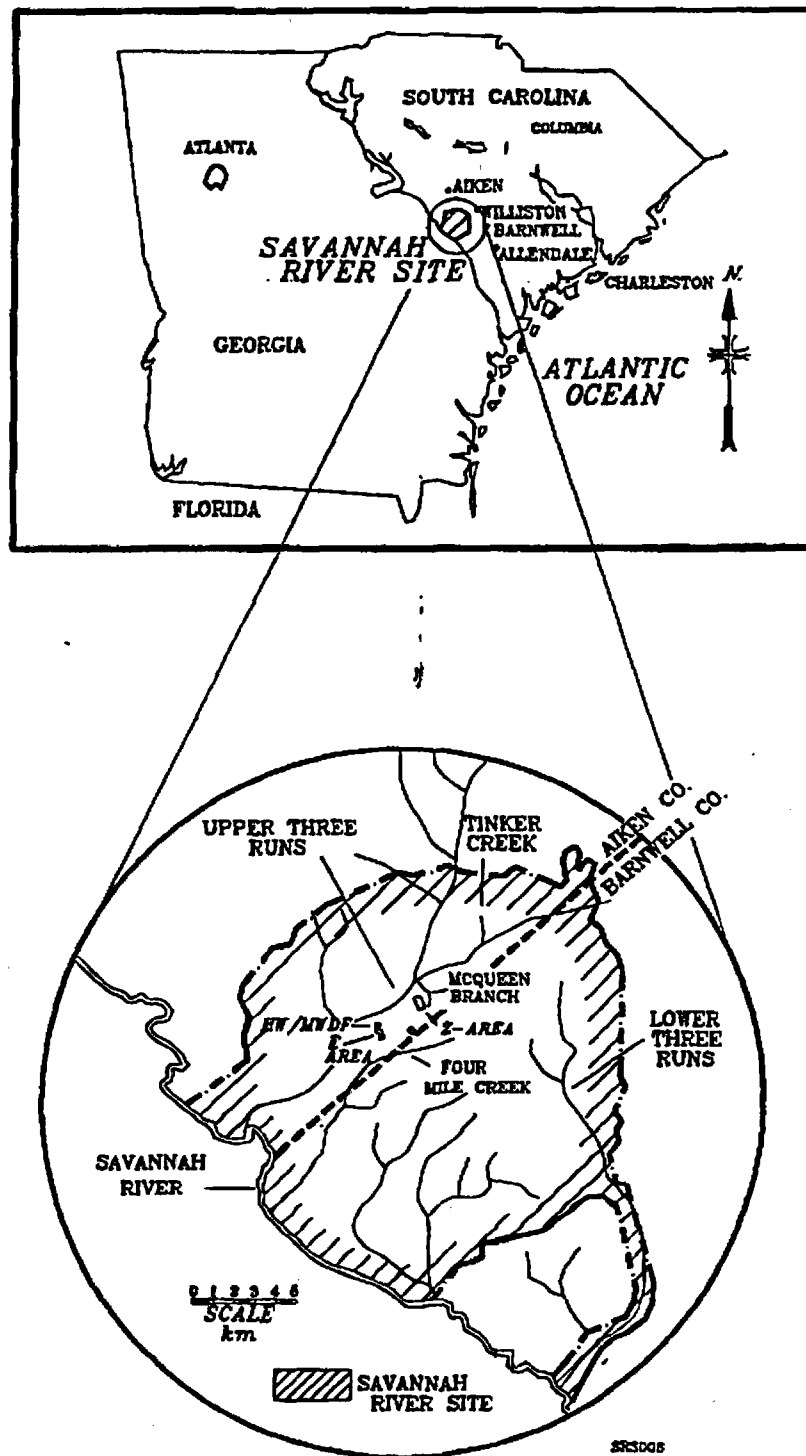


Fig. 1.1-1. Location map of the Savannah River Site.

The E-Area Vaults (EAVs) are only one part of an integrated radioactive waste management system that is being put in place at the SRS. As principal contractor and operator at SRS, the Westinghouse Savannah River Company (WSRC) will complete the design, construct and operate several facilities to manage and dispose of radioactive waste generated at the SRS. Assuming adequate funding is maintained at the SRS, all facilities that are a part of this integrated waste management system are projected to be in operation by the year 2000.

Before the SRS will comply completely with DOE Order 5820.2A, a separate RPA must be completed for at least three operating or planned disposal facilities at the SRS: 1) the EAVs solid waste disposal facility (SWDF), 2) the Saltstone Disposal Facility (SDF) (located in Z-Area), and 3) the Hazardous Waste/Mixed Waste Disposal Facility (HW/MWDF). To fulfill the RPA requirement of DOE Order 5820.2A for the EAV, the long-term radiological impacts on the environment and on the public due to solid waste disposal in E-Area have been assessed. Results of this assessment are documented in this report. An RPA has been completed for the SDF. An RPA has not been completed for the HW/MWDF since the construction and operation of this facility has been postponed. A description of the HW/MWDF is given in Sect. 2.8 along with a description of its integration with this RPA.

1.1 PURPOSE AND SCOPE

E-Area is the location of a new LLW disposal facility located at SRS. The objective of the EAV is to provide a new disposal and storage site for low-level, solid, non-hazardous radioactive waste to support continuing SRS operations. DOE Order 5820.2A defines low-level radioactive waste as waste that contains radioactivity and is not classified as high-level waste (HLW) (waste material that results from the reprocessing of spent nuclear fuel), transuranic waste, or spent nuclear fuel or 11e(2) by product material.

SRS operations further classify the LLW handled by EAV as low-activity waste (LAW), intermediate-activity waste (IAW) and tritiated waste. IAW consists of waste material that radiates greater than 200 mR/hr from an unshielded container at 5 cm. LAW consists of waste material that radiates less than 200 mR/hr from an unshielded container at 5 cm. Tritiated waste is waste that contains greater than 10 Ci of tritium per container regardless of the radiation rate. EAV will not dispose of or store liquid wastes, waste containing greater than 100 nCi/g of TRU isotopes, hazardous waste, or mixed (hazardous and radioactive) wastes.

Monitoring systems and procedures are in place to establish both the impact to the environment and the risks to operating personnel and off-site populations during normal operations and subsequent closure operations at the disposal site. Groundwater monitoring procedures are in place to provide baseline monitoring data and to confirm that disposal and closure operations do not adversely affect water quality. This RPA concentrates on establishing, with reasonable assurance, that LLW disposal in E-Area will meet the performance objectives of DOE Order 5820.2A after the disposal facility is closed. The objectives of the Order are described in Sect. 1.2.

Radiological and other hazards prior to closure have been analyzed in the Safety Analysis Report (SAR) for the operational period of the EAV (WSRC 1991a). In particular, the SAR for the EAV addresses the issues and hazards related to safety and radiological doses to on-site and off-site populations during active disposal operations and interim closure. The location of E-Area is well within the confines of the secured boundary of the SRS, thus precluding inadvertent access to the E-Area site by unauthorized personnel during active disposal operations. Furthermore, the distance to the present SRS site boundary obviates the need for extensive analysis of performance prior to closure and/or loss of institutional control.

1.2 PERFORMANCE OBJECTIVES

The specific performance objectives for solid waste disposal in E-Area are contained in DOE Order 5820.2A (U.S.DOE 1988a):

1. Protect public health and safety in accordance with standards specified in applicable EH Orders and other DOE Orders.
2. Assure that external exposure to the waste and concentrations of radioactive material which may be released to surface water, groundwater, soil, plants, and animals results in an effective dose equivalent (EDE) that does not exceed 25 mrem per year to a member of the general public. Releases to the atmosphere shall meet the requirements of 40 CFR 61 which limits the EDE to 10 mrem per year. Reasonable effort should be made to maintain releases of radioactivity in effluent to the general environment ALARA.
3. Assure that the EDE from all exposure pathways received by individuals who inadvertently may intrude into the facility after the loss of active institutional control (100 years) will not exceed 100 mrem per year for continuous exposure or 500 mrem for a single acute exposure.
4. Protect groundwater resources, consistent with Federal, State, and local requirements.

Compliance with the performance objective to protect groundwater resources is interpreted at SRS as meaning that concentrations of chemical and radioactive contaminants at any points of compliance should not exceed standards for public drinking water supplies established by the Environmental Protection Agency (EPA).

In this analysis, the point of compliance for groundwater protection requirements is taken to be that location more than 100 m from any disposed waste at which the predicted concentrations of contaminants in groundwater are the highest (Dodge et al. 1991). Requirements for protection of groundwater do not apply inside a 100-m buffer zone around the disposal units.

The performance objectives for disposal of LLW in the EAV given above require further interpretation with respect to three issues. The first is the time period over which the performance objectives for protection of off-site members of the public, inadvertent intruders, and groundwater resources should be applied. The second issue is the particular standards (i.e., numerical limits) for radionuclides that should be applied to protection of groundwater resources. The third issue is the inclusion of doses from radon and its decay products in the doses calculated in the intrusion scenarios.

1.2.1 Time for Compliance with Performance Objectives

The various performance objectives for LLW disposal in DOE Order 5820.2A do not specify a time period over which they are to be applied. Therefore, the implication is that all performance objectives apply at any time after disposal.

The DOE is actively considering a change in policy regarding the time for compliance with the performance objectives. In the near future, the DOE is expected to adopt a policy that compliance with the performance objectives would be required only for 10,000 years after disposal but would not be required thereafter. In addition, however, if the predicted doses to off-site individuals or inadvertent intruders or the predicted levels of contaminants in groundwater outside the 100-m buffer zone have not attained their maximum values within the 10,000-year compliance period, the DOE is expected to require that the analysis be continued beyond 10,000 years until such time as the peak doses or contaminant levels are attained. Any calculations beyond the 10,000-year compliance period would be used primarily to provide additional information and perspective on the performance of disposal facilities.

Although strict compliance with the performance objectives beyond 10,000 years would not be required, the results of any analyses beyond 10,000 years could be used by the DOE in rendering judgments on the overall acceptability of disposal facilities.

In accordance with the expected change in DOE policy, the following approach to the time period for compliance with the performance objectives has been taken in this RPA.

- 1) The performance objectives for protection of off-site members of the public, inadvertent intruders, and groundwater resources are applied for 10,000 years after disposal.
- 2) If calculated doses to off-site members of the public or inadvertent intruders or calculated contaminant levels in groundwater do not attain their maximum values during the 10,000-year compliance period, the calculations are continued in time until the peak values are obtained.

1.2.2 Performance Objective for Groundwater Protection

DOE Order 5820.2A does not specify either dose or concentration limits for radionuclides in groundwater. Therefore, there is some ambiguity in applying the performance objective even though, as described previously, the performance objective is interpreted as requiring that concentrations of contaminants in groundwater should not exceed values specified in EPA standards for public drinking water supplies (40 CFR Part 141).

In the RPA for the EAV, three different options for specifying maximum contaminant levels (MCLs) of radionuclides in groundwater are considered. The three options, each of which is consistent with EPA standards for radioactivity in drinking water, are described below.

Option 1

In the first option, the MCLs for radionuclides in groundwater are those specified in current EPA standards for radioactivity in drinking water, which were promulgated in 1976. The current standards include: 1) a limit on concentration of 5 pCi/L for Ra-226 and Ra-228 combined; 2) a limit on concentration of 15 pCi/L for gross alpha-particle activity, including Ra-226 but excluding radon and uranium; and 3) a limit on dose equivalent to whole body or any organ of 4 mrem per year from all beta/gamma-emitting radionuclides. The current standards also specify that the concentration of any beta/gamma-emitting radionuclide causing a dose equivalent of 4 mrem to whole body or any organ shall be calculated on the basis of a drinking water intake of 2 L/day and data for converting activity intakes of radionuclides to dose published by the U.S. Department of Commerce (1963), except the MCLs are given as 20,000 pCi/L for tritium (H-3) and 8 pCi/L for Sr-90.

A possible drawback of the approach specified by the EPA for calculating MCLs for beta/gamma-emitting radionuclides is that the concentration limits in water corresponding to a dose equivalent to whole body or any organ of 4 mrem are based on internal dosimetry data (U.S. Department of Commerce 1963) which are now outdated. The dosimetric and metabolic models for radionuclides used to obtain the data in the Department of Commerce report essentially are those recommended in Publication 2 of the International Commission on Radiological Protection (ICRP 1959), but these data have been superseded by data based on the models in ICRP Publication 30 (1979). Although the more recent internal dosimetry data developed by the ICRP have been adopted for use by the EPA (Eckerman et al. 1988) and DOE (1988b), these data have not yet been incorporated in the EPA standards for radioactivity in drinking water. Because these standards use outdated internal dosimetry data for beta/gamma-emitting radionuclides, the MCLs for most radionuclides calculated as specified by the EPA would not correspond to the specified limit on dose equivalent of 4 mrem to whole body or any organ. This consideration leads to the second option for the performance objective adopted for use in this analysis.

Option 2

In the second option, the EPA's current MCLs of 5 pCi/L for Ra-226 and Ra-228 combined and 15 pCi/L for gross alpha-particle activity, including Ra-226 but excluding radon and uranium, and the limit on dose equivalent of 4 mrem per year to whole body or any organ from all beta/gamma-emitting radionuclides are retained. However, the dose limit for any beta/gamma-emitting radionuclide is converted to a concentration limit using the internal dosimetry data from ICRP Publication 30 (1979) that has been adopted for use by the DOE (1988b). Thus, for beta/gamma-emitting radionuclides, the second option uses the same primary standard (i.e., dose limit) as the current EPA standards, but the secondary standards (i.e., concentration limits) are based on up-to-date internal dosimetry data; and, in this option, the MCLs for all beta/gamma-emitting radionuclides correspond, based on the best available information, to the dose limit of 4 mrem per year to whole body or any organ.

Option 3

In the third option, the MCLs for radionuclides in groundwater are those specified in the EPA's proposed revisions of the drinking water standards (DWS) for radionuclides (EPA 1991). The proposed standards include: 1) separate limits on concentration of 20 pCi/L for Ra-226 and Ra-228; 2) a limit on concentration of 20 µg/L for uranium, 3) a limit on concentration of 15 pCi/L for gross alpha-particle activity, excluding Ra-226, uranium, and Rn-222; and 4) a limit on EDE of 4 mrem per year for all beta/gamma-emitting radionuclides. The proposed concentration limit for uranium is based on prevention of chemical toxicity in the kidney, rather than limitation of radiation dose, and corresponds to an activity concentration of 14 pCi/L for naturally occurring uranium with its normal isotopic abundances. The proposed standards also include a concentration limit of 300 pCi/L for Rn-222, but the Energy Policy Act of 1992 directs the EPA not to issue a standard for radon in drinking water at the present time. Final revisions of the DWS for radionuclides have not yet been promulgated.

The proposed revisions of the DWS for radionuclides described above differ from the current standards in two respects that are potentially important for this RPA. First, the proposed revisions include an MCL for uranium, whereas uranium is unregulated in current standards. Second, the proposed revisions include a limit on EDE for beta/gamma-emitting radionuclides, whereas the dose limit in current standards applies to whole body or any organ. For radionuclides that preferentially irradiate only one or a few body organs (e.g., I-129, Pu-239) a limit on EDE of 4 mrem corresponds to a considerably different MCL than a limit on dose equivalent of 4 mrem to whole body or any organ, even when the same dosimetric and metabolic model is used. Internal dosimetry data based on ICRP Publication 30 (1979) presumably would be used to convert the dose limit of 4 mrem EDE to radionuclide-specific MCLs.

Summary

Three different options for specifying the performance objective for protection of groundwater resources have been used in this analysis. These options are summarized as follows:

- 1) Current EPA standards for radionuclides in drinking water, including the method prescribed by the EPA for calculating MCLs for beta/gamma-emitting radionuclides based on internal dosimetry data from ICRP Publication 2 (1959) and the specified MCLs for H-3 and Sr-90;
- 2) Current EPA standards for radionuclides in drinking water, except all MCLs for beta/gamma-emitting radionuclides are calculated from the prescribed dose limit using updated internal dosimetry data based on ICRP Publication 30 (1979); and

- 3) Proposed revisions of the EPA standards for radionuclides in drinking water, with MCLs for beta/gamma-emitting radionuclides calculated using internal dosimetry data based on ICRP Publication 30 (1979), except no standard for radon is assumed.

Option 1 will be used in this RPA to assess compliance with the groundwater protection performance objective; for uranium, a compliance limit of 20 $\mu\text{g/L}$ from Option 3 will be used. The SRS is one of the DOE sites designated as being on the National Priority List (NPL) by the Comprehensive Environmental Response, Compensation, and Liability Act (CERCLA) (40 CFR 300). As a result, all groundwater at SRS is regulated by CERCLA. Under CERCLA, the MCLs promulgated under the Safe Drinking Water Act (40 CFR 141) are used as applicable or relevant and appropriate requirements (ARARs). Thus, even though they use out-dated dose methodology, the current MCLs (Option 1) should be used for compliance. Where the current MCLs do not specify a limit (as in the case of uranium), a proposed MCL can be used as an ARAR. Thus the compliance limit for uranium is 20 $\mu\text{g/L}$. In most, but not all, cases Option 1 produces the most restrictive MCLs (see Table 3.2-1).

1.2.3 Radon

Radon-222 is produced by the decay of uranium-234 and -238. Radon can be a potentially significant contributor to doses in intruder scenarios. The current DOE Waste Management Order, 5820.2A, does not provide guidance as to whether doses from radon are to be included in assessing compliance with the performance objectives. However, the DOE Waste Management Order is now being revised. As a result of guidance provided by the Performance Assessment Task Team, the draft DOE Order, 5820.2B (U.S.DOE 1994), excludes dose from radon and its decay products in assessing compliance with the general population and intruder protection requirements. A separate exhalation objective is set for radon: "the limit for radon exhalation rate from the ground surface to air will be 20 $\text{pCi/m}^2\text{s}$

(0.7 Bq/m²s)*. This performance objective is taken from Subpart Q of 40 CFR 61 [National Emission Standards for Hazardous Air Pollutants (NESHAPs)], which addresses radon emissions from DOE storage and disposal facilities that contain radium (except uranium mill tailings, which are covered under a separate regulation). In this performance assessment (PA), results from intrusion scenarios will be presented to include doses from radon and its decay products. However, compliance will be assessed by excluding the dose from radon and its decay products. Compliance for radon will be assessed versus the radon exhalation rate stated above.

2. DISPOSAL FACILITY DESCRIPTION

In this chapter of the EAV RPA, characteristics which may either govern the impact of the EAVDF or be impacted by the EAV are described. In Sect. 2.1, regional characteristics of the SRS and vicinity are described that focus on geography, demography, meteorology, seismicity, hydrogeology, quality of surface waters and groundwaters, soils, ecology, and the existing radiological environment. Sect. 2.2, organized similarly to Sect. 2.1, concentrates on characteristics specific to E-Area.

In Sect. 2.3, the classification of solid waste sent to E-Area for disposal, the projected composition of the solid waste, and the physical facilities that are used to dispose of solid waste are described. The solid waste properties are described in Sect. 2.4. The disposal vaults and the projected site layout that are used as a basis for this assessment of long-term performance at the EAV are described in Sect. 2.5. The radionuclide contaminants that are pertinent to assessing long-term performance are described in Sect. 2.6. In Sect. 2.9, the site closure concept used to complete this assessment is described.

2.1 REGIONAL CHARACTERISTICS

The EAVDF is located within the SRS in an area designated as E-Area. Before describing the physical facility, the geography, demography, meteorology, seismicity, hydrogeology, surface water hydrology, water quality, soils, and ecology of the SRS relevant to assessing the facility's performance are described.

2.1.1 Geography of the Region

The SRS occupies about 780 km² in Aiken, Barnwell, and Allendale counties on the Upper Atlantic Coastal Plain of southwestern South Carolina (Fig. 2.1-1). The center of the SRS is approximately 40 km southeast of Augusta, GA; 32 km south of Aiken, SC; 160 km from the Atlantic Coast; and is bounded on the southwest by the Savannah River, for about 28 km. The Fall Line, which separates the Atlantic Coastal Plain physiographic province from the Piedmont physiographic province, is approximately 50 km northwest of the central SRS.

In addition to the Savannah River, other prominent geographical features within 80 km of the SRS are Thurmond Lake, Par Pond and L-Lake. Thurmond Lake is the largest nearby public recreational area. This reservoir is on the Savannah River and is about 64 km upstream of the center of the SRS. Par Pond is a 11 km² reactor cooling water impoundment that lies in the eastern sector of the SRS. L-Lake is a 4 km² reactor cooling water impoundment that lies in the southern sector of the SRS (Fig. 2.1-2).

The elevation of the SRS ranges from 24 m above sea level (ASL) at the Savannah River to about 122 m ASL in the upper northwest portion of the site. The Pleistocene Coastal terraces and the Aiken Plateau form two distinct physiographic subregions at the SRS (WSRC 1992a). The Pleistocene Coastal terraces are below 82 m in elevation, with the lowest terrace constituting the present flood plain of the Savannah River and the higher terraces characterized by gently rolling topography. The relatively flat Aiken Plateau occurs above 82 m.

The Aiken Plateau is dissected by numerous streams. Because of the large number of tributaries to small streams on the SRS site, no location on the site is far from a flowing stream, most of which drain to the Savannah River.

The dominant vegetation on the SRS is forest, with types ranging from scrub oak communities on the driest areas to bald cypress and black gum in the swamps. Pine forests cover more area than any other forest type. Land utilization presently is about 56% in pine forests, 35% in hardwoods, 7% in SRS facilities and open fields, and 2% in water (WSRC 1992a).

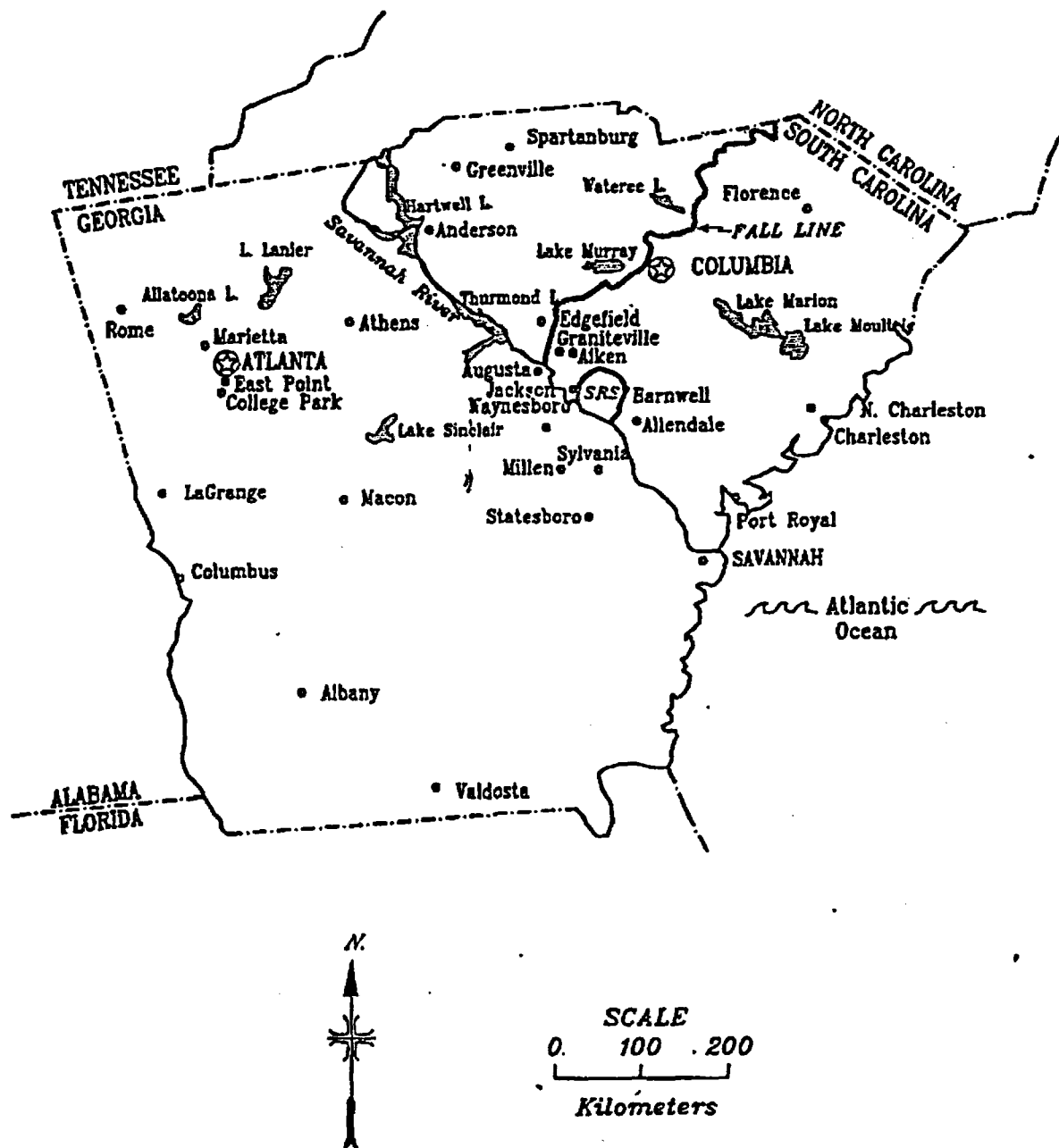


Fig. 2.1-1. SRS regional location map.

SRS081

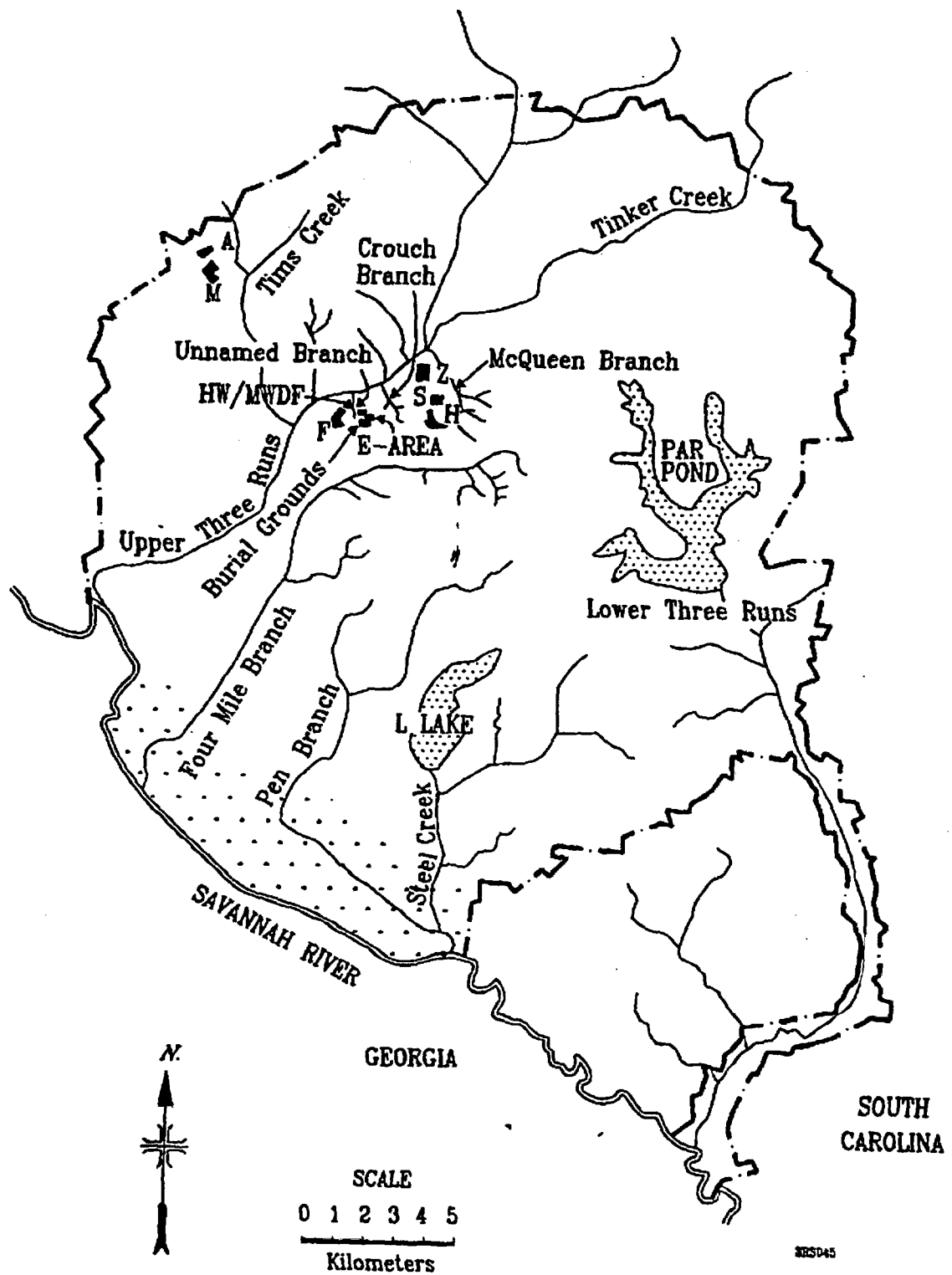


Fig. 2.1-2. Facility location map of the SRS, showing surface drainage.

Rev. 0

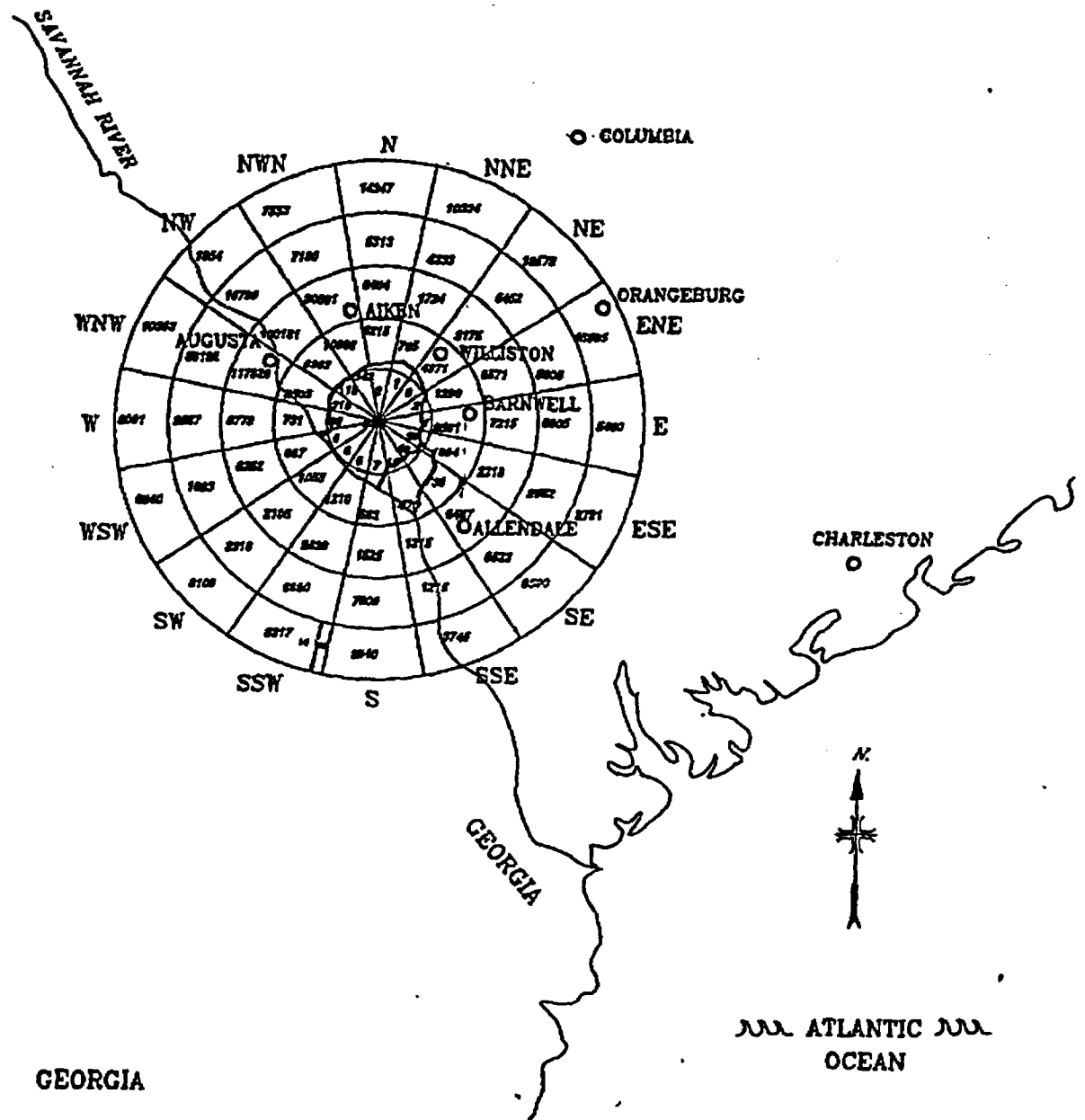
Except for three roadways and a railway that are near the edge of the SRS, public access to the SRS is restricted to guided tours, controlled deer hunts, and authorized environmental studies. Figure 2.1-2 shows the major areas at the SRS and their location within the site boundary. The major production areas located at the site include: Raw Materials (M Area), Separations (F and H Areas), Waste Management Operations (E, F, and H Areas), and Defense Waste Processing (S and Z Areas) (WSRC 1992). Administrative and support services, the Savannah River Technology Center and the Savannah River Ecology Laboratory are located in A-Area.

2.1.2 Demography

The population within 80 km of the SRS consists of a permanent (resident) and transient population, the latter of which includes industrial, recreational, and casual components. The distribution of the permanent populations within a 80 km radius of the SRS, based on 1980 U. S. Census data, is illustrated in Fig. 2.1-3. The data were assembled by geographical division formed by subdividing the study area into 16 radial segments centered on the north overlain by concentric circles with radii of 16, 32, 48, 64, and 80 km. The area within the 16 km radii are DOE-owned properties within the SRS. There are no permanent population groups within this area.

The major residential population centers 80 km from the approximate SRS plant center point are Augusta, Georgia, about 40 km to the northwest; Aiken, South Carolina, about 32 km to the north; and Orangeburg, South Carolina, about 79 km to the east northeast (Fig. 2.1-1). In 1980, the estimated population within the 80 km radius around the SRS was approximately 553,000 (Cook et al. 1987). More than 50% of the population is in the Augusta, Georgia - South Carolina Standard Metropolitan Statistical Area (SMSA) which includes Richmond and Columbia Counties in Georgia, Aiken County in South Carolina, and the Fort Gordon Military Reservation. Between 1980 and 2030, the residential population within the 80 km radius of the SRS is projected to increase from 553,000 to 845,000, or 53% (Cook et al. 1987).

SOUTH CAROLINA



SRS010

Fig. 2.1-3 Population distribution within an 80-km radius of the central SRS.

Rev. 0

The growth characteristics of the cities and towns around the SRS are similar to those of the rest of the state. There is a distinct pattern of population increase in the areas just outside cities. Cities of Aiken and North Augusta, South Carolina are major urban centers with populations over 25,000. No other major urban centers are expected to develop in this area.

The transient population consists almost entirely of the SRS work force. The Fort Gordon Military Reservation, Alvin W. Vogtle Nuclear Power Plant, and Chem-Nuclear Systems employ approximately 4500, 3400, and 300, respectively.

2.1.3 Meteorology

The regional climate of the SRS is classified as humid subtropical, characterized by short, mild winters and long, warm and humid summers. Summer usually lasts from May through September, at which time daytime temperatures are frequently above 90°F. Winter conditions alternate between warm, moist subtropical air from the Gulf of Mexico and cool, dry polar air. Less than one-third of all winter days have a minimum temperature below freezing. Annual average precipitation, computed from daily meteorological data collected at a SRS meteorological tower from 1952 to 1992, is 124 cm yr⁻¹ (Fig. 2.1-4). Extreme conditions, such as sustained winds, tornadoes, and maximum 24-h rainfall are not expected to impact the post-closure integrity of the disposal facility.

2.1.4 Hydrogeology

The surface of the Upper Atlantic Plain Province on which SRS is located slopes gently seaward. This province is underlain by a seaward dipping wedge of unconsolidated and semi-consolidated sediments that extends and progressively thickens from the Fall Line southeastward to the edge of the continental shelf. The sediments increase in thickness to more than 1.2 km near the coast of South Carolina and were deposited on the seaward sloping basement rock surface. Basement rocks consist of Late Precambrian and Paleozoic metamorphic and

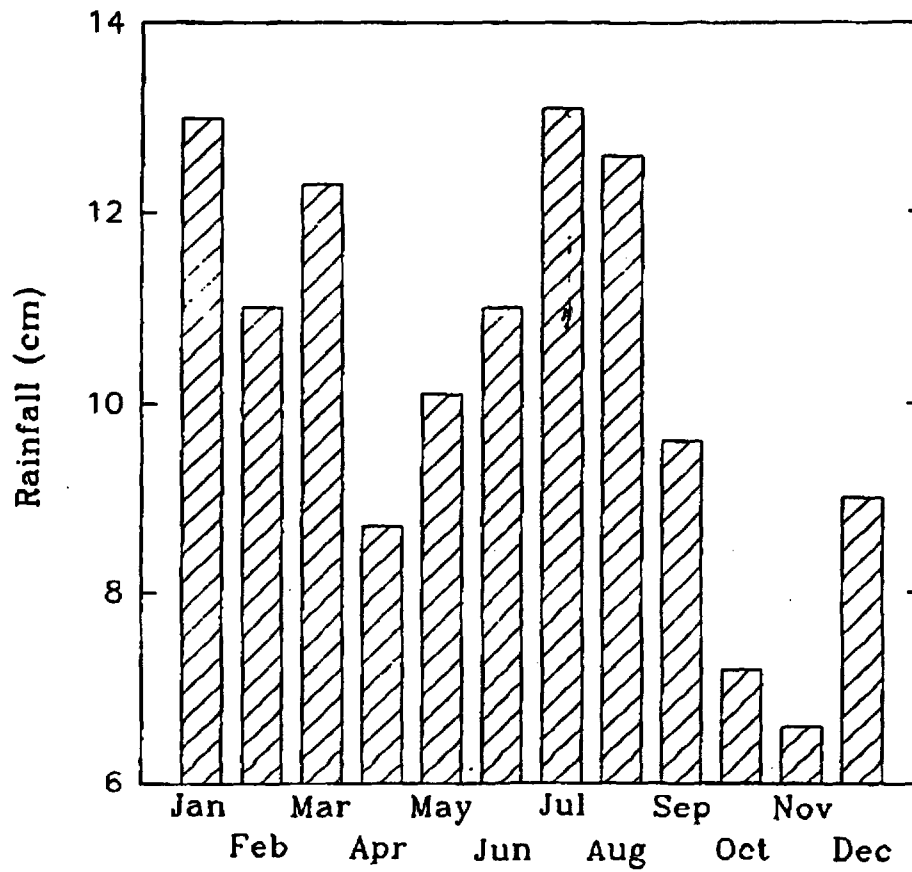


Fig. 2.1-4. Average rainfall at SRS: 1952 - 1992.

Rev. 0

igneous rocks and locally of Triassic siltstones and claystones. The Triassic rocks were deposited in fault-bound basins trending NE-SW within the igneous and metamorphic rocks.

SRS is underlain by a sequence of sediments that ranges in thickness from 180 to 370 m and in age from Cretaceous to Recent (WSRC 1992a). The sediments consist primarily of interbedded and unconsolidated gravels, sands, silts, clays, and limestones which were deposited in near-shore marine environments. Locally, the system can be highly heterogeneous and exhibit significant variability in texture both horizontally and vertically. Layers that are regionally extensive tend to thin in the direction of the Fall Line and can pinch out in the subsurface, adding to the complexity of the groundwater system. Vertical leakage is known to occur between layers. Deep dissection of the Aiken Plateau throughout SRS by streams has cut into the upper units which form the groundwater flow system. Consequently, portions of the uppermost aquifers can be isolated, horizontally, from the same units in other areas at SRS.

Numerous investigators have described the coastal plain sediments based upon lithologic and age criteria (WSRC 1991b). More recently, attempts have been made to define hydrostratigraphic units based upon features that relate to their ability to store and transmit water. The most recent classification system proposed for SRS (Aadland 1990) is presented in Fig. 2.1-5 along with correlating stratigraphic nomenclature of earlier investigators. The nomenclature of Aadland 1990 will be utilized throughout this report. The reader is referred to Appendix E for an in-depth discussion of the hydrostratigraphy of SRS.

Following is an overview of the groundwater hydrology associated with the hydrologic units identified in Fig. 2.1-5. Appendix E documents the hydrology of the bedrock formations and the Coastal Plain sediments. In this section, the hydrology of the upper Coastal Plain sediments, specifically Aquifer System II (Fig. 2.1-5) is summarized. Aquifer System I underlies Aquifer System II and is separated by confining System I - II. This confining system is comprised of the Ellenton Clays, which are greater than 30 m thick and act to retard groundwater flow between the units. Also, vertical hydraulic gradients are in the upward direction across the confining unit in the vicinity of the EAVDF. Thus, Aquifer System I is hydraulically isolated from surface disposal activities, and is not of interest for contaminant studies.

COMPARISION OF HYDROSTRATIGRAPHIC UNITS USED AT SRS						
GEOLOGIC AGE	PRESENT NOMENCLATURE	SRP BASELINE HYDROGEOLOGIC STUDY		PROPOSED NOMENCLATURE AADLAND (1980)		
UNKNOWN	UPLAND	UPLAND UNIT		AQUIFER UNIT I/II/C	AQUIFER UNIT IIB ZONE 2	AQUIFER SYSTEM II
TERTIARY	TOBACCO ROAD SAND	GROUP BARWELL	TOBACCO ROAD		CONFINING ZONE IIB ₁ - IIB ₂	
	IRWINTON SAND MBR.		DRY BRANCH			
	TWIGGS CLAY MBR.		Tan clay			
	DRY BRANCH FM. (Gd/line Lendine Mbr.)					
	SANTEE FORMATION	McBEAN FORMATION			AQUIFER UNIT IIB ZONE 1	SYSTEM I-II CONFINING
	CAWCAW MEMBER	Green clay			CONFINING UNIT IIA - IIB	
	CONGAREE FM.	CONGAREE			AQUIFER UNIT IIA	
	FISHBURNE FM. (Four Mile Mbr.)	WILLIAMSBURG FM.				
	WILLIAMSBURG FM. (Snapp Member)					SYSTEM I AQUIFER
	REHMS FORMATION (Ellenton Mbr.)	ELLENTON FM.				
CRETACEOUS	PEEDEE FM. (Steel Creek Mbr.)	PEEDEE FORMATION		CONFINING UNIT I/IIB-I/II/C	SYSTEM I AQUIFER	
	BLACK CREEK FM.	BLACK CREEK FM.		CONFINING UNIT I/IIA - I/II/B		
	MIDDENDORF FM.	MIDDENDORF FM.		AQUIFER UNIT I/IIA		
	CAPE FEAR FM.	CAPE FEAR FM.		CONFINING SYSTEM I		
	TRAISSIC OR PALEOZOIC BASEMENT				PALEOZOIC - TRIASSIC BASEMENT HYDROLOGIC SYSTEM	

SRS111

Fig. 2.1-5. Hydrologic and stratigraphic units underlying the SRS.

Aquifer System II is divided into individual units that are further subdivided into zones. These units and zones primarily relate to hydrogeological characteristics. The units and zones which comprise the aquifer system are as follows (GeoTrans 1992):

<u>Nomenclature of Aadland (1990)</u>	<u>Common Nomenclature</u>
---------------------------------------	----------------------------

Aquifer System II

Aquifer Unit IIB, Zone 2	Water Table
Confining Unit IIB1-IIB2	Tan Clay
Aquifer Unit IIB, Zone 1	Barnwell/McBean Aquifer
Confining Unit IIA-IIB	Green Clay
Aquifer Unit IIA	Congaree Aquifer
Confining System I-II	Ellenton Clays

2.1.4.1 Hydrogeology of Aquifer Unit IIA (Congaree Aquifer)

Aquifer Unit IIA consists of the clastic sediments of the Congaree Formation and the glauconite-bearing sands and clays of the lowermost Santee Limestone Formation. Aquifer Unit IIA is an aquifer that consists predominantly of fine-to-coarse quartz sand. Clay laminae occur throughout the formation, but they are too thin and discontinuous to be effective seals except locally. Confining Unit IIA - IIB, identified as the "green clay" layer, or Caw Caw member of the Santee Formation, is characterized by rapid facies changes. The permeability of this layer varies greatly from place to place but in most parts of SRS is low enough to form a competent layer between overlying and underlying aquifer units.

The potentiometric surface map for Aquifer IIA, illustrated in Appendix E, shows that flow directions for this unit are convergent toward Upper Three Runs (UTR) Creek. These flow directions reflect that UTR Creek has completely incised Confining Unit IIA-IIB and is a discharge area for Aquifer Unit IIA. Four Mile Creek does not incise Confining Unit IIA-IIB (Parizek and Root 1986), and thus, does not influence the groundwater flow

directions of Aquifer Unit IIA. Elsewhere on the SRS, Aquifer Unit IIA behaves as a confined to semi-confined aquifer (WSRC 1992a). Hydraulic gradients in this unit increase with proximity to UTR Creek. Near UTR Creek, groundwater flow velocities are likely to be proportionately higher, reflecting the increase in hydraulic gradient.

2.1.4.2 Hydrogeology of Aquifer Unit IIB, Zone 1 (Barnwell/McBean)

Aquifer Unit IIB, Zone 1 consists of clastic and carbonate sediments of the Santee Formation and the Dry Branch Formation of the Barnwell Group that lie above the Confining Unit IIA-IIB (Green Clay). Porosity and permeability of Aquifer Unit IIB, Zone 1 strata vary greatly, depending on the dominant lithology and amount of clay present at any particular location. Nowhere on the SRS, however, do the clays in this zone form effective aquitards.

Aquifer Unit IIB, Zone 1 is incised by many of the streams on the SRS, including UTR, McQueen and Crouch Branches. Thus, horizontal flow directions in this zone are affected to a large degree by the incision of drainage ways into the zone.

2.1.4.3 Hydrogeology of Aquifer Unit IIB, Zone 2 (Water Table)

Aquifer Unit IIB, Zone 2 is comprised of the Irwinton Sand Member and the Tobacco Road Formation of the Barnwell Group and the Upland Unit. The Irwinton Sand Member consists of moderately-to-poorly sorted quartz sand with interlaminated clays abundant in places. The Tobacco Road Sand consists of gravels, sands, and appreciable clay layers, but these are discontinuous and do not form an effective regional aquitard. Due to its stratigraphic position, the Tobacco Road Formation is frequently the formation in which the water table occurs in inter-stream areas. Thickness of this formation is extremely variable, but can be as much as 15 m in places. The Upland Unit consists of a mixture of gravel and sand with some finer textured sediments and occurs in thicknesses up to 21 m in some parts of SRS. This unit forms the surficial deposits in the inter-stream upland areas and is part of the vadose zone.

Aquifer Unit IIB, Zone 2 overlies Confining Zone IIB₁-IIB₂, which consists of the Twiggs Clay Member commonly known as the "Tan Clay". Confining Zone IIB₁-IIB₂ varies from 0.6 to 3 m in thickness where present. Like Aquifer Unit IIB, horizontal flow directions in Aquifer Unit IIB, Zone 2, are strongly influenced by incision of the unit by surface water drainage ways.

2.1.5 Seismicity

The susceptibility of the SRS, and particularly E-Area, to seismic motion is of interest to establish if E-Area is suitable for waste disposal. Seismic events could result in cracking of the vaults. Cracking could be fairly severe if liquefaction of supporting soils were to take place. However, liquefaction of supporting soils is not considered to be a potential problem at the SRS based on a review of previous studies at the SRS (URS/Blume 1982). Below is a discussion of seismic zones that are known to exist in the vicinity of the SRS, and the expected intensity associated with seismic activity in these zones at the SRS.

2.1.5.1 Location of Nearby Seismic Zones

The SRS is located in the interior of the North American plate. In the past 200 years the nearest zones of concentrated seismic activity in the region are centered in the Charleston-Summerville area of South Carolina and near Bowman, SC, which is 60 km northwest of Summerville, SC (Fig. 2.1-6). Recent seismic activity in the Charleston area, probably including the earthquake of 1886, has originated largely or entirely in the basement beneath the Coastal Plain sediments. The seismicity in the Charleston area is believed to occur at the intersection of the Ashley River fault and the Woodstock fault, at minimum depths of 4 km and 8 km, respectively. Seismicity associated with the Bowman seismic zone occurs along a border fault of a buried Triassic basin, extending to a depth of about 6 km (WSRC 1992a).

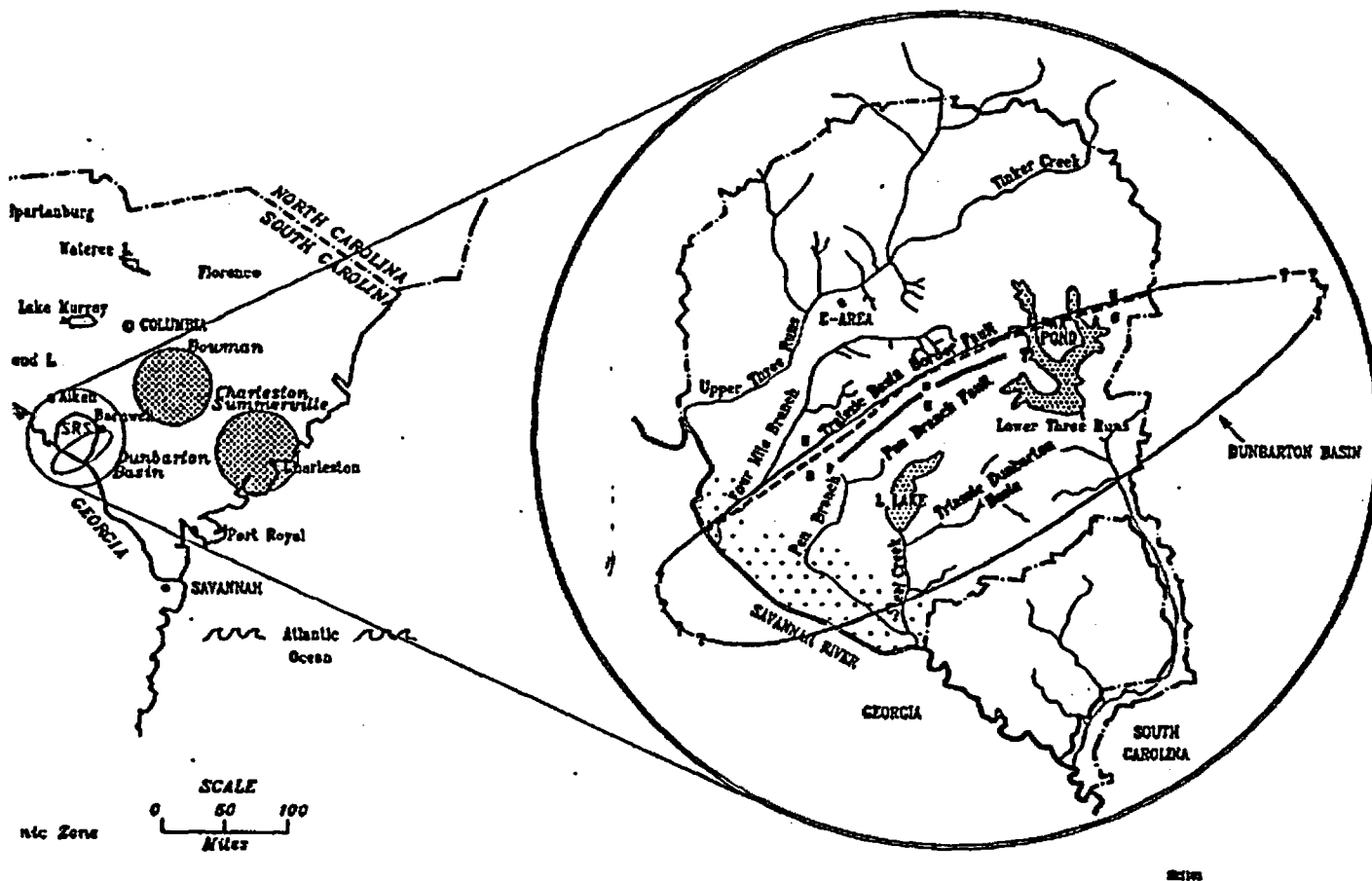


Fig. 2.1-6. Location of the Bowman and Charleston-Summerville seismic zones, and the Dunbarton Basin on the SRS.

Underlying the Coastal Plain sediments of the central and southern portions of the SRS is a Triassic-Jurassic rift basin within the crystalline basement. This basin, called the Dunbarton Triassic basin, is located in the Aiken Plateau, about 50 km southeast of the Fall Line (Fig. 2.1-6). Associated with this basin on the SRS are at least two faults; the northern border fault and a parallel fault, the Pen Branch fault, which may coincide with the border fault. These faults do not extend upward into post-Oligocene sediments at SRS.

Faulting has also been recognized in sediments as young as Oligocene in the Atlantic Coastal Plain sediments of South Carolina. Faulting has been postulated to occur in these sediments based on structure-contour mapping of the Eocene-Oligocene unconformity, which lies between 30 and 61 m below the surface, in the vicinity of Charleston, and about 100 km from the SRS, faulting has been postulated to occur in these sediments. A shallow fault, associated with a 16-km wide graben of Oligocene and Miocene rocks which crosses beneath the Savannah River from Georgia into South Carolina, is postulated about 56 km southeast of the SRS. It is not currently possible to relate these shallow faults to modern earthquakes that occur at depths greater than about 2 km.

2.1.5.2 Intensities of Historical Earthquakes

The largest known earthquake to affect the site region was the Charleston earthquake of 1886. This Modified Mercalli Intensity (MMI) X earthquake struck Charleston SC, on August 31, 1886. The greatest intensity felt at the SRS has been estimated at MMI VI-VII (felt by all; everyone runs outdoors; damage negligible in buildings of good structure, but considerable in poorly built structures) as a result of the Charleston earthquake (WSRC 1992a). Minor tremors from aftershocks of the 1886 Charleston event were also felt in the area where the SRS is now located. Intensities of these tremors were estimated to be equal to or less than MMI IV.

Seismic activity, producing earthquakes of estimated MMI up to V to VII, has been present in the Bowman area (about 95 km northeast of SRS) over the last 200 years (WSRC 1992a). These earthquakes produced motion at the SRS of less than 0.1 g (Stephenson

1993). An earthquake (MMI VIII) that struck Union County, SC (about 160 km north-northeast of the SRS) in 1913 was felt at Aiken (6 km north-northwest of SRS) with a MMI of II-III (vibration indoors like a passing truck).

Two earthquakes of MMI III or less have occurred with epicentral locations within the boundaries of the SRS (Stephenson et al., 1985; Stephenson 1988). A MMI III earthquake occurred in June 1985 at the SRS, as did a MMI I-II earthquake in August 1988. Neither of the earthquakes triggered the seismic alarms at the SRS facilities, which are triggered when ground accelerations equal or exceed .002 g. The epicenters of these earthquakes appear to be located within about six miles of the intersection of a northwest-trending fault and the northeast-trending border fault at the northern edge of the Dunbarton Triassic basin, and are relatively shallow (1 to 3 km below the earth's surface).

2.1.5.3 Projected Recurrence of Earthquakes

According to Bollinger et al. (1989), the recurrence interval for a Charleston size shock (MMI X) for the Charleston area and for the Coastal Plain is on the order of 1000 years, at the 95% confidence level. A recurrence of the 1886 Charleston earthquake would result in an intensity of MMI VII at the SRS (URS/Blume 1982). Recurrence of earthquakes associated with other known seismic zones in the region are not expected to be of greater intensity, nor cause greater shaking at the SRS (WSRC 1992a).

2.1.6 Surface Water Hydrology

The Savannah River cuts a broad valley approximately 76 m deep through the Aiken Plateau, on which most of the SRS sits. The Savannah River Swamp lies in the floodplain along the Savannah River and averages about 2.4 km wide. Upper Three Runs Creek, Fourmile Branch, Tinker Creek, Pen Branch, Steel Creek, and Lower Three Runs Creek (Fig. 2.1-2) are the major tributaries of the Savannah River that occur on the SRS. Three breaches of the natural levee occur at the confluences of the Savannah River with Beaver Dam Creek, Fourmile Branch, and Steel Creek, allowing discharge of these streams to the

river. During swamp flooding, water from Beaver Dam Creek and Fourmile Branch flows through the swamp that parallels the river and combines with the Pen Branch flow. Pen Branch joins Steel Creek about 0.8 km above its mouth.

Surface water is held in artificial impoundments and natural wetlands on the Aiken Plateau. Par Pond, the largest impoundment on the SRS, is located in the eastern part of the SRS, covering about 11 km². A second impoundment, L Lake, lies in the southern portion of SRS and covers approximately 4 km². The waters drain from Par Pond and L Lake to the south, via Lower Three Runs Creek and Steel Creek, respectively, into the Savannah River. Lowland and upland marshes, and natural and man-made basins on the SRS retain water intermittently.

Near the SRS, the flow of the Savannah River has been stabilized by the construction of upstream reservoirs. The yearly average flow is approximately 290 m³ s⁻¹. From the SRS, river water usually reaches the coast in five to six days, but may take as few as three days. At low flow, which usually occurs in autumn months, the Savannah River is about 100 m wide and 3 to 5 m deep, with an average flow of approximately 160 m³ s⁻¹.

2.1.7 Water Quality and Usage

2.1.7.1 Groundwater

The sand beds that comprise Aquifer System I are an important source of water for wells in localities neighboring the SRS. Most municipal and industrial water supplies in Aiken County, SC are developed in Aquifer System I. In Barnwell and Allendale counties, some municipal users are supplied from the shallower Aquifer Zones IIA and IIB. Private domestic supplies in all of these counties are primarily obtained from Aquifer System I.

Municipal and industrial groundwater use in the vicinity of the SRS indicated total pumpage from Aquifer System I on the order of 1 m³ s⁻¹; 0.2 m³ s⁻¹ from Aquifer Unit IIA; and up to 0.04 m³ s⁻¹ from Aquifer Zone IIB₁. The SRS uses up to 0.4 m³ s⁻¹ on site, from Aquifer System I (Cook et al. 1987).

Water quality parameters for groundwater at the SRS are likely to be quite variable. Parameters specific to E-Area are presented in Sect. 2.2 below.

2.1.7.2 Surface Water

Water from the Savannah River is used for drinking water at two locations below the SRS. About 160 km downstream of SRS, The Beaufort-Jasper Water Treatment Plant at Hardeeville, SC, withdraws about $0.3 \text{ m}^3 \text{ s}^{-1}$ for a consumer population of approximately 51,000. The Cherokee Hill Water Plant at Port Wentworth, GA, about 160 km downstream of the SRS, presently withdraws about $2 \text{ m}^3 \text{ s}^{-1}$ for a consumer population of about 20,000. The Savannah River is also used for commercial and sport fishing and for recreational boating. Surface water quality is presently monitored by the Environmental Monitoring Section and the Savannah River Technology Center at the SRS (Cummins et al. 1990). Surface water is characterized with respect to radiological and non-radiological aspects, both on site and downstream of the SRS. Some water quality characteristics of the Savannah River upstream of the SRS, classified as a Class B water by the South Carolina Department of Health and Environmental Control (SCDHEC), are listed in Table 2.1-1. The temperature, dissolved oxygen, and pH values reflected in this table are within the standards required for Class B waters (Cummins et al. 1990). Other water quality parameters listed in this table are within the ranges observed in previous years (Cummins et al. 1990), indicating that the quality of the Savannah River is not being degraded at the point of measurement.

2.1.8 Soils

Most of the soils at the SRS are sandy over a loamy or clayey subsoil. The distribution of soil types is very much influenced by the creeks on the site, with colluvial deposits on hill-tops and hillsides giving way to alluvium in valley bottoms (Dennehy et al. 1989). Road cuts and excavations on interstream areas near the SRS commonly expose a deeply developed soil profile. Two horizons are apparent; the A horizon may be up to 3 m thick, and typically consist of structureless fine- to medium-grained quartz sand, and the lower B horizon, which may be from 0.6 to 3 m in thickness, contains iron and aluminum compounds leached from the overlying material.

**Table 2.1-1. Water quality of the Savannah River
above SRS (Cummins et al. 1990)**

Parameter	Units	No. of Analyses	Arithmetic Mean	Max	Min
Temperature	°C	12	18	27	10
pH	pH	12		7.4	6.2
Dissolved oxygen	mg/L	12	8.0	9.6	6.4
Alkalinity	mg/L	12	21	24	17
Conductivity	umhos/cm	12	84	104	61
Turbidity	NTU	12	6.9	18	2.3
Suspended solids	mg/L	12	13	22	6.0
Volatile solids	mg/L	12	2.3	4.0	1.0
Total dissolved solids	mg/L	12	62	76	46
Total solids	mg/L	12	74	86	58
Fixed residue	mg/L	12	10	19	5.0
Chemical oxygen demand	mg/L	12	9.7	17	7.0
Chloride	mg/L	12	7.8	11	4.6
Nitrogen (as NO ₂ /NO ₃)	mg/L	12	0.32	0.99	0.15
Sulfate	mg/L	12	7.8	11	6.0
Phosphorus (as PO ₄)	mg/L	12	0.09	0.16	0.05
Nitrogen (as NH ₃)	mg/L	12	0.13	0.34	<0.02
Cadmium	mg/L	4	<0.01	<0.01	<0.01
Mercury	μg/L	4	<0.20	0.20	<0.20
Chromium	mg/L	4	<0.02	<0.02	<0.02

Weathering effects are evident. In some areas, intense weathering has produced tensional soil fractures as a result of volume reduction. These fractures are dominant features in shallow exposures such as drainage ditches or roadside embankments. Average soil erosion rates for the area surrounding the SRS, much of which is cropland, range from 1.5 to 2.0 kg m⁻² yr⁻¹. (U.S. Department of Agriculture 1985) Employing the Universal Soil Loss Equation to predict erosion at the SRS under different vegetative conditions, Horton and Wilhite (1978) estimate that the presence of natural successional forests would reduce erosion by a factor of 400 to 500 over cropland erosion.

2.1.9 Ecology

2.1.9.1 Aquatic Ecology

Flora in the Savannah River basin and in creeks on the SRS site is diverse and seasonally variable. Several species of diatoms, green algae, yellow-green algae, and blue-green algae are present. In seasonally flooded areas, bald cypress and tupelo gum thrive. In less severely flooded areas, oak, maple, ash, sweet gum, ironwood, and other species, less tolerant of flooding, are found. In the river swamp formed by the Savannah River in the vicinity of the SRS, herbaceous growth is sparse. A number of macrophytes, such as cattail and milfoil, are found in areas receiving sufficient sunlight.

The fish communities in the Savannah River and in creeks on the SRS are very diverse. Redbreast sunfish, spotted sucker, channel catfish, and flat bullhead are the dominant species. Sunfish, crappies, darters, minnows, American shad, and striped bass are also abundant.

Macroinvertebrate communities are largely comprised of true flies, mayflies, caddisflies, stoneflies, and beetles. Leaf litter input is high, but is rapidly broken down by macroinvertebrate shredders. The Asiatic clam is found in the Savannah River and its larger tributary streams.

2.1.9.2 Terrestrial Ecology

Prior to its acquisition by the U. S. Government in 1951, approximately one-third of the SRS was cropland, about half was forested, and the remainder was floodplain and swamp. Since that time, the U. S. Forest Service has reclaimed many previously disturbed areas through natural plant succession or by planting pine trees. As was noted in Sect. 2.1.1, 91% is now pine or hardwood forests, with the remaining 9% divided between SRS facilities and water bodies.

A variety of vascular plants exist on the site. Scrub oak communities cover the drier sandy areas, which includes predominantly longleaf pine, turkey oak, bluejack oak, blackjack oak, dwarf post oak, three awn grass, and huckleberry (U.S.DOE 1987). On the more fertile, dry uplands, white oak, post oak, southern red oak, mockernut hickory, pignut hickory, and loblolly pine predominate, with an understory of sparkleberry, holly, greenbriar, and poison ivy. Pine trees cover more area than any other tree genus.

The heterogeneity of the vegetation on the SRS supports a diverse wildlife population. Several species of reptiles and amphibians are present due to the variety of aquatic and terrestrial habitats. These include snakes, frogs, toads, salamanders, turtles, lizards, and alligators. More than 213 species of birds have been identified on the SRS. Burrowing animals at the SRS include: Peromyscus polionotus, known commonly as the Old Field Mouse; Blarina brevicauda, known as the Short Tail Shrew; Scalopus aquaticus, known as the Eastern Mole; Pogonomyrmex badius, known as the Harvester Ant; Dorymyrmex pyramicus, known as the Pyramid Ant; and earthworms (Briese and Smith 1974; Davenport 1964; Golley and Gentry 1964; Smith 1971; Van Pelt 1966).

2.1.10 Existing Radiological Environment

All human beings are exposed to sources of ionizing radiation which include naturally occurring and man-made sources. The average dose contribution estimates from various sources to individuals were obtained from recent reports of the National Council on Radiation Protection and Measurements (NCRP) and the EPA. On average, a person living in the

Central Savannah River Area (CSRA) receives an annual radiation dose of 379 mrem (Cummins et al. 1990). The average dose contributions from the various radiation sources to an individual in the CSRA are given in Fig. 2.1-7.

The major source of radiation exposure to an average member of the public in the CSRA is attributed to naturally-occurring radiation. This naturally-occurring radiation is often referred to as natural background radiation. Natural sources of radiation include cosmic radiation from outer space, cosmogenic radionuclides formed by interaction of cosmic radiation with elements in the earth's atmosphere, terrestrial radiation from natural radioactive materials in the ground, radiation from radionuclides occurring naturally in the body, and inhaled or ingested radionuclides of natural origin. The amount of exposure an individual receives depends on their location. Table 2.1-2 compares national averages for exposure to natural background radiation to average exposures in the vicinity of the SRS.

The average annual dose to people in the U.S. from cosmic radiation is about 27 mrem, which is lower than estimated for the vicinity of the SRS because a large fraction of the U.S. population lives near sea level, where cosmic radiation is lower. A report published by the EPA gives a specific outdoor cosmic radiation dose for Augusta, GA of about 41 mrem (Oakly 1972). When shielding and the time spent indoors are considered, the annual average cosmic radiation dose for the CSRA population is about 33 mrem, about 22% higher than the national average. The average annual EDE from terrestrial gamma radiation is about 28 mrem in the U.S. This annual EDE varies geographically across the U.S. Values from the SRS vicinity include 43 mrem for Augusta, GA, 23 mrem for Charleston, SC, and 68 mrem for Columbia, SC (Oakly 1972).

The major contributors to the annual EDE for internal radionuclides are the short-lived decay products of radon (mostly ^{222}Rn), which contribute an average EDE of about 200 mrem per year. This dose estimate is based on an average radon concentration of about 1 pCi/L (NCRP 1987). The results of long term measurements in living areas of about 30,000 homes in the U.S. suggest that the mean radon concentration levels are about 3.6 pCi/L for the U.S. population and about 1 pCi/L for South Carolina (Alter and Oswald 1988). The average EDE from other internal radionuclides is about 39 mrem per year, which is predominantly

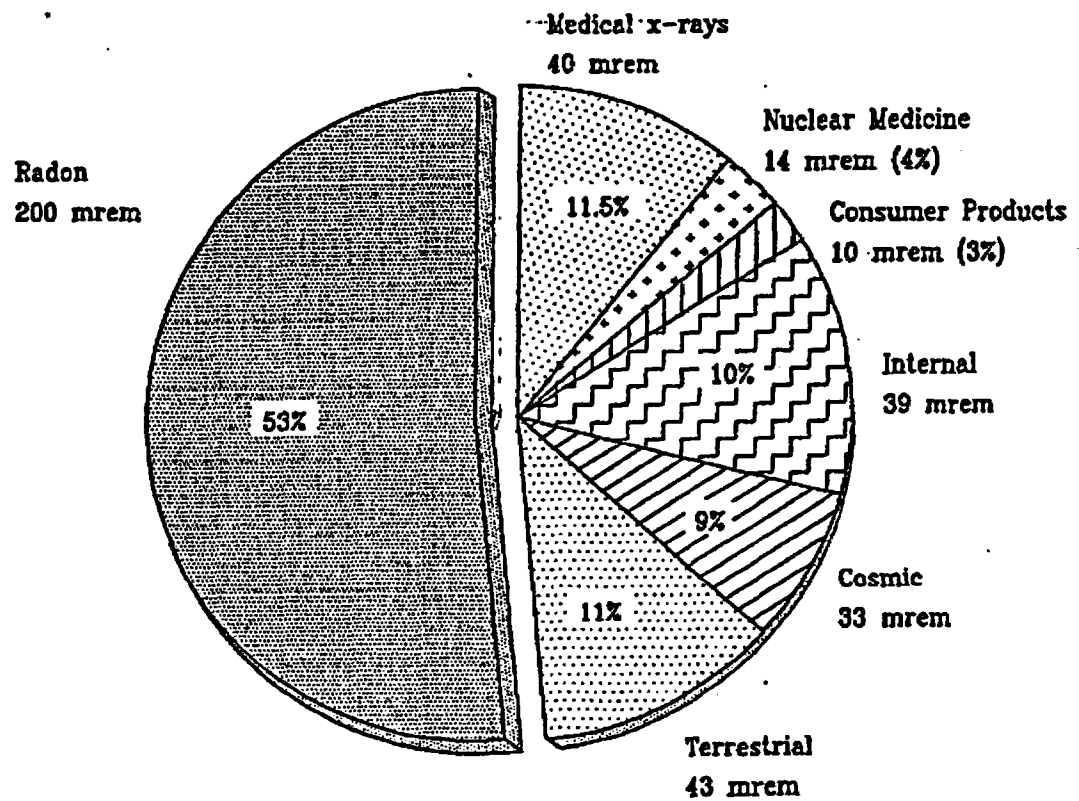


Fig. 2.1-7 The total average effective dose equivalent from various sources in the Central Savannah River Area.

SRS072

Table 2.1-2. Comparison of natural radiation doses near SRS with U.S. averages^a

Natural Radioactivity	Annual Average EDE (mrem)	
	50-mile radius of SRS	U.S. Average
Cosmic radiation	33	27
Terrestrial radiation	43	28
Internal radiation ^b	239	240
Total	315	295

^a Cummins et al. 1990.

^b Approximately 200 mrem of the dose from internal radiation is attributed to radon exposure. An EPA study, which was scheduled to be published in 1991, will update the information on the U.S. distribution of doses from radon. Preliminary information suggests that the U.S. average dose from radon may be higher than 200 mrem.

attributed to the naturally occurring radioactive isotope of potassium, ^{40}K . The concentration of ^{40}K in human tissues is similar in all parts of the world (NCRP 1987).

A wide range of consumer products also contain sources of ionizing radiation. The U.S. average annual EDE to an individual is about 10 mrem (NCRP 1987).

Radiation is an important tool of diagnostic medicine and cancer treatment. The average annual EDE to all individuals from all medical examinations is 54 mrem (about 40 mrem for diagnostic x-rays and 14 mrem for nuclear medicine procedures). The actual EDEs to individuals who receive such medical exams is much higher than these values, because not everyone receives such exams each year (NCRP 1989).

There are a few additional minor sources of radiation that contribute to the average EDEs to individuals in the U.S. About 1,320,000 people performed radiation work in 1980 and received an average dose of 110 mrem per year (Cummins et al. 1990). This exposed population represents only about one half of 1% of the U.S. population. The dose to the general public from nuclear fuel cycle facilities, such as uranium mines, mills, fuel processing plants, nuclear power plants, and transportation routes, has been estimated at less than 1 mrem per year.

Small doses to individuals occur as a result of radioactive fallout from atmospheric atomic bomb tests emissions of radioactive materials from other nuclear facilities, such as DOE facilities; emissions from mineral extraction facilities; and transportation of radioactive materials. The combination of these sources contributes less than 1 mrem per year to the average dose to an individual (Cummins et al. 1990).

Environmental monitoring is performed at the SRS to demonstrate that releases of radionuclides from the site do not exceed the radiation protection guidelines for the general public. Thousands of samples are collected and analyzed each year. Materials monitored include: air, groundwater, drinking water, milk, food stuffs, SRS streams and basins, vegetation, rainwater, Savannah River water, soil and sediments, fish, and wildlife. These samples are collected in defined ways from on site, at the site perimeter, and at locations up to 160 km from SRS. The samples are analyzed for specific radionuclides. Measurements of environmental gamma radiation are also made at numerous on-site and off-site locations (Cummins et al. 1990).

The non-radiological environment is also monitored at SRS. The materials sampled in the non-radiological program include: air, groundwater, Savannah River sediment, SRS streams and outfalls, and fish. In addition to laboratory analyses, water and air quality measurements are routinely made in the field. Non-radiological compounds monitored include nitrate, some heavy metals, and some chlorinated organics.

An environmental monitoring program has been maintained continuously in the SRS region since 1951. Public reports have been published since 1959 dealing with various aspects of the environmental program at SRS. In 1985, the on-site and off-site environmental monitoring reports were merged into a single publication. Recent monitoring results specific to E-Area, that provide information on the existing radiological environment at the EAV disposal site, are provided in Sect. 2.2.5.

2.2 E-AREA SITE DESCRIPTION

The following is a discussion of site characteristics specific to E-Area, that were not covered explicitly in the above discussion on regional characteristics.

2.2.1 E-Area Location, Description, and Land Use

The E-Area at the SRS, where the EAVDF is located, consists of approximately 200 acres, and is situated immediately north of the current LLW burial grounds (Fig. 2.1-2). Construction on the EAVDF began in October of 1989. The site is an elbow-shaped, cleared area of 100 acres, curving to the northwest on an interfluvial plateau in the center of SRS. The site slopes from an elevation of 290 feet in the southernmost corner to an elevation of 250 ft in the northernmost corner. Runoff is to the north and east toward UTR Creek and two of its ephemeral tributaries, Crouch Branch to the east of the EAVDF and an unnamed branch to the west. UTR Creek is approximately 2500 feet north of the facility boundary. The nearest perennial stream is approximately 1200 feet northeast of the boundary. A topographic map showing elevations and the local streams in the vicinity of E-Area is provided in Fig. 2.2-1.

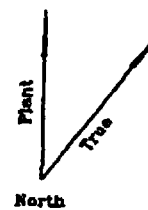
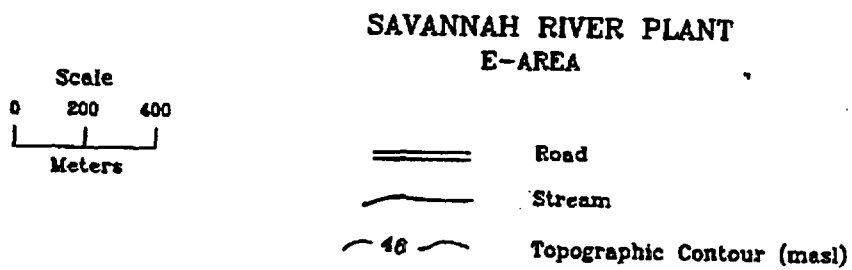
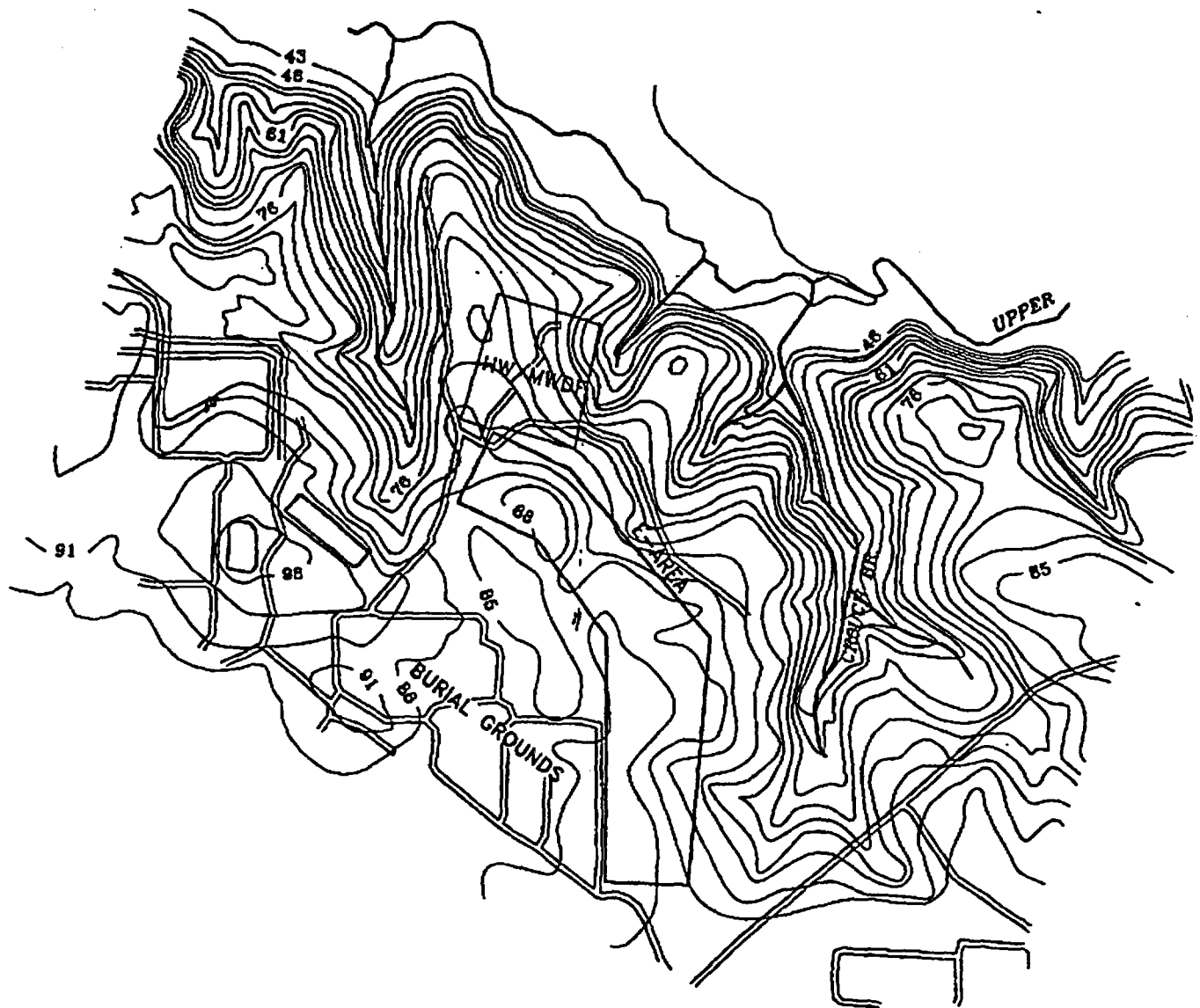


Fig. 2.2-1. Topographic map of the vicinity of E-Area.

889118

2.2.2 Hydrogeology of E-Area

The hydrogeology of the upper coastal plains sediments comprising Aquifer System II are discussed in this section. As previously mentioned, this is the only aquifer system that can be impacted by shallow waste disposal activities. The groundwater flow system beneath the EAVDF is relatively constrained and acts to force the groundwater to flow toward nearby surface water discharge zones.

Groundwater flow directions in Aquifer Units IIB, Zones 1 and 2, are northward toward discharge areas along Crouch Branch, UTR Creek, and the unnamed branch. Groundwater flow in these units cannot move southward because natural hydraulic gradients prevent such an occurrence. Vertical-flow directions are downward and some groundwater flows from these units across Confining Unit IIA - IIB into Aquifer IIA.

Horizontal-flow directions in Aquifer Unit IIA are directly toward UTR Creek, which is the regional discharge zone for this unit in the vicinity of the EAVDF. Aquifer Unit IIA is a zone of vertical-flow convergence. Groundwater flow is into the unit from both overlying and underlying aquifers. Natural groundwater gradients prevent the possibility of any contaminants migrating any deeper than Aquifer Unit IIA.

Much of the hydrogeologic information specific to E-Area comes from well boring logs and water level data from a series of wells placed in E-Area. A location map of these wells is provided in Fig. 2.2-2. Two lithologic cross-sections developed from this information are shown in Fig. 2.2-3 and 2.2-4.

Aquifer Unit IIA (Congaree) unconformably overlies Confining System I-II (Ellenton Clays) and ranges from 16 to 33 m thick within the GSA, which includes E-Area. The Unit dips 1.5 to 1.7 m per km to the south and southeast. The hydraulic head distribution for Aquifer Unit IIA declines, in general, from the southeast to the northwest following the trend of UTR Creek, the potentiometric map of this unit is presented in Fig. E.2-2. The horizontal gradient in this unit, beneath the EAVDF, is approximately 0.005. At E-Area, the aquifer unit is under confined conditions except along the fringe of UTR Creek. In this area, Aquifer Unit IIA converts to water-table conditions because Confining Unit IIA-IIB (Green Clay) is completely stripped away by UTR Creek.

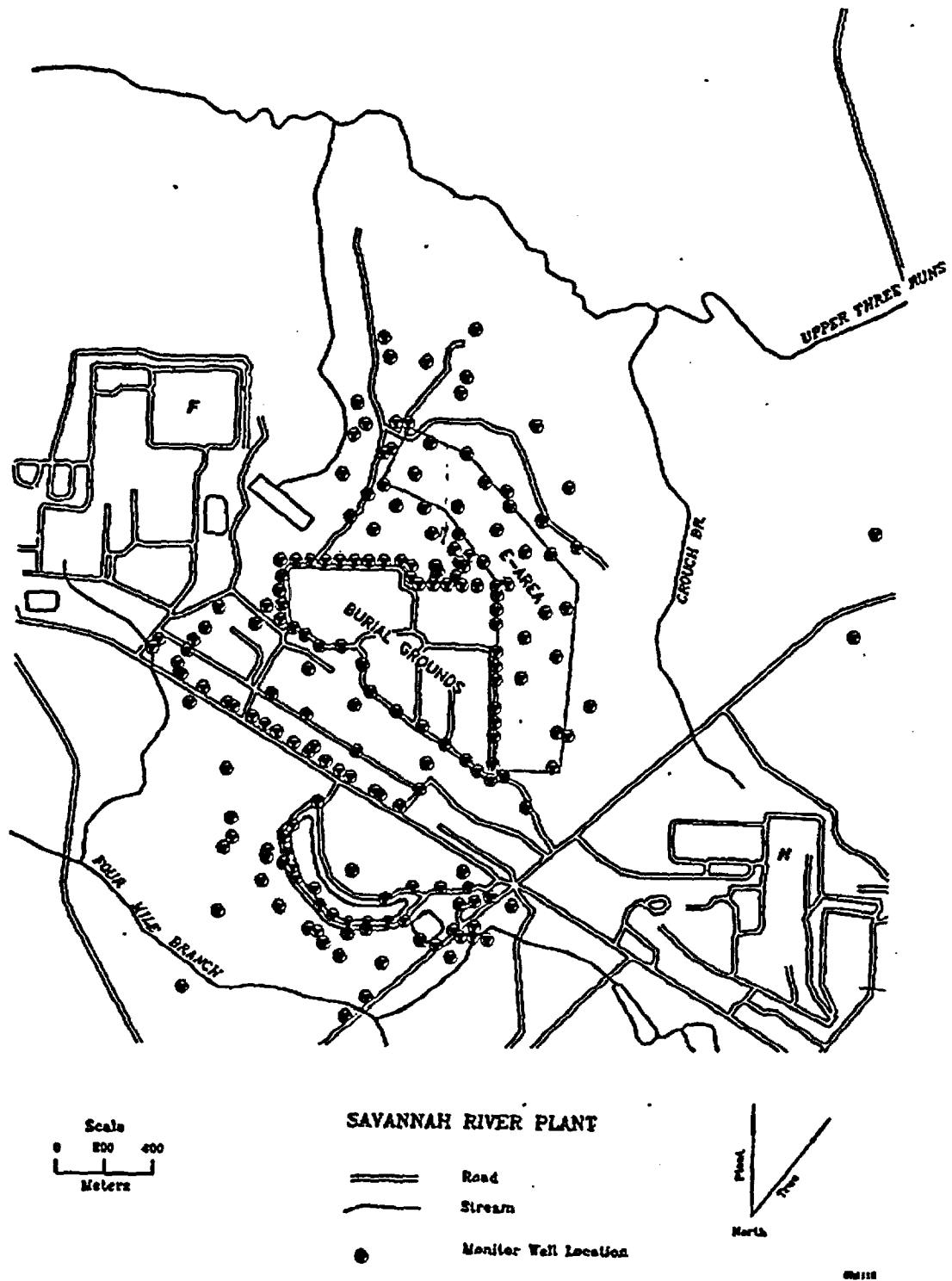
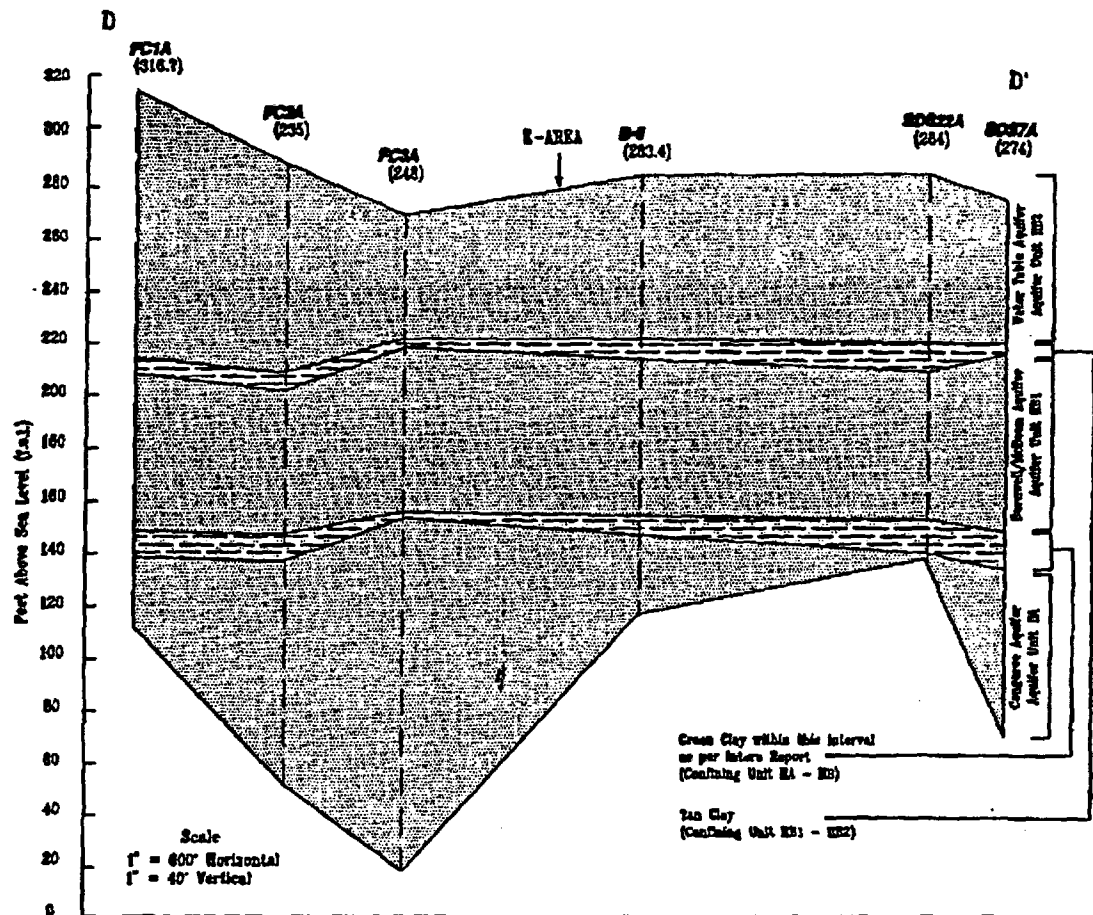


Fig. 22-2. Location of groundwater wells at E-Area.



EXPLANATION

	SAND	Loose to dense, orange and red, fine to coarse, moist sand.
	CLAYEY SAND	Medium to dense, olive brown to dark green, interbedded silty sand.
	CLAY	Dense, yellow to grey, plastic, heavy minerals.
SD04		Well number
(001)		Elevation



Cross-section location map

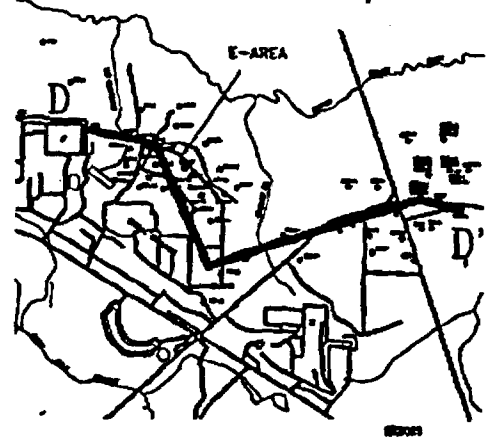
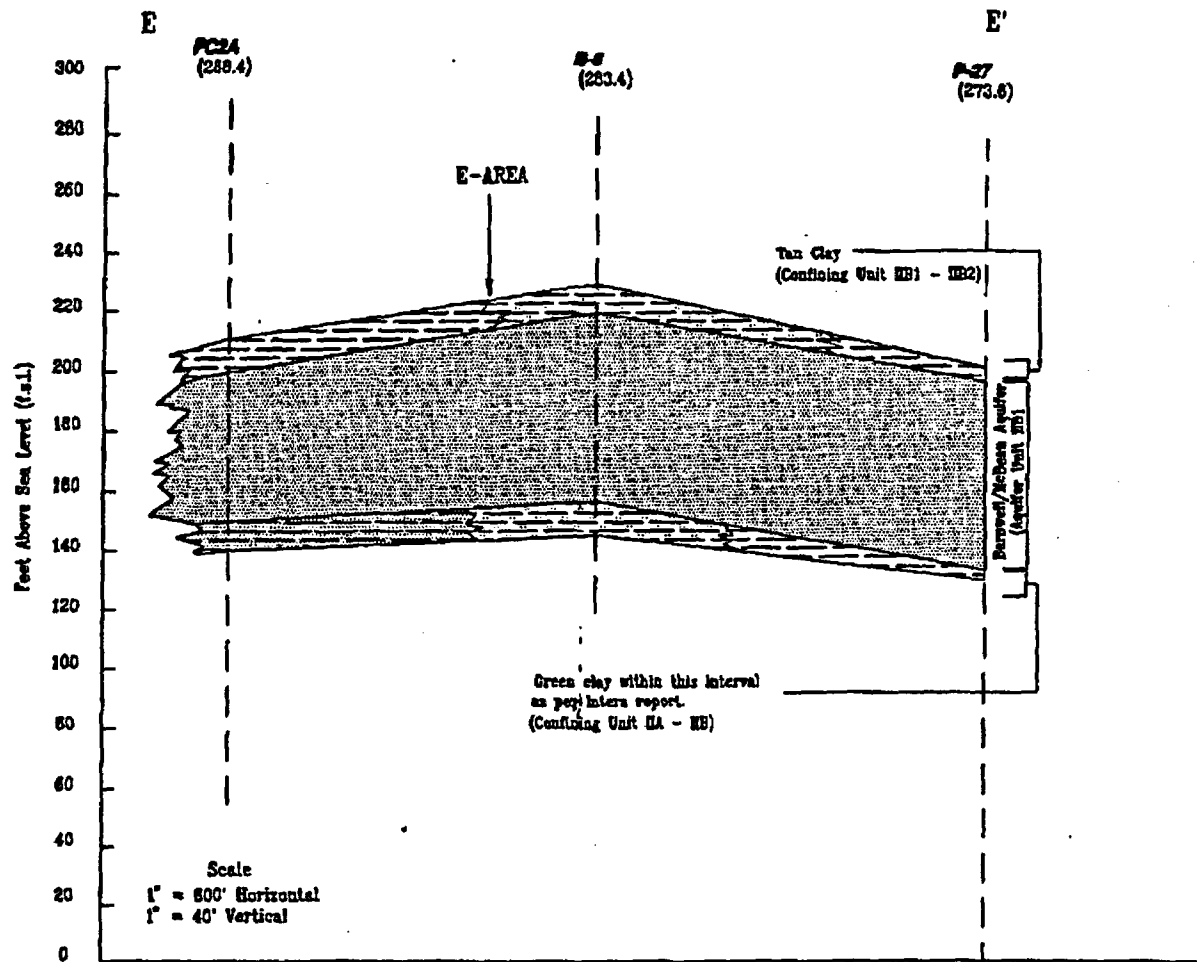


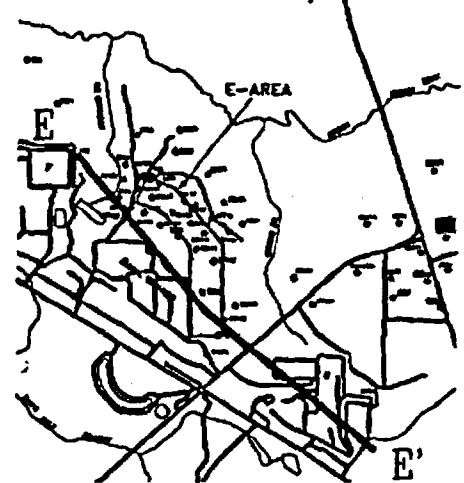
Fig. 2.2-3. Lithologic cross-section, D-D', in the vicinity of E-Area.



EXPLANATION

	SAND	Loose to dense, orange and red, fine to coarse, moist sand.
	CLAYEY SAND	Medium to dense, brown to red clay, with fine grained, green-gray sand.
	CLAY	Dense, yellow to grey, plastic, heavy mineral.
	SILT CLAY	Medium to dense, dark olive gray, with silt lens.
W-4	Well number	
(001)	Elevation	

Cross-section location map



SR5000

Fig. 2.2-4. Lithologic cross-section, E-E', in the vicinity of E-Area.

Confining Unit IIA-IIB (Green Clay) at E-Area separates Aquifer Unit IIA and Aquifer Unit IIB. The vertical component of flow in Aquifer Unit IIB, Zone 1 (Barnwell/McBean), is downward across the Confining Unit IIA-IIB (Green Clay) into Aquifer Unit IIA (Congaree). Confining Unit IIA-IIB (Green Clay) is more competent than Confining Zone IIB1-IIB2 (Tan Clay), but there is evidence of some leakage near E-Area.

Aquifer Unit IIB, Zone 1 (Barnwell/McBean) overlies Confining Unit IIA-IIB (Green Clay) and underlies Confining Zone IIB1-IIB2 (Tan Clay). This zone ranges in thickness from 12 to 28 m. It thins toward the western portion of the GSA, in the vicinity of the H-Area seepage basins. Aquifer Unit IIB, Zone 1 (Barnwell/McBean) dips approximately 1.5 to 1.7 m per km to the southeast. UTR Creek has eroded through Confining Zone IIB1-IIB2 (Tan Clay), and Aquifer Unit IIB, Zone 1 (Barnwell/McBean). Heads decline toward the bounding streams of UTR Creek, McQueen Branch, and Four Mile Branch as shown in Fig. E.2-4. A groundwater divide exists within this unit and acts to separate groundwater flow in the aquifer to the north and south. The divide follows the east-west trend of the topographic upland between UTR Creek and Four Mile Branch and is situated to the south of the EAVDF. The divide is not located symmetrically between these two lateral boundaries because of the deep incisement of UTR Creek, and instead is shifted slightly to the south.

Confining Zone IIB1-IIB2 (Tan Clay) separates underlying Aquifer Unit IIB, Zone 1 (Barnwell/McBean) from overlying Aquifer Unit IIB, Zone 2 (water table) and consists of multiple-discontinuous clay layers. The vertical component for the flow of water in the water table is downward across Confining Zone IIB1-IIB2 (Tan Clay) into Aquifer Unit IIB, Zone 1 (Barnwell/McBean). Confining Zone IIB1-IIB2 (Tan Clay) is a leaky aquitard with the degree of leakage across the confining zone being variable. Leakage depends on the magnitude of the head difference across the confining zone and the local permeability of the confining zone.

Aquifer Unit IIB, Zone 2 (water table), is the uppermost aquifer and is under unconfined conditions. Aquifer Unit IIB, Zone 2, has a downward hydraulic flow direction toward lower units. The hydraulic head distribution and flow directions are very similar to the Aquifer Unit IIB, Zone 1 (Barnwell/McBean), thus, flow directions are sub-parallel to flow directions in that unit. A groundwater divide exists in the interstream upland with hydraulic heads decreasing toward the bounding streams. Configuration of the water table is shown in Fig. E.2-5.

The water table occurs in Aquifer Zone IIB (water table) at E-Area. The historic high water level under the EAV is estimated to range between 71.6 and 74.8 m above mean sea level (MSL) (Amidon 1990). A review of well data available for E-Area suggests average water table elevations on the order of 69 m to 71 m above MSL. In the northeast section of the facility, where disposal of the intermediate-activity LLW is planned, the average water table elevation is estimated to be 69 m, with a historic high water level of approximately 71.7 m above MSL. The direction of flow is effected by the creeks in all aquifer units.

Measured hydraulic conductivities of the hydrologic zones described above are listed in Table 2.2-1.

Table 2.2-1 Summary of hydraulic conductivities reported for Aquifer System II

Hydrologic Units	Horizontal Hydraulic Conductivity (cm yr ⁻¹) ¹	Vertical Hydraulic Conductivity (cm yr ⁻¹) ¹
Aquifer Unit IIB, Zone 2	4.1×10^3 to 1.8×10^4	—
Confining Zone IIB ₁ -IIB ₂	0.19 to 3.8	0.04 to 13
Aquifer Unit IIB, Zone 1	2.3×10^3 to 2.3×10^5	—
Confining Unit IIA-IIB	0.44 to 5	0.2 to 1.4
Aquifer Unit IIA	2.0×10^4	—

¹ Source: WSRC 1991b.

Hydraulic characteristics of unsaturated soil near E-Area are reported in Appendix E. Soil water content - soil water pressure relationships for soil samples taken from two locations in the General Separations Areas (GSA) are provided, as are relationships between hydraulic conductivity and water content. The disparity between the relationships at the two areas are indicative of the heterogeneous nature of soils at the SRS.

2.2.3 Surface Water in the Vicinity of E-Area

The watershed of UTR Creek drains about 500 km² of the Upper Coastal Plain northeast of the Savannah River. Significant tributaries to this creek are Tinker Creek, which is a headwaters branch that comes in northeast of E-Area, and Tims Branch, which connects up west of E-Area (Fig. 2.1-2). There are no lakes or flow control structures on UTR Creek or its tributaries. The stream channel has a low gradient and is meandering. Its floodplain ranges in width from 0.4 to 1.6 km and is heavily forested with hardwoods.

UTR Creek is gauged at three points within SRS: 1) near the northern SRS boundary; 2) just upstream of the Tinker Creek confluence; and 3) about 5 km above the confluence with the Savannah River. The average discharge at the two northernmost gauges normalized to drainage area is 0.013 m³ s⁻¹ km⁻², ranging from 0.006 m³ s⁻¹ km⁻² to 0.06 m³ s⁻¹ km⁻² (Dennehy et al. 1989). Maximum flows are attributed to excess precipitation runoff.

Two smaller tributaries of UTR Creek, Crouch Branch and an unnamed branch, are located northeast and west, respectively, of the E-Area. Both Crouch Branch and the unnamed tributary receive runoff from E-Area. Crouch Branch has a drainage area of about 2.8 km² and the drainage area of the unnamed tributary has not been determined. One set of data from gauging stations on Crouch Branch reflects less than a full year's gauging results (Dennehy et al. 1989). At that time, the southeastern United States was in a drought condition. These data thus represent a low-flow condition, in which all streamflow is from groundwater discharge. Discharge rates as a function of gauge height could not be developed due to the low flow. Seepage investigations on one particular day indicated that Crouch Branch gained groundwater at an average rate of 0.010 m³ s⁻¹ km⁻¹ of stream length. The average number for UTR Creek at Z-Area, which is on the east side of Crouch Branch, was 0.16 m³ s⁻¹ km⁻¹. Stream-flow measurements for Crouch Branch and the unnamed branch were also conducted as part of this investigation. Flow rates were 1.78 and 0.68 cfs for Crouch and unnamed branch, respectively. This information is presented in Appendix C.

2.2.4 Water Quality and Usage in the E-Area Vicinity

Currently, groundwater in Aquifer Unit IIA (Congaree), Aquifer Units IIB1 (Barnwell/McBean), and IIB2 (water table) is monitored in E-Area. Results of chemical analyses of water samples from five wells upgradient from EAV are presented in Table 2.2-2 (Cummins et al. 1990, Aadland 1990). In general, water from the lower Aquifer Unit IIA (Congaree) tends to be higher in dissolved calcium and magnesium concentrations, higher in dissolved sulfate, and higher in dissolved silica concentrations than water from Aquifer Units IIB1 (Barnwell/McBean) and IIB2 (water table). Dissolved nitrate concentrations in water from Aquifer Unit IIA (Congaree) were significantly lower than in water from Aquifer Units IIB1 (Barnwell/McBean) and IIB2 (water table). The different chemistry of the zones has partially been attributed to the dissolution reactions that occur as water from the upper Aquifer Unit IIB2 (water table) moves downward through the lower calcite-bearing portion of Aquifer Unit IIB1 (Barnwell/McBean), and through the silica-bearing illite/smectite minerals in the Confining Unit IIA-IIB (Green Clay). (Aadland 1990, Dennehy et al. 1989). Differences in nitrate concentrations may be due to the activity of nitrate-reducing bacteria (Dennehy et al. 1989). Elevated pH levels are attributed to well construction problems rather than groundwater contamination (Cummins et al. 1990).

Water from the creeks local to E-Area are not currently used for human consumption. Some water quality characteristics of UTR Creek downstream of E-Area, classified as a Class B water by the SCDHEC, are listed in Table 2.2-3. The temperature, dissolved oxygen, and pH values reflected in this table are within the standards required for Class B waters (Cummins et al. 1990). Other water quality parameters listed in this table are within the ranges observed in previous years (Cummins et al. 1990), indicating that the quality of UTR Creek is not being degraded at the point of measurement.

Table 22-2. Concentration of dissolved elements in groundwater in Aquifer Unit IIA and Units IIB1 and IIB2 near E-Area (Cummins et al. 1990)

Parameter	Aquifer Unit IIA (Congaree) (BGO 6A)		Aquifer Unit IIA (Congaree) (BGO 10A)		Aquifer Zone IIB ₁ (Barnwell/McBean) (BGO 6C)		Aquifer Zone IIB ₁ (Barnwell/McBean) (BGO 10C)		Aquifer Zone IIB ₂ (Water Table) (BGO 6D)	
	Min	Max	Min	Max	Min	Max	Min	Max	Min	Max
Ca (mg/L)	36.9	57	32	61	19.9	23	5.97	26.4	20.1	21.2
Mg (mg/L)	1.32	1.42	1.25	1.6	0.464	0.516	0.307	0.95	0.818	1.1
Na (mg/L)	2.19	2.35	2.04	2.66	2.21	3.75	5.45	6.59	2.39	2.93
K (mg/L)	0.73	1.07	<0.5	5.2	<0.5	0.679	0.762	4.49	0.783	1.07
Cl (mg/L)	2.7	3	2.7	3.1	2	2.2	2.1	2.6	1.5	1.8
SO ₄ (mg/L)	8.5	9.2	8.9	10.6	<1	<5	1.8	5	1.6	<5
pH	7.1	7.6	6.6	7.6	6.9	7.2	7.6	10.5	6	6.7
Cd (μg/L)	<0.002	<0.004	<0.002	<0.004	<0.002	<0.002	<0.002	<0.004	<0.002	<0.002
NO ₃ as N (mg/L)	<0.05	<0.1	<0.05	<0.1	0.68	1.01	0.19	0.48	<0.1	0.2
Total PO ₄ (mg/L as P)	0.05	0.114	<0.05	0.106	0.12	0.155	<0.05	0.24	<0.05	0.108
SiO ₂ (mg/L)	39.2	44.3	38	46.1	9.53	10.4	14.4	22.1	8.09	10.5

Table 2.2-3. Water quality of UTR Creek at Road A (Cummins et al. 1990)

Parameter	Units	No. of Analyses	Mean	Max	Min
Temperature	°C	12	18	32	8.7
pH	pH	12		7.7	6.4
Dissolved oxygen	mg/L	12	8.9	11	7.3
Alkalinity	mg/L	12	4.3	6.0	1.0
Conductivity	umhos/cm	12	28	40	23
Turbidity	NTU	12	2.5	4.2	1.6
Suspended solids	mg/L	12	8.1	15	2.0
Volatile solids	mg/L	12	3.7	7.0	1.0
Total dissolved solids	mg/L	12	27	32	20
Total solids	mg/L	12	35	41	26
Fixed residue	mg/L	12	4.6	8.0	1.0
Chemical oxygen demand	mg/L	12	8.7	18	3.0
Chloride	mg/L	12	1.8	2.6	0.31
Nitrogen (as NO ₂ /NO ₃)	mg/L	12	0.11	0.14	0.08
Sulfate	mg/L	12	3.2	4.0	2.0
Phosphorus (as PO ₄)	mg/L	12	0.03	0.12	<0.02
Nitrogen (as NH ₃)	mg/L	12	0.05	0.14	<0.02
Cadmium	mg/L	4	<0.01	<0.01	<0.01
Mercury	μg/L	4	<0.20	<0.20	<0.20
Chromium	mg/L	4	<0.02	0.02	<0.02

2.2.5 Existing Radiation and Chemical Environment at E-Area

The environmental monitoring program at the SRS includes the assessment of radionuclides in the groundwater and in stream sediments. Additional monitoring is performed for the air pathway and river water. The background level of interest at the E-Area site location for this RPA is predominantly the long term concentrations related to the groundwater pathway.

Several wells were installed to obtain background data for the EAVDF and to monitor the EAV Disposal Facility after startup. Wells in the region of the EAV were monitored at the water table, Barnwell/McBean and Congaree aquifer zones. Because the flow of water in Aquifer Unit IIA (Congaree) is toward the UTR Creek, wells were monitored in that unit in the Burial Grounds and Mixed Waste Management Facility regions upgradient of EAVs.

During 1991, results from several wells monitored at EAVs and upgradient to EAVDF contained contaminants above DWS (Table 2.2-4). Tritium concentrations exceeded the applicable standard in Aquifer Units IIB1-IIB2 (Barnwell/McBean; water table) and in Aquifer Unit IIA (Congaree). In the upgradient wells (located at the Burial Grounds and MWMF), 3 of the 15 wells observed exceeded the DWS for tritium concentration. In Aquifer Unit IIA (Congaree), 1 of 2 wells monitored at EAVs exhibited elevated levels of tritium. Total radium concentration was above the PDWS in 1 of 15 EAV wells. Tritium concentration levels have also exceeded PDWS in downgradient wells of the EAVDF (Table 2.2-5 and Table 2.2-6). Tetrachloroethylene exceeded primary drinking water standards (PDWS) in 2 of 15 upgradient wells and trichloroethylene concentrations were exceeded in 5 of the 15 wells sampled. In the region of EAVs, tetrachloroethylene and trichloroethylene exceeded PDWS in 1 of 15 and 2 of 15 wells sampled, respectively. The migration of tritium and solvents toward UTR Creek is partly due to the plume associated with the Burial Grounds facility (643-7E, 643-7E, 643-28E) (WSRC 1992a). The migration of contaminants from the Burial Grounds to EAV contributes to the elevated levels of tritium prior to startup of the vaults. The wells used in this assessment of the existing groundwater-water quality and radionuclide content are shown in Fig. 2.2-5.

Table 2.2-4. Maximum constituent results exceeding applicable standards for wells at the EAVDF (Arnett et al. 1991).

Constituent	Unit	Standard	Maximum Result
Aquifer Unit IIA (Burial Grounds, Mixed Waste Management Facility)			
Alkalinity (as CaCO ₃)	mg/l	100	385
Americium-241	μCi/ml	6.3×10^{-9}	3.9×10^{-8}
Specific conductance	μS/cm	100	1,840
Lead	mg/l	0.015	0.020
pH	pH	≥8.5	13
Tetrachloroethylene	mg/l	0.0050	0.0055
Total dissolved solids	mg/l	200	435
Trichloroethylene	mg/l	0.0050	0.023
Tritium	μCi/ml	2.0×10^{-5}	1.5×10^{-4}
Aquifer Units IIB1-IIB2 (E-Area Vaults)			
Alkalinity (as CaCO ₃)	mg/l	100	109
Gross alpha	μCi/ml	1.5×10^{-8}	2.6×10^{-8}
Specific conductance	μS/cm	100	470
pH	pH	≥8.5	11
Tetrachloroethylene	mg/l	0.0050	0.0065
Total radium	μCi/ml	5.0×10^{-9}	1.7×10^{-8}
Trichloroethylene	mg/l	0.0050	0.0090
Tritium	μCi/ml	2.0×10^{-5}	9.8×10^{-5}
Aquifer Unit IIA (E-Area Vaults)			
Alkalinity (as CaCO ₃)	mg/l	100	1,300
Gross alpha	μCi/ml	1.5×10^{-8}	1.5×10^{-8}
Nonvolatile beta	μCi/ml	5.0×10^{-8}	9.2×10^{-8}
Specific conductance	μS/cm	100	5,030
Lead	mg/l	0.015	0.052
pH	pH	≥8.5	13
Total dissolved solids	mg/l	200	1,490
Total radium	μCi/ml	5.0×10^{-9}	8.1×10^{-9}
Tritium	μCi/ml	2.0×10^{-5}	1.8×10^{-4}

Table 2.2-5. Groundwater monitoring results for the EAVDF (Cummins et al. 1990)

Constituent	Unit	March 1990	May 1990	August 1990	November 1990
WELL: BG 96					
pH	pH	5.5	5.7	4.3	5.6
Specific conductance	$\mu\text{S}/\text{cm}$	48	34	35	29
Alkalinity	meq/L	6	6	6	4
TDS	mg/L	43	35	27	29
Cadmium	mg/L	<0.002	<0.002	<0.002	<0.002
Tritium	$\mu\text{Ci}/\text{mL}$	1.3×10^{-5}	1.0×10^{-5}	9.9×10^{-6}	7.0×10^{-7}
Chloride	mg/L	3.5	2.3	2.4	2.8
Chromium	mg/L	<0.004	<0.004	0.01	<0.004
Iron	mg/L	0.034	0.033	0.028	0.38
Lead	mg/L	<0.006	0.018	<0.003	0.004
Manganese	mg/L	0.013	<0.002	0.003	<0.002
Silver	mg/L	<0.002	<0.002	<0.002	<0.002
Sodium	mg/L	2.09	1.83	2.4	1.6
Total phosphates (as P)	mg/L	0.06	0.21	0.2	0.07
Zinc	mg/L	0.025	0.011	0.023	0.007
Nitrate (as N)	mg/L	1.1	1.04	1.15	0.78
Sulfate	mg/L	<5	<1	<1	<1
Phenols	mg/L	<0.005	<0.005	<0.005	<0.005
Total organic carbon	mg/L	2	2	<1	<1
WELL: BG 101					
pH	pH	5	5.1	3.9	5.1
Specific conductance	$\mu\text{S}/\text{cm}$	24	21	20	21
Alkalinity	meq/L	1	1	1	1
TDS	mg/L	54	27	34	36
Tritium	$\mu\text{Ci}/\text{mL}$	3.3×10^{-4}	3.0×10^{-4}	3.3×10^{-4}	3.2×10^{-4}
Cadmium	mg/L	<0.002	<0.002	<0.002	<0.002
Chloride	mg/L	1.9	1.9	2	2.2
Chromium	mg/L	<0.004	<0.004	<0.004	<0.004
Iron	mg/L	<0.004	0.03	0.031	0.017
Lead	mg/L	<0.006	0.011	0.004	0.004
Manganese	mg/L	0.007	0.008	0.009	0.008
Silver	mg/L	<0.002	<0.002	<0.002	<0.002
Sodium	mg/L	1.55	1.61	2	1.5
Total phosphates (as P)	mg/L	0.65	0.14	0.13	0.11
Zinc	mg/L	0.091	0.081	0.092	0.11
Nitrate (as N)	mg/L	0.66	0.62	0.71	0.57
Sulfate	mg/L	<5	<1	<1	<1
Phenols	mg/L	<0.005	<0.005	<0.005	<0.005
Total organic carbon	mg/L	<1	2	<1	<1

Table 2.2-5. (cont.)

Constituent	Unit	March 1990	May 1990	August 1990	November 1990
OTHER ANALYSES					
WELL: BG 96					
Aluminum	mg/L	<0.02	<0.02	<0.02	0.047
Beryllium	mg/L	<0.005	<0.003	<0.003	<0.003
Calcium	mg/L	3.89	3.39	4.3	2.28
Cobalt	mg/L	<0.004	<0.004	<0.004	<0.004
Carbonate	mg/L	<1	<1	-	-
Iodine	mg/L	<0.1	<0.1	<0.1	<0.1
Potassium	mg/L	<0.5	<0.5	<0.5	<0.5
Magnesium	mg/L	0.499	0.35	0.43	0.322
Nitrite (as N)	mg/L	<0.01	<0.01	<0.01	<0.4
Antimony	mg/L	<0.003	<0.003	<0.003	<0.003
Silica	mg/L	7.18	13	7.4	6.4
Total carbon	mg/L	8	6	10	7.04
Total inorganic carbon	mg/L	6	4	10	6.04
Uranium	mg/L	<1	<1	<1	<1
Vanadium	mg/L	<0.02	<0.01	<0.01	<0.01
WELL: BG 101					
Aluminum	mg/L	<0.02	0.067	0.028	<0.02
Beryllium	mg/L	<0.005	<0.003	<0.003	<0.003
Calcium	mg/L	1.26	1.27	1.5	0.93
Cobalt	mg/L	<0.004	<0.004	<0.004	<0.004
Carbonate	mg/L	<1	<1	-	-
Iodine	mg/L	<0.1	<0.1	<0.1	<0.1
Potassium	mg/L	<0.5	<0.5	<0.5	<0.5
Magnesium	mg/L	0.324	0.332	0.38	0.32
Nitrite (as N)	mg/L	<0.01	<0.01	<0.01	<0.01
Antimony	mg/L	<0.003	<0.003	<0.003	<0.003
Silica	mg/L	5.39	7.4	7.1	6.8
Total carbon	mg/L	6	6	10	6
Total inorganic carbon	mg/L	6	4	10	6
Uranium	mg/L	<1	<1	<1	<1
Vanadium	mg/L	<0.02	<0.01	<0.01	<0.01

Table 22-6. Monitoring well results of radionuclides in groundwater for the EAVDF (Cummins et al 1990)

Constituent	Unit	Aquifer Unit IIA		Aquifer Unit IIB, Zone IIB1		Aquifer Unit IIB, Zone IIB2	
		Well: BGO 6A		Well: BGO 6C		Well: BGO 6D	
		Min	Max	Min	Max	Min	Max
Americium-241	PCL	<0.2000	<0.3000	0.7400	0.7400	ND	ND
Cobalt-60	PCL	<2.000	<3.000	<4.000	<4.000	ND	ND
Cesium-137	PCL	<2.000	<3.000	<3.000	<3.000	ND	ND
Gross alpha	PCL	<3.000	<6.000	<3.000	<5.000	<3.000	<4.000
Nonvolatile beta	PCL	<2.000	<6.000	3.200	<5.000	2.600	5.300
Tritium	PCML	<0.7000	<1.000	990.0	1750.0	1700	1.18×10^4
Nickel-59	PCL	<90.00	<100.0	<90.00	<90.00	ND	ND
Nickel-63	PCL	<9.000	<10.00	<10.00	<10.00	ND	ND
Neptunium-237	PCL	<3.000	<6.000	<7.000	<7.000	ND	ND
Plutonium-239/240	PCL	<0.2000	<0.2000	<0.0400	<0.0400	ND	ND
Strontium-90	PCL	<0.9000	<1.000	<1.000	<1.000	ND	ND
Technetium-99	PCL	<4.000	<4.000	11.00	11.00	ND	ND
Total Radium	PCL	<1.000	1.000	<1.000	1.500	1.200	3.400
Uranium-234	PCL	0.2800	4.200	0.3000	<0.3000	ND	ND
Uranium-238	PCL	<0.0300	0.8700	<0.2000	<0.2000	ND	ND
Total Activity	PCL	ND	ND	1.00×10^4	2.5×10^5	1150	9.40×10^5
Constituent	Unit	Well: HSB 85A		Well: HSB 85B		Well: HSB 85C	
		Min	Max	Min	Max	Min	Max
		<0.2000	0.6100	<0.2000	0.7500	<0.1000	<0.2000
		<3.000	<4.000	<3.000	<6.000	<2.000	<6.000
		<2.000	<5.000	<4.000	<3.000	<2.000	<6.000
		<2.000	<4.000	<2.000	<5.000	<2.000	<3.000
		<4.000	<5.000	<5.000	8.100	<4.000	9.800
		<1.000	<1.000	<0.700	1.300	1.400	3.200
		<100.0	<100.0	<90.00	<100.0	<90.00	<100.0
		<8.000	<10.00	<9.000	<10.00	<8.000	<10.00
		<4.000	<10.00	<9.000	<10.00	<3.000	<10.00
		<0.0500	<0.2000	<0.0900	<0.2000	<0.0600	<1.000
		<0.7000	<1.000	<0.7000	<1.000	3.100	<0.7000
		<3.000	<5.000	<3.000	<8.000	3.400	<10.00
		<1.000	1.200	<1.000	<1.000	<1.000	1.400
		<0.0400	<2.000	<0.0400	<0.9700	<0.0500	6.300
		<0.0300	<2.000	0.2300	<0.0200	<0.0200	<2.000
		ND	ND	ND	ND	ND	ND
		Well: BGX 4A		Well: BGX 8D		Well: BGX 6D	
		Min	Max	Min	Max	Min	Max
		<2.000	2.000	<2.000	<2.000	<2.000	<2.000
		2.000	4.000	0.3000	4.300	<2.000	<2.000
		<0.700	<0.700	1.026	1034	3.500	4.100
		0.600	4.800	1.50	5.30	1.700	4.300
		ND	ND	1013	1027	4.450	5.950

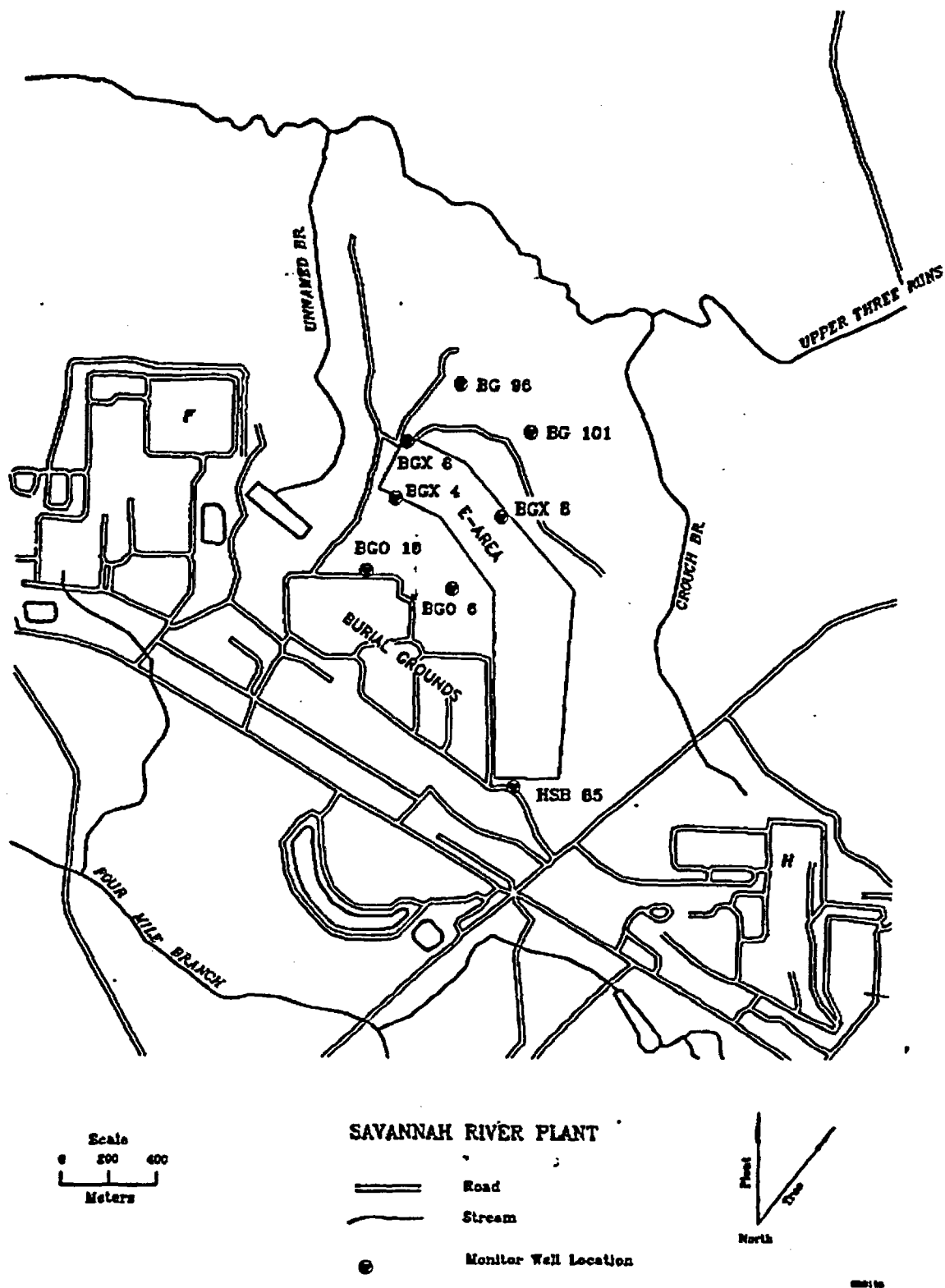


Fig. 22-5. Location of E-Area monitoring wells used to assess the groundwater quality and radionuclide activities.

23 DESCRIPTION OF E-AREA OPERATIONS, FACILITIES, AND FEED STREAMS

The EAVDF is part of an integrated waste disposal system being installed at the SRS. The EAVDF is regulated by DOE Orders and other Federal regulations that are applicable to disposal of low-level radioactive solid waste.

23.1 Description of the Waste Types at E-Area

The EAVs are to provide a new disposal and storage site for solid, low-level, non-hazardous radioactive waste. The U.S. DOE Order 5820.2A defines low-level radioactive waste as waste that contains radioactivity and is not classified as HLW (waste material that results from the reprocessing of spent nuclear fuel), TRU, spent nuclear fuel or 11c(2) byproduct material.

SRS operations further classify LLW into three categories to assist in the reduction of radiological risks to workers at the site. LAW, IAW, and Tritiated Waste. IAW consists of waste material that radiates ≥ 200 mR/h at 5 cm from the unshielded outer disposal container. LAW is defined as waste material that radiates < 200 mR/h at 5 cm from the unshielded outer disposal container. Tritiated Waste is waste material that contains greater than trace quantities of tritium regardless of the radiation rate. For waste acceptance purposes, trace quantities of tritium has been defined as 10 curies of tritium per waste container. The EAV will not dispose of or store liquid wastes, TRU waste, hazardous wastes, or mixed (both hazardous and radioactive) wastes.

24 E-AREA VAULTS WASTE COMPOSITION

24.1 Physical Characteristics of Waste Types

24.1.1 Low Activity Waste (LAW)

LAW will be disposed of in the Low Activity Waste Vault (LAWV). Most of the LAW

will be received in standard $1.2 \times 1.2 \times 1.8$ m metal containers (B25 boxes), but some waste will also be received in standard $0.6 \times 1.2 \times 1.8$ m containers (B12 boxes) or 210-L drums. The LAW may also be received in non-standard engineered concrete or metal containers. These containers shall be preapproved by Solid Waste Management prior to their receipt at the EAV.

The LAW will include job control waste, scrap metal, and contaminated soil and rubble. Job control waste will consist of potentially contaminated protective clothing including plastic suits, shoe covers, lab coats, and plastic sheeting. Scrap metal will be contaminated tools, process equipment, and laboratory equipment. Soil and rubble will be generated from demolition and cleanup activities. Historically, the majority of this waste has been generated by the HLW tank farms. Larger volumes of waste disposed at EAV are anticipated from environmental restoration activities as facilities are decommissioned and old waste sites are remediated.

2.4.1.2 Intermediate Activity Waste (IAW)

The Intermediate Level Non-Tritium Vault (ILNTV) will be used for disposal of IAW. IAW consists of job control waste, scrap hardware, and contaminated soil and rubble. Job control waste is primarily highly contaminated lab coats, plastic suits, shoe covers, plastic sheeting, etc. This material is assumed to be combustible and is contaminated primarily with fission products. Scrap hardware waste will consist of reactor hardware, reactor fuel and target fittings, jumpers, and used canyon and tank farm equipment contaminated with fission products and/or induced activity.

All of the IAW will be packaged in engineered metal or concrete containers that have been approved by Solid Waste Management. The containers will be remotely placed into the vault in layers. IAW containers will be grouted in place to provide better waste isolation, reduce dose to operators, and improve stacking of additional containers.

2.4.1.3 Tritiated Waste

Tritiated waste will be disposed in the Intermediate Level Tritium Vault (ILTV). This facility consists of two cells, one for each of the two subcategories of tritiated waste. Tritium crucibles will be disposed in the first cell. This waste form is generated by the tritium facilities in the process used to recover tritium from target assemblies. The crucibles will be over-packed into a stainless-steel container that is about 0.5 m in diameter and 6.1 m in length. The crucible cell is specially designed with vertical silos to receive waste. All other tritiated waste will be disposed of in the bulk tritiated waste cell. This waste will consist of job control waste and used process equipment that is contaminated with tritium. Bulk tritiated waste will be disposed in engineered metal or concrete containers.

2.4.2 Waste Packaging

Many different containers will be received at the EAV. However, all containers are required by the Operational Safety Requirements (OSRs) to be engineered concrete or metal containers that have been approved by Waste Management. A procedure has been written that defines this approval process and requires Solid Waste Management Engineering, Solid Waste Management Operations, and Solid Waste Management Maintenance to concur that the container can be safely handled, will not impair vault space utilization, and will satisfactorily contain the waste contents.

Standardized B25 and B12 containers will be used for a majority of the waste. These standardized containers have already received approval for acceptance at the EAV. Other containers are specific to the generator or the waste form. These containers will be approved for either one time use or unlimited use, depending on the circumstances.

242.1 Container Descriptions

Standard Containers

The B25 and B12 are carbon steel boxes that have been used in the past for waste disposal in the SWDF. The boxes are similar in construction with the exception of size. The B25 is a 2.5 m³ container that is approximately 1.2 m high, 1.2 m wide, and 1.8 m long. It is typically constructed of 14-gauge carbon steel (1.9 mm) but some B25s are constructed of 12-gauge carbon steel (2.6 mm) to allow use in the compactor. The B12 is a 1.3 m³ container that is approximately 0.6 m high, 1.2 m wide, and 1.8 m long and is typically constructed of 12-gauge carbon steel.

The B12 and B25 containers are constructed with a rubber-gasket seal between the lid and the container conforming to ASTM-D-1056 with a gasket compression of 20 to 30%. The interior and exterior of each container is coated with a zinc chromate primer. The exteriors are given an additional coating of alkyd enamel and a finish coat of paint conforming to ASTM-D-16-75.

DOT 210-L drums will also be received as a standard container. Use of these containers is restricted to situations where use of a B25 is not practical. Drums will be banded together and banded to a fire-resistant pallet prior to shipment to the EAV.

Non-Standard Containers

For waste that cannot be placed in a standard container, specific size and weight limits have been specified. Maximum dimensions for containers to be emplaced in the LAWV are 4.3 m high × 7.3 m wide × 15.2 m long. The maximum dimensions for containers to be emplaced in the Intermediate Vaults are 7.3 m high × 10.7 m long × 6.1 m wide. The maximum uniform load on the vault floor cannot exceed 4.9×10^6 kg m⁻² for the Intermediate Level Vaults and 2.8×10^6 kg m⁻² for the LAWV.

Tritium Crucibles

Tritium crucibles will be packaged in a stainless steel overpack container. The overpack will be an 0.46-m diameter pipe which is approximately 6.1 m long. The lid will be sealed to the overpack with a compression O-ring. The O-ring will not prevent off-gassing of tritium in the ILTV crucible silos. The ILTV is designed to receive 142 of these tritium crucible overpacks.

2.4.3 Radioactive Inventory of Waste Types

2.4.3.1 Low Activity Waste (LAW)

The radioactive content of LAW is primarily fission products from the tank farms and Separations. Waste contaminated with uranium will be received from M-Area. Waste will also be received from off-site facilities, which will have a variety of radionuclides.

2.4.3.2 Intermediate Activity Waste (IAW)

Depending on the origin of this waste, it can contain either fission products or induced activity contamination. The induced activity waste will be mostly metal reactor hardware and fittings that have been exposed to a high neutron field. This waste generates a high radiation field but the activity is fairly immobile due to the metal matrix. Job control waste and process piping from Separations and High Level Waste Management will be contaminated with fission products. These fission products will be both loose and fixed surface contamination.

2.4.3.3 Tritiated Waste

The large majority of activity in this waste will be tritium. However, Cobalt-60 and Zinc-65 will also be present due to the activation of impurities during tritium production.

2.5 DESCRIPTION OF THE E-AREA VAULTS DISPOSAL SITE

As presently planned, the EAVDF will contain several large concrete vaults divided into cells. Each of the cells will be filled with LAW, IAW, and tritium waste, as appropriate. The EAV provides primary containment of the waste.

The bottom of the vaults will be approximately 8 m above the average water table height (Sect. 2.2.2) beneath the E-Area site, thus avoiding disposal of waste in a zone of water table fluctuation. Design requirements mandate that the bottom of the vault structures be at least 3 m above the historical maximum water table height. Run-on and runoff controls are installed to minimize site erosion during the operational period.

2.5.1 Site Layout and Capacity

The EAV site will be located on a 200-acre site (Fig. 2.5-1) immediately north of the current LLW burial site; of the 200 acres, only 100 acres have been developed at this time. The nearest SRS boundary to the EAVs is about 11 km to the west. The EAVDF is in a relatively level highland region of SRS at about 90 m ASL.

For the purposes of this RPA, it was assumed that 100 acres would provide disposal capacity for 20 years of SRS operations, which would include 10 ILNTVs, 10 ILTVs, and 21 LAWVs.

2.5.1.1 Intermediate-Level Nontritium Vaults

There are ten ILNTVs designated for use by the EAV project. Three vaults are oriented in a general north-south direction, and the remaining seven vaults are oriented in a general east-west direction (Fig. 2.5-1). Each vault consists of seven cells or subdivided sections within the vault structure and provide approximately $5.7 \times 10^3 \text{ m}^3$ of waste disposal capacity. The base of the ILNTVs are at elevations ranging between approximately 76.4 m and 79.1 m above MSL.

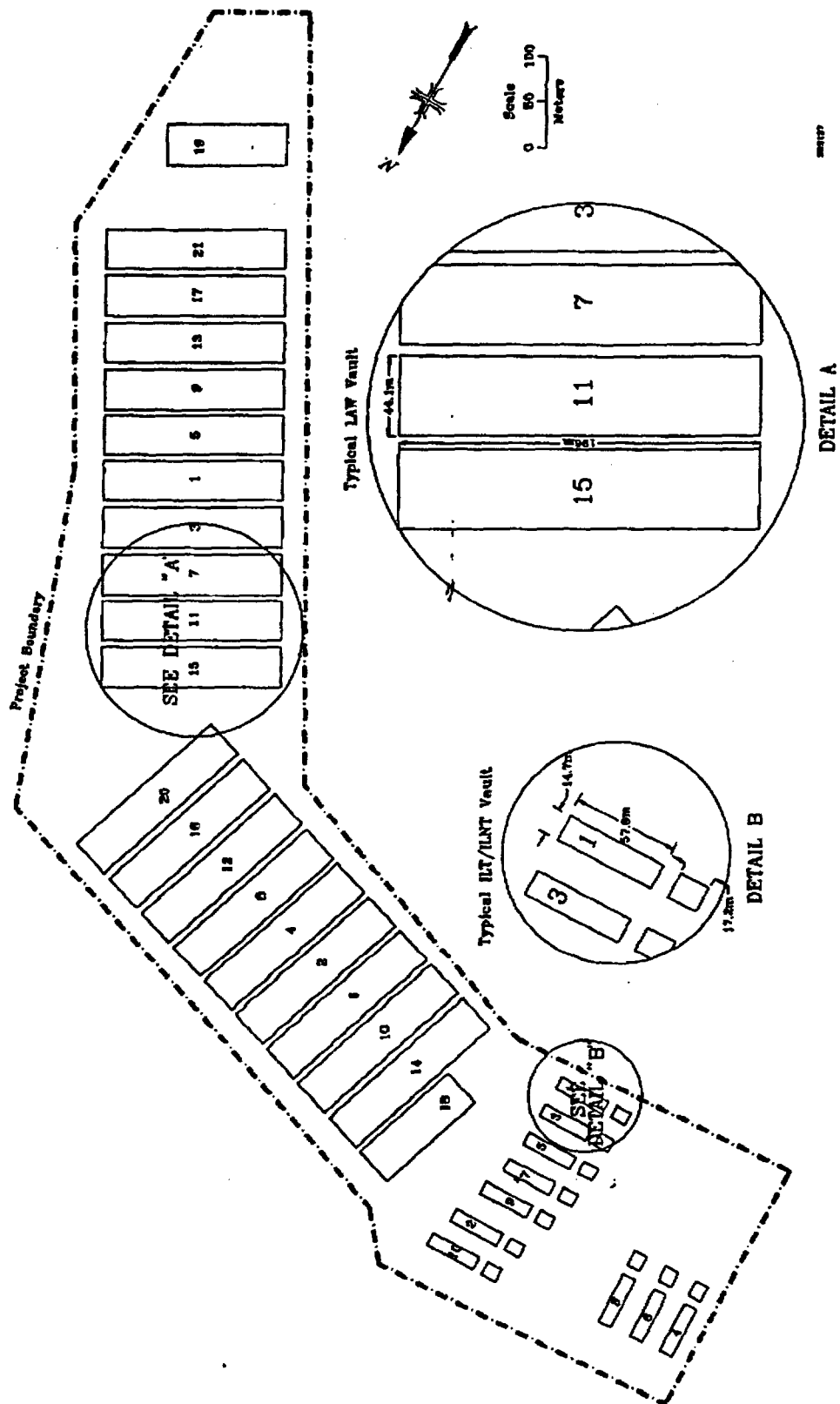


Fig. 2.5-1. Projected vault layout in the EAYDF.

2.5.1.2 Intermediate-Level Tritium Vaults

Ten ILTVs are designated for use by the EAV project. Three vaults are oriented in a general north-south direction and the remaining seven vaults are oriented in a general east-west direction (Fig. 2.5-1). Each vault consists of two cells or subdivided sections within the vault structure and provides approximately $1.6 \times 10^3 \text{ m}^3$ of waste disposal capacity. As originally conceived one cell in each vault would be fitted with a silo system to permit the disposal of tritium crucibles. As operations change at SRS, the need for additional or fewer silo cells will be evaluated. The base of the ILTVs are, like the ILNTVs, at elevations ranging between approximately 76.4 m and 79.1 m above MSL.

2.5.1.3 Low-Activity Waste Vaults

There are 21 LAWVs designated for use by the EAV project. Ten vaults are oriented in a general northeast-southwest direction, and eleven vaults are oriented in a general east-west direction (Fig. 2.5-1). Nineteen vaults consist of three major subdivisions (modules) with each module containing four cells. The remaining two vaults consist of two modules with each module containing four cells. Each three-module vault provides approximately $4.8 \times 10^4 \text{ m}^3$ of waste disposal capacity that will accommodate more than 12,000 B-25 boxes (waste containers). Each two-module vault provides approximately $3.2 \times 10^4 \text{ m}^3$ of waste disposal capacity that will accommodate more than 8,000 B-25 boxes. The base of the LAWs are at elevations ranging between approximately 84.0 m to 84.7 m above MSL.

2.5.2 Vault Descriptions

The EAV consists of three types of structures to house four designated waste types and the necessary roadways to allow waste container delivery.

One type of structure is partitioned into two segments (the ILTV and ILNTV) and receives two categories of waste. The ILNTV receives waste radiating $\geq 200 \text{ mR/h}$ at 5 cm from the exterior of the outer disposal container. The ILTV receives waste which is

contaminated with more than trace quantities of tritium. Administratively, the lower limit for the ILTV is 10 Ci of tritium per waste package. These two vaults share a similar design, are adjacently located, share waste handling equipment, and will be closed as one facility.

The second type of structure is designated as the LAWV. The LAWV is designed to receive waste radiating <200 mR/h at 5 cm from the exterior of the outer disposal container. The third facility is the long-lived waste storage building (LLWSB). The LLWSB is designed to provide covered, long term storage for waste containing long lived isotopes which exceed performance criteria for disposal. This waste would eventually be removed to a suitable disposal facility.

2.5.2.1 Intermediate-Level Non-tritium Vaults

There are currently ten ILNT vaults planned for the EAV. These vaults are subsurface concrete structures approximately 58 m long, 15 m wide, and 8.8 m high (Fig. 2.5-2). The end exterior walls are 0.8 m thick, the side exterior walls are 0.6 m thick, and interior walls are 0.5 m thick. All walls are structurally mated to a base slab, which is 0.8 m thick and extends past the outside of the exterior walls approximately 0.6 m. The 0.8 m base slab rests on two layers of crushed stone placed on the compacted subsurface. Each ILNTV consists of seven cells and provides approximately 5.7×10^3 m³ of waste disposal capacity.

The floor of each cell slopes to a drain which runs to a sump in the base slab for each cell. Any water accumulating in the sump can be monitored and removed through a 0.15-m - diameter riser pipe at the top of the wall. Any water that collects under the vault will flow to dry wells between the ILNTVs and the ILTVs. Access to the dry well can be obtained through a man hole at grade level.

The operating cell can be covered with reinforced concrete slabs, known as shielding tees, to reduce the radiation level at the edge of the vault. The profile of these tees are in the shape of the letter "T" so that they can be interlocked to provide 0.5 m of shielding. Each cell is also provided with a metal rain cover that is installed over each cell when not operating to minimize the infiltration of rain water.

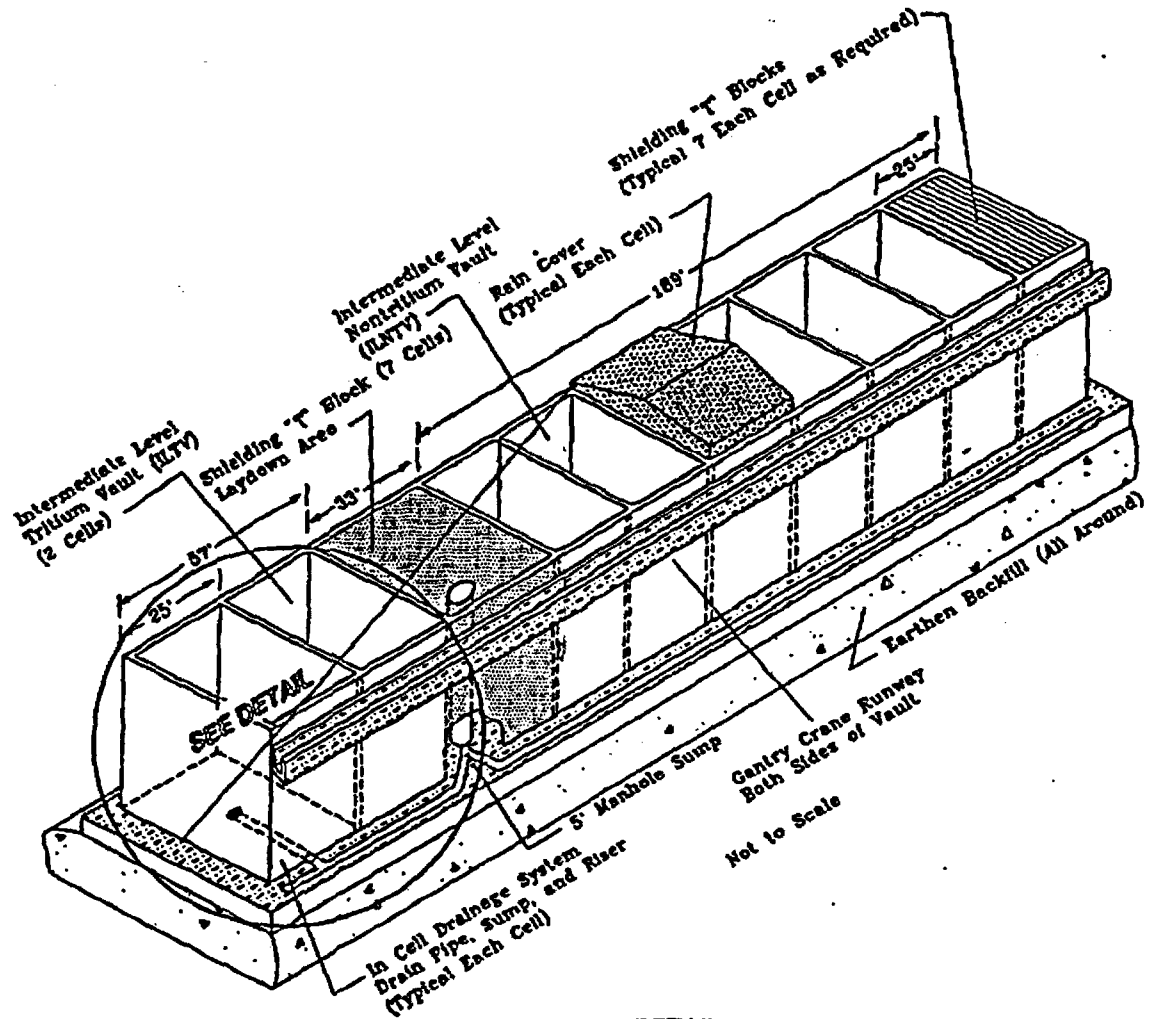
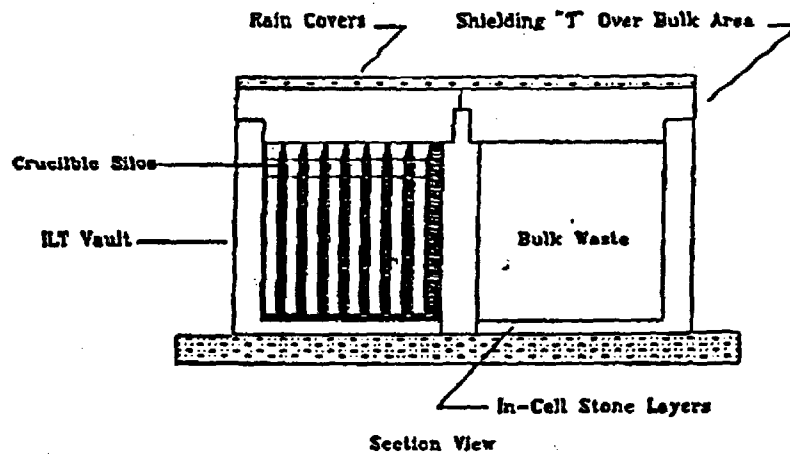
**DETAIL**

Fig. 2.5-2. General arrangement of the ILNT and ILT vaults.

225116

2.5.2.2 Intermediate-level Tritium Vaults

There are currently ten ILTVs planned for the EAV. Similar to the ILNTV, these vaults are subsurface concrete structures approximately 17 m long, 15 m wide, and 8.8 m high (Fig. 2.5-2). The wall and slab thicknesses are identical to ILNTV. Each ILNTV is composed of 2 cells.

One of the two cells is equipped with 142 silos, for tritium crucible overpacks. A 1-m - thick shielding plug will be used to reduce radiation exposure from the disposed crucibles. A plug will be installed in each silo after a crucible has been placed into it.

Both cells on the ILTV will be covered with metal raincovers when the vault is not operating.

2.5.2.3 Low Activity Waste Vaults

Twenty-one LAWVs are designated for construction in the EAV. These subsurface concrete structures consist of two or three modules depending on the vault location. Each module contains four cells. There are to be nineteen three-module vaults. Each will be approximately 200 m long, 44 m wide, and 8.2 m high (Fig. 2.5-3). There are plans for two vaults consisting of two modules. These vaults are approximately 130 m long, 44 m wide, and 8.2 m high. All exterior walls in the LAWVs will be 0.6 m thick and structurally mated to a 0.8-m thick footer. Interior cell walls are 0.3 m thick. The floor slab is 0.3 m thick and is not mated to the footer or walls.

2.5.2.4 Seismic Qualification

As documented on the Structural Design Criteria (S2889-306-25-0) the EAVs were designed and constructed to be maximum resistance structures after closure. In accordance with Site Specification 7096, a maximum resistance structure shall be designed to withstand a 0.2 g earthquake event.

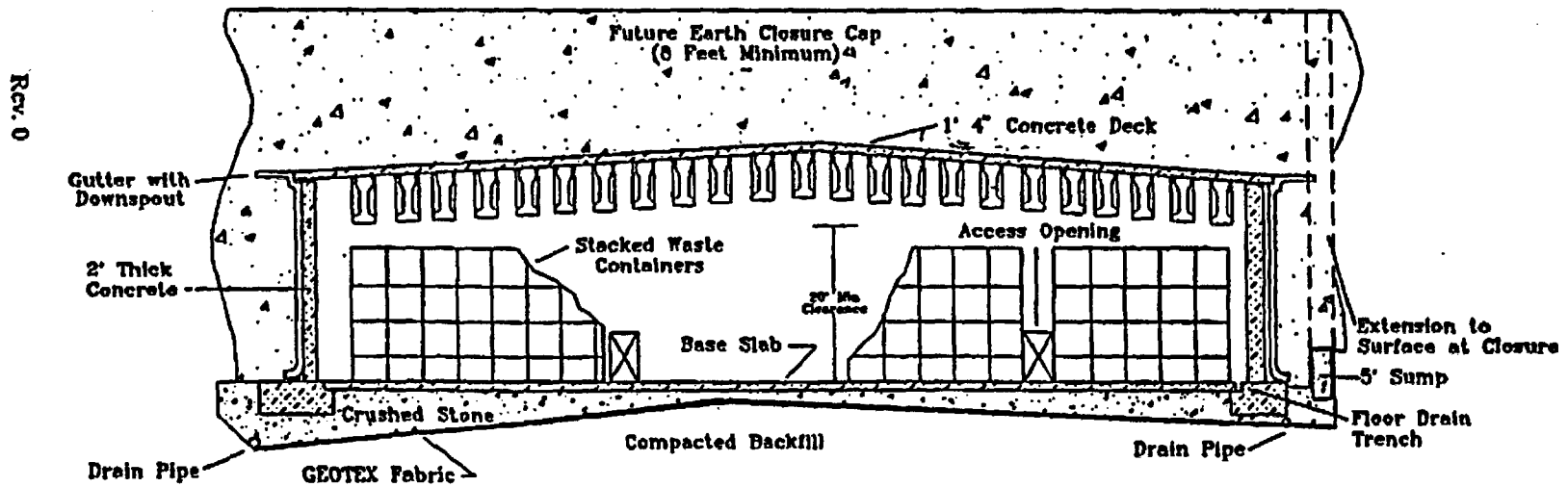


Fig. 2.5-3. Typical section through LAWV cell.

2.6 PROPOSED TRENCHES FOR DISPOSAL OF SUSPECT SOIL

Between 2800 and 5600 m³ of soil from regulated areas is designated as potentially contaminated soil (i.e., "suspect soil") at the SRS annually (Cook 1991). Non-vault disposal of a portion of this soil is being considered for the EAVDF.

Five below-grade trenches containing suspect soil are considered in this RPA for the EAVDF. The dimensions of each trench are 6 m wide by 200 m long by 6 m deep. The conceptual layout of the trenches is shown in Fig. 2.6-1. The location of these trenches is assumed to be near the LAW vaults, but not close enough to the LAW vaults to receive enhanced infiltration resulting from diversion of water from the vault roofs. The suspect soil is assumed to be placed in the trenches to a depth of 4.8 m, allowing for 1.2 m of a clean soil cover in the trenches. This clean soil is in addition to the final soil and clay cover that will overlay the trenches when final closure of the EAVDF occurs. No engineered barriers are assumed to exist beneath the trenches, and the base of the trenches are assumed to be at an elevation of approximately 84 m ASL, like the LAW vaults. The potential source of radionuclides to the E-Area environment and to inadvertent intruder posed by these trenches is evaluated in this RPA of the EAVDF in Appendix I, and radionuclide limits for disposal of suspect soil in such trenches are provided.

2.7 PROPOSED NAVAL REACTOR COMPONENT DISPOSAL

Within E-Area, disposal of up to 100 stainless steel casks containing naval reactor (NR) components is proposed. The NR waste is composed of activated metals and can include control rods, control rod drive mechanisms (CRDM's), resin vessels, adapter flanges, and similar equipment. The high shielding shipping/disposal containers reduce the safety risks involved in the disposal of NR wastes.

Rev. 0

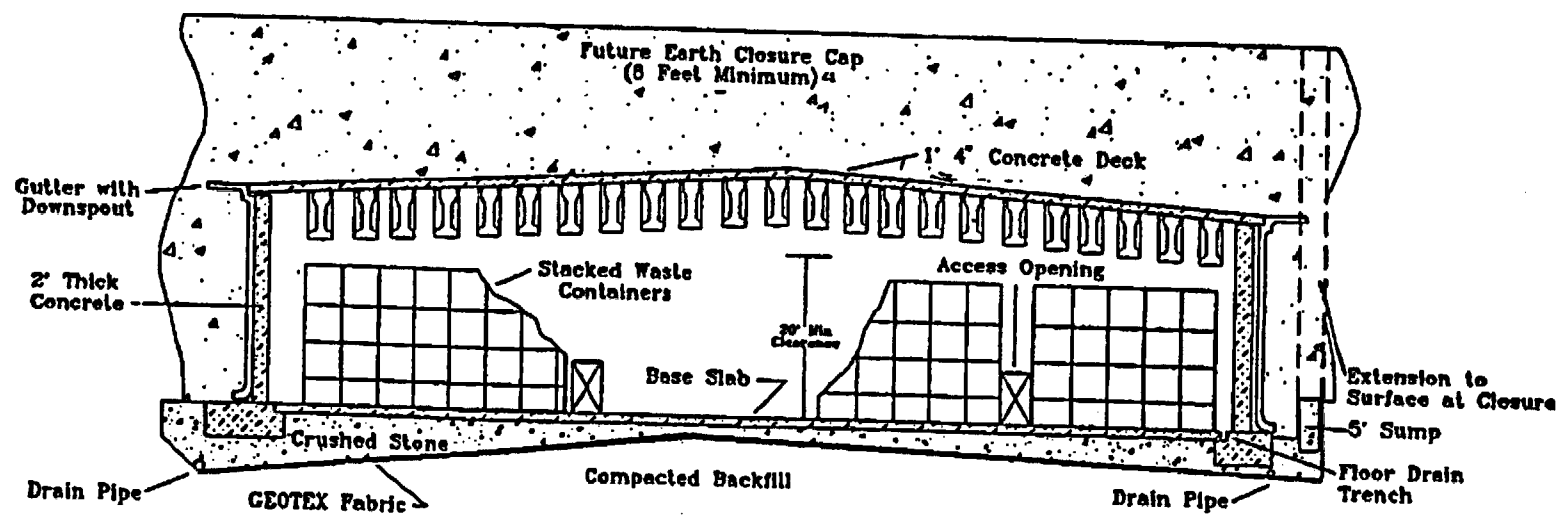


Fig. 2.5-3. Typical section through LAWV cell.

2.6 PROPOSED TRENCHES FOR DISPOSAL OF SUSPECT SOIL

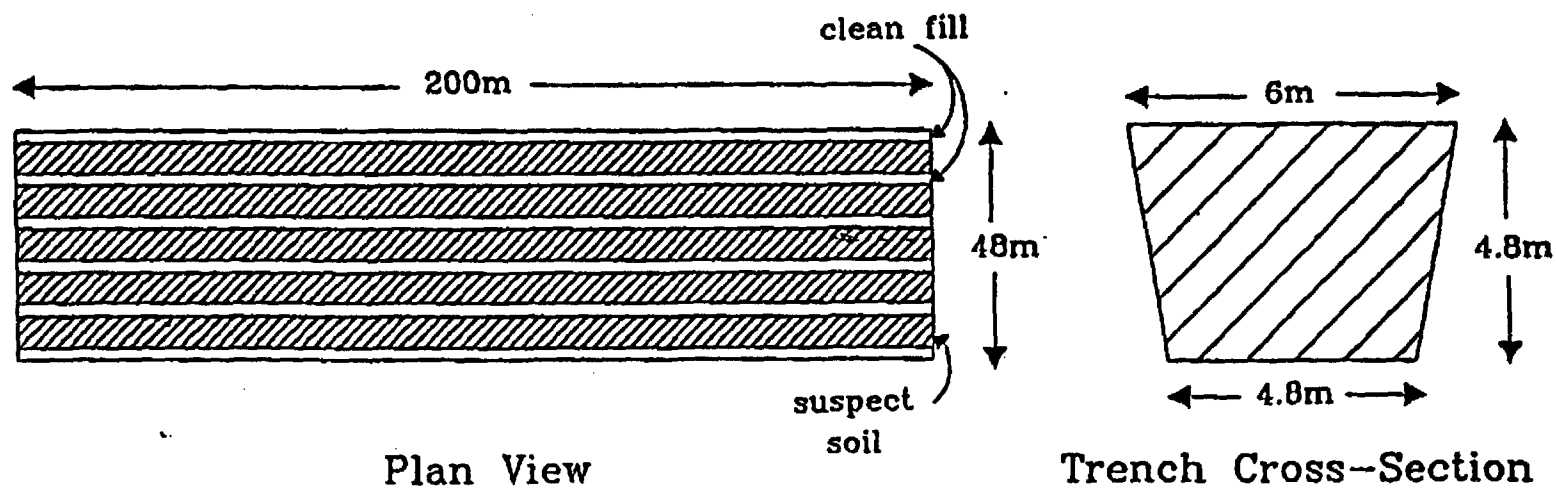
Between 2800 and 5600 m³ of soil from regulated areas is designated as potentially contaminated soil (i.e., "suspect soil") at the SRS annually (Cook 1991). Non-vault disposal of a portion of this soil is being considered for the EAVDF.

Five below-grade trenches containing suspect soil are considered in this RPA for the EAVDF. The dimensions of each trench are 6 m wide by 200 m long by 6 m deep. The conceptual layout of the trenches is shown in Fig. 2.6-1. The location of these trenches is assumed to be near the LAW vaults, but not close enough to the LAW vaults to receive enhanced infiltration resulting from diversion of water from the vault roofs. The suspect soil is assumed to be placed in the trenches to a depth of 4.8 m, allowing for 1.2 m of a clean soil cover in the trenches. This clean soil is in addition to the final soil and clay cover that will overlay the trenches when final closure of the EAVDF occurs. No engineered barriers are assumed to exist beneath the trenches, and the base of the trenches are assumed to be at an elevation of approximately 84 m ASL, like the LAW vaults. The potential source of radionuclides to the E-Area environment and to inadvertent intruder posed by these trenches is evaluated in this RPA of the EAVDF in Appendix I, and radionuclide limits for disposal of suspect soil in such trenches are provided.

2.7 PROPOSED NAVAL REACTOR COMPONENT DISPOSAL

Within E-Area, disposal of up to 100 stainless steel casks containing naval reactor (NR) components is proposed. The NR waste is composed of activated metals and can include control rods, control rod drive mechanisms (CRDM's), resin vessels, adapter flanges, and similar equipment. The high shielding shipping/disposal containers reduce the safety risks involved in the disposal of NR wastes.

Rev. 0



2-57

WSRC-RP-94-218

Fig. 2.6-1. Conceptual drawing of proposed suspect soil trenches.

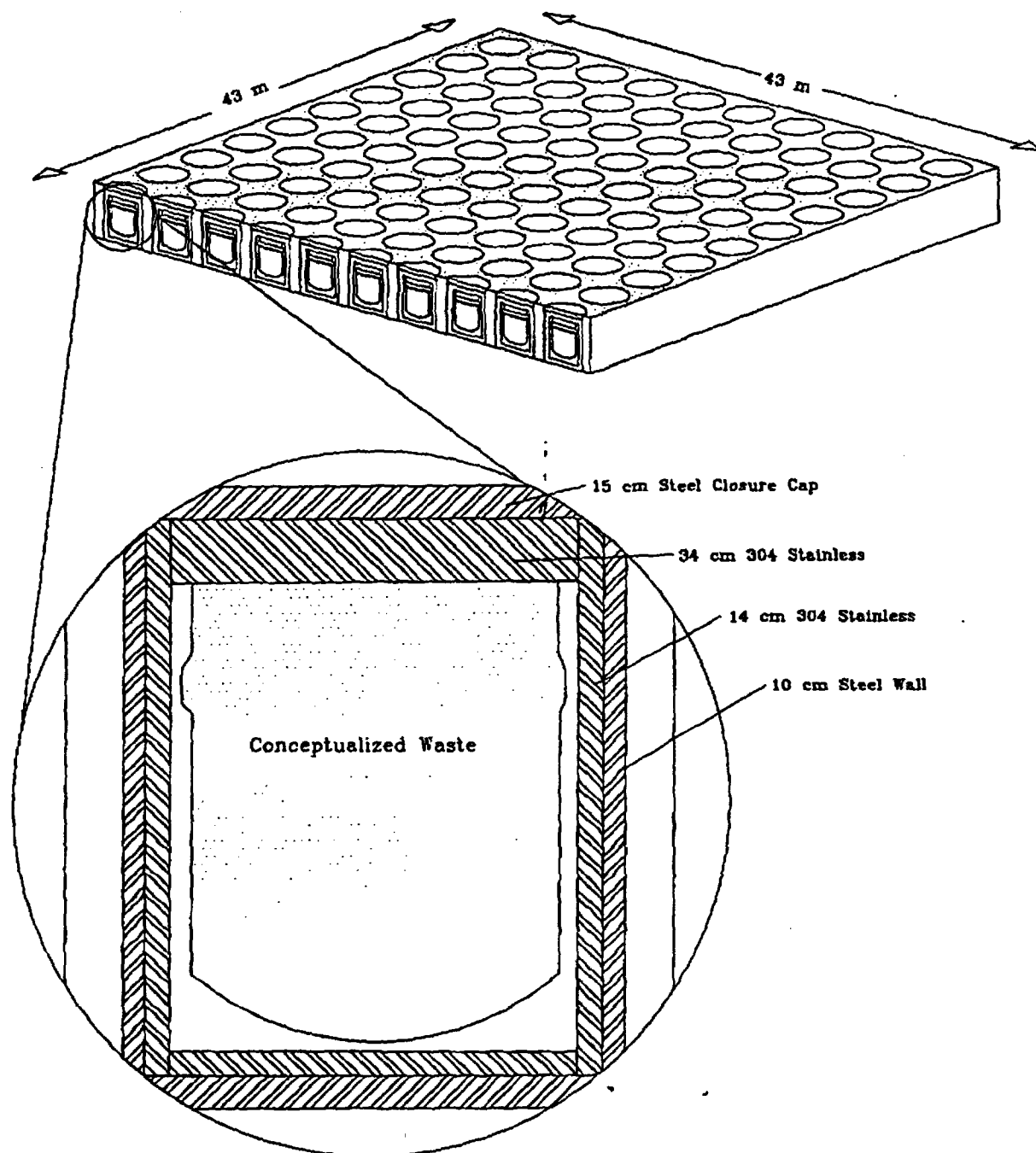
At least 41 containers are planned to be accepted for disposal at E-Area initially, although up to 100 containers may be delivered. The proposed layout of the containers is shown in Fig. 2.7-1. The life expectancy and shielding capacity of the shipping/disposal casks are determined by the specifications of the containers. A detail of the proposed NR waste package is shown in Fig. 2.7-2. Each cylindrical disposal container will have outside dimensions of 3.2 m in diameter and 5.4 m high. The container outer wall is 10-cm-thick carbon steel with a 15 cm base. The stainless steel inner layer is 14 cm thick with a 10 cm base and a 34 cm top plate. The disposal container is expected to be sealed with a 15 cm steel closure cap. The interior volume of the shipping/disposal cask is approximately 27 m³. The metal volume of the waste is approximately 3.5 m³. Approximately 3.8×10^3 m³ (1 gal) of water will be present initially in each cask.

The expected inventory of radionuclides for the first 41 NR waste shipments is listed in Table 2.7-1. A separate analysis of the performance of these waste packages is provided in Appendix L.

2.8 HAZARDOUS WASTE/MIXED WASTE DISPOSAL FACILITY

The HW/MWDF will be located in E-Area, Fig. 2.8-1, near the northeast corner of the 200 acre EAVDF. The facility will provide a Resource Conservation and Recovery Act (RCRA) permitted disposal facility for treated hazardous and MW that cannot be disposed in existing or planned facilities at SRS. The site of the HW/MWDF (Fig. 2.8-1) is a square shaped, wooded area of 0.15 km² (36 acres).

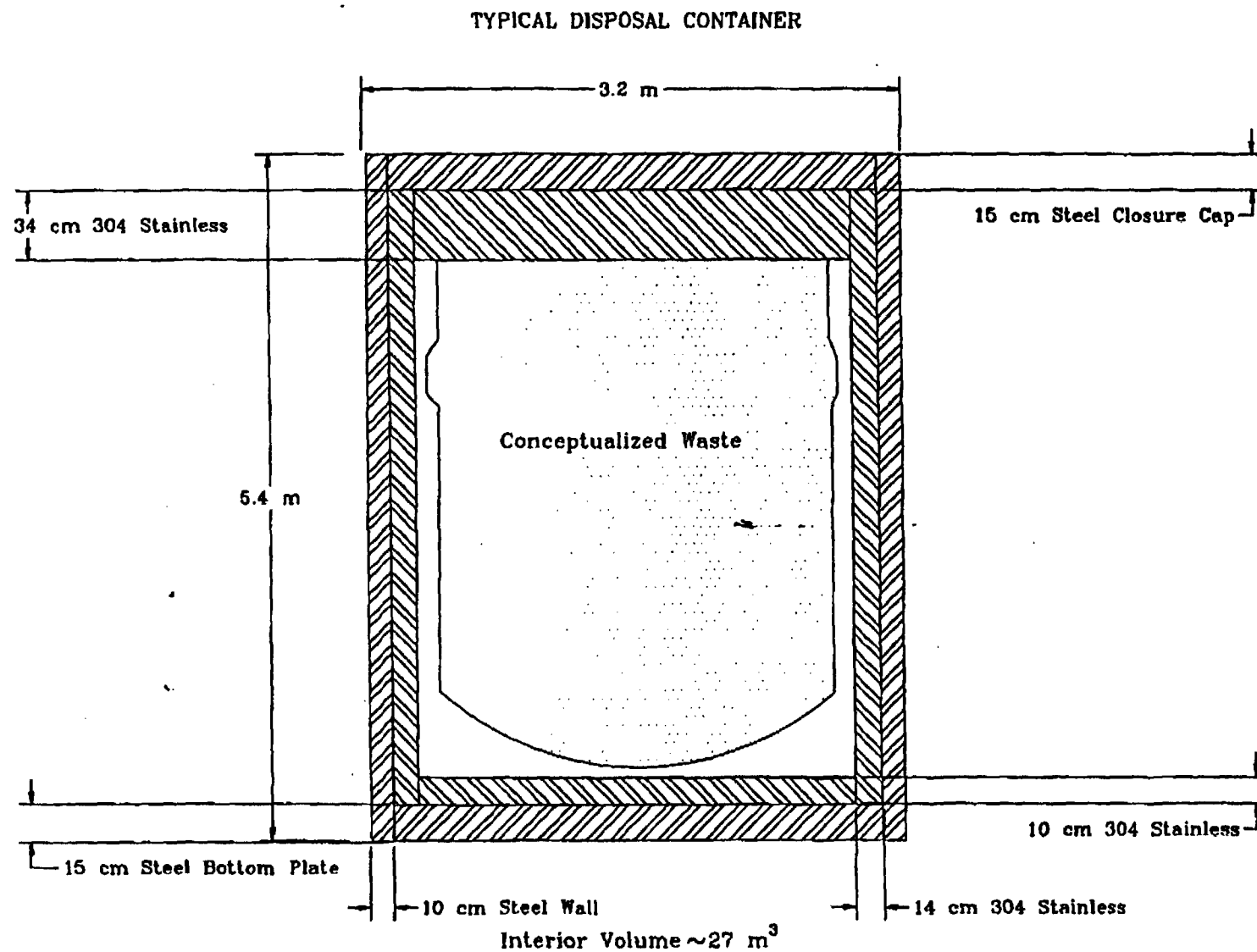
A separate RPA will be prepared at a later date to determine the performance of the HW/MWDF. The results from the HW/MWDF RPA will be evaluated to determine if it impacts the results determined in this RPA for the EAVs.



Dimensions 3.2 m X 5.4 m
Interior Volume ~27 m³

Fig. 2.7-1. Conceptual layout of 100 NR waste disposal containers.

Rev. 0



2-60

WSRC-RP-94-218

SRS152

Fig. 2.7-2. Typical NR waste disposal container.

Table 2.7-1. NR waste radioactive inventory

No. of units	1	8	8	16	8	Total all casks, Ci
Description	CBDC Hardware	Core Barrel	Holddown Barrels	CB/TS/CH Hardware	Adapter Flanges	
Isotopes:						
C14	3.12×10^{-1}	3.09×10^{-1}	---	1.10×10^1	1.61×10^{-3}	1.79×10^2
Co58	1.49×10^1	1.40×10^2	1.79×10	2.10×10^4	3.78×10^{-2}	3.37×10^5
Co60	2.96×10^2	5.92×10^3	5.79×10^1	4.50×10^4	1.45×10^{-1}	7.68×10^5
Cr51	1.82×10^{-1}	1.53×10^1	1.63×10^{-1}	8.10×10^3	2.84×10^{-5}	1.30×10^5
Cs137	1.22×10^{-2}	3.20×10^{-4}	2.80×10^{-4}	6.30×10^{-3}	6.32×10^{-5}	1.18×10^{-1}
Fe55	2.14×10^2	3.69×10^3	2.17×10^1	2.10×10^4	2.62×10^{-1}	3.66×10^5
Fe59	5.08×10^{-2}	7.80×10^{-1}	1.09×10^{-2}	1.50×10^2	4.40×10^{-4}	2.41×10^3
H3	9.55×10^{-3}	1.62×10	---	5.80×10^{-1}	---	2.22×10^1
Hf181	4.51×10^{-3}	7.00×10^{-4}	6.30×10^{-4}	2.61×10^3	1.41×10^{-4}	4.18×10^4
I129	1.25×10^{-6}	---	---	---	---	1.25×10^{-6}
In113	---	---	---	4.40×10^3	---	7.04×10^4
In114	---	---	---	5.50×10^2	---	8.80×10^3
Mn54	3.10×10	2.32×10^1	1.80×10^{-1}	5.70×10^2	8.46×10^{-3}	9.31×10^3
Nb94	6.41×10^{-3}	1.60×10^{-4}	1.40×10^{-1}	3.20×10^{-1}	3.22×10^{-5}	6.25×10
Nb95	4.11×10^{-2}	2.40×10^{-3}	2.20×10^{-3}	1.50×10^5	4.66×10^{-4}	2.40×10^6
Ni59	2.83×10	6.32×10^1	7.83×10^{-1}	2.10×10^2	4.83×10^{-4}	3.87×10^3
Ni63	3.82×10^2	6.32×10^3	7.83×10^1	2.90×10^4	4.80×10^{-2}	5.16×10^5
Pu239	2.49×10^{-5}	---	---	---	1.00×10^{-7}	2.57×10^{-5}
Pu241	8.86×10^{-4}	2.30×10^{-5}	2.10×10^{-5}	4.73×10^{-4}	4.70×10^{-6}	8.84×10^{-3}
Sb125	---	---	---	1.20×10^4	---	1.92×10^5
Sc46	3.26×10^{-3}	---	---	---	---	3.26×10^{-3}
Sn113	---	---	---	4.40×10^3	---	7.04×10^4
Sn119m	---	---	---	5.50×10^4	---	8.80×10^5

2-62
Table 2.7-1. (continued)

WSRC-RP-94-218

No. of units	1	8	8	16	8	Total all casks, Ci
Description	CBDC Hardware	Core Barrel	Holddown Barrels	CB/TS/CH Hardware	Adapter Flanges	
Isotopes:						
Sn123	---	---	---	1.50×10^3	---	2.40×10^4
Sr90	1.21×10^{-2}	3.20×10^{-4}	2.80×10^{-4}	2.90×10^1	6.32×10^{-5}	4.64×10^2
Ta182	2.86×10	---	---	1.10×10^3	---	1.76×10^4
Tc99	3.32×10^{-4}	3.69×10	---	---	---	2.95×10^1
Y90	1.21×10^{-2}	3.20×10^{-4}	2.80×10^{-4}	---	6.32×10^{-5}	1.74×10^{-2}
Zr95	---	1.00×10^{-3}	9.40×10^{-4}	---	2.33×10^{-4}	1.74×10^{-2}
Zn65	1.29×10^{-1}	---	---	---	---	1.29×10^{-1}
Totals, Ci	916.47	16,178.10	160.97	3.57×10^5	0.50	5.84×10^6

Total Curies: 5.84×10^6 (total curie content for all 41 casks)

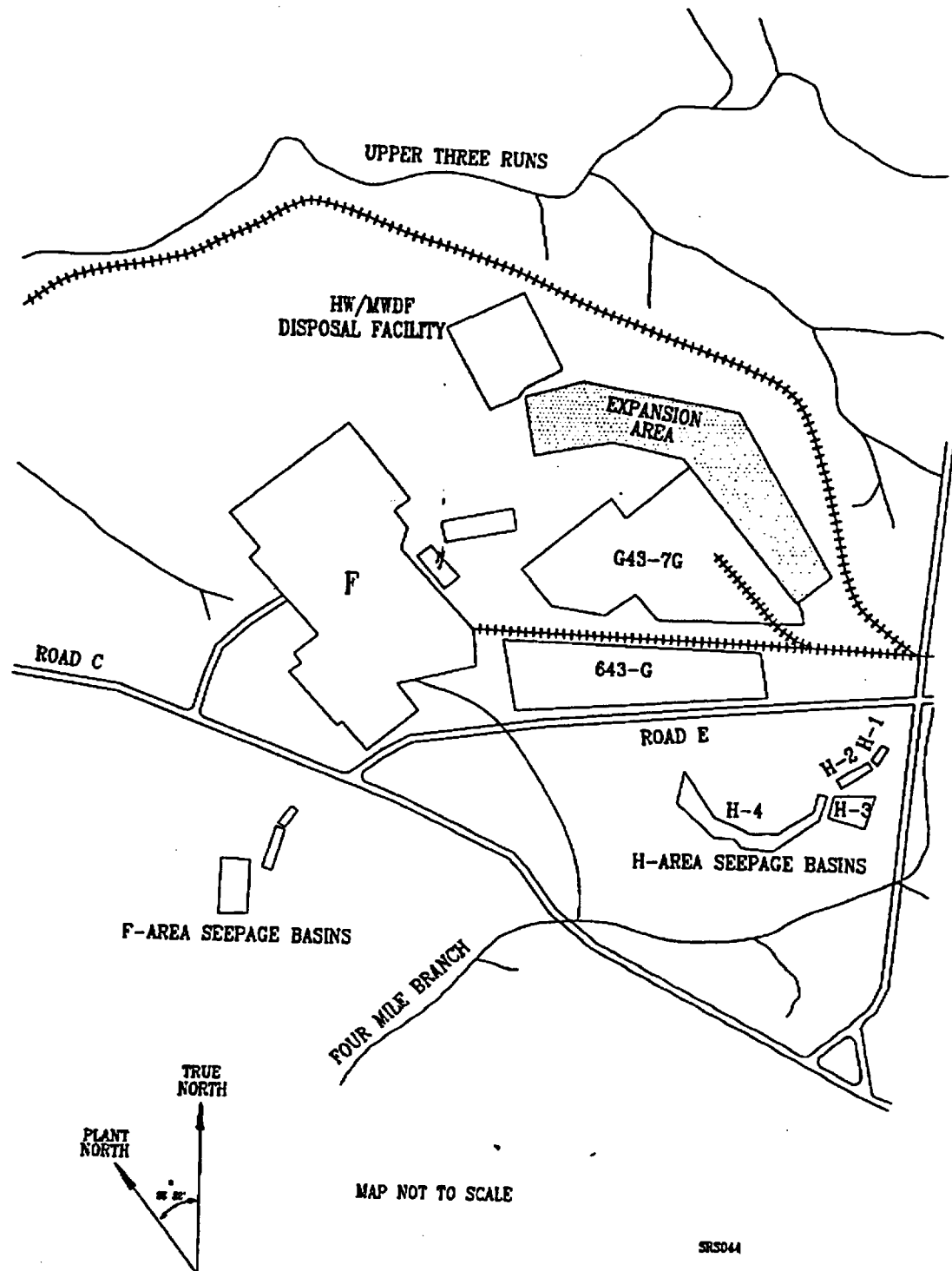


Fig. 2.8-1. Location map for HW/MWDF.

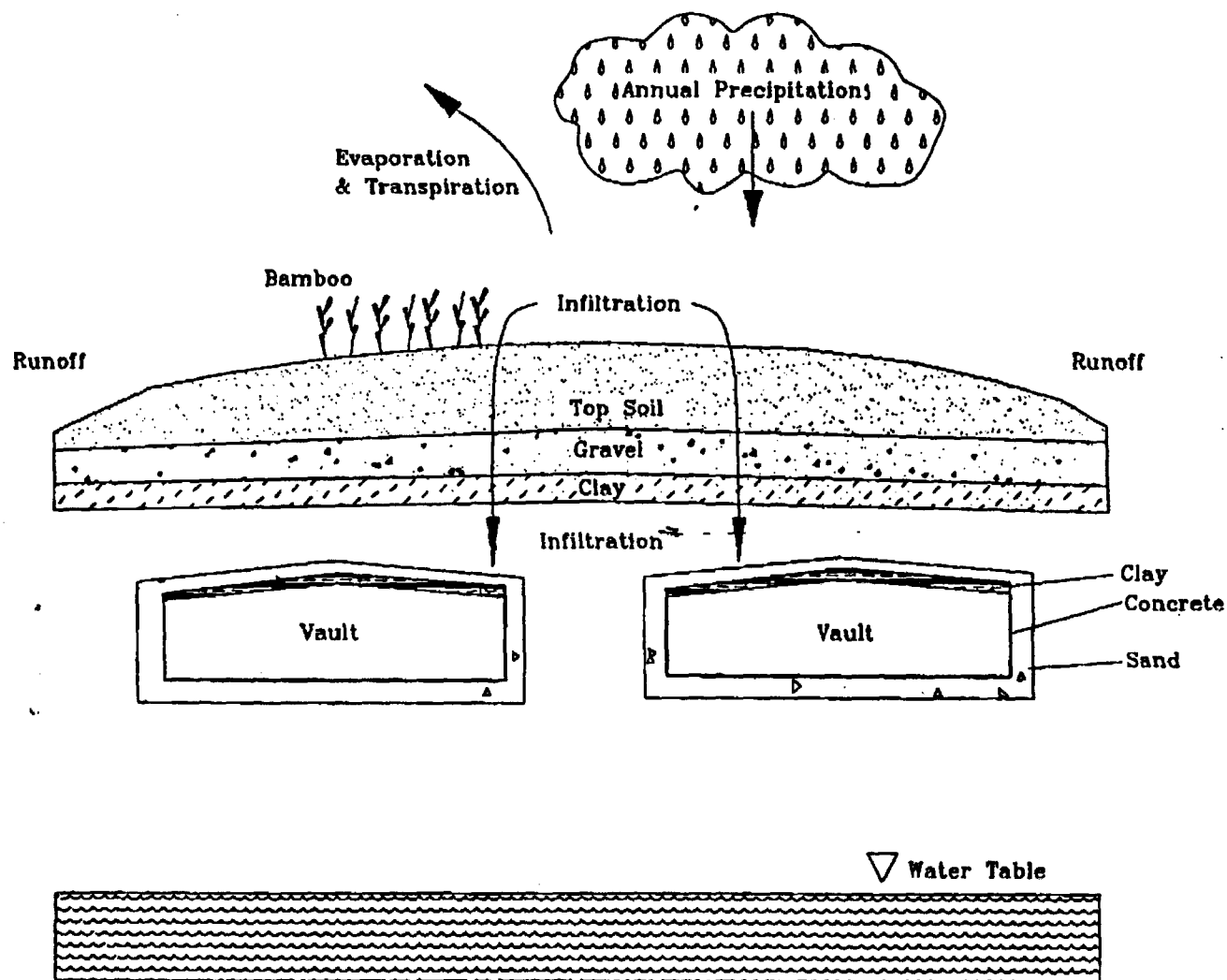
2.9 E-AREA CLOSURE CONCEPT

One of the key objectives of any closure of a waste disposal site is to limit moisture flux through the waste, thus minimizing contamination of the underlying groundwater. Because the EAVs are designed as a controlled release facility, proper closure to meet the objective of limiting moisture through the waste will be an integral part of long-term acceptability of the disposal site. Because backfilling and final closure of the EAVs will be delayed for several years, a detailed closure design has not been fully developed for the EAVs. Thus an integral part of the EAV RPA required that a closure concept be described and subsequently tested in models that simulate the performance characteristics of the proposed closure concept.

2.9.1 Physical Description of the EAVs Closure Concept

Closure concepts developed for this assessment are illustrated in Fig. 2.9-1 and Fig. 2.9-2. Figure 2.9-1 represents the closure concept with an intact cover (moisture barrier) (see Sect. 3.1.3.1 for a discussion of cover degradation), while Fig. 2.9-2 represents the degraded cover system, in which the properties of the moisture barrier have reverted to that of the surrounding soil (see Sect. 3.1.3.1). Closure operations will begin near the end of the active disposal period in the EAVs, i.e., after most or all of the vaults have been constructed and filled. Backfill of Burma Road sand will be placed around the vaults and above a clay cap, which will be emplaced on top of each vault. Above this layer of backfill, a laterally extensive moisture barrier will be installed. This moisture barrier will consist of 0.76 m of clay and an overlying layer of 0.3 m of gravel. A geotextile fabric will be placed on the gravel layer, and a second backfill layer, approximately 0.76 m thick, will be placed over the moisture barrier. Finally, 0.15 m layer of topsoil will be placed on the top layer of backfill to complete disposal operations at E-Area. This sequence of layers along with a minimum backfill of 0.43 m will provide a minimum of 2.9 m of cover for each vault.

Rev. 0



SR5113a

Fig. 2.9-1. Vault closure concept (2 cm/year infiltration).

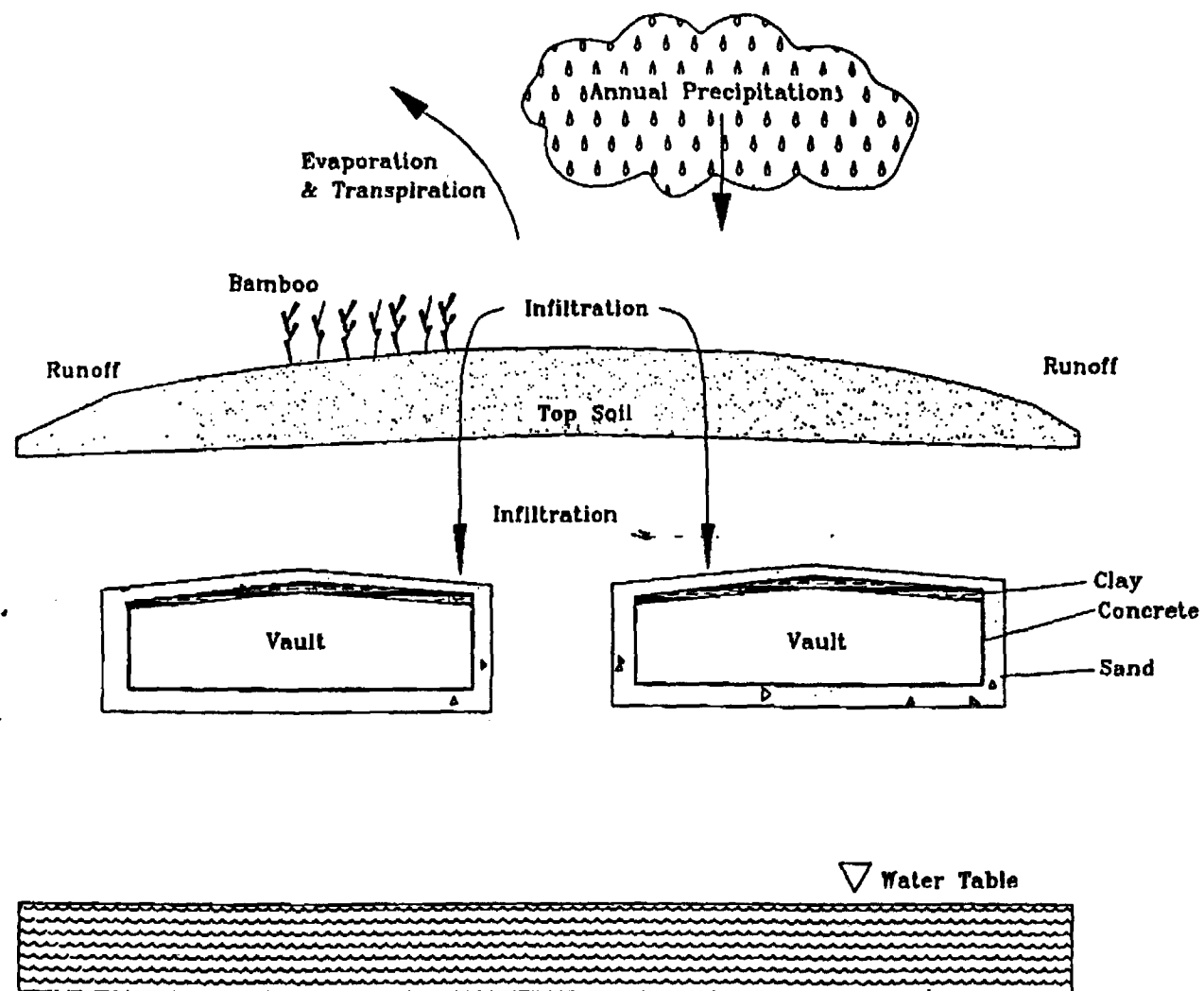


Fig. 2.9-2. Vault closure concept (40 cm/year infiltration).

SR9113

Final closure of the EAVs will be accomplished by constructing a drainage system and revegetating the site. The drainage system will consist of a system of rip-rap lined ditches that intercept the gravel layer of the moisture barrier. These ditches will divert surface runoff and water intercepted by the moisture barrier away from the disposal site. The drainage ditches will be constructed between rows of vaults and around the perimeter of the EAVDF.

The topsoil will be revegetated with bamboo. A study conducted by the USDA Soil Conservation Service (Salvo and Cook 1993) has shown that the two species of bamboo (*Phyllostachys bisetii* and *Phyllostachys rubromarginata*) will quickly establish a dense ground cover which will prevent the growth of pine trees, the most deeply rooted naturally occurring plant type at SRS. Bamboo is a shallow-rooted climax species which evapotranspires year-round in the SRS climate, thus, removing a large amount of moisture from the soil and decreasing the infiltration into the underlying disposal system.

2.9.2 Functional Description of the E-Area Closure Concept

Performance requirements for the closure concept are expressed in terms of hydraulic properties for the various soil layers (Thompson 1991). These properties are listed in Table 2.9-1. The topsoil and upper backfill layer serve to store and distribute infiltrating water. These layers intercept incoming water and redirect a significant portion in the horizontal direction to drainage ditches installed at the EAVDF. Computer simulations of flow through the cover show that the gravel drainage layer will carry away a major portion of the water that would normally infiltrate at the EAVDF (40 cm/year). The vertical moisture flux through the cover will be limited to less than 2 cm/year, based on the hydraulic properties of the closure system.

Table 2.9-1 Values for hydraulic properties of vault closure design

Layer Description	Hydraulic Conductivity (cm/s)
Clay	1.0×10^{-7}
Gravel	0.5
Backfill	1.0×10^{-5}

2.9.3 Post Closure Groundwater Monitoring

Post-closure monitoring of groundwater quality will serve to verify that the EAVDF is performing according to expectations and to allow differentiation of future EAVDF contaminant plumes from previously existing contaminant plumes.

Numerous groundwater monitoring wells have already been installed in the vicinity of the EAVDF to permit monitoring of contaminant plumes emanating from existing facilities. These wells are currently being sampled on a routine basis to define the current extent of contaminant plumes and to establish groundwater quality trends. Additional wells may be installed immediately surrounding the EAVDF at a later date to supplement this network if it is determined that it does not provide adequate monitoring of the EAVDF.

Continued monitoring in the post-closure period will allow establishment of future trends such that deviations due to EAVDF operation will be apparent. Statistical evaluation methodology will form the basis for making such a determination. An adequate methodology has not yet been developed but is expected to be developed for application at the Z-Area. The methodology will be described in the "Statistical Evaluation Plan" which is required in order to obtain the Industrial Waste Permit from SCDHEC for operation of the Saltstone Facility. When the methodology is developed it will serve as a guide for similar applications at the EAVDF.

3. ANALYSIS OF PERFORMANCE

The methods used to analyze the long-term performance of the EAVDF are described in this chapter. Source term development is discussed first, in Sect. 3.1. This section includes a list of radionuclides considered, potential mechanisms of contaminant release from the facility, and of potential mechanisms responsible for loss of integrity of the engineered barriers of the EAVs.

Following the source term discussion, potential receptors are identified in Sect. 3.2 by recognizing the time periods of concern in this RPA, the potentially significant pathways to human exposure, and exposure scenarios that should be evaluated for both off-site members of the public and inadvertent intruders. In this section, the EAV radionuclides of interest in the analysis have been determined by a screening process which eliminates radionuclides that, under unrealistically conservative conditions, are insignificant with respect to potential human exposures.

The conceptual models developed and the computational approach used to assess the performance of the EAVs are also described in this chapter. The conceptual models are derived from technical information presented in Chapter 2. These models embody a number of simplifying assumptions to facilitate the computational analysis required to assess long-term performance of the EAVs.

An overall conceptual model was used to prepare the RPA for E-Area and is illustrated schematically in Fig. 3.0-1. This overall conceptual model indicates the linkage of 1) a source term submodel (Sect. 3.1), which considers mechanisms of release of radionuclides from ILT, ILNT, and LAW vaults, 2) a near-field submodel (Sect. 3.3.1), which addresses movement of released constituents within the EAVs and through the unsaturated zone around the facility, 3) an environmental transport submodel, which addresses potential transport pathways including groundwater (Sect. 3.2.2 and 3.3.2), and 4) a dose submodel (Sect. 3.3.3) which relies on the exposure/intruder scenarios developed in Sect. 3.2.3 and 3.2.4. The computational methods used to implement the conceptual models are described in Sect. 3.4.

Conceptual Model

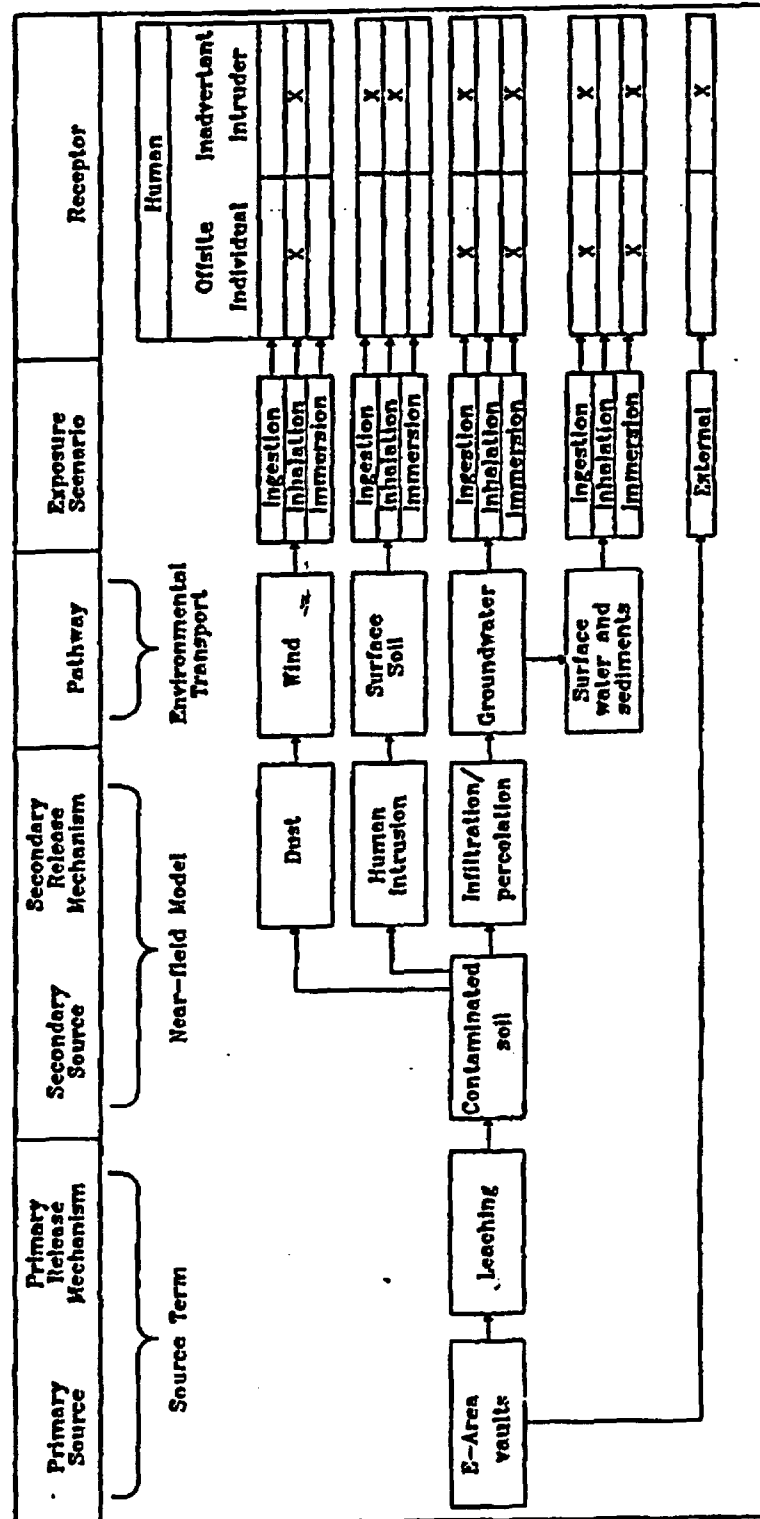


Fig. 3.0-1. Overall conceptual model for the Radiological Performance Assessment of the E-Area Vaults Disposal Facility.

3.1 SOURCE TERM

This section includes discussions of factors affecting the rate at which radionuclides are released from the disposal facility. Source term considerations are typically a large source of uncertainty. The uncertainty starts with trying to project future disposal practices and is compounded by uncertainties related to release mechanisms from the waste form. Once the contaminant is released from the waste forms, then the effectiveness and longevity of the concrete vault must be considered. The source term is also affected by the rate at which water percolates through the engineered cover. Thus, degradation of the cover is also addressed in this section. Each of these topics are discussed in the following paragraphs.

3.1.1 Radionuclides of Interest

The purpose of the PA for the EAVs was to determine the allowable inventory of radionuclides in a given vault type based upon the performance objectives for dose. Since the specific radionuclides that may be encountered in the waste during disposal operations is not known, a conservative screening method was used to determine the allowable inventories of a large suite of radionuclides which may be encountered during disposal operations. These limits are called "trigger values " and indicate the inventory at which the performance objectives may be exceeded. A detailed, site-specific analysis is recommended for a given radionuclide before additional inventories above the trigger value (TV) are placed in E-Area for disposal. The TVs for all radionuclides of interest in the EAVDF are provided in Appendix C. Radionuclides which have relatively small TVs, such that an allowable inventory above the TV is desirable, are included in the detailed site-specific analyses. The screening analysis for determining the TVs is described in detail in Sect. 3.2.3.4 and 3.2.4.4.

3.1.2 Release Mechanisms

Estimating the release of radionuclides from the E-Area disposal facility is difficult because of the variety of contaminated material that will be disposed in the vaults. Conceptually, waste within boxes (B-25 steel) or activated metals disposed in vaults will remain immobile until contacted by water that has leaked into the vaults. Defensible prediction of water movement in the vaults and of the effectiveness of boxes and activated metals in retarding waste release is not possible without developing a conservative simplified conceptual model. The key features of the conceptual model are:

- Waste is immobile until contacted by water.
- The water entering the vault will have a composition that can be represented as a mixture of concrete pore fluid and local groundwater equilibrated with soil levels of carbon dioxide gas.
- The presence of steel and activated metals in the vaults will result in the formation of corrosion products (i.e., hydrous Fe[III] oxides) and lead to reducing conditions inside the vaults.
- The entire inventory of the vault is available to react with the reducing water inside the vault (i.e., continuously stirred tank reactor source term model).
- The aqueous concentrations of radionuclides are controlled by sorption (represented with a K_d or isotherm) onto corrosion products (LAW/ILNT/ILT vaults) or grout (ILNT/ILT) with a solubility limited (oxide and hydroxide phases) upper concentration.
- Contaminated water exiting the vault will interact with the concrete vault and radionuclides will be chemically retarded by the vault wall.

The contaminant release rate will be a function of several physical and chemical factors. The most important factors are:

- water flux into the vault,
- water composition (pH and redox) in the vault,

- physical state (e.g., integrity) and properties (e.g., hydraulic conductivity) of the vault, and
- physical, chemical, and transport properties of the contaminants.

A detailed discussion of geochemical calculations is provided in Appendix D.

3.1.3 Engineered Barriers Degradation and Failure

The following two sections address degradation of the engineered cover and the concrete vaults. Degradation of the cover is addressed first. In general, cover degradation is considered in a binary fashion (i.e., it is assumed to be functional or it is assumed to be non-functional). Vault degradation is addressed in the second section. The primary mode of vault degradation is expected to be cracking and eventual failure of the roof. Subsequent flow and transport conceptual models are based on the conclusions of these two sections, and the detailed discussion in Appendix K.

3.1.3.1 Cover Degradation

Degradation of the cover is expected to occur by a number of processes. Potential processes are erosion; penetration by plants and animals; external events such as settling or slumping, or a seismic event; and human intrusion. These processes will reduce the effectiveness of the cover to limit the vertical moisture flux. Over the period of analysis, the net flux through the cover is expected to approach the background levels for the site, i.e., 40 cm/year.

As presently conceived in the closure concept (Sect. 2.8), shallow-rooted bamboo will be planted on the disposal site and a system of drainage ditches will be constructed to handle surface runoff and diverted infiltration. As specified in DOE Order 5820.2A, active institutional control is assumed for only 100 years. During this time, periodic site inspection would reveal any degradation of the overlying cover and drainage system and corrective actions would be taken. Cover degradation during this first 100 years is likely to be minimal. Sheet erosion will occur, but the bamboo vegetative cover would minimize the effects of this

disturbance. Return of the SRS land to unrestricted use after 100 years may result in a usage conversion to agricultural practices, consistent with past and current land use in the SRS vicinity. Row crop farming, which is consistent with historical practices in the vicinity, would increase the erosive effects of precipitation. Soil erosion rates for cropland in the vicinity of the SRS are on the order of $1.7 \text{ kg m}^{-2} \text{ yr}^{-1}$ (Sect. 2.1.8). Erosion is reduced several hundred fold if a dense vegetative cover is present (Sect. 2.1.8). This suggests that there will be little erosion as long as the bamboo vegetative layer has not been cleared; however, the cover may be eroded down to the gravel layer in as little as 800 years after the bamboo vegetative layer is cleared. However, erosion of the gravel layer is difficult to predict. In this analysis, it is assumed that the cover remains functional until the roof of the vault fails and thus, no longer provides support for the cover.

3.1.3.2 Vault Degradation

The concrete vaults are expected to degrade slowly through a combination of physical, chemical, and mechanical processes (Walton et al. 1990). Physical and mechanical degradation processes that produce cracking are of primary concern, because of the concomitant increase in permeability. Shrinkage cracks occur as a result of the temperature cycling during curing of concrete structures, and thus are present before the facility closure cover is constructed. This allows for filling of the outer portion of the cracks, in the vault walls or roof, with epoxy prior to closure. Cracking might occur after the vaults have been covered as a result of degradation of the epoxy used to fill shrinkage cracks, foundation settling, or rebar expansion due to corrosion.

The principal chemical processes that disrupt the integrity of concrete structures are: sulfate attack, carbonation, calcium hydroxide leaching, and rebar corrosion. The effects of these processes on EAV degradation have been analyzed using the methodology described in Walton, et al. (1990). The methodology quantifies the extent of concrete degradation in terms of the penetration depth. This depth is the amount of wall thickness that has degraded. The analysis of chemical degradation effects and structural considerations are discussed in detail in Appendix K. A brief discussion of the mechanisms affecting vault durability are provided in the following sections.

Sulfate attack

Concrete degrades by sulfate and/or magnesium attack when sulfate or magnesium ions in the pore-fluid migrate into the concrete and react with the cement paste. Sulfate reacts with tri-calcium aluminate in the cement paste to form calcium aluminum sulfates. Magnesium reacts with hydroxide ions to form magnesium hydroxide. The products of these reactions have considerably greater volume than the compounds they replace. The expansive reactions can result in disruption of the concrete.

The major sources of sulfate and magnesium at the site are from soil water. Concentrations of sulfate and magnesium in groundwater at the SRS (Sect. 2.2.4) are very low. Sulfate concentrations range from 0.27 to 15 ppm (2.81×10^{-6} to 1.56×10^{-4} mol/L) with a mean and median of 3.66 and 2 ppm (3.81×10^{-5} and 2.08×10^{-5} mol/L), respectively. Magnesium concentrations range from 0.14 to 8 ppm (5.76×10^{-6} to 3.29×10^{-4} mol/L) with a mean and median of 2.28 and 1.5 ppm (9.37×10^{-5} and 6.17×10^{-5} mol/L), respectively. The sum of Mg and SO_4 range from 0.57 to 18.5 ppm (1.51×10^{-5} to 3.77×10^{-4} mol/L) with a mean and median of 5.94 and 4.95 ppm (1.32×10^{-4} and 1.08×10^{-4} mol/L), respectively (Marine 1976).

The methodology developed by Atkinson and Hearne (1984) (and summarized in Walton et al. 1990) was used to assess the impact of sulfate and magnesium attack associated with the ingress of the soil-moisture.

Carbonation

Carbonation occurs when calcium in concrete reacts with carbon dioxide (CO_2) to form calcium carbonate. At the E-Area disposal site, carbon dioxide will be present in soil-air and dissolved in soil-water. Carbon dioxide will slowly migrate into the concrete, potentially leading to a carbonated zone. Concrete degradation, in this case, is associated with concrete expansion due to corrosion of the reinforcement bars (i.e., rebar). Typically, the pH of concrete is very high which is favorable to very low rebar corrosion. However, the carbonation reaction can reduce the pore-fluid pH which, in turn, makes the rebar susceptible to corrosion.

Carbonation may also result in potentially beneficial effects. For example, carbonate carried by the pore-fluid into cracks and pores of the vault structure may precipitate and reduce the effective porosity of the vaults. At the bottom of the vault, water which has percolated through the vault roof will be saturated with portlandite $\text{Ca}(\text{OH})_2$. The $\text{Ca}(\text{OH})_2$ can react with soil-air containing CO_2 , forming a calcium carbonate mass that then seals cracks and reduces effective pore sizes at any exposed surfaces of the vault structure.

The extent of carbonation was estimated using a shrinking core model (Walton et al. 1990). Carbonation was modeled as a uniform coating which forms on the surface of the concrete.

Calcium hydroxide leaching

Ingress of water into the vaults and flow of water around the vaults will provide a pathway for leaching of soluble components from the concrete. In particular, leaching of calcium hydroxide from the concrete can lead to loss of strength and increases in concrete permeability (Walton et al. 1990). Leaching is typically important in humid sites, such as the SRS, because high infiltration rates promote higher leaching rates.

The rate of leaching can be estimated using simple screening models or more complex numerical models. For this application, conservative screening calculations were performed. Two different simplifying assumptions were used in the calculations (Atkinson and Hearne 1984), namely: 1) concrete controlled leaching, and 2) geology controlled leaching. Concrete controlled leaching assumes that the leaching rate is limited by diffusion through the concrete into the surrounding soil. Once the calcium reaches the soil it is rapidly removed leading to a zero concentration boundary condition. If water is flowing around the vault, then a low concentration of calcium can conservatively be assumed in the soil moisture.

For the case of geology controlled leaching, diffusion of calcium into surrounding soils is assumed to limit the process. For this condition, the degradation effects are insignificant. This particular type of process, however, is only valid in diffusion dominated systems where water flow around the vault is low, such as beneath the vault or when infiltration is low.

Rebar corrosion

Corrosion of the reinforcing bars (rebar) is another possible mechanism of vault degradation. Corrosion occurs when iron in the rebar reacts with oxygen to form iron oxides. Corrosion of the rebar has two major effects on concrete structures: 1) corrosion lowers the strength of the rebar and 2) corrosion disrupts the integrity of the surrounding concrete.

Rebar is used in concrete structures to increase tensile strength. As the rebar corrodes, the tensile strength of the structure declines. For the EAVs, the structural role of the vault is essential to long-term isolation performance.

Iron oxides have a molar volume which is over twice that of steel. As rebar corrosion occurs, the volume occupied by the rebar will expand. The expansion leads to stress development around the reinforcement and eventually to disruption of the integrity of the concrete. This process is easily visible in old concrete structures where fractures and spalling of the concrete occur adjacent to corroded reinforcement.

Reinforcement corrosion is typically modeled in two stages: 1) initiation, and 2) active corrosion (Walton et al 1990). Initially the steel is protected from corrosion by a "passivating layer" of iron oxides on the metal surface. The stability of the passive layer is supported by the high pH of the concrete. Before significant corrosion can begin, the passive layer must be disrupted. This occurs when the pH of the concrete is lowered by carbonation or when aggressive anions (such as chloride) penetrate into the concrete to the depth of the steel.

As discussed previously, carbonation of the structure will occur too slowly to be a factor in concrete corrosion of the vaults. Accordingly, carbonation is even less of a factor in rebar corrosion. Concentrations of chloride ions in the soil moisture at the SRS are also too low to initiate active corrosion. Migration of chloride in the waste out to the rebar would control the time of the initiation stage noted above. To establish if rebar corrosion would significantly affect the rate of vault degradation, active corrosion was assumed to begin immediately after closure and no credit for the initiation lag time was taken in the corrosion calculations.

Once active corrosion begins, the corrosion rate may be limited by availability of oxygen. However, at very low oxygen concentrations, water can be used as a source of oxygen for corrosion (hydrogen evolution reaction). Because the thickness of concrete over the rebar

limits the availability of oxygen for rebar corrosion, hydrogen evolution was considered as an additional process for rebar corrosion. By combining the oxygen diffusion and hydrogen evolution reactions an estimate of the total rebar corrosion can be made.

3.2 PATHWAYS AND SCENARIOS

This section of the RPA addresses the time periods of concern and pathways to human exposure for EAV constituents potentially released in the manner described in Sect. 3.1 above. The information provided in this section is subsequently used in the development of models to evaluate doses potentially received as a result of releases of radionuclides from the EAVDF.

3.2.1 Time Periods of Concern

To assess the performance of the E-Area Disposal Facility, three time periods of concern are addressed: 1) the operational period; 2) the institutional control period; and 3) the post-institutional control period.

3.2.1.1 Operational Period

The operational period is defined as the period during which waste is actively emplaced. During this period, some vaults are sealed as an interim closure, prior to placement of the final closure cap. The facility is fenced and patrolled, preventing unauthorized access during this period.

The operational period for the E-Area Disposal Facility is expected to be at least 20 years. Doses to maximally exposed off-site individuals during this time period are addressed in the SAR for the E-Area Disposal Facility (WSRC 1991a), and are not considered part of this RPA.

3.2.1.2 Institutional Control Period

The institutional control period is the 100-year time interval specified in the DOE Order 5820.2A (U.S.DOE 1988a) following closure of a disposal site. Periodic maintenance and monitoring activities are conducted during this period. The disposal site is assumed to be stabilized and no longer operational during this period, but it will remain part of the SRS, and will therefore, be fenced and patrolled to eliminate the possibility of inadvertent intruders. During this period, doses to operational on-site personnel will be addressed in the SAR. While unlikely, doses to off-site individuals are addressed in this RPA. Realistically, this period is expected to continue for at least 100 years after closure of the EAVs, and possibly longer.

3.2.1.3 Post-Institutional Control Period

The final time period of concern is when the facility is no longer maintained by the SRS, and could be accessed by the public. The total duration of this period for the purpose of performance assessment depends on the time of predicted maximum impact with respect to potentially exposed individuals. Projections of conditions and activities during this period are uncertain and difficult to assess. However, because of the presence of long-lived radionuclides in the waste, the maximum off-site impact will occur many thousands of years after closure.

3.2.2 Transport Pathways

The purpose of this section is to identify potential pathways to human exposure to radionuclides potentially released from the EAV (Sect. 3.2.2.1), and to justify eliminating some of these pathways from further consideration (Sect. 3.2.2.2). The results of this section are used to develop exposure scenarios for off-site members of the public, which are discussed in Sect. 3.2.3.

3.2.2.1 Pathway Identification

Radionuclides released from the EAV to the geosphere have the potential of reaching humans through numerous pathways. Most conceivable pathways for a buried LLW source are indicated in Fig. 3.2-1. The pathways identified in this figure are for facilities undisturbed, from the standpoint of human intrusion. Pathways pertinent to intruder exposures are addressed separately in Sect. 3.2.4. In the list below, each pathway is briefly defined.

- (1) Leaching - migration of radionuclides from the wasteform by a combination of dissolution, diffusion, and advection.
- (2) Gaseous Diffusion - upward migration of gaseous radionuclides from the wasteform by diffusion through the caps and cover soils to the atmosphere.
- (3) Irrigation - contamination of cover soil by radionuclides which have reached groundwater which is subsequently used for irrigation.
- (4) Deposition - contamination of surface water by radionuclides which have reached the atmosphere; represents deposition of particulate associated radionuclides or gaseous species partitioning at the air-water interface.
- (5) Volatilization - partitioning of volatile radionuclide species present in surface water into air above the water body.
- (6) Discharge - discharge of radionuclides present in groundwater into surface water.
- (7) Recharge - movement of radionuclides into the groundwater from contaminated surface water.
- (8) Irrigation - contamination of cover soil by radionuclides which have reached surface water which is being subsequently used for irrigation.
- (9) Washload - contamination of surface water by soil containing radionuclides as a result of erosion by rain or irrigation water.
- (10) Deposition - contamination of cover soil by radionuclides which have reached the atmosphere and have become associated with airborne particulate matter.
- (11) Resuspension - Resuspension of soil-associated radionuclides as a result of wind erosion.

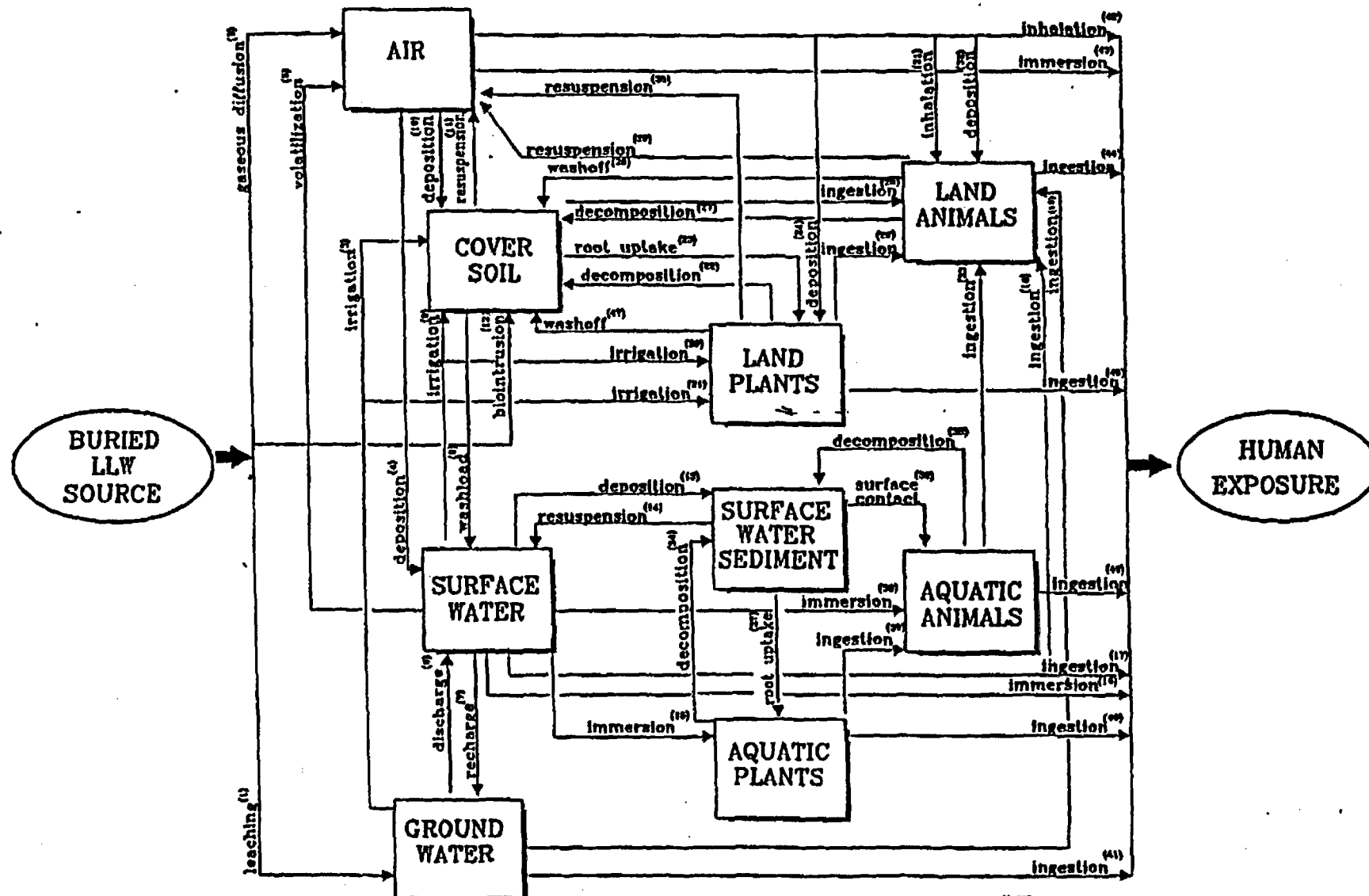


Fig. 3.2-1. Potential pathways to human exposure for undisturbed buried LLW.

- (12) **Biointrusion** - contamination of cover soil by soil-associated radionuclides that are brought to the surface from the vicinity of the wasteform by burrowing animals, such as rodents or ants, or by intruding plant roots.
- (13) **Deposition** - deposition of radionuclides in surface water that have partitioned onto suspended sediment.
- (14) **Resuspension** - resuspension of particulate-borne radionuclides in the sediment of surface water as a result of hydrodynamic forces at the sediment-water interface.
- (15) **Immersion** - contamination of aquatic plants by radionuclides in surface water attributable to the immersion of the plants in the contaminated water.
- (16) **Immersion** - human exposure to radionuclides as a result of immersion in contaminated surface water.
- (17) **Ingestion** - human exposure to radionuclides as a result of ingestion of radionuclides present in surface water.
- (18) **Ingestion** - contamination of terrestrial animals from their ingestion of radionuclides in surface water.
- (19) **Ingestion** - contamination of terrestrial animals from their ingestion of radionuclides in groundwater.
- (20) **Irrigation** - contamination of terrestrial plants as a result of irrigation with surface water containing radionuclides.
- (21) **Irrigation** - contamination of terrestrial plants as a result of irrigation with groundwater.
- (22) **Decomposition** - contamination of cover soil as a result of decomposition of terrestrial plants in the soil.
- (23) **Root uptake** - contamination of terrestrial plants by uptake through roots of soil water containing radionuclides.
- (24) **Deposition** - deposition of airborne radionuclides onto terrestrial plant surfaces.
- (25) **Ingestion** - ingestion of radionuclides by grazing animals as a result of contaminated soil ingestion.
- (26) **Ingestion** - ingestion of radionuclide-containing vegetation by terrestrial animals.
- (27) **Decomposition** - contamination of cover soil as a result of decomposition of terrestrial animals in the soil.

- (28) Washoff - contamination of surface soil as a result of washoff of externally contaminated terrestrial animals.
- (29) Resuspension - resuspension of surficial radionuclides on terrestrial animals to the atmosphere.
- (30) Resuspension - resuspension of surficial radionuclides on terrestrial plants to the atmosphere.
- (31) Inhalation - contamination of terrestrial animals as a result of inhalation of radionuclides in the atmosphere.
- (32) Deposition - surface contamination of terrestrial animals via deposition of particulate-borne radionuclides in the atmosphere.
- (33) Ingestion - contamination of terrestrial animals as a result of their ingestion of aquatic animals.
- (34) Decomposition - contamination of surface water sediment as a result of decomposition of aquatic plants in the sediment.
- (35) Decomposition - contamination of surface water sediment as a result of decomposition of aquatic animals in the sediment.
- (36) Surface contact - surface contamination of aquatic animals as a result of contact with contaminated sediment.
- (37) Root uptake - contamination of aquatic flora via radionuclide uptake through roots.
- (38) Immersion - contamination of aquatic animals as a result of immersion in surface water containing radionuclides.
- (39) Ingestion - contamination of aquatic animals as a result of their ingestion of aquatic plants containing radionuclides.
- (40) Ingestion - human exposure to radionuclides as a result of ingestion of contaminated aquatic flora.
- (41) Ingestion - human exposure to radionuclides as a result of ingestion of contaminated groundwater.
- (42) Inhalation - human exposure to radionuclides as a result of inhalation of airborne radionuclides.

- (43) Immersion - human exposure to radionuclides as a result of immersion in contaminated air.
- (44) Ingestion - human exposure to radionuclides as a result of ingestion of contaminated terrestrial animals.
- (45) Ingestion - human exposure to radionuclides as a result of ingestion of contaminated terrestrial plants.
- (46) Ingestion - human exposure to radionuclides as a result of ingestion of contaminated aquatic animals containing radionuclides.
- (47) Washoff - contamination of surface soil below vegetation due to rain-induced surface washoff.

3.2.2.2 Pathway Screening

The list in Sect. 3.2.2.1 above is generic in nature, and the significance of each pathway must be evaluated on a site-specific basis to develop an exposure model. Many pathways may be removed from consideration for particular sites because of a negligible contribution to human exposure.

For the EAVs, leaching and transport of radionuclides to the saturated zone (pathway (1)) is the predominant means that radionuclides may be subsequently transported in the environment. Thus, this pathway must be addressed in developing an exposure model, and is addressed in this RPA in the near-field model (Sect. 3.3.1). Other pathways which may contribute to human exposure are those tied to groundwater concentrations of contaminants. Irrigation with contaminated groundwater may lead to contamination of agricultural crops and animals (pathways (3), (21), (23), (25) and (26)). Discharge of contaminated groundwater to surface water (pathway (6)) may result in contamination of the aquatic ecosystem including the water body itself, sediment, and aquatic plants and animals (pathways (13), (14), (15), (34), (35), (36), (37), (38), and (39)). Ingestion of contaminated surface water, aquatic animals or groundwater by terrestrial animals (pathways (18), (33), and (19)) may lead to human exposure, and can be tied to groundwater contamination. Human exposure may occur as a result of direct human ingestion of contaminated surface water or groundwater (pathways (17) and (41)), as a result of consumption of contaminated food supplies (pathways (44), (45),

and (46)), and as a result of immersion in contaminated surface water during recreational activities such as swimming (pathway (16)). Consumption of contaminated aquatic plants (pathway (40)) was not considered in the EAV RPA because there is no indication that aquatic plants present in potentially-contaminated surface water in the vicinity of the SRS are consumed by humans.

Of the 47 pathways listed above, only 26 are accounted for in the above discussion. This leaves 21 pathways that are not considered significant for developing exposure scenarios discussed in the next section. The justification for neglecting these pathways is given below. Pathways that result in human exposure directly or indirectly as a result of atmospheric dispersion and deposition (pathways (2), (4), (5), (10), (11), (24), (28), (29), (30), (31), (32), (42), (43), and (47)) are not included in exposure scenarios for the following reason. The only potentially volatile radioactive components of the EAVs are H-3, C-14, and Rn-222. Atmospheric release of these compounds at the time of the operations is addressed in the EAV SAR (WSRC 1991a). Calculations providing an upper bound on doses received from volatilization of these radionuclides from the EAVDF after disposal (pathway (2)) are described in Sect. A.3. Pathways leading to exposure to resuspended contaminated soil (pathways (11), (42), and (43)) are addressed in the intruder exposure analysis (Sect. A.4). Other atmospheric pathways are indirect in nature; e.g., the contaminants must first be suspended or volatilized from one medium, then redeposited in another. These indirect pathways are not believed to be more significant than the direct pathways (2, 11, 42, and 43), and thus are not addressed in this RPA. Therefore, pathways 2, 11, 42, and 43 are included in the dose analysis.

Pathway (7) considers contamination of groundwater due to recharge by surface water. This pathway is not considered significant in the EAV RPA because some dilution of radionuclides in surface water can be expected for all streams, and thus concentrations in groundwater as a result of this pathway will always be lower than the concentrations which led to contamination of the surface water. Pathways (8) and (20), representing contamination of cover soil and terrestrial plants as a result of irrigation with contaminated surface water, respectively, are not considered important because of the relatively dilute concentration of radionuclides expected in surface water with respect to groundwater. Irrigation by groundwater is expected to be a more important pathway for radionuclides potentially reaching crops.

Contamination of surface water from erosion of contaminated soil (pathway (9)) was not considered significant, because buildup of radionuclides in surface soil would only result from radionuclides with high sorption potential. These radionuclides would not partition readily into the surface water if introduced as a result of erosive events. Pathways (22) and (27), representing the pathways of radionuclides to surface soil via decomposition of terrestrial plants and animals, were not considered significant relative to the exposure resulting from direct consumption of these potentially contaminated products.

Although surface water may receive contaminated groundwater, dilution is considerable in the nearby creeks. Because groundwater is expected to exceed surface water concentrations by orders of magnitudes, and direct ingestion of groundwater results in exposures exceeding less direct routes of exposure through aquatic food chains, surface-water pathways were dropped from further consideration.

Finally, contamination of cover soil over the EAVs as a result of biointrusion of burrowing animals or plant roots (pathway (12)) must be addressed. It is acknowledged that biointrusion is a potentially significant pathway of contamination of cover soil over a LLW facility, as is concluded in a study by McKenzie et al. (1983). For the humid southeast, where ground cover and soil moisture limit resuspension of soil, biointrusion is likely to result in contamination of soils over the facility, but probably not significant contamination off-site. Therefore, the relative significance of biointrusion to the inadvertent intruder is the issue of concern in addressing this pathway for this RPA.

Most of the burrowing animals identified as likely residents at the SRS (Sect. 2.1.9) do not burrow below 0.5 m (McKenzie et al. 1986). Only one burrower, the Florida Harvester Ant, is expected to burrow below 2 m, and then, only 5% of its burrows are expected to be that deep, resulting in very little potentially contaminated soil being moved. As the cover soil erodes, however, the significance of burrowers' activities may increase. Furthermore, if E-Area reverts to a hardwood, pine forest sometime after loss of institutional control, it is possible that deeper roots may contact contaminated soil above, or adjacent to, the vaults and translocate radionuclides to other plant organs. Radionuclides may subsequently be released back to the soil as roots and leaves wither and degrade. It is, therefore, likely that biointrusion may cause some mixing of the waste components with the soil column.

The significance of biointrusion is evaluated here by considering the effect of the mixed soil column on an inadvertent intruder. An inadvertent intruder, who is assumed to dig next to, into, or above the vaults, mixes the contaminated soil near the vaults with soil near the surface (Sect. 3.2.4). While it is not known how effective biointruders might be in causing mixing in the soil, the McKenzie et al. (1983) study of a reference humid site estimated that soil concentrations resulting from biointrusion are significantly lower than those resulting from intruder excavation activities, except for more biologically available compounds, where concentrations are of the same order of magnitude. The effect of burrowing animals or intrusive roots, then, is not expected to enhance the inadvertent intruder's contact with contaminated soil by more than a factor of two for any radionuclide. Doses that are calculated in this RPA are uncertain to the extent that a factor of two is inconsequential, and thus, the biointrusion pathway was neglected.

In summary, of the original 47 pathways identified in Fig. 3.2-1, only two are considered to be of possible consequence to exposures of off-site members of the public and to groundwater protection, and are considered further in this RPA. These pathways, related to contaminated groundwater, include: 1) leaching of the wasteform resulting in contamination of groundwater local to E-Area (pathway 1); and 2) contamination of agricultural crops and animals as a result of irrigation with contaminated groundwater (pathways 3, 21, 23, 25, 26). In the following section, the relative importance of these pathways is further addressed.

3.2.3 Exposures of Off-Site Members of the Public and Protection of Groundwater

As described in Sect. 1.2, disposal of low-level radioactive waste in the EAV must meet certain performance objectives for protection of off-site members of the public and sources of groundwater. In this section, the different exposure scenarios and pathways for off-site members of the public, which have been considered in the PA for the EAV are described. Requirements for groundwater protection assumed in this analysis also are described, and an analysis is presented which demonstrates the relative importance of the requirements for protection of off-site members of the public and sources of groundwater in determining the acceptability of waste disposals in the EAV. The greater importance of the assumed groundwater protection requirements is established, and a simple screening analysis to select those

radionuclides in the different disposal units that are considered for the groundwater pathway is presented.

3.2.3.1 Off-Site Members of the Public

This section discusses the requirements for protection of off-site members of the public and the exposure pathways assumed in the dose analysis for such individuals.

The performance objectives for LLW disposal specify that the EDE to off-site members of the public from all exposure pathways should not exceed 25 mrem per year (U.S.DOE 1988a). As described in Sect. 1.2.1, this performance objective is assumed to apply for 10,000 years after disposal. The nearest location from the disposal site for off-site members of the public depends on the time after disposal. During the period of active institutional control, i.e., for the first 100 years after facility closure, off-site members of the public are assumed to be located no closer to the disposal site than the present boundary of the SRS. However, after active institutional control ceases, off-site members of the public could be located as close as 100 m from any of the EAV.

As discussed in Sect. 3.1 and 3.2.2, the primary mechanism for mobilization and release of radionuclides from the EAV is expected to be infiltration of precipitation, and the primary pathway for subsequent exposures of off-site members of the public is expected to be transport of radionuclides in groundwater. Because of such factors as 1) the design and closure concept for the disposal units that are intended to inhibit infiltration of precipitation, 2) the considerable distance from the disposal site to the present boundary of the SRS, and 3) the expected discharge of contaminated groundwater to surface streams within the SRS and the considerable dilution in radionuclide concentrations provided by such discharge, it is reasonable to conclude that the dose analysis for off-site members of the public can focus on exposure pathways resulting from use of contaminated groundwater at distances from the disposal units as close as 100 m for the time period after active institutional control ceases.

Thus, in the dose analysis for the groundwater pathway, an off-site member of the public is assumed to use water from a well for domestic purposes, and the well is assumed to be at the location at least 100 m from the disposal units where the maximum concentrations of radionuclides in groundwater are predicted to occur after loss of active institutional control.

The following exposure pathways involving use of contaminated well water are assumed to occur:

- direct ingestion of contaminated water;
- ingestion of milk and meat from dairy and beef cattle that drink contaminated water;
- ingestion of vegetables grown in garden soil irrigated with contaminated water;
- direct ingestion of contaminated soil in conjunction with intakes of vegetables from the garden;
- external exposure to contaminated soil while working in the garden; and
- inhalation of radionuclides suspended into air from contaminated soil while working in the garden.

Rainfall normally is abundant at the SRS (see Sect. 2.1.3). Therefore, irrigation of a vegetable garden is assumed to occur only occasionally during the summer and only in small amounts relative to the annual rainfall (Murphy 1990). Irrigation of pasture grass ingested by dairy and beef cattle is neglected because agricultural land is not extensively irrigated near the SRS (U.S. Department of Commerce 1977; Baes and Sharp 1983).

Additional exposure pathways for off-site members of the public could involve release of radionuclides into the air and airborne transport to off-site locations. Radionuclides could be attached to particulates suspended into air from the ground surface, and volatile radionuclides (e.g., H-3, C-14, and isotopes of radon) could be released from the waste or contaminated soil. Exposures of off-site members of the public resulting from the air pathway are considered in this analysis.

3.2.3.2 Protection of Groundwater

This section discusses the assumed requirements for protection of groundwater that are applied to the PA for the EAV.

The performance objectives for LLW disposal specify that contamination of groundwater is to be limited in accordance with federal, state, and local standards (U.S.DOE 1988a). The State of South Carolina requires that concentrations of hazardous chemicals in groundwater be limited in accordance with federal DWS at any time after disposal. Presently, no federal, state, or local standards exist that limit radionuclides released to groundwater from the EAV. However, the SRS has established the objective of protecting groundwater for Site operations in accordance with EPA standards for contaminants in public drinking water supplies (40 CFR Part 141).

The performance objective for protection of groundwater resources assumed in this analysis is described in Sect. 1.2.2. Briefly, because there is some ambiguity in selecting particular numerical standards for radioactivity in drinking water to be applied to groundwater protection, three different options for specifying the performance objective are used in this analysis:

- 1) Current EPA standards for radionuclides in drinking water (40 CFR Part 141), including (a) the method prescribed in the standards for calculating MCLs for beta/gamma-emitting radionuclides from the specified dose limit based on internal dosimetry data from ICRP Publication 2 (1959), as tabulated by the Department of Commerce (1963), and (b) the specified MCLs for H-3 and Sr-90;
- 2) Current EPA standards for radionuclides in drinking water, except all MCLs for beta/gamma-emitting radionuclides are calculated from the specified dose limit using internal dosimetry data based on ICRP Publication 30 (1979); and
- 3) Proposed revisions of the EPA standards for radionuclides in drinking water (EPA 1991), with all MCLs for beta/gamma-emitting radionuclides calculated using internal dosimetry data based on ICRP Publication 30 (1979), except no standard for radon is assumed.

For all options, the performance objective is assumed to apply for 10,000 years after disposal (see Sect. 1.2.1). Some of the differences among the three options are summarized as follows.

All options specify concentration limits, rather than dose limits, for alpha-emitting radionuclides. The concentration limits for radium in the third option are higher than the first two options, and the third option is the only one that contains a limit for uranium.

In all options, a limit on dose equivalent is used to define limits on concentrations of beta/gamma-emitting radionuclides in water, but the resulting MCLs are different for all three options. The first two options use the same dose limit for whole body or any organ, but the internal dosimetry data used to obtain the MCLs from the dose limit differ substantially for most radionuclides. The third option differs from the first two in that a limit on EDE, rather than dose equivalent to whole body or any organ, is used. Thus, for most radionuclides, the resulting MCLs for the third option differ substantially from the values for the first two options.

The MCLs for the three options for specifying the performance objective for ground-water protection are given in Table 3.2-1. For all radionuclides except uranium in the third option, the MCLs are given in units of pCi/L to facilitate comparisons of the different options, even though the primary standard for beta/gamma-emitting radionuclides in all options is a dose limit rather than a limit on concentration. For naturally occurring uranium with its normal isotopic abundances, the MCL of 20 $\mu\text{g/L}$ corresponds to an activity concentration of 14 pCi/L.

For all alpha-emitting radionuclides, the MCLs in Table 3.2-1 are obtained directly from current EPA standards for radioactivity in drinking water (40 CFR Part 141) or the proposed revisions of the standards (EPA 1991). The MCLs for beta/gamma-emitting radionuclides for the different options are obtained as described below.

For the first option, the MCLs for H-3 and Sr-90 are the values specified in the current EPA standards. For any other beta/gamma-emitting radionuclide, the MCL is obtained, as specified in the current EPA standards, from the limit on dose equivalent of 4 mrem per year to whole body or any organ using the maximum permissible concentration (MPC) in water for an exposure time of 168 h obtained from a Department of Commerce (1963) tabulation. These MPCs apply to occupational exposure and are based on limits on dose equivalent of

Table 3.2-1. Maximum contaminant limits for radionuclides in groundwater corresponding to different options for groundwater protection requirement^a

Radionuclide	Option 1 ^b	Option 2 ^b	Option 3 ^{b,c}
H-3	20,000	90,000	60,900
C-14	6,400	2,600	3,200
Al-26	---	50	420 ^d
Co-60	130	110	220
Ni-59	530	5,500	27,000
Ni-63	80	1,600	9,900
Se-79	---	110	660 ^d
Rb-87	270	390	501
Sr-90	8	3	42
Zr-93	2,100	160	5,100
Nb-93m	1,100	1,000	10,500
Tc-99	800	420	3,800
Pd-107	---	3,200	37,000
Cd-113m	---	3	40 ^d
Sn-121m	---	320	2,260
Sn-126	---	30	290
I-129	0.5	0.6	21
Cs-135	800	800	790
Cs-137	160	110	120
Sm-151	1,100	1,500	14,000
Pb-210	0.3	0.07	1
Ra-226	5	5	20
Uranium	---	---	20 ^e
Am-242m	---	0.074	1.27
Other Alpha ^f	15	15	15

^a Different options are described in Sect. 1.2.2 and 3.2.3.2.

^b Values are in units of pCi/L, unless otherwise noted.

^c Value calculated by EPA (1991), unless otherwise noted.

^d Value calculated using ingestion dose conversion factor (DCF) from DOE compilation (U.S. DOE 1988b).

^e Value is in units of $\mu\text{g/L}$.

^f Adjusted gross alpha emitters (excluding Ra-226, U, and Rn-222).

5 rem per year to whole body or gonads, 30 rem per year to thyroid, or 15 rem per year to any other organ, whichever is more restrictive. Thus, the MCL in groundwater is obtained from the MPC in water by multiplying by the ratio of the applicable dose limit in the DWS to the dose limit used to obtain the MPC. For example, for Tc-99, which has the lower large intestine as the organ receiving the highest dose, the MPC in water for 168 h exposure in the Department of Commerce (1963) tabulation is multiplied by the factor 0.004/15 to obtain the MCL in groundwater.

For the second option, the MCL in groundwater for any beta/gamma-emitting radionuclide is obtained from (1) the dose limit of 4 mrem per year to whole body or any organ specified in the current EPA standards, (2) an assumed intake of contaminated water of 2 L/d (730 L/year), as also specified in the EPA standards, and (3) the dose per unit intake to whole body or the organ receiving the highest dose obtained from the DOE (1988b) compilation of internal DCFs, which are based on the dosimetric and metabolic models of ICRP Publication 30 (1979).

For the third option, the MCL in groundwater for most beta/gamma-emitting radionuclides is the value given by the EPA (1991). In a few cases, a value was not estimated by the EPA but is obtained from the limit on EDE of 4 mrem per year (EPA 1991), a water intake of 2 L/d, and the EDE per unit intake obtained from the DOE (1988b) compilation.

In comparing the second and third options for calculating MCLs for beta/gamma-emitting radionuclides, the change from a limit on dose equivalent to whole body or any organ to the same numerical limit on EDE results in substantial increases in the MCL in most cases. Again, essentially the same internal dosimetry models are used for both options.

3.2.3.3 Comparison of Performance Objectives for Protection of Off-Site Members of the Public and Groundwater

As described in Sect. 3.2.3.1 and 3.2.3.2, concentrations of radionuclides in groundwater at any location more than 100 m from the location of disposal units are limited by two performance objectives: 1) a maximum EDE of 25 mrem per year from all exposure pathways involving use of contaminated water and 2) various options for limiting dose from consumption of drinking water only or concentrations of radionuclides in groundwater. The first

performance objective assumes that use of contaminated groundwater is the only significant source of exposure for off-site members of the public. The question then arises as to which of the two performance objectives would be the more restrictive, i.e., would result in lower limits on acceptable concentrations of radionuclides in groundwater and, thus, in waste in the EAV. A similar question concerns whether exposure pathways other than ingestion of drinking water would contribute significantly to the dose from all exposure pathways.

In order to address the relative importance of the two performance objectives given above and the various exposure pathways listed in Sect. 3.2.3.1 that apply to use of contaminated groundwater, the doses from the pathways involving ingestion of milk and meat from dairy and beef cattle that drink contaminated water, ingestion of vegetables grown in garden soil irrigated with contaminated water, direct ingestion of contaminated soil from the vegetable garden in conjunction with vegetable intakes, external exposure to contaminated soil while working in the garden, and inhalation of radionuclides suspended into air while working in the garden must be investigated in relation to the dose from direct ingestion of contaminated water. For purposes of this analysis, the dose limit from drinking water only for beta/gamma-emitting radionuclides is assumed to be 4 mrem per year EDE, as in the third option for the performance objective for groundwater protection. With this choice, the same dosimetric quantity is used in the performance objectives for all exposure pathways and for drinking water only, but the results do not depend greatly on the choice of dose limits. The relative importance of the pathway involving ingestion of contaminated vegetables is considered first.

For direct consumption of radionuclides in drinking water, the dose to an exposed individual is given by

$$H_w = C_w U_w DCF_{in}$$

where

- H_w = EDE from drinking water pathway (rem/year),
- C_w = radionuclide concentration in groundwater ($\mu\text{Ci/L}$),
- U_w = consumption of drinking water (L/year), and

DCF_{ing} = EDE per unit activity of a radionuclide ingested, i.e., the ingestion dose conversion factor (rem/ μ Ci).

In determining compliance with the assumed groundwater protection requirement, a consumption rate of drinking water of 730 L/year (i.e., 2 L/d) is used. Therefore, the dose from direct consumption of contaminated groundwater is given by

$$H_w(\text{rem/year}) = (730 \text{ L/y})C_w(\mu\text{Ci/L})DCF_{ing}(\text{rem}/\mu\text{Ci}).$$

In order to estimate the dose per unit concentration of radionuclides in groundwater resulting from consumption of vegetables irrigated with contaminated water, a simple model developed by Baes and Sharp (1983) for estimating radionuclide concentrations in surface soil is used. In this model, the top layer of soil is treated as a well-mixed compartment, and radionuclides deposited in surface soil by irrigation are assumed to be removed from the soil compartment by infiltrating water according to a first-order leaching process as well as by radioactive decay. The removal rate constant describing the leaching process is given by

$$\lambda_1 = (V_w / \theta) / [d(1 + \rho K_d / \theta)],$$

where

λ_1 = fraction of activity in soil compartment removed by leaching per year,

V_w = infiltration rate of water in soil (m/year),

θ = volumetric water content of soil (dimensionless),

d = depth of soil compartment (m),

ρ = bulk density of soil, and

K_d = equilibrium solid/solution distribution coefficient for a radionuclide.

The density of soil and the distribution coefficient must be expressed in compatible units; e.g., if K_d is given in units of mL/g (or L/kg), then ρ must be expressed in g/cm³. Since radioactive decay also removes activity from soil, the total removal rate constant for a radionuclide in the

surface soil compartment is given by

$$\lambda = \lambda_1 + \lambda_r$$

where λ_r is the radiological decay constant (y^{-1}).

In the linear-compartment model described above, the equilibrium activity of a radionuclide in the surface soil compartment is simply the ratio of the input rate of activity to the total removal rate constant. The input rate of activity by irrigation used in this analysis is estimated as follows. At the SRS, the growing of vegetables normally requires irrigation only occasionally during the summer months. On the basis of experience with crop management at the site (Murphy 1990), an amount of irrigation equal to 0.2 m/year is considered to be applied to a vegetable garden. This amount corresponds to application of 2.5 cm once a week during the two hottest summer months. This amount of irrigation probably is more than would occur in most years, since one reported experiment required watering only on one or two occasions during the summer (Murphy 1990). Over a unit area of 1 m², the assumed irrigation rate corresponds to 0.2 m³, or 200 L/year. The unit area is arbitrary and is used only to obtain radionuclide concentrations in soil in the desired units of $\mu\text{Ci}/\text{m}^3$. Therefore, the average concentration of radionuclides input to surface soil per year from use of contaminated irrigation water, which is denoted by I_r , is given by

$$I_r (\mu\text{Ci}/\text{m}^3 \text{ per year}) = [(200 \text{ L/y per m}^2) / d(\text{m})] C_w (\mu\text{Ci}/\text{L}),$$

where

d = depth of surface soil layer, and

C_w = concentration of a radionuclide in groundwater.

From the equations derived above, the equilibrium concentration of radionuclides in surface soil from use of contaminated groundwater for irrigation then is given by

$$C_s (\mu\text{Ci}/\text{m}^3) = I_r / \lambda = [(200 \text{ L/y per m}^2) / d(\text{m})] C_w (\mu\text{Ci}/\text{L}) / \lambda (y^{-1}).$$

Given this concentration of a radionuclide in surface soil, the dose from ingestion of contaminated vegetables (see Eqs. A.4-2 and A.4-3) is given by

$$H_v = B_v(C_s/\rho)U_vDCF_{ing}$$

where

- H_v = EDE from vegetable intakes (rem/year),
- B_v = plant-to-soil concentration ratio for a radionuclide (dimensionless),
- ρ = bulk density of soil,
- U_v = consumption rate of vegetables (kg/year), and
- DCF_{ing} = ingestion dose conversion factor (rem/ μ Ci).

If C_s is expressed in units of μ Ci/ m^3 and U_v in units of kg/year, then the density of soil in this equation must be expressed in units of kg/m^3 .

Given the equation for the dose from consumption of contaminated vegetables, as derived using the model of Baes and Sharp (1983) for retention of radionuclides in surface soil, and the equation for the dose from direct consumption of drinking water, a direct comparison of the relative importance of the two exposure pathways can be obtained. Using the equations for H_w , H_v , and C_s derived above, the ratio of the doses from the drinking water and vegetable pathways is given by

$$H_w/H_v = [(3.65 \text{ m}^2) d(m) \rho(kg/m^3) \lambda(y^{-1})] / [B_v U_v(kg/y)].$$

This ratio does not depend on the radionuclide concentration in groundwater or the ingestion DCF.

In this analysis, the following radionuclide-independent parameter values are used:

- 1) a depth of the soil compartment (d) of 0.3 m, which is a typical depth of the root zone for vegetation;
- 2) a water infiltration rate through soil of 0.4 m/year, which is the average infiltration rate of precipitation at the SRS (see Appendix A.1.1.2) and is appropriate when irrigation is considerably less than the total precipitation;
- 3) a volumetric water content of soil

(6) of 0.3 (Baes and Sharp 1983); 4) a bulk density of soil (ρ) of 1,400 kg/m³, or 1.4 g/cm³ (Baes and Sharp 1983); and 5) a consumption of contaminated vegetables of 90 kg fresh weight per year, which is half of the estimated total consumption of vegetables by an average adult (Rupp 1980; Hamby 1992). It should be noted that if the removal rate constant, λ , is dominated by the contribution from leaching, λ_1 , then the ratio of the doses from the drinking water and vegetable pathways does not depend on the depth of the soil compartment, d .

The equation for H_w/H_v given above has been evaluated for the radionuclides Tc-99, Sn-126, Pu-239, and Cs-137. Tc-99 represents radionuclides with a high plant-to-soil concentration ratio (B_v) but a low distribution coefficient (K_d); Sn-126 has intermediate values of B_v and K_d ; Pu-239 has a low value of B_v but a high K_d ; and Cs-137 has an intermediate value of B_v and a high K_d , but its half-life is sufficiently short that the equilibrium concentration in soil is determined primarily by the half-life rather than the leaching constant, λ_1 . In implementing the model, it is important to recognize that B_v and K_d are correlated; i.e., radionuclides with high plant-to-soil concentration ratios have low distribution coefficients resulting in relatively low equilibrium concentrations in soil, and vice versa (Baes et al. 1984; Sheppard 1985). Thus, evaluating the model for these four radionuclides should give results that are representative of any other important radionuclides in the EAV.

The radionuclide-specific parameter values used for the example calculations are listed as follows:

Tc-99 —	$B_v = 0.65,$	$K_d = 1.5 \text{ mL/g};$
Sn-126 —	$B_v = 0.0026,$	$K_d = 250 \text{ mL/g};$
Pu-239 —	$B_v = 0.000019,$	$K_d = 4,500 \text{ mL/g};$
Cs-137 —	$B_v = 0.013,$	$K_d = 1,000 \text{ mL/g}.$

The values of B_v for each radionuclide are given in Table A.4-7 and were obtained from the compilation of Baes et al. (1984). The values of K_d also were obtained from Baes et al. (1984). These data do not necessarily apply to soils at the SRS but are expected to be reasonably representative.

For the model and parameters described above, the following comparisons of the dose from direct consumption of drinking water and the dose from consumption of vegetables

irrigated with contaminated water are obtained. The dose from the drinking water pathway exceeds the dose from the vegetable pathway by about a factor of 15 for Tc-99, a factor of 25 for Sn-126, a factor of 190 for Pu-239, and a factor of 30 for Cs-137. If removal by radioactive decay were not taken into account for Cs-137 (e.g., if the analyses were performed for Cs-135 instead), the dose from the vegetable pathway would be about the same as the dose from the drinking water pathway. Isotopes of Cs represent an extreme case where the plant-to-soil concentration ratio relative to the distribution coefficient is higher than for almost all other elements (Sheppard 1985), and a similar result would not be expected for most long-lived radionuclides that reasonably could be present in significant quantities in the EAV.

The analysis presented above illustrates that the dose from direct consumption of drinking water is expected to be equal to or greater than the dose from ingestion of vegetables contaminated with irrigation water from the same source; and, for most radionuclides, the dose from drinking water is expected to be substantially greater. This conclusion is expected to apply to all radionuclides that could be present in the EAV.

The next pathways considered in this comparison are consumption of milk and meat from dairy and beef cattle that drink contaminated water. The doses from ingestion of contaminated milk (m) and meat (f) are given by

$$H_m = C_m U_m DCF_{ing},$$

$$H_f = C_f U_f DCF_{ing},$$

respectively, where

H_m, H_f = EDE from milk or meat intakes (rem/year),

C_m, C_f = radionuclide concentration in milk ($\mu\text{Ci/L}$) or meat ($\mu\text{Ci/kg}$),

U_m, U_f = consumption rate of milk (L/year) or meat (kg/year), and

DCF_{ing} = ingestion dose conversion factor (rem/ μCi).

Dairy and beef cattle are assumed to drink only contaminated groundwater, and the radionuclide concentrations in milk and meat are given by

$$C_m = C_w Q_m F_m,$$

$$C_f = C_w Q_f F_f,$$

respectively, where

C_w = radionuclide concentration in groundwater ($\mu\text{Ci/L}$),

Q_m, Q_f = consumption rate of water by dairy or beef cattle (L/d), and

F_m, F_f = ratio of equilibrium radionuclide concentration in milk ($\mu\text{Ci/L}$) or meat ($\mu\text{Ci/kg}$) to daily intake by dairy or beef cattle ($\mu\text{Ci/d}$).

In implementing the model for the milk and meat pathways, a consumption rate of water by dairy and beef cattle of 60 L/d and 50 L/d, respectively, and a consumption rate of milk and meat by an exposed individual of 110 L/year and 90 kg/year, respectively, are used (NRC 1977). If the transfer coefficients for the milk and meat pathways (F_m and F_f) recommended by Baes et al. (1984) are used, the following comparison of the dose from the drinking water pathway and the doses from the milk and meat pathways is obtained. The dose from the drinking water pathway exceeds the dose from the milk and meat pathways by about a factor of 10 for Tc-99, a factor of 3 for Sn-126, a factor of 5 for Cs-137, and 5 orders of magnitude for Pu-239.

The analysis presented above illustrates that the dose from direct ingestion of drinking water is expected to be considerably greater than the dose from ingestion of milk and meat obtained from dairy and beef cattle that drink contaminated water from the same source. This conclusion is expected to apply to all radionuclides that could be present in the EAV.

The next pathway considered in this comparison is direct ingestion of contaminated soil in conjunction with vegetable intakes. For a given concentration of a radionuclide in garden soil, a direct comparison of the doses from the vegetable and soil ingestion pathways can be obtained from the results given in Tables A.4-8 and A.4-9, respectively, of Appendix A.4.

The dose from the drinking water pathway relative to the dose from the soil ingestion pathway then is the product of two factors: 1) the ratio of the doses from the vegetable and soil ingestion pathways obtained from the tables listed above and 2) the ratio of the doses from the drinking water and vegetable pathways obtained previously in this section. Using this procedure, the dose from the drinking water pathway is found to exceed the dose from the soil ingestion pathway by about 4 orders of magnitude for Tc-99, a factor of 200 for Sn-126, 3 orders of magnitude for Cs-137, and an order of magnitude for Pu-239.

The analysis presented above illustrates that the dose from direct ingestion of drinking water is expected to be considerably greater than the dose from direct ingestion of contaminated soil from a vegetable garden that is contaminated with irrigation water from the same source. This conclusion should apply to all radionuclides that could be present in the EAV.

The next pathway considered in this comparison is external exposure to contaminated soil while working in the vegetable garden. For a given concentration of a radionuclide in garden soil, a direct comparison of the doses from the vegetable and external exposure pathways can be obtained from the results given in Tables A.4-8 and A.4-10, respectively, of Appendix A.4. The dose from the drinking water pathway relative to the dose from the external exposure pathway then is the product of two factors: 1) the ratio of the doses from the vegetable and external exposure pathways obtained from the tables listed above and 2) the ratio of the doses from the drinking water and vegetable pathways obtained previously in this section. Using this procedure, the dose from the drinking water pathway is found to exceed the dose from the external exposure by about 50% for Sn-126 and a factor of 70 for Cs-137. The dose from the external exposure pathway is essentially zero for Tc-99 and Pu-239.

The analysis presented above illustrates that the dose from direct ingestion of drinking water is expected to be greater than the dose from external exposure to contaminated soil while working in a vegetable garden that is contaminated with irrigation water from the same source. This conclusion is expected to apply to all photon-emitting radionuclides that could be present in the EAV.

The final pathway considered in this comparison is inhalation exposure to radionuclides suspended into air from contaminated soil while working in the vegetable garden. For a given concentration of a radionuclide in garden soil, a direct comparison of the doses from the vegetable and inhalation pathways can be obtained from the results given in Tables A.4-8 and A.4-12, respectively, of Appendix A.4. The dose from the drinking water pathway relative to the dose from the inhalation pathway then is the product of two factors: 1) the ratio of the doses from the vegetable and inhalation pathways obtained from the tables listed above and 2) the ratio of the doses from the drinking water and vegetable pathways obtained previously in this section. Using this procedure, the dose from the drinking water pathway is found to exceed the dose from inhalation exposure by about 8 orders of magnitude for Tc-99, 5 orders of magnitude for Sn-126, 7 orders of magnitude for Cs-137, and a factor of 350 for Pu-239.

The analysis presented above illustrates that the dose from direct ingestion of drinking water is expected to be much greater than the dose from inhalation exposure while working in a vegetable garden that is contaminated with irrigation water from the same source. This conclusion should apply to all radionuclides that could be present in the EAV.

The comparison of the doses from the drinking water pathway and the vegetable, milk and meat, soil ingestion, external exposure, and inhalation pathways for the same concentration of particular radionuclides in water may be summarized as follows: for Tc-99, the dose from the drinking water pathway exceeds the dose from all other pathways by about a factor of 6; for Sn-126, the dose from all other pathways is about the same as the dose from the drinking water pathway; for Cs-137, the dose from the drinking water pathway exceeds the dose from all other pathways by about a factor of 4; and, for Pu-239, the dose from the drinking water pathway exceeds the dose from all other pathways by about a factor of 8. These results should be representative of those that would be obtained for any other radionuclides that could be present in the EAV.

Given the doses for the drinking water pathway relative to the doses for the other exposure pathways involving use of contaminated groundwater from the same source, as obtained above, the following conclusions are obtained.

First, for all beta/gamma-emitting radionuclides, the performance objective for protection of groundwater resources — i.e., a dose limit of either 4 mrem per year to whole body or any organ or 4 mrem per year EDE from the drinking water pathway only — should be more restrictive than the performance objective for protection of off-site members of the public — i.e., a dose limit of 25 mrem per year EDE from all exposure pathways — because the dose from the drinking water pathway only is expected to be greater than the dose from all other exposure pathways combined. Thus, if the performance objective for groundwater protection is met, then the performance objective for protection of off-site individuals also will be met without the need for analysis of the dose from exposure pathways other than drinking water.

Second, for alpha-emitting radionuclides, the performance objective for protection of groundwater resources, which is expressed in terms of concentration limits rather than limits on dose equivalent, may result in doses from the drinking water pathway only that exceed the performance objective for protection of off-site members of the public. For example, the current MCL for Pu-239 in groundwater of 15 pCi/L (see Table 3.2-1) corresponds to an EDE of nearly 50 mrem per year, assuming consumption of 2 L/d of water and the ingestion DCF for Pu-239 given in Table A.4-2. In these cases, the dose limit in the performance objective for off-site individuals would be more restrictive and, in principle, the contributions to the dose from the exposure pathways other than drinking water would need to be considered in demonstrating compliance with the performance objective. However, the contribution from the other exposure pathways is expected to be no more than a few tens of percent, and should be much less for many radionuclides, in which case the other pathways essentially can be neglected in estimating dose. That is, in cases where the performance objective for off-site individuals from all exposure pathways applies, demonstrations of compliance with the performance objective reasonably need to take into account only the dose from the drinking water pathway. In other cases where the MCL for an alpha-emitting radionuclide corresponds to a dose less than the performance objective for off-site individuals, compliance with the MCL would ensure that the dose limit for all exposure pathways would be met without need for further analysis.

Therefore, the general conclusion from this analysis is that only the drinking water pathway needs to be considered for off-site releases of radionuclides in groundwater. In cases where the MCL in groundwater corresponds to a dose equivalent less than the performance objective for off-site individuals of 25 mrem per year from all exposure pathways, compliance with the MCL would ensure that the dose to off-site individuals would be substantially less than the performance objective. In cases where the MCL in groundwater corresponds to a dose equivalent greater than the performance objective for off-site individuals, the dose from all exposure pathways other than drinking water would be insignificant compared with the dose from the drinking water pathway, particularly when the uncertainties in estimating maximum concentrations of radionuclides in groundwater at locations more than 100 m from any disposal units are taken into account.

3.2.3.4 Screening of Radionuclides for Groundwater Pathway

As demonstrated in the previous section, limitation of concentrations of radionuclides in groundwater at any location beyond the boundary of the 100-m buffer zone around the disposal facility is the only concern in the dose analysis for off-site individuals. Although a large number of radionuclides are present in waste placed in the EAV, only a few radionuclides are of interest in estimating the allowable inventories at E-Area. This section presents the results of a simple screening analysis for determining TVs for radionuclides in groundwater. A more detailed analysis of releases from the disposal facility and transport in groundwater is required for those radionuclides for which an allowable inventory above the TV is desirable.

Screening calculations have been made on a large suite of 730 radionuclides (Appendix C) which may be encountered during disposal operations (Appendix C). These radionuclides were selected because they represent all radionuclides having published DCFs (U.S.DOE 1988b). Initial screening utilized spreadsheet calculations that take no credit for the engineered barriers. The travel time to the compliance point was estimated based on the conservative assumption of a five year flow period and retardation due to sorption on the soil.

The waste concentrations (Wc) in Ci/L for a unit inventory can be calculated as follows:

$$\text{ILTV Wc} = \text{Unit inventory (Ci/Vault)} / 803,310 \text{ (L/Vault)}$$

$$\text{ILNTV Wc} = \text{Unit inventory (Ci/Vault)} / 5,880,450 \text{ (L/Vault)}$$

$$\text{LAWV Wc} = \text{Unit inventory (Ci/Vault)} / 48,138,500 \text{ (L/Vault)}.$$

The screening doses were calculated based on a contaminant travel time (CTT), which is used for the decay time:

$$\text{CTT} = 5 \text{ years} * \text{Rf}.$$

Values for the radionuclide-specific retardation factors (Rf) in soils are provided in Appendix C, Table C.1-3. Values on the conservative end of available ranges of values were selected in most cases.

For the majority of the radionuclides, no special calculations were required to account for daughter products. For these radionuclides, the concentration at the receptor (Cr) for a unit inventory of the radionuclides of interest is obtained using:

$$\text{Cr (Ci/L)} = \text{Wc} * \text{EXP}(-(\text{decay constant}) * \text{CTT}) / (\text{Rf} * \text{Porosity}).$$

Values for the decay constant are provided in Appendix C, Table C.1-3. The porosity is assumed to be 0.5.

The screening dose (D) for a unit inventory of a given radionuclide is obtained using the ingestion DCF and consumption rate (I) (assumed to be 730 L/year):

$$\text{D (mrem/year per Ci/vault)} = \text{Cr} * \text{DCF} * \text{I}.$$

Ingrowth of daughters for actinides requires a slightly more complicated method for computing the dose. A weighted DCF that accounts for progeny contributions must be calculated. The waste concentrations are calculated in the same manner as previously and the

CTT is computed using the R_f for the parent. This CTT is used as the time for decay and ingrowth in the RADDECAY computer code. The results of RADDECAY are used to determine the fraction of the parent remaining and the fraction of the progeny at time = CTT. These daughter fractions (DF_i) are used in the calculation of the weighted DCFs. The radionuclide-specific weighted dose conversion factor (WDCF_i) including retardation effects for the *i*th progeny is calculated using:

$$WDCF_i = DCF_i * DF_i / R_{fi}$$

where DCF_i, DF_i, and R_{fi} are the ingestion DCF, Fraction of the progeny remaining at time CTT, and retardation factor for the *i*th progeny, respectively. Table C.1-4. in Appendix C is a tabulation of these values.

A concentration/consumption factor (CCF) is necessary to obtain the dose. The CCF is obtained using:

$$CCF(Ci/year) = (W_c(Ci/L) / Porosity) * I(L/year)$$

where W_c represents the concentration of the parent.

The dose for a given parent is then calculated with:

$$D(mrem/year) = CCF(Ci/year) * \text{Sum}(WDCF_i)(mrem/Ci)$$

where $\text{Sum}(WDCF_i)$ represents the summation of WDCF_i for the parent and each progeny to be considered.

The TV, based on the groundwater pathway, is then determined from the performance objective dose of interest and the dose per unit inventory of the radionuclide.

$$TV (Ci/vault) = \frac{\text{Performance Objective Dose of Interest (4 mrem/year)}}{D (mrem/year per Ci/vault)}$$

The algorithm used in the screening spreadsheet for radionuclides without significant progeny was:

$$TV = 4 \text{ mrem/yr} \cdot Rf \cdot \text{porosity} \cdot \text{vault volume(L)} / \text{EXP}(-\text{decay constant(1/yr)} \cdot 5 \text{ yr} \cdot Rf) \\ \cdot \text{DCF(mrem/pCi)} \cdot 730 \text{ L/yr} \cdot 1\text{E}+12 (\text{pCi/Ci})$$

In thirty-five years of operations SRS has disposed of a total of about 10 million curies, so any radionuclide with a TV over $1\text{E}+15$ was immediately eliminated from further consideration. A greatly reduced list of radionuclides was then examined in light of SRS operations. Radionuclides not produced by either fission or neutron activation were removed from the list. The only naturally occurring radionuclides retained were U and Th, the only radioactive raw materials used at SRS. This process resulted in the following radionuclides being considered in detailed groundwater analysis:

H-3, C-14, Ni-59, Se-79, Sr-90, Tc-99, Sn-126, I-129, Cs-135, Th-232, U-233, U-234, U-235, U-236, U-238, Np-237, Pu-238, Pu-239, Pu-240, Pu-242, Pu-244, Am-241, Am-243, Cm-244, Cm-248, and Cf-252.

3.2.4 Exposure Scenarios for Inadvertent Intruders

As described in Sect. 1.2, disposal of low-level radioactive waste in the EAV must meet a performance objective for protection of inadvertent intruders onto the disposal site. In particular, after loss of active institutional control at 100 years after facility closure, the EDE to an intruder should not exceed 100 mrem per year for scenarios involving continuous exposure or 500 mrem for scenarios involving a single acute exposure (U.S.DOE 1988a). These dose limits apply to the sum of dose equivalents from all exposure pathways that are assumed to occur in a given exposure scenario for an inadvertent intruder. As described in Sect. 1.2.1, this performance objective is assumed to apply for 10,000 years after disposal.

As described in Sect. 1.2.3, this performance objective is interpreted in this RPA to exclude doses from radon and its daughter products. A separate performance objective of 20 pCi/m²-s for the radon exhalation rate is used to assess compliance for radon. The analysis of radon exhalation is presented in Appendix A.3.7.

In this section, the different exposure scenarios for an inadvertent intruder which have been considered in the PA for the EAV are described. An important assumption in all scenarios is that an intruder has no prior knowledge of the existence of a waste disposal facility at the site. Therefore, after active institutional control ceases, certain exposure scenarios are assumed to be precluded only by the physical state of the disposal facility, i.e., the integrity of the engineered barriers used in facility construction. Passive institutional controls, such as permanent marker systems at the disposal site and public records of prior land use, also could prevent inadvertent intrusion after active institutional control ceases, but the use of passive institutional controls is not assumed in this analysis.

3.2.4.1 Chronic Exposure Scenarios for Inadvertent Intruders

Three distinct scenarios resulting in chronic exposure of inadvertent intruders are considered in the dose analysis for the EAV. Two of these scenarios, which usually are referred to as the agriculture (or homesteader) and post-drilling scenarios, have often been applied in other intruder dose analyses for LLW disposal (NRC 1981; Oztunali and Roles 1986; Kennedy and Peloquin 1988; ORNL 1990). The third scenario considered in this analysis is referred to as the resident scenario. As noted previously, all chronic exposure scenarios for inadvertent intruders are subject to a limit on EDE of 100 mrem per year.

In previous intruder dose analyses, such as those referred to above, the agriculture scenario usually was found to be more important than the post-drilling scenario; i.e., the agriculture scenario usually results in higher doses per unit concentration of radionuclides in the disposal facility than the post-drilling scenario. Thus, the agriculture scenario usually results in lower concentrations of radionuclides that would be acceptable for disposal. However, as discussed later in this section, the agriculture scenario possibly could be less important than the post-drilling scenario under certain circumstances.

The following sections describe the assumptions for the agriculture, resident, and post-drilling scenarios.

Agriculture scenario

The agriculture scenario assumes that an intruder comes onto the site after active institutional control ceases and establishes a permanent homestead, including on-site sources of water and foodstuffs. Waste in disposed units is assumed to be accessed when an intruder constructs a home directly on top of a disposal facility and the foundation of the home extends into the facility itself. All waste in the disposal facility at the time the foundation is dug is assumed to be physically indistinguishable from native soil.

In the agriculture scenario, some of the waste exhumed from the disposal facility is assumed to be mixed with native soil in the intruder's vegetable garden. The following exposure pathways involving exhumed waste or waste remaining in the exposed disposal facility on which the intruder's home is located then are assumed to occur:

- ingestion of vegetables grown in contaminated garden soil;
- direct ingestion of contaminated soil, primarily in conjunction with intakes of vegetables from the garden;
- external exposure to contaminated soil while working in the garden or residing in the home on top of the disposal facility;
- inhalation of radionuclides attached to soil particles that are suspended into air from contaminated soil while working in the garden or residing in the home; and
- inhalation of volatile radionuclides released into air from contaminated soil while working in the garden or residing in the home.

For the last exposure pathway listed above, the only radionuclides of concern would be H-3, C-14, and isotopes of radon.

The agriculture scenario also assumes that the intruder's entire supply of water for domestic use is obtained from a well on the disposal site. The well is assumed to be placed at the location beyond the 100-m buffer zone around disposal units where the maximum

concentrations of radionuclides in groundwater are predicted to occur. The following exposure pathways involving use of contaminated well water then are assumed to occur:

- direct ingestion of contaminated water;
- ingestion of milk and meat from dairy and beef cattle that drink contaminated water;
- ingestion of vegetables grown in garden soil irrigated with contaminated water;
- direct ingestion of contaminated soil in conjunction with intakes of vegetables from the garden;
- external exposure to contaminated soil while working in the garden; and
- inhalation of radionuclides suspended into air from contaminated soil while working in the garden.

These pathways are the same as those assumed in Sect. 3.2.3 for off-site members of the public who use contaminated groundwater or surface water for domestic purposes. Again, since rainfall normally is abundant at the SRS (see Sect. 2.1.3), irrigation of a vegetable garden is assumed to occur only occasionally during the summer and only in small amounts relative to the annual rainfall (Murphy 1990), and irrigation of pasture grass ingested by dairy and beef cattle is neglected because extensive irrigation of agricultural land is not practiced near the SRS (U.S. Department of Commerce 1977; Baes and Sharp 1983). In the performance assessment for the agriculture scenario, the potential importance of the exposure pathways resulting from use of contaminated well water at the disposal site compared with the exposure pathways resulting from direct intrusion into the disposal facility is described below.

In accordance with the performance objectives for off-site releases of radionuclides described in Sect. 1.2, concentrations of radionuclides in groundwater beyond the 100-m buffer zone around disposal units would be limited either by the MCLs for radionuclides in drinking water or by a limit on EDE of 25 mrem per year from all exposure pathways, whichever is more restrictive. Thus, as shown by the analysis in Sect. 3.2.3.3, the maximum EDE in any year that could result from use of contaminated groundwater on the disposal site, taking into account all of the exposure pathways listed above, is only a small fraction (i.e., about 25% or less) of the maximum EDE to an intruder from all exposure pathways of 100 mrem per year. Therefore, for purposes of demonstrating compliance with the dose limit for inadvertent intruders, only the exposure pathways involving direct intrusion into the

disposal facility need to be considered, and the exposure pathways involving use of contaminated well water can be neglected.

In this analysis, direct intrusion into disposal units is assumed to be precluded for the period of time after loss of active institutional control when the concrete roof on the vaults and other engineered barriers, such as the top layer of uncontaminated grout in the ILNT and ILT vaults, maintain their structural and physical integrity. That is, intact engineered barriers used in constructing disposal units are assumed to preclude direct access to waste in the disposal facility by the types of equipment that normally would be used in digging a foundation for a home at the SRS.

Resident scenario

As in the agriculture scenario described above, the resident scenario assumes that an intruder excavates a foundation for a home on top of a disposal facility. During excavation, however, the intruder is assumed to encounter an intact concrete roof or other engineered barrier above the waste that cannot easily be penetrated by the types of excavation equipment normally used at the SRS. That is, the presence of intact engineered barriers is assumed to preclude direct intrusion into the waste during excavation. But instead of abandoning the site, the intruder constructs a home directly on top of the intact barrier and, thus, establishes a permanent residence at that location.

From the definition of the resident scenario, the primary exposure pathway of concern is external exposure to photon-emitting radionuclides during the time the intruder resides in the home on the disposal site. The presence of intact barriers would preclude any ingestion exposures and most inhalation exposures. Some exposures to radon could occur during indoor residence on top of intact engineered barriers, e.g., as a result of crack formation in concrete. However, such exposures should be much less than exposures to radon in the agriculture scenario when excavation into waste is assumed to occur and residence in a home on top of exposed waste becomes credible. Therefore, potential exposures to radon are ignored in the resident scenario, but such exposures essentially are captured in the agriculture scenario.

The resident scenario is assumed to occur at any time after loss of active institutional control over the disposal facility. However, even though the concentrations of most radionuclides in the disposal facility will decrease monotonically with time, due to radioactive decay and migration from the disposal facility, the dose in the resident scenario is not necessarily the highest at 100 years after facility closure. At this time, the concrete roof on top of the vaults is assumed to be intact. Therefore, at the earliest time the resident scenario could occur, the concrete roof provides a substantial amount of shielding that greatly reduces the external dose compared with the dose from unshielded waste. For the ILNT and ILT vaults, the layer of uncontaminated grout on top of the waste provides a considerable amount of additional shielding. At some later time, however, the concrete roof is assumed to have lost its integrity and most of the layer of uncontaminated grout is assumed to have weathered to soil-equivalent material. These processes presumably take hundreds to thousands of years or more. Therefore, for long-lived radionuclides that are retained in the waste for long periods of time, the external dose in the resident scenario would be considerably higher long after active institutional control ceases, when excavation essentially to the depth of the waste could occur, than at 100 years after disposal, when excavation only to the depth of the top of the concrete roof is credible.

Thus, for the resident scenario, the maximum dose to an inadvertent intruder and the time at which the maximum dose occurs depend on 1) the half-lives and concentrations of the important photon-emitting radionuclides in the waste, 2) the time period over which the engineered barriers above the waste lose their integrity and can easily be excavated, and 3) the rate at which the important radionuclides migrate from the disposal facility. However, the maximum dose for this scenario can be estimated by considering two bounding cases:

1) intrusion at 100 years after disposal in the presence of an intact concrete roof, but with no reduction in radionuclide inventories at disposal except by radioactive decay; and 2) intrusion at a much later time after disposal when exposure to essentially unshielded waste is credible, but again with no reduction in radionuclide inventories except by radioactive decay. The first bounding case takes into account radionuclides of both shorter and longer half-lives and the shielding provided by the concrete roof and any other barriers between the waste and the roof, whereas the second bounding case applies to time periods when only long-lived

radionuclides presumably are present, but the waste is assumed to be unshielded. In both cases, self-shielding provided by the waste and any encapsulating materials is taken into account in estimating external dose.

In this analysis, the two bounding cases for the resident scenario described above are evaluated. The analyses of the bounding cases take into account differences in the design of the engineered barriers for the three types of disposal units in E-Area, i.e., the types and thicknesses of the different barriers in each unit.

Comparison of agriculture and resident scenarios

From the definition of the resident scenario, this scenario can be regarded as a variation of the agriculture scenario in which only one of the exposure pathways is potentially important — namely, external exposure while residing in the home located on top of the disposal facility. Therefore, since this exposure pathway is essentially the same in the two scenarios and the agriculture scenario includes other exposure pathways that are not relevant for the resident scenario, the agriculture scenario probably will be more important than the resident scenario. That is, the dose per unit concentration of radionuclides in disposed waste probably will be higher in the agriculture scenario than in the resident scenario. Thus, the agriculture scenario is expected to be more restrictive in regard to determining acceptable disposals.

However, the tentative conclusion about the relative importance of the agriculture and resident scenarios could be incorrect if the removal rate of radionuclides from the waste by infiltrating water were comparable to or greater than the degradation rate of the engineered barriers above the waste. If such an occurrence were possible, then the external dose that would result at the time the engineered barriers have degraded to soil-equivalent material, but not any of the encapsulated waste itself, could be greater than the total dose from all exposure pathways that would result at a later time when a significant layer of waste also has weathered to soil. This could particularly be the case for the ILNT vaults in which the waste is grouted. In addition, shorter-lived radionuclides could be important in the resident scenario at 100 years after disposal, when all engineered barriers are presumed to be intact, but would be unimportant in the agricultural scenario at much later times. Therefore, the resident scenario, as well as the agriculture scenario, is considered in the intruder dose analysis.

Post-Drilling scenario

The post-drilling scenario assumes that an intruder who resides permanently on the disposal site drills through a disposal unit in constructing a well for a domestic water supply. Following construction of the well, the contaminated material brought to the surface during drilling operations, which is assumed to be indistinguishable from native soil, is assumed to be mixed with native soil in the intruder's vegetable garden. The exposure pathways involving ingestion of contaminated vegetables, ingestion of contaminated soil, and external and inhalation exposures while working in the garden then are the same as the pathways described previously for the agriculture scenario. In the post-drilling scenario, however, external and inhalation exposures while residing in the home on the disposal site, which are important in the agriculture scenario, are not relevant, because all drilling waste is assumed to be mixed with native soil in the garden and the intruder's home is assumed not to be located directly on top of exposed waste.

As in the agriculture scenario, the post-drilling scenario assumes that the intruder's entire supply of water is obtained from the on-site well, and the exposure pathways from use of contaminated well water are the same as those described previously for the agriculture scenario. Again, however, because of the stringent requirement on allowable contamination of groundwater at the disposal site in comparison with the maximum allowable dose to an intruder from all exposure pathways, demonstrations of compliance with the dose limit for inadvertent intruders for the post-drilling scenario can be based only on the exposure pathways involving direct intrusion into solid waste; i.e., the exposure pathways involving use of contaminated well water can be neglected.

In this analysis, as in the agriculture scenario, drilling through a disposal unit is assumed to be precluded during the time when the concrete vaults and any other engineered barriers maintain their integrity. Thus, in most cases, the post-drilling scenario involving drilling through a disposal facility is assumed not to be credible until the same time as the agriculture scenario involving direct excavation into a disposal facility. The basis for this assumption is that the types of drill bits normally used in constructing wells in the soft sand and clay soils at the SRS could not easily penetrate an intact concrete vault or other engineered barrier.

Therefore, in attempting to drill directly through a disposal facility, it seems reasonable to assume that an intruder would encounter considerable resistance and, instead of taking extraordinary measures to obtain a drill bit designed to penetrate through hard rock, would move the drilling operation to a different location away from the disposal facility.

For the LAW vaults, however, the post-drilling scenario conceivably could occur before the agricultural scenario. Because of the void space above the waste, the concrete roof could collapse but still consist primarily of large, intact pieces that would not be removed by normal excavation procedures. Thus, after collapse of the roof, drilling between intact sections of the roof could occur.

Comparison of agriculture and post-drilling scenarios

Previous analyses of the agriculture and post-drilling scenarios (Oztunali and Roles 1986; Kennedy and Peloquin 1988; ORNL 1990) have shown that the dose to an intruder per unit concentration of radionuclides in excavated material should be considerably greater for the agriculture scenario than for the post-drilling scenario, provided the assumptions for the exposure pathways in the two scenarios are reasonably consistent. The principal reasons for the greater doses in the agriculture scenario are 1) the greater volume of waste exhumed during construction of a foundation for a home compared with the volume of waste exhumed during drilling of a well, which results in greater concentrations of radionuclides in contaminated soil in the intruder's vegetable garden, and 2) the doses from external and inhalation exposure while residing in a home on the disposal site, which contribute to the dose for the agriculture scenario but are not relevant for the post-drilling scenario.

However, if the post-drilling scenario could occur before the agriculture scenario (e.g., if the use of drill bits that could easily penetrate intact concrete vaults and waste forms were assumed), then previous analyses have shown that the dose from the post-drilling scenario could exceed the dose from the agriculture scenario (ORNL 1990). Whether or not this is the case depends on the concentrations of the particular radionuclides in the waste and the assumed difference in time between the first credible occurrences of the post-drilling and

agriculture scenarios. Therefore, the post-drilling scenario is included in the intruder dose analysis for the EAV. As noted previously, this scenario could be particularly important for the LAW vaults if the roof should collapse long before it loses its physical integrity and resembles soil.

3.2.4.2 Acute Exposure Scenarios for Intruders

Three distinct scenarios resulting in acute exposure of inadvertent intruders have commonly been applied to LLW disposal facilities. These scenarios usually are referred to as the construction, discovery, and drilling scenarios (NRC 1981; Oztunali and Roles 1986; Kennedy and Peloquin 1988). As noted previously, all acute exposure scenarios for inadvertent intruders are subject to a limit on EDE of 500 mrem. The following sections describe the three acute exposure scenarios and their potential importance in the intruder dose analysis for the EAV.

Construction scenario

The chronic agriculture scenario described in Sect. 3.2.4.1 is based on the assumption that an intruder builds a home on the disposal site, with the foundation extending into a disposal unit. The construction scenario considers exposures during the short period of time for digging a foundation and building a home.

During construction, the relevant exposure pathways are assumed to be inhalation of radionuclides suspended into air from an uncovered disposal unit and external exposure to photon-emitting radionuclides in the disposal unit. Ingestion exposure is assumed to be unimportant during normal work activities. The potential importance of the construction scenario arises primarily from the assumption that construction activities result in airborne concentrations of radionuclides that are substantially higher than those during normal activities while inhabiting the site, as in the agriculture scenario. The construction scenario also assumes external exposure to unshielded waste, whereas in the agriculture scenario shielding during indoor residence on the disposal site usually is taken into account.

From its definition, the construction scenario would occur at the same time as the agriculture scenario. Therefore, the dose analysis for the two scenarios would be based on the same concentrations of radionuclides. Previous calculations (Kennedy and Peloquin 1988) provide a direct comparison of doses for the two scenarios. For a few radionuclides, the dose per unit concentration could be slightly higher for the construction scenario but, for most radionuclides, the dose per unit concentration is expected to be much greater for the agriculture scenario. This result assumes a reasonable exposure time for the construction scenario and the use of a reasonably consistent set of assumptions for the exposure pathways in the two scenarios. Therefore, since the dose limit for the acute construction scenario is a factor of 5 higher than the dose limit for the chronic agriculture scenario, the agriculture scenario always will be more restrictive and the construction scenario generally can be neglected in demonstrating compliance of the EAV with the performance objective for protection of inadvertent intruders.

Discovery scenario

As in the resident scenario described in Sect. 3.2.4.1, the discovery scenario assumes that an intruder attempts to dig into a disposal facility while excavating a foundation for a home on the disposal site, but encounters an intact concrete roof or other engineered barrier which cannot easily be penetrated by the types of excavating equipment that normally would be used at the SRS. However, in distinction from the resident scenario, the intruder soon decides to abandon digging at that location and moves elsewhere. Since intact engineered barriers are assumed not to be breached during excavation, the primary exposure pathway for this scenario is external exposure to photon-emitting radionuclides in the disposal facility during the time the intruder digs at the site and the barriers are uncovered. The presence of intact barriers is assumed to preclude any significant inhalation or ingestion exposures.

From its definition, the discovery scenario would occur at the same time as the resident scenario. Furthermore, the relevant exposure pathway — namely, external exposure to photon-emitting radionuclides in the waste — is essentially the same in the discovery and resident scenarios. Other than the exposure time, the only difference is the shielding factor

during indoor residence, which is relevant only for the resident scenario. Therefore, since the exposure time for the discovery scenario presumably would be no more than 100 h (ORNL 1990), which is considerably less than a reasonable exposure time for indoor residence in the resident scenario, and the dose limit for the discovery scenario is a factor of 5 greater than the dose limit for the resident scenario, the resident scenario always will be more restrictive and the discovery scenario generally can be neglected in demonstrating compliance of the EAV with the performance objective for protection of inadvertent intruders.

Drilling scenario

The chronic post-drilling scenario described in Sect. 3.2.4.1 is based on the assumption that an intruder drills a well directly through a disposal unit. The drilling scenario considers exposures during the short period of time for drilling and construction of the well.

During well drilling and construction, the most important exposure pathway is assumed to be external exposure to uncovered drilling wastes confined to a pile near the well. Although some radionuclides in the drilling waste could be suspended into the air and inhaled during well drilling and construction, inhalation exposures are expected to be relatively unimportant due to such factors as the initial water content of the drilling wastes, the small volume of the waste produced, and the absence of direct mechanical disturbance of the waste pile. Ingestion exposure also is assumed to be unimportant during normal drilling activities. The potential importance of the drilling scenario arises primarily from the assumption that an intruder could be located near an unshielded waste pile for a substantial period of time.

From its definition, the drilling scenario would occur at the same time as the post-drilling scenario. Therefore, the dose analyses for the two scenarios would be based on the same concentrations of radionuclides. Previous calculations (Kennedy and Peloquin 1988) provide a direct comparison of doses for the two scenarios. For all radionuclides, the dose per unit concentration for the drilling scenario is expected to be at least an order of magnitude less than the dose per unit concentration for the post-drilling scenario, provided a reasonable exposure time for the drilling scenario and a reasonably consistent set of assumptions for the exposure pathways in the two scenarios are used. Therefore, the post-drilling scenario always will be more restrictive and the drilling scenario generally can be neglected in demonstrating

compliance of the EAV with the performance objective for protection of inadvertent intruders.

Summary of Acute Exposure Scenarios

In this section, three scenarios for acute exposure of inadvertent intruders were discussed, i.e., the construction, discovery, and drilling scenarios. However, an evaluation of these scenarios has shown that all three scenarios can be neglected for purposes of demonstrating compliance of the EAV with the performance objective for protection of intruders because the chronic agriculture, resident, and post-drilling scenarios will always be more restrictive.

3.2.4.3 Summary of Exposure Scenarios for Inadvertent Intruders

Several chronic and acute exposure scenarios for inadvertent intruders have been considered for use in the PA for the EAV. However, on the basis of previous analyses and considerations of how these scenarios would apply to the EAV, it is evident that only the following three chronic exposure scenarios need to be included in the PA:

- an agriculture scenario involving direct intrusion into disposal units at times after the engineered barriers above the waste have lost their structural and physical integrity and can be penetrated by the types of excavation procedures normally used at the SRS;
- a resident scenario involving permanent residence in a home located either on top of an intact concrete roof or other engineered barrier, which first could occur upon loss of active institutional control at 100 years after facility closure, or on top of intact but essentially exposed waste at times after the engineered barriers have lost their integrity; and
- a post-drilling scenario involving exhumation of waste from a disposal unit at times after drilling through a disposal unit becomes credible.

Estimates of dose for all of these scenarios are considered in this analysis. All acute exposure scenarios would be less restrictive in regard to demonstrating compliance with the performance objective for protection of inadvertent intruders and, thus, are not considered further in this analysis.

As described in Sect. 1.2.1, compliance with the performance objective for protection of inadvertent intruders is assumed to be required for 10,000 years after disposal. However, in cases where the maximum dose to an inadvertent intruder is predicted to occur beyond 10,000 years after disposal, the calculations are carried out until the time the maximum dose occurs to provide additional information and perspective on the performance of disposal units. Consideration of potential doses beyond 10,000 years is particularly important for disposal of uranium, due to the very long time required for ingrowth of its radiologically significant decay products.

A comparison of the relative importance of the chronic exposure scenarios for inadvertent intruders considered in this analysis requires a detailed analysis of each scenario based on the expected long-term performance of the engineered barriers in the different types of disposal units. Therefore, all three scenarios are evaluated in this analysis. An important purpose of the analysis of the different scenarios is to determine minimal requirements for the performance of the engineered barriers in order for the performance objective for inadvertent intruders to be met.

3.2.4.4 Screening of Radionuclides for Intruder Dose Analyses

Screening calculations have been made on a suite of 730 radionuclides (Appendix C). These radionuclides were selected because they represent all radionuclides having published DCFs (U.S. DOE 1988b). However, only a few radionuclides are potentially important in estimating doses to inadvertent intruders according to the different scenarios considered in this analysis. This section presents the results of a simple screening analysis for selecting the radionuclides that are potentially of concern for protection of inadvertent intruders.

The commitment that active institutional control will be maintained over the disposal site for 100 years after facility closure is an important factor in eliminating many radionuclides from consideration in the intruder dose analysis. In particular, any radionuclide with a half-life substantially less than 5 years can be neglected, because the inventory at 100 years after disposal will be reduced to innocuous levels by radioactive decay for any reasonable inventory at the time of disposal. Then, dose analyses for the agriculture, resident, and post-drilling scenarios can be used for further screening of radionuclides in each case. In particular, the dose analysis presented in Appendix A.4 can be used in screening of radionuclides for these scenarios.

The intruder dose analysis in Appendix A.4 shows that the agricultural scenario is the most restrictive, and that the EDE per unit concentration of any radionuclide in the waste at the time this scenario could occur would be less than 10 mrem per year per $\mu\text{Ci}/\text{m}^3$, unless the radionuclide decays to radon. Therefore, for any radionuclide except those which produce radon, the limit on EDE of 100 mrem per year possibly could be exceeded only if the concentration at the time this scenario occurs is greater than $10 \mu\text{Ci}/\text{m}^3$. The screening analysis for selecting radionuclides for the intruder scenarios then assumes that the scenarios occur at 100 years after disposal, which is the earliest possible time, and that a safety factor of 10 should be applied in reducing the minimum concentration of concern estimated above.

From the assumptions described above, a radionuclide would be of potential concern only if the concentration in the waste 100 years after disposal, taking into account only the concentration at disposal and the reduction in concentration due to radioactive decay over 100 years, could be greater than $1 \mu\text{Ci}/\text{m}^3$. A spreadsheet was created to calculate the vault inventory for each radionuclide which, after 100 years of radioactive decay, would produce a concentration of $1 \mu\text{Ci}/\text{m}^3$. This inventory was then used as the TV to decide if more detailed calculations were required.

The algorithm used in the spreadsheet was derived in the following manner:

If X is the concentration, in Ci/m^3 , in the vault at the time of disposal, and the target concentration is $1 \mu\text{Ci}/\text{m}^3$, then for 100 years of decay:

$$1 \mu\text{Ci}/\text{m}^3 = X(\text{Ci}/\text{Vault}) * \text{EXP}(-\text{decay constant}(1/\text{yr}) * 100 \text{ yr}) \\ * 1\text{E}+06 \mu\text{Ci}/\text{Ci} / \text{Vault Volume}(\text{L}/\text{Vault}) * 1\text{E}-03(\text{m}^3/\text{L})$$

Solving for X

$$X = \frac{1\mu\text{Ci}/\text{m}^3 \cdot 1\text{E-}06\text{Ci}/\mu\text{Ci} \cdot \text{Vault Volume (L/vault)} \cdot 1\text{E-}03 \text{ m}^3/\text{L}}{\text{EXP}(-\text{decay constant}(1/\text{yr}) \cdot 100 \text{ yr})}$$

The equation above is what was implemented in the spreadsheet. The spreadsheets for each of the vault types and the suspect soil disposal trenches are included as Tables C.1-1 through C.1-4 in Appendix C.

In thirty-five years of operations SRS has disposed of a total of about 10 million curies, so any radionuclide with a TV over $1\text{E}+15$ was immediately eliminated from further consideration. A greatly reduced list of radionuclides was then examined in light of SRS operations. Radionuclides not produced by either fission or neutron activation were removed from the list. The only naturally occurring radionuclides retained were U and Th, the only radioactive raw materials used at SRS. This process resulted in the following radionuclides, including radiologically significant long-lived decay products, being considered in the detailed intruder analysis:

H-3, C-14, Co-60, Ni-59, Ni-63, Se-79, Sr-90, Zr-93, Nb-93m, Tc-99, Pd-107, Cd-113m, Sn-126, I-129, Cs-135, Cs-137, Sm-151, Pb-210, Ra-226, Th-229, Th-230, Th-232, Pa-231, U-232, U-233, U-234, U-235, U-236, U-238, Np-237, Pu-238, Pu-239, Pu-240, Pu-241, Pu-242, Pu-244, Am-241, Am-243, Cm-243, Cm-244, Cm-245, Cm-246, Cm-247, Cm-248, Cf-249, Cf-250, and Cf-251.

3.3 MODELS AND ASSUMPTIONS

Having defined potential mechanisms of release of radionuclides and other contaminants from the EAVDF (Sect. 3.1) and the human exposure scenarios and radionuclides believed to be most significant to this RPA (Sect. 3.2), this section describes the models adopted and assumptions made to carry out the computations necessary to estimate doses.

3.3.1 Near-Field Model

The current conceptual models for screening, and intact and degraded vault analyses are discussed in the following sections. Screening analyses were conducted first to identify radionuclides that must be considered in the detailed analysis. Three sets of conditions for the vaults were considered for the detailed analysis: intact, cracked, and completely failed. Concrete degradation calculations were combined with structural calculations to determine the timing and extent of cracking and the timing of failure. Further details are provided in the following paragraphs.

Screening calculations were used to reduce the list of contaminants that need to be considered in detailed analyses. The screening calculations assumed no credit for performance of the engineered features at the site. The basis for the calculations were conservative groundwater travel time and distribution coefficients appropriate for conditions at the site. Release from the waste form and container degradation were not considered. In essence, the calculations assume that the receptor consumes 2 L/d of the pore fluid that would be present if the radionuclides were deposited directly in the groundwater. Details for the screening calculations are documented in Sect. 3.2.3.4 and the results are summarized in Sect. 4.1.1. More detail regarding the conceptual models for the vault calculations are provided below.

3.3.1.1 Conceptual Model for Vaults

In the conceptual model for water movement, water infiltrates at the surface and either undergoes evapotranspiration back through the surface and out of the domain or it infiltrates. The majority of this infiltrating water is diverted around the engineered barrier; however, some water penetrates the barrier and perches above the concrete vault. Most of this perched water flows through the sand layer surrounding the vault and down to the water table, but some water penetrates the lower barrier and concrete roof and flows through the waste form. So a minute portion of the water that infiltrates from the surface flows through the vault. The process is illustrated in Fig. 3.3-1.

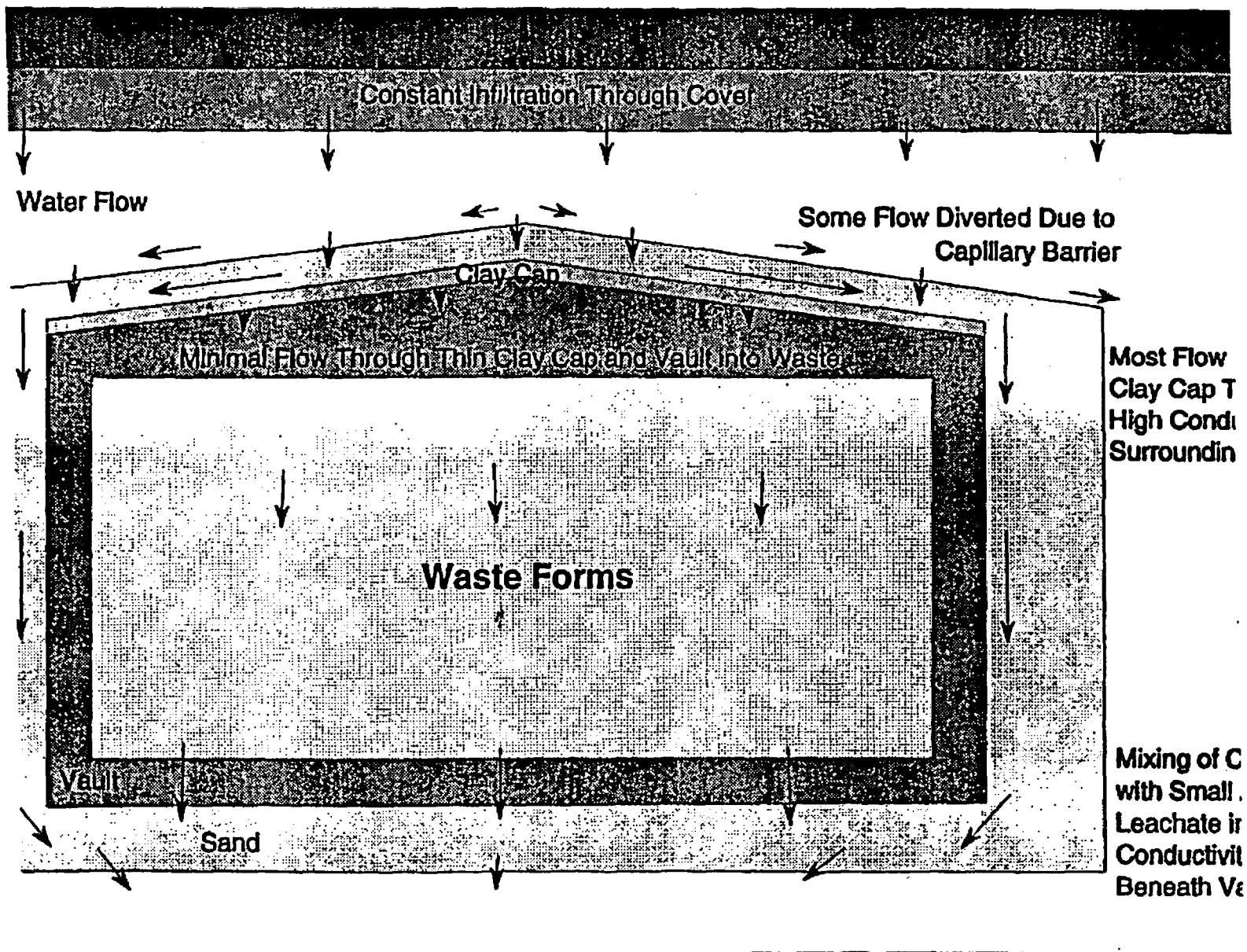


Fig. 3.3-1. Flow path through near-field vadose zone.

Not

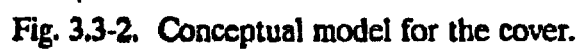
The flow regime in the subsurface was separated into four regions for purposes of analysis. The first region is the soil and sediments near the surface where evaporation and transpiration have a dynamic role in reversing the downward movement of water due to gravity. Below this region, but above the concrete vault, is the region that includes the engineered barrier which has the purpose of diverting the majority of the infiltrating water around the concrete vault, and thus, reducing the amount of water contacting the vault (see Fig. 3.3-2). The last region extends down to the water table and consists of backfill, the concrete vault, the waste form, and high permeability sand surrounding the vault (see Fig. 3.3-3 and Fig. 3.3-4).

An assumption inherent in dividing the flow regime in this manner is that contaminants escaping the vault cannot diffuse upwards through the top engineered barrier (cover). Rather, advection dominates transport outside the vault in the conductive soils and these contaminants are swept horizontally past the vault and down to the water table. Results show that the amount of diffusion upwards is minimal in the humid environment at SRS.

The conceptual model for transport involves several processes. These processes are diffusion, advection, adsorption, and radioactive decay. Each of these processes occurs within each of the five material types.

Assumptions involving degradation of both the engineered barrier and the vault are included in the conceptual model. As previously mentioned (Sect. 3.1.3.1, Cover Degradation), the degradation of the engineered barrier is difficult to quantify at this point. For the purposes of this analysis, it is assumed that the cover continues to function as designed until the roof of the vault collapses, which results in subsidence and failure of the cover.

Figure 3.3-4 illustrates the assumptions regarding waste form degradation for the LAW vault. Due to uncertainties in predicting degradation of the containers, it is assumed that the containers have completely degraded and collapsed (voids inside and between boxes are compacted) at the start of the simulation yielding a large void above the waste. Given that minimal flow is predicted in the vault during the time frame that the container could be intact (e.g., the first few hundred years at most), this assumption has minimal impact on the results. In general, the assumption of complete package failure results in more concentrated waste and the waste is closer to the release point. Since the ILNT/ILT vaults are backfilled with grout and voids are minimized, subsidence of the waste form is not expected, and thus, a significant void at the top of the vault is not expected.



Rev. 0

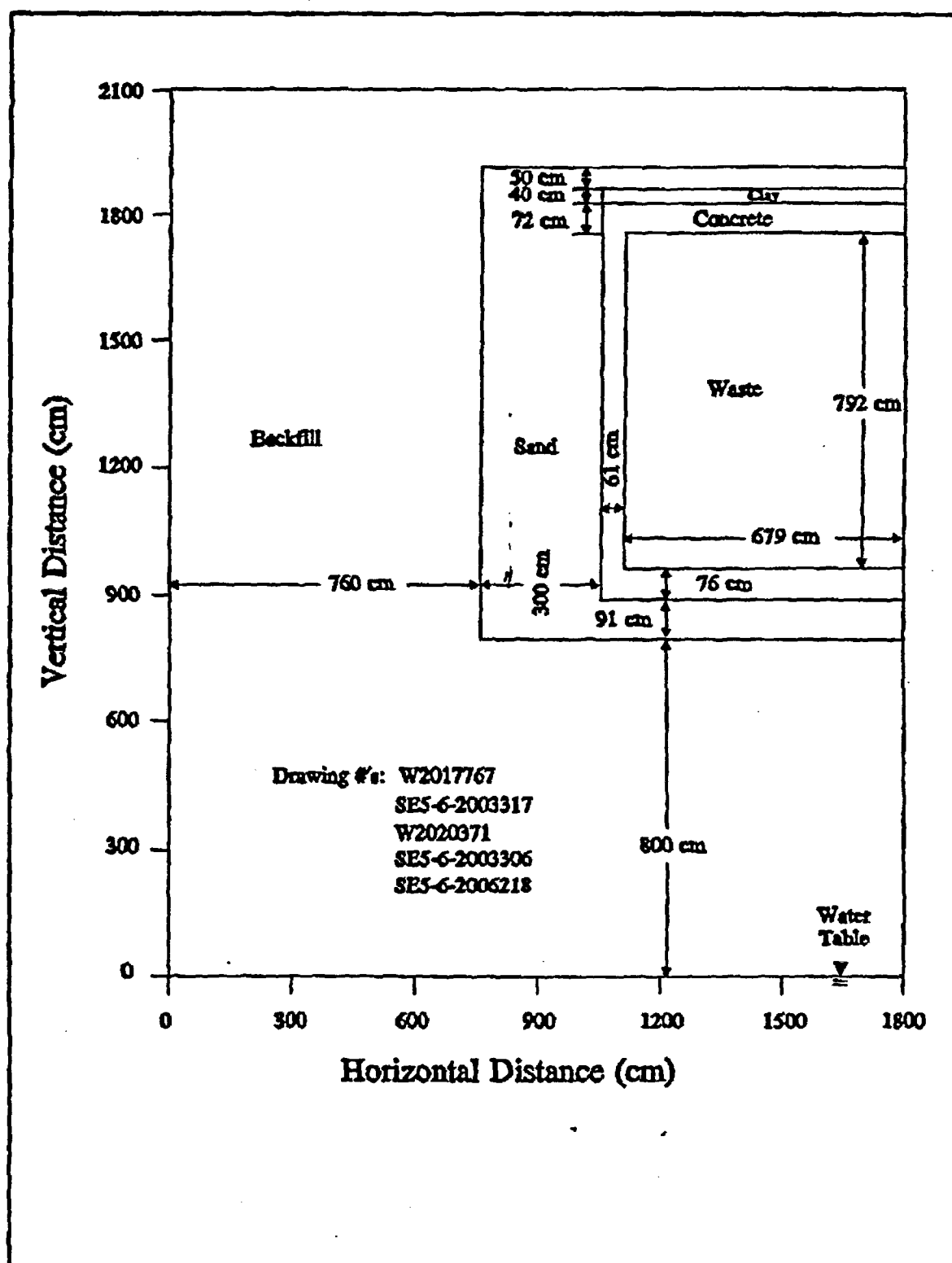


Fig. 3.3-3. Conceptual model for the ILNT and ILT vaults.

Rev. 0

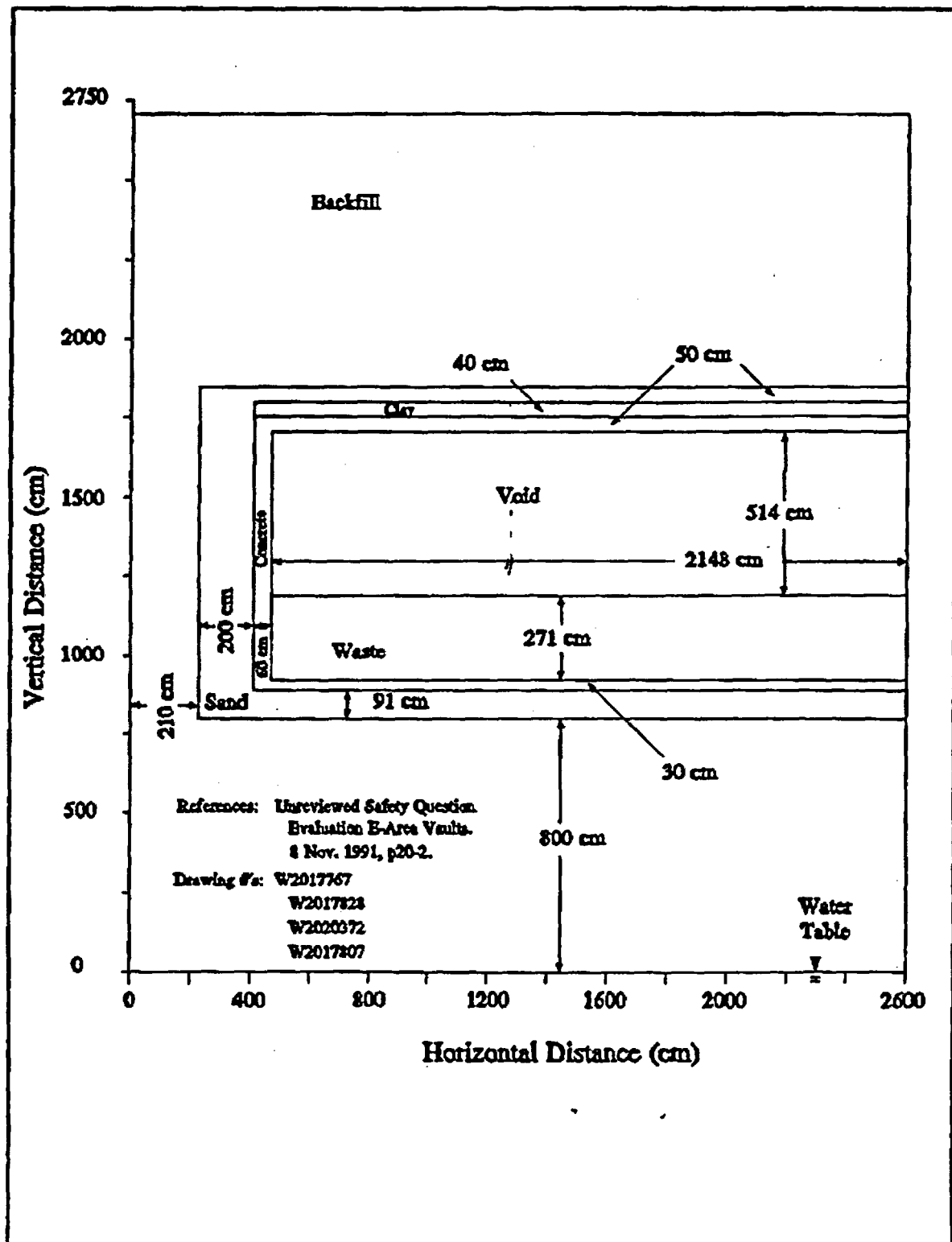


Fig. 3.3-4. Conceptual model for the LAW vault.

Rev. 0

The time required for the construction of the barrier and the vault is minimal compared to the period considered in this study. Therefore, the vault and engineered cover are assumed to be emplaced instantaneously.

For the intact barrier scenario, a constant amount of water passes through the barrier. No consideration is given to the time required for water to begin passing through the barrier. Thus, the upper flux in the vault domain is kept constant during the entire simulation while the vault is intact. It is also assumed that flow around the vault is at steady state for the entire time the vault is assumed to remain intact. This assumption is discussed further in Appendix A.1.2.

Numerical simulation has, at its heart, averaging of spatial properties on the field scale in order to fit the problem into a numerical model. The conceptual model used to provide a framework for the numerical simulation of the near-field movement of water and contaminants from the EAV relies heavily on this averaging. The subsurface is treated as if it consists of six material types: 1) the backfill or native soil; 2) clay; 3) gravel; 4) concrete; 5) waste form; and 6) sand. Each of these materials are treated as if they are homogeneous and isotropic. No spatial variation is accounted for within any of the materials.

Flow through each of these mediums is assumed to behave as flow through porous media. Correspondingly, the hydraulic properties for each material type are assumed to be adequately described by the following hydraulic parameters: saturated hydraulic conductivity, effective porosity, and moisture characteristic curves. The moisture characteristic curves describe the nonlinear relationship between the matrix potential or pressure head, the moisture content, and the hydraulic conductivity.

Two different analytic expressions are used for describing the moisture characteristic curve. The van Genuchten (1978) and Mualem (1976) equations were used to describe this nonlinear relationship for every material type except the backfill and waste form, and void zone of the LAW vault. The equations are given as follows:

$$\theta(\psi) = \theta_r + \frac{(\theta_s - \theta_r)}{[1 + (\alpha\psi)^n]^m}$$

and

$$K(\psi) = K_s \frac{[1 - (\alpha\psi)^{n-1}][1 + (\alpha\psi)^{-n}]}{[1 + (\alpha\psi)^n]^{m+2}}$$

where

- θ = the volumetric moisture content (cm^3/cm^3),
- θ_r = the residual moisture content (cm^3/cm^3),
- θ_e = the effective porosity (cm^3/cm^3),
- ψ = the suction pressure head (cm),
- K_s = the saturated hydraulic conductivity (cm/s),
- α and n = fitting parameters, and
- m = $1 - 1/n$.

The α parameter has units of inverse length and is indicative of the air entry pressure. The n parameter is dimensionless and controls the degree of nonlinearity in the moisture characteristic curve. Table 3.3-1 gives a summary of the hydraulic and van Genuchten parameters used for all the materials.

Table 3.3-1. Summary of hydraulic and van Genuchten fitting parameters

Material	K_s (cm/s)	θ_r	θ_e	α (1/cm)	n
Backfill	1.0×10^{-5}	0.439	0.088	7.50×10^{-2}	1.70
Clay	1.0×10^{-7}	0.386	0.340	1.75×10^{-3}	1.51
Gravel	0.5	0.380	0.010	8.19×10^{-2}	3.70
Concrete	1.0×10^{-10}	0.150	0.147	5.98×10^{-4}	3.43
Sand	1.0×10^{-3}	0.375	0.074	5.51×10^{-2}	2.50
Waste Form (ILNT & ILT)	1.0×10^{-10}	0.150	0.147	5.98×10^{-4}	3.43

The backfill, void and waste form, within the LAW vault were described using the Stone correlation curve (Stone 1973). The equation for this curve is given as:

$$\psi = P_1 + P_2(1-S_w) + P_3(1-S_w)^3$$

and

$$K(S_w) = K_r K_{ro} \left(\frac{S_w - S_{wr}}{1 - S_{wr}} \right)$$

where

$$S_w = \frac{\theta - \theta_r}{\theta_s - \theta_r}$$

The fitted Stone parameters for the backfill moisture characteristic curve were:

P_1 = fitting parameter, = 0 cm,

P_2 = fitting parameter, = 120 cm,

P_3 = fitting parameter, = 600 cm,

K_{ro} = relative permeability at 100% saturation, = 1.0,

S_{wr} = residual moisture saturation, = 0.22, and

K_r = saturated hydraulic conductivity, = 1.0×10^{-5} cm/s.

The development of these moisture characteristic curves and data sources, for each of the material types, will be discussed in turn.

Backfill

Backfill soils were taken to have the same moisture characteristic curve as the native soil. Gruber's (1980) study of soil near the E-Area was determined to be the most complete because it included analyses of hydraulic conductivity. Sampled data for the soil from Gruber's study was analyzed with the RETC (van Genuchten 1988) code. The code uses a

least square curve fit to generate the van Genuchten parameters, as well as the saturated hydraulic conductivity. This fitting can occur on either moisture content versus hydraulic conductivity data or pressure head versus moisture content data. Analysis of the pressure versus moisture content data showed the backfill soil to be highly drainable. This was not expected for a silt sand soil. Previous studies (INTERA 1989) have used both the pressure versus moisture content and the hydraulic conductivity versus moisture content data sets to estimate a moisture characteristic curve. However, based on professional judgement, only the K versus θ data was used to determine the moisture characteristic curve parameters. As a comparison, Stone's curve was then graphically fitted to the resulting θ versus ψ van Genuchten fitted curve. Both curves are shown in Fig. 3.3-5. As can be seen, the Stone curve does not mimic known behavior at the dry end of the curve; however, this is not a problem in the simulation study because the soils remain wet and in that portion of the Stone curve, that shows a good match with the van Genuchten curve. In order to be consistent in our implementation of moisture characteristic curves, the van Genuchten curve was used for the backfill soil. The van Genuchten fitting parameters used were $\alpha = 0.075 \text{ cm}^{-1}$, and $n = 1.7$. The saturated hydraulic conductivity used was $1.0 \times 10^{-5} \text{ cm/s}$. Porosity and residual moisture content were 0.439 and 0.088 respectively.

Gravel

The gravel to be used in constructing the engineered barrier was previously analyzed by the University of Texas (INTERA 1989). Coarse sand, glacial outwash, and stony soil were studied to determine the best representation of gravel. A hydraulic conductivity of 0.5 cm/s , and porosity of $\phi = 0.38$ were suggested. Data from the University of Texas report was analyzed with the RETC code to obtain van Genuchten parameters for the gravel. The resulting parameters were $\alpha = 0.0819 \text{ cm}^{-1}$, and $n = 3.70$, and $\theta_r = 0.01 \text{ cm}^3/\text{cm}^3$. Figure 3.3-6 shows data from several soils and the University of Texas recommended curve, which represents the more drainable end of the spectrum. This is essentially the same curve used by INTERA (1989) in their study of the saltstone vault to represent the gravel moisture characteristic curve.

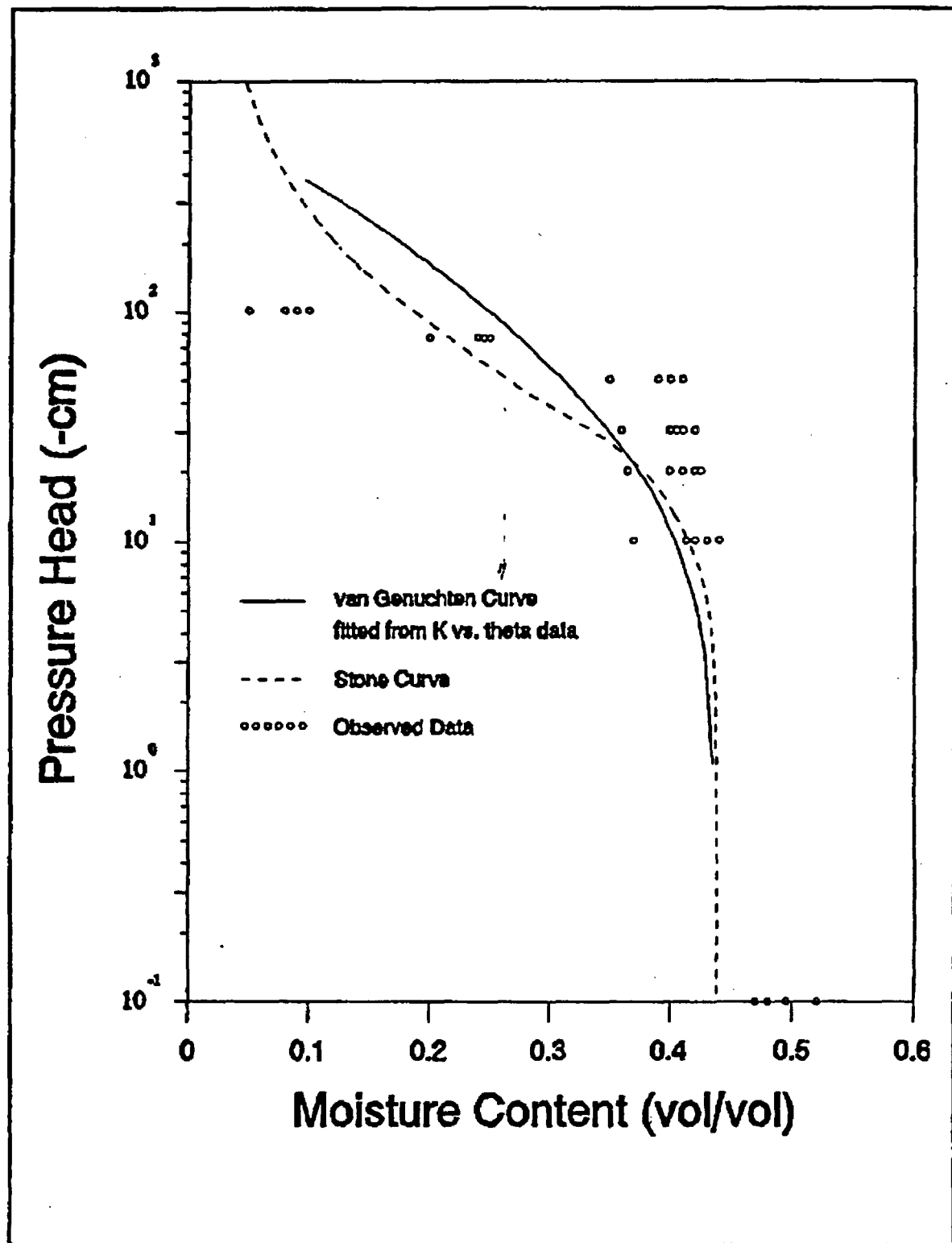


Fig. 3.3-5. Fitted moisture characteristic curve for the backfill soil.

Rev. 0

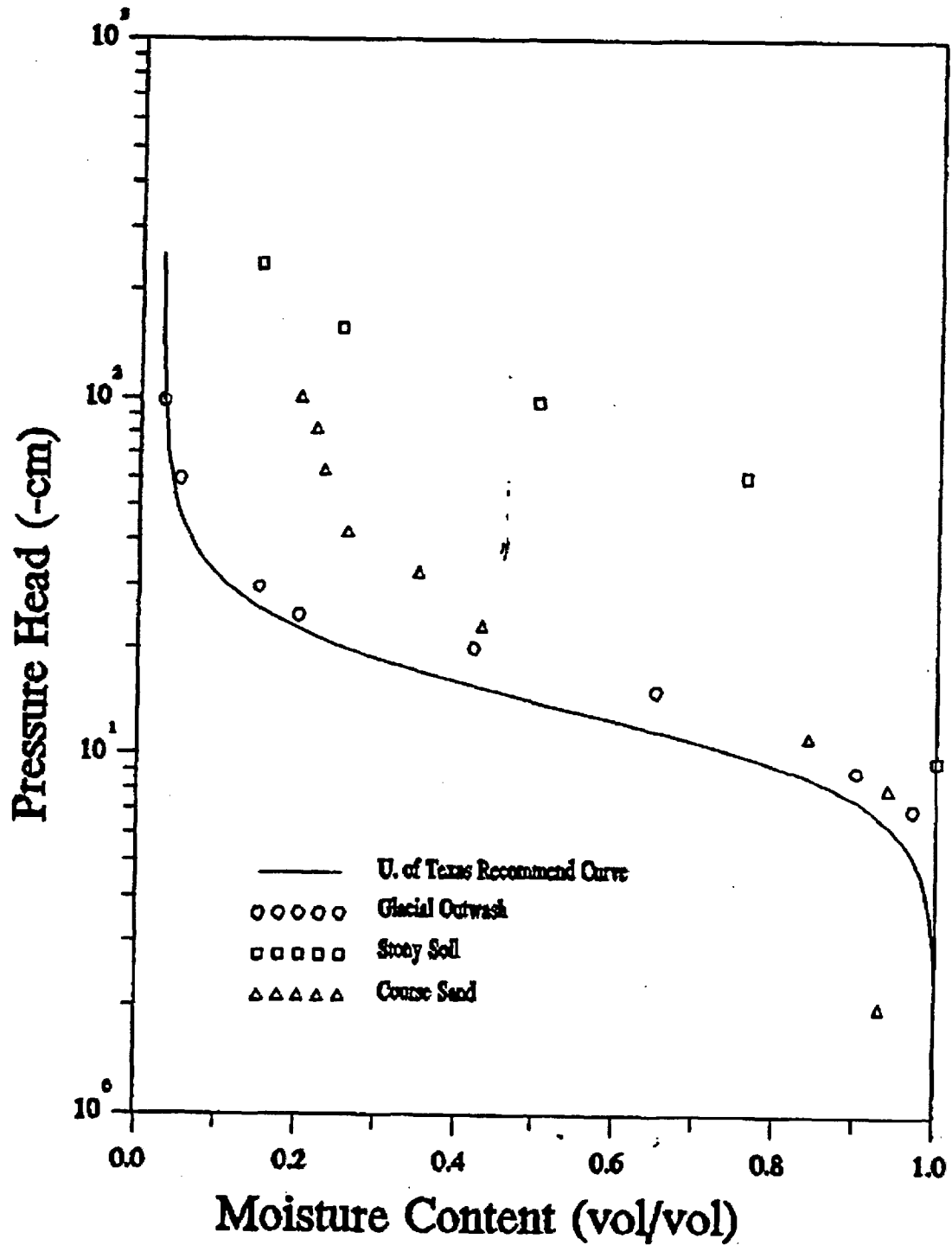


Fig. 3.3-6. Fitted moisture characteristic curve for the gravel soil.

Rev. 0

Clay

A clay cap was not considered in the INTERA (1989) study so there is no previous example to follow. The clay soil used in the engineered moisture barrier cover will be taken from the vicinity of SRS. A contracted study on Dixie clay and Grace clay (Yu et al. 1993) was the source of information for the clay data. Hydraulic parameters given for the Dixie clay were used. The hydraulic parameters were: saturated hydraulic conductivity $k_{sat} = 1.0 \times 10^{-7}$ cm/s, porosity of $\phi = 0.386$, Van Genuchten parameters $\alpha = 1.75 \times 10^{-3}$ cm⁻¹, and $n = 1.51$, and $\theta_r = 0.34$ cm³/cm³. Based on considerations of *in-situ* hydraulic conductivity versus laboratory measured values, it was decided to use a k_{sat} of 1.0×10^{-7} cm/s. In general, it is assumed that *in-situ* values would be larger than laboratory values.

Sand

Sand was also tested for its hydraulic performance (Yu et al. 1993). The saturated hydraulic conductivity was reported as $k_{sat} = 1.0 \times 10^{-3}$ cm/s. Porosity and residual moisture content were, $\phi = 0.375$ and $\theta_r = 0.074$. The van Genuchten fitting parameters used in describing the moisture characteristic curve were, $\alpha = 0.051$ and $n = 2.43$.

Waste Form

Since the waste in the ILNT and ILT vaults is to be grouted in place or enclosed in concrete, it was assumed that the moisture characteristics of grout are similar to that of concrete. The moisture characteristic curve used was the same as that for the concrete. Water flow through the LAW vault waste was assumed to be controlled by the surrounding concrete. Thus, during the intact period of the simulation, the hydraulic parameters were the same as the concrete. From the end of the intact period to the end of the simulations, the LAW vault waste was assumed to have the same hydraulic properties as sand.

Concrete

Samples of concrete to be used for the EAVs were tested to determine their hydraulic parameters by Core Labs (Yu et al. 1993). Results from this analysis gave the following parameters for the E-Area concrete. Saturated hydraulic conductivity, k_{sat} , was 1.0×10^{-10} cm/s, $\alpha = 5.98 \times 10^{-4}$ cm⁻¹, $n = 3.43$, and $\theta_r = 0.147$ cm³/cm³. An effective porosity of $\phi = 0.15$ was used in the model.

The molecular diffusivities assumed for each soil type are:

- 158 cm²/year for the soil and sand,
- 0.315 cm²/year for the concrete,
- 0.158 cm²/year for the ILNT and LAW vault wastes, and
- 47 cm²/year for the clay.

The longitudinal dispersivities for each soil type were:

- 10 cm - for soil and sand,
- 5 cm - for the concrete, ILNT waste, LAW waste, and clay.

The transverse dispersivity was 2 cm for all material types. The transport partition coefficients used in the simulations are given in Table 3.3-2. All transport simulations were conducted assuming a unit concentration as the initial mass in the waste forms.

3.3.1.2 Conceptual Model for Degraded Vault

Two steps of degradation are considered in the detailed flow and transport models: cracking and collapse. The cover is assumed to fail at vault collapse due to the loss of support from the roof of the vault. When the cover fails, the flow field is assumed to be at equilibrium with the background infiltration rate (40 cm/year). Variations in the failed cover

Table 3.3-2. Partition coefficients used in PORFLOW near-field simulations, mL/g

	Soil	Concrete ^a	ILNT Waste ^a	LAW Waste ^a	Sand ^b	Clay ^b
H	0	0	0	0	0	0
C	2 ^c	5000	5000	0	5	1
Ni	300 ^d	1000	1000	1200	400	650
Se	5 ^c	0	200	170	150	740
Sr	10 ^f	10	10	3	15	110
Tc	0.36 ^f	700	1	0	0.1	1
Sn	130 ^d	200	200	50	130	670
I	0.6 ^f	30	30	0	1	1
Cs	100 ^f	20	2	0	280	1900
Ra	500	10	10	60	500	9100
Th	3000 ^d	5000	5000	2200	3200	5800
U	50 ^c	5000	200	6000	35	1600
Np	10 ^c	5000	2000	750	5	55
Pu	100 ^f	5000	5000	2000	550	5100
Am	150 ^f	5000	5000	3700	1900	8400
Cm	150 ^h	5000	5000	3700	4000	6000
Bk	150 ^h	5000	5000	3700	1900	8400
Cf	150 ^h	5000	5000	3700	1900	8400

^a All values from NAGRA (Allard 1985) except Cs-135 from Oblath (1985).

^b All values from Sheppard and Thibault (1990). Berkelium and californium were assumed to be the same as americium.

^c Source: McIntyre (1988).

^d Source: Sheppard and Thibault (1990).

^e NEA data base (Ticknor and Ruegger 1989).

^f Source: Hoeffner (1985).

^g Source: Looney et al. (1987).

^h Assumed to be the same as americium.

infiltration rate are considered in the sensitivity analysis. In all cases, the flow field is maintained at steady state while the transport processes are occurring. At the time of cracking and the time of collapse, new flow fields are obtained for use during the respective time frame.

Parameter values from Sect. 3.3.1.1 will be used for all soils. Parameters for the engineered features are obtained from concrete degradation and structural calculations. The approach for degradation modeling is introduced in Sect. 3.1.3 and discussed in detail in Appendix K. The results of the degradation modeling identify estimates of the times that cracking and collapse occur and the changes in concrete permeability when cracking occurs. Changes in other parameters are based on engineering judgement.

The parameters used for the degraded cases are identified in Tables 3.3-3 and 3.3-4. Tables 3.3-3 and 3.3-4 identify the times for the step changes as t_1 and t_2 . Table 3.3-5 provides the times considered best estimates for the step changes in the LAW and ILNT/ILT vaults. Details regarding the degradation calculations are provided in Appendix K.

The material properties used for the backfill, clay, and sand do not change over time for all types of vaults as shown in Tables 3.3-3 and 3.3-4. Also, the material properties for the waste are assumed to be degraded initially for the LAW vault, and thus, do not change with time. The grouted waste forms for the ILNT/ILT vaults are assumed to increase in permeability at the first step change and remain at the larger permeability for the duration of the simulation. Geochemical properties for the waste form are assumed to persist for the duration of the simulations.

The concrete properties for the vault also vary with time based on the degradation calculations in Appendix K. The roof, walls, and floor were treated separately as shown in Tables 3.3-3 and 3.3-4. Note that the times of the step changes are different for the different vaults. The floor actually fails at roughly the same time for all vaults. However, the time of failure for the roof is different. The hydraulic conductivity for the cracked concrete was estimated using an analytic solution as part of the degradation calculations discussed in Appendix K.

Table 3.3-3. LAW vault parameters

	TIME	k_{sat}	Infiltration, cm/year	Porosity
Placement of vaults; all systems work as designed				
Backfill	$t_0 - t_1$	1×10^{-5}	4	0.44
Clay	$t_0 - t_1$	1×10^{-7}	4	0.39
Concrete (roof)	$t_0 - t_1$	1×10^{-10}	4	0.15
Concrete (floor)	$t_0 - t_1$	1×10^{-10}	4	0.15
Concrete (walls)	$t_0 - t_1$	1×10^{-10}	4	0.15
Sand	$t_0 - t_1$	1×10^{-3}	4	0.38
Void	$t_0 - t_1$	1×10^{-3}	4	0.99
Waste	$t_0 - t_1$	1×10^{-3}	4	0.33
Cracks penetrate the floor and walls, and the roof				
Backfill	$t_1 - t_2$	1×10^{-5}	4	0.44
Clay	$t_1 - t_2$	1×10^{-7}	4	0.39
Concrete (roof)	$t_1 - t_2$	1×10^{-7}	4	0.15
Concrete (floor)	$t_1 - t_2$	1×10^{-8}	4	0.15
Concrete (walls)	$t_1 - t_2$	1×10^{-3}	4	0.15
Sand	$t_1 - t_2$	1×10^{-3}	4	0.38
Void	$t_1 - t_2$	1×10^{-3}	4	0.99
Waste	$t_1 - t_2$	1×10^{-3}	4	0.33
Roof collapses, but moisture flux out the vault prevents filling of vault, evapotranspiration yields lower infiltration				
Backfill	$t_2 - t_3$	1×10^{-5}	40	0.44
Clay	$t_2 - t_3$	N/A		
Concrete (roof)	$t_2 - t_3$	N/A		
Concrete (floor)	$t_2 - t_3$	1×10^{-3}	40	0.15
Concrete (walls)	$t_2 - t_3$	1×10^{-3}	40	0.15
Sand	$t_2 - t_3$	1×10^{-3}	40	0.38
Void	$t_2 - t_3$	N/A		
Waste	$t_2 - t_3$	1×10^{-3}	40	0.33

t_0 = beginning of simulation, 0 years

t_1 = cracks penetrate roof

t_2 = roof collapse

t_3 = beyond peak release of each nuclide

Table 3.3-4. ILNT vault parameters

	TIME	k_{sat}	Infiltration, cm/year	Porosity
Placement of vaults; all systems work as designed				
Backfill	$t_0 - t_1$	1×10^{-5}	4	0.44
Clay	$t_0 - t_1$	1×10^{-7}	4	0.39
Concrete (roof)	$t_0 - t_1$	1×10^{-10}	4	0.15
Concrete (floor)	$t_0 - t_1$	1×10^{-10}	4	0.15
Concrete (walls)	$t_0 - t_1$	1×10^{-10}	4	0.15
Sand	$t_0 - t_1$	1×10^{-3}	4	0.38
Waste	$t_0 - t_1$	1×10^{-10}	4	0.50
Cracks penetrate the roof, while the floor and walls remain intact				
Backfill	$t_1 - t_2$	1×10^{-5}	4	0.44
Clay	$t_1 - t_2$	1×10^{-7}	4	0.39
Concrete (roof)	$t_1 - t_2$	1×10^{-7}	4	0.15
Concrete (floor)	$t_1 - t_2$	1×10^{-10}	4	0.15
Concrete (walls)	$t_1 - t_2$	1×10^{-3}	4	0.15
Sand	$t_1 - t_2$	1×10^{-3}	4	0.38
Waste	$t_1 - t_2$	1×10^{-3}	4	0.50
Roof collapses, but moisture flux out the vault prevents filling of vault, evapotranspiration yields lower infiltration				
Backfill	$t_2 - t_3$	1×10^{-5}	40	0.44
Clay	$t_2 - t_3$	N/A		
Concrete (roof)	$t_2 - t_3$	N/A		
Concrete (floor)	$t_2 - t_3$	1×10^{-3}	40	0.15
Concrete (walls)	$t_2 - t_3$	1×10^{-3}	40	0.15
Sand	$t_2 - t_3$	1×10^{-3}	40	0.38
Waste	$t_2 - t_3$	1×10^{-5}	40	0.50

t_0 = beginning of simulation, 0 years

t_1 = cracks penetrate roof

t_2 = roof collapse

t_3 = beyond peak release of each nuclide

Table 3.3-5. Degradation times for vaults, years

Vault State	ILNT/ILT	LAW
Intact, $t_0 - t_1$	0 to 575	0 to 1400
Cracked, $t_1 - t_2$	575 to 1050	1400 to 3100
Failed, $t_2 - t_3$	1050 to end	3100 to end

The conceptual model for the analytic solution assumes, as discussed in Sect. 3.1.3.5, that: 1) fractures occur at regular intervals as determined by the structural calculations; 2) that all fractures open simultaneously at the time specified in Table 3.3-5; 3) the fractures are assumed to be continuous and open and filling or plugging by soils or precipitates is not considered; 4) the fracture is saturated with water; and 5) water drains freely at the base of the fracture. These assumptions should yield a conservative estimate of the hydraulic conductivity and flow rates through out the fractures.

The PORFLOW (ACRI 1993) computer code is used to conduct the flow and transport calculations using the assumptions discussed in the previous paragraphs. The analyses are conducted in an iterative fashion. The first set of analyses address intact conditions for the vault and cover for the first time frame (Sect. 3.3.1.1). The second and third time frames are addressed using the parameters in Tables 3.3-3 and 3.3-4. Fractures are modeled as an increase in the effective hydraulic conductivity of the concrete. The material properties and assumptions discussed previously represent the base case values for the input parameters. Sensitivity analyses are conducted to address the impacts of changes in the base case on performance.

3.3.2 Groundwater Transport Model

A brief summary of the conceptual model of the subsurface transport of radionuclides in the saturated zone is provided here, while a more detailed description is given in Appendix A.2. Radionuclides that leach from the EAVs will eventually reach the water table unless their half-lives are sufficiently short relative to the transport time in the unsaturated zone. Radionuclides that reach the water table, as determined in the near-field models for both intact and degraded vaults (Sect. 3.3.1), would be transported in the saturated zone beneath the facility to discharge points along nearby streams; specifically, UTR Creek, unnamed, and Crouch Branches (Fig. 2.1-2). The five hydrologic units (Appendix A.2) of interest, are Aquifer Unit IIA (Congaree Aquifer), Confining Unit IIA-IIB (Green Clay), Aquifer Unit IIB, Zone 1 (Barnwell/McBean Aquifer), Confining Zone IIB₁-IIB₂ (Tan Clay), and Aquifer Unit IIB, Zone 2 (water table). All units are dissected by the three creeks to some degree, except for Aquifer Unit IIA and Confining Unit IIA-IIB, which are incised only by UTR Creek.

The computer code PORFLOW (ACRI 1993) was used to simulate groundwater flow under the EAVDF. PORFLOW is a three dimensional code capable of simulating multi-phase fluid flow in variably saturated porous or fractured media. The PORFLOW computer code is described in detail in Appendix B.5. The purpose of this section is to briefly describe the system simulated with this computer code with respect to the physical boundaries of the model domain, the assumptions made regarding the hydrologic characteristics within that domain, and the assumptions made regarding physical characteristics of the porous media and chemical characteristics of the radionuclides that affect mass transport in groundwater. A more in-depth treatment of the conceptual saturated flow and transport model is provided in Appendix A.2. A description of the method by which the conceptual model described below is represented by PORFLOW simulations is provided in Sect. 3.4.2.

3.3.2.1 Model Domain

The hydrologic setting at E-Area is conceptualized as a three-dimensional domain, due to the divergent nature of the flow in the aquifers of interest. The model domain in the saturated zone beneath the EAVs is defined by the lateral and vertical extent of interest; i.e., that volume which could potentially be impacted by contamination due to waste disposal in the EAVDF. The lateral extent of the model domain was selected not only to assure simulation of the zone of interest but also to permit a reasonable representation of naturally occurring flow boundaries within the model domain. For example, the domain extent on the west, south, and east sides coincide approximately with groundwater divides in Aquifer Units IIB, Zones 1 and 2.

Vertically, the domain is divided into five layers corresponding to the three aquifer units and the two confining units that separate them. All five units potentially will be impacted by the release of radionuclides from the EAVs and will be the units through which the radionuclides will be transported. The upper unit, Aquifer Unit IIB, Zone 2, is the water table and is the unit within which the upper surface of the zone of saturation occurs. Beneath this unit is Confining Unit IIB₁-IIB₂ (or the Tan Clay), which separates it from the Aquifer Unit IIB,

Zone 1 (Barnwell/McBean). Beneath Aquifer IIB, Zone 1, is Confining Unit IIA-IIB (the Green Clay), which separates it from Aquifer Unit IIA (the Congaree Aquifer). The two confining layers both have relatively low hydraulic conductivities and, thus, act to confine the aquifer units which underlie each.

The lower unit, Aquifer IIA, is the lowermost unit of interest because units below this will not be impacted by any long-term releases from the EAVs. Beneath Aquifer IIA is Confining Unit I-II (Ellenton Clays), which separates it from the underlying Aquifer Unit I. Piezometric levels measured near the EAVDF indicate that there is an upward gradient across Confining Unit I-II, which means that the vertical component of flow is upward in this low-permeability unit. Consequently, Aquifer Unit IIA is a zone of groundwater convergence, vertically, and flow within the unit is horizontal in the direction of the discharge zone at UTR Creek. Within the saturated zone model, the base of the Aquifer Unit IIA is the base of the flow field. All of the above mentioned units are described in greater detail within Appendix E.

3.3.2.2 Model Assumptions

Use of the groundwater model described above involves several key assumptions relating to how the model is used to make projections of contaminant migration into the future and how the hydrologic system beneath the EAVDF is represented within the model. One of the primary assumptions is that recharge will remain constant during the future time period that is simulated, and therefore, a steady-state flow will prevail. Since there is no way to project long-term trends in this component of the hydrologic budget, an assumption of steady recharge at a rate close to what occurs today is reasonable. This assumption is embodied in the basic simulation strategy to create a steady-state flow field and then allow contaminants to migrate through that flow field in a transient mode. Other assumptions relate to how the flow field is represented within the model, how certain processes of contaminant migration are simulated, and the validity of these representations. These assumptions are identified below.

Boundary Conditions

Assumptions of boundary conditions are important because they constrain the simulation solution. Boundary types consist of constant head, constant flux, and the special case of constant flux where the flux = 0 (or no flow). In all cases, an effort was made to match natural flow boundaries as closely as possible. Boundaries used in the saturated zone model are described on an unit by unit basis.

Aquifer Unit IIA - The lower boundary of the model domain is the base of Aquifer Unit IIA. This plane is set as a constant flux boundary with the flux being set equal to the calculated inflow from below. The calculation utilized measured hydraulic gradients and estimates of the Ellenton Confining Unit vertical hydraulic conductivity. The western and eastern edges of the domain for this unit are set as no-flow boundaries, while the southern edge of the domain is set as a constant-flux boundary. The southern boundary is an area of inflow and the flux was set based upon known gradients and hydraulic conductivities. The eastern and western edges of the domain are sub-parallel to flow directions in this unit, and therefore, no-flow boundaries are the most valid representations of natural conditions. The area of primary interest within this model is that area south of UTR Creek, hence, the constant-head nodes used to represent this stream from the northern boundary of the area of interest. Although flow enters the stream nodes from the north, the trace of UTR Creek acts as an internal no-flow boundary in this unit since flow converges from both the north and south to these nodes.

Aquifer Unit IIB1 - Three sides of this aquifer unit are represented as no-flow boundaries. The extent of the model domain on the eastern, southern, and western edges was selected to allow a general conformance with sub-regional groundwater divides, which occur within this unit. In theory, these divides delineate vertical planes across which flow cannot occur, hence, the no-flow designation is thought to be the most valid way to represent natural conditions. The northern edge of this unit is truncated by erosion south of UTR Creek and the free-water surface defines the northern extent to which groundwater can flow.

Aquifer Unit IIB2 - Boundaries to this unit are treated in an identical fashion as Aquifer Unit IIB1, no-flow boundaries on three sides and a free-water surface to the north. The ground-water divides in both units are sub-parallel, and hence, the domain extent is representative of these boundaries in both units.

Confining Units IIA-IIB and IIB1-IIB2 - In theory, flow directions in aquitards is nearly vertical, hence, the amount of horizontal flow in the units is negligible. This fact supports the representation of lateral boundaries on the east, south, and west edges of the model domain as no-flow boundaries. At their northern extent each of these units is truncated by erosion south of UTR Creek. In the area north of the "outcrop" position, the vertical hydraulic conductivity for nodes of these layers was increased to the extent where flow is not impeded.

Internal streams - Two tributaries of UTR Creek enter from the south and are discharge areas of Aquifer Units IIB1 and IIB2 within the model domain. These tributaries are Crouch Branch, located east and north of the EAVDF, and an unnamed branch located west and north of the EAVDF. Measurements of flow rates were taken at multiple locations along each of the streams to delineate rates of gain along different stream segments. Measurements were taken at a relatively dry time period so that measured stream flows would directly reflect groundwater discharge. Model nodes closest to the bed of each of these streams was designated as a "stream node". Initially, constant fluxes were assigned to each of these nodes at a rate equal to the measured stream flow gain. Once calibration was achieved, designations of the stream nodes were changed to constant-heads, set at the elevation of the stream bed.

Hydraulic Characteristics

The five units conceptualized for the groundwater model are assumed to be homogenous and anisotropic. Vertical and horizontal hydraulic conductivity values, K_v and K_h , were assigned uniformly within each layer. In all cases, K_v was assigned at a lower value than K_h , but the ratio was kept constant within each layer. Incorporation of vertical to horizontal

anisotropy is supported by extensive hydrologic and geologic evidence. Values of hydraulic conductivity for the groundwater flow and transport simulations are documented in Table 3.3-6.

Table 3.3-6. Hydraulic conductivities for saturated zone simulations

Hydrologic Unit	Horizontal Hydraulic Conductivity (cm yr ⁻¹)	Vertical Hydraulic Conductivity (cm yr ⁻¹)
Aquifer Unit IIB2	4.0×10^4	1.0×10^4
Confining Zone IIB1-IIB2	6.4×10^1	4.3×10^1
Aquifer Unit IIB1	4.1×10^4	3.1×10^4
Confining Unit IIA-IIB	3.0	2.0
Aquifer Unit IIA	4.2×10^5	4.2×10^4

Each of the five units was also assumed to be homogenous with respect to specific storage and porosity. Porosity was set at 0.3 for the aquifer units and at 0.4 for the aquitard units. Specific storage was assumed to be uniform throughout the entire flow field at 0.0001.

Mass Transport

Mass transport in the saturated zone occurs by advective, diffusive, and dispersive processes, but is hindered by sorptive processes. It is assumed that the use of partitioning coefficients, K_d 's, which remain constant throughout the simulation is a valid method of representation of the sorption phenomenon for each contaminant species. Although these coefficients are known to vary with changing geochemical conditions, there is no transport code available which can simulate time or spatially-varying K_d 's. The K_d 's assumed for Aquifer Units IIA, IIB1, and IIB2 are listed in the soil column of Table 3.3-2. For Confining Units IIA-IIB and IIB1-IIB2, the K_d 's assumed are listed in the clay column of Table 3.3-2.

Dispersion was simulated by assuming longitudinal and transverse dispersivities of 3 m and 0.3 m, respectively, assigned uniformly in all layers. Diffusion does not significantly contribute to contaminant transport within the saturated zone. Values of the aquifer matrix specific parameters assumed in the mass transport simulations are listed in Table 3.3-7.

Table 3.3-7. Aquifer matrix-specific mass transport parameters

Matrix Property	Property Value Used
Effective diffusion coef.	$5 \times 10^{-10} \text{ m}^2 \text{ s}^{-1}$
Longitudinal dispersivity	3 m
Transverse dispersivity	0.3 m
Matrix dry bulk density	2650 kg m^{-3}
Total porosity	0.40
Effective porosity	0.30

3.3.3 Models for Dose Estimation

As described in Sect. 3.2.3 and 3.2.4, two basic exposure situations are considered in the PA for the EAV. The first is exposure of members of the general public following transport of radionuclides beyond the boundary of the disposal site, and the second is exposure of inadvertent intruders at the disposal site following loss of active institutional control at 100 years after facility closure. In each case, models for calculating radiation dose from estimated concentrations of radionuclides in the environment are required.

3.3.3.1 Models for Estimating Dose to Off-Site Individuals

The different transport pathways for exposure of off-site members of the public following release of radionuclides from the EAV are discussed in Sect. 3.2.2. The two principal pathways of concern are transport in groundwater following mobilization of radionuclides by

infiltrating precipitation and transport in air following releases of volatile radionuclides to the atmosphere. An analysis of the atmospheric pathway is presented in Appendix A.3. This section discusses the analysis for the groundwater pathway beyond the boundary of the 100-m buffer zone around the disposal site.

For transport of radionuclides via the groundwater pathway, an analysis presented in Sect. 3.2.3.3 shows that the only exposure pathway of concern for off-site members of the public is direct consumption of contaminated drinking water obtained from a well located beyond the boundary of the 100-m buffer zone around the disposal site. Either the performance objective for protection of groundwater resources determines allowable releases to groundwater, in which case only the drinking water pathway is of concern, or doses from other pathways involving use of contaminated groundwater are relatively insignificant. Therefore, doses from other exposure pathways involving other use of contaminated groundwater need not be considered in the dose analysis for off-site members of the public.

The model used to estimate dose from the drinking water pathway is presented in Appendix A.4.5.1. The inputs to the model are the maximum concentrations of radionuclides in groundwater at any location beyond the boundary of the 100-m buffer zone at any time after disposal, as obtained from the models for mobilization and transport of radionuclides described in Sect. 3.3.1 and 3.3.2. The model for the drinking water pathway is summarized in Table A.4-6 of Appendix A.4. For each radionuclide, the factor in this table gives the EDE in rem per year from the drinking water pathway for a unit concentration in groundwater of 1 $\mu\text{Ci/L}$. Thus, the annual dose from any radionuclide is simply obtained by multiplying the estimated maximum concentration in groundwater by the factor given in this table.

3.3.3.2 Models for Estimating Dose to Inadvertent Intruders

The different exposure scenarios and exposure pathways for inadvertent intruders assumed for the EAV are discussed in Sect. 3.2.4. The principal exposure scenarios of concern involve direct intrusion into disposal units. Doses to inadvertent intruders resulting from use of contaminated groundwater obtained from a well on the disposal site should be negligible compared with the doses from direct intrusion into solid waste, because the maximum

permissible doses from the groundwater pathway are only a small fraction of the dose limits for inadvertent intruders from all exposure pathways. An analysis in Appendix A.3 discusses doses to inadvertent intruders following release of volatile radionuclides to the atmosphere.

The discussion of possible exposure scenarios for inadvertent intruders in Sect. 3.2.4 shows that only three scenarios need be considered in the analysis for the EAV. All of these scenarios involve chronic exposure and, thus, are subject to a limit on EDE from all exposure pathways of 100 mrem per year. These scenarios include 1) an agriculture scenario involving direct intrusion into disposal units at any time after the concrete vaults and any other engineered barriers above the waste have lost their structural and physical integrity and excavation into the waste becomes credible, 2) a resident scenario involving permanent residence in a home located immediately above an intact concrete roof or other engineered barrier at any time after loss of active institutional control, and 3) a post-drilling scenario involving exhumation of waste from a disposal unit at any time after drilling through a disposal unit becomes credible. The discussion in Sect. 3.2.4 shows that other scenarios involving chronic or acute exposure either are not credible for the EAV, would result in lower doses than the scenarios considered in the analysis, or are subject to a higher dose limit in the case of acute exposure scenarios (i.e., 500 mrem) and, thus, would be less restrictive than the chronic exposure scenarios considered in the analysis.

The models for estimating dose for the three chronic exposure scenarios for inadvertent intruders considered in this analysis are presented in Appendix A.4.5.2. The inputs to the model for each scenario are the maximum concentrations of radionuclides in the disposal facility at any time after the scenario is first assumed to be credible. The concentrations of radionuclides in disposal units over time are estimated using the initial concentrations at disposal corrected for radioactive decay. Depletion of radionuclide inventories in disposal units due to removal by infiltrating water also is considered in some cases, particularly for long-lived isotopes of uranium. In these cases, the ingrowth of radiologically significant decay products at times long after disposal is potentially important in the intruder dose analysis. The models for the agriculture, resident, and post-drilling scenarios are summarized in Tables A.4-14, A.4-15, and A.4-16, respectively, of Appendix A.4. For each radionuclide and exposure scenario, the factor in the appropriate table gives the EDE in rem per year for a unit

concentration in the disposal facility of $1 \mu\text{Ci}/\text{m}^3$. Thus, for any scenario, the annual dose from any radionuclide is simply obtained by multiplying the estimated concentration in the disposal facility at the time intrusion is assumed to occur by the factor given in the table for that scenario. The calculation of radionuclide concentrations in disposal facilities on the basis of concentrations in disposed waste is described in Sect. 4.1.5.

3.4 PERFORMANCE ANALYSIS METHODOLOGY

This section describes the computational methods used to implement conceptual models for release and transport of EAV constituents. As discussed previously, the PORFLOW-3D computer code was used for the flow and transport simulations. The simulations were conducted for three time frames: intact (as-built) vault, cracked vault, and failed roof over the vault. Separate analyses were conducted for concrete degradation and resulting structural changes to determine the timing and changes that occur when moving from one time frame to the next.

Analyses of potential pathways of transport of EAV constituents through the environment (Sect. 3.2.2) to receptors (Sect. 3.2.3 and 3.2.4) indicate that soil and groundwater concentrations will dominate the performance of the facility. Thus, the computational analyses focussed on determining concentrations in these media as the vault changes with time, and on doses received as a result of such concentrations.

These analyses were aided by the use of computer codes, which are described in detail in Appendix B. Integration of the results of various computations was accomplished in the manner outlined in Fig. 3.4-1. The manner in which each of the computer codes and analytical techniques were adapted to address the conceptual model is described in detail in the following sections.

3.4.1 Near-Field Model Analysis

Computational software (i.e., WingZ, Mathematica) and sophisticated computer codes (i.e., MINTEQ, PORFLOW) were used in the near-field analysis of the E-Area PA. The software and computer codes were applied to analyze or predict: 1) degradation of the

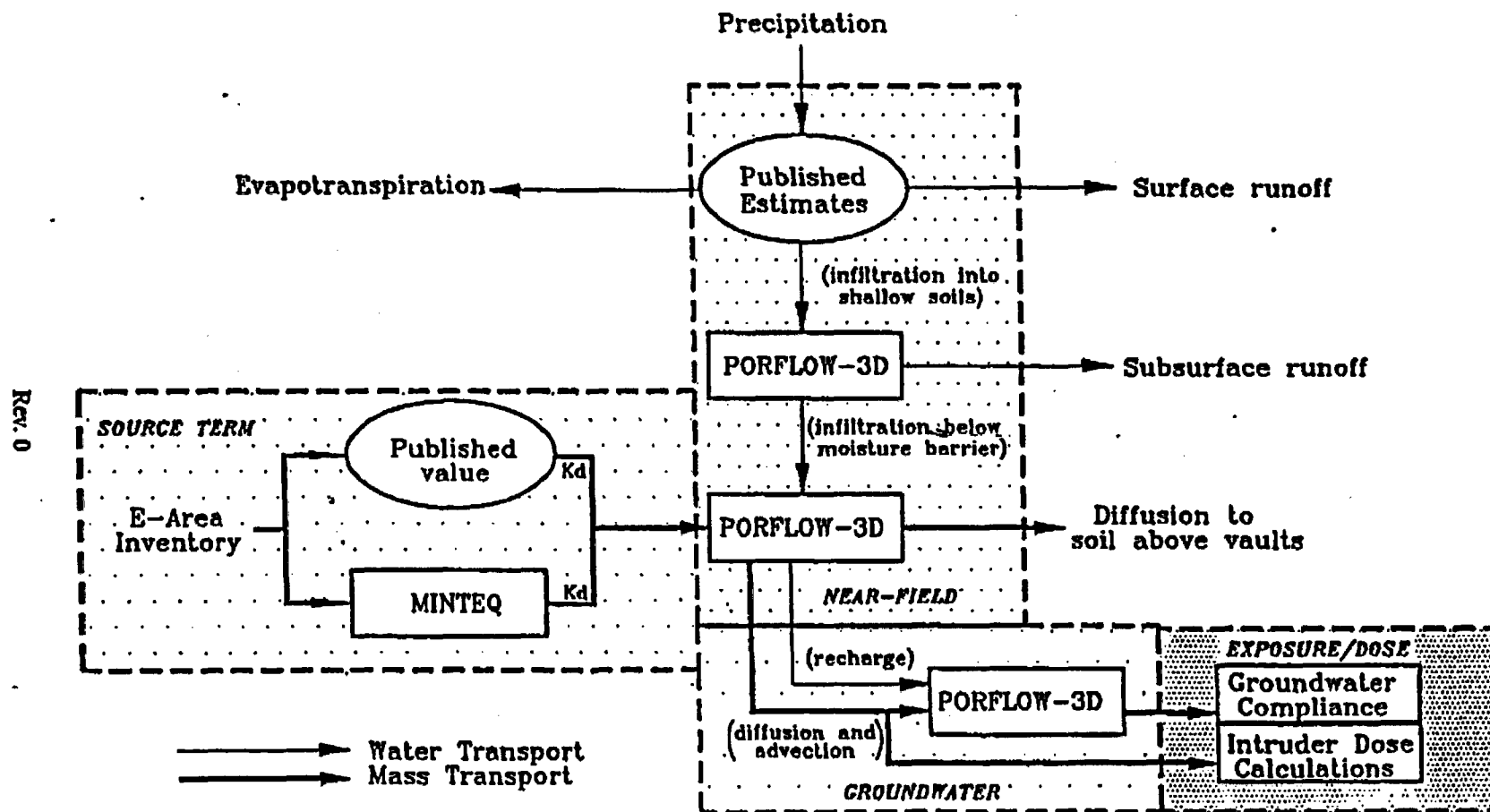


Fig. 3.4-1. Integration of computational methods for the Radiological Performance Assessment of the EAVs.

concrete; 2) screening of insignificant radionuclides; 3) geochemical conditions in the wasteform pore-fluid; 4) water flow patterns and travel-times through the vadose zone; and 5) contaminant migration patterns and fluxes to the aquifer.

A complex sequence of computations and computer simulations were performed to answer the following technical questions:

- Which of the numerous radionuclides in the wasteforms are likely to control the long-term performance of the disposal systems?
- What are the pore-fluid concentrations of the key contaminants in the wasteforms and what geochemical conditions may control the release rates?
- What is the average infiltration rate into the vadose zone?
- What are the likely water flow paths and average travel-times through the cover materials and vaults?
- What rate do the vaults degrade and how does the hydraulic conductivity of the vault change with time?
- As the cover and vaults degrade, what quantities (i.e. concentrations and fluxes) of contaminants will reach the underlying aquifer?

This section describes the computational methods and simulation approaches that were used in the near-field analysis. Methods and approaches have been divided into several sections. Both intact and degraded vault conditions were used in the PA.

Contaminant Inventory Computations

Due to the uncertainty associated with estimating future inventories, an initial activity of one curie within the model domain was used for all radionuclides. This approach was used to establish limits on the quantities of radionuclides that could be placed in the vaults rather than determining if a given inventory was acceptable. In some cases, solubility-limited simulations were made. These cases required an estimate of the initial inventory. The approach for obtaining this inventory is described in Sect. 3.1.

Concrete Degradation Computations

The general methodology of Walton et al. (1990) was used in conjunction with structural calculations to investigate degradation of the structural and hydraulic properties of the vault (Sect. 3.1.3 and Appendix K). The methodology, which consists of empirical relationships and diffusion and structural submodels, provides a basis for predicting the degradation penetration depth. To specialize the methodology for the vaults, mathematical relationships were modified to account for the specific composition of the concrete (e.g., water-to-cement ratio, carbonate content, thickness, etc.) and the pore-water chemistry (pH, carbonate, sulfate and magnesium concentrations, etc.) of the vadose zone.

Infiltration and Fluid Flow Computations

Net moisture flux at the soil surface and through the vadose zone are two primary factors controlling contaminant release and transport rates in the vadose zone. Estimates of the average annual infiltration rate at the site were obtained from previous investigations (Appendix A.1.1). The estimated infiltration rate was then used as a boundary condition for two-dimensional simulations of water flow through the clay and gravel cover and the subsurface region containing the vaults and waste.

Two-dimensional simulations of water flow through the vadose zone were performed using the PORFLOW code. These computations were used, in turn, to:

- estimate the net moisture flux through the cover (i.e., gravel-clay layers),
- define the primary flow paths (i.e., streamlines) from the soil surface, through the cover materials, backfill and vault, to the water table, and
- estimate the water travel-times (i.e., residence times) along the flow paths.

Fluid flow simulations were performed for two distinct subregions of a portion of a single vault. These subregions consisted of: 1) soil, gravel, and clay and 2) backfill, vault, and wasteform. The PORFLOW computer code was used for the flow and transport simulations.

3.4.1.1 Screening Calculations

Screening calculations for the EAVs at the SRS were conducted to limit the scope of future iterations of the PA. For simplicity and efficiency, the approach used for the screening calculations considers site characteristics (in the form of a conservative travel time and distribution coefficients) and excludes the benefits of engineered features of the vault. In this regard, the calculations should be considered conservative. Since E-Area inventories are indeterminate, a set of TVs were calculated using the screening approach. The TVs can be used to identify future waste streams (with larger inventories of given radionuclides) that require more detailed analysis. The TVs are based on extremely conservative calculations, and thus, are not limits for disposal. The simplistic nature of the calculations allowed the use of commercially available spreadsheet software.

3.4.1.2 Flow and Transport Analysis

Implementation of the conceptual near-field model of flow and transport was accomplished in the manner summarized below. Details of the simulation techniques are provided in Appendix A.1.2.

Contaminant Transport Computations

Mass transport simulations were performed to predict the distribution of the key contaminants as a function of such factors as their initial concentrations, solubilities, pore-water velocities and dispersivities. For consistency with the fluid flow computations, the PORFLOW code was used to perform two-dimensional simulations of contaminant transport. These simulations were performed for the two subregions described previously (i.e., engineered barrier and vault) and were carried out until peak concentration was obtained.

Three distinct time periods, corresponding to the stages of vault degradation, were simulated. The three stages correspond to the times when the vault is intact, cracked, and when it completely fails. Hydrologic and transport properties were adjusted at the times when the vault is projected to crack and when it subsequently fails. The timing of the changes in the vault was estimated using the degradation calculations discussed previously. The times used for the base case calculations are best estimates. Appendix K describes the ranges of conditions considered and the resulting ranges of predicted time of failure.

Changes in material properties were estimated using degradation calculations and (or) engineering judgment. The hydraulic conductivity of the cracked concrete is estimated using a semi-analytic solution. The semi-analytic solution assumes a series of equally spaced parallel cracks through the roof and floor of the vault (Sect. 3.3.1.2). Determination of the presence or absence of perched water on a fractured vault is a prerequisite to determining the potential for flow to occur through the cracks. The determination of effective permeability of cracked vaults is necessary to quantify how rapidly the water available above can be conducted through the fractured media. Since the simplified model is steady-state, all fractures are assumed to open at the time of cracking predicted by the structural models. Computational analyses are described in Appendix K.

Pore Fluid Geochemistry Computations

In order to model mass transport in heterogeneous media the concentrations of contaminants in the pore fluid of the wasteforms must be estimated and related to total concentrations in the porous media (contaminant on or in the solid phase plus contaminant in aqueous phase).

The problem of relating total inventory to pore fluid concentrations in wasteforms is complicated by several factors including: 1) precipitation/dissolution reactions involving contaminants; 2) complex formation in solution; and 3) sorption. All of these processes are poorly understood and difficult to quantify.

The chemical complexities of wasteforms were simplified to be consistent with models which consider only reversible linear sorption (i.e., K_d 's). Within this context two general approaches are possible:

- 1) Use theoretical geochemical codes (such as MINTEQ) to estimate K_d 's of each contaminant. Assume the contaminants are released from the solid by linear reversible sorption.
- 2) Obtain K_d 's from pertinent literature for each contaminant.

Both of these approaches are used to compute initial pore solutions in the manner described in Sect. A.1.2.2. The results of the first approach are documented in Appendix D. The remainder of the contaminants of interest used only the second approach to address contaminant/cement reactions (see Table 3.3-2 for K_d 's obtained).

The primary output of the flow and transport computations were: 1) fluid concentration distributions in the vault for use in intruder calculations, and 2) mass flux histories at the water table. The mass flux histories at the water table were used as input into the mass transport simulations for groundwater (Sect. 3.4.2.). In addition, the transport computations were performed in a manner allowing parametric sensitivity analysis to gain insight regarding:

- impacts of cover effectiveness on performance,
- impact of wasteform distribution coefficients on performance, and
- the impacts of hydrologic parameters on performance.

3.4.2 Groundwater Flow and Mass Transport

The code PORFLOW (Appendix B.4), developed by Analytical and Computational Research, Inc. (ACRI), was used to simulate groundwater flow and contaminant transport in E-Area. In this section, the means by which the conceptual model for groundwater (described in Sect. 3.3.2) was translated into a computer-simulated model are described.

3.4.2.1 Groundwater Flow Simulations

The problem domain consisted of a volume defined by a surface water drainage, a drainage divide, and five hydrostratigraphic units as described in Sect. 3.3.2. The model area was discretized into a three-dimensional model consisting of a 38 by 30 by 28 grid as illustrated in Fig. 3.4-2. The five horizontal zones corresponding to the hydrostratigraphic units of interest, specifically Aquifer Unit IIB2 (water table), Confining Zone IIB1-IIB2 (Tan Clay), Aquifer IIB1 (Barnwell/McBean Aquifer), Confining Unit IIA-IIB (Green Clay), and Aquifer Unit IIA (Congaree Aquifer), were defined in the model input by specifying different hydrologic characteristics for each zone.

The northern model boundary, defined by UTR Creek, was designated as a constant head boundary for all of the hydrostratigraphic units. The tributary streams of Crouch and an unnamed Branch are simulated within the problem domain. The western and eastern boundaries for the problem domain were placed at significant distances to minimize influences and were defined as no-flow boundaries because they coincide approximately with groundwater divides in the upper two aquifers. The southern boundary was located along the watershed divide. For Aquifer Unit IIB2 and IIB1 and Confining Units IIB1-IIB2 and IIA-IIB, the watershed divide was defined as a no-flow boundary consistent with Toth's (1962) approach for defining regional flow. For Aquifer Unit IIA (Congaree Aquifer), the southern boundary was defined as a constant-flux boundary, reflecting the regional flow characteristics of this aquifer. The base of Aquifer Unit IIA was considered as a constant flux boundary reflecting small quantities of recharge from the underlying Ellenton Formation.

Hydraulic parameters used in the model are discussed in Sect. 3.3.2 and A.2. Recharge to the system of 40 cm/year was used based on the analysis in Appendix A.1.1.

Model calibration

Using the saturated flow option of PORFLOW, steady-state groundwater flow conditions were simulated and a potentiometric map for the Aquifer Unit IIB2 (water table aquifer) was generated based on the head values calculated by the model (Fig. 3.4-3). To calibrate the

REV. 0

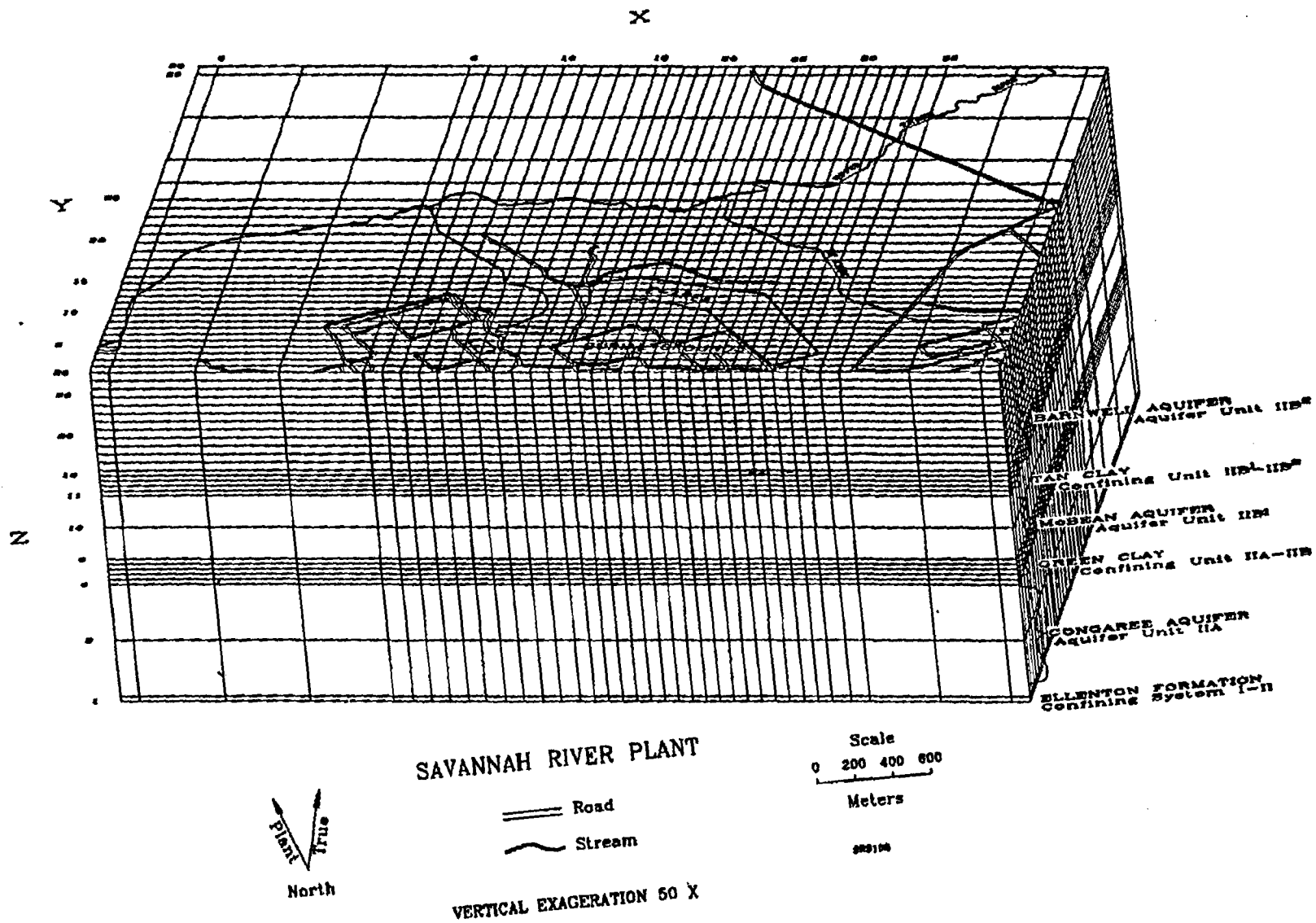
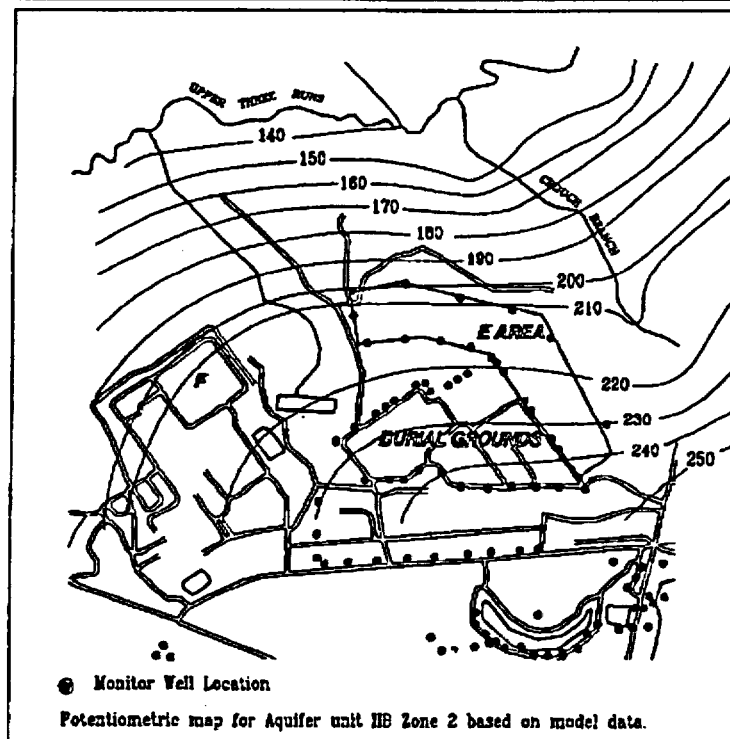
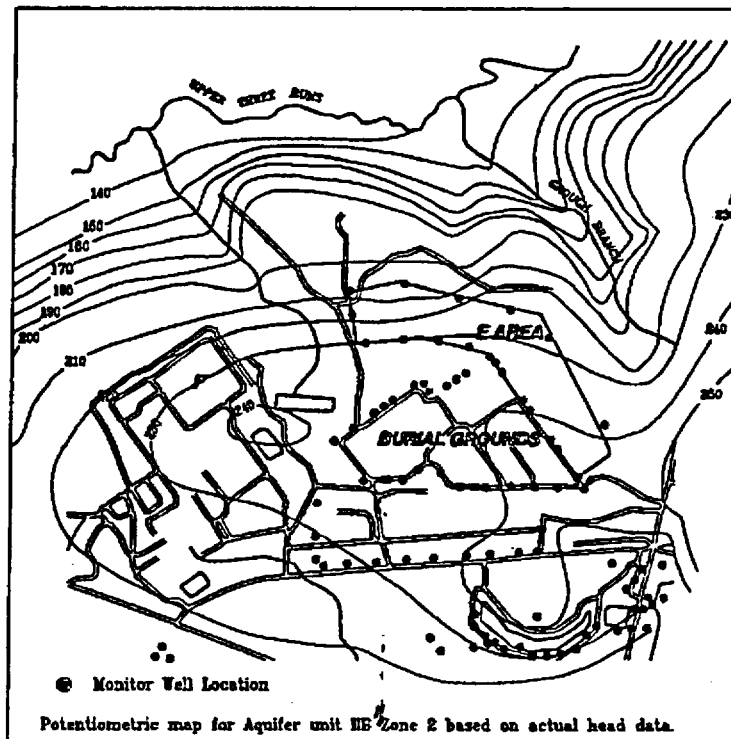


Fig. 3.4-2. Model domain for PORFLOW simulations of groundwater at E-Area.



Scale
0 250 500
Meters



Fig. 3.4-3. Actual potentiometric surface for Aquifer Unit IIB, Zone 2 (water table), and simulated surface for Aquifer Unit IIB, Zone 2.

groundwater flow model, the model-based potentiometric map was compared with potentiometric maps generated from actual water level data from E-Area. Hydraulic parameters were adjusted within the range of observed values to attain the closest comparison between the two types of maps. This calibration process was also completed for Aquifer Unit IIB1 (Barnwell/McBean Aquifer) (Fig. 3.4-4) and for Aquifer Unit IIA (Congaree) (Fig. 3.4-5). The impact of hydraulic parameters in obtaining a calibrated model are discussed in Sect 4.2.2, where a sensitivity analysis of PORFLOW is described.

Model validation

True validation of the calibrated PORFLOW model requires that the model be capable of accurately predicting flow and transport responses when changes in flow conditions occur. Data are not available to carry out such an exercise. However, local stream flow data were obtained at selected locations along the surface creeks (Fig. 3.4-6) using conventional stream gaging techniques and used to evaluate the predictive capability of the groundwater flow model with respect to discharge to the creeks. The data collected are provided in Appendix C.2.

3.4.2.2 Contaminant Transport Simulations

Contaminant transport simulations used to assess the impact of the EAVs on the underlying groundwater system were dependent on the calibrated flow model and the source input values from the overlying unsaturated zone. Data files for contaminant transport simulations relied on the groundwater flow velocity vectors calculated from the steady-state simulations. During actual contaminant transport, the flow simulation portion of the model was disabled and advective movement of the contaminants were calculated from the steady-state velocity values.

Contaminant fluxes at the water table, obtained as described in Sect. 3.4.1, were injected at nodes that corresponded to the water table elevation beneath the vaults. Areas where contamination was injected into the groundwater system are shown in Fig. 3.4-7.

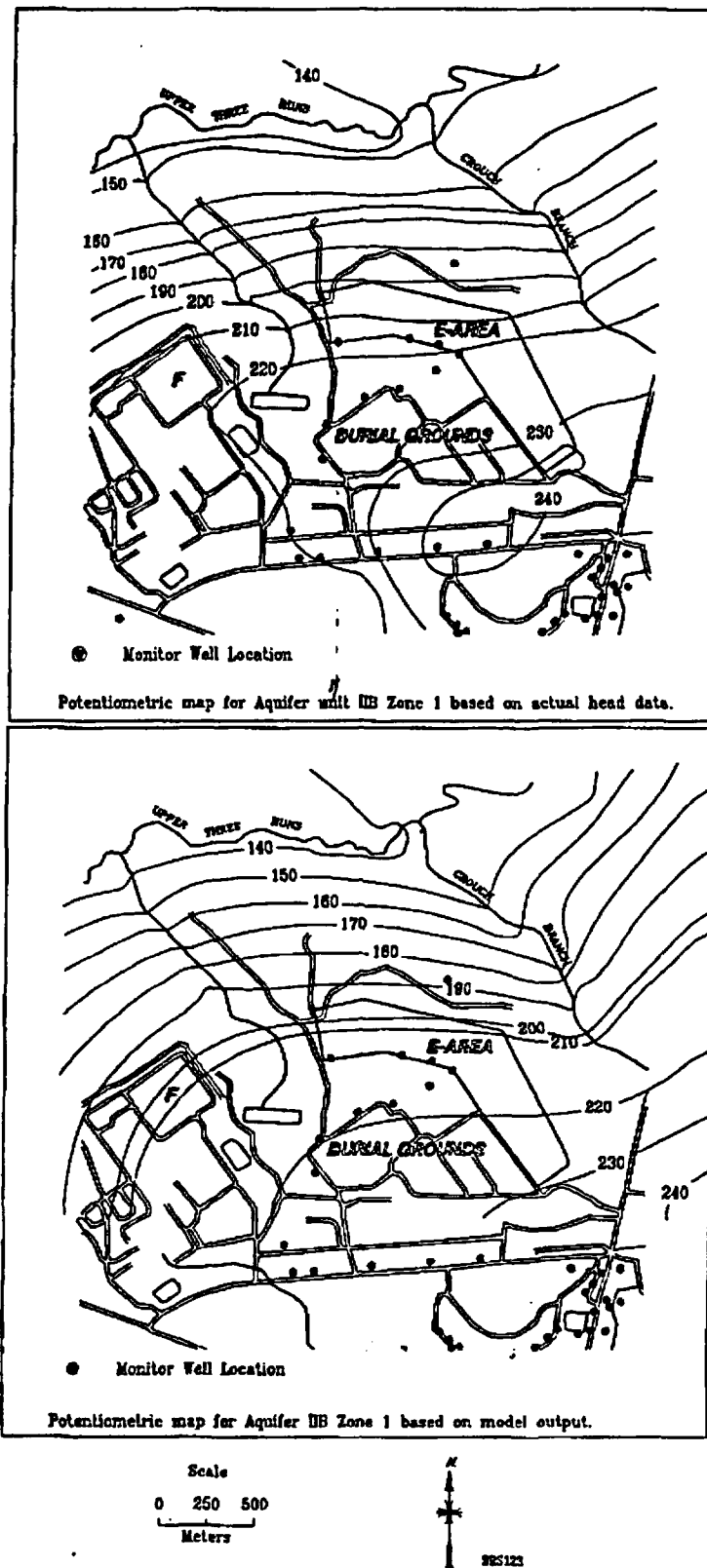


Fig. 3.4-4. Actual potentiometric surface for Aquifer Unit IIB, Zone 1 (Barnwell/McBean), and simulated surface for Aquifer Unit IIB, Zone 1.

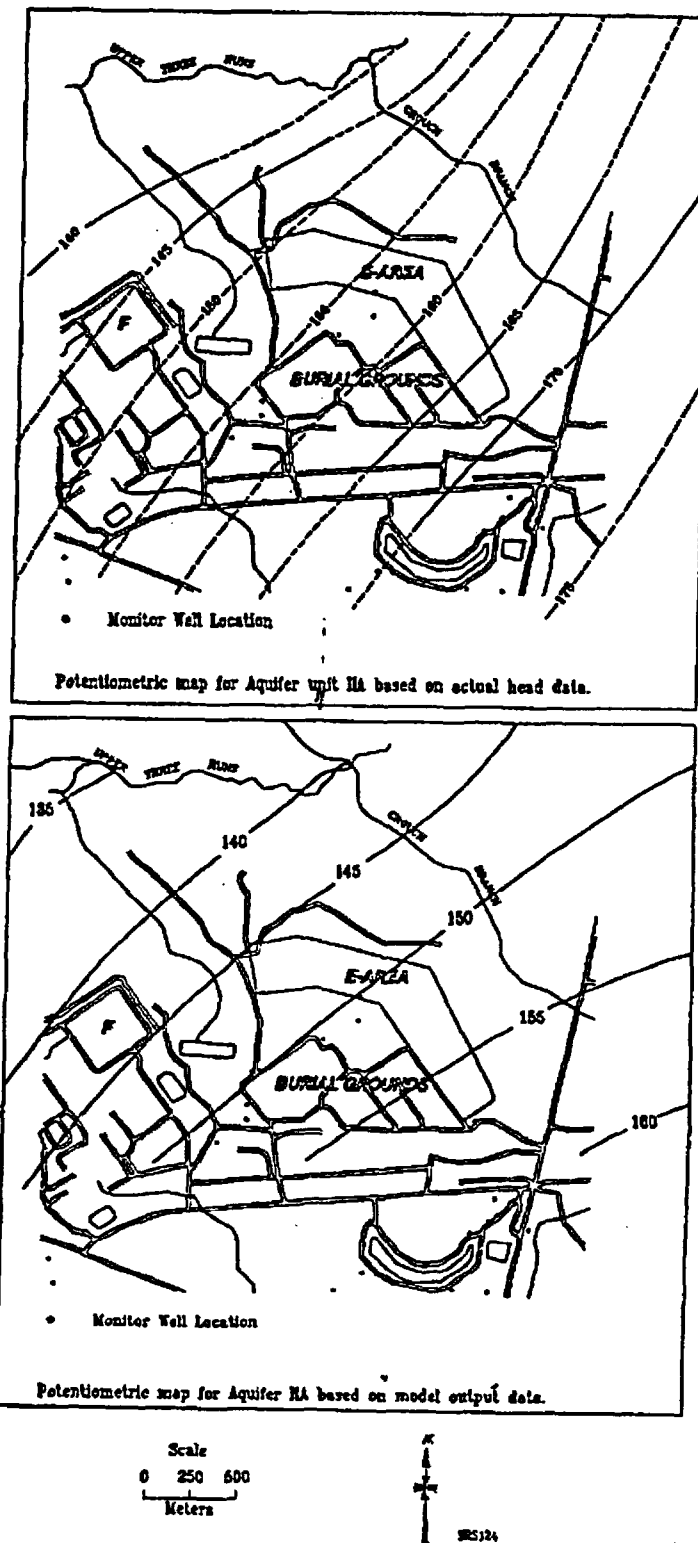


Fig. 3.4-5. Actual potentiometric surface for Aquifer Unit IIA (Congaree) and simulated surface for Aquifer Unit IIA.

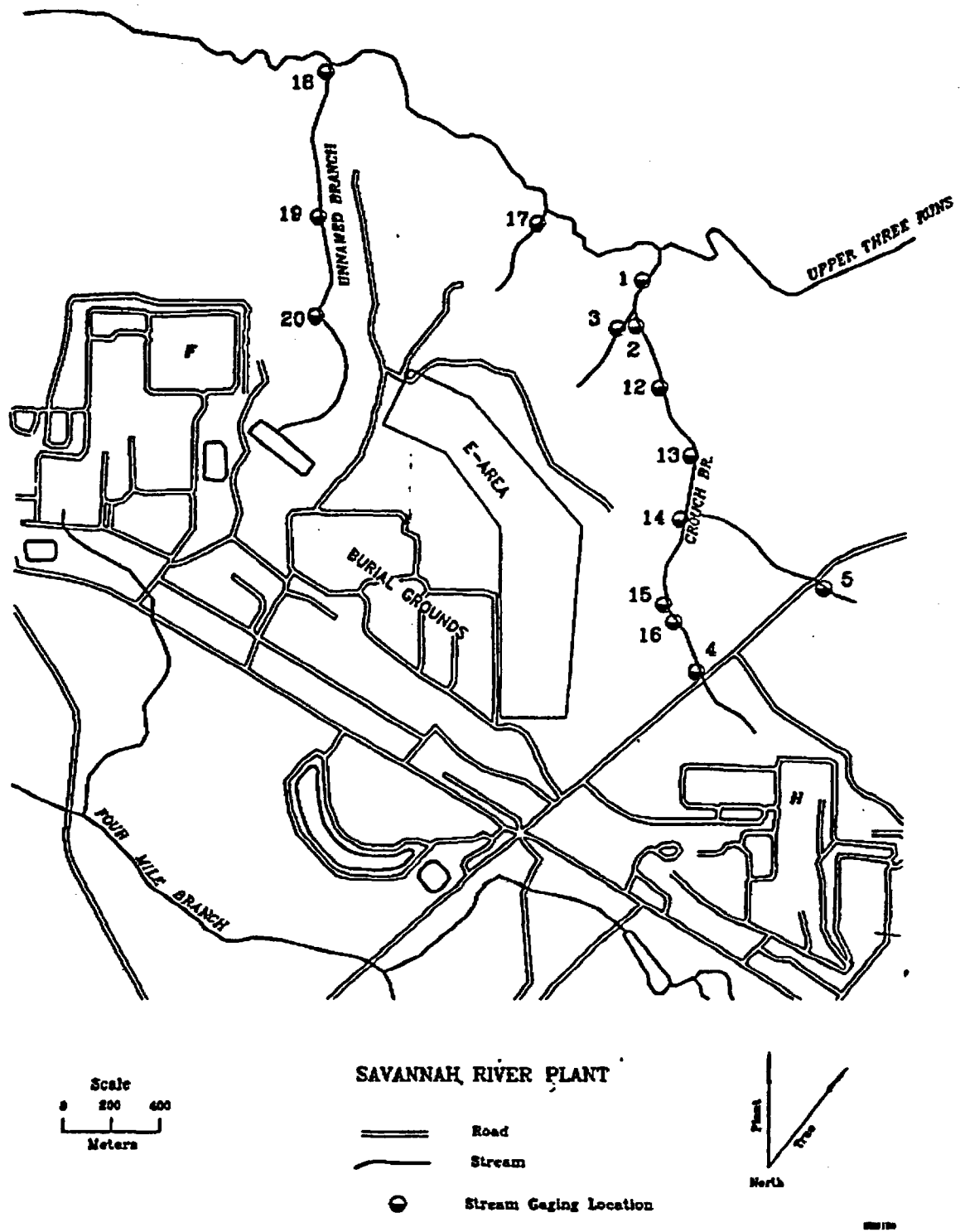
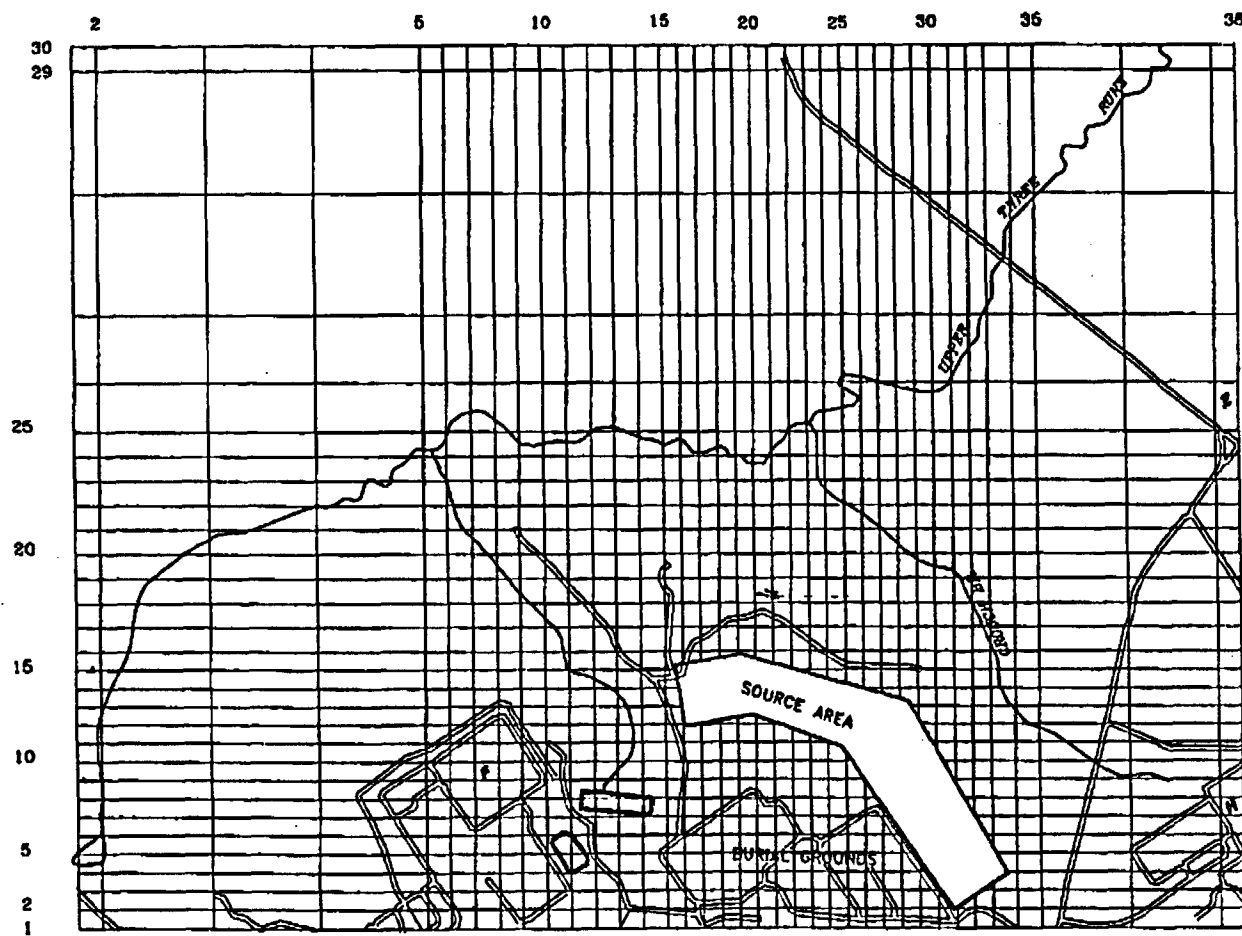


Fig. 3.4-6. Locations of stream-gaging stations in creeks near E-Area.

Rev. 0



== Road
— Stream

Scale
0 200 400
Meters

Fig. 3.4-7. Illustration of EAV source area in PORFLOW grid.

3.4.3 Methods for Dose Analysis

3.4.3.1 Protection of Off-Site Individuals and Groundwater

Calculations of the maximum concentrations of radionuclides in groundwater at any location beyond the 100-m buffer zone were obtained from the models to generate source terms and describe transport in the near-field region and groundwater (Sect. 3.4.1 and 3.4.2).

Doses to the off-site members of the public resulting from use of contaminated groundwater beyond the 100-m buffer zone around all disposal units were not directly estimated. Rather, comparisons of maximum predicted groundwater concentrations with the more restrictive of either MCLs (Table 3.2-1) or allowable concentrations based on the 25-mrem per year performance objective were made. The allowable concentrations were calculated by dividing 25 mrem per year by the EDE per unit concentration in drinking water (Table A.4-6, Sect. A.4). These calculations are simple, were performed by hand, and checked several times for accuracy.

3.4.3.2 Intruder Dose Analysis

Doses to inadvertent intruders into the EAV following loss of active institutional control were estimated. The different exposure scenarios assumed in the analysis are discussed in Sect. 3.2.4 and the models and parameter values are presented in detail in Appendix A.4. Because of the hypothetical and prospective nature of the intruder scenarios and dose estimates, simple multiplicative-chain models which assume that the concentrations of radionuclides are in equilibrium in all parts of the intruder's exposure environment are used in the intruder dose analysis. The use of such models had the advantage that unnecessarily complex computer codes are avoided. The models and data bases presented in Appendix A.4 describe the calculations in their entirety.

In practice, the models are sufficiently simple that all calculations can be performed by hand, and this approach normally was used. The calculations were checked several times for accuracy.

3.5 QUALITY ASSURANCE (QA)

Contributors to this RPA conducted pertinent activities of the project under the guidance of the provisions of the American National Standards Institute (ANSI)/American Society of Mechanical Engineers (ASME) Nuclear Quality Assurance (NQA)-1 Program Requirements for Nuclear Facilities (NRC 1989), as required by the DOE Order 5820.2A (U.S.DOE 1988a). The manner in which the nineteen basic elements of NQA-1 are implemented by Oak Ridge National Laboratory (ORNL), the RPA coordinator, is shown in Table 3.5-1. In this table, the ORNL documented QA procedure which implements the specified element of NQA-1 is listed. Some aspects of all nineteen elements of NQA-1 applied to this RPA. Procedures are documented in the ORNL QA Manual (*Oak Ridge National Laboratory Quality Assurance Manual* current edition), the ORNL Pollutant Assessments Group Procedures Manual (1992), and the Software QA Plan (*Software Quality Assurance Plan for PORFLOW* 1991) produced specifically for the PORFLOW computer code used in this assessment. Table 3.5-2 presents similar information for INEL.

Software QA plans were written by each DOE contractor contributing to this RPA, addressing the provisions of ASME NQA-2a, Part 2.7, *Quality Assurance Requirements of Computer Software for Nuclear Facility Applications*. These QA plans were transmitted to WSRC for review and approval.

Copies of the Software QA Plans submitted are in Appendix F. A surveillance was conducted by WSRC at all contractor sites after the RPA project was underway, for the purpose of evaluating adherence to governing QA procedures described in the submitted QA plans and general project integration. Observations and findings from these surveillances are on file at WSRC. Corrective action was taken in response to these findings, and responses made to observations.

Table 3.5-1. Implementation of NQA-1 by ORNL for the EAVDF RPA

NQA-1 basic element	Implementing ORNL QA procedures ^a	Location of project-specific procedure
1. Organization	QA-L-1-100	a,b,c
2. Quality Assurance Program	QA-L-2-100 QA-L-2-101 QA-L-2-103 QA-L-2-105 QA-L-2-106	a,b,c,d,e
3. Design Control	QA-L-3-100 QA-L-3-101 QA-L-3-102	b,c
4. Procurement Document Control	QA-L-4-100 QA-L-4-101	b,c
5. Instructions, Procedures, and Drawings	QA-L-5-100	b,c
6. Document Control	QA-L-6-100	c
7. Control of Purchased Items and Services	QA-L-7-100 QA-L-7-101 QA-L-7-102	b,c
8. Identification and Control of Items	QA-L-8-100	b,c
9. Control of Processes	QA-L-9-100	b,c
10. Inspection	QA-L-10-100	b,c
11. Test Control	QA-L-11-100	b,c
12. Control of Measuring and Test Equipment	QA-L-12-100	b,c
13. Handling, Storage, and Shipping	QA-L-13-100	b,c
14. Inspection, Test, and Operating Status	QA-L-14-100 QA-L-14-101	b,c

Table 3.5-1. (continued)

NQA-1 basic element	Implementing ORNL QA procedures ^a	Location of project-specific procedure
15. Control of Nonconforming Items	QA-L-15-100	b,c
16. Corrective Action	QA-L-16-100 QA-L-16-101 QA-L-16-102 QA-L-16-103	b,c
17. Quality Assurance Records	QA-L-17-100	b,c
18. Audits and Surveillances	QA-L-18-100 QA-L-18-101 QA-L-18-102	b,c
19. Software	QA-L-19-100	b,c

- ^a Source: Oak Ridge National Laboratory Quality Assurance Manual (current edition).
- ^b Source: Software Quality Assurance Plan for PORFLOW-3D (1991), Appendix F.
- ^c Source: ORNL Pollutant Assessments Group Procedures Manual (1992).
- ^d Source: U.S.DOE (1991).
- ^e Source: Quality Assurance Program Requirements for Nuclear Facilities (1989).

Table 3.5-2. Implementation of NQA-1 by INEL for the EAVDF RPA

NQA-1 basic element	Implementing INEL QA procedures^a	Location of project-specific procedure
1. Organization	QP-1	•
2. Quality Assurance Program	QP-2 QP-2 QP-2 QP-2 QP-2	•
3. Design Control	QP-3 QP-3 QP-3	•
4. Procurement Document Control	QP-4 QP-4	•
5. Instructions, Procedures, and Drawings	QP-5	•
6. Document Control	QP-6	•
7. Control of Purchased Items and Services	QP-7 QP-7 QP-7	•
8. Identification and Control of Items	QP-8	•
9. Control of Processes	QP-9	•
10. Inspection	QP-10	•
11. Test Control	QP-11	•
12. Control of Measuring and Test Equipment	QP-12	•
13. Handling, Storage, and Shipping	QP-13	•
14. Inspection, Test, and Operating Status	QP-14 QP-14	•

Table 3.5-2. (continued)

NQA-1 basic element	Implementing INEL QA procedures ^a	Location of project-specific procedure
15. Control of Nonconforming Items	QP-15	•
16. Corrective Action	QP-16 QP-16 QP-16 QP-16	•
17. Quality Assurance Records	QP-17	•
18. Audits and Surveillances	QP-18 QP-18 QP-18	•
19. Software	EG&G-EELS-106666	•

^a Source: EG&G Idaho Inc. *Quality Manual - Policy and Procedures* (current edition).

^b Source: *Software Quality Assurance Plan for PORFLOW-3D* (1993), Appendix F.

4. RESULTS OF ANALYSIS

In this chapter, the results of the analysis of performance of the EAV, conducted in accordance with the conceptual models and methodologies described in the previous chapter, are presented. Predicted releases to the environment, resulting concentrations, results of dose analysis, and allowable inventories are presented in Sect. 4.1. The results of the sensitivity and uncertainty analyses that were conducted to gain perspective on the meaning of the results are provided in Sect. 4.2.

4.1 ANALYSIS RESULTS

In this section, results of the computational analyses that estimate the potential radiological impact of the EAV are provided. Maximum concentrations of radionuclides in exposure media and estimated doses based on these maximum values are tabulated. The radionuclide concentrations in groundwater are provided in Sect. 4.1.3.

In Sect. 4.1.1, the results of a screening analysis for the groundwater pathway are presented. Since the specific radionuclides that may be encountered in the waste during disposal operations are not known, a conservative screening method was used to determine the allowable inventories of a large suite of radionuclides, which may be encountered during disposal operations. These limits are called "trigger values" (TVs) and indicate the inventory at which the performance objectives may be exceeded. A detailed, site-specific analysis is recommended for a given radionuclide before additional inventories above the TVs are placed in E-Area for disposal. Radionuclides which have relatively small TVs are included in the detailed site-specific analysis, especially if an inventory above the TV is likely to occur in future waste.

In Sect 4.1.2, the near-field model results are presented. The predicted unsaturated flow field through the facility and estimated fluxes of radionuclide constituents in the waste to the water table are described.

In Sect. 4.1.3, concentrations of radionuclides in groundwater are presented. The compliance point for groundwater protection requirements is assumed to be the point of maximum concentration in groundwater at least 100 m from the disposal units (see Sect. 1.2).

The results of the dose analysis are presented in Sect. 4.1.4 and 4.1.5. In Sect. 4.1.4, the estimated maximum concentrations of radionuclides in groundwater at the point of compliance are used to obtain estimates of dose to off-site members of the public and determine allowable disposal inventories. Sect. 4.1.5 presents the results of the dose analysis for inadvertent intruders into solid waste in disposal units.

4.1.1 Screening Results for the Groundwater Pathway

Screening calculations to establish TVs were calculated for all radionuclides and are described in Sect. 3.2.3.4.

Radionuclides which have relatively small TVs, such that an allowable inventory above the TV is likely to occur, have been selected as needing further attention in the RPA (Sect. 3.2.3.4). Radionuclides requiring further attention based on these calculations for each vault are given in Table 4.1-1. Appendix C provides the TVs for all radionuclides. The trigger levels represent the inventory of the given radionuclide that would yield a dose of 4 mrem per year using the screening approach. The trigger levels are not limits for disposal; rather, they indicate inventory levels that will require more detailed consideration if larger quantities of a radionuclide will need to be disposed. Likewise, if the projected inventory is below the trigger level, the radionuclide can be disposed of without further analysis. Note, however, that other pathways may be more limiting than the groundwater pathway (e.g., intrusion).

4.1.2 Near-Field Model Results

Water movement and contaminated transport through the near-field portion of the waste disposal system were simulated to determine the overall performance of the system. The simulations were performed in two stages as discussed in Sect. 3.3.1.1. Both the simulation of the engineered barrier and of the vault will be discussed in turn.

Table 4.1-1. Trigger values for radionuclides selected for detailed groundwater analyses.

Nuclide	Trigger Value (Ci/vault)	
	LAWV	ILNT
H-3	2.8×10^0	3.4×10^{-1}
C-14	7.0×10^{-1}	8.5×10^{-2}
Ni-59	1.1×10^3	1.3×10^2
Se-79	4.1×10^{-1}	5.1×10^{-2}
Sr-90	2.5×10^1	3.1×10^0
Tc-99	2.8×10^{-1}	3.5×10^{-2}
Sn-126	5.2×10^0	6.3×10^{-1}
I-129	1.9×10^{-3}	2.3×10^{-4}
Cs-135	9.3×10^0	1.1×10^0
Th-232	1.6×10^{-1}	1.9×10^{-2}
U-233	1.2×10^{-1}	1.5×10^{-2}
U-234	1.2×10^{-1}	1.5×10^{-2}
U-235	6.3×10^{-2}	7.7×10^{-3}
U-236	1.3×10^{-1}	1.6×10^{-2}
U-238	1.3×10^{-1}	1.6×10^{-2}
Np-237	1.7×10^{-3}	2.1×10^{-4}
Pu-238	3.2×10^2	3.9×10^1
Pu-239	1.6×10^{-2}	2.0×10^{-3}
Pu-240	2.0×10^{-2}	2.4×10^{-3}
Pu-241	3.1×10^1	3.8×10^0
Pu-242	1.6×10^{-2}	2.0×10^{-3}
Pu-244	1.7×10^{-2}	2.0×10^{-3}
Am-241	4.4×10^0	5.4×10^{-1}
Am-243	2.7×10^{-2}	3.3×10^{-3}
Cm-244	7.3×10^0	9.0×10^{-1}
Cm-248	4.2×10^{-3}	5.1×10^{-4}
Cf-252	5.5×10^2	6.7×10^1

4.1.2.1 Engineered Barrier Simulation

The PORFLOW computer code was used to simulate the engineered barrier's effectiveness in reducing the amount of infiltrating water reaching the vault. The engineered barrier consisted of two soil layers. The upper layer was comprised of highly conductive gravel overlying a layer of low permeability clay; this system was surrounded by native backfill soil. In the design of the barrier these layers are sloped from 2 to 5%. As a measure of conservatism, the slope was taken to be 2%.

The hydraulic characteristics of each of the material types used in the simulation were discussed in Sect. 3.3.1.1. The simulation domain was 1000 cm wide and 600 cm high. Although the barriers will be emplaced over the entire vault system, it was only necessary to simulate the end 500 cm of the barrier in order to determine its performance. The physical domain simulated is shown in Fig. 3.3-2. In this simulation, the orientation of gravity was rotated clockwise in the simulation to account for the 2% slope of the barrier.

The boundary conditions for the simulation consisted of no-flow boundaries for each lateral direction. The left boundary, or boundary away from the barrier, could be considered no-flow since it was far enough away from the barrier so that the flow field was not affected and remained vertical. Admittedly, this is slightly in error due to the orientation of gravity. The placement of the right no-flow boundary is arbitrary; based on the results of the simulation it is adequately placed. Results showed that extending the simulation domain further to the right to include more of the barrier, would not change vertical flow through the barrier. The upper boundary was assigned a prescribed flux of 40 cm/year based on the results of the infiltration study (see Appendix A.1.1). The bottom boundary was also arbitrarily placed far enough away to eliminate any influence on the flow field near the barrier and was assigned a pressure head of zero.

The simulation domain was discretized into a grid of 22 horizontal and 63 vertical nodes. The grid spacing in both the horizontal and vertical directions was variable in order to improve the definition of the flow field near the barrier.

The simulation was carried out in several stages. Initially, the entire domain was treated as if it were all backfill to establish a uniform flow field. Then, the clay layer was included and the simulation was run in a transient mode until equilibrium was achieved. The gravel layer was then added and the simulation was run in a transient mode until the flow field equilibrated. Steady-state saturation is shown in Fig. 4.1-1.

In addition to monitoring the convergence of the flow field to steady state, the total water mass balance for the domain was also monitored. Until the addition of the gravel layer, the mass balance was exactly correct to the third decimal place. Upon placement of the gravel layer, the mass balance gained a slight amount of mass. The water flux in the top was 4.0×10^4 cm/year, which was exactly correct based on the 1000 cm width and the flux of 40 cm/year. The flux out the bottom was 4.014×10^4 cm/year. This corresponds to a mass balance error of 0.35%. We judged this to be adequate for determining the effectiveness of the barrier at diverting water based on these two observations: 1) the numerical techniques of reducing the time step and refining the grid about the barrier were both tried, but neither improved the mass balance; and 2) a close inspection of the numerical solution showed that the slight increase of water in the system occurred within the gravel.

The flux across two planes within the simulation domain was monitored to determine how effective the barrier was at diverting water. One flux plane extended from the left simulation boundary to the edge of the clay layer. The other flux plane went from the edge of the clay layer to the right simulation boundary. The flux through the left and right planes was 3.992×10^4 and 2.218×10^2 cm/year, respectively. The sum of these two fluxes matches the total flux out the bottom of the simulation. So, the barrier diverts approximately 99.4% of the infiltrating water.

To determine the flow rate through the moisture barrier, the gravity corrected vertical fluxes through a plane beneath the clay layer were plotted. The results are shown in Fig. 4.1-2. From this plot, it can be seen that the left boundary was placed far enough away from the edge of the barrier so as not to influence the results, because the flux at the left boundary matches the overall infiltration rate of 40 cm/year. The large amount of water being diverted around the barrier shows up as the large downward dip in the graph. Some

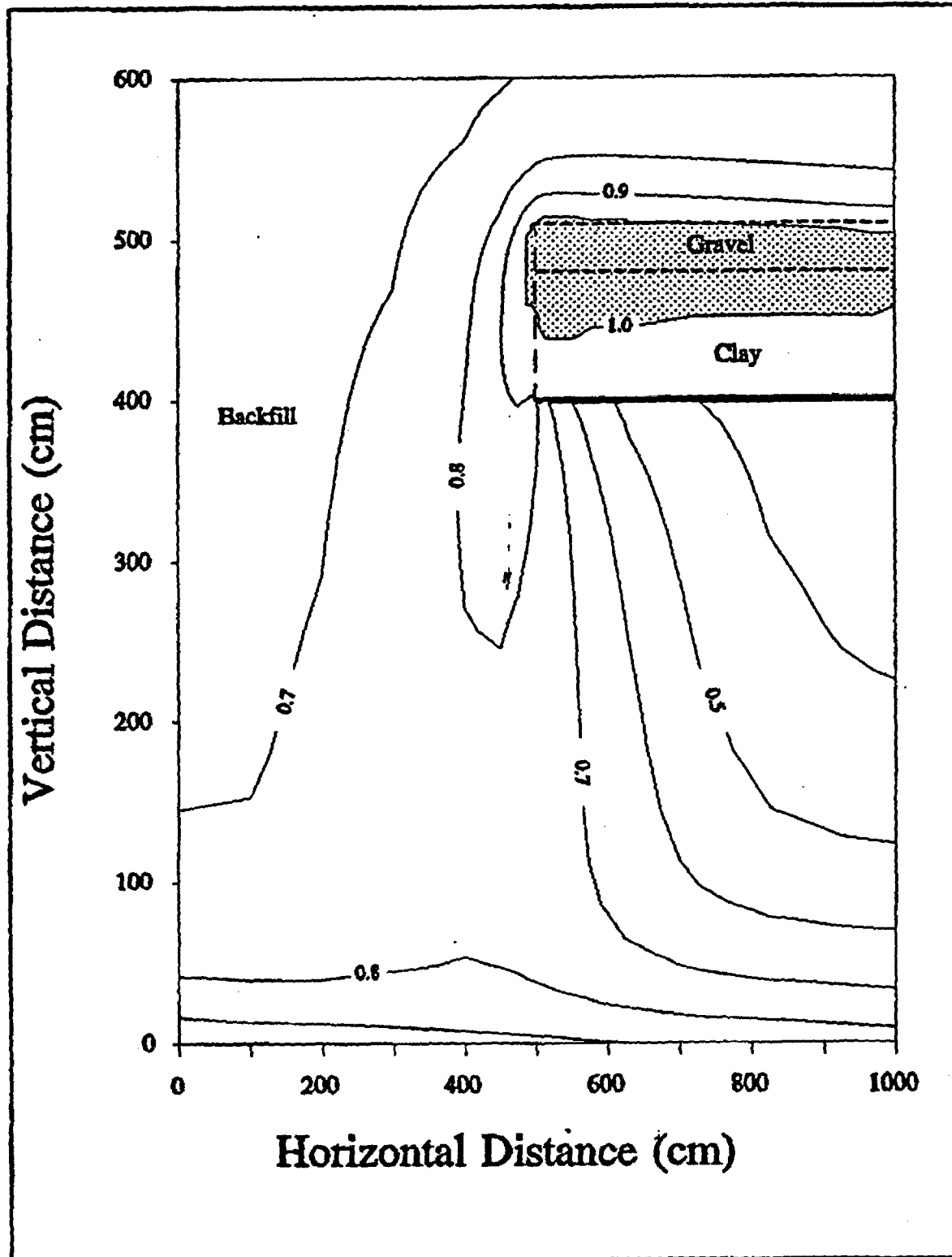


Fig. 4.1-1. Engineered barrier steady-state saturation

Rev. 0

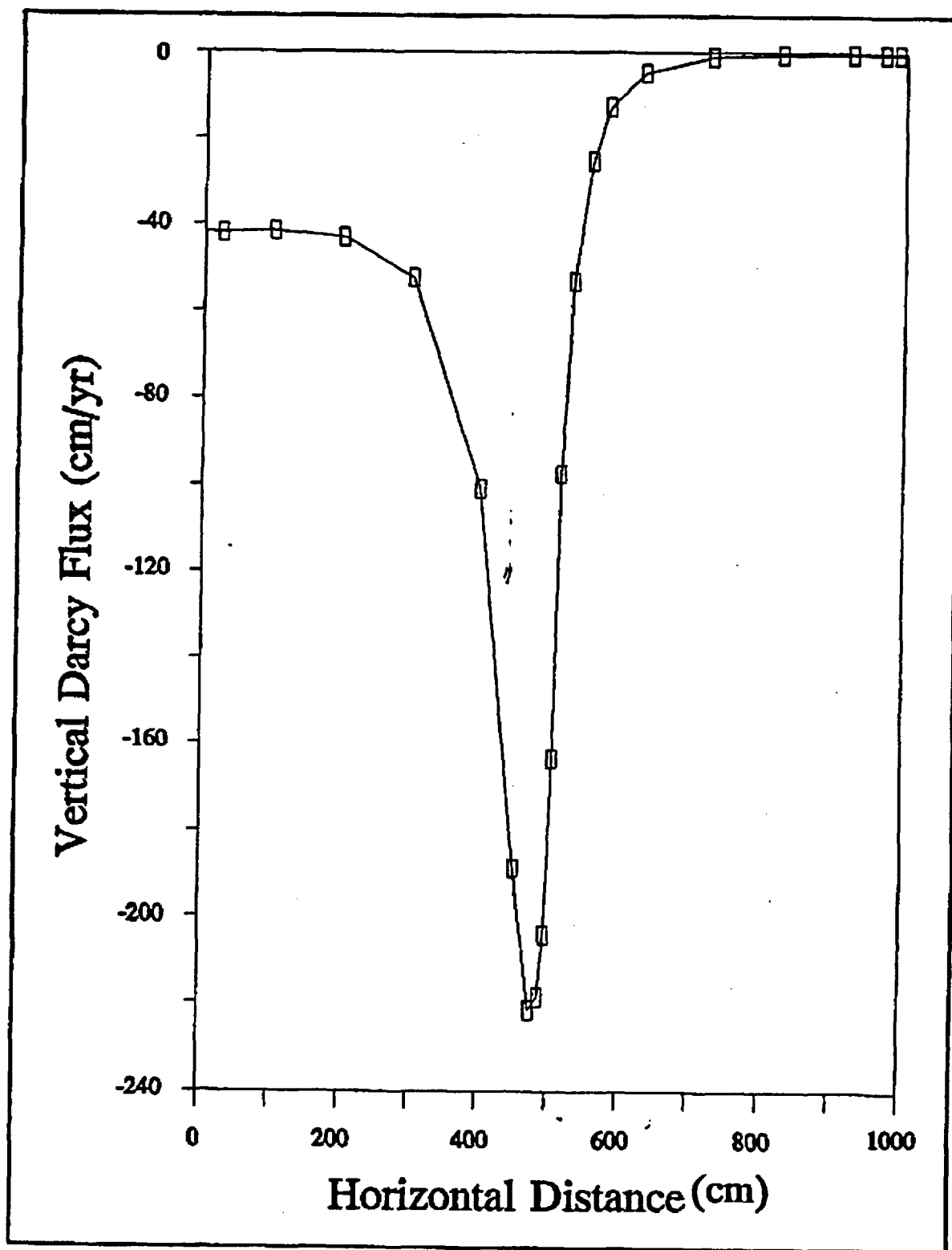


Fig. 4.1-2. Vertical fluxes beneath the engineered barrier.

Rev. 0

water infiltrates around the end of the barrier, as can be seen by the elevated infiltration rate, which extends past 500 cm, the beginning of the gravel/clay barrier. And lastly, it appears that 500 cm of the barrier was an adequate length to establish a constant flow rate through the barrier. The vertical flux through the barrier stabilizes about 300 cm in from the end of the barrier at a value of 0.45 cm/year. While it would be appropriate to use this value as the infiltration rate for water reaching the vault, WSRC determined a more conservative value of 4 cm/year should be used as the infiltration rate through the barrier.

4.1.2.2 Vault and Waste Form Simulations

The similarities between the ILNT and ILT allowed the same conceptual design to be used for both types of vaults, whereas, the LAW vault required a different conceptual design (see Sect. 3.3.1.1). Likewise, for the simulations of solute transport the same flow fields were used for the ILNT and ILT vaults and a separate flow field was generated for the LAW vault. The physical domain in the simulation consisted of a vertical half-plane of the vaults and the surrounding backfill soil (see Figs. 3.3-3 and 3.3-4). This domain is rectangular with the vault superimposed on the right side. Since the roof of the vault slopes from the center out to the edge to increase the flow of water around the vault, the gravity vector was shifted to account for the sloped roofs. The domain was discretized into a computational grid of 46 by 72 nodes for the ILNT and ILT vaults. The LAW vault domain was discretized into a computational grid of 71 by 76 nodes. In order to make the transition from one flow field to the next easier, the same computational domain was used for all simulations.

As mentioned previously in Sect. 3.3.1.1, a three-step process was used to simulate the performance of the vaults over time. In the first time period, all engineered systems are assumed to remain intact and function as designed, so the flux into the domain was 4 cm/year. In the second period, some of the engineered barriers are assumed to begin to fail. Specifically, cracks are assumed to penetrate the entire width of the vault walls, floor, and ceiling. This was simulated by increasing the concrete permeability which causes an increase of water flowing through the vault instead of being diverted around the vault. The third and final step of the simulations was a complete failure of the members supporting the vault ceiling, causing

the ceiling to collapse. The failure of the vaults has two significant impacts on the flow of moisture through the domain. The first is the breach in the engineered barrier, causing a higher flux of water (40 cm/year) entering the domain. Second, the loss of integrity of the vault allows more water to flow through the vaults rather than being diverted around by the roof.

The upper boundary for water flow in each simulation is treated as a prescribed flux boundary with the assigned value fixed to 4 cm/year before the collapse of the vaults and increased to 40 cm/year after the failure. Because of symmetry, both lateral boundaries are prescribed as no-flux boundaries. The lateral boundary away from the vault is located halfway between adjacent vaults and the flow field there is strictly vertical. The inner boundary is located at the midpoint of the vault and the flow field is also vertical. The bottom boundary is located at the water table so a prescribed head of 0 cm is appropriate. The boundary conditions for the transport simulations were assigned as follows. Again using symmetry, the lateral boundary conditions are assigned to be no-flux. A conservative approach to the lower boundary condition is to assign a zero concentration, which serves to maximize the diffusive flux out of the domain. The upper boundary condition was also set to zero as it is the most appropriate with the flow boundary condition.

The procedure used for simulating the flow and transport in the vault region consisted of the following:

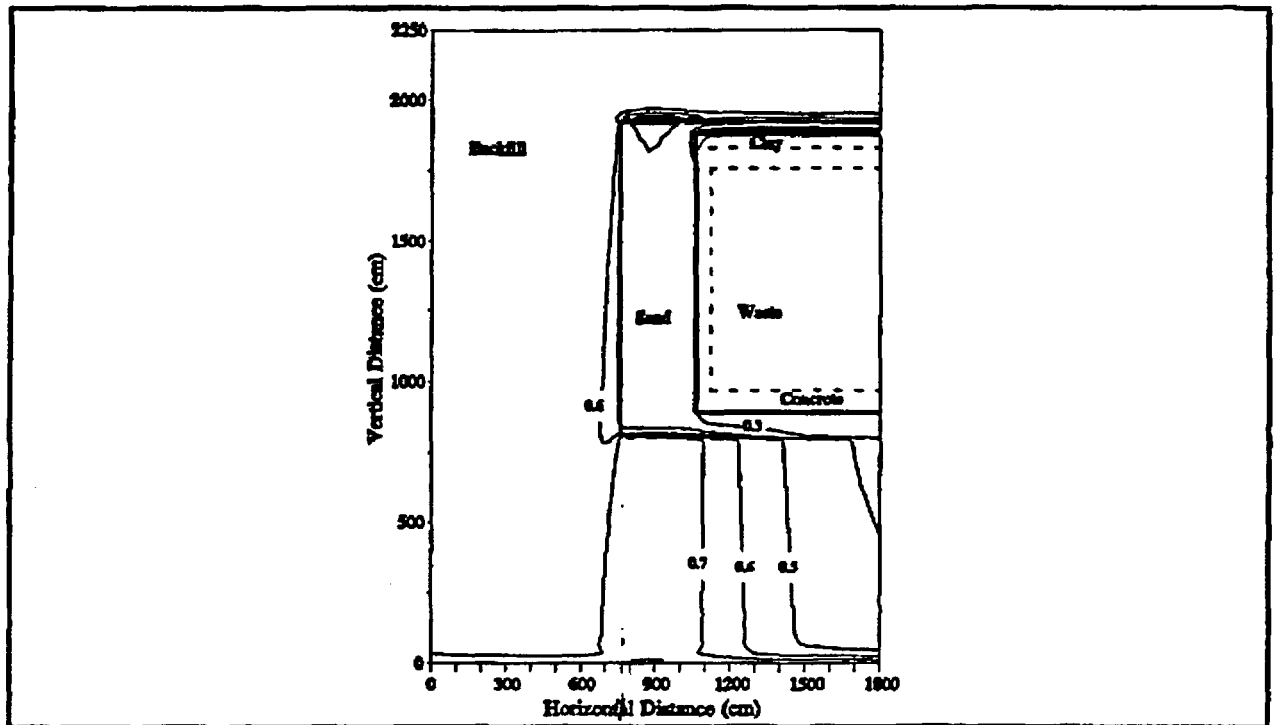
- First a domain consisting entirely of backfill was simulated with the 4 cm/year upper boundary in order to obtain a uniform initial pressure head and saturation distribution.
- The vault and waste form were then superimposed on the model space, and the upper flow boundary was kept at 4 cm/year. This new system was simulated until it reached steady state. The results of this simulation were used for the first time period in which the vault is assumed to remain intact.
- The next step was to change the hydraulic parameters to those of the cracked vault in the input file and make another flow simulation. The resulting flow field was used for the intermediate time period transport simulations.

- The final flow field was then simulated using hydraulic properties of the collapsed vault. This flow field was used for the final time interval of the transport simulations.
- The flow fields, calculated from the above steps, were used for each step of the transport simulations.
- With the exception of the solubility limited runs, all transport runs simulated a total of 200,000 years. The solubility limited runs continued until all of the mass had dissolved out of the solid phase.

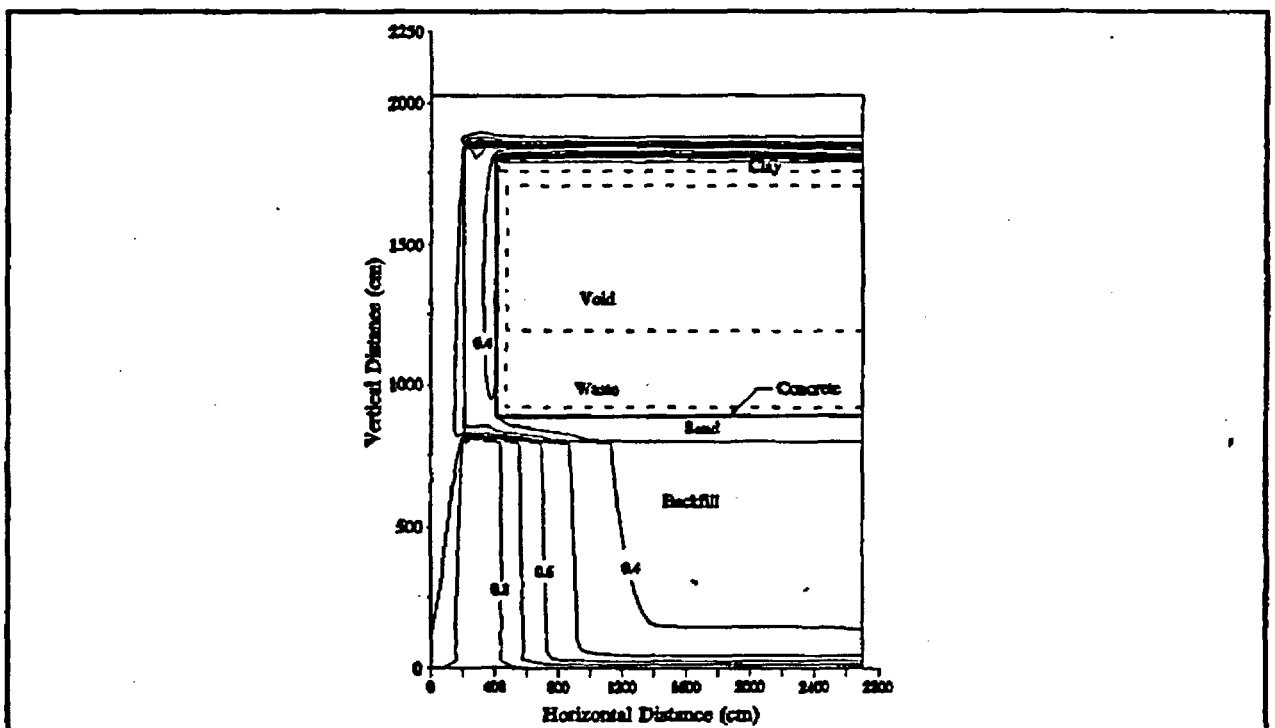
Table 4.1-2 defines the simulation time for each state of the vault. Steady-state saturation fields for each time period are shown in Figs. 4.1-3, 4.1-4, and 4.1-5. The success of the flow simulation was determined by three methods. The first was by monitoring the local convergence of the flow simulation in relation to a specified convergence criterion. The PORFLOW code allows a simulation to proceed even though convergence may not be achieved at a particular time step. This was the case during the initial time steps of the flow simulation. However, as the simulations continued, the results began to converge to the specified convergence criterion. The second method involved monitoring the flow of water through the domain. Monitoring of an internal flux plane around the upper and lower boundaries allows a check to confirm if the correct amount of water was flowing through the domain. Mass balance for each flow field matched exactly (to four significant digits), except for the flow field for the intact LAW vault simulation, where the error was 0.4%, which was judged to be acceptable.

Table 4.1-2. Simulation time for each state of the vault

Vault State	ILNT	LAW
Intact	0 to 575 years	0 to 1400 years
Cracked	575 to 1050 years	1400 to 3100 years
Failed	1050 to end	3100 to end



(a)



(b)

Fig. 4.1-3. Steady state saturation for the Intact period for the ILNT (a), and LAW (b) vaults.

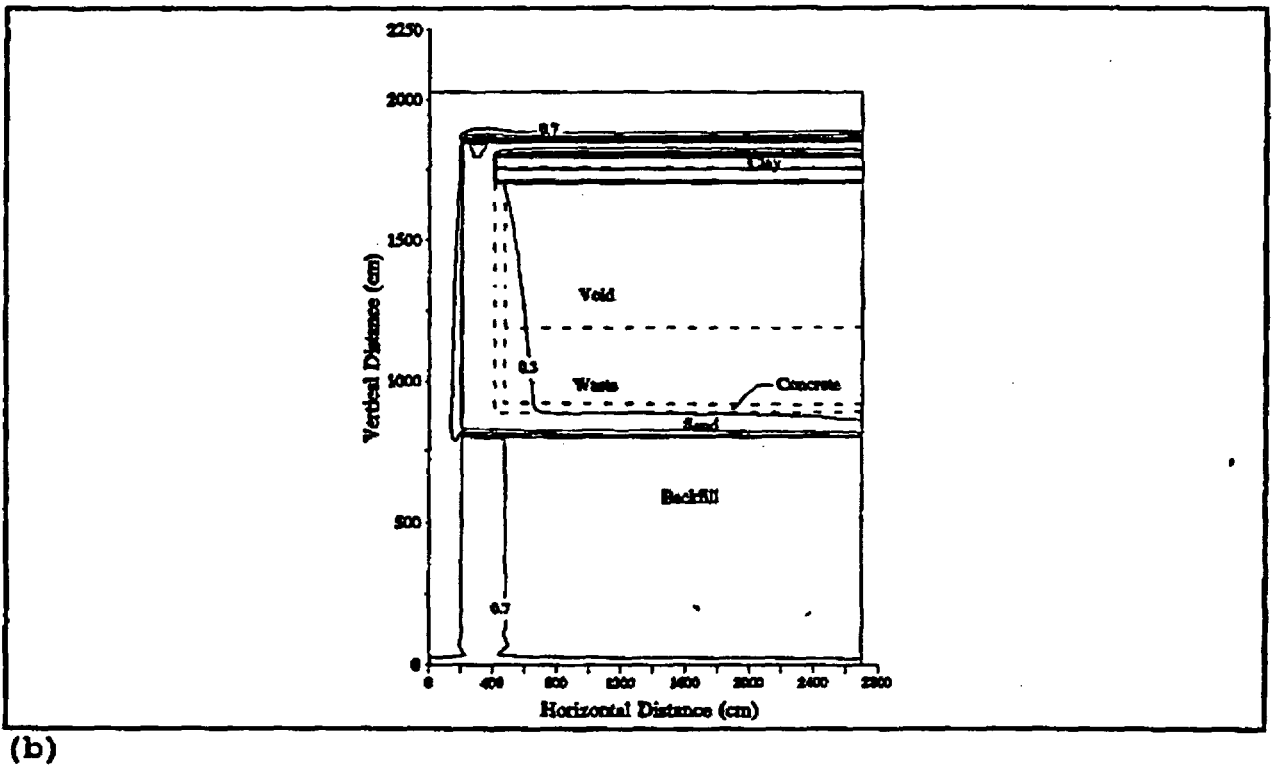
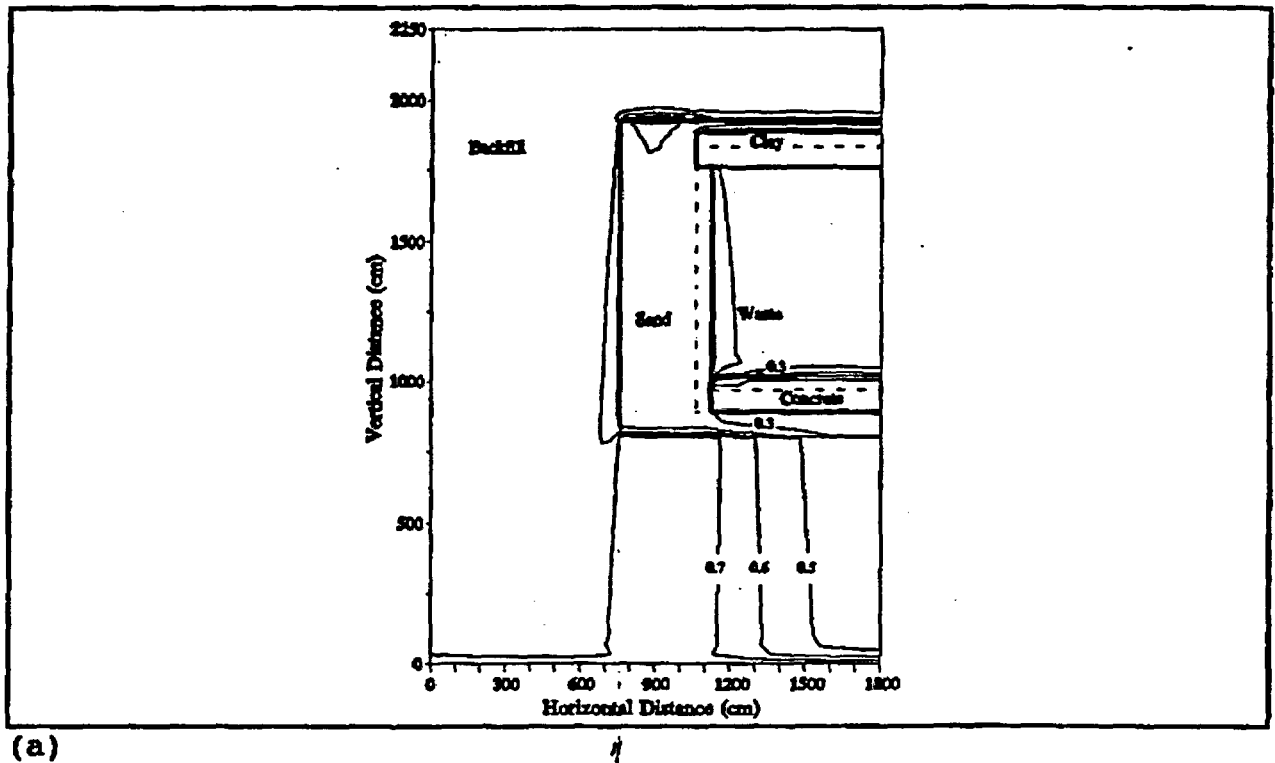
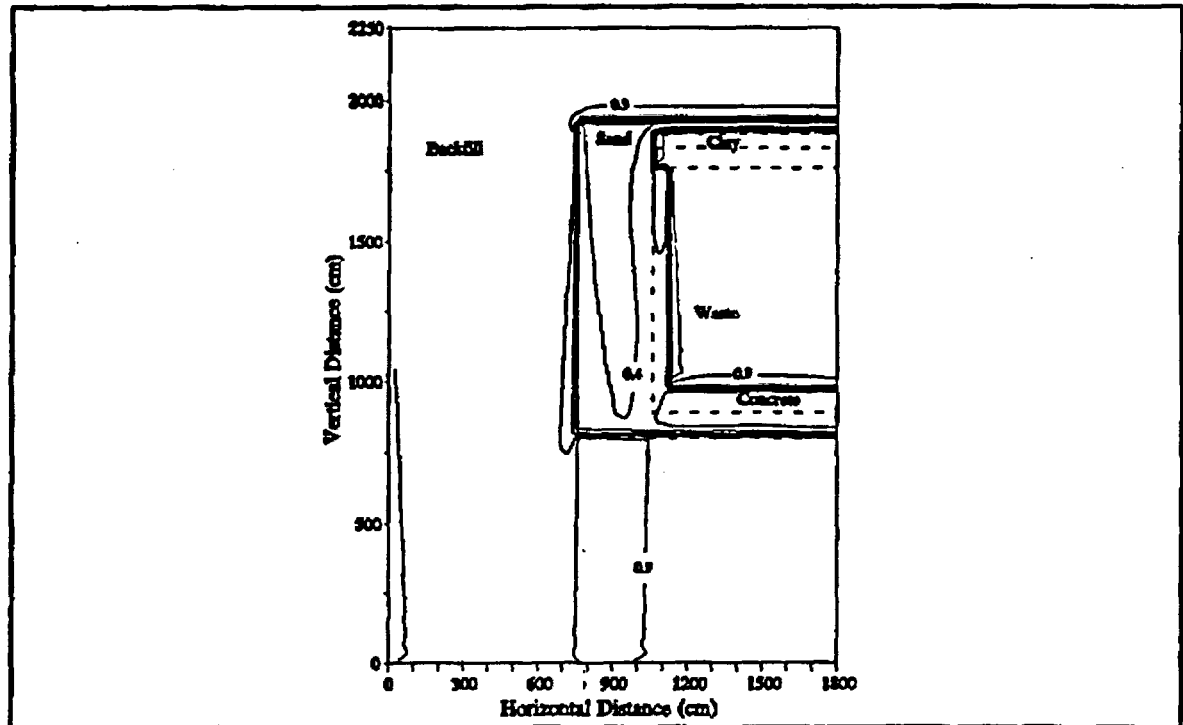
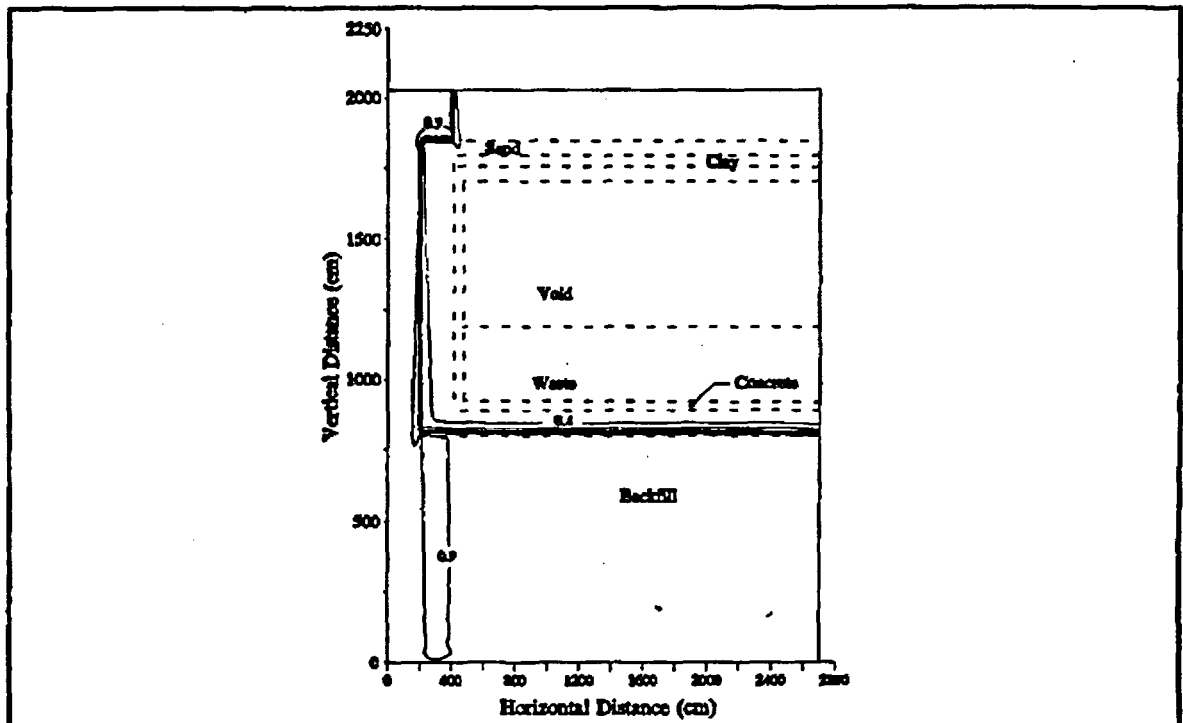


Fig. 4.1-4. Steady state saturation for the Cracked period for the ILNT (a), and LAW (b) vaults.



(a)



(b)

Fig. 4.1-5. Steady state saturation for the Failed period for the ILNT (a), and LAW (b) vaults.

The third method, in which a flow simulation was judged to be at steady state, was to monitor the maximum and minimum x and y velocities, pressures, and saturations. The simulations were continued until the maximums and minimums remained constant to at least 3 significant digits. The success of the transport simulation was determined through a similar mass balance approach. For each contaminant considered, all the initial mass was contained within the vault. The mass of contaminant leaving the simulation domain, via the top and bottom boundaries, was integrated over the entire simulation. For these two boundaries, the amount that left via the top boundary was always negligible. The sum of the exiting mass and the mass remaining in the domain at the end of the simulation was compared to the initial mass (for those radionuclides with a short enough half life to have an impact decay was factored into the equation). The transport mass balance errors were all less than 1%.

The flux of each radionuclide to the aquifer is needed to predict the groundwater concentration. The peak flux to the water table for each nuclide and its corresponding time are given in Table 4.1-3. Isotopes of U and Pu are not included in this table, as the fluxes of these isotopes were estimated in a different manner described below. Graphical representations of the flux to the aquifer for selected nuclides are given in Appendix A.1.4.1.

Solubility-limited simulations were conducted for isotopes of Pu and U in both vaults. The only modification to the above process for the solubility-limited simulations was to use the estimated solubility limit for each element as described in Appendix D. The initial concentrations for Pu isotopes were based upon an assumed initial inventory of 150 Ci/vault of each nuclide. The initial mass assumed for U isotopes in the transport simulations was 10,000 kg/vault. The assumed initial inventories were chosen to exceed the solubility limit. The solubility limit is the controlling factor in this type of simulation and not the initial mass.

Because the initial mass for each of the nuclides was much greater than the solubility limit, the pore water concentration coming out of the waste form was equal to the solubility-limited concentration for several thousand years. Consequently, the only reduction of the pore water concentration in the waste comes from decay during travel out of the vault and to the water table. Table 4.1-4 lists the solubility limit assumed for each nuclide and the peak flux (Ci/year) entering the aquifer from all of the ILNT and LAW vaults.

Table 4.1-3. Peak fractional mass flux release to the aquifer for EAV radionuclides except isotopes of U and Pu

Nuclide	ILNT Vaults (10)		LAW Vaults (21)	
	Fractional Flux (pCi/year-pCi)	Time (year)	Fractional Flux (pCi/year-pCi)	Time (year)
³ H	9.7×10^{-14}	114	5.9×10^{-11}	85
¹⁴ C	1.7×10^{-06}	12,000	1.4×10^{-04}	4,800
⁵⁹ Ni	5.0×10^{-05}	14,500	2.2×10^{-04}	9,300
⁷⁹ Se	2.9×10^{-04}	2,000	2.3×10^{-03}	3,300
⁹⁰ Sr	1.3×10^{-16}	975	$<1 \times 10^{-20}$	$<1,000$
⁹⁰ Y	3.2×10^{-19}	975	N/A	N/A
⁹⁹ Tc	7.4×10^{-04}	1,700	1.8×10^{-03}	3,200
¹²⁶ Sn	2.5×10^{-04}	5,600	6.7×10^{-04}	5,100
¹²⁹ I	8.1×10^{-04}	1,100	4.3×10^{-03}	1,700
¹³⁵ Cs	7.7×10^{-04}	2,700	8.6×10^{-04}	4,700
²³² Th	1.1×10^{-05}	110,000	3.0×10^{-05}	55,800
²³⁷ Np	2.7×10^{-04}	24,800	2.3×10^{-04}	6,200
²⁴¹ Am	3.0×10^{-11}	7,700	4.0×10^{-11}	7,400
²⁴³ Am	1.2×10^{-06}	19,700	3.2×10^{-05}	12,400
²⁴⁴ Cm	$<1 \times 10^{-20}$	$>1,000$	$<1 \times 10^{-20}$	$<1,000$
²⁴⁵ Cm	1.0×10^{-06}	24,200	2.8×10^{-05}	14,800
²⁴⁶ Cm	2.4×10^{-07}	20,900	1.1×10^{-05}	13,900
²⁴⁷ Cm	1.2×10^{-05}	56,500	9.7×10^{-05}	16,000
²⁴⁸ Cm	1.0×10^{-05}	48,300	9.4×10^{-05}	16,000
²⁴⁹ Bk	N/A	N/A	$<1 \times 10^{-20}$	$<1,000$
²⁴⁹ Cf	4.3×10^{-15}	6,900	2.7×10^{-12}	7,100
²⁵¹ Cf	1.1×10^{-10}	10,600	3.2×10^{-08}	8,900
²⁵² Cf	$<1 \times 10^{-20}$	$<1,000$	$<1 \times 10^{-20}$	$<1,000$

Table 4.1-4. Solubility limit and peak flux to the aquifer for isotopes of U and Pu*

Nuclide	Solubility Limit, g/cc	ILNT Vaults (10)		LAW Vaults (21)	
		Flux, Ci/yr	Time, year	Flux, Ci/yr	Time, year
²³³ U	7.2×10^{-11}	1.7×10^{-3}	106,000	4.8×10^{-2}	41,200
²³⁴ U	7.2×10^{-11}	1.0×10^{-3}	92,900	3.1×10^{-2}	44,200
²³⁵ U	7.2×10^{-11}	4.0×10^{-7}	83,100	1.3×10^{-6}	44,200
²³⁶ U	7.2×10^{-11}	1.2×10^{-5}	90,400	3.3×10^{-4}	27,600
²³⁸ U	7.2×10^{-11}	6.2×10^{-4}	86,600	1.7×10^{-6}	39,200
²³⁸ Pu	1.0×10^{-13}	6.7×10^{-18}	3,111	6.4×10^{-16}	4,410
²³⁹ Pu	1.0×10^{-13}	5.3×10^{-6}	64,300	1.8×10^{-5}	21,400
²⁴⁰ Pu	1.0×10^{-13}	7.6×10^{-6}	38,800	4.3×10^{-5}	29,100
²⁴¹ Pu	1.0×10^{-13}	$<10^{-50}$	1,050	$<10^{-50}$	522
²⁴² Pu	1.0×10^{-13}	5.0×10^{-7}	102,000	1.3×10^{-6}	22,000
²⁴⁴ Pu	1.0×10^{-13}	4.7×10^{-9}	99,300	1.3×10^{-7}	18,800

* Based on 150 Ci/vault for Pu and 10,000 kg/vault for U.

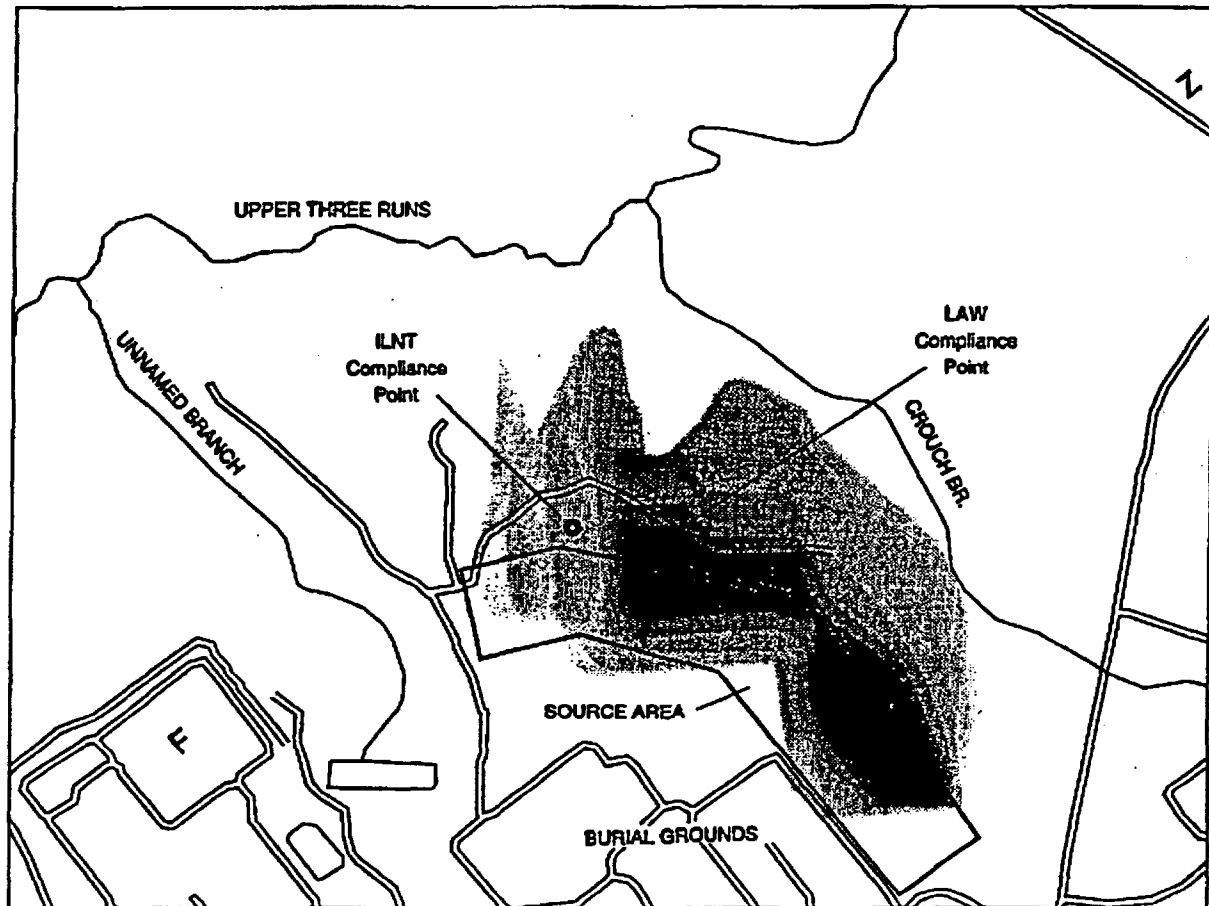
4.1.3 Groundwater Concentrations

Groundwater concentrations at the compliance point for groundwater protection were predicted by using the near-field results, which supplied the contaminant flux to the water table as a function of time. Fractional fluxes were specified as the source term to groundwater and the concentrations at the compliance point were specified as pCi/cc-Ci. In other words, the groundwater concentration (pCi/cc) was based upon an initial inventory in each set of vaults of one curie. The results could then be used to determine the allowable inventory limits for the EAVs. For uranium and plutonium isotopes, which are solubility limited, the flux to the water table based on an assumed inventory (Sect. 4.1.2.2) was specified as the source term to the groundwater and the concentrations at the compliance point were specified as pCi/cc. The compliance point is assumed to be the point of maximum concentration in groundwater at least 100 m from the edge of the facility, and was determined by surveying the groundwater simulation results to locate this point. The potential for plume overlap from the ILNT and LAW vaults was evaluated to determine if the overlap of these plumes resulted in a groundwater concentration greater than from ILNT or LAW vaults alone. It was determined that the maximum groundwater concentrations were not located in the area of plume overlap (see Fig. 4.1-6).

Tables 4.1-5 and 4.1-6 provide the maximum predicted contaminant concentrations at the compliance point for groundwater protection, and the time of occurrence. Results for the ILNT and LAW vaults are provided in Tables 4.1-5 and 4.1-6, respectively.

Radioactive daughter contributions to groundwater concentrations were considered in the following ways. For radionuclides that are relatively short-lived (with half-lives less than 1000 years) and that decay to longer-lived radioactive progeny, daughter contributions to groundwater radioactivity per Ci of parent activity originally in all of the vaults were estimated in the following manner. First, it was conservatively assumed that the parent radionuclide decays completely to the daughter in the vaults. This assumption neglects the loss of parent through leaching and the gradual, rather than instantaneous, nature of daughter ingrowth. The initial activity of the daughter per Ci of original inventory of parent was calculated from:

$$A_{D0} = A_{P0} \frac{\lambda_D}{\lambda_P} = \frac{\lambda_D}{\lambda_P}$$



SRS157

SAVANNAH RIVER PLANT

H-3 Contours, Water Table, K=16, 130 Years

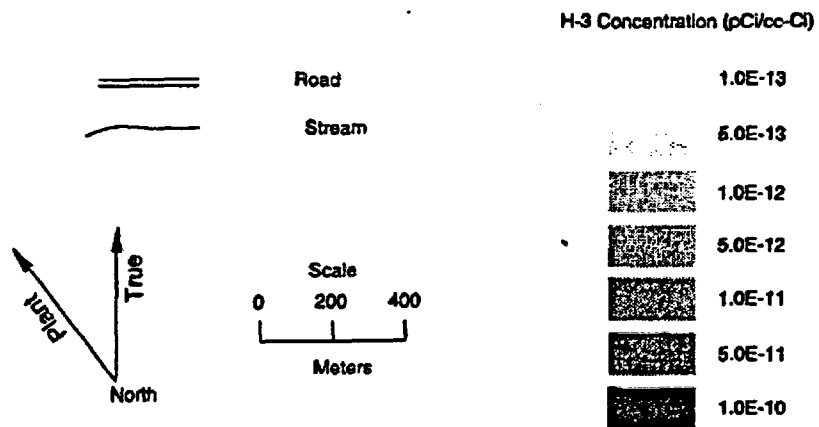


Fig. 4.1-6. Contaminant plume overlap for the LAW and ILNT vaults at E-Area.

Rev. 0

Table 4.1-5. Predicted groundwater compliance concentration for the ILNT vaults

Radionuclides	Groundwater Conc. at 10,000 years, (pCi/cc-Ci) ^a	Peak Groundwater Conc., (pCi/cc - Ci) ^a	Time of Peak Groundwater Conc., (years)
Am-241	---	6.4×10^{-12}	9,000
Np-237	$8.9 \times 10^{-7} e$	$2.8 \times 10^{-6} e$	27,000
Am-243	2.3×10^{-7}	1.2×10^{-5}	27,000
Bk-249	---	---	---
Cm-245	$3.7 \times 10^{-12} e$	$1.2 \times 10^{-9} e$	33,000
C-14	6.5×10^{-5}	8.7×10^{-5}	12,300
Cf-249	---	5.9×10^{-16}	7,900
Cm-245	$1.5 \times 10^{-9} e$	$5.0 \times 10^{-7} e$	33,000
Cf-251	4.7×10^{-11}	9.4×10^{-11}	13,000
Cm-247	$3.6 \times 10^{-12} e$	$2.1 \times 10^{-8} e$	76,000
Cf-252	---	---	---
Cm-248	$1.0 \times 10^{-12} e$	$2.5 \times 10^{-9} e$	72,000
Cm-244	---	---	---
Pu-240	$7.3 \times 10^{-6} e,d$	$1.2 \times 10^{-4} e,d$	66,000
Cm-245	3.6×10^{-8}	1.2×10^{-5}	33,000
Cm-246	1.8×10^{-8}	1.9×10^{-6}	27,000
Cm-247	6.2×10^{-8}	3.7×10^{-4}	76,000
Cm-248	1.3×10^{-7}	3.2×10^{-4}	72,000
Cs-135	---	4.2×10^{-3}	6,700
H-3	---	2.7×10^{-12}	130
I-129	---	9.4×10^{-2}	1,400
Ni-59	3.0×10^{-5}	9.4×10^{-4}	32,000
Np-237	4.4×10^{-3}	1.4×10^{-2}	27,000
Sc-79	---	7.4×10^{-3}	3,000
Sn-126	2.5×10^{-3}	2.8×10^{-3}	12,000
Sr-90	---	2.7×10^{-17}	1,100
Tc-99	---	4.1×10^{-2}	1,800
Th-232	4.0×10^{-17}	1.5×10^{-4}	300,000

see footnotes at end of table

Table 4.1-5. (continued)

Radionuclides	Groundwater Conc. at 10,000 years, (pCi/cc)	Peak Groundwater Conc., (pCi/cc)	Time of Peak Groundwater Conc. (years)
U-233	3.5×10^{-3}	8.1×10^{-2}	160,000
Th-229	2.3×10^{-11}	---	---
U-234	2.3×10^{-3}	5.5×10^{-2}	150,000
Th-230	4.0×10^{-18}	---	---
Ra-226	3.9×10^{-3}	---	---
U-235	6.9×10^{-6}	1.9×10^{-4}	110,000
Pa-231	3.2×10^{-6} ^e	---	---
U-236	2.4×10^{-5}	5.8×10^{-4}	230,000
Th-232	1.3×10^{-19}	---	---
U-238	1.4×10^{-7}	3.0×10^{-6}	140,000
U-234	$\leq 2.3 \times 10^{-3}$	---	---
Th-230	6.4×10^{-24}	---	---
Ra-226	6.2×10^{-9}	---	---
Pu-238	---	9.7×10^{-20}	3,300
U-234	$\leq 2.3 \times 10^{-3}$	---	---
Th-230	3.5×10^{-24}	---	---
Ra-226	3.4×10^{-9}	---	---
Pu-239	4.7×10^{-6}	1.5×10^{-4}	220,000
U-235	$\leq 6.9 \times 10^{-6}$	---	---
Pa-231	2.1×10^{-11}	---	---
Pu-240	7.3×10^{-6}	1.2×10^{-4}	66,000
Pu-242	2.7×10^{-7}	2.4×10^{-5}	500,000
Pu-244	2.1×10^{-9}	2.5×10^{-7}	400,000

- ^a Except for isotopes of plutonium and uranium, for which groundwater concentrations are based on solubility limits, and thus, are expressed in pCi/cc per any inventory in the vaults.
- ^b Peak groundwater concentration at the compliance point for groundwater protection occurred before 10,000 years.
- ^c Units for radioactive daughters are pCi/cc per Ci of parent activity originally in vaults.
- ^d Assumes Pu-240 reaches same concentration based on solubility-limited calculations as a daughter of Cm-244.
- ^e Ac-227 daughter accounted for in EDE.

Table 4.1-6. Predicted groundwater compliance concentration for the LAW vaults

Radionuclides	Groundwater Conc. at 10,000 years, (pCi/cc-Ci) ^a	Peak Groundwater Conc., (pCi/cc - Ci) ^a	Time of Peak Groundwater Conc., (years)
Am-241	---	1.1×10^{-12}	8,700
Np-237	$3.2 \times 10^{-7} c$	$3.2 \times 10^{-7} c$	10,000
Am-243	4.2×10^{-6}	3.7×10^{-5}	18,000
Bk-249	---	---	---
Cm-245	$1.1 \times 10^{-10} c$	$3.8 \times 10^{-9} c$	21,000
C-14	---	1.5×10^{-3}	5,400
Cf-249	---	5.0×10^{-14}	8,100
Cm-245	$4.5 \times 10^{-8} c$	$1.5 \times 10^{-6} c$	21,000
Cf-251	3.1×10^{-9}	3.5×10^{-9}	11,000
Cm-247	$1.7 \times 10^{-10} c$	$1.3 \times 10^{-8} c$	23,000
Cf-252	---	---	---
Cm-248	$2.3 \times 10^{-11} c$	$1.6 \times 10^{-9} c$	23,000
Cm-244	---	---	---
Pu-240	$1.6 \times 10^{-5} cd$	$9.5 \times 10^{-5} cd$	45,000
Cm-245	1.1×10^{-6}	3.7×10^{-5}	21,000
Cm-246	5.7×10^{-7}	1.0×10^{-5}	19,000
Cm-247	3.0×10^{-6}	2.2×10^{-4}	23,000
Cm-248	3.0×10^{-6}	2.1×10^{-4}	23,000
Cs-135	---	6.7×10^{-4}	8,400
H-3	---	2.1×10^{-10}	97
I-129	---	2.4×10^{-2}	1,800
Ni-59	3.4×10^{-5}	2.1×10^{-4}	21,000
Np-237	1.6×10^{-3}	1.6×10^{-3}	10,000
Sc-79	---	5.1×10^{-3}	3,600
Sn-126	4.7×10^{-4}	4.7×10^{-4}	10,000
Sr-90	---	1.5×10^{-22}	520
Tc-99	---	1.9×10^{-2}	3,400
Th-232	1.2×10^{-17}	2.3×10^{-5}	210,000
see footnotes at end of table			

Fig. 4.1-6. (continued)

Radionuclide	Groundwater Conc. at 10,000 years, (pCi/cc)	Peak Groundwater Conc., (pCi/cc)	Time of Peak Groundwater Conc., (years)
U-233	1.0×10^{-1}	4.1×10^{-1}	260,000
Th-229	1.4×10^{-11}	---	---
U-234	6.2×10^{-2}	2.9×10^{-1}	200,000
Th-230	1.6×10^{-17}	---	---
Ra-226	2.5×10^{-1}	---	---
U-235	2.0×10^{-5}	1.3×10^{-4}	230,000
Pa-231	$2.1 \times 10^{-4}^c$	---	---
U-236	7.0×10^{-4}	3.9×10^{-3}	320,000
Th-232	8.2×10^{-20}	---	---
U-238	3.4×10^{-6}	2.0×10^{-5}	230,000
U-234	$\leq 6.2 \times 10^{-2}$	---	---
Th-230	2.6×10^{-23}	---	---
Ra-226	4.0×10^{-7}	---	---
Pu-238	---	1.2×10^{-18}	4,800
U-234	$\leq 6.2 \times 10^{-2}$	---	---
Th-230	1.3×10^{-23}	---	---
Ra-226	2.1×10^{-7}	---	---
Pu-239	1.0×10^{-5}	6.4×10^{-5}	160,000
U-235	$\leq 2.0 \times 10^{-5}$	---	---
Pa-231	1.3×10^{-9}	---	---
Pu-240	1.6×10^{-5}	9.5×10^{-5}	45,000
Pu-242	7.7×10^{-7}	1.0×10^{-5}	620,000
Pu-244	7.1×10^{-8}	1.5×10^{-6}	660,000

- ^a Except for isotopes of plutonium and uranium, for which groundwater concentrations are based on solubility limits, and thus, are expressed in pCi/cc per any inventory in the vaults.
- ^b Peak groundwater concentration at the compliance point for groundwater protection occurred before 10,000 years.
- ^c Units for radioactive daughters are pCi/cc per Ci of parent activity originally in vaults.
- ^d Assumes Pu-240 reaches same concentration based on solubility-limited calculations as a daughter of Cm-244.
- ^e Ac-227 daughter accounted for in EDE.

where

A_{D0} = initial activity of the daughter, Ci,

A_{P0} = initial activity of the parent (= 1 Ci),

λ_D = radioactive decay constant ($.693/T_{1/2}$) of the daughter (yr^{-1}), and

λ_P = radioactive decay constant of the parent (yr^{-1}).

The peak concentration of the daughter, per Ci of parent radionuclide, was then calculated by multiplying the initial activity of the daughter per Ci of parent activity (A_{D0}) by the 10,000-year and peak groundwater concentration of the daughter (pCi/cc-Ci). The daughter concentration is expressed in terms of pCi/cc of daughter per Ci of parent activity.

For relatively long-lived radionuclides with short-lived daughters, the EDEs used in this PA (Table A.4-6 of Appendix A.4) consider that short-lived daughters are in secular equilibrium with the parent radionuclide. Therefore, separate accounting of these daughters does not need to be carried out in the groundwater simulations.

Several radionuclides in the inventory lists for both the ILNT and LAW vaults are long-lived parents of potentially radiologically-significant daughters. Radiologically-significant daughters are defined here as radioactive decay products that may reach the groundwater compliance point by 10,000 years in concentrations that are significant with respect to the 10,000-year concentration of the parent. Consideration is given to the fact that the allowable concentration of the daughter may be less than that of the parent, as is the case with some decay products of uranium isotopes. The long-lived parents of decay products that fall into this category include Np-237, Cm-246, Cm-247, Cm-248, isotopes of uranium, and isotopes of plutonium. The following discussion provides the rationale for neglecting or considering decay products of these radionuclides in the groundwater-based dose analysis for off-site individuals.

First, note that for the uranium and plutonium decay products of the long-lived radionuclides listed, solubility limits are applied in the waste. Although uranium and plutonium decay products may also be produced in transit from the waste to the compliance point in groundwater, the production during transport is minimal because transit times are

small compared to half-lives of the parent radionuclides. Therefore, the peak groundwater concentrations calculated for the uranium and plutonium isotopes as parent radionuclides can be assumed to constitute an upper bound on the peak groundwater concentration of these isotopes as decay products.

For Np-237, U-233 is the first daughter of interest, since the short-lived daughter Pa-233 will never exceed the Np-237 concentration in groundwater based on its considerably greater sorption on surfaces (K_d exceeds that of Np by a factor of 100; Sheppard and Thibault 1990). As noted above, uranium is considered to be solubility limited at the source in this assessment, and thus, the compliance-point groundwater concentration of this Np-237 decay product will never exceed the value calculated for U-233 considered as the parent radionuclide. The only decay product of U-233 that is relatively long-lived is Th-229. By 10,000 years, the maximum production of Th-229 is approximately 1% of the original Np-237 activity. Because Th-229 is much more strongly sorbed than Np-237, and can only reach a small fraction of the Np-237 activity in the source, it was not deemed a radiologically-significant radionuclide in the Np-237 decay chain. Therefore, radioactive decay products of Np-237 were not considered further in the analysis.

For Cm-246, the only long-lived decay products are Pu-242 and U-238, which are both considered to be solubility-limited at the source. Thus, radioactive decay products of Cm-246 were not considered further in the groundwater analysis.

For Cm-247, the long-lived decay products are Am-243, Pu-239, and U-235. Am-243 is assumed to sorb similarly to Cm-247 and can be, therefore, assumed to travel at the same rate. At 10,000 years, the activity of Am-243 relative to that of Cm-247 is approximately 60%, and this activity relationship can be assumed to hold at the groundwater compliance point. Therefore, Am-243 should be considered as a potentially radiologically-significant daughter. Aside from solubility-limited uranium and plutonium isotopes in the Cm-247 decay chain, Pa-231 is the only other long-lived radionuclide. However, the ingrowth of Pa-231 in 10,000 years is less than $1 \times 10^{-4}\%$, because of the very long-lived U-235 intermediary, and thus, is not considered radiologically significant.

For Cm-248, no long-lived radionuclides other than isotopes of uranium and plutonium achieve significant activities relative to that of the parent in this decay chain. Thus, radioactive decay products of Cm-248 were not considered further in the groundwater analysis.

For U-233, which is considered solubility-limited, the long-lived Th-229 decay product is of potential significance. By delaying loss of U-233 from the waste due to solubility limitations, the U-233 source of Th-229 in the waste remains for a long time. By 10,000 years, assuming a negligible amount of U-233 is lost from the waste, the Th-229 activity may reach close to 60% of the U-233 initial activity. Thorium is also slowly leached from the waste due to its high sorption potential ($K_d = 3000 \text{ mL/g}$). A conservative estimate of the peak activity of Th-229 in the ILNT vaults in the first 10,000 years after disposal is $5.8 \times 10^5 \text{ Ci}$, based on an initial U-233 content of 10,000 kg in each of 10 vaults. This Th-229 activity is conservatively assumed to be present in the 10 ILNT vaults at the time of disposal. For the LAW vaults, a similar calculation results in an initial activity of the Th-229 daughter in the 21 LAW vaults of $1.2 \times 10^6 \text{ Ci}$ of Th-229. Ten thousand-year groundwater concentrations of the Th-229 daughter of U-233 are estimated by multiplying the assumed initial activity of Th-229 by the pCi/cc-Ci concentrations of Th-232 in Tables 4.1-5 and 4.1-6, and are reported with the U-233 parent concentration. Because Th-229 decays more rapidly than Th-232, this adds additional conservatism to the result.

For U-234, potentially radiologically-significant daughters include Th-230, Ra-226, and short-lived decay products. The shorter-lived decay products are included in the EDE for Ra-226. As with U-233, the Th-230 concentration in the waste can be estimated at 10,000 years by assuming negligible loss of U-234 and Th-230 from the waste. However, because Ra-226 is more mobile than Th-230 and solubility-limited U-234, estimating the peak concentration of Ra-226 in the waste up to 10,000 years is more difficult. Therefore, the ingrowth and loss via leaching and decay of these decay products of U-234 were simulated rigorously in the PORFLOW runs for U-234 for the ILNT vaults, and the 10,000-year value is reported as pCi/cc with the U-234 concentration in Table 4.1-5. Observations from the ILNT and LAW vault simulation results allow parallels to be drawn for the Th-230 and Ra-226 contributions to groundwater concentrations for the LAW vaults. For Th-232, the ratio of the 10,000-year peak groundwater concentration for the LAW vaults to the 10,000-year concentration for the ILNT vaults is approximately four. Therefore, assuming this same ratio for the daughter calculations, the groundwater concentration of the Th-230 daughter of U-234 in the LAW vaults was estimated. For Ra-226, no simulations of this isotope were carried out.

However, the overall ratio of 10,000-year groundwater concentrations from LAW to ILNT vaults ranges up to about a factor of 65 (Tables 4.1-5 and 4.1-6). Assuming for Ra-226 that the ratio of 10,000-year groundwater concentrations from LAW to ILNT vaults is 65, the Ra-226 groundwater concentration resulting from decay of U-234 in the LAW vaults was estimated.

For U-235, the only potentially radiologically-significant decay products include Pa-231 and Ac-227. Both of these daughter radionuclides exhibit similar sorption behavior, and thus, can be assumed to travel similarly. Assuming negligible transport of U-235 in 10,000 years, the activity of Pa-231 and Ac-227 can achieve activities approaching 20% of the original U-235 activity. However, the mobility of Pa-231 and Ac-227 will limit the peak activity of the radionuclides in the waste, due to continuous leaching during production by decay. Because the ingrowth and loss via leaching and decay of these decay products are not readily estimated, PORFLOW runs simulating these processes were carried out for the U-235 chain in the ILNT vaults. As with U-234, daughter concentrations arising from U-235 in LAW vaults were estimated from LAW:ILNT vault 10,000-year concentration ratios, assuming an upper-end value of 65 for this ratio.

For U-236, ingrowth of all potentially radiologically-significant decay products is limited by ingrowth of the first member of the decay chain, Th-232, which has a half-life of 1.5×10^{10} years. All other members of the decay chain are short-lived, and can be assumed in equilibrium with Th-232 during transit. Assuming no leaching of the parent, U-236, and no leaching of the daughters, the maximum activity of any daughter is less than 5×10^{-5} % of the initial U-236 activity. Groundwater concentrations of Th-232, as a daughter of U-236, were conservatively estimated by assuming that this 10,000-year activity is present at the time of disposal. Based on the 10,000 kg/vault U-236 initial inventory, this corresponds to an initial activity of 3.3×10^{-3} Ci in the 10 ILNT vaults, and 6.8×10^{-3} Ci of Th-232 in the LAW vaults. Ten thousand-year groundwater concentrations of the Th-232 daughter of U-233 are calculated by multiplying the assumed initial activity of Th-232 by the pCi/cc-Ci concentrations in Tables 4.1-5 and 4.1-6, and are reported with the U-233 parent concentration.

For U-238, the first long-lived radiologically-significant daughter in the decay chain is U-234. The decay products of U-234 are considered for the U-234 parent in the waste. By 10,000 years, assuming no leaching of uranium isotopes, the activity of U-234 will be approximately 3% of that of U-238. Therefore, a conservative estimate of the contribution of the U-234 daughters to the U-238 chain is based on the assumption that the initial activity of the U-234 daughter of U-238 is 1 Ci for the 10 ILNT vaults and 2.1 Ci for the LAW vaults, or 3% of the initial 10,000 kg U-238/vault. Using this method to estimate initial inventory of U-234, the results of the U-234 daughter simulations were scaled to these initial activities to derive groundwater concentrations of Th-230 and Ra-226 arising from U-238.

For Pu-238, the first radiologically-significant decay product is U-234. The peak activity of U-234 in the waste relative to the initial activity of Pu-238 in the waste can be estimated according to the procedures described above for short-lived parents with longer-lived daughters. This method uses the ratio of the half-lives of parent-to-daughter to conservatively estimate ingrowth. Because the ingrowth and loss of decay products of U-234 were simulated with PORFLOW, these results can be used to estimate the groundwater concentrations of the decay products of Pu-238. The initial activity of U-234 in ILNT and LAW vaults arising from decay of Pu-238 was estimated to be 3.6×10^{-4} Ci per Ci of Pu-238 initially present. With 150 Ci of Pu-238 assumed initially in each vault, the total inventory of U-234 arising from Pu-238 is 0.54 Ci for the 10 ILNT vaults, and 1.1 Ci for the LAW vaults. The 10,000-year groundwater concentrations for Th-230 and Ra-226 were calculated by scaling the results of the U-234 daughter calculations to these initial inventories of U-234 in each vault type. The results are presented with the Pu-238 concentrations in Tables 4.1-5 and 4.1-6.

For Pu-239, other than solubility-limited U-235, the potentially radiologically-significant daughters are Pa-231 and Ac-227. Assuming no leaching of Pu-239 or U-235, the activity of U-235 is approximately 9×10^{-5} % of the original activity of Pu-239 at 10,000 years after disposal. This corresponds to U-235 activities of 1.4×10^{-3} Ci for all 10 of the ILNT vaults, and 2.8×10^{-3} Ci for all 21 of the LAW vaults. Conservatively assuming that these activities exist initially, the daughter contributions to groundwater concentrations can be estimated using the results of the U-235 PORFLOW simulations, which consider transport of decay products, described previously.

For Pu-240, Pu-242, and Pu-244, other than solubility-limited uranium isotopes, there are no potentially radiologically-significant decay products. For Pu-240, very long-lived Th-232 limits ingrowth of other decay products to less than $10^{-7}\%$ of the initial activity of Pu-240. For Pu-242, very long-lived U-238 and U-235 limit ingrowth of decay products to less than $10^{-9}\%$ of the initial activity of Pu-242. Finally, for Pu-244, Th-232 again limits ingrowth to less than $10^{-7}\%$ of the initial activity of Pu-244. Therefore, decay products of these radionuclides were not considered further in the groundwater analysis.

4.1.4 Dose Analysis for Off-Site Releases of Radionuclides

As described in Sect. 3.2.3.3, the only exposure pathway of concern for off-site releases of radionuclides via the groundwater pathway is direct consumption of groundwater obtained from a well located beyond the 100-m buffer zone around the disposal units. For beta/gamma-emitting and some alpha-emitting radionuclides, the performance objective for protection of groundwater resources, which requires consideration of the drinking water pathway only, is more restrictive than the performance objective for protection of off-site members of the general public, which requires consideration of all exposure pathways involving use of contaminated groundwater. For some alpha-emitting radionuclides, the performance objective for off-site individuals is more restrictive than the performance objective for groundwater protection, due to the high doses per unit activity intake by ingestion, but in these cases the dose from all exposure pathways involving use of contaminated groundwater is only marginally greater than the dose from the drinking water pathway alone. This conclusion assumes that off-site releases of volatile radionuclides (i.e., H-3 and C-14) also can be neglected in the dose analysis beyond the buffer zone (see Appendix A.3).

In order to determine which performance objective is more restrictive for each radionuclide, the MCLs from Table 3.2-1 were compared to the results of the model for estimating dose from the drinking water pathway for off-site individuals. The annual EDEs, in rem per year, from the drinking water pathway per unit concentration ($1 \mu\text{Ci/L}$) of radionuclides in

groundwater (from Table A.4-6 of Appendix A.4) are summarized in Table 4.1-7. The radionuclides in this table were selected by the screening analysis described in Sect. 4.1.1, and all potentially significant decay products are included.

For comparison to MCLs, the performance objective of 25 mrem per year for off-site individuals is divided by the EDEs in Table 4.1-7 to derive the concentration limit in drinking water for each radionuclide based on this dose limit. The results of this calculation, converted to appropriate units, and the MCLs from Table 3.2-1 are listed in Table 4.1-8 for comparison. These results indicate that the 25 mrem per year performance objective is more restrictive for most of the alpha-emitting radionuclides, with the exception of Ra-226, Th-230, U-235, and U-238.

The dose analysis for the drinking water pathway is based on the predicted maximum concentrations of radionuclides in groundwater at any location beyond the 100-m buffer zone and at any time up to 10,000 years after disposal. These concentrations for the different disposal units in E-Area are presented in Tables 4.1-5 and 4.1-6. The groundwater concentrations in these tables represent activity concentrations per unit activity (Ci) in all (not each) of the 10 ILNT vaults or all (not each) of the 21 LAW vaults, except for the Pu and U isotopes. Maximum groundwater concentrations for Pu and U isotopes are based on solubility limits in the vaults for 150 Ci of each Pu isotope and 10,000 kg of each U isotope initially in each vault of each type.

The allowable inventories derived for the drinking water pathway from off-site releases of radionuclides are given in Table 4.1-9. These inventories (Ci) are calculated for all isotopes except for those of Pu and U in the following manner. First, the most restrictive performance objective based in Table 4.1-8 is selected by choosing the lowest allowable groundwater concentration of the two values given for each radionuclide. Second, the lowest allowable groundwater concentration is divided by the maximum groundwater concentration up to 10,000 years, per Ci of inventory in either the ILNT or LAW vaults. Because U and Pu isotopes are assumed to be solubility limited in the vaults, a linear relationship between groundwater concentration and initial inventory does not exist and the allowable inventory cannot be calculated. However, the calculated groundwater concentrations for Pu and U can

Table 4.1-7. Annual EDEs from drinking water pathway per unit concentration of radionuclides in groundwater^a

Radionuclide ^b	Annual EDE (rem/y per $\mu\text{Ci/L}$)	Radionuclide ^b	Annual EDE (rem/y per $\mu\text{Ci/L}$)
H-3	4.6×10^{-2}	Pa-231 + d	1.1×10^4
C-14	1.5	U-232 + d	1.5×10^3
Al-26	9.5	U-233	2.0×10^2
Ni-59	1.5×10^{-1}	U-234	1.9×10^2
Ni-63	3.9×10^{-1}	U-235	1.8×10^2
Se-79	6.1	U-236	1.8×10^2
Rb-87	3.5	U-238 + d	1.8×10^2
Sr-90 + d	1.0×10^2	Np-237	2.8×10^3
Zr-93 ^c	1.2	Pu-238	2.8×10^3
Nb-93m	3.9×10^{-1}	Pu-239	3.1×10^3
Tc-99	9.5×10^{-1}	Pu-240	3.1×10^3
Pd-107	1.0×10^{-1}	Pu-242	3.0×10^3
Cd-113m	1.1×10^2	Pu-244	2.9×10^3
Sn-121m	9.5×10^{-1}	Am-241	3.3×10^3
Sn-126 + d	1.3×10^1	Am-242m ^e	3.1×10^3
I-129	2.0×10^2	Am-243	3.3×10^3
Cs-135	5.2	Cm-245	3.3×10^3
Sm-151	2.5×10^{-1}	Cm-246	3.3×10^3
Pb-210 + d	4.9×10^3	Cm-247	3.0×10^3
Ra-226 + d ^d	8.0×10^2	Cm-248	1.2×10^4
Th-229 + d	2.9×10^3	Cf-249	7.4×10^3
Th-230	3.9×10^2	Cf-251	3.4×10^3
Th-232 + d	3.5×10^3		

^a Results are obtained from Table A.4-6 of Appendix A.4.

^b "+ d" denotes short-lived decay products that are assumed to be in secular equilibrium with parent radionuclide; see Table A.4-1 of Appendix A.4 for decay products and branching fractions.

^c Value does not include possible contributions from Nb-93m decay product.

^d Value does not include possible contributions from Pb-210 decay product.

^e Value does not include possible contributions from Pu-238 decay product.

Table 4.1-8 Comparison of MCLs and allowable groundwater concentrations based on the 25 mrem per year performance objective for off-site individuals

Radionuclide	MCL, ^a pCi/L	Allowable Concentration Based on 25 mrem per year, pCi/L
H-3	20,000	540,000
C-14	6,400	16,000
Ni-59	530	160,000
Se-79	660 ^b	4,100
Sr-90	8	250
Tc-99	800	26,000
Sn-126	290 ^b	1,900
I-129	0.5	120
Cs-135	800	4,800
Ra-226	15	31
Ac-227	5.3	— ^c
Pa-231	2.4	2.3
Th-229	15	8.6
Th-230	15	64
Th-232	15	7.1
U-233	190,000 (20 µg/L) ^b	125
U-234	124,000 (20 µg/L) ^b	132
U-235	428 (20 µg/L) ^b	139
U-236	1,270 (20 µg/L) ^b	139
U-238	6.66 (20 µg/L) ^b	139
Np-237	15	8.9
Pu-238	15	8.9
Pu-239	15	8.1
Pu-240	15	8.1

Table 4.1-8. (continued)

Radionuclide	MCL, ^a pCi/L	Allowable Concentration Based on 25 mrem per year, pCi/L
Pu-242	15	8.3
Pu-244	15	8.6
Am-241	15	7.6
Am-243	15	7.6
Cm-244	15	(based solely on Pu-240) ^d
Cm-245	15	7.6
Cm-246	15	7.6
Cm-247	15	8.3
Cm-248	15	2.1
Bk-249	15	(based solely on Cm-245) ^d
Cf-249	15	3.4
Cf-251	15	7.4
Cf-252	15	(based solely on Cm-248) ^d

^a Option 1, Table 3.2-1, unless otherwise noted.

^b Option 3, Table 3.2-1.

^c EDE of Pa-231 parent considers contribution of Ac-227.

^d EDE not provided in Table 4.1-7 because groundwater concentration of parent negligible.

Table 4.1-9. Calculated allowable inventories based on the groundwater pathway
(for off-site doses up to 10,000 years after disposal)^a

Radionuclide	ILNT Vaults (10)	LAW Vaults (21)
	Inventory, Ci	Inventory, Ci
H-3	7.4×10^{12}	9.5×10^{10}
C-14	9.9×10^4	7.4×10^4
Ni-59	1.8×10^4	1.6×10^4
Se-79	8.9×10^1	1.3×10^2
Sr-90	3.0×10^{14}	5.3×10^{10}
Tc-99	2.0×10^1	4.2×10^1
Sn-126	1.2×10^2	6.2×10^2
I-129	5.3×10^3	2.1×10^2
Cs-135	1.9×10^2	1.2×10^3
Th-232	1.8×10^{14}	5.9×10^{14}
Np-237	2.0	5.6
Am-241 ^b	1.0×10^4	2.7×10^4
Am-243	3.3×10^4	1.8×10^3
Cm-244 ^c	5.4×10^4	5.4×10^4
Cm-245	2.1×10^5	6.9×10^5
Cm-246	4.2×10^5	1.3×10^4
Cm-247	1.3×10^5	2.8×10^3
Bk-249 ^b	2.1×10^6	6.9×10^7
Cm-248	1.6×10^4	7.0×10^2
Cf-249 ^b	5.1×10^6	1.7×10^5
Cf-251 ^b	1.6×10^8	2.4×10^6
Cf-252 ^b	2.1×10^9	9.1×10^7
U-233 ^b	Solubility limited ^d	Solubility limited ^d
Th-229 ^c	3.6×10^{14} ($>>10^5$ kg) ^f	1.2×10^{15} ($>>2.1 \times 10^5$ kg) ^g
U-234 ^b	Solubility limited ^d	Solubility limited ^d
Th-230 ^c	1.0×10^{20} ($>>10^5$ kg) ^f	5.2×10^{21} ($>>2.1 \times 10^5$ kg) ^g
Ra-226 ^c	8.0×10^5 ($>10^5$ kg) ^f	2.6×10^4 ($<2.1 \times 10^5$ kg) ^g
U-235 ^b	Solubility limited ^d	Solubility limited ^d
Pa-231 ^c	1.6×10^5 ($>>10^5$ kg) ^f	5.0×10^5 ($>2.1 \times 10^5$ kg) ^g
U-236 ^b	Solubility limited ^d	Solubility limited ^d
Th-232 ^c	3.5×10^{20} ($>>10^5$ kg) ^f	1.2×10^2 ($>>2.1 \times 10^5$ kg) ^g
U-238 ^b	Solubility limited ^d	Solubility limited ^d
U-234 ^c	Solubility limited ^d	Solubility limited ^d
Th-230 ^c	3.4×10^{23} ($>>10^5$ kg) ^f	1.7×10^{23} ($>>2.1 \times 10^5$ kg) ^g
Ra-226 ^c	2.7×10^7 ($>>10^5$ kg) ^f	8.8×10^5 ($>>2.1 \times 10^5$ kg) ^g
Pu-238 ^b	Solubility limited ^d	Solubility limited ^d
U-234 ^c	Solubility limited ^d	Solubility limited ^d
Th-230 ^c	2.7×10^{23}	1.6×10^{23}
Ra-226 ^c	2.2×10^9	7.5×10^7
Pu-239 ^b	Solubility limited ^d	Solubility limited ^d
U-235 ^c	Solubility limited ^d	Solubility limited ^d
Pa-231 ^c	1.6×10^{21}	5.6×10^7
Pu-240	Solubility limited ^d	Solubility limited ^d
Pu-242	Solubility limited ^d	Solubility limited ^d
Pu-244	Solubility limited ^d	Solubility limited ^d

^a Based on lower of the two allowable concentrations listed in Table 4.1-8.

^b Includes contributions of potentially radiologically-significant daughter(s).

^c Based on solubility-limited Pu-240 with a total initial inventory of 150 Ci/vault of Pu-240. Parent inventory based on ratio of half-lives (Sect. 4.1.3).

^d Assumed initial inventory of 10,000 kg/vault for each uranium isotope.

^e Inventory limit listed is for U or Pu parent.

^f Expression in parentheses indicates that the inventory limit, in Ci, always exceeds and usually greatly exceeds, the assumed initial inventory of 10^5 kg U for the 10 ILNT vaults.

^g Expression in parentheses indicates that the inventory limit, in Ci, always exceeds the assumed initial inventory of 2.1×10^5 kg U for the 21 LAW vaults, with one exception (U-234).

^h Assumed initial inventory of 150 Ci/vault for each plutonium isotope.

be directly compared to the most restricted allowable groundwater limit from Table 4.1-8 to evaluate whether up to 150 Ci of Pu/vault (for any of the Pu isotopes evaluated) and/or 10,000 kg of U/vault (for any of the U isotopes evaluated) are acceptable for disposal. Inventory limits for U and Pu isotopes based on radiologically significant daughters were calculated by dividing the 10,000-year groundwater concentrations by the assumed initial inventory of the parent (U or Pu isotope), in Ci, and following the procedure described above for the radionuclides other than isotopes of U and Pu.

4.1.5 Dose Analysis for Inadvertent Intruders

As demonstrated in Sect. 3.2.4, the following exposure scenarios are of concern for inadvertent intruders onto the disposal site following loss of active institutional control at 100 years after facility closure:

- an agriculture scenario involving direct excavation into disposal units at times after the engineered barriers above the waste have lost their structural and physical integrity and can be penetrated by normal excavation procedures at the SRS;
- a resident scenario involving permanent residence in a home located either on top of an intact concrete roof or other engineered barrier, which first could occur at any time after loss of active institutional control, or on top of intact but exposed waste at times after all engineered barriers have lost their integrity; and
- a post-drilling scenario involving removal by drilling of waste from a disposal unit at times after drilling through a disposal unit becomes credible. The results of the dose analysis for the different exposure scenarios for inadvertent intruders are presented in the following sections.

The general approach to the dose analysis for any exposure scenario for inadvertent intruders is described below.

Because the isotopic composition of waste intended for disposal in the EAV is not known, the dose analysis for inadvertent intruders is used to estimate limits on inventories of

radionuclides that would be acceptable for disposal. For a known volume of disposal units of the same type, limits on radionuclide inventories are equivalent to limits on average concentrations in disposed waste. The estimated limits on radionuclide inventories are based on the performance objective for protection of inadvertent intruders described in Sect. 1.2, i.e., a limit on EDE of 0.1 rem per year for scenarios involving chronic exposure. The procedure for estimating limits on inventories of radionuclides for the different types of disposal units, based on the dose analysis for each exposure scenario for inadvertent intruders, is described as follows.

For an assumed exposure scenario and particular type of disposal unit, the EDE (rem/year) to an inadvertent intruder from exposure to a given radionuclide can be expressed as

$$H = (I_0/V) \times \text{SDCF} \times G \times F, \quad (\text{Eq. 4.1-1})$$

where

- I_0 = inventory of radionuclide in disposal units at time of disposal (μCi),
- V = volume of waste in disposal units (m^3),
- SDCF = scenario dose conversion factor for radionuclide (rem/year per $\mu\text{Ci}/\text{m}^3$),
- G = geometrical correction factor (dimensionless), and
- F = fraction of initial inventory of radionuclide remaining in disposal units at time intrusion occurs.

In this equation, scenario dose conversion factor (SDCF) is the annual dose to an inadvertent intruder for the assumed exposure scenario per unit concentration of a radionuclide based on the assumption that intrusion occurs only into the regions of disposal units that are occupied by waste. The SDCFs for the agriculture, resident, and post-drilling scenarios are estimated in Appendix A.4, and the results are summarized in Table 4.1-10, 4.1-11, and 4.1-12, respectively. The correction factors G and F then take into account that the average radionuclide concentration encountered by an inadvertent intruder would be less than the average concentration in disposed waste and that the dose would be correspondingly reduced.

Table 4.1-10. SDCFs for agriculture scenario for inadvertent intruders^a

Radionuclide ^b	Annual EDE (rem/y per $\mu\text{Ci}/\text{m}^3$)	Radionuclide ^b	Annual EDE (rem/y per $\mu\text{Ci}/\text{m}^3$)
H-3	3.9×10^{-6}	Pa-231 + d	8.3×10^{-4}
C-14	1.5×10^{-5}	U-232 + d ^c	2.3×10^{-3}
Al-26	3.9×10^{-3}	Rn-220	1.0×10^{-2} ^f
Co-60	3.5×10^{-3}	U-233	1.1×10^{-5}
Ni-59	6.8×10^{-8}	U-234	1.1×10^{-5}
Ni-63	1.8×10^{-7}	U-235 + d	1.8×10^{-4}
Se-79	1.2×10^{-6}	U-236	1.0×10^{-5}
Rb-87	1.9×10^{-6}	U-238 + d	3.9×10^{-5}
Sr-90 + d	1.8×10^{-4}	Np-237 + d	5.0×10^{-4}
Zr-93 ^c	4.5×10^{-8}	Pu-238	3.4×10^{-5}
Nb-93m	1.9×10^{-8}	Pu-239	4.0×10^{-5}
Tc-99	1.1×10^{-5}	Pu-240	4.0×10^{-5}
Pd-107	3.2×10^{-8}	Pu-241	7.7×10^{-7}
Cd-113m	1.3×10^{-4}	Pu-242	3.8×10^{-5}
Sn-121m	4.7×10^{-7}	Pu-244	3.7×10^{-5}
Sn-126 + d	2.6×10^{-3}	Am-241	5.6×10^{-5}
I-129	8.3×10^{-5}	Am-242m + d	6.0×10^{-5}
Cs-135	1.2×10^{-6}	Am-243 + d	2.5×10^{-4}
Cs-137 + d	7.7×10^{-4}	Cm-243	1.6×10^{-4}
Sm-151	1.4×10^{-8}	Cm-244	2.0×10^{-5}
Eu-154	1.7×10^{-3}	Cm-245	1.1×10^{-4}
Eu-155	4.0×10^{-5}	Cm-246	4.0×10^{-5}
Pb-210 + d	3.0×10^{-4}	Cm-247 + d	4.4×10^{-4}
Ra-226 + d ^d	2.7×10^{-3}	Cm-248	1.4×10^{-4}
Rn-222	1.2×10^{-1} ^f	Cf-249	4.6×10^{-4}
Th-229 + d	4.3×10^{-4}	Cf-250	1.7×10^{-5}
Th-230	1.1×10^{-5}	Cf-251	1.6×10^{-4}
Th-232 + d ^e	3.6×10^{-3}		
Rn-220	1.0×10^{-2} ^f		

^a Results are obtained from Table A.4-14 of Appendix A.4.

^b "+ d" denotes short-lived decay products that are assumed to be in secular equilibrium with parent radionuclide; see Table A.4-1 for decay products and branching fractions.

^c Value assumes that Nb-93m is present in secular equilibrium.

^d Value assumes that Pb-210 is present in secular equilibrium.

^e Dose from radon decay product is listed separately.

^f Dose is normalized to unit concentration of parent radionuclide.

Table 4.1-11. SDCFs for resident scenario for inadvertent intruders^a

Radionuclide ^b	Annual EDE (rem/y per $\mu\text{Ci}/\text{m}^3$)		
	No shielding ^c	45-cm shielding ^d	100-cm shielding ^e
Al-26	3.9×10^{-3}	1.1×10^{-4}	2.8×10^{-6}
Co-60	---	8.8×10^{-5}	1.2×10^{-6}
Sn-121m	4.2×10^{-7}	---	---
Sn-126 + d	2.6×10^{-3}	2.2×10^{-5}	8.4×10^{-8}
I-129	2.8×10^{-6}	---	---
Cs-137 + d	7.6×10^{-4}	6.6×10^{-6}	2.2×10^{-8}
Eu-154	---	3.2×10^{-5}	3.5×10^{-7}
Eu-155	---	6.3×10^{-10}	---
Ra-226 + d	2.4×10^{-3}	6.0×10^{-5}	1.3×10^{-6}
Th-229 + d	3.5×10^{-4}	2.6×10^{-6}	3.5×10^{-8}
Th-232 + d	3.5×10^{-3}	1.1×10^{-4}	4.1×10^{-6}
Pa-231 + d	4.2×10^{-4}	1.1×10^{-6}	3.5×10^{-9}
U-232 + d	2.2×10^{-3}	9.2×10^{-5}	3.8×10^{-6}
U-235 + d	1.7×10^{-4}	3.9×10^{-8}	2.3×10^{-12}
U-238 + d	2.9×10^{-5}	3.0×10^{-7}	2.5×10^{-9}
Np-237 + d	2.4×10^{-4}	4.6×10^{-7}	2.8×10^{-10}
Am-241	9.5×10^{-6}	---	---
Am-242m + d	1.5×10^{-5}	6.2×10^{-8}	5.2×10^{-10}
Am-243 + d	2.0×10^{-4}	1.1×10^{-7}	4.2×10^{-11}
Cm-243	1.3×10^{-4}	4.9×10^{-8}	2.0×10^{-11}
Cm-245	7.4×10^{-5}	5.3×10^{-9}	---
Cm-247 + d	4.0×10^{-4}	1.3×10^{-6}	1.3×10^{-9}
Cf-249	4.2×10^{-4}	1.2×10^{-6}	1.1×10^{-9}
Cf-251	1.2×10^{-4}	3.1×10^{-8}	---

^a Results are obtained from Table A.4-15 of Appendix A.4.

^b "+ d" denotes short-lived decay products that are assumed to be in secular equilibrium with parent radionuclides; see Table A.4-1 of Appendix A.4 for decay products and branching fractions.

^c Results apply to ILNT, LAW, and ILT vaults at times long after disposal when all engineered barriers above the waste have lost their integrity.

^d Results apply to LAW vaults at 100 years after disposal.

^e Results apply to ILNT and ILT vaults at 100 years after disposal.

Table 4.1-12. SDCFs for post-drilling scenario for inadvertent intruders^a

Radionuclide ^b	Annual EDE (rem/year per $\mu\text{Ci}/\text{m}^3$)	Radionuclide ^b	Annual EDE (rem/year per $\mu\text{Ci}/\text{m}^3$)
H-3	3.9×10^{-7}	Pa-231 + d	1.8×10^{-5}
C-14	1.5×10^{-6}	U-232 + d ^c	5.6×10^{-6}
Al-26	1.8×10^{-6}	Rn-220	2.1×10^{-6} ^f
Co-60	1.8×10^{-6}	U-233	7.5×10^{-7}
Ni-59	6.8×10^{-9}	U-234	7.3×10^{-7}
Ni-63	1.8×10^{-8}	U-235 + d	7.9×10^{-7}
Se-79	1.2×10^{-7}	U-236	6.9×10^{-7}
Rb-87	1.9×10^{-7}	U-238 + d	6.6×10^{-7}
Sr-90 + d	1.8×10^{-5}	Np-237	2.4×10^{-5}
Zr-93 ^e	3.5×10^{-9}	Pu-238	2.1×10^{-6}
Nb-93m	1.8×10^{-9}	Pu-239	2.5×10^{-6}
Tc-99	1.1×10^{-6}	Pu-240	2.5×10^{-6}
Pd-107	3.2×10^{-9}	Pu-241	4.8×10^{-8}
Cd-113m	1.3×10^{-5}	Pu-242	2.4×10^{-6}
Sn-121m	5.3×10^{-9}	Pu-244	2.3×10^{-6}
Sn-126 + d	1.4×10^{-6}	Am-241	3.1×10^{-6}
I-129	8.1×10^{-6}	Am-242m + d	3.0×10^{-6}
Cs-135	1.2×10^{-7}	Am-243 + d	3.2×10^{-6}
Cs-137 + d	1.2×10^{-6}	Cm-243	1.6×10^{-6}
Sm-151	9.3×10^{-10}	Cm-244	1.3×10^{-6}
Eu-154	8.4×10^{-7}	Cm-245	2.5×10^{-6}
Eu-155	2.6×10^{-8}	Cm-246	2.5×10^{-6}
Pb-210 + d	3.0×10^{-5}	Cm-247 + d	2.5×10^{-6}
Ra-226 + d ^e	3.2×10^{-5}	Cm-248	8.9×10^{-6}
Rn-222	1.3×10^{-5} ^f	Cf-249	2.7×10^{-6}
Th-229 + d	2.9×10^{-6}	Cf-250	1.0×10^{-6}
Th-230	3.4×10^{-7}	Cf-251	2.6×10^{-6}
Th-232 + d ^e	5.9×10^{-6}		
Rn-220	2.1×10^{-6} ^f		

^a Results are obtained from Table A.4-16 of Appendix A.4.

^b "+ d" denotes short-lived decay products that are assumed to be in secular equilibrium with parent radionuclide; see Table A.4-1 of Appendix A.4 for decay products and branching fractions.

^c Value assumes that Nb-93m is present in secular equilibrium.

^d Value assumes that Pb-210 is present in secular equilibrium.

^e Dose from radon decay product is listed separately.

^f Dose is normalized to unit concentration of parent radionuclides.

The geometrical correction factor, G , in Eq. 4.1-1 takes into account that a large-scale excavation into disposal units, as assumed in the agriculture and resident scenarios, would involve exposure to uncontaminated material between individual disposal units as well as disposed waste itself. This correction factor assumes, in essence, that excavation into disposal units would occur at random locations. Therefore, the geometrical correction factor is given by the fraction of the land area encompassed by the disposal units of a particular type that contains waste.

The values of the geometrical correction factor for the agriculture and resident scenarios assumed in this analysis for the different disposal types of units are given in Table 4.1-13. These values were estimated for the three vault types and the suspect soil trenches in the following manner. An envelope was drawn around each grouping of each vault type (Fig. 2.5-1) or trench (Fig. 2.6-1), representing the total land area occupied by vaults or trenches and uncontaminated soil between each disposal unit in a grouping. Using known vault and trench dimensions (Figs. 2.5-2, 2.5-3, and 2.6-1) and spacing, the correction factors were estimated by dividing the vault and trench areas in a grouping by the area of the corresponding envelope. The correction factors represent the fraction of land area occupied by the vaults or trenches and soil between these units that actually contains waste. For the post-drilling scenario, the geometrical correction factor is assumed to be unity for all disposal units, because an intruder is assumed to drill only through contaminated regions in each type of disposal unit. Any uncontaminated material above and below the waste that also would be exhumed by drilling is taken into account in estimating the SDCF for the post-drilling scenario in Table 4.1-12.

Table 4.1-13. Geometrical reduction factors (G) used in dose analyses for inadvertent intruders^a

Disposal Units	Reduction Factor
ILNT vaults	0.4
LAW vaults	0.8
ILT vaults	0.4
Suspect soil trenches	0.6

^a See Eq. 4.1-1; reduction factors apply to agriculture and resident scenarios but not to post-drilling scenario.

The parameter F in Eq. 4.1-1 takes into account that, between the time of disposal and the time that a scenario for inadvertent intrusion is assumed to occur, the initial inventories of radionuclides in the disposal units would be reduced by radioactive decay and by mobilization and transport in infiltrating water. This correction factor depends on the particular disposal unit as well as the radionuclide.

For any radionuclide in disposed waste, the parameter F is a monotonically decreasing function of time after disposal. Therefore, if a radionuclide does not produce radiologically significant long-lived decay products, the dose to an inadvertent intruder for a given scenario will attain its maximum value at the time after disposal when the scenario first becomes credible. However, if a radionuclide produces radiologically more significant long-lived decay products (e.g., U-238, which produces Ra-226), the maximum dose from the parent radionuclide and its decay products could occur long after the scenario first becomes credible, depending on the rate of buildup of activity of the decay product relative to the rate of removal of the parent radionuclide from the disposal units.

For any radionuclide and type of disposal unit, the value of the parameter F as a function of time after disposal is obtained from calculations performed by the PORFLOW computer code. Again, the fraction of the initial inventory remaining in disposal units at any time after disposal takes into account radioactive decay and removal from the disposal units by infiltrating water. For any radiologically significant long-lived decay products, the simplifying assumption is made that the inventory at any time after disposal is determined by (1) the remaining inventory of the parent radionuclide at that time and (2) the ratio of the activity of the decay product to the initial activity of the parent radionuclide as obtained from the Bateman equations. As described in Sect. 4.1.3, a similar approximation was used in accounting for long-lived decay products in the dose analysis for the groundwater pathway.

Since the objective of the intruder dose analysis is to establish limits on inventories of radionuclides for disposal, Eq. 4.1-1 can be rearranged to give

$$I_0 = (H \times V) / (SDCF \times G \times F).$$

Therefore, for a dose limit for inadvertent intruders of 0.1 rem per year and using a conversion factor for activity of 10^{-6} Ci/ μ Ci, the inventory limit for a radionuclide in a particular type of disposal unit for a given exposure scenario is given by

$$I_0(\text{Ci}) = [10^{-7} \times V(\text{m}^3)] / [\text{SDCF}(\text{rem-m}^3/\mu\text{Ci-y}) \times G \times F]. \quad (\text{Eq. 4.1-2})$$

The volume V depends only on the type of disposal unit, the SDCF depends only on the radionuclide and exposure scenario but not on the type of disposal unit, G depends only on the type of disposal unit and exposure scenario, and F depends on the time after disposal at which intrusion is assumed to occur and on the radionuclide and type of disposal unit.

Alternatively, the waste acceptance criteria (WAC) could be expressed in terms of limits on average concentrations of radionuclides in disposed waste. From Eq. 4.1-2, the limit on average concentration of a radionuclide is given by

$$C_0(\mu\text{Ci/m}^3) = 0.1 / [\text{SDCF}(\text{rem-m}^3/\mu\text{Ci-y}) \times G \times F]. \quad (\text{Eq. 4.1-3})$$

The model in Eqs. 4.1-2 and 4.1-3 for estimating limits on inventories or average concentrations of radionuclides in the different types of disposal units for the different exposure scenarios for inadvertent intruders is implemented in the following sections.

4.1.5.1 Dose Analysis for Agriculture Scenario

The SDCFs obtained from the model for estimating dose to inadvertent intruders for the agriculture scenario are summarized in Table 4.1-10. The remainder of this section discusses application of the results in Table 4.1-10 and the model in Eqs. 4.1-1 through 4.1-3 to the different disposal units in E-Area.

ILNT Vaults

Because of the design of the ILNT vaults, the agriculture scenario involving direct excavation into the waste is not expected to become credible for a considerable period of time

after disposal. Since the waste will be located well below the ground surface, a considerable amount of erosion will need to occur before the waste could be accessed by normal excavation procedures for a home. Then, the concrete roof and layer of uncontaminated grout above the waste are expected to preclude excavation into the waste for as long as they maintain their physical integrity. The assumed performance of the three barriers to excavation into waste is discussed below.

The current closure concept for the disposal units in E-Area calls for an earthen cover above the concrete roof of thickness about 2.9 m. As described in Sect. 2.1.8, the average erosion rate for cropland in the vicinity of the SRS is about 1.4 mm/year. This erosion rate probably is an upper-bound estimate for the earthen cover, because an estimated erosion rate for natural successional forests (see Sect. 2.1.8) is about 0.003 mm/year. Since an excavation for a home normally is assumed to extend no more than about 3 m below the ground surface (NRC 1981; Oztunali and Roles 1986) and since the total thickness of the concrete roof and layer of uncontaminated grout above the waste in the ILNT vaults is expected to be about 1.7 m (see Sect. 2.8), at least 2.7 m of the earthen cover would need to erode before a significant thickness of the waste (about 1 m) would be accessible during excavation and significant exposures according to the agriculture scenario could occur. Using the estimated erosion rates given above, the time required for 2.7 m of cover material to erode is estimated to be nearly 2,000 years and perhaps as long as 900,000 years. The very low erosion rate for natural successional forests is difficult to justify for such a long time period. However, the presence of a gravel layer about 0.9 m below the surface in the current closure concept undoubtedly would inhibit further erosion once the gravel layer is exposed. Therefore, erosion to a depth necessary to permit normal excavation into the waste presumably will not occur for at least several thousand years after disposal.

The models for degradation of the concrete roof are described in Sect. 3.1.3. As indicated in Table 3.3-4, the roof above an ILNT vault is expected to maintain its integrity for about 1,000 years after disposal, and collapse of the roof is expected to occur at about that time. If the roof were in the form of rubble after collapse, which probably represents a worst-case scenario, excavation through the collapsed roof could occur at that time.

After the concrete roof over an ILNT vault fails, the layer of uncontaminated grout above the waste presumably must weather almost entirely to soil-equivalent material before excavation into the waste would become credible. In order to estimate the weathering rate of grout, this material is assumed to resemble carbonate rock (e.g., limestone) in its weathering properties. Available data summarized by Ketelle and Huff (1984) indicate that the weathering rate of carbonate rock in regions near the SRS is in the range 35 to 100 mm per 1,000 years. For purposes of this analysis, a weathering rate for the layer of uncontaminated grout of 100 mm (0.1 m) per 1,000 years is assumed. This value applies to the expected infiltration rate of water in native soil of 40 cm/year (see Appendix A.1.1) and, thus, applies at times after the concrete roof has failed at about 1,000 years after disposal. A weathering rate at the upper end of the range of reported values for carbonate rock is chosen, because grout should have a somewhat higher porosity than average carbonate rock and, thus, should be correspondingly more susceptible to weathering by infiltrating water.

The nominal thickness of the layer of uncontaminated grout above the waste in the ILNT vaults is 3 ft (90 cm). By assuming that essentially all of this grout layer must weather to soil-equivalent material in order for excavation into the waste to become credible, and using the estimated weathering rate given above, the time required for weathering of the grout at the normal infiltration rate of water is estimated to be about 9,000 years. This estimate shows that even in the absence of a concrete roof, the layer of uncontaminated grout above the waste should prevent excavation into the waste for many thousands of years after disposal.

The analysis described above assumes that excavation into the waste could occur as soon as the concrete roof has failed and the layer of uncontaminated grout above the waste has weathered to soil-equivalent material and the waste becomes accessible by excavation. This assumption probably is conservative because the space between waste packages in the ILNT vaults will be backfilled with grout, and the top layer (about 1 m) of this grout presumably must weather to soil-equivalent material before significant excavation into the waste could occur. The weathering rate of this material presumably would be about the same as for the grout layer above the waste described above. Therefore, about 10,000 years presumably would be required for a layer 1 m thick to weather to soil-equivalent material. This time is in addition to the time required for weathering of the grout above the waste.

In summary, an analysis of the expected performance of the earthen cover above the ILNT vaults and the concrete roof and layers of grout in the vaults indicates that excavation into the waste probably is not credible for at least 20,000 years after disposal. The layer of gravel in the earthen cover, which will be placed about 3.5 m above the waste, presumably will be quite erosion resistant, and a typical excavation to a depth of about 3 m below the ground surface would not access waste in the presence of the gravel layer. Even if the gravel layer were subject to the same erosion rate as native soil, the time required for a sufficient thickness of the cover to erode so that about 1 m of waste would be accessible by excavation should be at least several thousand years and could approach one million years if the current erosion rate for natural successional forests at the SRS is maintained.

The concrete roof above the vaults, the layer of uncontaminated grout above the waste, and the grouting of the waste itself also are expected to be effective barriers to excavation into the waste for many thousands of years after disposal. Although the roof is expected to collapse at about 1,000 years after disposal, the presence of large, intact pieces of the roof may preclude excavation for a considerable period of time thereafter. However, even if a collapsed roof were not a deterrent to excavation, the layer of uncontaminated grout above the waste is expected to maintain its integrity for about 10,000 years after disposal (i.e., for about 9,000 years after the roof collapses), and the grouting of the waste itself is expected to preclude excavation into a layer of waste about 1 m thick for about another 10,000 years after disposal.

From the analysis of the earthen cover and engineered barriers for the ILNT vaults presented above, it is clear that only long-lived radionuclides in the waste possibly could be of concern in an analysis of the agriculture scenario for inadvertent intruders. In this analysis, results are presented for three different times after disposal. The first is at 10,000 years after disposal, which is the maximum time of compliance with the performance objective for protection of inadvertent intruders (see Sect. 1.2.1). The analysis at this time is based on the pessimistic assumption that the agriculture scenario reasonably could occur then. Again, however, the scenario may not be credible until long after 10,000 years, based on the expected performance of the earthen cover and engineered barriers. The second time is at

20,000 years after disposal, which is the earliest time that the engineered barriers are expected to have failed sufficiently to permit excavation into a layer of waste about 1 m thick. Again, however, excavation into the waste at this time may be a pessimistic assumption if the gravel layer in the earthen cover prevents erosion to a depth sufficient to permit excavation at the depth of the waste. The third time is far into the future (i.e., at 200,000 to 2,000,000 years) when all barriers to excavation presumably have failed. Results at these far future times are presented only for U-234, U-235, and U-238, and the purpose of the analysis is to capture possible exposures to long-lived decay products which would reach their peak values only at very long times after disposal. A similar analysis was considered for Np-237, but in this case removal of the parent radionuclide from the vaults by mobilization and transport in water is sufficiently rapid to more than compensate for the long-term buildup of U-233 and Th-229 decay products.

The results of the dose analysis for the agriculture scenario at the various times after disposal are given in Table 4.1-14. The results are calculated using Eqs. 4.1-2 and 4.1-3. The SDCFs for the long-lived radionuclides of concern are given in Table 4.1-10, the geometrical reduction factor for the ILNT vaults of 0.4 is obtained from Table 4.1-13, and the fraction of the initial inventory of radionuclides remaining in the vaults at the various times after disposal, which takes into account radioactive decay and mobilization and transport in water, was calculated using the PORFLOW computer code. The results of the analysis are given in two forms, both of which are based on the dose limit for inadvertent intruders of 0.1 rem per year. The first set of results is in the form of limits on average concentrations of radionuclides in the waste. This type of result is useful because the concentrations in individual waste packages cannot exceed the limits for Class-C waste established by the NRC in 10 CFR Part 61 (DOE 1988a). The second set of results is in the form of limits on total activity of radionuclides in each vault.

For Th-232, U-234, and U-238, two sets of concentration and inventory limits are calculated for each time after disposal listed in Table 4.1-13. The first set of results include the contributions to the dose to inadvertent intruders from radon decay products (i.e., Rn-220 for Th-232 and Rn-222 for U-234 and U-238), but the second set of results excludes the contributions from radon. The dose limit for inadvertent intruders in the present performance

Table 4.1-14. Results of dose analysis for intruder agriculture scenario for ILNT vaults^a

Radionuclide	SDCF ^b (rem/y per $\mu\text{Ci}/\text{m}^3$)	Time (y)	F ^c	Concentration Limit ^d ($\mu\text{Ci}/\text{m}^3$)	Inventory Limit ^e (Ci)
C-14	1.5×10^{-5}	1×10^4 2×10^4	3.0×10^{-1} 8.8×10^{-2}	5.6×10^4 1.9×10^5	3.2×10^2 1.1×10^3
Al-26	3.9×10^{-3}	1×10^4 2×10^4	9.9×10^{-1} 9.8×10^{-1}	6.5×10^1 6.5×10^1	3.7×10^{-1} 3.7×10^{-1}
Ni-59	6.8×10^{-8}	1×10^4 2×10^4	8.3×10^{-1} 3.6×10^{-1}	4.4×10^6 1.0×10^7	2.5×10^4 5.8×10^4
Se-79	1.2×10^{-6}	1×10^4 2×10^4	3.8×10^{-2} 3.4×10^{-2}	5.5×10^6 6.1×10^6	3.1×10^4 3.5×10^4
Rb-87	1.9×10^{-6}	1×10^4 2×10^4	1.0 1.0	1.3×10^5 1.3×10^5	7.5×10^2 7.5×10^2
Zr-93	4.5×10^{-8}	1×10^4 2×10^4	1.0 1.0	5.6×10^6 5.6×10^6	3.2×10^4 3.2×10^4
Tc-99	1.1×10^{-5}	1×10^4 2×10^4	1.8×10^{-2} 1.5×10^{-2}	1.3×10^6 1.5×10^6	7.2×10^3 8.6×10^3
Pd-107	3.2×10^{-8}	1×10^4 2×10^4	1.0 1.0	7.8×10^6 7.8×10^6	4.5×10^4 4.5×10^4
Sn-126	2.6×10^{-3}	1×10^4 2×10^4	5.8×10^{-2} 4.1×10^{-2}	1.7×10^3 2.3×10^3	9.5 1.3×10^1
I-129	8.3×10^{-5}	1×10^4 2×10^4	2.5×10^{-3} 2.5×10^{-3}	1.2×10^6 ^f 1.2×10^6 ^f	4.6×10^2 4.6×10^2
Cs-135	1.2×10^{-6}	1×10^4 2×10^4	1.1×10^{-2} 1.1×10^{-2}	1.9×10^7 1.9×10^7	1.1×10^5 1.1×10^5
Th-232 ^g	1.4×10^{-2}	1×10^4 2×10^4	1.0 1.0	1.8×10^1 ^g 1.8×10^1 ^g	1.0×10^{-1} ^g 1.0×10^{-1} ^g
Th-232 ^h	3.6×10^{-3}	1×10^4 2×10^4	1.0 1.0	6.9×10^1 ^h 6.9×10^1 ^h	4.0×10^{-1} ^h 4.0×10^{-1} ^h
U-233	1.1×10^{-3}	1×10^4 2×10^4	9.6×10^{-1} 9.2×10^{-1}	2.4×10^4 2.5×10^4	1.3×10^2 1.4×10^2
U-234	1.1×10^{-5}	1×10^4	9.7×10^{-1}	3.2×10^1 ^g	1.8×10^{-1} ^g
Th-230	1.1×10^{-5}		8.5×10^{-2}	1.3×10^3 ^h	7.5
Ra-226 ^g	1.2×10^{-1}		6.6×10^{-2}		
Ra-226 ^h	2.7×10^{-3}		6.6×10^{-2}		
U-234	1.1×10^{-5}	2×10^4	9.4×10^{-1}	1.5×10^1 ^g	8.5×10^{-2} ^g
Th-230	1.1×10^{-5}		1.6×10^{-1}	6.4×10^2 ^g	3.7
Ra-226 ^g	1.2×10^{-1}		1.4×10^{-1}		
Ra-226 ^h	2.7×10^{-3}		1.4×10^{-1}		

4-47
Table 4.1-14. (continued)

WSRC-RP-94-218

Radionuclide	SDCF ^b (rem/y per $\mu\text{Ci}/\text{m}^3$)	Time (y)	F ^c	Concentration Limit ^d ($\mu\text{Ci}/\text{m}^3$)	Inventory Limit ^e (Ci)
U-234	1.1×10^{-5}	2×10^5	5.7×10^{-1}	3.5^g	$2.0 \times 10^{-2}^g$
Th-230	1.1×10^{-5}		5.9×10^{-1}	$1.6 \times 10^2^h$	$8.9 \times 10^{-1}^h$
Ra-226 ^g	1.2×10^{-1}		5.9×10^{-1}		
Ra-226 ^h	2.7×10^{-3}		5.9×10^{-1}		
U-235	1.8×10^{-4}	1×10^4	1.0	7.4×10^2	4.2
Pa-231	8.3×10^{-4}		1.9×10^{-1}		
U-235	1.8×10^{-4}	2×10^4	1.0	5.3×10^2	3.0
Pa-231	8.3×10^{-4}		3.5×10^{-1}		
U-235	1.8×10^{-4}	1×10^6	1.0	2.5×10^2	1.4
Pa-231	8.3×10^{-4}		1.0		
U-236	1.0×10^{-5}	1×10^4	1.0	2.5×10^4	1.4×10^2
		2×10^4	1.0	2.5×10^4	1.4×10^2
U-238	3.9×10^{-5}	1×10^4	1.0	$1.9 \times 10^3^g$	$1.1 \times 10^1^g$
U-234	1.1×10^{-5}		2.8×10^{-2}	$6.1 \times 10^3^h$	$3.4 \times 10^1^h$
Th-230	1.1×10^{-5}		1.2×10^{-3}		
Ra-226 ^g	1.2×10^{-1}		7.9×10^{-4}		
Ra-226 ^h	2.7×10^{-3}		7.9×10^{-4}		
U-238	3.9×10^{-5}	2×10^4	1.0	$5.1 \times 10^2^g$	2.9^g
U-234	1.1×10^{-5}		5.5×10^{-2}	$5.0 \times 10^3^h$	$2.9 \times 10^1^h$
Th-230	1.1×10^{-5}		4.7×10^{-3}		
Ra-226 ^g	1.2×10^{-1}		3.8×10^{-3}		
Ra-226 ^h	2.7×10^{-3}		3.8×10^{-3}		
U-238	3.9×10^{-5}	2×10^6	1.0	2.1^g	$1.2 \times 10^{-2}^g$
U-234	1.1×10^{-5}		1.0	$8.9 \times 10^1^h$	$5.1 \times 10^{-1}^h$
Th-230	1.1×10^{-5}		1.0		
Ra-226 ^g	1.2×10^{-1}		1.0		
Ra-226 ^h	2.7×10^{-3}		1.0		
Np-237	5.0×10^{-4}	1×10^4	9.7×10^{-1}	5.1×10^2	2.9
U-233	1.1×10^{-5}		4.2×10^{-2}		
Th-229	4.3×10^{-4}		1.5×10^{-2}		
Np-237	5.0×10^{-4}	2×10^4	7.4×10^{-1}	6.4×10^2	3.7
U-233	1.1×10^{-5}		6.2×10^{-2}		
Th-229	4.3×10^{-4}		3.5×10^{-2}		
Pu-239	4.0×10^{-5}	1×10^4	7.5×10^{-1}	8.3×10^3	4.8×10^1
		2×10^4	5.6×10^{-1}	1.1×10^4	6.4×10^1
Pu-240	4.0×10^{-5}	1×10^4	3.4×10^{-1}	1.8×10^4	1.0×10^2
		2×10^4	1.2×10^{-1}	5.2×10^4	3.0×10^2
Pu-242	3.8×10^{-5}	1×10^4	9.8×10^{-1}	6.7×10^3	3.8×10^1
		2×10^4	9.6×10^{-1}	6.9×10^3	3.9×10^1

Table 4.1-14. (continued)

Radionuclide	SDCF ^b (rem/y per $\mu\text{Ci}/\text{m}^3$)	Time (y)	F ^c	Concentration Limit ^d ($\mu\text{Ci}/\text{m}^3$)	Inventory Limit ^e (Ci)
Pu-244	3.7×10^{-5}	1×10^4	1.0	6.8×10^3	3.9×10^1
		2×10^4	1.0	6.8×10^3	3.9×10^1
Am-243	2.5×10^{-4}	1×10^4	3.9×10^{-1}	2.6×10^3	1.5×10^1
		2×10^4	1.5×10^{-1}	6.7×10^3	3.8×10^1
Cm-245	1.1×10^{-4}	1×10^4	4.4×10^{-1}	5.2×10^3	2.9×10^1
		2×10^4	2.0×10^{-1}	1.1×10^4	6.5×10^1
Cm-246	4.0×10^{-5}	1×10^4	2.3×10^{-1}	2.7×10^4	1.5×10^2
		2×10^4	5.4×10^{-2}	1.2×10^5	6.6×10^2
Cm-247	4.4×10^{-4}	1×10^4	1.0	5.7×10^2	3.2
		2×10^4	1.0	5.7×10^2	3.2
Cm-248	1.4×10^{-4}	1×10^4	9.8×10^{-1}	1.8×10^3	1.0×10^1
		2×10^4	9.6×10^{-1}	1.9×10^3	1.1×10^1

^a Concentration and inventory limits are obtained from Eqs. 4.1-2 and 4.1-3.

^b Values are obtained from Table 4.1-10.

^c Fraction of initial inventory of radionuclide remaining in disposal units at time scenario is assumed to occur.

^d Limit on average concentration in disposed waste.

^e Limit on inventory per vault; volume of each vault is assumed to be $5.7 \times 10^3 \text{ m}^3$.

^f Value exceeds NRC's Class-C limit in 10 CFR Part 61 of $8 \times 10^4 \mu\text{Ci}/\text{m}^3$, which applies to individual waste packages at DOE disposal sites (U.S.DOE 1988a).

^g Results include contribution to dose from radon decay product.

^h Results exclude contribution to dose from radon decay product.

objective in DOE Order 5820.2A (U.S.DOE 1988a) presumably includes contributions from radon. However, as described in Sect. 1.2.3, a revision of the DOE Order is being considered in which the dose limit in the performance objective for inadvertent intruders specifically excludes contributions from radon, and a separate limit on radon flux rate to the atmosphere would be imposed to provide an additional constraint on acceptable disposals of radionuclides that produce radon.

The results in Table 4.1-14 may be interpreted as follows. For all radionuclides except the isotopes of uranium which produce long-lived decay products, the maximum dose would occur at the time after disposal at which the agriculture scenario first becomes credible, and the results at 10,000 or 20,000 years represent lower-bound estimates of limits on average concentrations and inventories of radionuclides in waste. For U-234, U-235, and U-238, the results at times far beyond 10,000 or 20,000 years represent worst-case estimates of concentration and inventory limits at times when the buildup of decay products has reached equilibrium with the parent radionuclide.

LAW Vaults

Because of the presence of an earthen cover and concrete roof above the LAW vaults, the agriculture scenario involving direct excavation into the waste is not expected to become credible for a considerable period of time after disposal. However, these disposal units will not include a layer of uncontaminated grout above the waste, and the waste itself will not be grouted after disposal.

As described previously in the dose analysis for the ILNT vaults, the erosion rate of the earthen cover should be no greater than 1.4 mm/year and could be as low as 0.003 mm/year. For the LAW vaults, the earthen cover also is about 2.9 m thick, and the thickness of the concrete roof is about 50 cm. Thus, for a layer of waste about 1 m thick to be accessible during excavation, about 1.4 m of the cover material would need to be removed by erosion. Based on the erosion rates given above, the time period required for this amount of erosion should be at least 1,000 years and could be as long as 500,000 years. These estimates do not take into account the presence of a gravel layer at about 0.9 m below the surface, which presumably would inhibit erosion once it is exposed.

The models for degradation of the concrete roof indicate that the roof above the LAW vault should maintain its integrity for about 3,000 years after disposal, and collapse of the roof is expected to occur at about that time. If the roof were in the form of rubble after collapse, then excavation through the collapsed roof could occur at that time.

The assumption that excavation through the concrete roof could occur immediately following collapse of the roof would be pessimistic if most of the roof were in large pieces. Excavation through the collapsed roof would become more likely after most of the roof has weathered to soil-equivalent material. As previously described with the ILNT vaults, the weathering rate of concrete is assumed to be about 0.1 m per 1,000 years. Therefore, since a collapsed roof presumably could weather from both top and bottom and the thickness of the roof is about 0.5 m, the time required for essentially all of the concrete to weather to soil is expected to be about 2,000 years. Thus, taking into account that the roof is not expected to collapse for about 3,000 years, the estimated time at which excavation through the roof could occur is about 5,000 years after disposal.

From the analysis of the earthen cover and concrete roof for the LAW vaults presented above, it is again clear that only long-lived radionuclides in the waste possibly could be of concern in an analysis of the agriculture scenario for inadvertent intruders. In this analysis, results are presented for four different times after disposal. The first is at 3,000 years after disposal, and the analysis is based on the pessimistic assumption that the agriculture scenario reasonably could occur at the time that the concrete roof is expected to collapse. This assumption is pessimistic because it assumes that erosion of the cover material below the gravel layer has occurred and that excavation of the collapsed roof would be credible. The second time is at 5,000 years after disposal, when the concrete roof presumably has weathered to soil-equivalent material and excavation into the waste could occur. This assumption is pessimistic again because erosion of the cover material below the gravel layer again is presumed to have occurred. Finally, results are presented for U-234, U-235, and U-238 at 10,000 years after disposal, which is the maximum time of compliance with the performance objective for protection of inadvertent intruders, and at times far into the future (i.e., at 200,000 to 2,000,000 years) when the doses due to buildup of radiologically significant decay products could attain their maximum values. Similar calculations were performed for Np-237

and its long-lived decay products, but in this case the maximum dose occurs when the agriculture scenario first becomes credible, due to the rapid depletion of the parent radionuclide in the vaults by mobilization and transport in water compared with the buildup of decay products U-233 and Th-229.

The results of the dose analysis for the agriculture scenario at the various times after disposal are given in Table 4.1-15. These results were obtained as described previously for the ILNT vaults, except the geometrical reduction factor for the LAW vaults is 0.8 (see Table 4.1-13). For Th-232, U-234, and U-238, two sets of results again are given, one including the contributions to dose from radon and the other excluding the contributions from radon. For all radionuclides except U-234, U-235, and U-238, the maximum dose would occur at the time after disposal at which the agriculture scenario first becomes credible, and the results at 3,000 or 5,000 years after disposal represent lower-bound estimates of limits on average concentrations and inventories of radionuclides in waste. For U-234, U-235, and U-238, the results at 10,000 years represent the best estimates of the concentration and inventory limits during the 10,000-year compliance period for protection of inadvertent intruders, and the results at times far beyond 10,000 years represent worst-case estimates of limits at times when the buildup of decay products has reached equilibrium with the parent radionuclide.

ILT Vaults

The ILT vaults will be constructed in the same manner as the ILNT vaults, i.e., with an earthen cover about 2.9 m thick, a concrete roof about 90 cm thick, a layer of uncontaminated grout above the waste about 90 cm thick, and grouting of the waste in the vaults. Therefore, essentially the same assumptions used previously in the analysis of the agriculture scenario for the ILNT vaults apply to the ILT vaults. In particular, the scenario may not be credible until long after 10,000 years due to burial of the waste below the ground surface, the slow erosion rate expected for the earthen cover with a gravel layer, and the slow weathering rate of the layers of grout in the vaults.

Table 4.1-15. Results of dose analysis for intruder agriculture scenario for LAW vaults^a

Radionuclide	SDCF ^b (rem/y per $\mu\text{Ci}/\text{m}^3$)	Time (y)	F ^c	Concentration Limit ^d ($\mu\text{Ci}/\text{m}^3$)	Inventory Limit ^e (Ci)
C-14	1.5×10^{-5}	3×10^3 5×10^3	6.9×10^{-1} 4.5×10^{-1}	1.2×10^4 1.9×10^4	5.8×10^2 8.9×10^2
Al-26	3.9×10^{-3}	3×10^3 5×10^3	1.0 1.0	3.2×10^1 3.2×10^1	1.5 1.5
Ni-59	6.8×10^{-3}	3×10^3 5×10^3	9.7×10^{-1} 9.6×10^{-1}	1.9×10^6 1.9×10^6	9.1×10^4 9.2×10^4
Se-79	1.2×10^{-6}	3×10^3 5×10^3	9.3×10^{-1} 4.3×10^{-2}	1.1×10^5 2.4×10^6	5.4×10^3 1.2×10^5
Rb-87	1.9×10^{-6}	3×10^3 5×10^3	1.0 1.0	6.6×10^4 6.6×10^4	3.2×10^3 3.2×10^3
Zr-93	4.5×10^{-3}	3×10^3 5×10^3	1.0 1.0	2.8×10^6 2.8×10^6	1.3×10^5 1.3×10^5
Tc-99	1.1×10^{-5}	3×10^3 5×10^3	8.7×10^{-1} 2.2×10^{-2}	1.3×10^4 5.2×10^5	6.3×10^2 2.5×10^4
Pd-107	3.2×10^{-3}	3×10^3 5×10^3	1.0 1.0	3.9×10^6 3.9×10^6	1.9×10^5 1.9×10^5
Sn-126	2.6×10^{-3}	3×10^3 5×10^3	9.8×10^{-1} 6.6×10^{-1}	4.9×10^1 7.3×10^1	2.4 3.5
I-129	8.3×10^{-5}	3×10^3 5×10^3	1.5×10^{-4} 1.1×10^{-4}	1.0×10^{7f} 1.4×10^{7f}	3.8×10^3 3.8×10^3
Cs-135	1.2×10^{-6}	3×10^3 5×10^3	1.0 3.2×10^{-1}	1.0×10^5 3.3×10^5	5.0×10^3 1.6×10^4
Th-232 ^g	1.4×10^{-2}	3×10^3 5×10^3	1.0 1.0	8.9 ^g 8.9 ^g	4.3×10^{-1g} 4.3×10^{-1g}
Th-232 ^h	3.6×10^{-3}	3×10^3 5×10^3	1.0 1.0	3.5×10^{1h} 3.5×10^{1h}	1.7 1.7
U-233	1.1×10^{-5}	3×10^3 5×10^3	9.9×10^{-1} 9.8×10^{-1}	1.1×10^4 1.2×10^4	5.5×10^2 5.6×10^2
U-234	1.1×10^{-5}	3×10^3	9.9×10^{-1}	8.6×10^{1g}	4.1 ^g
Th-230	1.1×10^{-5}		2.7×10^{-2}	2.9×10^{3h}	1.4×10^{2h}
Ra-226 ^g	1.2×10^{-1}		1.2×10^{-2}		
Ra-226 ^h	2.7×10^{-3}		1.2×10^{-2}		
U-234	1.1×10^{-5}	5×10^3	9.9×10^{-1}	4.0×10^{1g}	1.9 ^g
Th-230	1.1×10^{-5}		4.4×10^{-2}	1.5×10^{3h}	7.4×10^{1h}
Ra-226 ^g	1.2×10^{-1}		2.6×10^{-2}		
Ra-226 ^h	2.7×10^{-3}		2.6×10^{-2}		
U-234	1.1×10^{-5}	1×10^4	9.7×10^{-1}	1.6×10^{1g}	7.6×10^{-1g}
Th-230	1.1×10^{-5}		8.5×10^{-2}	6.6×10^{2h}	3.2×10^{1h}
Ra-226 ^g	1.2×10^{-1}		6.6×10^{-2}		
Ra-226 ^h	2.7×10^{-3}		6.6×10^{-2}		

4-53
Table 4.1-15. (continued)

WSRC-RP-94-218

Radionuclide	SDCF ^b (rem/y per $\mu\text{Ci}/\text{m}^3$)	Time (y)	F ^c	Concentration Limit ^d ($\mu\text{Ci}/\text{m}^3$)	Inventory Limit ^e (Ci)
U-234	1.1×10^{-5}	2×10^5	5.7×10^{-1}	1.8^f	$8.5 \times 10^{-2}^g$ 3.8^h
Th-230	1.1×10^{-5}		5.9×10^{-1}		
Ra-226 ^g	1.2×10^{-1}		5.9×10^{-1}		
Ra-226 ^h	2.7×10^{-3}		5.9×10^{-1}		
U-235	1.8×10^{-4}	3×10^3	1.0	5.4×10^2	2.6×10^1
Pa-231	8.3×10^{-4}		6.2×10^{-2}		
U-235	1.8×10^{-4}	5×10^3	1.0	4.8×10^2	2.3×10^1
Pa-231	8.3×10^{-4}		1.0×10^{-1}		
U-235	1.8×10^{-4}	1×10^4	1.0	3.7×10^2	1.8×10^1
Pa-231	8.3×10^{-4}		1.9×10^{-1}		
U-235	1.8×10^{-4}	1×10^6	1.0	1.3×10^2	6.0
Pa-231	8.3×10^{-4}		1.0		
U-236	1.0×10^{-5}	3×10^3	1.0	1.3×10^4	6.0×10^2
		5×10^3	1.0	1.3×10^4	6.0×10^2
U-238	3.9×10^{-5}	3×10^3	1.0	$2.9 \times 10^3^g$ $3.2 \times 10^3^h$	$1.4 \times 10^2^g$ $1.5 \times 10^2^h$
U-234	1.1×10^{-5}		8.5×10^{-3}		
Th-230	1.1×10^{-5}		1.1×10^{-4}		
Ra-226 ^g	1.2×10^{-1}		3.7×10^{-5}		
Ra-226 ^h	2.7×10^{-3}		3.7×10^{-5}		
U-238	3.9×10^{-5}	5×10^3	1.0	$2.2 \times 10^3^g$ $3.1 \times 10^3^h$	$1.1 \times 10^2^g$ $1.5 \times 10^2^h$
U-234	1.1×10^{-5}		1.4×10^{-2}		
Th-230	1.1×10^{-5}		3.1×10^{-4}		
Ra-226 ^g	1.2×10^{-1}		1.4×10^{-4}		
Ra-226 ^h	2.7×10^{-3}		1.4×10^{-4}		
U-238	3.9×10^{-5}	1×10^4	1.0	$9.3 \times 10^2^g$ $3.0 \times 10^3^h$	$4.5 \times 10^1^g$ $1.5 \times 10^2^h$
U-234	1.1×10^{-5}		2.8×10^{-2}		
Th-230	1.1×10^{-5}		1.2×10^{-3}		
Ra-226 ^g	1.2×10^{-1}		7.9×10^{-4}		
Ra-226 ^h	2.7×10^{-3}		7.9×10^{-4}		
U-238	3.9×10^{-5}	2×10^6	1.0	1.0^g $4.5 \times 10^1^h$	$5.0 \times 10^{-2}^g$ 2.1^h
U-234	1.1×10^{-5}		1.0		
Th-230	1.1×10^{-5}		1.0		
Ra-226 ^g	1.2×10^{-1}		1.0		
Ra-226 ^h	2.7×10^{-3}		1.0		
Np-237	5.0×10^{-4}	3×10^3	1.0	2.5×10^2	1.2×10^1
U-233	1.1×10^{-5}		1.3×10^{-2}		
Th-229	4.3×10^{-4}		1.7×10^{-3}		
Np-237	5.0×10^{-4}	5×10^3	8.9×10^{-1}	2.8×10^2	1.3×10^1
U-233	1.1×10^{-5}		2.0×10^{-2}		
Th-229	4.3×10^{-4}		3.9×10^{-3}		
Pu-239	4.0×10^{-5}	3×10^3	9.2×10^{-1}	3.4×10^3	1.6×10^2
		5×10^3	8.7×10^{-1}	3.6×10^3	1.7×10^2
Pu-240	4.0×10^{-5}	3×10^3	7.3×10^{-1}	4.3×10^3	2.1×10^2
		5×10^3	5.9×10^{-1}	5.3×10^3	2.5×10^2

4-54
Table 4.1-15. (continued)

WSRC-RP-94-218

Radionuclide	SDCF ^b (rem/y per $\mu\text{Ci}/\text{m}^3$)	Time (y)	F ^c	Concentration Limit ^d ($\mu\text{Ci}/\text{m}^3$)	Inventory Limit ^e (Ci)
Pu-242	3.8×10^{-5}	3×10^3 5×10^3	9.9×10^{-1} 9.9×10^{-1}	3.3×10^3 3.3×10^3	1.6×10^2 1.6×10^2
Pu-244	3.7×10^{-5}	3×10^3 5×10^3	1.0 1.0	3.4×10^3 3.4×10^3	1.6×10^2 1.6×10^2
Am-241	5.6×10^{-5}	3×10^3 5×10^3	8.1×10^{-3} 3.3×10^{-4}	2.8×10^5 ^f 6.8×10^6 ^f	— —
Am-243	2.5×10^{-4}	3×10^3 5×10^3	7.5×10^{-1} 6.2×10^{-1}	6.7×10^2 8.1×10^2	3.2×10^1 3.9×10^1
Cm-245	1.1×10^{-4}	3×10^3 5×10^3	7.8×10^{-1} 6.6×10^{-1}	1.5×10^3 1.7×10^3	7.0×10^1 8.3×10^1
Cm-246	4.0×10^{-5}	3×10^3 5×10^3	6.5×10^{-1} 4.8×10^{-1}	4.8×10^3 6.5×10^3	2.3×10^2 3.1×10^2
Cm-247	4.4×10^{-4}	3×10^3 5×10^3	1.0 1.0	2.8×10^2 2.8×10^2	1.4×10^1 1.4×10^1
Cm-248	1.4×10^{-4}	3×10^3 5×10^3	9.9×10^{-1} 9.9×10^{-1}	9.0×10^2 9.0×10^2	4.3×10^1 4.3×10^1
Cf-249	4.6×10^{-4}	3×10^3 5×10^3	2.7×10^{-3} 5.2×10^{-5}	1.0×10^5 ^f 5.2×10^6 ^f	— —
Cf-251	1.6×10^{-4}	3×10^3 5×10^3	9.9×10^{-2} 2.1×10^{-2}	7.9×10^3 3.7×10^4	3.8×10^2 1.8×10^3

- ^a Concentration and inventory limits are obtained from Eqs. 4.1-2 and 4.1-3.
- ^b Values are obtained from Table 4.1-10.
- ^c Fraction of initial inventory of radionuclide remaining in disposal units at time scenario is assumed to occur.
- ^d Limit on average concentration in disposed waste.
- ^e Limit on inventory per vault; volume of each vault is assumed to be $4.8 \times 10^4 \text{ m}^3$.
- ^f Value exceeds NRC's Class-C limit in 10 CFR Part 61 of $8 \times 10^4 \mu\text{Ci}/\text{m}^3$, which applies to individual waste packages at DOE disposal sites (U.S.DOE 1988a).
- ^g Results include contributions to dose from radon decay product.
- ^h Results exclude contributions to dose from radon decay product.
- ⁱ Limit for individual waste packages at DOE disposal sites is 100 nCi/g (about $2 \times 10^5 \mu\text{Ci}/\text{m}^3$) for all alpha-emitting, transuranic radionuclides with half-lives greater than 5 years (U.S.DOE 1988a).

The results of the dose analysis for the agriculture scenario at various times after disposal are given in Table 4.1-16. The results were obtained as described previously for the ILNT vaults. For Th-232, U-234, and U-238, two sets of results again are given, one including the contributions from radon and the other excluding the contributions from radon. The calculations again were performed at 10,000 and 20,000 years after disposal for all long-lived radionuclides and at 200,000 to 2,000,000 years for U-234, U-235, and U-238, when the dose from buildup of radiologically significant long-lived decay products could attain its maximum value. However, the results at 10,000 years, which is the maximum time of compliance with the performance objective for protection of inadvertent intruders, and at 20,000 years, which is the earliest time that the concrete and grout barriers in the vaults are expected to have failed sufficiently to permit excavation into a significant amount of waste, may be pessimistic based on the expected erosion resistance of the earthen cover, particularly the gravel layer. The only difference between the results for the ILT vaults in Table 4.1-16 and for the ILNT vaults in Table 4.1-14 is the volume of waste per vault, which is used only to convert the limits on average concentrations of radionuclides in disposed waste to limits on inventory per vault.

4.1.5.2 Dose Analysis for Resident Scenario

Two bounding assumptions have been used in the dose analysis for the resident scenario for inadvertent intruders. In the first case, the intruder is assumed to reside in a home located immediately on top of an intact concrete roof or other engineered barrier above a disposal unit, and the scenario is assumed to be credible immediately following loss of active institutional control at 100 years after disposal. In the second case, the home is assumed to be located immediately on top of the waste in a disposal unit, but the scenario is assumed not to occur until the concrete roof and any other engineered barriers above the waste have lost their integrity and can be penetrated during excavation.

In both bounding cases for the resident scenario, the intruder is assumed not to excavate into the waste itself while constructing a home on the disposal site. Thus, the only exposure pathway of concern for this scenario is external exposure to photon-emitting radionuclides in the waste while residing in the home. The only differences between the two bounding cases

Table 4.1-16. Results of dose analysis for intruder agriculture scenario for ILT vaults

Radionuclide	SDCF ^b (rem/y per $\mu\text{Ci}/\text{m}^3$)	Time (y)	F ^c	Concentration Limit ^d ($\mu\text{Ci}/\text{m}^3$)	Inventory Limit ^e (Ci)
C-14	1.5×10^{-5}	1×10^4 2×10^4	3.0×10^{-1} 8.8×10^{-2}	5.6×10^4 1.9×10^5	4.4×10^1 1.5×10^2
Al-26	3.9×10^{-3}	1×10^4 2×10^4	9.9×10^{-1} 9.8×10^{-1}	6.5×10^1 6.5×10^1	5.2×10^{-2} 5.2×10^{-2}
Ni-59	6.8×10^{-3}	1×10^4 2×10^4	8.3×10^{-1} 3.6×10^{-1}	4.4×10^6 1.0×10^7	3.5×10^3 8.2×10^3
Se-79	1.2×10^{-6}	1×10^4 2×10^4	3.8×10^{-2} 3.4×10^{-2}	5.5×10^6 6.1×10^6	4.4×10^3 4.9×10^3
Rb-87	1.9×10^{-6}	1×10^4 2×10^4	1.0 1.0	1.3×10^5 1.3×10^5	1.0×10^2 1.0×10^2
Zr-93	4.5×10^{-3}	1×10^4 2×10^4	1.0 1.0	5.6×10^6 5.6×10^6	4.4×10^3 4.4×10^3
Tc-99	1.1×10^{-5}	1×10^4 2×10^4	1.8×10^{-2} 1.5×10^{-2}	1.3×10^6 1.5×10^6	1.0×10^3 1.2×10^3
Pd-107	3.2×10^{-3}	1×10^4 2×10^4	1.0 1.0	7.8×10^6 7.8×10^6	6.3×10^3 6.3×10^3
Sn-126	2.6×10^{-3}	1×10^4 2×10^4	5.8×10^{-2} 4.1×10^{-2}	1.7×10^3 2.3×10^3	1.3 1.9
I-129	8.3×10^{-5}	1×10^4 2×10^4	2.5×10^{-3} 2.5×10^{-3}	1.2×10^6 f 1.2×10^6 f	6.4×10^1 6.4×10^1
Cs-135	1.2×10^{-6}	1×10^4 2×10^4	1.1×10^{-2} 1.1×10^{-2}	1.9×10^7 1.9×10^7	1.5×10^4 1.5×10^4
Th-232 ^g	1.4×10^{-2}	1×10^4 2×10^4	1.0 1.0	1.8×10^1 ^h 1.8×10^1 ^h	1.4×10^{-2} ^h 1.4×10^{-2} ^h
Th-232 ^h	3.6×10^{-3}	1×10^4 2×10^4	1.0 1.0	6.9×10^1 ^h 6.9×10^1 ^h	5.5×10^{-2} ^h 5.5×10^{-2} ^h
U-233	1.1×10^{-5}	1×10^4 2×10^4	9.6×10^{-1} 9.2×10^{-1}	2.4×10^4 2.5×10^4	1.9×10^1 2.0×10^1
U-234	1.1×10^{-5}	1×10^4	9.7×10^{-1}	3.2×10^1 ^g	2.5×10^{-2} ^g
Th-230	1.1×10^{-5}		8.5×10^{-2}	1.3×10^3 ^h	1.0
Ra-226 ^g	1.2×10^{-1}		6.6×10^{-2}		
Ra-226 ^h	2.7×10^{-3}		6.6×10^{-2}		
U-234	1.1×10^{-5}	2×10^4	9.4×10^{-1}	1.5×10^1 ^g	1.2×10^{-2} ^g
Th-230	1.1×10^{-5}		1.6×10^{-1}	6.4×10^2 ^h	5.1×10^{-1} ^h
Ra-226 ^g	1.2×10^{-1}		1.4×10^{-1}		
Ra-226 ^h	2.7×10^{-3}		1.4×10^{-1}		

4-57
Table 4.1-16. (continued)

WSRC-RP-94-218

Radionuclide	SDCF ^b (rem/y per $\mu\text{Ci}/\text{m}^3$)	Time (y)	F ^c	Concentration Limit ^d ($\mu\text{Ci}/\text{m}^3$)	Inventory Limit ^e (Ci)
U-234	1.1×10^{-5}	2×10^5	5.7×10^{-1}	3.5^f	$2.8 \times 10^{-3}^g$
Th-230	1.1×10^{-5}		5.9×10^{-1}	$1.6 \times 10^2^h$	$1.3 \times 10^{-1}^h$
Ra-226 ^g	1.2×10^{-1}		5.9×10^{-1}		
Ra-226 ^h	2.7×10^{-3}		5.9×10^{-1}		
U-235	1.8×10^{-4}	1×10^4	1.0	7.4×10^2	5.9×10^{-1}
Pa-231	8.3×10^{-4}		1.9×10^{-1}		
U-235	1.8×10^{-4}	2×10^4	1.0	5.3×10^2	4.3×10^{-1}
Pa-231	8.3×10^{-4}		3.5×10^{-1}		
U-235	1.8×10^{-4}	1×10^6	1.0	2.5×10^2	2.0×10^{-1}
Pa-231	8.3×10^{-4}		1.0		
U-236	1.0×10^{-5}	1×10^4	1.0	2.5×10^4	2.0×10^1
		2×10^4	1.0	2.5×10^4	2.0×10^1
U-238	3.9×10^{-5}	1×10^4	1.0	$1.9 \times 10^3^g$	1.5^g
U-234	1.1×10^{-5}		2.8×10^{-2}	$6.1 \times 10^3^h$	4.9^h
Th-230	1.1×10^{-5}		1.2×10^{-3}		
Ra-226 ^g	1.2×10^{-1}		7.9×10^{-4}		
Ra-226 ^h	2.7×10^{-3}		7.9×10^{-4}		
U-238	3.9×10^{-5}	2×10^4	1.0	$5.1 \times 10^2^g$	$4.0 \times 10^{-1}^g$
U-234	1.1×10^{-5}		5.5×10^{-2}	$5.0 \times 10^3^h$	4.0^h
Th-230	1.1×10^{-5}		4.7×10^{-3}		
Ra-226 ^g	1.2×10^{-1}		3.8×10^{-3}		
Ra-226 ^h	2.7×10^{-3}		3.8×10^{-3}		
U-238	3.9×10^{-5}	2×10^6	1.0	2.1^g	$1.7 \times 10^{-3}^g$
U-234	1.1×10^{-5}		1.0	$8.9 \times 10^1^h$	$7.1 \times 10^{-2}^h$
Th-230	1.1×10^{-5}		1.0		
Ra-226 ^g	1.2×10^{-1}		1.0		
Ra-226 ^h	2.7×10^{-3}		1.0		
Np-237	5.0×10^{-4}	1×10^4	9.7×10^{-1}	5.1×10^2	4.1×10^{-1}
U-233	1.1×10^{-5}		4.2×10^{-2}		
Th-229	4.3×10^{-4}		1.5×10^{-2}		
Np-237	5.0×10^{-4}	2×10^4	7.4×10^{-1}	6.4×10^2	5.1×10^{-1}
U-233	1.1×10^{-5}		6.2×10^{-2}		
Th-229	4.3×10^{-4}		3.5×10^{-2}		
Pu-239	4.0×10^{-5}	1×10^4	7.5×10^{-1}	8.3×10^3	6.7
		2×10^4	5.6×10^{-1}	1.1×10^4	8.9
Pu-240	4.0×10^{-5}	1×10^4	3.4×10^{-1}	1.8×10^4	1.5×10^1
		2×10^4	1.2×10^{-1}	5.2×10^4	4.2×10^1
Pu-242	3.8×10^{-5}	1×10^4	9.8×10^{-1}	6.7×10^3	5.4
		2×10^4	9.6×10^{-1}	6.9×10^3	5.5
Pu-244	3.7×10^{-5}	1×10^4	1.0	6.8×10^3	5.4
		2×10^4	1.0	6.8×10^3	5.4

4-58
Table 4.1-16. (continued)

WSRC-RP-94-218

Radionuclide	SDCF ^b (rem/y per $\mu\text{Ci}/\text{m}^3$)	Time (y)	F ^c	Concentration Limit ^d ($\mu\text{Ci}/\text{m}^3$)	Inventory Limit ^e (Ci)
Am-243	2.5×10^{-4}	1×10^4	3.9×10^{-1}	2.6×10^3	2.1
		2×10^4	1.5×10^{-1}	6.7×10^3	5.3
Cm-245	1.1×10^{-4}	1×10^4	4.4×10^{-1}	5.2×10^3	4.1
		2×10^4	2.0×10^{-1}	1.1×10^4	9.1
Cm-246	4.0×10^{-5}	1×10^4	2.3×10^{-1}	2.7×10^4	2.2×10^1
		2×10^4	5.4×10^{-2}	1.2×10^5	9.3×10^1
Cm-247	4.4×10^{-4}	1×10^4	1.0	5.7×10^2	4.5×10^1
		2×10^4	1.0	5.7×10^2	4.5×10^1
Cm-248	1.4×10^{-4}	1×10^4	9.8×10^{-1}	1.8×10^3	1.5
		2×10^4	9.6×10^{-1}	1.9×10^3	1.5

^a Concentration and inventory limits are obtained from Eqs. 4.1-2 and 4.1-3.

^b Values are obtained from Table 4.1-10.

^c Fraction of initial inventory of radionuclide remaining in disposal units at time scenario is assumed to occur.

^d Limit on average concentration in disposed waste.

^e Limit on inventory per vault; volume of each vault is assumed to be $8.0 \times 10^2 \text{ m}^3$.

^f Value exceeds NRC's Class-C limit in 10 CFR Part 61 of $8 \times 10^4 \mu\text{Ci}/\text{m}^3$, which applies to individual waste packages at DOE disposal sites (U.S.DOE 1988a).

^g Results include contribution to dose from radon decay product.

^h Results exclude contribution to dose from radon decay product.

are the time at which the scenario is assumed to become credible, as described above, and the amount of shielding between the source region (i.e., the waste) and the receptor location.

The SDCFs obtained from the model for estimating dose to an inadvertent intruder for the resident scenario are summarized in Table 4.1-11. The remainder of this section discusses application of the results in Table 4.1-11 and the model in Eqs. 4.1-1 through 4.1-3 to the different disposal units in E-Area. The resident scenario is potentially relevant for any disposal units constructed with engineered barriers above the waste.

ILNT Vaults

As described previously, the ILNT vaults will be constructed with a concrete roof of average thickness about 90 cm and a layer of uncontaminated grout above the waste of thickness about 90 cm. Thus, the total thickness of the engineered barriers is about 1.8 m, and this thickness of shielding would apply to the resident scenario for the ILNT vaults at 100 years after disposal when all engineered barriers are assumed to be intact and impenetrable by normal excavation procedures.

As described in Appendix A.4.4, the 1.8 m thickness of shielding in the ILNT vaults is sufficient to reduce the external dose to very low levels for any conceivable concentrations of photon-emitting radionuclides in the waste. Therefore, in the dose analysis for the ILNT vaults at 100 years after disposal, the conservative assumption is made that only the layer of uncontaminated grout above the waste is present to provide shielding. For purposes of this analysis, the thickness of the grout layer is assumed to be 100 cm. This value is slightly greater than the planned thickness and is intended to take into account the somewhat greater shielding provided by any metal waste containers and waste forms in the ILNT vaults compared with the shielding provided by soil-equivalent material.

The results of the dose analysis for the resident scenario at 100 years after disposal are given in Table 4.1-17. The results are calculated in the same manner as those for the agriculture scenario using Eqs. 4.1-2 and 4.1-3, and the SDCFs are those for 100 cm of shielding in Table 4.1-11.

Table 4.1-17. Results of worst-case dose analysis for resident scenario for ILNT vaults at 100 years after disposal^a

Radionuclide	SDCF ^b (rem/y per $\mu\text{Ci}/\text{m}^3$)	F ^c	Concentration limit ($\mu\text{Ci}/\text{m}^3$)	Inventory limit ^e (Ci)
Al-26	2.8×10^{-6}	1.0	8.9×10^4	5.1×10^2
Co-60	1.2×10^{-6}	2.0×10^{-6}	1.0×10^{11}	5.9×10^8
Sn-126	8.4×10^{-8}	1.0	3.0×10^6	1.7×10^4
Cs-137	2.2×10^{-8}	1.0×10^{-1}	1.1×10^8	6.5×10^5
Eu-154	3.5×10^{-7}	3.8×10^{-4}	1.9×10^9	1.1×10^7
Th-232	4.1×10^{-6}	1.0	6.1×10^4	3.5×10^2
U-232	3.8×10^{-6}	3.8×10^{-1}	1.7×10^5	9.9×10^2
U-235	2.3×10^{-12}	1.0	—	—
U-238	2.5×10^{-9}	1.0	—	—
Np-237	2.8×10^{-10}	1.0	f	—
Am-242m	5.2×10^{-10}	6.3×10^{-1}	f	—
Am-243	4.2×10^{-11}	9.9×10^{-1}	f	—
Cm-243	2.0×10^{-11}	8.8×10^{-2}	f	—
Cm-247	1.3×10^{-9}	1.0	f	—
Cf-249	1.1×10^{-9}	8.2×10^{-1}	f	—

- ^a Concentration and inventory limits are obtained from Eqs. 4.1-2 and 4.1-3.
- ^b Values are obtained from Table 4.1-11 for 100 cm of shielding.
- ^c Fraction of initial inventory of radionuclides remaining in disposal units at time scenario is assumed to occur.
- ^d Limit on average concentration in disposal waste.
- ^e Limit on inventory per vault; volume of each vault is assumed to be $5.7 \times 10^3 \text{ m}^3$.
- ^f Limit for individual waste packages at DOE disposal sites is 100 nCi/g (about $2 \times 10^5 \mu\text{Ci}/\text{m}^3$) for all alpha-emitting transuranic radionuclides with half-lives greater than 5 years (U.S.DOE 1988a).

The results in Table 4.1-17 are expected to be quite pessimistic, and thus, the derived concentration and inventory limits are identified as worst-case conditions. As described above, the assumed thickness of shielding of 100 cm for these calculations greatly underestimates the amount of shielding that would be provided by an intact concrete roof and the uncontaminated layer of grout above the waste. For the long-lived isotopes of uranium, the calculated concentration limit is greater than the specific activity, and the calculated limits are not included in the table.

As described previously, the second bounding case for the resident scenario for the ILNT vaults is based on the assumption that the intruder's home is located immediately on top of exposed waste in a disposal unit, but that the excavation for the home does not penetrate into the waste itself, because the grouting at the depth of the top layer of waste is still intact. Therefore, this variation of the resident scenario could not reasonably occur until the concrete roof above the vaults has lost its integrity and the layer of uncontaminated grout above the waste has weathered to soil-equivalent material. An analysis described previously in presenting the results for the agriculture scenario indicates that the second bounding case for the resident scenario first could occur at about 10,000 years after disposal.

The results of the dose analysis for the resident scenario at 10,000 years after disposal are given in Table 4.1-18 and again are obtained using Eqs. 4.1-2 and 4.1-3. The SDCFs in this case are those for no shielding in Table 4.1-11. Only long-lived radionuclides, including long-lived decay products of the isotopes of uranium and neptunium, are of concern at this time.

The assumption that residence on top of exposed waste could occur at 10,000 years after disposal may also be pessimistic for the ILNT vaults. Even if the top layer of the earthen cover would erode to the level of the gravel layer by that time, which would occur only if the erosion rate was comparable to the value presently observed for agriculture lands at the SRS, but was considerably greater than the erosion rate for natural forests at the site, the gravel layer presumably would be quite resistant to further erosion. Since the top of the gravel layer will lie about 3.5 m above the top layer of waste and an excavation for a home is assumed to extend no more than 3 m below the ground surface, an excavation at 10,000 years probably would not extend to the depth of waste, and the additional shielding provided by the remaining layer of uncontaminated material between the bottom of the excavation and the waste has not been taken into account in the dose analysis.

**Table 4.1-18. Results of dose analysis for resident scenario
for ILNT vaults at 10,000 years after disposal^a**

Radionuclide	SDCF ^b (rem/year per $\mu\text{Ci}/\text{m}^3$)	F ^c	Concentration limit ($\mu\text{Ci}/\text{m}^3$)	Inventory limit ^e (Ci)
Al-26	3.9×10^{-3}	9.9×10^{-1}	6.5×10^1	3.7×10^{-1}
Sn-126	2.6×10^{-3}	5.8×10^{-2}	1.7×10^3	9.5
I-129	2.8×10^{-6}	2.5×10^{-3}	3.6×10^7 ^f	4.6×10^2
Th-232	3.5×10^{-3}	1.0	7.1×10^1	4.1×10^{-1}
U-234	—	9.7×10^{-1}	1.6×10^3	9.0
Ra-226	2.4×10^{-3}	6.6×10^{-2}		
U-235	1.7×10^{-4}	1.0	1.0×10^3	5.7
Pa-231	4.2×10^{-4}	1.9×10^{-1}		
U-238	2.9×10^{-3}	1.0	8.1×10^3	4.6×10^1
Ra-226	2.4×10^{-3}	7.9×10^{-4}		
Np-237	2.4×10^{-4}	9.7×10^{-1}	1.0×10^3	5.9
Th-229	3.5×10^{-4}	1.5×10^{-2}		
Am-243	2.0×10^{-4}	3.9×10^{-1}	3.2×10^3	1.8×10^1
Cm-245	7.4×10^{-5}	4.4×10^{-1}	7.7×10^3	4.4×10^1
Cm-247	4.0×10^{-4}	1.0	6.3×10^2	3.6

^a Concentration and inventory limits are obtained from Eqs. 4.1-2 and 4.1-3.

^b Values are obtained from Table 4.1-11 for the case of no shielding.

^c Fraction of initial inventory of radionuclides remaining in disposal units at time scenario is assumed to occur.

^d Limit on average concentration in disposal waste.

^e Limit on inventory per vault; volume of each vault is assumed to be $5.7 \times 10^3 \text{ m}^3$.

^f Value exceeds NRC's Class-C limit in 10 CFR Part 61 of $8 \times 10^4 \mu\text{Ci}/\text{m}^3$, which applies to individual waste packages at DOE disposal sites (U.S.DOE 1988a).

In contrast to the dose analysis for the agriculture scenario, there is no need to perform a dose analysis for the resident scenario at times beyond the time at which residence on top of exposed waste first becomes credible. At later times, the top layer of waste presumably would begin to weather to soil-equivalent material and the agriculture scenario, which always results in a higher dose per unit concentration of radionuclides, then becomes the scenario of concern.

LAW Vaults

As described previously, the LAW vaults will be constructed with a concrete roof of average thickness about 50 cm, but without a layer of uncontaminated grout above the waste. This thickness of shielding would apply to the resident scenario for the LAW vaults at 100 years after disposal when the concrete roof is assumed to be intact and impenetrable by normal excavation procedures.

As described in Appendix A.4.4, the nominal thickness of shielding provided by the concrete roof for the LAW vaults is assumed to be 45 cm. This value is slightly less than the planned thickness of the roof and is intended to take into account the somewhat reduced shielding provided by the waste itself due to the presence of void spaces in these disposal units.

The results of the dose analysis for the resident scenario at 100 years after disposal are given in Table 4.1-19. The results are calculated using Eqs. 4.1-2 and 4.1-3, and the SDCF_s are those for 45 cm of shielding in Table 4.1-11.

The assumption that the resident scenario could occur at 100 years after disposal probably is reasonable for the LAW vaults, because the thickness of the earthen cover above the vaults is approximately the same as the presumed maximum depth of an excavation in constructing a home. Therefore, significant erosion of the cover material would not be required in order for an excavation to uncover the roof of the vaults.

Table 4.1-19. Results of dose analysis for resident scenario for LAW vaults at 100 years after disposal^a

Radionuclide	SDCF ^b (rem/year per $\mu\text{Ci}/\text{m}^3$)	F ^c	Concentration limit ($\mu\text{Ci}/\text{m}^3$)	Inventory limit ^d (Ci)
Al-26	1.1×10^{-4}	1.0	1.1×10^3	5.5×10^1
Co-60	8.8×10^{-5}	2.0×10^{-6}	7.1×10^3	3.4×10^7
Sn-126	2.2×10^{-5}	1.0	5.7×10^3	2.7×10^2
Cs-137	6.6×10^{-6}	1.0×10^{-1}	1.9×10^5	9.1×10^3
Eu-154	3.2×10^{-5}	3.8×10^{-4}	1.0×10^7	4.9×10^5
Th-232	1.1×10^{-4}	1.0	1.1×10^3	5.5×10^1
U-232	9.2×10^{-5}	3.8×10^{-1}	3.6×10^3	1.7×10^2
U-235	3.9×10^{-8}	1.0	---	---
U-238	3.0×10^{-7}	1.0	---	---
Np-237	4.6×10^{-7}	1.0	/	---
Am-242m	6.2×10^{-8}	6.3×10^{-1}	/	---
Am-243	1.1×10^{-7}	9.9×10^{-1}	/	---
Cm-243	4.9×10^{-8}	8.8×10^{-2}	/	---
Cm-245	5.3×10^{-9}	9.9×10^{-1}	/	---
Cm-247	1.3×10^{-6}	1.0	/	---
Cf-249	1.2×10^{-6}	8.2×10^{-1}	/	---
Cf-251	3.1×10^{-6}	9.3×10^{-1}	/	---

- ^a Concentration and inventory limits are obtained from Eqs. 4.1-2 and 4.1-3.
- ^b Values are obtained from Table 4.1-11 for 45 cm of shielding.
- ^c Fraction of initial inventory of radionuclides remaining in disposal units at time scenario is assumed to occur.
- ^d Limit on average concentration in disposal waste.
- ^e Limit on inventory per vault; volume of each vault is assumed to be $4.8 \times 10^4 \text{ m}^3$.
- ^f Limit for individual waste packages at DOE disposal sites is 100 nCi/g (about $2 \times 10^5 \mu\text{Ci}/\text{m}^3$) for all alpha-emitting transuranic radionuclides with half-lives greater than 5 years (U.S.DOE 1988a).

However, the second bounding case for the resident scenario, based on an assumption that the intruder's home is located immediately on top of exposed but impenetrable waste in a disposal unit, is not relevant for the LAW vaults. This bounding case occurs only at a time when the concrete roof has failed and excavation to the depth of the waste could occur. As described previously, this time at which the concrete roof collapses is expected to be about 3,000 years after disposal for the LAW vaults. By this time, the waste forms and waste packages themselves presumably will have degraded to soil-equivalent material, because the waste in the LAW vaults will not be grouted. Therefore, at times after the concrete roof collapses, the agriculture scenario would become the scenario of concern and the resident scenario would no longer be relevant.

ILT Vaults

As described previously, the ILT vaults will be constructed in the same manner as the ILNT vaults, i.e., with a concrete roof of average thickness about 90 cm, a layer of uncontaminated grout above the waste of thickness about 90 cm, and grouting of the waste vaults. Thus, the dose analysis for the resident scenario for the ILT vaults is essentially the same as the previous analysis for the ILNT vaults. The only difference between the results for these two types of vaults is the assumed volume of waste per vault, which again is used only to convert the limits on average concentrations of radionuclides to limits on inventory per vault.

The results for the two bounding cases for the resident scenario — the first at 100 years after disposal when residence on top of an intact concrete barrier 100 cm thick is assumed to occur, and the second at about 10,000 years when residence on top of unshielded waste is assumed to occur — are given in Tables 4.1-20 and 4.1-21. As in the analysis for the ILNT vaults, the results at 100 years after disposal in Table 4.1-20, are expected to be quite pessimistic, because the assumed thickness of shielding of 100 cm considerably underestimates the thickness of an intact concrete roof and layer of uncontaminated grout above the waste. The analysis for the second bounding case at 10,000 years after disposal also would be pessimistic if the earthen cover above the vaults has eroded only to the level of the gravel layer by that time, because an excavation would not likely extend to the depth of the waste.

Table 4.1-20. Results of worst-case dose analysis for resident scenario for ILT vaults at 100 years after disposal^a

Radionuclide	SDCF ^b (rem/year per $\mu\text{Ci}/\text{m}^3$) ^c	F ^c	Concentration limit ($\mu\text{Ci}/\text{m}^3$)	Inventory limit ^e (Ci)
Al-26	2.8×10^{-6}	1.0	8.9×10^4	7.1×10^1
Co-60	1.2×10^{-6}	2.0×10^{-6}	1.0×10^{11}	8.3×10^7
Sn-126	8.4×10^{-8}	1.0	3.0×10^6	2.4×10^3
Cs-137	2.2×10^{-8}	1.0×10^{-1}	1.1×10^8	9.1×10^4
Eu-154	3.5×10^{-7}	3.8×10^{-4}	1.9×10^9	1.5×10^6
Th-232	4.1×10^{-6}	1.0	6.1×10^4	4.9×10^1
U-232	3.8×10^{-6}	3.8×10^{-1}	1.7×10^5	1.4×10^2
U-235	2.3×10^{-12}	1.0	---	---
U-238	2.5×10^{-9}	1.0	---	---
Np-237	2.8×10^{-10}	1.0	f	---
Am-242m	5.2×10^{-10}	6.3×10^{-1}	f	---
Am-243	4.2×10^{-11}	9.9×10^{-1}	f	---
Cm-243	2.0×10^{-11}	8.8×10^{-2}	f	---
Cm-247	1.3×10^{-9}	1.0	f	---
Cf-249	1.1×10^{-9}	8.2×10^{-1}	f	---

^a Concentration and inventory limits are obtained from Eqs. 4.1-2 and 4.1-3.

^b Values are obtained from Table 4.1-11 for 100 cm of shielding.

^c Fraction of initial inventory of radionuclides remaining in disposal units at time scenario is assumed to occur.

^d Limit on average concentration in disposal waste.

^e Limit on inventory per vault; volume of each vault is assumed to be $8.0 \times 10^2 \text{ m}^3$.

^f Limit for individual waste packages at DOE disposal sites is 100 nCi/g (about $2 \times 10^5 \mu\text{Ci}/\text{m}^3$) for all alpha-emitting transuranic radionuclides with half-lives greater than 5 years (U.S.DOE 1988a).

Table 4.1-21. Results of dose analysis for resident scenario for ILT vaults at 10,000 years after disposal^a

Radionuclide	SDCF ^b (rem/y per $\mu\text{Ci}/\text{m}^3$)	F ^c	Concentration limit ($\mu\text{Ci}/\text{m}^3$)	Inventory limit ^d (Ci)
Al-26	3.9×10^{-3}	9.9×10^{-1}	6.5×10^1	5.2×10^{-2}
Sn-126	2.6×10^{-3}	5.8×10^{-2}	1.7×10^3	1.3
I-129	2.8×10^{-6}	2.5×10^{-3}	3.6×10^7 ^f	2.9×10^4
Th-232	3.5×10^{-3}	1.0	7.1×10^1	5.7×10^{-2}
U-234 Ra-226	— 2.4×10^{-3}	9.7×10^{-1} 6.6×10^{-2}	1.6×10^3	1.3
U-235 Pa-231	1.7×10^{-4} 4.2×10^{-4}	1.0 1.9×10^{-1}	1.0×10^3	8.0×10^{-1}
U-238 Ra-226	2.9×10^{-5} 2.4×10^{-3}	1.0 7.9×10^{-4}	8.1×10^3	6.5
Np-237 Th-229	2.4×10^{-4} 3.5×10^{-4}	9.7×10^{-1} 1.5×10^{-2}	1.0×10^3	8.3×10^{-1}
Am-243	2.0×10^{-4}	3.9×10^{-1}	3.2×10^3	2.6
Cm-245	7.4×10^{-5}	4.4×10^{-1}	7.7×10^3	6.1
Cm-247	4.0×10^{-4}	1.0	6.3×10^2	5.0×10^{-1}

- ^a Concentration and inventory limits are obtained from Eqs. 4.1-2 and 4.1-3.
- ^b Values are obtained from Table 4.1-11 for the case of no shielding.
- ^c Fraction of initial inventory of radionuclides remaining in disposal units at time scenario is assumed to occur.
- ^d Limit on average concentration in disposal waste.
- ^e Limit on inventory per vault; volume of each vault is assumed to be $8.0 \times 10^2 \text{ m}^3$.
- ^f Value exceeds NRC's Class-C limit in 10 CFR Part 61 of $8 \times 10^4 \mu\text{Ci}/\text{m}^3$, which applies to individual waste packages at DOE disposal sites (U.S. DOE 1988a).

4.1.5.3 Dose Analysis for Post-Drilling Scenario

The SDCFs obtained from the model for estimating dose to inadvertent intruders for the post-drilling scenario are summarized in Table 4.1-12. The remainder of this section discusses application of the results in Table 4.1-12 to the different disposal units in E-Area. The model for estimating dose and limits on concentrations and inventories of radionuclides is given by Eqs. 4.1-1 through 4.1-3, except the geometrical correction factor (G) is not relevant for the post-drilling scenario when drilling is assumed to occur through the waste. The post-drilling scenario is potentially relevant for any disposal units constructed with engineered barriers.

ILNT Vaults

The post-drilling scenario assumes that the concrete roof, layer of uncontaminated grout above the waste, and grouting of the waste itself would preclude drilling into the waste for as long as these barriers remain intact. Therefore, since the waste in the ILNT vaults will be grouted, drilling into the waste is not expected to be a credible occurrence until the grout essentially has weathered to soil-equivalent material. Since weathering of the grout also is presumed to be a necessary condition for occurrence of the agriculture scenario involving excavation into the waste, the post-drilling and agriculture scenarios presumably would not occur until approximately the same time after disposal. Therefore, since the agriculture scenario always results in more restrictive disposal limits for radionuclides than the post-drilling scenario when the two scenarios are assumed to occur at the same time, the post-drilling scenario need not be considered further in the ILNT vaults, and limits on concentrations and inventories of radionuclides based on this scenario are not presented.

LAW Vaults

As described in previously, the concrete roof on the LAW vaults is expected to remain intact for about 3,000 years. At the time the roof is expected to collapse, drilling through the disposal units is presumed to be a credible occurrence because, in contrast to the ILNT

vaults, the waste in the LAW vaults will not be grouted and any waste forms and waste packages presumably will be sufficiently degraded that drilling through the waste would not be precluded.

The results of the dose analysis for the post-drilling scenario at 3,000 years after disposal are given in Table 4.1-22. The SDCFs are obtained from Table 4.1-12, and the concentration and inventory limits are calculated from Eqs. 4.1-2 and 4.1-3, except the parameter G is set equal to unity. As in the analysis for the agriculture scenario, results for Th-232, U-234, and U-238 are calculated including and excluding the contribution to the dose from radon decay products. The post-drilling scenario need not be considered at times substantially beyond 3,000 years, because the more restrictive agriculture scenario is presumed to become credible by about 5,000 years. At 3,000 years after disposal, only long-lived radionuclides in the waste are of concern for the post-drilling scenario.

ILT Vaults

The ILT vaults will be constructed in the same manner as the ILNT vaults. Therefore, the applicability of the post-drilling scenario will be the same in the two cases. As described previously in the discussion of the post-drilling scenario for the ILNT vaults, the post-drilling scenario need not be considered in establishing concentration and inventory limits of radionuclides in the ILT vaults, essentially because the more restrictive agriculture scenario could occur at the same time as the first credible occurrence of the post-drilling scenario. Therefore, results for the post-drilling scenario are not presented for the ILT vaults.

4.1.5.4 Summary of Dose Analysis for Inadvertent Intruders

A dose analysis for inadvertent intruders for the EAV has been performed on the basis of three assumed exposure scenarios:

- an agriculture scenario involving direct excavation into disposal units;
- a resident scenario involving residence in a home on top of intact engineered barriers above disposal units or on top of unshielded waste; and
- a post-drilling scenario involving removal of waste from disposal units by drilling.

Table 4.1-22. Results of dose analysis for post-drilling scenario for LAW vaults^a

Radionuclide	SDCF ^b (rem/year per $\mu\text{Ci}/\text{m}^3$)	F ^c	Concentration limit ^d ($\mu\text{Ci}/\text{m}^3$)	Inventory limit ^e (Ci)
C-14	1.5×10^{-6}	6.9×10^{-1}	9.7×10^4	4.6×10^3
Al-26	1.8×10^{-6}	1.0	5.5×10^4	2.7×10^3
Ni-59	6.8×10^{-9}	9.7×10^{-1}	1.5×10^7	7.3×10^5
Se-79	1.2×10^{-7}	9.3×10^{-1}	9.0×10^5	4.3×10^4
Zr-93	3.5×10^{-9}	1.0	2.9×10^7	1.4×10^6
Rb-87	1.9×10^{-7}	1.0	5.3×10^5	2.5×10^4
Tc-99	1.1×10^{-6}	8.7×10^{-1}	1.0×10^5	5.0×10^3
Pd-107	3.2×10^{-9}	1.0	3.1×10^7	1.5×10^6
Sn-126	1.4×10^{-6}	9.8×10^{-1}	7.3×10^4	3.5×10^3
I-129	8.1×10^{-6}	1.5×10^{-4}	8.2×10^7	3.8×10^3
Cs-135	1.2×10^{-7}	1.0	8.3×10^5	4.0×10^4
Th-232 ^e	8.0×10^{-6}	1.0	1.3×10^4 ^e	6.0×10^2 ^e
Th-232 ^h	5.9×10^{-6}	1.0	1.7×10^4 ^h	8.1×10^2 ^h
U-233	7.5×10^{-7}	9.9×10^{-1}	1.3×10^5	6.5×10^3
U-234	7.3×10^{-7}	9.9×10^{-1}	7.9×10^4 ^e	3.8×10^3 ^e
Th-230	3.4×10^{-7}	2.7×10^{-2}	9.1×10^4 ^h	4.4×10^3 ^h
Ra-226 ^e	4.5×10^{-5}	1.2×10^{-2}		
Ra-226 ^h	3.2×10^{-5}	1.2×10^{-2}		
U-235	7.9×10^{-7}	1.0	5.2×10^4	2.5×10^3
Pa-231	1.8×10^{-5}	6.2×10^{-2}		
U-236	6.9×10^{-7}	1.0	1.4×10^5	7.0×10^3
U-238	6.6×10^{-7}	1.0	1.5×10^5 ^e	7.2×10^3 ^e
U-234	7.3×10^{-7}	8.5×10^{-3}	1.5×10^5 ^h	7.2×10^3 ^h
Th-230	3.4×10^{-7}	1.1×10^{-4}		
Ra-226 ^e	4.5×10^{-5}	3.7×10^{-3}		
Ra-226 ^h	3.2×10^{-5}	3.7×10^{-5}		
Np-237	2.4×10^{-5}	1.0	4.2×10^3	2.0×10^2
U-233	7.5×10^{-7}	1.3×10^{-2}		
Th-229	2.9×10^{-6}	1.7×10^{-3}		
Pu-239	2.5×10^{-6}	9.2×10^{-1}	4.3×10^4	2.1×10^3

Table 4.1-22. (continued)

Radionuclide	SDCF ^b (rem/year per $\mu\text{Ci}/\text{m}^3$)	F ^c	Concentration limit ^d ($\mu\text{Ci}/\text{m}^3$)	Inventory limit ^e (Ci)
Pu-240	2.5×10^{-6}	7.3×10^{-1}	5.5×10^4	2.6×10^3
Pu-242	2.4×10^{-6}	9.9×10^{-1}	4.2×10^4	2.0×10^3
Pu-244	2.3×10^{-6}	1.0	4.3×10^4	2.1×10^3
Am-241	3.1×10^{-6}	8.1×10^{-3}	4.0×10^6 ^g	---
Am-242m	3.0×10^{-6}	1.1×10^{-6}	3.0×10^{10} ^h	---
Am-243	3.2×10^{-6}	7.5×10^{-1}	4.2×10^4	2.0×10^3
Cm-245	2.5×10^{-6}	7.8×10^{-1}	5.1×10^4	2.5×10^3
Cm-246	2.5×10^{-6}	6.5×10^{-1}	6.2×10^4	3.0×10^3
Cm-247	2.5×10^{-6}	1.0	4.0×10^4	1.9×10^3
Cm-248	8.9×10^{-6}	9.9×10^{-1}	1.1×10^4	5.4×10^2
Cf-249	2.7×10^{-6}	2.7×10^{-3}	1.4×10^7 ⁱ	---
Cf-251	2.6×10^{-6}	9.9×10^{-2}	3.9×10^5 ^j	---

^a Concentration and inventory limits are obtained from Eqs. 4.1-2 and 4.1-3 with G set equal to unity. Scenario is assumed to occur at 3,000 years after disposal.

^b Values are obtained from Table 4.1-12.

^c Fraction of initial inventory of radionuclides remaining in disposal units at time scenario is assumed to occur.

^d Limit on average concentration in disposal waste.

^e Limit on inventory per vault; volume of each vault is assumed to be $4.8 \times 10^4 \text{ m}^3$.

^f Value exceeds NRC's Class-C limit in 10 CFR Part 61 of $8 \times 10^4 \mu\text{Ci}/\text{m}^3$, which applies to individual waste packages at DOE disposal sites (U.S.DOE 1988a).

^g Results include contribution to dose from radon decay product.

^h Results exclude contribution to dose from radon decay product.

ⁱ Limit for individual waste packages at DOE disposal sites is 100 nCi/g (about $2 \times 10^5 \mu\text{Ci}/\text{m}^3$) for all alpha-emitting transuranic radionuclides with half-lives greater than 5 years (U.S.DOE 1988a).

For each of these scenarios, the performance objective for protection of inadvertent intruders is a limit on EDE of 100 mrem per year. As described in Sect. 1.2.1, this performance objective is assumed to apply for 10,000 years after disposal. However, an intruder dose analysis also has been performed for times beyond 10,000 years if the maximum dose could occur at such times.

Models for estimating dose to inadvertent intruders according to the assumed exposure scenarios were used to derive limits on average concentrations and inventories of radionuclides in the different types of disposal units, based on the performance objective for inadvertent intruders. The results of the analyses for the three exposure scenarios for the different types of disposal units in E-Area are summarized as follows.

ILNT Vaults

For the ILNT vaults, an analysis of the expected performance of the earthen cover above the vaults, the layer of uncontaminated grout above the waste, and the grout surrounding the waste itself has indicated that the agriculture scenario probably is not a credible occurrence until well beyond 10,000 years after disposal. A gravel layer, which should erode at a very slow rate compared with an assumed erosion rate for agriculture land at the SRS, will be located sufficiently far above the top layer of waste that normal excavation into the waste is not expected as long as the gravel layer is in place. Furthermore, the analysis indicates that about 20,000 years will be required for a significant thickness of waste to weather to soil-equivalent material, and thus, be subject to removal by excavation.

In Table 4.1-14, results based on a dose analysis for the agriculture scenario are presented for a sequence of times beginning at 10,000 years after disposal. However, for the purpose of demonstrating compliance with the performance objective for protection of inadvertent intruders, the most reasonable conclusion from the present analysis is that the agriculture scenario would not occur within the 10,000-year compliance period for the performance objective, and thus, would not provide a reasonable basis for establishing limits on concentrations and inventories of radionuclides for disposal.

Since the post-drilling scenario is assumed to be credible only after the concrete roof and grout layers have lost their integrity, this scenario presumably cannot occur for the ILNT vaults until about the same time as the agriculture scenario. Therefore, the post-drilling scenario also would not reasonably occur within the 10,000-year compliance period. Furthermore, the dose per unit concentration of radionuclides for the post-drilling scenario is always less than the value for the agriculture scenario. Therefore, it is reasonable to conclude that the post-drilling scenario also is not relevant for establishing disposal limits for the ILNT vaults.

The resident scenario could occur at 100 years after disposal, when a home could be built on top of an intact concrete roof, or at about 10,000 years after disposal, when an analysis of the performance of the engineered barriers indicates that excavation to the depth of the top of the waste in the vaults could become credible. Thus, of the different exposure scenarios for inadvertent intruders considered in this analysis, only the resident scenario reasonably can be used to establish disposal limits for the ILNT vaults. Results for the two bounding cases for the resident scenario are given in Table 4.1-17 and 4.1-18.

The estimated limits on concentrations and inventories of radionuclides for the ILNT vaults, as obtained from the analysis of the resident scenario at 100 and 10,000 years after disposal, are summarized in Table 4.1-23. The limits for any radionuclide are the more restrictive of the results in Tables 4.1-17 and 4.1-18. With the exception of the relatively short-lived radionuclides Co-60, Cs-137, and U-232, the disposal limits are based on the resident scenario at 10,000 years after disposal, because the shielding between the source and receptor locations is considerably less in the case of residence on unshielded waste compared with residence on an intact concrete barrier above the waste. The disposal limits for Co-60, Cs-137, and U-232 are undoubtedly pessimistic, because the planned thickness of the concrete roof and layer of uncontaminated grout above the waste is about 1.8 m thick but only 1 m of shielding was assumed in the dose analysis. The disposal limits for the other radionuclides also may be pessimistic. Erosion of the earthen cover to a depth below the top of the gravel layer appears unlikely within 10,000 years. If the gravel layer has not eroded away within 10,000 years, then an excavation for a home probably would not extend to the depth of the waste, and the shielding provided by a layer of uncontaminated material between the top of the waste and the bottom of the excavation was not considered in the dose analysis.

Table 4.1-23. Disposal limits of radionuclides for ILNT and ILT vaults based on analyses of exposure scenarios for inadvertent intruders^a

Radionuclide ^b	Concentration limit ^c ($\mu\text{Ci}/\text{m}^3$)	Inventory limit ^d (Ci)
Al-26	6.5×10^1	4.2×10^{-1}
Co-60	1.0×10^{11}	6.7×10^8
Sn-126	1.7×10^3	1.1×10^1
I-129	8.0×10^4	5.2×10^2
Cs-137	1.1×10^8	7.4×10^5
Eu-154	1.9×10^9	1.2×10^7
Th-232	7.1×10^1	4.7×10^{-1}
U-232	1.7×10^3	1.1×10^3
U-234	1.6×10^3	1.0×10^1
U-235	1.0×10^3	6.5
U-238	8.1×10^3	5.2×10^1
Np-237	1.0×10^3	6.7
Am-243	3.2×10^3	2.1×10^1
Cm-245	7.7×10^3	5.0×10^1
Cm-247	6.3×10^2	4.1

- ^a Values are more restrictive of limits for resident scenario at 100 and 10,000 years after disposal given in Table 4.1-17, 4.1-18, 4.1-20, and 4.1-21.
- ^b For radionuclides not listed, either there are no disposal limits based on scenarios for inadvertent intrusion or concentration limits in individual waste packages are restricted to limits for Class-C wastes specified in NRC's 10 CFR Part 61 (see Table 4.1-24).
- ^c Limit on average concentration in disposed waste.
- ^d Limit on inventory per vault, sum of ILNT and ILT limits.
- ^e Limit for Class-C waste specified in NRC's 10 CFR Part 61; limit applies to individual waste packages.

As indicated in Table 4.1-23, analyses of scenarios for inadvertent intrusion have established disposal limits for only a relatively few of the total number of radionuclides that could occur in the waste. For all other radionuclides of concern with half-lives sufficiently long that they possibly could exist in significant amount at 100 years after disposal when inadvertent intrusion first could occur, either there are no disposal limits based on the intruder dose analysis or the concentrations in individual waste packages are restricted to the limits for Class-C waste specified by the NRC in 10 CFR Part 61. Concentration limits for Class-C waste specified by the NRC are given in Table 4.1-24.

LAW Vaults

For the LAW vaults, all three exposure scenarios for inadvertent intruders are presumed to be credible during the 10,000-year compliance period, primarily because these vaults do not contain a layer of uncontaminated grout above the waste and the waste itself is not grouted. Based on an analysis of the collapse and subsequent degradation of the concrete roof for the LAW vaults, the agriculture scenario is most likely to become credible at about 5,000 years after disposal and the post-drilling scenario could occur at about 3,000 years. The only relevant resident scenario involves residence on an intact concrete roof at 100 years after disposal. Results for the three scenarios are given in Tables 4.1-15, 4.1-19, and 4.1-22.

The estimated limits on concentrations and inventories of radionuclides for the LAW vaults, as obtained from the analyses of the agriculture scenario at 5,000 to 10,000 years after disposal, the resident scenario at 100 years, and the post-drilling scenario at 3,000 years, are summarized in Table 4.1-25. The limits for any radionuclide are the most restrictive of the limits for the relevant scenarios. For most radionuclides, the disposal limits are based on the agriculture scenario at 5,000 to 10,000 years after disposal. However, for Co-60, Cs-137, and U-232, the limits are based on the resident scenario at 100 years after disposal, and the limits for Tc-99 are based on the post-drilling scenario at 3,000 years. Tc-99 represents an unusual case where a large fraction of the initial inventory of waste is predicted to be removed from the vaults by mobilization and transport in water between the times the post-drilling and

Table 4.1-24. Concentration limits of radionuclides for Class-C waste specified in NRC's 10 CFR Part 61^a

Radionuclide	Concentration limit ($\mu\text{Ci}/\text{m}^3$)
C-14 ^b	8.0×10^6
Ni-59 ^b	2.2×10^7
Ni-63 ^b	7.0×10^8
Sr-90	7.0×10^9
Tc-99	3.0×10^6
I-129	8.0×10^4
Cs-137	4.6×10^9
"	$1.0 \times 10^{12} \text{ }^d$
Pu-241	$3.5 \times 10^3 \text{ }^d$
Cm-242	$2.0 \times 10^4 \text{ }^d$

^a Limits from Table 1 and 2 of 10 CFR Part 61 apply to individual waste packages at DOE disposal sites (U.S.DOE 1988a).

^b If radionuclide occurs in form of activated metal, concentration limit is increased by factor of 10.

^c All alpha-emitting transuranic radionuclides with half-lives greater than 5 years.

^d Units are nCi/g; 1 nCi/g corresponds approximately to $2 \times 10^3 \mu\text{Ci}/\text{m}^3$.

Table 4.1-25. Disposal limits of radionuclides for LAW vaults based on analysis of exposure scenarios for inadvertent intruders^a

Radionuclide ^b	Concentration limit ^c ($\mu\text{Ci}/\text{m}^3$)	Inventory limit ^d (Ci)
C-14	1.9×10^4	8.9×10^2
Al-26	3.2×10^1	1.5
Co-60	7.1×10^8	3.4×10^7
Ni-59	1.9×10^6	9.2×10^4
Se-79	2.4×10^6	1.2×10^5
Rb-87	6.6×10^4	3.2×10^3
Zr-93	2.8×10^6	1.3×10^5
Tc-99	1.0×10^5	5.0×10^3
Pd-107	3.9×10^6	1.9×10^5
Sn-126	7.3×10^4	3.5
I-129	8.0×10^4 ^e	3.8×10^3
Cs-135	3.3×10^5	1.6×10^4
Cs-137	1.9×10^5	9.1×10^3
Eu-154	1.0×10^7	4.9×10^5
Th-232	8.9 ^f 3.5×10^1 ^e	4.3×10^{-1} ^f 1.7 ^e
U-232	3.6×10^3	1.7×10^2
U-233	1.2×10^4	5.6×10^2
U-234	1.6×10^1 ^f 6.6×10^2 ^e	7.6×10^{-1} ^f 3.2×10^1 ^e
U-235	3.7×10^2	1.8×10^1
U-236	1.3×10^4	6.0×10^2
U-238	9.3×10^2 ^f 3.0×10^3 ^e	4.5×10^1 ^f 1.5×10^2 ^e
Np-237	2.8×10^2	1.3×10^1
Pu-239	3.6×10^3	1.7×10^2
Pu-240	5.3×10^3	2.5×10^2
Pu-242	3.3×10^3	1.6×10^2
Pu-244	3.4×10^3	1.6×10^2

Table 4.1-25. (continued)

Radionuclide ^b	Concentration limit ^c ($\mu\text{Ci}/\text{m}^3$)	Inventory limit ^d (Ci)
Am-241	^e	---
Am-242m	^e	---
Am-243	8.1×10^2	3.9×10^1
Cm-245	1.7×10^3	8.3×10^2
Cm-246	6.5×10^3	3.1×10^2
Cm-247	2.8×10^2	1.4×10^1
Cm-248	9.0×10^2	4.3×10^1
Cf-249	^e	---
Cf-251	3.7×10^4	1.8×10^3

- ^a Values are most restrictive of limits for agriculture scenario at 5,000 or 10,000 years after disposal given in Table 4.1-14, resident scenario at 100 years after disposal given in Table 4.1-20, or post-drilling scenario at 3,000 years after disposal given in Table 4.1-23.
- ^b For radionuclides not listed, either there are no disposal limits based on scenarios for inadvertent intrusion or concentration limits in individual waste packages are restricted to limits for Class-C wastes specified in NRC's 10 CFR Part 61 (see Table 4.1-24).
- ^c Limit on average concentration in disposed waste.
- ^d Limit on inventory per vault.
- ^e Limit for Class-C waste specified in NRC's 10 CFR Part 61; limit applies to individual waste packages.
- ^f Results include contributions to dose from radon decay product.
- ^g Results exclude contributions to dose from radon decay product.
- ^h Limit for individual waste packages is based on requirement that concentration of all alpha-emitting transuranic radionuclides with half-lives greater than 5 years not exceed 100 nCi/g (about $2 \times 10^5 \mu\text{Ci}/\text{m}^3$).

agriculture scenarios are assumed to occur, due to the significant increase in infiltration at times beyond collapse of the vault roof at 3,000 years after disposal. Two sets of concentration and inventory limits are given for Th-232, U-234, and U-238. If exposures to radon decay products are taken into account in estimating doses to inadvertent intruders, which presumably is required by the present performance objective (U.S.DOE 1988a), then the lower of the disposal limits apply for each isotope. However, if the dose limit in the performance objective for protection of inadvertent intruders were to exclude doses from exposure to radon and a separate limit on radon flux rate to the atmosphere were imposed, as is presently being considered in revision of DOE Order 5820.2A, then the higher of the disposal limits apply.

ILT Vaults

The dose analysis for inadvertent intruders is essentially the same for the ILT vaults as for the ILNT vaults, because both types of vaults will be constructed in the same manner. Therefore, as in the case of the ILNT vaults, the only exposure scenario for inadvertent intruders that reasonably could be used to determine disposal limits of radionuclides for the ILT vaults is the resident scenario, evaluated at either 100 or 10,000 years after disposal.

The estimated limits on concentrations and inventories of radionuclides for the ILT vaults, as obtained from the analysis of the resident scenario at 100 and 10,000 years after disposal in Tables 4.1-20 and 4.1-21, are summarized in Table 4.1-26. With the exception of Co-60, Cs-137, and U-232, the disposal limits are based on the resident scenario at 10,000 years after disposal. As described previously for the ILNT vaults, the disposal limits for Co-60, Cs-137, and U-232 are expected to be quite pessimistic, because the amount of shielding between the source and receptor locations has been underestimated by a significant amount, and the disposal limits for the other radionuclides also may be pessimistic, because excavation to the depth of the waste appears unlikely within 10,000 years after disposal.

Table 4.1-26. Disposal limits of radionuclides for ILT vaults based on analyses of exposure scenarios for inadvertent intruders^a

Radionuclide ^b	Concentration limit ^c ($\mu\text{Ci}/\text{m}^3$)	Inventory limit ^d (Ci)
Al-26	8.9×10^4	7.1×10^1
Co-60	1.0×10^{11}	8.3×10^7
Sn-126	1.7×10^3	1.3
I-129	8.0×10^4 ^e	4.6×10^2
Cs-137	1.1×10^8	9.1×10^4
Eu-154	1.9×10^9	1.5×10^6
Th-232	7.1×10^1	5.7×10^{-2}
U-232	1.7×10^5	1.4×10^2
U-234	1.6×10^3	1.3
U-235	1.0×10^3	8.0×10^{-1}
U-238	8.1×10^3	6.5
Np-237	1.0×10^3	8.6×10^{-1}
Am-243	3.2×10^3	2.6
Cm-245	7.7×10^3	6.1
Cm-247	6.3×10^2	5.0×10^{-1}

- ^a Values are more restrictive of limits for resident scenario at 100 and 10,000 years after disposal given in Table 4.1-21 and 4.1-22, respectively.
- ^b For radionuclides not listed, either there are no disposal limits based on scenarios for inadvertent intrusion or concentration limits in individual waste packages are restricted to limits for Class-C wastes specified in NRC's 10 CFR Part 61 (see Table 4.1-24).
- ^c Limit on average concentration in disposed waste.
- ^d Limit on inventory per vault.
- ^e Limit for Class-C waste specified in NRC's 10 CFR Part 61; limit applies to individual waste packages.

4.2 SENSITIVITY AND UNCERTAINTY ANALYSES

To interpret the results provided in the previous section (Sect. 4.1), parameters and assumptions to which the results are most sensitive must be identified. The uncertainty associated with these parameters and assumptions must also be considered to determine the degree of confidence in the predicted results. A rigorous quantitative analysis of uncertainty is desirable, but such an analysis is not possible for all aspects of the analyses conducted for this RPA due to: 1) limits of our knowledge with respect to certain physical and functional characteristics or processes; 2) the inability to predict conditions in the future, especially beyond several decades; and 3) the inability to quantify uncertainty associated with the definition of a particular scenario. This last type of uncertainty can dominate the overall uncertainty in some cases.

In this section, sensitivity and uncertainty analyses are discussed separately for the following stages of the overall computational approach: 1) analysis of near-field transport to the water table from the vaults and subsequent groundwater transport; 2) dose analysis for off-site releases; and 3) dose analysis for inadvertent intruders.

4.2.1 Analysis of Near-Field and Groundwater Transport

In this RPA, the fractional fluxes of radionuclides to the water table were simulated in the near-field model with PORFLOW and used as a source to the saturated flow and transport model (also simulated with PORFLOW) to determine groundwater concentrations as a function of time and distance from the EAV. The sensitivity and uncertainty analysis of the near-field groundwater transport model is discussed in this section.

A sensitivity and uncertainty analysis was performed on the near-field and groundwater transport models with respect to selected parameters (Appendix J). The PORFLOW simulations of the ILNT vault system were evaluated in terms of the movement of ^{99}Tc from the vault area through the vadose zone and in groundwater. The study focusses on the sensitivity and uncertainty in model results with respect to the K_s s in the waste form, concrete and soil of the unsaturated zone, and with respect to timing of two different types of vault failure: roof cracking and roof collapse.

Sensitivity of, and uncertainty in, PORFLOW simulations of vault-contained low-level radioactive waste were evaluated in the Z-Area RPA (WSRC 1992b) with respect to variable infiltration rates and hydraulic and diffusive properties of the waste form, vaults, and soil. The results indicated a low sensitivity to infiltration rate, due to the flux-controlling nature of the low-conductivity concrete materials, and a high sensitivity to hydraulic conductivity, especially to that of the material with the lowest conductivity. Ultimately, the amount of water allowed to flow through the waste and reach the water table controls the final groundwater concentration. A large uncertainty in the hydraulic conductivity can translate to a large uncertainty in predicted results. However, the EAVs analysis is expected to be less sensitive to concrete hydraulic conductivities with respect to maximum groundwater concentrations, since most of the radionuclides of concern are long-lived and, thus, are available for transport after vault failure is assumed. Degradation of the low-conductivity concrete is considered to be complete in approximately 1000 years, during which time leaching or radioactive decay for most of the E-Area radionuclides of concern is minimal.

The analysis of the influence of K_d and timing parameters (Appendix J) together resulted in specification of distributions and bounds on values of five factors for the PORFLOW simulations in this analysis. The results of the sensitivity analysis indicated that the peak groundwater concentration was most sensitive to the concrete K_d assumed for ^{99}Tc (accounting for 96% of the response variability). This is likely due to the fact that concrete K_d s specified in this RPA are orders of magnitude larger than the waste or soil K_d s for ^{99}Tc , such that retardation in the concrete is the controlling geochemical factor in the simulations. The time that the peak occurred was also fairly sensitive to the time assumed between vault cracking and roof collapse. The amount of variability, or uncertainty, in the ^{99}Tc results was rather low for the range of parameter values tested. Calculated 95% tolerance limits indicated peak groundwater concentrations to range between 0.008 and 0.192 pCi/cc per Ci of ^{99}Tc in the ILNT vaults, while the time of the peak ranged from 780 to 5500 years with 95% confidence. The peak groundwater concentration of ^{99}Tc from Table 4.1-5 is 0.04 pCi/cc per Ci in the ILNT vaults, occurring at 1800 years, which is approximately the midpoint of these distributions. A cumulative distribution function of the maximum groundwater concentrations calculated in the uncertainty analysis (Fig. 4.2-1) indicated that although 50% of the calculated peak

MAXIMUM GROUNDWATER CONCENTRATION TC99

95% CONFIDENCE LIMITS ON DISTRIBUTION

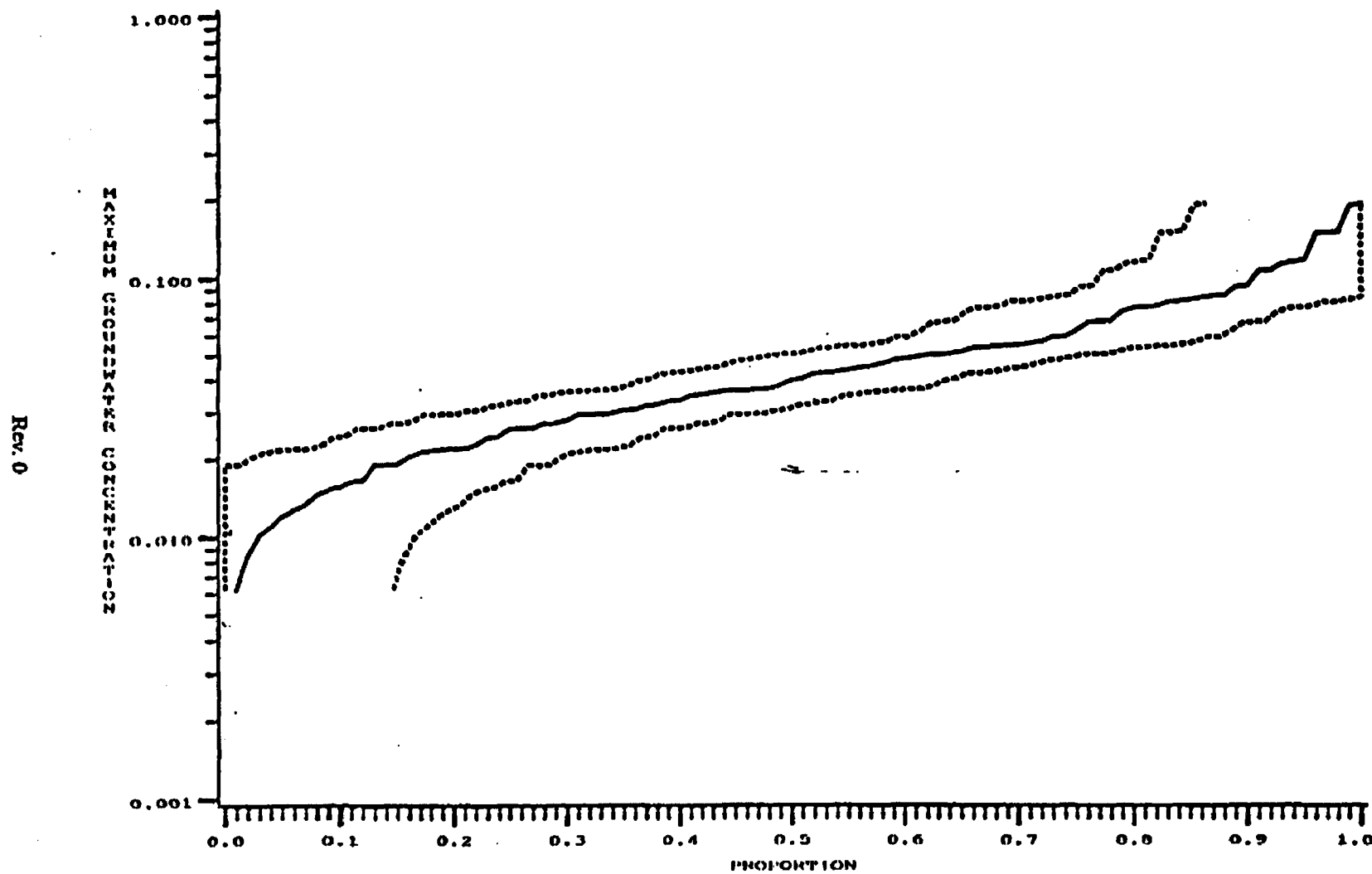


Fig. 4.2-1. Cumulative distribution function for peak groundwater concentration of ^{99}Tc , based on ranges of parameters specified in Appendix J.

groundwater concentrations appear to exceed the 0.04 pCi/cc per Ci inventory, less than 10% exceed 0.1 pCi/cc per Ci. Because the ranges of K_d s and timing of degradation events were specified to be very broad for the uncertainty analysis (Table J.1-1, Appendix J), the results of this analysis lend confidence in the RPA results for near-field transport.

A preliminary sensitivity analysis of the PORFLOW saturated flow and transport model indicates that simulation of flow is sensitive to the amount of recharge assumed and the horizontal and vertical saturated hydraulic conductivities of the five hydrologic units assumed in the model. The simulation of transport by groundwater is directly proportional to the flux of contaminant to the water table, but is insensitive to the diffusion coefficient because the transport in groundwater is advection-dominated. Sensitivity of the model to transverse and longitudinal dispersivities within the reasonable ranges for these parameters is low because the plume originating at the EAV facility is so broad.

Sensitivity to recharge under the facility was tested by varying the recharge rate between 0.2 and 40 cm/year under the area covered by the facility, and assuming 40 cm/year elsewhere in the model domain. Increasing recharge from 0.2 to 2 cm/year under the EAV results in only a slight increase in water levels and hydraulic gradients under the facility, and virtually no change in the contaminant concentration at the compliance point for a given flux of contaminant to the water table. This is likely due to the relative unimportance of either 0.2 or 2 cm/year recharge to the flow system under the facility. When recharge under the EAV is increased to 40 cm/year, the simulated elevation of the groundwater table and hydraulic gradient under the facility are observed to increase more dramatically, but contaminant concentrations at the point of compliance do not decrease as dramatically for a given flux of contaminant to the aquifer.

While the sensitivity and uncertainty analysis with respect to selected parameters for Tc-99 indicates low variability around the reported groundwater concentrations for Tc-99, groundwater concentrations for solubility-limited radionuclides (i.e., isotopes of U and Pu) have an additional type of associated uncertainty - that of the prescribed solubility limits. It is believed that the uncertainty associated with the solubility limits applied is largely governed by the changes in geochemistry that may occur over time, as the vaults degrade. It is very

difficult, if not impossible, to predict these changes and the effect they may have on solubility of U and Pu with a quantifiable degree of certainty because of the multitude of competing geochemical processes involved. Therefore, quantification of uncertainty associated with the groundwater concentrations of U and Pu isotopes was not attempted in this analysis.

4.2.2 Analysis of Dose Model from Off-Site Releases

As described in Sect. 4.1.4 and elsewhere, the drinking water pathway is the primary exposure pathway of concern for releases of radionuclides via the groundwater pathway beyond the 100-m buffer zone around disposal units. In this section, the sensitivity and uncertainty analysis of the model used to estimate dose from the drinking water pathway is discussed.

For a given concentration of a radionuclide in groundwater, the estimated dose from the drinking water pathway is given by Eq. (A.4-1) of Appendix A.4. In this equation, the dose per unit concentration of a radionuclide for the drinking water pathway is directly proportional to two parameters: 1) the consumption rate of drinking water from the affected source and 2) the ingestion DCF for the radionuclide. Both of these parameters are assumed to be fixed values for a reference adult as specified by regulatory authorities or international advisory groups. In this analysis, the assumed consumption rate of water of 2 L/d is the value normally specified by the EPA in demonstrating compliance with DWS for radionuclides; and the ingestion DCFs for radionuclides, which are given in Table A.4-2 of Appendix A.4, are values developed by the International Commission on Radiological Protection. Therefore, for purposes of this analysis, the dose from the drinking water pathway per unit concentration of any radionuclide in groundwater is assumed to be a prescribed value with no uncertainty.

In any population of exposed individuals, the intake rate of water and the ingestion DCFs for radionuclides are variables that could be described by a mean value and standard deviation. However, for the type of dose analysis presented in this report, it is customary to assume, as indicated above, that all exposed members of the general public are reference individuals who experience the same intake rates of water and the same doses per unit activity intakes of radionuclides by ingestion. The assumed intake rate of drinking water of 2 L/day is not likely to be exceeded by most individuals.

Although the dose per unit concentration of a radionuclide in water for a normal population would be subject to some uncertainty, this uncertainty undoubtedly will be much less than the uncertainty associated with estimates of the maximum concentrations of radionuclides in groundwater at any location beyond the 100-m buffer zone. Thus, the assumption of no uncertainty in the model for estimating dose from the drinking water pathway should have no effect on the overall uncertainty in the performance of the disposal facility with regard to meeting the performance objective for protection of groundwater resources.

4.2.3 Analysis of Dose Models for Inadvertent Intruders

The model for estimating dose to an inadvertent intruder, as represented by Eq. 4.1-1, is based on estimates of annual doses per unit concentration of radionuclides in disposed waste, the so-called SDCFs for the agriculture, resident, and post-drilling scenarios summarized in Tables 4.1-10, 4.1-11, and 4.1-12, respectively. This section discusses the sensitivity and uncertainty analysis of the models used to estimate the SDCFs for the different exposure scenarios for inadvertent intruders. The sensitivity and uncertainties in these models do not depend on similar considerations regarding depletion of radionuclide inventories in disposal units due to mobilization and transport in water, which are discussed in Sect. 4.2.1.

For each of the assumed exposure scenarios, the SDCFs for radionuclides are single values based on the models and parameter values presented in Appendix A.4.5. The parameter values adopted for use in the models for the different exposure pathways usually were intended to represent reasonable average conditions that might be experienced, rather than maximum possible conditions that would yield the highest estimates of dose. This approach was used in selecting parameter values related to human activities, such as the annual consumption of foodstuffs, breathing rate, and exposure times, and parameter values describing transport of radionuclides through environmental pathways to man, such as the elemental plant-to-soil concentration ratios and atmospheric mass loading of activity suspended from surface soil.

The exposure pathways considered in the dose analyses for an inadvertent intruder for the different exposure scenarios include consumption of vegetables grown in contaminated garden soil, direct consumption of contaminated garden soil, external exposure while working in the garden or during indoor residence, and inhalation exposure while working in the garden or during indoor residence. In implementing the models for the various exposure pathways, data specific to the SRS generally were not available for such important parameters as the elemental plant-to-soil concentration ratios in vegetables grown in contaminated garden soil and the airborne concentration of suspended radionuclides in particulate form. Therefore, generic parameter values obtained from the literature were used in all exposure pathway models, and the same data can be used to provide crude estimates of uncertainty.

For fission and activation products which do not emit significant intensities of high-energy photons (e.g., Sr-90 and Tc-99), the vegetable pathway is the only significant contributor to the total dose for the agriculture and post-drilling scenarios, and the dose for this pathway is directly proportional to the plant-to-soil concentration ratio. Data available in the literature, which often were obtained under conditions that may not be representative of the SRS, indicate that this parameter could be uncertain by as much as one-to-three orders of magnitude depending upon the radionuclide (Ng et al. 1982; Peterson 1983).

For actinide radioisotopes which do not emit significant intensities of high-energy photons (e.g., Pu-239), the soil ingestion and inhalation pathways are significant contributors to the total dose for the agriculture and post-drilling scenarios. In the model for the soil ingestion pathway, the intake rate of contaminated soil is the only parameter that is subject to variability. There are few data on the distribution of intake rates that could be used to support an uncertainty analysis, but the intake rate presumably is uncertain by at least an order of magnitude. In the model for the inhalation pathway, the dose is proportional to the atmospheric mass loading of suspended activity from surface soil. Generic data indicate that this parameter could be uncertain by two or three orders of magnitude (Anspaugh et al. 1975; Healy 1980).

The dose for the resident scenario is due entirely to external exposure; and, for radionuclides that emit significant intensities of high-energy photons (e.g., Cs-137, Ra-226), this pathway is the only significant contributor to the total dose for the agriculture scenario and is an important contributor to the total dose for the post-drilling scenario. The dose from external exposure depends on the assumed exposure time and the amount of shielding between the source and receptor locations, and it is not particularly meaningful to attempt to quantify uncertainties in these parameters. Particularly in the resident scenario, estimates of external dose could be uncertain by an order of magnitude or more if the assumed thickness of shielding provided by engineered barriers is in error by only a few tens of cm. As described in Appendix A.4.4, the assumed thicknesses of shielding for the types of disposal units constructed with engineered barriers probably result in overestimates of dose. External dose in the resident and agriculture scenarios also depends on the shielding factor for the walls of the home during indoor residence, but this parameter probably is uncertain by no more than a factor of two.

For some important parameters in the exposure pathway models, it is difficult to quantify the uncertainty even on the basis of generic data. An example of a parameter for which the uncertainty appears to be essentially unquantifiable is the assumed dilution factor for mixing of waste exhumed from disposal units with native soil in a vegetable garden. The dose from several exposure pathways in the agriculture scenario and from all exposure pathways in the post-drilling scenario is directly proportional to this dilution factor. An uncertainty analysis for this parameter could be based on estimated uncertainties in the volume of waste exhumed from disposal units, the fraction of exhumed waste that is mixed with soil in a vegetable garden, and the size of the garden. But, except for the assumed size of the garden, there are no data that could be used to support such an uncertainty analysis, essentially because the values are based primarily on assumptions presumed to be reasonable. The uncertainty in this dilution factor is probably an order of magnitude or more. However, it seems likely that the values chosen for use in this analysis tend to overestimate the average concentrations of radionuclides that would be found in contaminated soil in a vegetable garden. The dilution factor of 0.2 assumed in the agriculture scenario probably is conservative because exhumed

waste presumably would not be fertile material and, thus, soil containing a significantly larger fraction of exhumed material would not support plant growth. The dilution factor of 0.02 assumed in the post-drilling scenario is based on reasonable assumptions for the volume of drilling waste and the size of the vegetable garden, and the assumption that all drilling waste is mixed with native soil in the garden clearly is conservative.

The most important source of uncertainty in the estimates of the SDCFs for the different exposure scenarios probably is the definitions of the scenarios themselves, notwithstanding any parameter uncertainties that could be quantified and regardless of whether or not the results would reasonably represent the variability in doses that could be experienced at the SRS. The dose analyses for inadvertent intruders are based on assumptions that the exposure scenarios will occur as postulated, but many of the explicit or implicit assumptions used in defining the scenarios are open to question and, furthermore, are likely to be conservative.

In defining exposure scenarios, it seems reasonable to assume that an inadvertent intruder will establish a homestead within the boundary of the disposal facility at some time after loss of active institutional controls. However, several of the assumptions used in developing the particular exposure scenarios used in this analysis are less certain and probably pessimistic. For example, all scenarios assume that individuals will have no knowledge of prior waste disposal activities at the site, but this assumption seems unreasonable for times soon after loss of active institutional controls. Furthermore, even if knowledge of the disposal facility were lost, all exposure scenarios assume that an inadvertent intruder will build a home or drill a well at the location of disposal units, rather than in uncontaminated areas, and that exhumed waste will be mixed with uncontaminated soil in a vegetable garden. Particularly at the SRS, it may also be pessimistic to assume that an intruder would excavate to depths well below the ground surface in constructing a home, because most homes near the site do not have a basement.

By their very definitions, the exposure scenarios for inadvertent intruders assume conditions that probably tend to produce estimates of dose considerably greater than doses that reasonably could be received by most individuals who might come onto the disposal site. Therefore, it is not really the purpose of a dose analysis for inadvertent intruders to provide best estimates of dose that likely would be received and a quantification of uncertainties in

these estimates. Rather, the primary purpose of the analysis is to establish WAC in the form of limits on average concentrations (total inventories) of radionuclides in waste. Furthermore, quantitative estimates of uncertainties in calculated doses (and, thus, in limits on average concentrations or inventories of radionuclides) based on parameter uncertainty analyses may not be meaningful, because the results are conditional on the occurrence of the assumed exposure scenarios. Therefore, the most important factor in determining whether or not the WAC derived from dose analyses for inadvertent intruders are likely to be reasonable is the credibility of the assumed exposure scenarios—i.e., whether the assumed exposure scenarios reasonably could occur at a particular disposal facility—rather than any estimates of uncertainties in the results due to uncertainties in model parameters.

4.3 INTERPRETATION OF RESULTS

The results presented in Sect. 4.1 can be interpreted by comparing the calculated vault inventory limits and an estimated radionuclide inventory for disposal. As stated in Sect. 1, due to the changing nature of operations at SRS, it is impossible to make an accurate estimate at the present time as to the type and quantity of waste that will be disposed of in the EAVDF. However, an estimate based on several years of disposal while SRS was in production has been made (Reed 1992), and that will be used as the basis for the comparison. While this is a good measure of the usefulness of the vault structures as a method of disposal, this alone is not sufficient to address the question of whether there is reasonable assurance that all performance objectives of DOE Order 5820.2A are met. Further interpretation is necessary because limited data exist for performing realistic and definitive uncertainty analyses. Providing reasonable assurance requires consideration of: 1) sensitivities of results to parameters, assumptions and models; 2) uncertainties in models, parameters and scenarios; and 3) conservatisms, or lack thereof, inherent in the calculational approach or scenarios devised. In this section, some of the more significant observations made throughout this report are summarized and results are interpreted in terms of these observations.

Results presented in Sect. 4.1 indicate that the EAVDF will meet the performance objectives of DOE Order 5820.2A. The results are based on a number of assumptions, simplifications, and scenarios that, in most cases, erred on the side of conservatism. Therefore, the results are more likely to underestimate, rather than overestimate, the inventory allowable in each type of disposal.

4.3.1 Off-Site Doses and Groundwater Protection

For off-site releases, groundwater was demonstrated to be the only pathway of concern except for H-3 and C-14, which are limited by atmospheric emission (see Appendix A.3). Nine radionuclides were limited by the groundwater pathway, Ni-59, Se-79, Sr-90, Pd-107, I-129, Cs-135, Np-237, Am-241, and Cf-252 (based on the Cm-248 daughter). Consideration of solubility limitations on U and Pu isotopes prevents them from exceeding their respective MCLs. Although the solubility limits applied are believed to be reasonable for this waste, the long-term geochemistry is impossible to predict. As noted in Sect. 4.2.1, the uncertainty associated with the predicted groundwater concentrations of U and Pu, arising from uncertainty in long-term geochemistry, has not been addressed. Radioactive decay products of U and Pu isotopes that are potentially radiologically significant were not found to limit the inventory of U or Pu below the assumed initial inventory, with the exception of the Ra-226 daughter of U-234 in the LAW vaults. In this one case, it was estimated that U-234 would be limited to 2.6×10^4 Ci for all 21 LAW vaults, or about 200 kg/LAW vault.

As stated in Sect. 1.2, the current MCLs, promulgated under the Safe Drinking Water Act, are used in this RPA to assess compliance with the groundwater protection performance objective of DOE Order 5820.2A. For uranium a compliance limit of 20 $\mu\text{g/L}$ is used (EPA 1991).

Degradation of the vaults and the overlying closure cap were considered in this RPA because the engineered features of the facility are not expected to last indefinitely. An engineering study was commissioned to provide a basis for selecting degradation time for use in the analysis (Appendix K). As stated in Sect. 2.5.2.4, the EAVs were designed to withstand a 0.2 g earthquake after closure. Based on Sect. 2.1.5.2, seismic events are not expected to

produce accelerations at SRS greater than 0.1 g; thus, seismic events were considered less significant than other degradation mechanisms. Although many mechanisms potentially contributing to degradation are identified (Sect. 3.1.3), the impossibility of predicting the timing and magnitude of degradation processes renders the uncertainty associated with the degradation scenario high.

4.3.2 Inadvertent Intruders

Scenarios were developed and dose analyses were completed to estimate exposures to hypothetical inadvertent intruders. Acute exposure scenarios for inadvertent intruders were not included, because they would always be less restrictive in regard to demonstrating compliance with performance objectives than chronic exposure scenarios (Sect. 3.2.4.3). The four chronic exposure scenarios considered were: 1) an agricultural scenario with direct intrusion into the disposal vaults; 2) a resident scenario; 3) a post-drilling scenario; and 4) volatile transport. Some considerations are important for interpretation of the intruder results.

One consideration is the longevity of the engineered structures. If the vaults maintain their integrity for several hundred years then all of the radionuclides with relatively short half-lives decay away before intrusion into the waste is possible. As shown in Appendix K and Sect. 3.1.3.2, even in the conservative analysis presented, the vaults will be effective intruder barriers for at least 1,000 years.

The second consideration is the long-term dose in the agricultural scenario due to the buildup of radium and radon daughters from U-238 and U-234. As shown in Tables 4.1-14 and 4.1-15, doses from these isotopes exceed performance objectives at very long times after disposal. However, as stated in Sect. 1.2, this RPA assumes that only doses calculated out to 10,000 years after disposal are considered for compliance. Also, as stated in Sect. 1.2.3, dose from radon and its decay products will be excluded from inadvertent intruder dose for the purpose of assessing compliance. A separate performance objective for radon ($20 \text{ pCi/m}^2 \text{ s}$) is established. A conservative analysis of the radon exhalation rate from the EAVDF is presented in Appendix A.3.

Yet another consideration is the effect of long-term land use policy at SRS. Draft DOE Order 5820.2B (U.S.DOE 1994) considers the use of inadvertent intruder analyses to determine whether a site should be released for unrestricted use. Also, DOE Headquarters Offices of Environmental Restoration and Waste Management (EM) and Facilities Management (FM) are jointly sponsoring an effort to develop future use plans for each of the DOE sites. The expectation for SRS is that the EAVDF and surrounding land will be zoned for industrial use only and will be controlled in perpetuity. This will eliminate the potential for inadvertent intrusion. Table 4.1-9 presents acceptable inventory limits for the EAVDF derived only from the groundwater protection scenario. Long-term land use plans will be developed and implemented; however, because this effort is only now in the planning stage, this PA will conservatively establish inventory limits based on protection of inadvertent intruders. Future revisions of the PA will take appropriate credit for land use planning.

4.3.3 Disposal Limits for Waste at E-Area

Limiting inventories calculated from the groundwater pathway (Table 4.1-9) and intruder scenarios (Table 4.1-14 and Table 4.1-15) as well as the results of the atmospheric effluent analyses in Appendix A.3, have been combined in Table 4.3-1, which lists for each radionuclide the most restrictive of the three. The limiting inventories in Table 4.3-1 can be compared with an estimated vault inventory which is shown in Table 4.3-2 for the LAW vaults and Table 4.3-3 for the ILNT vaults. The estimated inventory (Reed 1992) is based on the average waste receipts at the SRS burial ground during the three year period 1986 through 1988. The average annual receipts were multiplied by a factor of 2.5 to provide a conservative inventory estimate.

None of the vault limits exceed the estimated inventory. Thus, the limits calculated in this PA are not expected to restrict waste receipts to the EAVDF.

The inventory limits calculated in this analysis are implemented through a set of WAC and managed through the SRS's computerized Waste Information Tracking System (WITS). The operating limits for the EAVs, as documented in the SRS WAC Manual (WSRC 1993), are derived from safety documentation and this PA. The WAC Manual is a compilation of

Table 43-1. E-Area Vault Disposal Facility performance-based inventory limits (Ci/vault) and limiting performance objectives

Radionuclide	LAW	ILNT & ILT (ILNT only for ^3H)	ILT
H-3	8.3×10^5 (air)	5.0×10^5 (air)	6.7×10^4 (air) JCW* 4.2×10^7 (air) crucibles
C-14	4.0×10^1 (air)	1.0×10^1 (air)	
Al-26	1.5 (a)	4.2×10^{-1} (r)	
Co-60	3.4×10^7 (r)	6.7×10^2 (r)	
Ni-59	7.6×10^2 (g)	1.8×10^3 (g)	
Se-79	6.2 (g)	8.9 (g)	
Rb-87	3.2×10^3 (a)	No limit #	
Sr-90	2.5×10^{12} (g)	3.0×10^{13} (g)	
Zr-93	1.3×10^5 (a)	No limit #	
Tc-99	2.0 (g)	2.0 (g)	
Pd-107	1.9×10^5 (a)	No limit #	
Sn-126	3.5 (a)	1.1×10^1 (r)	
I-129	1.0×10^{-3} (g)	5.3×10^{-4} (g)	
Cs-135	5.7×10^1 (g)	1.9×10^1 (g)	
Cs-137	9.1×10^3 (r)	7.4×10^5 (r)	
Eu-154	4.9×10^5 (r)	1.2×10^7 (r)	
Th-232	1.7 (a)	4.7×10^{-1} (r)	
U-232	1.7×10^2 (r)	1.1×10^3 (r)	
U-233	5.6×10^2 (a)	3.6×10^{13} (g)	
U-234	3.2×10^1 (a)	1.0×10^1 (r)	
U-235	1.8×10^1 (a)	6.5 (r)	
U-236	6.0×10^2 (a)	3.5×10^{19} (g)	
U-238	1.5×10^2 (a)	5.2×10^1 (r)	
Np-237	2.6×10^{-1} (g)	2.0×10^{-1} (g)	
Pu-239	1.7×10^2 (a)	1.6×10^{10} (g)	
Pu-240	2.5×10^2 (a)	No limit #	
Pu-242	1.6×10^2 (a)	No limit #	
Pu-244	1.6×10^2 (a)	No limit #	
Am-241	2.1×10^3 (g)	1.0×10^3 (g)	
Am-243	3.9×10^1 (a)	2.1×10^1 (r)	
Cm-245	8.3×10^1 (a)	5.0×10^1 (r)	
Cm-246	3.1×10^2 (a)	No limit #	
Cm-247	1.4×10^1 (a)	4.1 (r)	
Cm-248	4.3×10^1 (a)	No limit #	
Cf-249	8.1×10^3 (g)	5.1×10^5 (g)	
Cf-251	1.8×10^3 (a)	1.6×10^7 (g)	
Cf-252	4.3×10^6 (g)	2.1×10^8 (g)	

Note: (air) = atmospheric (Appendix A.3)
 (g) = groundwater protection (Table 4.1-9)
 (a) = intruder, agricultural scenario (Tables 4.1-14 and 4.1-15)
 (r) = intruder, resident scenario (Tables 4.1-17, 4.1-18, and 4.1-19).
 (*) = JCW = Job Control Waste
 (#) = Intrusion into waste in the Intermediate Level vaults is not credible until after 10,000 years (Sect. 4.1.5.1).

Table 43-2 Comparison of LAW vault calculated disposal limits with estimated inventory

Radionuclide	Disposal Limit Ci/Vault	Estimated Inventory Ci/Vault	Ratio
H-3	8.3×10^5	5.0×10^3	1.7×10^2
C-14	4.0×10^1	6.0×10^{-4}	6.7×10^3
Al-26	1.5	-----	-----
Co-60	3.4×10^7	2.4	1.4×10^7
Ni-59	7.6×10^2	0	-----
Se-79	6.2	5.5×10^{-6}	1.1×10^6
Rb-87	3.2×10^3	-----	-----
Sr-90	2.5×10^{13}	7.1×10^2	3.5×10^{15}
Zr-93	1.3×10^5	2.6×10^{-2}	5.0×10^6
Tc-99	2.0	2.0×10^{-4}	1.0×10^4
Pd-107	1.9×10^5	2.1×10^{-4}	9.1×10^8
Sn-126	3.5	3.4×10^{-3}	1.0×10^3
I-129	1.0×10^3	3.1×10^{-7}	3.2×10^3
Cs-135	5.7×10^1	1.3×10^{-3}	4.4×10^4
Cs-137	9.1×10^3	7.1×10^2	1.3×10^1
Eu-154	4.9×10^5	-----	-----
Th-232	1.7	3.4×10^{-3}	5.0×10^2
U-232	1.7×10^2	-----	-----
U-233	5.6×10^2	1.2×10^{-1}	4.7×10^3
U-234	3.2×10^1	1.9	1.7×10^1
U-235	1.8×10^1	1.7×10^{-2}	1.1×10^3
U-236	6.0×10^2	3.2×10^{-1}	1.9×10^3
U-238	1.5×10^2	5.5	2.7×10^1
Np-237	2.6×10^{-1}	3.2×10^{-7}	8.1×10^5
Pu-239	1.7×10^2	3.2×10^1	5.3
Pu-240	2.5×10^2	1.2×10^{-1}	2.1×10^3
Pu-242	1.6×10^2	2.2×10^{-7}	7.3×10^8
Pu-244	1.6×10^2	1.2×10^{-1}	1.3×10^3
Am-241	2.1×10^3	4.0×10^{-4}	3.3×10^6
Am-243	3.9×10^1	2.1×10^{-7}	1.9×10^8
Cm-245	8.3×10^1	1.2×10^{-1}	6.9×10^2
Cm-246	3.1×10^2	1.2×10^{-1}	2.4×10^3
Cm-247	1.4×10^1	1.2×10^{-1}	1.2×10^2
Cm-248	4.3×10^1	1.2×10^{-1}	3.6×10^2
Cf-249	8.1×10^3	1.2×10^{-1}	6.8×10^4
Cf-251	1.8×10^3	1.2×10^{-1}	1.5×10^4
Cf-252	4.3×10^6	6.0×10^{-17}	7.2×10^{22}

* Not included in Reed inventory. Calculated by ratio to Cs-137 from Table 2.4 of Cook et al. 1987

**Table 4.3-3 Comparison of ILNT and ILT vault calculated disposal limits
with estimated inventory**

Radionuclide	Disposal Limit Ci/Vault	Estimated Inventory Ci/Vault	Ratio
H-3	5.0×10^5	1.0×10^3	5.0×10^2
C-14	1.0×10^1	0	-----
Al-26	4.2×10^{-1}	-----	-----
Co-60	6.7×10^8	2.4×10^4	2.8×10^4
Ni-59	1.8×10^3	1.3×10^1	1.4×10^2
Se-79	8.9	8.0×10^{-4}	1.1×10^4
Rb-87	-----	-----	-----
Sr-90	3.0×10^{13}	1.3×10^4	2.3×10^9
Zr-93	-----	-----	-----
Tc-99	2.0	2.6×10^{-2}	7.7×10^1
Pd-107	-----	-----	-----
Sn-126	1.1×10^1	6.4×10^{-2}	1.7×10^2
I-129	5.3×10^{-4}	4.3×10^{-5}	1.2×10^1
Cs-135	1.9×10^1	2.4×10^{-2}	7.9×10^2
Cs-137	7.4×10^5	1.3×10^4	5.7×10^1
Th-232	4.7×10^{-1}	3.2×10^{-3}	1.5×10^2
U-232	1.1×10^3	-----	-----
U-233	3.6×10^{13}	2.7	1.3×10^{13}
U-234	1.0×10^1	4.4×10^{-2}	2.3×10^2
U-235	6.5	8.0×10^{-4}	8.1×10^3
U-236	3.5×10^{19}	3.8×10^{-3}	9.2×10^{21}
U-238	5.2×10^1	2.2×10^{-3}	2.4×10^4
Np-237	2.0×10^{-1}	2.5×10^{-3}	8.0×10^1
Pu-239	1.6×10^{10}	4.4×10^{-1}	3.6×10^{10}
Pu-240	-----	-----	-----
Pu-242	-----	-----	-----
Pu-244	-----	-----	-----
Am-241	1.0×10^3	5.6×10^{-2}	1.8×10^4
Am-243	2.1×10^1	2.8×10^{-5}	7.5×10^5
Cm-245	5.0×10^1	2.8	1.8×10^1
Cm-246	-----	-----	-----
Cm-247	4.1	2.8	1.5
Cm-248	-----	-----	-----
Cf-249	5.1×10^5	2.8	1.8×10^5
Cf-251	1.6×10^7	2.8	5.7×10^6
Cf-252	2.1×10^8	3.7	5.7×10^7

* Not included in Reed inventory. Calculated by ratio to Cs-137 from Table 2.4 of Cook et al. 1987

the radionuclide limits from a Safety Analysis Report (SAR), cell criticality limits, 100 nCi/g transuranic concentration limit, NRC Class C limits, and vault performance-based inventory limits. Each of these limits is converted into a hypothetical container limit. For each radionuclide, the most restrictive limit is then implemented as a WAC container limit for the waste generators.

As packages are received for emplacement in the various vaults, their package contents will be entered into WITS. Before emplacement of each package, WITS will compare the package contents with the 100 nCi/g transuranic limits and NRC Class C limits, and calculate the cell inventory (to ensure compliance with the cell criticality limits) and the total vault inventory (to ensure compliance with the PA-based limits). The SAR and PA-based limits are tracked as a sum-of-fractions of the individual radionuclide limits. For the PA-based limits, the total vault inventory for each radionuclide is divided by its corresponding limit. The sum of these fractions will be maintained less than one to ensure compliance with the limits. A similar procedure will be followed to ensure compliance with the SAR limits.

5. PERFORMANCE EVALUATION

The purpose of this site-specific RPA of the EAVDF at the SRS is to fulfill the DOE Order 5820.2A requirement that such an assessment be prepared and maintained for any LLW disposal facility located at a DOE field site. The RPA must provide reasonable assurance that the facility design and method of disposal will comply with the performance objectives of the order, which are concerned with protection of public health and safety, limiting doses to members of the general public and inadvertent intruders, and protecting groundwater resources. In this chapter of the RPA, a summary of how the results of the comprehensive analysis provide reasonable assurance that the performance objectives will be met, followed by consideration of design changes that are based on the results, and recommended data acquisition and research necessary to reduce conservatism in the results are presented.

5.1 COMPARISON TO PERFORMANCE OBJECTIVES

The performance objectives of DOE Order 5820.2A for LLW disposal are listed in Sect. 1.2. In essence, these objectives put forth dose limits for members of the general public and inadvertent intruders that are not to be exceeded at any point in time through consideration of credible pathways. The performance objectives include protection of groundwater resources consistent with Federal, State and local requirements.

For the groundwater protection performance objective, it has been determined that Option 1, as described in Sect. 1.2, is required to be used because of the interpretation of CERCLA regulations by the State of South Carolina. If the proposed drinking water standard is promulgated by the EPA (U.S.EPA 1991), the limits presented in this report must be recalculated.

This PA was prepared using reasonable, but conservative, parameter values to calculate disposal facility inventories that will meet the performance objectives. Implementation of these limits as waste acceptance criteria and a waste certification program will provide reasonable assurance that the performance objectives will be met.

5.2 DESIGN CHANGES REQUIRED TO MEET PERFORMANCE OBJECTIVES

The RPA process assumed the design described for the EAVs in Sect. 2.5 and the closure concept described in Sect. 2.9 of this report. Because the results indicate compliance with performance objectives, no changes to the design of EAVs and suspect soil trenches are recommended. However, the analysis of NR waste presented in Appendix L does not indicate compliance. Rather than indicating the need for design changes, the results presented in Appendix L indicate the need for additional data to reduce conservatism in the analysis (see Sect. 5.3).

However, as noted in Sect. 2.9, a final design for the closure is not now available; a closure concept was analyzed. As the closure design is developed, its performance for limiting infiltration into the waste will be evaluated versus the performance of the closure concept analyzed in this RPA.

5.3 DATA AND RESEARCH NEEDS

In addition to groundwater monitoring (Sect. 2.9.3 and H.2 - recommendation #6), near-field monitoring will be necessary to validate the predicted performance of the EAVDF. However, technology for accomplishing near-field monitoring, especially in terms of *in-situ* monitoring of non-volatile contaminants, is in a developmental stage. SRS will seek and implement appropriate monitoring technology as it becomes available. Meanwhile, SRS will continue to collect data from the various lysimeter programs at SRS. Such data may be useful for validation.

The analysis of naval reactor waste presented in Appendix L does not indicate compliance with performance objectives. However, as noted in Appendix L, the analysis is very conservative because of a lack of data specific to the NR wasteforms. Obtaining data on the composition and physical configuration of the wasteforms and on the expected lifetime of the welds in the disposal containers should enable the analysis to be revised to indicate compliance. Until the analysis is so revised, NR waste will only be received at E-Area for storage.

Although the RPA has indicated compliance with performance objectives for the EAVs and suspect soil trenches, a number of opportunities have been identified which would decrease the conservatism in the analysis. Because the RPA is to be maintained through time, and thus is a living document, further iterations of the RPA process will benefit greatly if these opportunities are explored. Reducing conservatism in the RPA should enable disposal limits to be increased, thus, enhancing the utility of the EAV. Several opportunities for reducing conservatism are discussed below.

The waste in the vaults could be represented more realistically. Presently, all of the waste containers are assumed to totally degrade immediately and the waste is represented as a single stirred tank. Corrosion rates of waste containers could be developed and incorporated into the RPA to take credit for the waste containers. Also, the waste, after container degradation, could be represented as a series of stirred tanks to more realistically represent the waste volume. Treatment of the waste prior to disposal, such as super-compaction, incineration, vitrification, etc., or addition of additives such as zeolite to waste packages, could be incorporated into the RPA to take credit for improved waste forms.

Because the predicted groundwater concentrations of U and Pu isotopes depend on the applied solubility limits for these elements, further research should be conducted to evaluate the appropriateness of the applied limits over the long-term. Geochemical degradation, although difficult to assess, is potentially an important aspect of PAs. Additional consideration of chemical solubility in the waste form for radionuclides with low disposal limits, such as Np-237, should be done. Geochemical modeling and/or laboratory experimentation will be required to determine solubility values.

Since collapse of the LAW vault roof is a significant contributor to doses from the EAV, any measures to prevent, or reduce the extent of, roof collapse would result in significantly increased vault limits. If for example, the LAW vault design and mode of waste emplacement were altered to enable minimizing voids (or filling voids with an inert material such as sand), the roof collapse scenario would be improved. Also, waste emplacement procedures could be implemented to provide for placement of packages containing higher concentrations of radionuclides of concern in intruder scenarios at the bottom of each vault. Another possibility to be considered is to alter the vault (or other disposal unit) design to provide deeper burial of the waste to deter intrusion. In addition, more realistic representation of the collapsed vault in the intruder scenarios to take credit for the presence of the concrete rubble should be considered. More realistic formulation of intrusion scenarios to take credit for practices in the southeastern USA, such as not generally constructing basements for private homes, should be considered. Credit for longer-term institutional control, such as limiting future land use through the Site Development Plan, should be considered.

Modeling of the degraded vaults could be improved by using a time distribution for the development of cracks and collapse of the roofs. Data would need to be developed to support the distributions.

Doses from I-129 in the RPA have been calculated without regard to the isotopic dilution with stable iodine that will take place. Because assimilated iodine is concentrated in the thyroid, and the thyroid has a limited capacity for iodine, consideration of the expected specific activity of I-129 (curies of I-129 per gram of iodine present in the environment) would lead to a more realistic assessment of the dose from I-129.

More rigorous implementation of the sum-of-fractions rule using the timing of doses to improve waste acceptance criteria from the RPA results should be considered.

Although vault design changes are not needed to meet performance objectives, disposal design could be optimized to ensure cost-effective LLW disposal. Alternative disposal technologies such as trench burial could be employed for certain waste types in addition to suspect soil. Further modeling is necessary to develop the appropriate disposal limits for each disposal technology to ensure that performance objectives will be met.

6. PREPARERS

Below is a list of contributors to this performance assessment effort, and the portions of the assessment for which they are responsible.

COOK, JAMES R., WSRC/SRTC, Geology, Geochemistry

M.S. Geochemistry
B.S. Geology

Experience: Mr. Cook has 15 years of experience at the Savannah Rive Site, 13 of which have been in various aspects of low-level waste research. Research topics have included site selection, site characterization, site closure, and performance assessment. Mr. Cook served on the revision team for Chapter 3 of DOE Order 5820.2A. He is a member of the Performance Assessment Task Team. He serves as the technical lead on the PA advisory team.

Contributions: WSRC Technical Leader of PA team. Screening Calculations.

DICKE, CRAIG A., INEL, Radionuclide Screening, Concrete Degradation, Geochemistry

M.S. Geology
B.S. Geology

Experience: Mr. Dicke has 6 years experience in modeling geochemical processes related to radioactive waste disposal.

Contributions: Analyzed the geochemistry of the vault environments, and provided K_d s for radionuclides in all media.

HIERGESELL, ROBERT A., WSRC/SRTC, Geology, Hydrology

M.S. Hydrology/Hydrogeology
B.S. Geology

Experience: Mr. Hiergesell has 16 years of experience relating to all aspects of groundwater investigations. Specific experience includes data collection and analysis, aquifer testing, and groundwater flow modeling.

Contributions: Participated in development and implementation of the three dimensional saturated zone flow model. Collected field data required to calibrate the saturated flow model.

HORWEDEL, JIM L., ORNL, Computer Analyst, Sensitivity and Uncertainty Analysis

M.A. Math Education

Experience: For the last 9 years, Mr. Horwedel has developed the GRESS software system for automation of sensitivity analysis capability into existing computer codes and has applied GRESS to a wide range of waste management and performance assessment analysis codes. Mr. Horwedel has written several drivers for automating the use of statistical sampling methods, such as Latin Hypercube Sampling, for a variety of computers.

Contributions: Performed all sensitivity and uncertainty analysis runs of PORFLOW for both the saturated and unsaturated models. Developed a driver to carry out these runs based on Latin Hypercube sampling procedures. Developed a post-processor to analyze the output of the multiple PORFLOW runs.

HSU, ROBERT H., WSRC/SRTC, R & D Management

D.E.S. Chemical Engineering
M.S. Chemical Engineering
B.S. Chemical Engineering

Experience: Dr. Hsu has 13 years of industrial experience in chemical processing, R&D, safety analysis and management. In his 10 years at SRS his assignments have included laboratory R&D, NRC-format safety analyses, and management of R&D groups. For the past year, he has managed an R&D group that develops technology for support of environmental restoration (soil and groundwater) and for treating, handling and disposing of low-level radioactive, mixed, hazardous, sanitary, and industrial aqueous wastes. The group has expertise in site closure, environmental transport, groundwater modeling and decontamination.

HUNT, PAUL D.

B.S. Nuclear Engineering

Experience: Mr. Hunt has seven years experience on the Navy's Nuclear Power Program and three years experience at the Savannah River Site. He has served as Manager, Low-Level Waste Cognizant Engineering for two years and is the engineering manager for the E-Area Vaults.

Contribution: Advisor to PA team.

KEARL, PETER M., ORNL/GJ, Groundwater Hydrology

M.S. Hydrology/Hydrogeology
B.S. Geology

Experience: Mr. Kearl has extensive experience (13+ years) with designing and installing groundwater monitoring networks to evaluate contaminant transport and for conducting regional aquifer studies. He has dealt with the hydraulics of fractured media as well as cavernous and porous media, and has conducted vadose zone characterizations. He also has several years experience with numerical modeling of groundwater flow.

Contributions: Evaluated the hydrogeologic environment at E-Area, and developed and implemented a three-dimensional saturated flow and transport model. Collected field data required to calibrate the saturated flow model.

KOCHER, DAVID C., ORNL, Exposure Scenario Development, Dose Calculations

Ph.D. Physics

Experience: Dr. Kocher has over 15 years experience in environmental health physics. He also has served on the Performance Assessment Task Team since its inception, and thus, has considerable insight into performance assessment issues.

Contributions: Developed exposure scenarios for intruders and off-site individuals, computed doses from environmental concentrations, and served in an advisory capacity for several other technical issues.

LANGTON, CHRISTINE A., WSRC/SRTC, Material Science

Ph.D. Material Science

M.S. Geochemistry

B.S. Geology

Experience: Dr. Langton has 10 years experience on developing and testing cement wasteforms and inorganic treatment processes for low-level and mixed wastes.

Contributions: Advisor to PA team.

LEVER, WILLIAM E., ORNL, Task Leader, Sensitivity and Uncertainty Analysis

Ph.D. Statistics

Experience: Dr. Lever has over twenty-five years of experience as a statistical consultant. He has been involved in a large number of physical science problems for both ORNL and the Oak Ridge Y-12 Plant.

Contributions: Determined through the analysis of simulated results from PORFLOW, the K_d and time factors that had the greatest influence on the simulated performance of the vault. The analysis was done through the use of Step-Wise Regression Techniques. The variability of the simulated results was examined through the use of confidence and tolerance intervals.

LORAH, STEVEN A., WSRC/SWME, Chemical Engineering

B.S. Chemical Engineering
B.S. Chemistry
B.S. Applied Mathematics

Experience: Mr. Lorah has 5 years of experience in Solid Waste Management at the Savannah River Site. Responsibilities have included technical support for the closure of F- and H-Area Seepage Basin at the SRS, and for the design and permitting of the Consolidated Incineration Facility (CIF). His most recent assignment has been the engineering support for the startup of E-Area Vaults.

Contributions: Input on the facility descriptions and concrete information in the PA Advisor to PA team.

LOWE, PAUL E., WSRC/SRTC, Quality Assurance

B.S. Industrial Engineering
Registered Professional Engineer (PE)

Experience: Mr. Lowe has over 20 years of high technology experience in aerospace, commercial nuclear, and DOE facilities. Six of these years have been in Radioactive Waste Program QA. Mr. Lowe has managed major projects and worked for companies such as Hughes Aircraft, Battelle Institute, as well as major nuclear utilities and consulting firms.

Contributions: Interpreted the Quality Assurance requirements of the PA and ensured SRTC and the National Laboratories performed their research in a manner consistent with good QA practice. This was accomplished by reviews and QA surveillances of all the contractors on the project.

MCDOWELL-BOYER, LAURA M., ORNL/GJ, Groundwater Hydrology

Ph.D. Civil/Environmental Engineering
M.S. Radiological Health Physics

Experience: Dr. McDowell-Boyer has eight years experience in radiological exposure assessments, has directed the development of a multi-media environmental transport model, studied mechanisms of subsurface contaminant migration, and modeled groundwater flow and transport.

Contributions: Evaluated the hydrogeologic environment at E-Area, assisted with the development and implementation of a three-dimensional saturated flow and transport model, and coordinated production of the final draft and final report of this PA effort. Co-principal investigator of PA.

MCVAY, CHARLES W., WSRC/SWO, Facility Manager EAV

B.S. Chemistry

Experience: Mr. McVay has 9 years of experience in the nuclear field. Seven years of experience were at the West Valley Demonstration Project in analytical chemistry analysis and laboratory analysis, waste management activities including remediation, and disposal and treatment. The 2 years of experience at Savannah River have been predominantly in startup activities with E-Area Vaults.

Contributions: Reviewed draft PA.

REED, SHAWN R., WSRC/SWME

B.S. Geology
B.S. Mechanical Engineering
M.S. Geophysics

Experience: Mr. Reed has 3½ years of experience in Solid Waste Management at the Savannah River Site. He functioned as the technical support engineer for the E-Area Vaults during the design phase and has been involved with the E-Area Vaults Performance Assessment for 2½ years.

Contributions: Advisor to PA team.

RODDY, NATHANIEL S., WSRC/SRTC, Engineer

B.S. Civil Engineering

Experience: Mr. Roddy has five years of experience at the Savannah River Site in the area of low-level waste programs. Research programs include closure cap evaluation utilizing the HELP computer code. He served as chairperson of the Process Requirements Team for the E-Area Vaults, and was responsible for the preparation of the PR document. Mr Roddy has served as an alternate Operational Readiness Review Board member for the EAV. He co-coordinated the Engineered Low-Level Trench-4 flood recovery. He is a member of the Performance Assessment advisory team.

Contributions: Advisor to PA team.

**SEITZ, ROGER R., INEL, Near-Field Degraded Vault Flow and Transport,
Radionuclide Screening**

**B.S. Mathematics
(pursuing M.S. in Chemical Engineering)**

Experience: Mr. Seitz has over nine years of experience in conducting performance assessments for high- and low-level waste disposal facilities. His experience is primarily in the area of flow and transport modeling in porous media with some additional experience in radiological dose calculations.

Contributions: Principal investigator for near-field modeling.

SMITH, CARY S., INEL, Unsaturated Zone Conceptual Design and Modeling

B.S. Mathematics

Experience: Mr. Smith's primary area of expertise is applied mathematics and mathematical modeling. Mr. Smith has spent two years working with groundwater flow and contaminant transport modeling. He is doing research on numerical algorithms for fluid flow and transport.

Contributions: Conducted numerical modeling of the fluid flow and contaminant transport for the moisture barrier, concrete vaults, and vadose zone.

SMITH, ROBERT, INEL, Geochemistry

M.S. Geochemistry and Geoscience

Ph.D. Geochemistry and Geoscience

Experience: Dr. Smith specializes in inorganic aqueous geochemistry, with emphasis on the modeling of water-rock system at ambient and elevated temperatures. His work focuses on characterizing chemical processes important in natural systems by the application of thermodynamic principals, kinetic theories and adsorption phenomenon. In addition, Dr. Smith has extensive experience in both domestic and international high-level nuclear waste repository design. He has numerous publications in the areas of geochemistry, mineralogy, and environmental science.

Contributions: Conducted geochemical modeling of the E-Area Vaults.

STEVENS, WILLIAM E., WSRC/SRTC, R & D Management

M.S. Chemical Engineering

B.S. Chemical Engineering

Experience: Mr. Stevens has 17 years of industrial experience in chemical processing, waste management, and environmental restoration. His assignments include process engineering, development engineering, and management of process and project engineering groups, maintenance groups, and R & D groups. For the past four years, he has managed an R & D group that develops technology for support of environmental restoration and minimizing, recycling, treating, handling, and disposing of low-level radioactive, mixed, hazardous, and sanitary waste. The group has expertise in site closure, environmental transport, groundwater modeling, and decontamination. Mr. Stevens is a licensed Professional Engineer.

Contribution: Advisor to PA team.

TAYLOR, GERALD E., WSRC/SWME

B.S. Civil/Structural Engineering

Experience: Mr. Taylor came to the Savannah River Site with 11 years experience at the Tennessee Valley Authority in the Hydraulic Investigations Branch in the Division of Nuclear Engineering. He has functioned as the Disposal Vault Project Engineer for 3 years.

Contribution: Advisor to PA team.

THORNE, DAVID J., ORNL/GJ, Task Group Leader

M.S. Radiological Health Physics

B.S. Geology

Experience: Mr. Thorne has five years experience in radiological transport and dose assessments. His experience includes source term development, contaminant transport modeling, dose and risk assessment, and environmental compliance. He is member of the Performance Assessment Task Team and serves as a research member of the IAEA's research program on Near-Surface Radioactive Waste Disposal Facility Performance Assessments.

Contributions: Integrated results of the various technical tasks and coordinated the production of the initial draft report. Provided technical support to the saturated flow modeling and analysis of volatile emissions release and dose. Co-principal investigator of PA.

WILHITE, ELMER L, WSRC/SRTC, Advisory Scientist

M.S. Inorganic Chemistry
B.S. Chemistry

Experience: Mr. Wilhite has twenty-two years experience at the Savannah River Site. Most of his experience (12 years) has been in low-level waste research. Other experience has included environmental research (3 years), high-level waste research (2 years), and analytical development supervision (3 years). Mr. Wilhite has contributed to the preparation of DOE Order 5820.2A and is currently chairman of the Peer Review Panel.

Contributions: Advisor to PA team.

WORLEY, BRIAN A., ORNL, Task Manager, Sensitivity and Uncertainty Analysis

Ph.D. Nuclear Engineering, Massachusetts Institute of Technology

Experience: Dr. Worley has been involved with reactor physics analysis of advanced reactors since 1977 at ORNL. He has experience in developing methods for sensitivity and uncertainty analysis for reactor systems and waste management systems. He has managed the development of sensitivity and uncertainty analysis work sponsored by ONWI and DOE/LLW since 1985.

Contributions: Provided management and oversight of the sensitivity and uncertainty analysis for the E-Area performance assessment.

YU, ANDREW, WSRC/SRTC, Chemical Engineering**Ph.D. Chemical Engineering**

Experience: Dr. Yu has thirteen years experience in modeling enhanced oil recovery processes prior to joining SRS in 1987. At SRS, he and his coworkers have recommended key design features of disposal vaults based on groundwater protection.

Contributions: Advisor to PA team. Participated in various aspects of the vadose zone model development.

7. REFERENCES

- Aadland, R. K. 1990. *Classification of Hydrostratigraphic Units at Savannah River Site, South Carolina*. Savannah River Laboratory, WSRC-RP-90-987. Westinghouse Savannah River Company, Aiken, SC.
- ACRI. 1993. *PORFLOW: A Model for Fluid Flow, Heat and Mass Transport in Multifluid, Multiphase Fractured or Porous Media, Version 2.50, Draft User's Manual*. Analytic and Computational Research, Inc., Bel Air, Calif.
- Allard, B. 1985. Radionuclide Sorption on Concrete. Nationale Genossenschaft fur die Lagerung Radioaktiver Abfalle report NAGRA-NTB-85-21 (November).
- Alter, H. W., and R. A. Oswald. 1988. Nationwide Distribution of Indoor Radon Measurements. *Radiation Protection Practice*. Proceedings of the Seventh International Congress of International Radiation Protection Association, Sydney: Pergamon Press.
- Amidon, M. B. 1990. *Re: Historic Water Table High at the Burial Ground Expansion Site (U)*. Internal Report. NMP-WMT-900953. Westinghouse Savannah River Company, Savannah River Site, Aiken, SC.
- Anspaugh, L. R., J. H. Shinn, P. L. Phelps, and N. C. Kennedy. 1975. Resuspension and Redistribution of Plutonium in Soils. *Health Phys.* 29:571.
- Arnett, M. W., L. K. Karapatakis, A. R. Mamatey, and J. L. Todd. 1991. *Savannah River Site Environmental Report for 1991*. WSRC-TR-92-186. Westinghouse Savannah River Company, Savannah River Site, Aiken, S.C.
- Atkinson, A., and Hearne. 1984. *An Assessment of the Long-Term Durability of Concrete in Radioactive Waste Repositories*. AERE-R11465. Harwell, U. K.
- Bacs, C. F. III, and R. D. Sharp. 1983. A Proposal for Estimation of Soil Leaching and Leaching Constants for Use in Assessment Models. *J. Environ. Qual.* 12:17.
- Bacs, C. F. III, R. D. Sharp, A. L. Sjoreen, and R. W. Shor. 1984. *A Review and Analysis of Parameters for Assessing Transport of Environmentally Released Radionuclides through Agriculture*. ORNL-5786. Oak Ridge National Laboratory.

- Bollinger, G. A., F. C. Davison, Jr., M. S. Sibol, and J. B. Birch. 1989. Magnitude Recurrence Relations for The Southeastern United States and its Subdivisions. *Journal of Geophysical Research*, 94(B3):2857-2873.
- Briese, L. A., and M. H. Smith. 1974. Seasonal Abundance and Movement of Nine Species of Small Mammals. *J. Mammal*, 55:615-629.
- Cook, J. R. 1991. *Technical Basis for Non-Vault Disposal of Suspect Soil (U)*. WSRC-RP-91-58. Westinghouse Savannah River Company, Savannah River Site, Aiken, S.C.
- Cook, J. R., M. W. Grant, and O. A. Towler. 1987. *Environmental Information Document - New Low-Level Radioactive Waste Storage/Disposal Facilities at the Savannah River Plant*. DPST-85-862. Savannah River Laboratory, E. I. du Pont de Nemours & Co., Inc., Aiken, SC.
- Cummins, C. L., D. K. Martin, and J. L. Todd. 1990. *Savannah River Site Environmental Report*. WSRC-IM-91-28, Volumes I and II. Westinghouse Savannah River Company, Savannah River Site, Aiken, SC.
- Davenport, L. B. 1964. Structure of Two Peromyscus polionotus Populations in Old-Field Ecosystems at the AED Savannah River Plant. *J. Mammal*, 45:95-113.
- Dennehy, K. F., D. C. Prowell, and P. B. McMahon. 1989. *Reconnaissance Hydrological Investigation of the Defense Waste Processing Facility and Vicinity*. E. I. du Pont de Nemours and Company Savannah River Laboratory, Aiken, SC.
- Dodge, R. L., W. R. Hansen, W. E. Kennedy, Jr., D. W. Layton, D. W. Lee, S. J. Maheras, S. M. Neuder, E. L. Wilhite, R. U. Curl, K. F. Grahn, B. A. Heath, and K. H. Turner. 1991. *Performance Assessment Review Guide for DOE Low-Level Radioactive Waste Disposal Facilities*. Prepared by Dames and Moore for Department of Energy Office of Environmental Restoration and Waste Management (DOE/LLW-93). Radioactive Waste Technical Support Program, Idaho National Engineering Laboratory EG&G Idaho, Inc. Idaho. Idaho.

- Eckerman, K. F., A. B. Wohlbarst, and A. C. B. Richardson. 1988. *Limiting Values of Radionuclide Intake and Air Concentration and Dose Conversion Factors for Inhalation, Submersion, and Ingestion*. Federal Guidance Report No. 11. EPA-520/1-88-020. U. S. Environmental Protection Agency, Washington, D.C.
- GeoTrans. 1992. *Groundwater Flow Model for the General Separations Area, Savannah River Site*. GeoTrans Project No: 3017-003. GeoTrans Inc., Sterling, Virginia.
- Golley, F. B., and J. B. Gentry. 1964. Bioenergetics of the Southern Harvester Ant, Pogonomyrmex badius. *Ecol.* 45:217-225.
- Gruber, P. 1980. *A Hydrologic Study of the Unsaturated Zone Adjacent to a Radioactive-Waste Disposal Site at the Savannah River Plant, Aiken, South Carolina*. M.S. Thesis, University of Georgia, Athens, Georgia.
- Hamby, D. M. 1992. Site-Specific Parameter Values for the Nuclear Regulatory Commission's Food Pathway Dose Model. *Health Phys.* 62:136.
- Healy, J. W. 1980. Review of Resuspension Models in Transuranic Elements in the Environment, p. 209. DOE/TIC-22800. Ed. by W. C. Hanson. U. S. Department of Energy, Washington, D. C.
- Hoeffner, S. L. 1985. *Radionuclide Sorption on Savannah River Plant Burial Ground Soil: A Summary and Interpretation of Laboratory Data*. DP-1702. E. I. du Pont de Nemours and Company, Savannah River Laboratory, Aiken, SC.
- Horton, J. H., and E. L. Wilhite. 1978. *Estimated Erosion Rate at the SRP Burial Ground*. DP-1493. E. I. du Pont de Nemours & Co., Inc., Savannah River Laboratory, Aiken, SC.
- INTERA. 1989. *Comparison of Unsaturated Flow and Transport Models with Volume and Nitrate Measurements from a Pilot-Scale, In-Situ Lysimeter with Different Geometry Low Level Radioactive Waste Designs*. INTERA Technologies report H01203R014. INTERA Technologies, Inc., Austin, Texas.
- ICRP. 1959. *Recommendation of the International Commission on Radiological Protection*. International Commission on Radiological Protection. Publication No. 2. Pergamon Press, New York.

- ICRP. 1979. *Limits for Intakes of Radionuclides by Workers*. International Commission on Radiological Protection. Publication 30, Part 1. *Ann. ICRP* 2. No. 3/4. Pergamon Press, Oxford, U.K.
- Kennedy, W. E., Jr., and R. A. Peloquin. 1988. *Intruder Scenarios for Site-Specific Low-Level Waste Classification*. DOE/LLW-71T. Idaho Operations Office, U. S. Department of Energy.
- Ketelle, R. H., and D. D. Huff. 1984. *Site Characterization of the West Chestnut Ridge Site*. ORNL/TM-9229. Oak Ridge National Laboratory, Oak Ridge, Tenn.
- Looney, B. B., Grant, M. W., and King, C. M. 1987. *Estimation of Geochemical Parameters for Assessing Subsurface Transport at the Savannah River Plant*. Savannah River Laboratory Environmental Information Document. DPST-85-904. E. I. du Pont de Nemours and Company, Savannah River Laboratory, Aiken, SC, p. 13.
- Marine, I. W. 1976. *Geochemistry of Ground Water at the Savannah River Plant*. DP-1356. E. I. du Pont de Nemours and Co, Savannah River Laboratory, Aiken, SC.
- Mualem, Y. 1976. A New Model for Predicting the Hydraulic Conductivity of Unsaturated Porous Media. *Water Resources Research*, 12(3):518-522.
- McIntyre, P. F. 1988. *Sorption Properties of Carbon-14 on Savannah River Plant Soil*. DPST-88-900. E. I. du Pont de Nemours and Company, Savannah River Laboratory, Aiken, SC.
- McKenzie, D. H., L. L. Cadwell, L. E. Eberhardt, W. E. Kennedy, Jr., R. A. Peloquin, and M. A. Simmons. 1983. *Relevance of Biotic Pathways to the Long-Term Regulation of Nuclear Waste Disposal; Topical Report on Reference Eastern Humid Low-Level Sites*. NUREG/CR-2675, PNL-4241, Vol. 3. Pacific Northwest Laboratory, Richland, Wash.
- McKenzie, D. H., L. L. Cadwell, W. E. Kennedy, Jr., L. A. Prohammer, and M. A. Simmons. 1986. *Relevance of Biotic Pathways to the Long-Term Regulation of Nuclear Waste Disposal, Phase II, Final Report*. NUREG/CR-2675, PNL-4241, vol. 6. Pacific Northwest Laboratory, Richland, Wash.

- Murphy, C. E., Jr. 1990. *Lysimeter Study of Vegetative Uptake from Saltstone*.
WSRC-RP-90-421. Westinghouse Savannah River Company.
- NCRP. 1987. *Ionizing Exposure of the Population of the United States*. Washington, D. C., NCRP report No. 93. National Council on Radiation Protection and Measurements.
- NCRP. 1989. *Exposure of the U. S. Population from Diagnostic Medical Radiation*. NCRP report No. 100. National Council on Radiation Protection and Measurements, Bethesda, MD.
- NRC. 1977. *Regulatory Guide 1.109. Calculation of Annual Doses to Man from Routine Releases of Reactor Effluents for the Purpose of Evaluating Compliance with 10 CFR Part 50, Appendix I*. Nuclear Regulatory Commission.
- NRC. 1981. *Draft Environmental Impact Statement on 10 CFR Part 61 "Licensing Requirements for Land Disposal of Radioactive Waste."* NUREG-0782. U. S. Nuclear Regulatory Commission, Washington D. C.
- NRC. 1989. *Quality Assurance Program Requirements for Nuclear Facilities*. ASME NQA-1-1989 Edition. The American Society of Mechanical Engineers.
- Ng, Y. C., C. S. Colsher, and S. E. Thompson. 1982. *Soil-to-Plant Concentration Factors for Radiological Assessments*. NUREG/CR-4370, UCID-19463. Lawrence Livermore National Laboratory, Livermore, Calif.
- Oak Ridge National Laboratory Quality Assurance Manual. Current Edition. Oak Ridge National Laboratory, Oak Ridge, Tenn.
- ORNL. 1990. *Performance Assessment for Continuing and Future Operations at SWSA 6*. Internal draft report. Oak Ridge National Laboratory, Oak Ridge, Tenn.
- ORNL Pollutant Assessments Group Procedures Manual. 1992. ORNL-6645/V2/R1. Oak Ridge National Laboratory, Oak Ridge, Tenn.
- Oakly, D. T. 1972. *Natural Radiation Exposure in the United States*. ORP/SID 72-1. U. S. Environmental Protection Agency, Washington, D. C.
- Oblath, S. B. 1985. *Effect of Groundwater on Saltstone Leaching*. Internal Report. DPST-85-504. E. I. du Pont de Nemours and Company, Savannah River Laboratory, Aiken, SC.

- Oztunali, O. I., and G. W. Roles. 1986. *Update of Part 61 Impacts Analysis Methodology*. NUREG/CR-4370. U. S. Nuclear Regulatory Commission and Envirosphere Company.
- Parizek, R. R., and R. W. Root. 1986. *Development of a Groundwater Velocity Model for the Radioactive Waste Management Facility, Savannah River Plant, South Carolina*. Pennsylvania State University, University Park, Penn.
- Peterson, H. T., Jr. 1983. Terrestrial and Aquatic Food Chain Pathways in *Radiological Assessment*. NUREG/CR-3332, ORNL-5968. Ed. by J. E. Till and H. R. Meyer. U. S. Nuclear Regulatory Commission and Oak Ridge National Laboratory, Oak Ridge, Tenn.
- Quality Assurance Program Requirements for Nuclear Facilities*. 1989. ASME NQA-2a, Part 2.7. The American Society of Mechanical Engineers.
- Reed, S. 1992. WER-WMT-929265. Reed-SR-Y5597, Westinghouse Savannah River Company, Aiken, SC.
- Rupp, E. M. 1980. Age Dependent Values of Dietary Intake for Assessing Human Exposures to Environmental Pollutants. *Health Phys.*, 39:151.
- Salvo, S. K., and Cook, J. R. 1993. Selection and cultivation of final vegetative cover for closed waste sites at the Savannah River Site, S.C. *Waste Management '93 Proceedings*, 2:1635-1637.
- Sheppard, M. I. 1985. Radionuclide Partitioning Coefficients in Soils and Plants and Their Correlation. *Health Phys.*, 49:106.
- Sheppard, M. I., and D. H. Thibault. 1990. Default Soil Solid/Liquid Partition Coefficients, K_{ds}, for Four Major Soil Types: A Compendium. *Health Physics*, 59:471-482.
- Smith, M. H. 1971. Food as a Limiting Factor in the Population Ecology of *Peromyscus polionotus* (Wagner). *Physiol. Zool.*, 40:31-39.
- Stephenson, D. E. 1988. *August 1988 Savannah River Plant Earthquake*. DPST-88-841. E. I. du Pont de Nemours & Company, Inc., Savannah River Laboratory, Aiken, SC.

- Stephenson, D. E. 1993. Personal Communication 12/14/93.
- Stephenson, D. E., P. Taiwani, and J. Rawlins. 1985. *Savannah River Plant Earthquake of June 1985*. DPST-85-583. E. I. du Pont de Nemours & Co., Inc., Savannah River Laboratory, Aiken, SC.
- Stone, H. L. 1973. Estimation of Three-Phase Relative Permeability and Residual Oil Data. *Journal of Canadian Petroleum Technology*, October - December.
- Thompson, D. G. 1991. *RE: Vault Closure Concept for Saltstone Vaults*. Internal report OPS-DTZ-91-0002. Westinghouse Savannah River Company, Savannah River Site, Aiken, SC.
- Ticknor, K. V., and Ruegger, B. 1989. *A Guide to the NEA's Sorption Data Base*. Version 2.0, 19 p.
- Toth, J. 1962. A theory of groundwater motion in small drainage basins in central Alberta. *J. Geophys. Res.*, 67:4375-4387.
- URS/Blume, J. A. and Associates, Engineers. 1982. *Update of Seismic Criteria for the Savannah River Plant*. 1, Geotechnical, DPE-3699. E.I. du Pont de Nemours and Company, Savannah River Laboratory, Aiken, SC.
- U. S. Department of Agriculture. 1985. *Site Specific Cropland Erosion Inventory*. Soil Conservation Service, Columbia, SC.
- U. S. Department of Commerce. 1963. *Maximum Permissible Body Burdens and Maximum Permissible Concentrations of Radionuclides in Air and Water for Occupational Exposure*. National Bureau of Standards Handbook 69. NCRP Report No. 22.
- U. S. Department of Commerce. 1977. *1974 Census of Agriculture*. Bureau of the Census, Agriculture Division.
- U.S.DOE. 1987. *Waste Management Activities for Groundwater Protection*, Savannah River Plant, Aiken, SC. Final Environmental Impact Statement, DOE/EIS-0120, Vol. 1. U. S. Department of Energy, Savannah River Plant, Aiken, SC.

- U.S.DOE. 1988a. *Radioactive Waste Management, Order 5820.2A*, U. S. Department of Energy, Washington, D.C.
- U.S.DOE. 1988b. *Internal Dose Conversion Factors for Calculation of Dose to the Public*. DOE/EH-0071. U. S. Department of Energy, Washington, D.C.
- U.S.DOE. 1991. *Analysis of the Environmental Impacts Resulting from Modifications in the Defense Waste Processing Facility*. Environmental Division, Savannah River Operations Office, U. S. Department of Energy, Aiken, SC.
- U.S.DOE. 1994. *Waste Management (draft)*. Order 5820.2B. U. S. Department of Energy, Washington, D.C.
- U.S.EPA. 1991. 40 CFR Parts 141 and 142 - National Primary Drinking Water Regulations; Radionuclides; Proposed Rule. *Federal Register*, 56:33050.
- van Genuchten, M. Th. 1978. *Calculating the Unsaturated Hydraulic Conductivity with a New Closed-Form Analytic Model*. Report 78-WR-08. Water Resources Program, Department of Civil Engineering, Princeton University, Princeton, NJ.
- van Genuchten, M. Th. 1988. *RETC, F77 FORTRAN Code*. June.
- Van Pelt, A. F. 1966. Activity and Density of Old-Field Ants of the Savannah River Plant, South Carolina. *J. Elisha Mitchell Sci. Soc.*, 2:343-351.
- Walton, J. C., L. E. Plansky, and R. W. Smith. 1990. *Models for Estimation of Service Life of Concrete Barriers in Low-Level Radioactive Waste Disposal*. NUREG/CR-5542, EGG-2597. U.S. Nuclear Regulatory Commission, Washington, D.C.
- WSRC. 1991a. *Burial Ground Operation Safety Analysis Report Addendum - E-Area Vaults (U)*. DPSTSA-200-10, SUPP-8, Addendum 1. DOE Review Draft. Westinghouse Savannah River Company, Savannah River Site, Aiken, SC.
- WSRC. 1991b. *Burial Grounds Expansion (U) - Hydrogeologic Characterization, Savannah River Site*. WSRC-RP-91866. Prepared by Sirrine Environmental, Inc., for Westinghouse Savannah River Company, Aiken, SC.
- WSRC. 1992a. *Safety Analysis 200 Area Replacement Tritium Facility*. WSRC-SA-1-1. Savannah River Laboratory, Westinghouse Savannah River Company, Aiken, SC.

- WSRC. 1992b. *Radiological Performance Assessment for the Z-Area Saltstone Disposal Facility*. WSRC-RP-92-1360. Savannah River Laboratory, Westinghouse Savannah River Company, Aiken, SC.**
- WSRC. 1993. *Procedure Manual 1S*. Westinghouse Savannah River Company, Savannah River Site Waste Acceptance Criteria. Chapter 3.10, Rev. 1 Interim.**
- Yu, A. D., C. A. Langton, and M. G. Serrato. 1993. *Physical Properties Measurements Program*. WSRC-93-894.**

687581
WSRC-RP-94-218

RADIOLOGICAL PERFORMANCE ASSESSMENT FOR THE E-AREA VAULTS DISPOSAL FACILITY (U)

APPENDICES A through M

April 15, 1994

*Authenticated
Mary Mullis
5/16/94*

Rev. 0

APPENDIX A

DETAILS OF MODELS AND ASSUMPTIONS

A.1 NEAR-FIELD MODEL

Appendix A.1 provides details of models and assumptions that support the information provided in Sect. 3.3 and 3.4 of the main body of the RPA report.

A.1.1 Infiltration

The process of infiltration is defined as the flow of water from the ground surface and into the soil. This is contrasted with the process of evaporation, and transpiration (i.e., evapotranspiration). In order to assess the performance of EAV an estimate of the infiltration rate at SRS is needed.

An idealized cross section of the vadose, or unsaturated soil, zone representing the infiltration area is shown in Fig. A.1-1. Water infiltrates at the surface and either undergoes evapotranspiration back through the surface and out of the domain or it infiltrates down to the underlying aquifer. The upper region in Fig. A.1-1, the dynamic zone, consists of the sediments near the surface where evaporation and transpiration have a dynamic role in reversing the downward movement of water due to gravity. The remaining region consists of the vadose zone. In the vadose zone, soil pores contain gases and water. Water is typically transported downward by gravity and capillarity.

A.1.1.1 Past Infiltration Studies

Past studies of infiltration at or near the SRS offer estimates of average infiltration rates. Hubbard and Englehardt (1987) used the CREAMS computer code to calculate a water balance for the old SRS burial ground (643-G) for the period 1961-1986. The CREAMS code, developed by the U.S. EPA, considers daily rainfall records, site vegetation, climatic characteristics, and soil properties. Daily rainfall records from F Separations Area were used in the simulation. Soils, vegetation, and climatic characteristics of the burial ground site

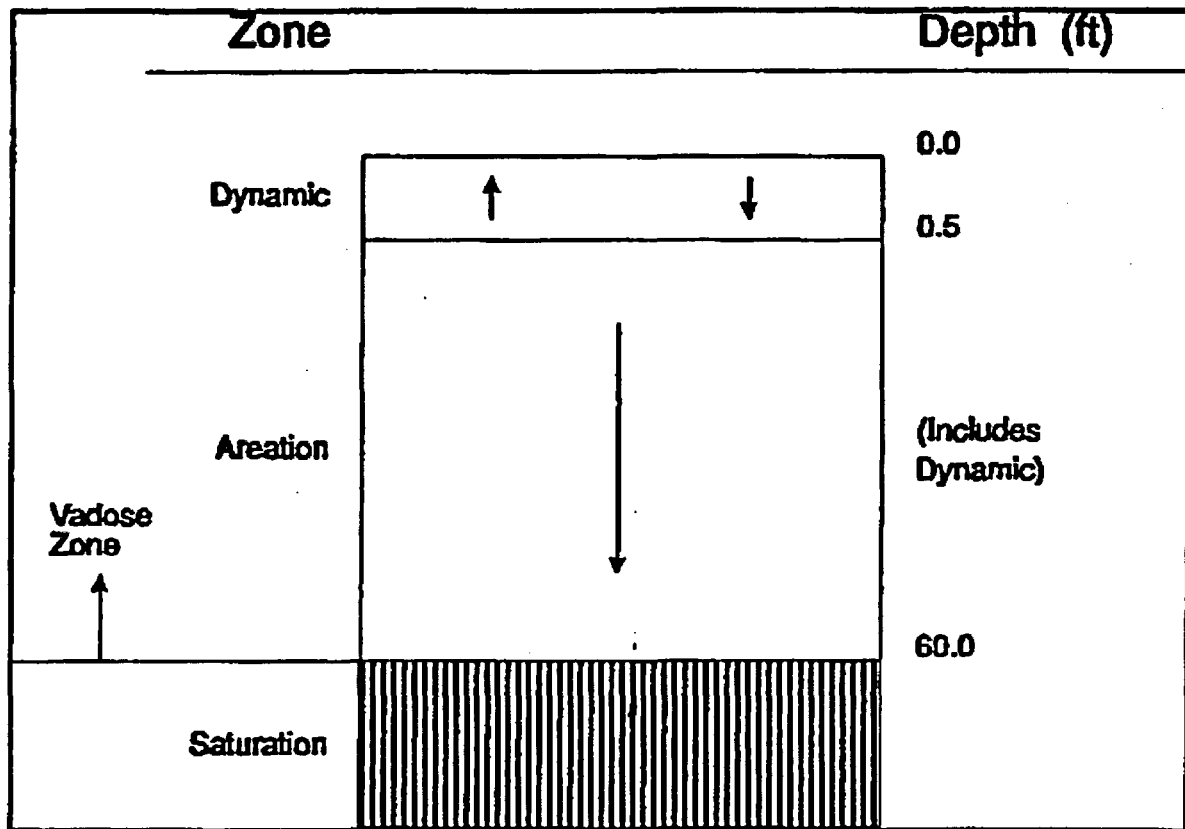


Fig. A.1-1. Idealized cross-section of the SRS vadose zone.

were used for the hydrologic parameters in the model. The average annual infiltration rate was estimated to be 37 cm or about 1/3 of annual average precipitation. Observed extremes for infiltration were 81 cm in 1964 and 10 cm in 1968.

To estimate the net infiltration for time intervals corresponding to pumping of the Tank 24 lysimeter, INTERA Technologies (1986) estimated discrete event evaporation using these bases:

- maximum evaporation is limited to 80% of pan evaporation rates;
- if evaporation exceeds the precipitation by more than 10% of the pan rate, an infiltration deficit can remove water from the soil;
- the maximum infiltration deficit per month is assumed to be 20% of the pan rate; and

- the infiltration deficit accumulates until it is overcome by subsequent precipitation exceeding evaporation.

The algorithm developed from these bases was then used to estimate infiltration rates during discrete periods of precipitation. A yearly infiltration total for the period February 1984 through August 1985 was determined to be approximately 24 cm.

Parizek and Root (1986) used a water balance method, where stream flow measurements were subtracted from annual precipitation to yield an estimated evaporation at 64% of the total annual precipitation. This estimate gives an average annual infiltration value of 45 cm for a grassland and intermittently forested portion of the SRS near the LLW burial site.

Dennehy and McMahon (1987) conducted a field study of water movement in the unsaturated zone at 4 grass-covered test trenches located at the SRP LLW burial site. The study consisted of monitoring actual evapotranspiration, monitoring soil water, and water movement using field techniques and computer simulations. The results of the study relevant to net infiltration were:

- 43 cm of infiltration neglecting runoff occurred between June 1984 and July 1985;
- precipitation on trenches infiltrated the trench cap and moved vertically into the trench backfill; and
- infiltration mainly occurred during the winter and spring.

A.1.1.2 Summary of Infiltration into the Vadose Zone

Past estimates of infiltration at the SRS have ranged from 22 to 45 cm/year. Using the mean of the observed and predicted infiltration studies at the SRS results in an infiltration value of 37 cm/year. This mean infiltration value of 37 cm/year was rounded to one significant figure for the RPA; i.e., 40 cm/year for the infiltration at the EAVs.

A1.1.3 Infiltration Through the Clay Cap

PORFLOW (ACRI 1993) was used to estimate the average infiltration rate of water through the upper clay cap given the infiltration estimated for the vadose zone in Sect. A.1.1.2. Infiltration rate through the clay cap was determined by simulating a case with a yearly infiltration into the native soil overlying the vault of 40 cm/year. The gravel layer above the vault provides a zone of high conductivity to remove water from above the vaults. Clay underlying the gravel serves as an additional barrier because of its low hydraulic conductivity. The domain of the cover simulation is shown in Fig. A.1-2. The code recorded infiltration over time for several locations under the clay cap. The infiltration rate in the zone below the edge of the cap was used as a conservative estimate of infiltration beneath the cap. Infiltration in the center of the cap may be approximately two orders of magnitude lower than this estimate, based on the hydraulic conductivity of clay.

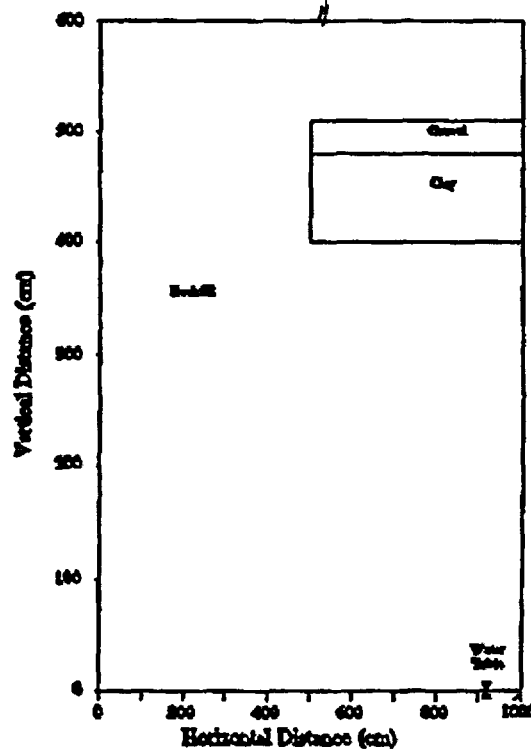


Figure A.1-2. Domain of the cover simulation

A.1.2 Flow and Mass Transport Through Vaults

In this section of Appendix A, details supporting the conceptual near-field model for each state of the vaults, intact, cracked, and failed (briefly described in Sect. 3.3.1.1), and the computational analysis (briefly described in Sect. 3.4.1.1) are provided.

A.1.2.1 Conceptual Model for Near-Field Analysis of the Vaults

As noted in Sect. 3.3.1, the near-field environment is defined as the portion of the subsurface environments extending from the ground surface to the water table. The flow regime in the subsurface was separated into three regions for purposes of analysis. The first region is the sediments near the surface where evaporation and transpiration have a dynamic role in reversing the downward movement of water due to gravity. Below this region, but above the concrete vaults, is the region that includes the engineered moisture barrier, composed of clay and an overlying gravel layer which is expected to divert much of the infiltrating water around the facility. The last region consists of the backfill sediment, soils underlying the EAV, the concrete vault, and the waste form, and extends down to the water table.

Assumptions specific to analysis of flow of water through the first region near the surface are discussed in Appendix A.1.1. The remainder of this section will address assumptions relevant to flow through the moisture barrier and flow and mass transport through the vaults and surrounding soil.

Flow Through the Moisture Barrier

Flow through the moisture barrier required assumptions regarding the hydraulic characteristics of the layered clay, gravel, and backfill soil. As noted in Sect. 3.3.1.1, the conceptual model used to provide a framework for the numerical simulation of the near-field movement of water and contaminants from the EAV relies on averaging of spatial properties for these three material types. To the extent possible, characteristics of these materials are site-specific.

Hydraulic properties of each of these porous media can be adequately described by the following hydraulic parameters: saturated hydraulic conductivity, effective porosity, and moisture characteristic curves. Moisture characteristic curves describe the nonlinear relationship between the matrix potential or pressure head, the moisture content, and the hydraulic conductivity. These properties were discussed in Sect. 3.3.1.1.

Flow and Mass Transport Through Waste Form, Vaults, and Surrounding Soil

Like the moisture barrier, flow of water through the concrete vaults and soils surrounding the vaults is a function of the hydraulic properties of the different porous materials present. Hydraulic parameters were defined for these materials in the same manner as for the moisture barrier materials, and the values used are listed in Table 3.3-1. For the backfill sediments and underlying soils, the same parameter definitions used for the backfill portion of the moisture barrier analysis are also used. It is reasonable to expect that all backfill soils will originate from the E-Area vicinity, and will therefore, be similar to native soils underlying the facility. The basis for the hydraulic parameters for all soil types is provided in Sect. 3.3.1. Additionally, a basis for the degradation times and changes in hydraulic conductivity are given in Appendix K.

Mass transport in the near-field model is governed by several processes: diffusion, advection, dispersion, sorption, and radioactive decay. In order to address these processes quantitatively, values for dispersivities, diffusion coefficients, liquid: solid partition coefficients (i.e., K_d 's) for the concrete, waste form, clay, sand, and backfill, and half-lives of radioactive decay for all constituents not screened from further consideration in Sect. 3.2.3 and 3.2.4 must be developed.

Longitudinal and transverse dispersion of a contaminant plume will occur, but the degree to which this may occur at E-Area is unknown. Dispersion is largely a function of the heterogeneity of the porous material encountered, which may reduce the concentration in a plume, but may also reduce the travel time of the leading edge of a plume at a downstream location. Although concrete may intuitively seem to be relatively homogeneous, fractures will increase dispersion of a plume passing through this material. The dispersivities assumed for each

material are listed in Table A.1-1. Based on conservatism relative to peak plume concentrations, the dispersivities were assigned values as low as possible that still maintained an adequate numerical mass balance.

Table A.1-1. Longitudinal and transverse dispersivities used in the PORFLOW near-field model

Porous Material	Longitudinal Dispersivity (cm)	Transverse Dispersivity (cm)	Eff Diffusion Coefficient (cm ² /year)
Backfill	10	2	110
Concrete	5	1	.32

Calculation of the effective diffusive flux of a constituent out of a porous material, requires values of the effective diffusion coefficient (molecular diffusion coefficient corrected for tortuosity of the porous medium). Tortuosity cannot be measured directly, but effective diffusion coefficients can be obtained empirically for conservative (i.e., nonsorbing, non-chemically reactive) compounds. For a given material, it is expected that the effective diffusivities for various radionuclides and non-radioactive compounds would be similar because molecular diffusivities in water do not vary significantly. Table A.1-1 lists the effective diffusion coefficients used for the various materials.

Sorption of radionuclides by the waste form will result in lower initial pore solution concentrations. During mass transport of radionuclides partitioned into the liquid phase, sorption will serve to retard the movement of the contaminants relative to water. Sorption is often characterized by K_d s, which assume linear, reversible, sorption at equilibrium. The K_d s used in this assessment are specific to the material to which they are assigned. K_d values used in this analysis are provided in Sect. 3.3.1.

A.1.2.2 Near-Field Flow and Transport Simulations

As noted in Sect. 3.4.1, computational analysis of the near-field model relied on the PORFLOW (Appendix B.4) computer code to simulate flow and mass transport. This complex code was necessary to address flow through the several adjacent materials in the unsaturated near-field environment, all of which possess different hydraulic properties. Details of the simulations of flow through the moisture barrier and flow and mass transport through the waste forms, vaults, and vadose zone are provided in this section. The PORFLOW code was chosen from a list of three dimensional variably saturated flow codes presently available (Appendix B.4).

Simulation of Flow Through the Moisture Barrier

The simulation of flow through the moisture barrier was performed using the PORFLOW code to determine the effectiveness of the barrier. This engineered barrier consists of a double layer of highly conductive gravel overlying clay. The surrounding material is composed of backfill soil. A 2% slope was used in the simulation as a conservative measure of performance, based on preliminary closure concept information indicating the slope of the clay layer will range between 2 and 5% (Thompson 1991).

The assumed hydraulic characteristics of each of the material types used in the simulations were discussed previously in Sect. 3.3.1.1. The simulation domain was 1000 cm wide and 600 cm high. Although the barriers will be placed over the entire facility, it was only necessary to simulate the end 500 cm of the barrier to determine its performance. This allows consideration of flow around the end of the barrier in addition to flow through the barrier.

The two-dimensional domain developed for the moisture barrier analyses is illustrated in Fig. 4.1-1. This figure also shows simulation results for saturation. It should be noted that the orientation of gravity was rotated clockwise in the simulation to account for the effort of the 2% slope of the barrier on flow rate.

Boundary conditions for this domain are as follows. The upper boundary is a constant flux boundary, representing the average annual infiltration rate into the soil, estimated in Appendix A.1.1 to be 40 cm/year. The lateral boundaries are assumed to be no-flow boundaries. This imposes an assumption that lateral flow in this region can be neglected. This is reasonable, as long as lateral diversion of water by the clay layer simulated occurs far from these boundaries within the domain. The lateral boundary conditions assume only vertical flow parallel to the boundaries, although vertical flow in this case is 2% off from the direction of gravity, due to the orientation of gravity at 2% off the vertical. The placement of the right no-flow boundary at 500 cm from the edge of the moisture barrier was somewhat arbitrary, based on judgement that the edge effect of the barrier would not be significant at this distance. From Fig. 4.1-1, the simulated saturation field supports this judgement, as it appears to be approaching an equilibrium near the right boundary, where saturation contours indicate predominantly vertical flow. The lower boundary was placed far enough away so as not to influence the flow field near the moisture barrier, and was assigned a pressure head of zero, in effect simulating the water table.

The simulation was carried out in several stages. Initially, the entire domain was treated as if it was all backfill, such that a uniform flow field was predicted. Then, the clay layer was included and the simulation was conducted in a transient mode until steady state was achieved. Lastly, the gravel layer was added to the simulation domain, and a simulation was conducted in transient mode until the pressure field (Fig. 4.1-1) maintained constant values.

During the course of these simulations, the predicted pressure field was monitored, as was the total water mass balance for the simulation domain. The maximum water mass balance error observed in these simulations was less than 3%, which was considered adequate for the purpose of determining the effectiveness of the barrier in diverting water. Reasonable efforts to improve the mass balance failed. A close inspection of the numerical solution showed that a slight increase in water in the system originated within the gravel layer, and persisted through the clay.

The flux across two planes (two-dimensional domains assume a unit width in the third dimension, such that a plane is of unit width) within the simulation domain was monitored to determine how effective the barrier was at diverting water. One flux plane extended from the left simulation boundary edge of the clay layer at 500 cm, representing flux through the region not covered by clay, but receiving diverted water from the gravel layer overlying the clay. The other flux plane went from the edge of the clay layer to the right simulation boundary at 1000 cm, representing the region of the domain "protected" by the clay. A comparison of the two fluxes indicated that 99.5% of the total water flux across the upper boundary was being diverted through the plane to the left of the assumed-intact clay layer.

To evaluate the flow rate through the moisture barrier, the vertical fluxes through a plane beneath the clay layer were plotted. The results are shown in Fig. 4.1-2. The results indicated that the left boundary (no-flow condition assumed) was far enough away from the moisture barrier such that the assumption of negligible lateral flow at this boundary from the gravel drainage layer is reasonable. The flux adjacent to this boundary is 40 cm/year in the vertical direction, parallel to the boundary. The large amount of water being diverted around the barrier is represented in Fig. 4.1-2 by the peak flux occurring in approximately the center of the domain. Inspection of Fig. 4.1-2, also indicates that an elevated infiltration rate extends past 500 cm, into the region covered by the clay, representing infiltration around the end of the barrier into the protected region. Finally, it appears that 500 cm of the barrier was an adequate length to establish a constant flow rate through the barrier. The vertical flux through the barrier stabilizes about 300 cm in from the end of the barrier at a value of 0.45 cm/year. While it would be appropriate to use this value as the infiltration rate for water reaching the vault, SRS determined a more conservative value of 4 cm/year should be used as the infiltration rate through the barrier. This is due, in part, to the fact that the hydraulic conductivity of the clay as measured in the laboratory was approximately 1.0×10^{-8} cm/s. It was felt that a more appropriate value for the *in situ* saturated hydraulic conductivity would be 1.0×10^{-7} cm/s, which is consistent with liners in RCRA clay liners. Using this saturated hydraulic conductivity and assuming unit gradient conditions the flux through the cover would be approximately 4 cm/year.

Simulation of Flow and Mass Transport Through the Vadose Zone

The second part of the near-field analysis consisted of simulating water flow and solute transport in the region below the moisture barrier, which includes the vault and waste form. This simulation was performed using the PORFLOW computer code using double precision. The physical domain in the simulation consisted of a vertical half-plane of the vaults and the surrounding backfill soil (Figs. 3.3-3 and 3.3-4). The simulation domain was rectangular with the vault superimposed on the left side. While the actual vaults have sloping roofs to increase the flow of water around the vault, the roof was assumed to be flat in the simulation, for ease of computation. This was conservative because it allowed more water to perch, and thus, penetrate the vault. The process used to simulate the vaults is discussed in Sect. 4.1.2.2.

The ILNT physical domain simulated was 1800 cm wide, 2100 cm high, and LAW vault domain was 2700 cm wide, and 2050 cm high. The computational grids for the ILNT/ILT model was 46×72 , while the much larger LAW vault was simulated with a grid of 71×76 nodes. Spacing of the nodes varied in the domain with a maximum vertical distance in the ILNT/ILT vault of 90 cm in the center of the waste zone, and a maximum of 100 cm in the horizontal direction in the backfill zone at the side of the vault. The minimum node spacing occurred at every soil boundary and was 10 cm for both the vertical and horizontal directions. The maximum node spacing for the LAW vault was 50 cm in both the horizontal and vertical directions, each occurred in the backfill zone. The minimum node spacing in the horizontal direction was 5 cm at the sand-backfill interface, while the minimum node spacing in the vertical direction was 10 cm at each soil interface.

The upper boundary for water flow in each simulation was treated as a prescribed flux boundary with the assigned value dependent on the assumption regarding whether the moisture barrier remained intact. Both lateral boundaries were assumed to be no-flux boundaries. The left lateral boundary, away from the vault, was located halfway between adjacent vaults, where the flow field is essentially vertical. The inner boundary is located at the midpoint of a transverse section of a vault, where the flow field is also essentially vertical. The bottom boundary is located at the water table, such that a prescribed pressure head of zero is appropriate.

The boundary conditions for mass transport (i.e., boundary conditions on concentration, rather than fluid pressure) simulations were assigned as follows. No-flux conditions were assigned at the lateral boundaries, based on assumptions of symmetry between vaults and at the midpoint within the vaults. The lower boundary condition was a prescribed zero concentration, which corresponds to a condition where contaminants are swept away from the water table surface fast enough to render the concentration relatively low. This assumption serves to maximize the simulated diffusive flux through the domain, which is driven by concentration gradients, and thus, is conservative. The upper boundary condition was also specified as a zero concentration boundary, which is reasonable because mass transport is expected to be predominantly downward once contaminants are out of the vaults.

Since the void in the LAW vault is not a porous media, it required special consideration. In order to maintain conservatism, it was necessary to assume the travel time through the void was minimal. However, during the intact time period only a small amount of water is expected to enter the void resulting in small average velocities. Therefore, the saturated hydraulic conductivity in the void was set equal to that of concrete (1.0×10^{-10} cm/s). After cracking, the void's saturated hydraulic conductivity was increased to that of sand (1.0×10^{-3} cm/s). By doing this it was possible to allow the movement of water through the void space to be maximized upon cracking and maintain mass balance during the intact period.

Since the waste containers are expected to corrode and lose their integrity much faster than the vault, it was assumed that upon placement of the waste the boxes were completely corroded and compacted. This required an estimate of the effective height of the waste zone. A brief discussion of the assumptions used to calculate the height of the waste inside the LAW vault is given below.

Assumptions:

A Porosity of 50% is assumed in the waste inside the B-25 boxes.

As the B-25 boxes compact and corrode the volume of pores in the waste decrease by 50%.

LAW vaults are filled to the capacity of 12,000 B-25 boxes.

B-25 boxes are filled to 85% capacity.

Void Inside B-25 Boxes:

Fraction of inside of box that is void = 0.15

Fraction of inside of box that is waste = 0.425

Fraction of inside of box that is pores = 0.425

$$\begin{aligned}\text{Void} &= (\text{Initial Void}) + (\text{Compaction Factor}) (\text{Initial Pore Fraction}) \\ &= (0.15) + (0.5) (0.425) \\ &= 0.3625\end{aligned}$$

Void Outside B-25 Boxes:

Volume of B-25 Box: 113 ft³

Volume of Cell: 159,753 ft³

$$\begin{aligned}\text{Void} &= 1 - \frac{(\text{Volume of Boxes})}{(\text{Total Volume})} \\ &= 1 - \frac{(113 \text{ ft}^3/\text{box}) (12000 \text{ box/vault})}{(159,753 \text{ ft}^3/\text{cell}) (12 \text{ cell/vault})} \\ &= 0.293\end{aligned}$$

Total Void:

$$\begin{aligned}\text{Total Void} &= (\text{Void Inside Boxes}) + (\text{Void Outside of Boxes}) \\ &= 0.3625 + 0.293 \\ &= 0.655\end{aligned}$$

Height of Waste and Void:

Inside height of LAW Vault = 785 cm

$$\begin{aligned}\text{Void Depth} &= (785 \text{ cm}) (0.655) = 514 \text{ cm} \\ \text{Waste Depth} &= (785 - 514) \text{ cm} = 271 \text{ cm}\end{aligned}$$

All of the waste was assumed to be uniformly distributed in the bottom 271 cm of the LAW vault. The same process was followed for the ILNT/ILT vaults; however, the results indicated that the waste would occupy all but 9% of the total height. Based on this result, it was determined that a void would not be considered for the ILNT/ILT vault system, although collapse of the ILNT/ILT roof was incorporated into the modeling study.

A2 GROUNDWATER FLOW AND MASS TRANSPORT MODEL AND SIMULATIONS

This section of Appendix A provides details of the conceptual model adopted for simulating flow and mass transport through the saturated hydrologic zones beneath the EAVs (Sect. A.2.1), and details related to simulation of the model using the PORFLOW computer code (Sect. A.2.2).

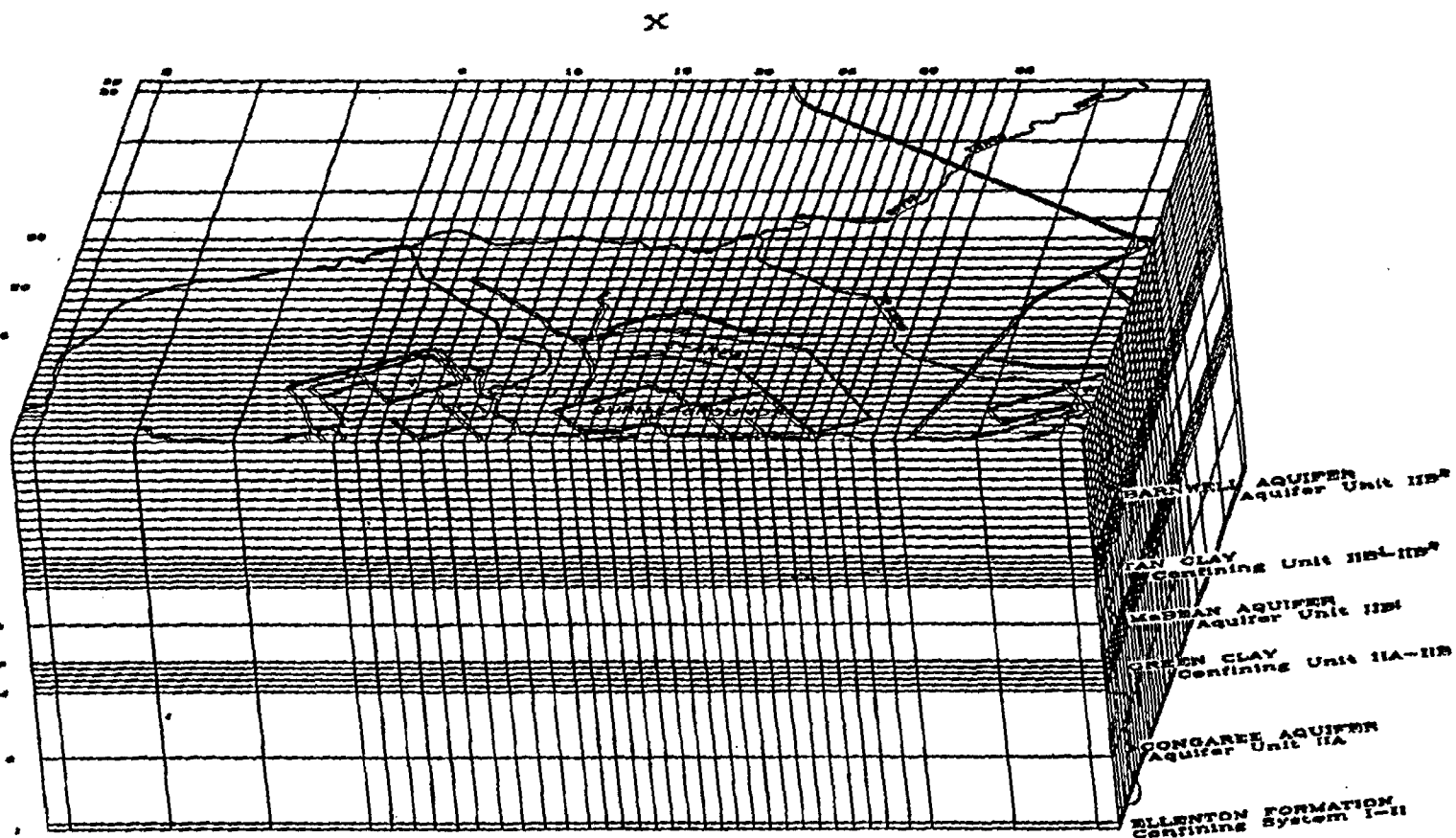
A.2.1 Conceptual Saturated Flow and Transport Model

Based on the piezometric data at E-Area (Sect. 3.4.2), it is apparent that the groundwater flow field is highly variable within and among the hydrologic units in the vicinity of E-Area. A three-dimensional representation of the groundwater flow system was chosen to allow the divergent lateral flow to be simulated (Fig. A.2-1).

The conceptual model for saturated flow was developed from data obtained in the E-Area wells and available regional data. The E-Area wells shown in Fig. A.2-2, provided site-specific information on the lithology and hydrologic properties of the subsurface units. Lithologic cross-sections (Sect. 2.2.2) developed from site wells were used to identify hydrologic units. Data from single well hydraulic tests and pump tests were used to group units according to similar hydrologic characteristics. Regional hydrogeologic data provided information on potentiometric surfaces, from which hydraulic gradients were estimated. Regional topographic maps were used to estimate pressure heads and gradients in the nearby streams. Local streams were gaged to estimate the quantity of groundwater discharge.

REV. 0

N



SAVANNAH RIVER PLANT



== Road
~ Stream

VERTICAL EXAGGERATION 50 X

Scale
0 200 400 600
Meters

WSR100

Fig. A2-1. Model domain for PORFLOW simulation of groundwater in E-Area vicinity.

A-15

WSRC-RP-94-218

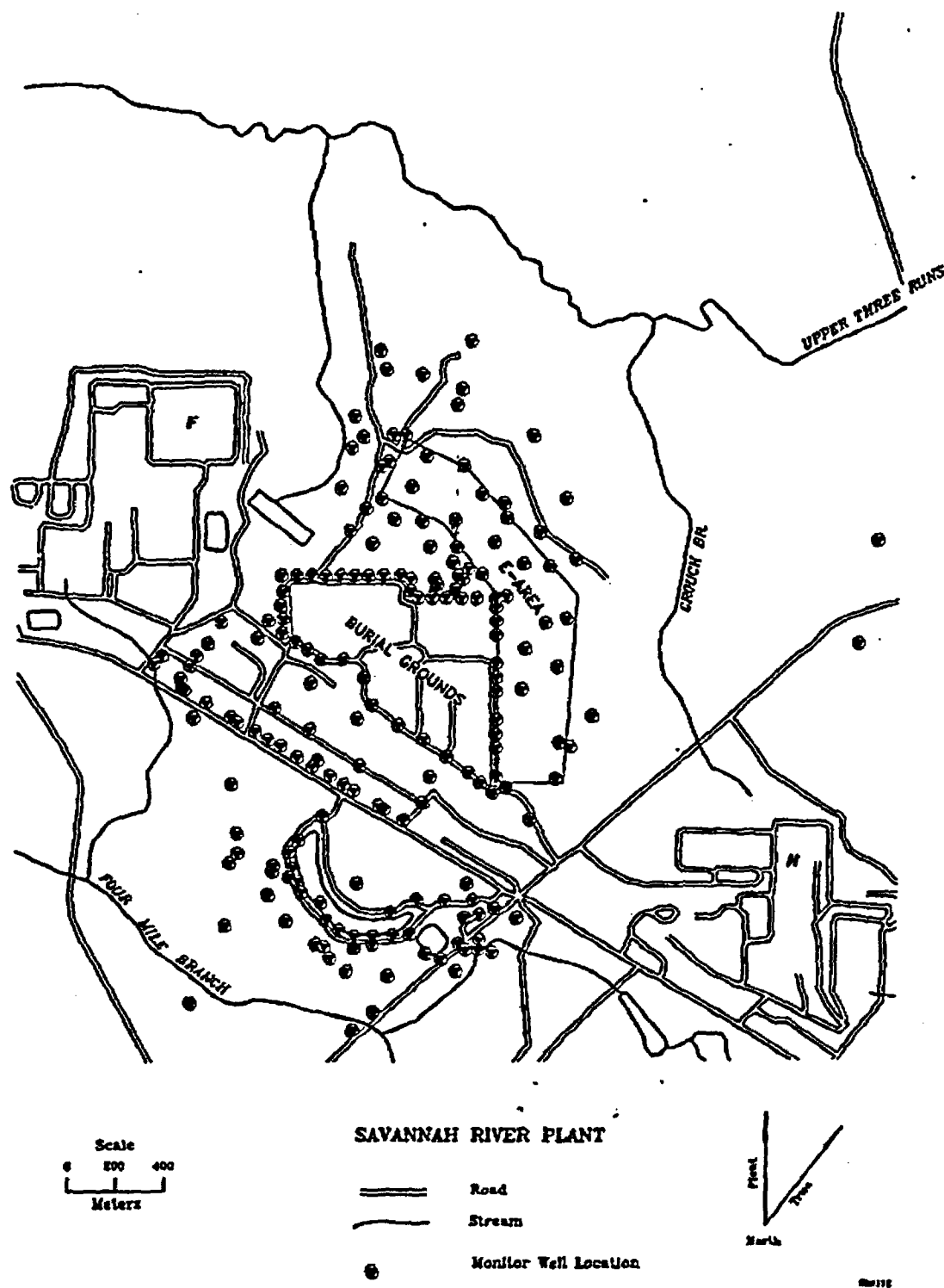


Fig. A.2-2. Location of E-Area groundwater wells.

Rcv. 0

In Sect. A.2.1.1, the boundaries selected for the model domain are defined and the basis for these boundaries are justified. Section A.2.1.2 identifies the five hydrologic units assumed. Characteristics of these units that affect flow are described in Sect. A.2.1.3. Properties that affect mass transport are described in Sect. A.2.1.4.

A.2.1.1 Model Boundaries

Before a model of the saturated zone beneath the EAVs was conceptualized, the area of potential concern was defined. This was done by: 1) evaluating hydrologic data available for the SRS, particularly for E-Area (Sect. 2.1.5, 2.2.2 and Appendix E), to identify the likely areas of potential contamination and 2) to further limit these boundaries by considering the exposure scenarios of concern, which are outlined in Sect. 3.2.3 and 3.2.4 in this report. The vertical extent of the model is described first according to the lower and upper boundaries of the model domain. The areal extent of the model and its boundaries are then described.

Vertical Extent of Model

The model boundaries for the vertical extent of the E-Area conceptual groundwater model domain are described in terms of the hydrological units underlying E-Area, which were identified in Sect. 2.1.5. According to the regional geological and hydrological data, Aquifer Unit IIA (Congaree Aquifer) is the lowermost hydrostratigraphic unit which could potentially be affected by the planned facility. The lower boundary of the domain (i.e., constant flux boundary) is assumed to be the contact between Aquifer Unit IIA and Confining System I-II (Ellenton Clays) (Fig. 2.1-5). There is a considerable thickness of the low-permeability geologic constituents of Confining System I-II (Sect. 2.1.5) separating the two units. In addition, Christiansen and Gordon (1983) indicated that the lower sand aquifer (Aquifer System I) has a higher piezometric head than the overlying Aquifer Unit IIA, thus forming an effective barrier to downward flow from Aquifer Unit IIA. However, the same quantities of recharge to the Congaree from the underlying formations is expected due to a substantial upward gradient. Consequently, the base of the problem domain is simulated as a constant flux boundary.

The upper boundary limit in the vertical extent of the model domain is defined by the water table, assumed to be a constant flux boundary defined by the average annual recharge. The upper boundary of the vertical domain occurs in Aquifer Unit IIB, Zone 2 (water table).

Lateral extent of the model

The upper hydrologic units included in the model [Aquifer Unit IIB, Zone 2 (water table), and Aquifer Unit IIB, Zone 1 (Barnwell/McBean)] are partially drained by the three creeks surrounding E-Area. Groundwater in these upper units discharges into the creeks around E-Area. Groundwater from Aquifer Unit IIB, Zone 1, discharges through the green clay into the underlying Aquifer Unit IIA (Fig. A.2-1). The lowermost unit, Aquifer Unit IIA, is partially dissected only by UTR Creek.

The eastern and western model boundaries for all hydrologic units are located at a substantial distance from the creek (Fig. A.2-1). As mentioned in Sect. 3.3.2.2, the horizontal extent of the model domain was selected to coincide wherever possible with naturally occurring sub-regional groundwater flow boundaries. Selecting model boundaries so that the streams that are included within the flow field allows simulation of the effect of the creeks on groundwater flow. UTR Creek forms the northern boundary of the problem domain and incises all of these units. Stream gaging surveys indicate significant groundwater discharge from all units to UTR Creek. Flow rates in Crouch and unnamed Branches increase from their upper reaches towards UTR Creek, suggesting significant groundwater discharge from the water-table units which they incise.

The southern boundary is defined by the drainage divide. Measured potentiometric surfaces for Aquifer Units IIB, Zones 1 and 2, in this region (Fig. E.2-2, E.2-4, and E.2-5) indicate that flow is away from this divide and toward the creeks.

The presence of the creeks serve to limit the lateral extent of flow, especially those creeks that completely incise a hydrologic unit. The upper units are completely incised by UTR Creek (Aquifer Units IIB, Zones 1 and 2), (Appendix E) and partially by Crouch and unnamed Branches. Aquifer Unit IIA is partially incised by only UTR Creek. All available hydrogeologic information suggests that the entire contaminant plume will eventually discharge to the surface streams near E-Area.

A2.1.2 Hydrologic Units

Five simplified hydrologic units (Fig. 2.1-5) are included in the groundwater conceptual model: Aquifer Unit IIB, Zone 2, makes up the upper zone containing the water table aquifer, Confining Unit IIB1-IIB2 (Tan Clay) is a semi-confining unit separating the water table unit and Aquifer Unit IIB, Zone 1 (Barnwell/McBean), Confining Unit IIA-IIB (Green Clay) is a confining zone between Aquifer Unit IIB, Zone 1, and the underlying aquifer, Aquifer Unit IIA (Congaree Aquifer). These five units were identified based on similar lithology and hydrologic characteristics. The five units are characterized by spatially-averaged hydrologic parameters, which are obtained in pump tests. Anisotropy, which is likely to exist as a result of lithologic heterogeneity, is assumed for each unit by assigning vertical hydraulic conductivities that are less than horizontal conductivities. Hydrologic characteristics of the units making up these conceptual units are described in detail in Appendix E.

A2.1.3 Hydrogeologic Properties

The hydrogeologic properties chosen to represent the five simplified hydrologic units in the groundwater model are based on previous field, laboratory, and modeling studies at SRS.

The existing horizontal hydraulic conductivity data, listed in Table 2.2-1 for all hydrologic units at E-Area, indicate horizontal conductivities ranging over several orders of magnitude for the aquifer units simulated in this RPA. The range, as well as the value used in simulations, are listed in Table A.2-1. Values used in simulations were chosen from the range of measured values, when available, based on the calibration procedure described in Sect. 3.4.2.1.

Table A.2-1. Measured and assumed hydraulic conductivities for saturated hydrologic units

Hydrologic Unit	Horizontal hydraulic conductivity (cm yr ⁻¹)		Vertical hydraulic conductivity (cm yr ⁻¹)
	Measured range (Geotrans 1992)	Value used in simulations	Value used in simulations
Aquifer Unit IIB, Zone 2	4.1×10^3 to 1.8×10^4	4.0×10^4	1.0×10^4
Confining Unit IIB1-IIB2	0.19 to 3.8	6.4×10^1	4.3×10^1
Aquifer Unit IIB, Zone 1	2.3×10^3 to 2.3×10^5	4.1×10^4	3.1×10^4
Confining Unit IIA-IIB	0.44 to 5.0	3.0	2.0
Aquifer Unit IIA	2.0×10^4	4.2×10^5	4.2×10^4

A.2.1.4 Properties Affecting Mass Transport

Mass transport in the saturated zone occurs by advective, diffusive, and dispersive processes, but is hindered by sorptive processes. In the saturated zone, advective transport is sufficiently high to render diffusive transport relatively insignificant. Mechanical dispersion, which causes spreading of a contaminant plume, is a property of the aquifer matrix and flow characteristics that have not been measured in aquifers underlying the SRS. Dispersion is not expected to be important for the EAV, however, because the area of the source (i.e., area of the EAV), and thus, the potential area of a contaminant plume originating from the facility, is large. Spreading of the plume from such a large source will not significantly reduce concentrations at a point 100 m from the facility, the compliance point for groundwater protection assumed in this RPA. Thus, reasonable dispersivities for longitudinal and transverse dispersion were selected from a reputable groundwater textbook (Freeze and Cherry 1979). The longitudinal and transverse dispersivities selected are 3 m and 0.3 m respectively.

Other characteristics of the porous media that affect mass transport simulations include density and porosity of the media. Matrix density of the media is a property used by the simulation code PORFLOW to calculate retardation based on sorption coefficients, or K_d 's. For the five hydrologic units of interest, a matrix density of 2650 kg/m^3 is used, based on an average value provided by Freeze and Cherry (1979). The total porosity of all units was based on data contained in Table A.2-2. An effective porosity was determined, based on an average value from de Marsily (1986).

Table A.2-2. Total porosities - E-Area

Zone(s)	Total θ (%)
Aquifer Unit IIB, Zone 2	40
Confining Unit IIB1-IIB2	40
Aquifer Unit IIB, Zone 1	40
Confining Unit IIA-IIB	40
Aquifer Unit IIA	40

Characteristics of contaminants that are needed to simulate mass transport are sorption coefficients (Sect. 3.3.1) and half-lives of radioactive decay (Appendix C). Sorption of a continuous source of contaminants on solid surfaces is often viewed as reversible, achieving equilibrium instantaneously, and applies only to immobile surfaces (i.e., sorption on mobile colloids is not considered). This view of sorption is represented by a K_d , and is the view adopted for this RPA. This representation of sorption serves to retard the computed arrival of a plume of contaminants at a given location, rather than lower the ultimate concentration. However, extending the transit time of a contaminant can allow for radioactive decay or microbial degradation processes to reduce the concentration before the plume reaches a critical receptor location. These decay processes will be important for radionuclides with half-lives significantly less than the transit time in groundwater.

The value of K_d varies with the contaminant and the media to a large degree. The values used for the saturated zone are consistent with those used in the near-field model (Table 3.3-2), and were site-specific when possible.

A.2.2 Saturated Flow and Transport Simulations

In this section, the method for simulating the conceptual saturated flow and transport is described in detail. In Sect. A.2.2.1, details of the design of the input file for the PORFLOW computer code simulations are given. In Sect. A.2.2.2, the initial optimization study that was done, to ascertain that code simulations were producing credible results is discussed.

A.2.2.1 Simulation Design

Groundwater flow and mass transport simulations were conducted with PORFLOW based on the conceptual model discussed in Sect. A.2.1. The model was calibrated by comparing hydraulic head values calculated by PORFLOW with actual head values from site monitoring wells. Calibration was based on an average annual recharge of 40 cm. The calibration process is discussed in detail in Sect. 3.4.2.

After completing the groundwater flow simulations, and generating a predicted steady-state flow field, separate input files were developed for transport simulations. These input files consisted of the concentration boundary conditions and transport parameters described in Sect. A.2.1.4 above, and rely on the results of the steady-state flow simulations for the specification of the velocity vectors. The velocity vectors are used in the transport simulations in computing advective and dispersive transport of potential contaminants.

A.3. ANALYSIS OF ATMOSPHERIC EFFLUENT

Volatile emissions, such as HTO (tritiated water vapor), HT, $^{14}\text{CO}_2$, and isotopes of radon are expected to occur at LLW disposal facilities in varying quantities that depend on the initial disposal activities of each volatile isotope or radioactive parent, disposal method, and the surrounding physiochemical environment.

The purpose of this section is to estimate an upper bound of the potential impact of ^3H and ^{14}C in terms of off-site individual and inadvertent intruder doses associated with the EAVDF. The impacts from the release of radons are described in Sect. A3.7.

A3.1 Dose Analysis of Tritium Crucibles in the ILT Vaults

Tritium is produced by irradiation of lithium isotopes by the neutron flux produced in nuclear reactors at the SRS. The ^3H is extracted as a gas by vacuum melting irradiated Li-Al alloy targets in stainless steel crucibles such that only a small residual of less than 500 Ci ^3H is left in the alloy when the crucibles are discarded. The tritium crucibles are placed into sealed 46-cm-diameter steel pipe overpacks and placed into lined concrete silos in the ILT vaults, with a capacity of 142 crucibles for each vault.

A3.1.1 Previous Studies

Orebaugh and Wallace (1989) produced a modeling study titled *Quantification of Hazards Associated with the Decay and Storage/Disposal of Tritium Crucibles*. This study evaluated the release of ^3H from the crucibles for various scenarios including: Case I, a tritium crucible sealed with moist air inside; Case II, plug shrinkage vents the crucible to moist air; Case III, vented crucibles stored in a sealed concrete vault; and Case IV, Case III with an engineered vent. This study evaluated the impact of the corrosion reaction between Al and H_2O producing H_2 gas. The study provides ^3H flux rates from the crucibles, which were used in this RPA to determine the impact to the intruder and off-site individuals from tritiated water vapor released from the EAV ILT vaults.

A3.1.2 Intruder Dose Analysis

An analysis was performed for the intruder based upon the flux rate determined by Orebaugh and Wallace (1989). Modeling results for Case III of this study were used in which vented crucibles are stored in a sealed concrete vault. This assumes that the vault is not

ventilated, therefore, the source of HTO would be maximized in the vault. The epoxy plugged crucibles are assumed to vent due to shrinkage of the plug. Near saturated vault walls were assumed requiring an aqueous diffusion pathway. Wet vault walls were assumed to ensure saturated air at all times in the vault.

The Orebaugh and Wallace (1989) study assumed that: 1) the air in the vault is always water saturated; 2) all 250 plugged crucibles, each containing 500 Ci of ^3H , are releasing hydrogen and tritium to the vault (NOTE: presently only 142 crucibles are planned per vault making this analysis conservative); and 3) hydrogen diffuses out of the vault through an aqueous pathway (i.e., saturated concrete). The hydrogen and tritium diffuse out of the crucibles into the vault, and gradually increase the concentration of both isotopes in the vault atmosphere. The concentration in the soil is assumed to always be zero. The flux through all the vault walls at the time of the maximum tritium concentration in the vault air was less than 1 mCi yr^{-1} .

Assuming that the intruder's house resides directly on top of the vault, the steady-state concentration in the house may be determined simply by:

$$C_{ss} = \frac{\left(\frac{q}{a}\right)}{h} \quad \text{Eq. A.3.1}$$

where

- C_{ss} = steady-state air concentration in house, Ci m^{-3} ,
- q = HTO flux rate into house, $\text{Ci m}^{-2} \text{ yr}$,
- a = air exchange rate in house, 8760 yr^{-1} ,
- h = height of the ceiling in house, 2.4 m.

The inhalation dose to the intruder is calculated as follows:

$$D = C_{ss} * B_r * DCF \quad \text{Eq. A.3.2}$$

where

- D = inhalation dose, mrem yr⁻¹,
 C_a = steady-state air concentration, Ci m⁻³,
 B_r = breathing rate (8000 m³ yr⁻¹),
 DCF = inhalation dose conversion factor (6.3×10^4 mrem Ci⁻¹).

Assuming a 1 mCi yr⁻¹ flux out of the top of the ILT vault (i.e., 15 m by 7.6 m) enters directly into the house of the intruder, a steady-state concentration was determined to be 4.2×10^{-10} Ci m⁻³ using Eq. A3.1. The inhalation committed EDE to the intruder in the house was determined to be 2.1×10^{-1} mrem yr⁻¹ using Eq. A3.2. The dose calculation is for inhalation only; however, it is considered bounding for the all-pathway dose to the intruder since the intruder is assumed to reside in the house all year. Thus, the dose from a more realistic full pathway analysis would result in doses which are equivalent to or less than those determined for the inhalation pathway only.

The tritium inventory limit for the tritium crucibles in the ILT vault is determined from:

$$I = I_0 * \frac{D}{D_0} \quad \text{Eq. A3.3}$$

where

- I = allowable inventory, Ci vault⁻¹,
 I_0 = initial inventory used in the calculation, Ci vault⁻¹,
 D = allowable intruder dose objective, (100 mrem yr⁻¹),
 D_0 = dose from the initial inventory, mrem yr⁻¹.

Using Eq. A3.3, and the assumed initial inventory of 500 Ci per crucible or 1.25×10^5 Ci of ³H, the allowable inventory for tritium crucibles in the ILT vaults was determined to be 6.0×10^7 Ci vault⁻¹.

The ILT vaults are predicted to crack 575 years post-closure and to fail at 1050 years (Appendix K). These times are sufficiently long to preclude significant inhalation doses at the time of failure, even for the large allowable inventory calculated above.

A.3.1.3 Off-Site Individual Dose Analysis

The dose to an individual located at the SRS site boundary before the 100 year institutional control period was evaluated using the Orebaugh and Wallace (1989) report for Case IV, which involved a vented engineered vault with barometric pumping. This is the expected scenario for the off-site individual since the vault will be intact during the institutional control period. A vented vault is allowed to breathe, by variations in barometric pressure. The report indicates that daily pressure excursions of 0.01 atm are expected. The resulting concentration of HTO at this pressure was determined to be 5.2×10^{-7} Ci L⁻¹ and the release rate through a 1-cm vent pipe of 2.6×10^1 Ci yr⁻¹ from each vault. The release rate is adjusted to account for the ten ILT vaults providing releases of ³H. The nearest off-site individual is assumed to reside continuously at the SRS site boundary located 5 km from E-Area. A maximum EDE dose of 0.06 mrem yr⁻¹ was calculated for all pathways by AIRDOS-PC (U.S.EPA 1989) utilizing the August, GA windfile. The AIRDOS-EPA input and output information is provided in Appendix C. The dose results for this analysis indicate that the maximum inventory of ³H crucibles (i.e., 250,000 Ci/vault) in the ILT vaults will not exceed the performance objective of 10 mrem yr⁻¹ for an off-site individual from the airborne pathway.

A.3.2 Dose Analysis of ³H in JCW in the ILT Vaults

A.3.2.1 Intruder Dose Analysis

The basis of this analysis is to determine the allowable inventory of ³H in the ILT job control waste vaults. Since ³H in the vapor form is derived from the concentrations in the pore water, the ratio of the concentration in the vapor form to that in the water phase was

determined as follows:

$$H = \frac{C_{\text{vapor}} \text{ (g/m}^3 \text{ of air)}}{C_{\text{water}} \text{ (g/m}^3 \text{ of water)}} \quad \text{Eq. A.3.4}$$

The concentration of water in air at 10 °C and 100 percent relative humidity can be determined as follows:

$$C \text{ (g/m}^3\text{)} = \frac{A_{vp}}{R \times T} \times MW \quad \text{Eq. A.3.5}$$

where

- A_{vp} = actual vapor pressure (0.012 bars),
- R = gas constant ($8.314 \times 10^{-5} \text{ bar m}^3 \text{ mol}^{-1} \text{ } ^\circ\text{K}^{-1}$),
- T = temperature (283 °K),
- MW = molecular weight (18 g mol⁻¹).

This results in a water concentration in the air of 9.2 g m⁻³. Assuming that concentration of H-3 in water is equal to the concentration in the vapor:

$$\frac{1 \text{ Ci}}{m_{\text{(H}_2\text{O)}}^3} \times \frac{1 \text{ m}_{\text{(H}_2\text{O)}}^3}{10^6 \text{ g}_{\text{(H}_2\text{O)}}} \times \frac{9.2 \text{ g}_{\text{(H}_2\text{O)}}}{m_{\text{(air)}}^3} = \frac{9.2 \times 10^{-6} \text{ Ci H-3}}{m_{\text{(air)}}^3}$$

Therefore,

$$H = \frac{9.2 \times 10^{-6} \text{ Ci/m}_{\text{(air)}}^3}{1 \text{ Ci/m}_{\text{(H}_2\text{O)}}^3} \quad \text{Eq. A.3.6}$$

Using this relationship, the ³H concentration in the vapor phase can be determined from the concentration in the water phase in the vault. It was assumed that the vaults each contained 1.0 Ci vault⁻¹ at the time of closure, which results in 3.6×10^{-3} Ci vault⁻¹ at the end of institutional control (i.e., 100 years post-closure). The ILT JCW vaults have a volume of

803 m³ vault⁻¹. Assuming that the waste within each ILT vault is saturated and has a porosity of 0.50, the volume of water in each vault would be about 400 m³ vault⁻¹. The corresponding ³H concentration in the water within the vault is 9.0 × 10⁻⁶ Ci m⁻³. Using the relationship developed in Eq. A.3.6, the ³H concentration in the vapor phase would be 8.3 × 10⁻¹¹ Ci m⁻³. Assuming this vapor concentration is at the top surface of the vault, then the flux at the ground surface is given by Eq. A.3.7:

$$J = D \left(\frac{C_o}{x} \right) \quad \text{Eq. A.3.7}$$

where

- J = flux at the soil surface, Ci m⁻² yr⁻¹;
- D = diffusion coefficient in air, 754 m² yr⁻¹, (CRC 1981),
- C_o = source concentration, Ci m⁻³,
- x = soil thickness, 1 m.

The allowable ³H inventory was determined by use of Eq. A.3.2 and A.3.3 to be 6.7 × 10⁴ Ci vault⁻¹ based upon an intruder dose of 100 mrem. The dose calculated is for inhalation exposure only; however, it is considered bounding for the all pathway dose to the intruder since the intruder is assumed to reside in the house all year.

A.3.2.2 Off-Site Dose Analysis

The dose to an individual located at the SRS site boundary before the 100 year institutional control period was evaluated in the following manner. Potential exposure is estimated by first calculating the ³H concentration in pore water per Ci in each vault. Assuming 400 m³ of pore water per vault, the ³H concentration in pore water is 2.5 × 10⁻³ Ci m⁻³. From Eq. A.3.6, the vapor phase ³H concentration is 2.3 × 10⁻⁸ Ci m⁻³. The flux at the soil surface was determined using Eq. A.3.7. This results in a flux at the soil surface above the

ILT vault of $1.7 \times 10^5 \text{ Ci m}^2 \text{ yr}^{-1}$. This flux is assumed to occur over all 10 of the ILT vaults resulting in a release of $1.1 \times 10^2 \text{ Ci yr}^{-1}$ for an area source of $6.4 \times 10^2 \text{ m}^2$. The off-site atmospheric transport was modeled with the AIRDOS-PC computer code (U.S.EPA 1989) using the Augusta, GA windfile (Appendix C). The nearest off-site individual is assumed to reside continuously at the SRS site boundary located 5 km from E-Area. The maximum EDE from all pathways was determined to be $2.5 \times 10^6 \text{ mrem yr}^{-1}$. The AIRDOS-PC input and output file information is provided in Appendix C. The allowable ^3H inventory was determined using Eq. A.3.3, and was calculated to be $4.0 \times 10^6 \text{ Ci vault}^{-1}$ based upon the atmospheric performance objective dose of 10 mrem yr^{-1} .

A.3.3 Dose Analysis of ^3H in JCW in the ILNT Vaults

A.3.3.1 Intruder Dose Analysis

Using the relationship in Eq. A.3.6, the ^3H concentration in the vapor phase can be determined from the concentration in the water phase in the vault. It is assumed that the vaults each contained $1.0 \text{ Ci vault}^{-1}$ at the time of closure, which results in $3.6 \times 10^3 \text{ Ci vault}^{-1}$ at the end of institutional control (i.e., 100 years post-closure). The ILNT vaults have a volume of $5880 \text{ m}^3 \text{ vault}^{-1}$. Assuming that the waste within each ILNT vault is saturated and has a porosity of 0.50, the volume of water in each vault would be $2940 \text{ m}^3 \text{ vault}^{-1}$. Therefore, the ^3H concentration in the water within the vault is $1.2 \times 10^6 \text{ Ci m}^{-3}$. Using the relationship developed in Eq. A.3.6, the ^3H concentration in the vapor phase would be $1.1 \times 10^{11} \text{ Ci m}^{-3}$. Assuming this vapor concentration in Eq. A.3.7 and using Eqs. A.3.1 and A.3.2, the intruder's dose from inhalation would be $2.0 \times 10^4 \text{ mrem yr}^{-1}$. The allowable ^3H inventory was determined by use of Eq. A.3.3, and was calculated to be $5.0 \times 10^5 \text{ Ci vault}^{-1}$ based upon an intruder dose of 100 mrem. The dose calculated is for inhalation exposure only; however, it is considered bounding for the all pathway dose to the intruder since the intruder is assumed to reside in the house all year.

A3.3.2 Off-Site Dose Analysis

The dose to an individual located at the SRS site boundary before the 100 year institutional control period was evaluated using the equation for the flux given in Eq. A.3.7. The ^3H concentration in pore water per Ci in each vault is $3.4 \times 10^{-4} \text{ Ci m}^{-3}$, based on $2.94 \times 10^3 \text{ m}^3$ of pore water. From Eq. A.3.6, the vapor phase ^3H concentration is $3.1 \times 10^{-9} \text{ Ci m}^{-3}$. This results in a flux at the soil surface above each ILNT vault of $2.3 \times 10^{-6} \text{ Ci m}^{-2} \text{ yr}^{-1}$. This flux is assumed to occur over all 10 of the ILNT vaults resulting in a release of $2.0 \times 10^{-2} \text{ Ci yr}^{-1}$ for an area source of $8.7 \times 10^3 \text{ m}^2$. The off-site atmospheric transport was modeled with the AIRDOS-PC computer code (U.S.EPA 1989) using the Augusta, GA windfile (Appendix C). The nearest off-site individual is assumed to reside continuously at the SRS site boundary located 5 km from E-Area. The maximum EDE from all pathways was determined to be $4.5 \times 10^{-6} \text{ mrem yr}^{-1}$. The AIRDOS-PC input and output file information is provided in Appendix C. The allowable ^3H inventory was determined using Eq. A.3.3, and was calculated to be $2.2 \times 10^6 \text{ Ci vault}^{-1}$ based upon the atmospheric performance objective dose of 10 mrem yr^{-1} .

A3.4 Dose Analysis of ^{14}C in the ILNT Vaults

The waste form expected to contain ^{14}C in the ILNT vaults is mainly job control waste. C-14 is assumed to be in the form of $^{14}\text{CO}_2$ and contained in B-25 boxes.

A3.4.1 Intruder Dose Analysis

The initial activity of ^{14}C in an ILNT vault containing job control waste is assumed to be 1 Ci. Each ILNT vault has a volume of 5880 m^3 . Assuming a porosity within the waste of 0.50, the void volume in each ILNT vault is 2940 m^3 . This results in a ^{14}C vault concentration of $3.4 \times 10^{-4} \text{ Ci m}^{-3}$ of void space at the end of the institutional control period (i.e., 100

years post-closure). Assuming this is the vapor phase concentration of $^{14}\text{CO}_2$, the flux of ^{14}C at the surface of 1 m of overlying soil, determined for the ILNT vault based on Eq. A.3.7 using a diffusion coefficient of $4.4 \times 10^2 \text{ m}^2 \text{ yr}^{-1}$ (CRC 1981), is $1.5 \times 10^{-1} \text{ Ci m}^{-2} \text{ yr}^{-1}$.

The projected area of each ILNT vault is 870 m^2 . At a flux rate of $1.5 \times 10^{-1} \text{ Ci m}^{-2} \text{ yr}^{-1}$ per Ci of ^{14}C in each ILNT vault, the entire ^{14}C inventory would be released in much less than a year. Therefore, the flux rate was adjusted to reflect total release within the first year. Per Ci of ^{14}C in the ILNT vault, total release in a year gives a flux rate of $1/870 \text{ Ci m}^{-2} \text{ yr}^{-1}$, or $1.1 \times 10^{-3} \text{ Ci m}^{-2} \text{ yr}^{-1}$. From Eq. A.3.1, the resulting air concentration in the intruder's house is $5.2 \times 10^{-5} \text{ Ci m}^{-3}$. The dose to the intruder was determined to be 10 mrem yr^{-1} , based upon Eq. A.3.2, using a DCF of $2.4 \times 10^4 \text{ mrem Ci}^{-1}$. The allowable inventory of ^{14}C in the ILNT vaults was determined to be 10 Ci per vault using Eq. A.3.3 and a performance objective of 100 mrem yr^{-1} . The dose calculated is for inhalation exposure only; however, it is considered bounding for the all-pathway dose to the intruder since the intruder is assumed to reside in the house all year.

A.3.4.2 Off-Site Dose Analysis

The dose to an individual located at the SRS site Boundary before the 100-year institutional control period was evaluated using the ^{14}C flux determined above, i.e., $1.1 \times 10^{-3} \text{ Ci m}^{-2} \text{ yr}^{-1}$. This flux is assumed to occur over all 10 ILNT vaults resulting in a release of 9.6 Ci yr^{-1} for an area source of $8.7 \times 10^3 \text{ m}^2$. The off-site atmospheric transport was modeled with the AIRDOS-PC computer code (U.S.EPA 1989) using the Augusta, GA windfile (Appendix C). The nearest off-site individual is assumed to reside continuously at the SRS site boundary located 5 km from E-Area. The maximum EDE from all pathways was determined to be $1.2 \times 10^{-1} \text{ mrem yr}^{-1}$. The AIRDOS-PC input and output file information is provided in Appendix C. The allowable ^{14}C inventory was determined using Eq. A.3.3, and was calculated to be 83 Ci per vault, based upon the atmospheric performance objective dose of 10 mrem yr^{-1} .

A3.5 Dose Analysis of ^3H in JCW in the LAW Vaults

A3.5.1 Intruder Dose Analysis

Using the relationship in Eq. A.3.6, the ^3H concentration in the vapor phase can be determined from the concentration in the water phase in the vault. It is assumed that the vaults each contained $1.0 \text{ Ci vault}^{-1}$ at the time of closure, which results in $3.6 \times 10^{-3} \text{ Ci vault}^{-1}$ at the end of institutional control (i.e., 100 years post-closure). The LAW vaults have a volume of approximately $47,000 \text{ m}^3 \text{ vault}^{-1}$ (for the smaller 2-module vaults). Assuming that the waste in each vault is saturated and has a porosity of 0.50, the volume of water in each vault would be $2.4 \times 10^4 \text{ m}^3 \text{ vault}^{-1}$. Therefore, the ^3H concentration in the water within each vault is approximately $1.5 \times 10^{-7} \text{ Ci m}^{-3}$ (1.0×10^{-7} for the larger vaults). Using the relationship developed in Eq. A.3.6, the ^3H concentration in the vapor phase would be $1.4 \times 10^{-12} \text{ Ci m}^{-3}$. Assuming this vapor concentration in Eq. A.3.7 and using Eqs. A.3.1 and A.3.2, the intruder's dose from inhalation would be $2.5 \times 10^{-5} \text{ mrem yr}^{-1}$. The allowable ^3H inventory was determined by use of Eq. A.3.3, and was calculated to be $4.0 \times 10^6 \text{ Ci vault}^{-1}$ based upon an intruder dose of 100 mrem. The dose calculated is for inhalation exposure only; however, it is considered bounding for the all pathway dose to the intruder since the intruder is conservatively assumed to reside in the house all year.

A3.5.2 Off-Site Dose Analysis

The dose to an individual located at the SRS site boundary before the 100 year institutional control period was evaluated using the equation for the flux given in Eq. A.3.7. The vapor-phase concentration of ^3H is calculated from Eq. A.3.6, assuming an initial pore water ^3H concentration of $4.2 \times 10^{-5} \text{ Ci m}^{-3}$ (or 1 Ci divided by $2.4 \times 10^4 \text{ m}^3$ pore water per vault). The ^3H concentration in the vault vapor phase, $3.9 \times 10^{-10} \text{ Ci m}^{-3}$, leads to a ^3H flux at the soil surface above each LAW vault of $2.9 \times 10^{-7} \text{ Ci m}^{-2} \text{ yr}^{-1}$. This flux was assumed to occur over all 21 of the LAW vaults resulting in a release of $5.2 \times 10^{-2} \text{ Ci yr}^{-1}$ for an area source

computer code (U.S.EPA 1989) using the Augusta, GA windfile (Appendix C). The nearest off-site individual is assumed to reside continuously at the SRS site boundary located 5 km from E-Area. The maximum EDE from all pathways was determined to be 1.2×10^5 mrem yr^{-1} . The AIRDOS-PC input and output file information is provided in Appendix C. The allowable ^3H inventory was determined using Eq. A.3.3, and was calculated to be 8.3×10^5 Ci vault $^{-1}$ based upon the atmospheric performance objective dose of 10 mrem yr^{-1} .

A.3.6 Dose Analysis of ^{14}C in the LAW Vaults

The waste form expected to contain ^{14}C in the LAW vaults is mainly job control waste. C-14 is assumed to be in the form of $^{14}\text{CO}_2$ and contained in B-25 boxes.

A.3.6.1 Intruder Dose Analysis

The initial activity of ^{14}C in a LAW vault containing job control waste is assumed to be 1 Ci. Each LAW vault has a volume of approximately 47,000 m^3 . Assuming a porosity within the waste of 0.50, the void volume in each LAW vault is 2.4×10^4 m^3 . This results in a ^{14}C vault concentration of 4.2×10^{-5} m^3 of void space at the end of the institutional control period (i.e., 100 years post-closure). Assuming this is the vapor phase concentration of $^{14}\text{CO}_2$, the flux of ^{14}C at the surface of 1 m of overlying soil, determined for a LAW vault based on Eq. A.3.7 using a diffusion coefficient of 4.4×10^2 $\text{m}^2 \text{yr}^{-1}$ (CRC 1981), is 1.8×10^{-2} Ci $\text{m}^{-2} \text{yr}^{-1}$.

The projected area of each LAW vault is 8800 m^2 . At a flux rate of 1.8×10^{-2} Ci $\text{m}^{-2} \text{yr}^{-1}$ per Ci of ^{14}C in each LAW vault, the entire ^{14}C inventory would be released in less than a year. Therefore, the flux rate was adjusted to reflect total release within the first year. Per Ci of ^{14}C in the LAW vault, total release in a year gives a flux rate of $1/8800$ Ci $\text{m}^{-2} \text{yr}^{-1}$, or 1.1×10^{-4} Ci $\text{m}^{-2} \text{yr}^{-1}$. From Eq. A.3.1, the resulting air concentration in the intruder's house is 5.2×10^{-9} Ci m^{-3} . The dose to the intruder was determined to be 1 mrem yr^{-1} , based upon Eq. 4.3.2, using a DCF of 2.4×10^4 mrem Ci $^{-1}$. The allowable inventory of ^{14}C in the LAW vaults was determined to be 100 Ci per vault using Eq. A.3.3 and a performance objective of

100 mrem yr⁻¹. The dose calculated is for inhalation exposure only; however, it is considered bounding for the all-pathway dose to the intruder since the intruder is assumed to reside in the house all year.

A3.6.2 Off-Site Dose Analysis

The dose to an individual located at the SRS site Boundary before the 100-year institutional control period was evaluated using the ¹⁴C flux determined above, i.e., 1.1×10^{-4} Ci m⁻² yr⁻¹. This flux is assumed to occur over all 21 LAW vaults resulting in a release of 20 Ci yr⁻¹ for an area source of 1.8×10^5 m². The off-site atmospheric transport was modeled with the AIRDOS-PC computer code (U.S.EPA 1989) using the Augusta, GA windfile (Appendix C). The nearest off-site individual is assumed to reside continuously at the SRS site boundary located 5 km from E-Area. The maximum EDE from all pathways was determined to be 2.5×10^{-1} mrem yr⁻¹. The AIRDOS-PC input and output file information is provided in Appendix C. The allowable ¹⁴C inventory was determined using Eq. A.3.3, and was calculated to be 40 Ci per vault, based upon the atmospheric performance objective dose of 10 mrem yr⁻¹.

A3.7 Analysis of Radon Flux

The release of radon from the EAVDF was calculated using the PORFLOW code. Besides having the capability to model groundwater flow and transport, the PORFLOW code can also model radioactive decay and diffusion. The case that was modeled was that of the LAW vault at 10,000 years. At this time it is assumed that the vault has failed, and the waste has formed a layer 2.7 m thick with a uniform distribution of waste constituents. A 2-m thick layer of soil was assumed to cover the waste in the failed vault. A unit concentration of U-234 was allowed to decay for 10,000 years through the intermediate daughters, Th-230 and Ra-226, producing Rn-222. The radon was allowed to diffuse upward as it was produced, and the flux of radon emanating from the top of the 2-m soil cover was calculated. The

parameters used in this calculation were:

Rn-222 Half Life:	1.05×10^{-2} year (3.8 days)
Ra-226 Half Life:	1.62×10^3 year
Th-230 Half Life:	7.70×10^4 year
U-234 Half Life:	2.45×10^5 year
Diffusivity of Rn:	2×10^6 cm ² /year
Density of waste and soil	1.6 g/cm ³
Effective porosity	0.1

The simulation results give a radon flux of 1.0×10^{-6} units per cm³/year from the soil cover. In order to compare this with a performance objective of 20 pCi/m²-s, the following unit's conversions had to be made:

If we assume that the initial units were mol/cm³, converting units gives:

$$\begin{aligned}
 1 \text{ mol/cm}^3 &= > 1.0 \times 10^{-6} \text{ mol/cm}^2\text{-yr} * 222 \text{ g/mol} * 1.5 \times 10^5 \text{ Ci/g} = 3.3 \times 10^1 \text{ Ci/cm}^2\text{-yr} \\
 &= > 3.3 \times 10^1 \text{ Ci/cm}^2\text{-yr} * 10^{12} \text{ pCi/Ci} * 10^4 \text{ cm}^2/\text{m}^2 * 3.2 \times 10^{-8} \text{ yr/s} \\
 &= 1.1 \times 10^{10} \text{ pCi/m}^2\text{-s}
 \end{aligned}$$

Since we now know that 1 mol/cm³ of U-234 will produce 1.1×10^{10} pCi/m²-yr as a radon flux, a simple ratio can be used to determine the U-234 concentration, in Ci/m³, that will produce a Rn-222 flux of 20 pCi/m²-s.

$$\begin{aligned}
 X \text{ mol/cm}^3 / 1 \text{ mol/cm}^3 &= 20 \text{ pCi/m}^2\text{-s} / 1.1 \times 10^{10} \text{ pCi/m}^2\text{-s} \\
 X &= 1.8 \times 10^{-9} \text{ mol/cm}^3 * 234 \text{ g/mol} * 6.2 \times 10^{-3} \text{ Ci/g} * 10^6 \text{ cm}^3/\text{m}^3 \\
 X &= 2.6 \times 10^{-3} \text{ Ci/m}^3
 \end{aligned}$$

This is equivalent to 125 Ci per LAW vault with a volume of 4.8×10^4 m³, which is about two and a half orders of magnitude greater than the allowable inventory for ²³⁴U based on intruder results, which include the dose from Rn-222 (Sect. 4.1.5.2). The conceptual model used here is applicable to failed ILNT vaults as well. The concentration of 2.6×10^{-3} Ci/m³ would give an inventory limit of 15 Ci per ILNT vault with a volume of 5,880 m³.

A sensitivity analysis was performed on the effect of the thickness of soil cover over the waste. The results were fluxes of 1.6×10^{-6} and 5.7×10^{-7} for cover thicknesses of 1 m and 3 m, respectively.

The results for 1 m of cover are applicable to trench disposal of suspect soil (Appendix I). If transport of uranium from the trench is conservatively ignored, then using the same analysis as above gives:

$$\begin{aligned} 1 \text{ mol/cm}^3 &= > 1.6 \times 10^{-6} \text{ mol/cm}^2\text{-yr} \cdot 222 \text{ g/mol} \cdot 1.5 \times 10^5 \text{ Ci/g} = 5.3 \times 10^1 \text{ Ci/cm}^2\text{-yr} \\ &= > 5.3 \times 10^1 \text{ Ci/cm}^2\text{-yr} \cdot 10^{12} \text{ pCi/Ci} \cdot 10^4 \text{ cm}^2/\text{m}^2 \cdot 3.2 \times 10^{-8} \text{ yr/s} \\ &= 1.7 \times 10^{10} \text{ pCi/m}^2\text{-s} \end{aligned}$$

Since we now know that 1 mol/cm³ of U-234 will produce 1.7×10^{10} pCi/m²-yr as a radon flux, a simple ratio can be used to determine the U-234 concentration, in Ci/m³, that will produce a Rn-222 flux of 20 pCi/m²-s.

$$\begin{aligned} X \text{ mol/cm}^3 / 1 \text{ mol/cm}^3 &= 20 \text{ pCi/m}^2\text{-s} / 1.7 \times 10^{10} \text{ pCi/m}^2\text{-s} \\ X &= 1.2 \times 10^{-9} \text{ mol/cm}^3 \cdot 234 \text{ g/mol} \cdot 6.2 \times 10^{-3} \text{ Ci/g} \cdot 10^6 \text{ cm}^3/\text{m}^3 \\ X &= 1.7 \times 10^{-3} \text{ Ci/m}^3 \end{aligned}$$

Since the disposal volume of each trench is 5,200 m³, the limiting inventory due to radon generation is:

$$1.7 \times 10^{-3} \text{ Ci/m}^3 \cdot 5,200 \text{ m}^3 = 8.8 \text{ Ci per trench}$$

The input file used to produce the 2-m cover case is presented in Fig. A.3-1.

```

/TITLE E-Area Radon Diffusion, 1-0
/ 200 cm of soil on top of 270 cm of waste
/ J. R. Cook, P. S. Lee & A. B. Yu
/ 2/8/94, 2/16/94, 2/22/94
/
/*****
GRID 3 by 48
SCALE 1.0000
COORDINATE X
      -1.8      8.8      1.0
SCALE 1.0000
COORDINATE Y RANGE 470
/
ZONE 1 is from ( 1, 1) to ( 3, 48) & soil
/
DENSITY = 0.0.
/
GRAVITY components are: 0.0, 0.0
/
Density of fluid is constant and equal to 0.01 gm/cc
/
FOR 1 Soil
MATERIAL PROPERTIES: rho 1.60 gm/cc, n_eff = 0.1, n_tot = 0.1, ndiff = 0.1
/MULT VAN n = 1.70 alpha = 7.5e-2 sr = 0.058
/NYDR az = 1.e-3 bx = 315.0 by = 315.0 bz = 315.0
TRANSPORT for C kd = 0.00, D = 0.000, al = 10.0, at = 2.0 & C is U-234
TRANSPORT for C2 kd = 0.00, D = 0.000, al = 10.0, at = 2.0 & C is Th230
TRANSPORT for C3 kd = 0.00, D = 0.000, al = 10.0, at = 2.0 & C is Ra226
TRANSPORT for C4 kd = 0.00, D = 2.e+6, al = 10.0, at = 2.0 & C2 is Rn222
/
LOCATE subregion ( 1, 1) to ( 3, 48) with ID=SOIL
LOCATE subregion ( 1, 21) to ( 3, 48) with ID=U234
/
SET C2 to 0.0 in ID=SOIL
SET C3 to 0.0 in ID=SOIL
SET C4 to 0.0 in ID=SOIL
SET C to 0.0 in ID=SOIL
SET C to 1.0 in ID=U234
/
DECAY half life for C is 2.45E+05 transform to Th230 is 1.00
DECAY half life for C2 is 7.70E+04 transform to Ra226 is 1.00
DECAY half life for C3 is 1.62E+03 transform to Rn222 is 1.00
DECAY half life for C4 is 1.04E+02
/
BOUND C -1 FLUX = 0.
BOUND C +1 FLUX = 0.
BOUND C -2 FLUX = 0.
BOUND C +2 FLUX = 0.
/
BOUND C2 -1 FLUX = 0.
BOUND C2 +1 FLUX = 0.
BOUND C2 -2 FLUX = 0.
BOUND C2 +2 FLUX = 0.
/
BOUND C3 -1 FLUX = 0.
BOUND C3 +1 FLUX = 0.
BOUND C3 -2 FLUX = 0.
BOUND C3 +2 FLUX = 0.
/
BOUND C4 -1 FLUX = 0.
BOUND C4 +1 FLUX = 0.
BOUND C4 -2 VALU = 0.

```

Fig. A3-1. PORFLOW input file for radon calculations.

```

PROPERTY for C C2 C3 C4 is NARN mean
MATRIX in X and Y directions for C and C2 C3 C4 in 3 sweeps using ADI
RELAX P = 0.7
/
DIAGNOSTIC mode for C and C4 at ( 2, 20) every 100 steps
OUTPUT every 900000 steps
/
/FLUX BALANCE for C in 'run.flx' for ID=SOIL every 50 steps
/FLUX BALANCE for C in 'run.flx' for ID=M234 every 50 steps
FLUX BALANCE for C4 in 'run.flx' for ID=SOIL every 100 steps
FLUX BALANCE for C4 in 'run.flx' for ID=M234 every 100 steps
/
TIME=0.
/
CONV for C4 REFE; GLOS mode; value = 1.0e-04, max 5 iter, 2 4
/HISTORY for C (25, 50) every 20 in 'run.his'
//////////
DISABLE FLOW
//////////
SOLV C C2 C3 C4 500000 Init 1.e-5 Inc 1.005 max 100.0 min 1.e-9 2.0 900000
OUTPUT C C2 C3 C4 NOW
/
SAVE C C4 in 'run.arc'
END

```

Fig. A.3-1. (continued).

Rev. 0

A4 DOSE ANALYSIS FOR OFF-SITE INDIVIDUALS AND INADVERTENT INTRUDERS

A4.1 Introduction

This appendix presents the models and data bases used to estimate EDEs per unit concentration of radionuclides in particular exposure media following disposal of LLW in the EAV. The dose analysis considers two groups of exposed individuals:

- off-site individuals, i.e., members of the public who reside beyond the boundary of the disposal facility; and
- inadvertent intruders, i.e., individuals who come onto the disposal site following loss of active institutional control.

Off-site individuals may be exposed to radionuclides released from the disposal facility at any time after disposal. During the period of active institutional control over the disposal site, which is assumed to last for 100 years after facility closure (U.S.DOE 1988a), off-site individuals are assumed to be restricted to locations beyond the present boundary of the SRS. However, after the period of active institutional control, off-site individuals could be located anywhere beyond the boundary of the buffer zone around the disposal facility, which is assumed to be no more than 100 m from the disposal units. Inadvertent intrusion onto the disposal site is assumed to be precluded by active institutional control until 100 years after facility closure. No credit is taken in this analysis for any passive institutional controls (e.g., marker systems at the disposal site, public records of land use) that could prevent inadvertent intrusion for some time after the period of active institutional control.

The PA for the EAV assumes that releases of radionuclides to groundwater due to infiltration of precipitation through disposal units is the principal mechanism for transport of radionuclides to off-site locations. However, potential doses to off-site individuals resulting from airborne releases of radionuclides also were considered (see Appendix A.3). Potential doses to inadvertent intruders are estimated by assuming that certain scenarios for direct intrusion into disposal units occur.

The following sections discuss the exposure scenarios and exposure pathways assumed for off-site individuals or inadvertent intruders and the models and parameter values used in calculating annual EDEs to these groups of individuals for each exposure pathway. For exposures to contaminated groundwater, the results of the dose analysis are summarized in the form of annual EDEs per unit concentration of radionuclides in water. For exposures resulting from direct intrusion into disposal units, the results are summarized in the form of annual EDEs per unit concentration of radionuclides in solid waste at the time intrusion is assumed to occur.

A.4.2. Radionuclides of Importance for Dose Analyses

As indicated in Appendix C, waste in the EAV potentially contains a large number of radionuclides. However, only a relatively few radionuclides are potentially important in the dose analyses for off-site individuals or inadvertent intruders. Most of the radionuclides either could occur only in very low concentrations or are sufficiently short-lived that they would decay to innocuous levels before off-site transport via the groundwater pathway or inadvertent intrusion onto the disposal site could occur.

The radionuclides which have been considered in the dose analyses for the EAV, either for off-site individuals or for inadvertent intruders, are listed in Table A.4-1. These radionuclides were selected on the basis of conservative screening analyses for exposures of off-site individuals via the groundwater pathway and exposures of inadvertent intruders, as described in Sects. 3.2.3.4 and 3.2.4.4, respectively. The exposure scenarios which have been considered for each radionuclide are indicated in the table and are described in Sect. A.4.3. All other radionuclides listed in Appendix C can be neglected in the dose analyses for off-site individuals and inadvertent intruders, because their concentrations would be sufficiently low that they could not result in doses that exceed a very small fraction of the applicable limits for either group of individuals.

**Table A.4-1. Radionuclides considered in dose analyses
for off-site individuals or inadvertent intruders**

Radionuclide ^a	Half-life ^b	Applicable scenarios ^c
H-3	12.28 y	1,2,4
C-14	5730 y	1,2,4
Al-26	7.2×10^5 y	1,2,3,4
Co-60	5.271 y	2,3,4
Ni-59	7.5×10^4 y	1,2,4
Ni-63	100.1 y	1,2,4
Se-79	6.5×10^4 y	1,2,4
Rb-87	4.73×10^{10} y	1,2,4
Sr-90	28.6 y	1,2,4
Y-90 (1.0)	64.1 h	
Zr-93	1.53×10^6 y	1,2,4
Nb-93m	14.6 y	1,2,4
Tc-99	2.13×10^5 y	1,2,4
Pd-107	6.5×10^6 y	1,2,4
Cd-113m	13.7 y	1,2,4
Sn-121m	55 y	1,2,4
Sn-126	1.0×10^5 y	1,2,3,4
Sb-126m (1.0)	19.0 m	
Sb-126 (0.14)	12.4 d	
I-129	1.57×10^7 y	1,2,4
Cs-135	2.3×10^6 y	1,2,4
Cs-137	30.17 y	1,2,3,4
Ba-137m (0.946)	2.552 m	
Sm-151	90 y	1,2,4
Eu-154	8.8 y	2,3,4
Eu-155	4.96 y	2,3,4
Pb-210	22.26 y	1,2,4
Po-210 (1.0)	138.378 d	

See end of table for footnotes.

Table A.4-1. (continued)

Radionuclide ^a	Half-life ^b	Applicable scenarios ^c
Ra-226	1600 y	1,2,3,4
Rn-222 (1.0)	3.8235 d	
Pb-214 (1.0)	26.8 m	
Bi-214 (1.0)	19.9 m	
Th-229	7.34×10^3 y	1,2,3,4
Ra-225 (1.0)	14.8 d	
Ac-225 (1.0)	10.0 d	
Fr-221 (1.0)	4.8 m	
Bi-213 (1.0)	45.65 m	
Tl-209 (0.0216)	2.20 m	
Th-230	7.7×10^4 y	1,2,4
Th-232	1.405×10^{10} y	1,2,3,4
Ra-228 (1.0)	5.75 y	
Ac-228 (1.0)	6.13 h	
Th-228 (1.0)	1.9132 y	
Ra-224 (1.0)	3.62 d	
Rn-220 (1.0)	55.61 s	
Pb-212 (1.0)	10.643 h	
Bi-212 (1.0)	60.55 m	
Tl-208 (0.3593)	3.053 m	
Pa-231	3.276×10^4 y	1,2,3,4
Ac-227 (1.0)	21.773 y	
Th-227 (0.9862)	18.718 d	
Ra-223 (1.0)	11.434 d	
Pb-211 (1.0)	36.1 m	
Bi-211 (1.0)	2.13 m	
Tl-207 (0.99727)	4.77 m	
U-232 ^d	72 y	1,2,3,4
U-233	1.5952×10^5 y	1,2,4

See end of table for footnotes.

Table A.4-1. (continued)

Radionuclide ^a	Half-life ^b	Applicable scenarios ^c
U-234	2.445×10^5 y	1,2,4
U-235	7.038×10^8 y	1,2,3,4
Th-231 (1.0)	25.52 h	
U-236	2.3415×10^7 y	1,2,4
U-238	4.468×10^9 y	1,2,3,4
Th-234 (1.0)	24.10 d	
Pa-234m (1.0)	1.17 m	
Pa-234 (0.0016)	6.70 h	
Np-237	2.14×10^6 y	1,2,3,4
Pa-233 (1.0)	27.0 d	
Pu-238	87.75 y	1,2,4
Pu-239	24,131 y	1,2,4
Pu-240	6569 y	1,2,4
Pu-241	14.4 y	1,2,4
Pu-242	3.758×10^5 y	1,2,4
Pu-244	8.26×10^7 y	1,2,4
Am-241	432.2 y	1,2,3,4
Am-242m	152 y	1,2,3,4
Am-242 (0.99524)	16.02 h	
Cm-242 (0.823)	163.2 d	
Np-238 (0.00476)	2.117 d	
Am-243	7.38×10^3 y	1,2,3,4
Np-239 (1.0)	2,355 d	
Cm-243	28.5 y	2,3,4
Cm-244	18.11 y	2,4
Cm-245	8.5×10^3 y	1,2,3,4
Cm-246	4.75×10^3 y	1,2,4
Cm-247	1.56×10^7 y	1,2,3,4
Pu-243 (1.0)	4.956 h	

See end of table for footnotes.

Table A4-1. (continued)

Radionuclide ^a	Half-life ^b	Applicable scenarios ^c
Cm-248	3.39×10^5 y	1,2,4
Cf-249	350.6 y	1,2,3,4
Cf-250	13.08 y	2,4
Cf-251	900 y	1,2,3,4

^a Indented entries are radiologically significant short-lived decay products of parent radionuclide listed. With each decay product, branching fraction in decay of parent radionuclide is given in parentheses.

^b Values from Kocher (1981).

^c 1 = groundwater transport pathway, off-site individuals;
 2 = agriculture scenario, inadvertent intruders;
 3 = resident scenario, inadvertent intruders;
 4 = post-drilling scenario, inadvertent intruders.

^d Short-lived decay products Th-228, Ra-224, Rn-220, Pb-212, Bi-212, and Tl-208 are listed under Th-232.

As indicated in Table A.4-1, some radionuclides included in the dose analyses decay to short-lived radionuclides that are potentially important for at least one exposure pathway. In all such cases, the doses from a parent radionuclide and its short-lived decay products are combined by assuming that the decay products are in secular equilibrium with the parent, and the activity concentrations of the decay products take into account the decay branching fractions given in Table A.4-1. Long-lived decay products of uranium and Np-237 that could be significant in the dose analyses (i.e., Ra-226, Th-229, Th-230, Pa-231, and U-233) also are included in the table. However, these radionuclides are not assumed to be in secular equilibrium with their respective parent radionuclides, because buildup of the activity of decay products occurs over a very long time. Thus, in these cases, the activity of the long-lived decay products over time should be considered explicitly in the dose analyses, as is also the case when a radionuclide produces a longer-lived decay product.

A.4.3 Assumed Exposure Scenarios and Exposure Pathways

This section briefly describes the exposure scenarios and exposure pathways assumed in the dose analyses for off-site individuals and inadvertent intruders. A more detailed description of the assumed exposure scenarios, including the justification for neglecting other scenarios in the dose analyses, is given in Sects. 3.2.3 and 3.2.4. The model equations and parameter values for each exposure pathway then are presented in Sect. A.4.5.

A.4.3.1 Exposure Scenarios and Pathways for Off-Site Individuals

The PA for the EAV assumes that radionuclides are transported to off-site locations principally via the groundwater pathway. Off-site transport via atmospheric releases also was considered (see Appendix A.3).

As described in Sect. 3.2.3, off-site individuals are assumed to use contaminated groundwater for domestic purposes, and the following exposure pathways involving use of contaminated water are assumed to occur: 1) direct ingestion of the contaminated drinking

water; 2) ingestion of milk and meat from dairy and beef cattle that drink contaminated water; 3) ingestion of vegetables grown in garden soil irrigated with contaminated water; 4) direct ingestion of contaminated soil in conjunction with intakes of vegetables from the garden; 5) external exposure to contaminated soil while working in the garden; and 6) inhalation of radionuclides suspended into air from contaminated soil while working in the garden. Irrigation of pasture grass consumed by dairy and beef cattle is assumed to be unimportant, because irrigation of pasture is not widely practiced near the SRS. The relative importance of the different exposure pathways for off-site individuals is summarized below.

As described in Sect. 3.2.3.1 and 3.2.3.2, off-site releases of radionuclides via the groundwater pathway are assumed to be subject to two dose limits that are consistent with the performance objectives for LLW disposal (U.S.DOE 1988a): 1) a limit on EDE of 25 mrem per year from all exposure pathways and 2) a limit on EDE of 4 mrem per year from consumption of 2 L/day of drinking water from a contaminated source. The latter performance objective is used to limit concentrations of radionuclides in groundwater at locations beyond the 100-m buffer zone around the disposal units.

In Sect. 3.2.3.3, an analysis was performed to compare the importance of the two performance objectives for off-site releases of radionuclides listed above. The analysis showed that, at the SRS, the performance objective for protection of groundwater is expected to be more restrictive for any radionuclide than the performance objective for protection of off-site individuals from all exposure pathways. That is, if the lower dose limit for direct consumption of contaminated groundwater is met, then the higher dose limit for all exposure pathways also will be met without the need for further analysis of the pathways involving use of contaminated groundwater other than direct consumption of drinking water.

Therefore, in the dose analysis for off-site individuals, only the following exposure pathway needs to be considered:

- direct ingestion of contaminated drinking water from a source of groundwater beyond the 100-m buffer zone around disposal units.

This exposure pathway must be considered at any time after disposal. Therefore, for example, in the analysis of groundwater transport for U-234/U-238 and Np-237 in disposed waste, buildup of the long-lived decay products Th-230/Ra-226 and U-233/Th-229, respectively, must be taken into account in the analysis for the groundwater pathway.

A.4.3.2 Exposure Scenarios and Pathways for Inadvertent Intruders

In estimating doses to inadvertent intruders after the period of active institutional control (i.e., at any time beyond 100 years after closure of the disposal facility), it is assumed that such individuals could establish a permanent homestead on the site. Furthermore, it is assumed that an intruder has no *a priori* knowledge of waste disposal activities at the site. Inadvertent intruders are assumed to receive radiation exposures from use of contaminated groundwater obtained from a well on the disposal site and from direct intrusion into waste disposal units. Exposures of inadvertent intruders to volatile releases of H-3 and C-14 are considered separately in Appendix A.3. However, exposures to radon and its short-lived decay products are considered in this appendix.

Exposures of inadvertent intruders to radionuclides in contaminated groundwater are assumed to occur in conjunction with any of the scenarios involving direct intrusion into waste disposal units described below, and the exposure pathways involving use of contaminated groundwater are assumed to be the same as those listed in Sect. A.4.3.1 for off-site individuals. However, because the requirement for protection of groundwater beyond the 100-m buffer zone (i.e., the limit on EDE of 4 mrem per year from direct consumption of groundwater) is much more stringent than the dose limits for protection of inadvertent intruders taking into account all exposure pathways (i.e., limits on EDE of 100 mrem per year for chronic exposures and 500 mrem for a single acute exposure), exposures to contaminated groundwater can be neglected in the dose analysis for inadvertent intruders (see Sect. 3.2.4.1).

For direct intrusion into disposal units after loss of active institutional control, exposures are assumed to occur according to one of three scenarios, which are called the agriculture, resident, and post-drilling scenarios. Other scenarios which were considered but shown to be less important are discussed in Sect. 3.2.4. The three scenarios considered in this analysis and their associated exposure pathways are described as follows.

In the agriculture scenario, an intruder is assumed to build a home directly on top of disposal units, and the foundation is assumed to extend into the units themselves. Radioactive wastes exhumed during excavation for the foundation are assumed to be indistinguishable from native soil, and some of the exhumed waste is assumed to be mixed with native soil in the intruder's vegetable garden. The following pathways involving exposure to radionuclides in solid waste then are assumed to occur:

- ingestion of vegetables grown in contaminated garden soil;
- direct ingestion of contaminated soil, primarily in conjunction with intakes of vegetables from the garden;
- external exposure to contaminated soil while working in the garden or residing in the home on top of the disposal units; ;
- inhalation of radionuclides attached to soil particles that are suspended into air from contaminated soil while working in the garden or residing in the home; and
- inhalation of volatile radionuclides released into air from contaminated soil while working in the garden or residing in the home.

Inhalation of the volatile radionuclides H-3 and C-14 while working in the garden or residing in the home is considered separately in Appendix A.3. Inhalation of radon and its short-lived decay products is considered in this appendix.

In the resident scenario, an intruder also is assumed to excavate at the location of disposal units, but is assumed to encounter an intact engineered barrier (e.g., a reinforced concrete roof) used in constructing the disposal units which cannot readily be penetrated by the types of excavation equipment normally used near the SRS. Therefore, instead of excavating into the waste, the intruder is assumed to build a home immediately on top of the intact engineered barrier. Since waste in the disposal facility is not directly accessed during excavation, due to the assumed impenetrability of the engineered barriers, the only exposure pathway of concern for this scenario is external exposure to photon-emitting radionuclides in the waste while residing in the home. While exposure to radon could occur during residence

on top of intact engineered barriers, such exposures presumably would be much less than those occurring in the agriculture scenario when residence on top of unshielded waste is assumed to be credible. Therefore, potential exposures to radon are ignored in the resident scenario but are captured in the agriculture scenario.

In the post-drilling scenario, an intruder is assumed to access solid waste by drilling through a disposal unit, e.g., for the purpose of constructing a well for the intruder's domestic water supply. During drilling, a small volume of waste is brought to the surface, and all of the drilling waste is assumed to be mixed with native soil in the intruder's vegetable garden. The following pathways involving exposure to radionuclides in the solid waste then are assumed to occur:

- ingestion of vegetables grown in contaminated soil;
- direct ingestion of contaminated soil, primarily in conjunction with intakes of vegetables from the garden;
- external exposure to contaminated soil while working in the garden;
- inhalation of radionuclides attached to soil particles that are suspended into air from contaminated soil while working in the garden; and
- inhalation of volatile radionuclides released into air from contaminated soil while working in the garden.

As in the agriculture scenario, inhalation of the volatile radionuclides H-3 and C-14 while working in the garden is considered in Appendix A.3, and inhalation of radon and its short-lived decay products is considered in this appendix.

The pathways listed above for the post-drilling scenario correspond to some of the pathways for the agriculture scenario. However, in the post-drilling scenario, external and inhalation exposures while residing in the home are not relevant, because all drilling waste is assumed to be mixed with soil in the intruder's vegetable garden and the intruder's home is not located on top of disposal units.

A4.4 Dose Conversion Factors for Internal and External Exposure

From the descriptions of the assumed exposure scenarios and pathways given in Sect. A.4.3, doses to off-site individuals and inadvertent intruders are assumed to result from ingestion, inhalation, and external exposure. This section presents the factors used in the dose analyses to convert intakes of radionuclides via ingestion and inhalation to internal doses and to convert concentrations of radionuclides in the environment to external dose rates.

The internal DCFs for ingestion and inhalation of radionuclides are given in Tables A.4-2 and A.4-3, respectively. These factors give 50-year committed EDEs per unit activity intake. The entries for any short-lived decay products of a longer-lived radionuclide do not take into account the branching fraction in the decay of the parent radionuclide; i.e., the values for each decay product assume the same unit intake of activity (1 μCi). Dose conversion factors are listed for a short-lived decay product only if ingestion or inhalation of the decay product would contribute significantly to the dose from intakes of the parent radionuclide and the decay product in secular equilibrium. Dose conversion factors for inhalation of isotopes of radon and their short-lived decay products are not listed in Table A.4-3. Rather, as described with the agriculture scenario in Sect. A.4.5.2, a natural analog model based on the known doses from exposure to radon per unit concentration of Ra-226 or Th-232 in soil is used to estimate inhalation doses from radon in waste. The internal DCFs in Table A.4-3 are those currently recommended for use by the U.S.DOE (1988b) in assessing radiation doses to the public.

For some radionuclides, more than one DCF for ingestion or inhalation has been tabulated by the U.S.DOE (1988b). Whenever ingestion DCFs are given for two GI-tract absorption fractions, the value corresponding to the higher absorption fraction is adopted in Table A.4-2, because radionuclides that are transported in water or through terrestrial food-chains should be in relatively soluble form and more easily absorbed in the GI tract. This choice does not always give the higher ingestion DCF, but the value corresponding to the lower GI-tract absorption fraction differs from the adopted value in such cases by less than 10%. If inhalation DCFs are given for more than one lung clearance class, the clearance class

Table A.4-2. Internal dose conversion factors for ingestion of radionuclides^a

Radionuclide ^b	f_1^c	Rem/ μ Ci Ingested	Radionuclide ^b	f_1^c	Rem/ μ Ci Ingested
H-3	1.0	6.3×10^5	Th-229	0.0002	3.5
C-14	—	2.1×10^3	Ra-225	0.2	3.1×10^1
Al-26	0.01	1.3×10^2	Ac-225	0.001	9.5×10^2
Co-60	0.3	2.6×10^2	Th-230	0.0002	5.3×10^1
Ni-59	0.05	2.0×10^4	Th-232	0.0002	2.8
Ni-63	0.05	5.4×10^4	Ra-228	0.2	1.2
Se-79	0.8	8.3×10^3	Th-228	0.0002	3.8×10^1
Rb-87	1.0	4.8×10^3	Ra-224	0.2	3.3×10^1
Sr-90	0.3	1.3×10^1	Pb-212	0.2	4.1×10^2
Y-90	0.0001	1.0×10^2	Pa-231	0.001	1.1×10^1
Zr-93	0.002	1.6×10^3	Ac-227	0.001	1.4×10^1
Nb-93m	0.01	5.3×10^4	Ra-223	0.2	5.5×10^1
Tc-99	0.8	1.3×10^3	U-232 ^d	0.05	1.3
Pd-107	0.005	1.4×10^4	U-233	0.05	2.7×10^1
Cd-113m	0.05	1.5×10^1	U-234	0.05	2.6×10^1
Sn-121m	0.02	1.3×10^3	U-235	0.05	2.5×10^1
Sn-126	0.02	1.7×10^2	U-236	0.05	2.5×10^1
Sb-126	0.1	9.0×10^3	U-238	0.05	2.3×10^1
I-129	1.0	2.8×10^1	Th-234	0.0002	1.3×10^2
Cs-135	1.0	7.1×10^3	Np-237	0.001	3.9
Cs-137	1.0	5.0×10^2	Pu-238	0.001	3.8
Sm-151	0.0003	3.4×10^4	Pu-239	0.001	4.3
Eu-154	0.001	9.1×10^3	Pu-240	0.001	4.3
Eu-155	0.001	1.3×10^3	Pu-241	0.001	8.6×10^2
Pb-210	0.2	5.1	Pu-242	0.001	4.1
Po-210	0.1	1.6	Pu-244	0.001	4.0
Ra-226	0.2	1.1	Am-241	0.001	4.5

See end of table for footnotes.

Table A-4-2 (continued)

Radionuclide ^a	f _i ^c	Rem/ μ Cl Ingested	Radionuclide ^a	f _i ^c	Rem/ μ Cl Ingested
Am-242m	0.001	4.2	Cm-246	0.001	4.5
Cm-242	0.001	1.1×10^{-1}	Cm-247	0.001	4.1
Am-243	0.001	4.5	Cm-248	0.001	1.6×10^1
Cm-243	0.001	2.9	Cm-249	0.001	4.6
Cm-244	0.001	2.3	Cm-250	0.001	1.9
Cm-245	0.001	4.5	Cm-251	0.001	4.6

- ^a Values adopted by U.S.DOE (1988b) give 50-year committed EDEs per unit activity ingested.
- ^b Indented entries are radiologically significant short-lived decay products of parent radionuclide listed. Dose-rate conversion factors for decay products do not take into account branching fraction in decay of parent.
- ^c Fraction of ingested radionuclide absorbed into blood from GI tract.
- ^d Entries for short-lived decay products Th-228, Ra-224, and Pb-212 are listed under Th-232.

Table A4-3. Internal dose conversion factors for inhalation of radionuclides^a

Radionuclide ^b	Clearance Class ^c	Rem/ μ Ci inhaled	Radionuclide ^b	Clearance Class ^c	Rem/ μ Ci inhaled
H-3		6.3×10^5	Ra-226	W	7.9
C-14 ^d		2.1×10^3	Rn-222 ^f		
Al-26	D	7.9×10^2	Th-229	Y	1.7×10^3
Co-60	Y	1.5×10^1	Th-230	Y	2.6×10^2
Ni-59 ^e	D	1.3×10^3	Th-232	Y	1.1×10^3
Ni-63 ^e	D	3.0×10^3	Th-228	Y	3.1×10^2
Se-79	W	8.9×10^3	Rn-220 ^f		
Rb-87	D	3.3×10^3	Pa-231	W	1.3×10^3
Sr-90	D	2.3×10^1	Ac-227	D	6.7×10^3
Y-90	Y	8.2×10^3	U-232 ^g	Y	6.7×10^2
Zr-93	D	3.2×10^1	U-233	Y	1.3×10^2
Nb-93m	Y	2.8×10^2	U-234	Y	1.3×10^2
Tc-99	D	8.4×10^4	U-235	Y	1.2×10^2
Pd-107	Y	1.3×10^2	U-236	Y	1.2×10^2
Cd-113m	D	1.6	U-238	Y	1.2×10^2
Sn-121m	D	5.8×10^3	Np-237	W	4.9×10^2
Sn-126	D	8.6×10^2	Pu-238	W	4.6×10^2
Sb-126	D	4.6×10^3	Pu-239	W	5.1×10^2
I-129	D	1.8×10^1	Pu-240	W	5.1×10^2
Cs-135	D	4.5×10^3	Pu-241	W	1.0×10^1
Cs-137	D	3.2×10^2	Pu-242	W	4.8×10^2
Sm-151	W	2.9×10^2	Pu-244	W	4.8×10^2
Eu-154	W	2.6×10^1	Am-241	W	5.2×10^2
Eu-155	W	3.9×10^2	Am-242m	W	5.1×10^2
Pb-210	D	1.3×10^1	Cm-242	W	1.7×10^1
Po-210	W	8.1	Am-243	W	5.2×10^2

See end of table for footnotes.

Table A.4-3. (continued)

Radionuclide ^a	Clearance Class ^c	Rem/ μ Ci inhaled	Radionuclide ^a	Clearance Class ^c	Rem/ μ Ci inhaled
Cm-243	W	3.5×10^2	Cm-246	W	5.4×10^2
Cm-244	W	2.7×10^2	Cm-247	W	4.9×10^2
Cm-245	W	5.4×10^2			

- ^a Values adopted by U.S.DOE (1988b) give 50-year committed EDEs per unit activity inhaled.
- ^b Indented entries are radiologically significant short-lived decay products of parent radionuclide listed. Dose-rate conversion factors for decay products do not take into account branching fraction in decay of parent.
- ^c Clearance from respiratory passages for radionuclides in particulate form in a matter of days (D), weeks (W), or years (Y).
- ^d Radionuclide is assumed to be in organic form.
- ^e Radionuclide is assumed to be in inorganic form.
- ^f Inhalation doses from radon and its short-lived decay products are estimated using model described with agriculture scenario in Sect. A.4.5.2.
- ^g Entries for short-lived decay products Th-228 and Rn-220 are listed under Th-232.

giving the highest value usually is adopted in Table A.4-3, because there is little information for most elements on the expected chemical forms and their solubilities in waste or soil and the choice of the highest inhalation DCF may result in conservative overestimates of inhalation doses. However, Sr-90 and Tc-99 are assumed to be Class D because their solubility in the environment is expected to be relatively high, and all isotopes of Th are assumed to be Class Y because Th in the environment is expected to be highly insoluble.

Dose conversion factors for external exposure give dose-equivalent rates per unit concentration of radionuclides in the environment. These factors depend on the distribution of radionuclides in the source region, the amount of self-shielding provided by material in the source region, and the shielding provided by any uncontaminated material between the source region and the location of an exposed individual. Therefore, separate sets of DCFs are required for the assumed pathways involving external exposure to 1) activity in contaminated soil while working in the vegetable garden in the agriculture and post-drilling scenarios, 2) activity in exposed waste while residing in the home at the disposal site in the agriculture and resident scenarios, and 3) activity in waste shielded by intact engineered barriers while residing in the home at the disposal site in the resident scenario.

For external exposure to radionuclides in disposal units or in soil in the vegetable garden, the source region is assumed to be a uniformly contaminated slab of infinite lateral extent. Depending upon the particular exposure scenario and pathway, the slab is assumed to have either finite or infinite thickness, and the shielding provided by any uncontaminated material between the source and receptor locations is taken into account. The idealized distributions of radionuclides in the source region assumed in the dose analysis are reasonable, because radionuclides should be dispersed throughout the source regions and only about 1 m of soil-equivalent material between the source and receptor locations provides essentially complete shielding (Kocher and Sjoreen 1985).

In all calculations of external dose, an exposed individual is assumed to be located at a distance of 1 m above ground. In all cases, the shielding provided by 1 m of air is negligible compared with the shielding provided by the material in the source region itself or by the thickness of any uncontaminated material (e.g., an intact concrete roof) between the source and receptor locations.

For external exposure while working in the vegetable garden, the source region is assumed to be a uniformly contaminated slab of soil with a thickness of 15 cm, which is a typical depth of a plowed layer in a garden. The external dose-rate conversion factors for this case are given in Table A.4-4.

For external exposure while residing in the home in the agriculture scenario, the source region is assumed to be a slab of soil-equivalent material of essentially infinite thickness. This is a good approximation because sources more than 1 m below the surface would not contribute significantly to the dose (Kocher and Sjoeren 1985). No shielding is assumed between the source region and the receptor location other than that provided by the material in the source region itself. Shielding provided by the walls of the home during indoor residence is taken into account in the dose analysis itself (see Eq. A.4-8). The external dose-rate conversion factors for this case are given in the column in Table A.4-5 labeled "No shielding".

For external exposure while residing in the home in the resident scenario, the source region also is assumed to be a slab of soil-equivalent material of infinite thickness. As described in Sect. 3.2.4.2, the maximum external dose in the resident scenario can be bounded by considering two limiting cases. The first involves exposure to both shorter- and longer-lived photon-emitting radionuclides and photon-emitting daughters at the time active institutional control ceases at 100 years after facility closure when an intact concrete roof and any other engineered barriers on top of the waste provide a considerable amount of shielding. The second case involves exposure only to longer-lived photon-emitting radionuclides and photon-emitting daughters at a time long after disposal when the concrete roof and any other engineered barriers above the waste have lost their physical integrity and exposure to waste with no external shielding could occur.

As described in Sect. 2.9, the closure concept for the ILNT and ILT vaults includes a layer of uncontaminated grout about 3 ft (90 cm) thick on top of the waste and a concrete roof of variable thickness, the average thickness being about 3 ft (90 cm). The closure concept for the LAW vaults does not include a layer of uncontaminated grout on top of the waste, and the concrete roof is about 50 cm thick.

Table A.4-4. External dose-rate conversion factors for radionuclides uniformly distributed in 15 cm of surface soil^a

Radionuclide ^b	Dose-rate factor (rem/y per $\mu\text{Ci}/\text{m}^3$)	Radionuclide ^b	Dose-rate factor (rem/y per $\mu\text{Ci}/\text{m}^3$)
Al-26	9.0×10^{-3}	Pa-231	1.1×10^{-4}
Co-60	8.5×10^{-3}	Th-227	3.1×10^{-4}
Sn-121m	1.2×10^{-6}	Ra-223	3.6×10^{-4}
Sn-126	9.2×10^{-5}	Pb-211	1.7×10^{-4}
Sb-126m	5.2×10^{-3}	Bi-211	1.5×10^{-4}
Sb-126	9.5×10^{-3}	Tl-207	1.1×10^{-5}
I-129	8.1×10^{-6}	U-232 ^c	---
Cs-137	---	U-235	4.4×10^{-4}
Ba-137m	2.0×10^{-3}	Th-231	2.3×10^{-5}
Eu-154	4.1×10^{-3}	U-238	---
Eu-155	1.1×10^{-4}	Th-234	1.5×10^{-5}
Ra-226	---	Pa-234m	4.9×10^{-5}
Pb-214	7.8×10^{-4}	Pa-234	6.3×10^{-3}
Bi-214	5.1×10^{-3}	Np-237	4.9×10^{-5}
Th-229	2.0×10^{-4}	Pa-233	6.0×10^{-4}
Ra-225	6.9×10^{-6}	Am-241	2.7×10^{-5}
Ac-225	3.9×10^{-5}	Am-242m	1.1×10^{-6}
Fr-221	9.2×10^{-5}	Am-242	3.1×10^{-5}
Bi-213	4.4×10^{-4}	Np-238	1.8×10^{-3}
Tl-209	6.8×10^{-3}	Am-243	8.9×10^{-5}
Th-232	---	Np-239	4.6×10^{-4}
Ac-228	3.2×10^{-3}	Cm-243	3.5×10^{-4}
Pb-212	4.2×10^{-4}	Cm-245	2.1×10^{-4}
Bi-212	6.3×10^{-4}	Cm-247	1.0×10^{-3}
Tl-208	1.1×10^{-2}	Pu-243	4.9×10^{-5}
		Cf-249	1.1×10^{-3}
		Cf-251	3.2×10^{-4}

^a Values from Eckerman and Ryman (1993) give EDE rates from external exposure per unit activity concentration in soil at distance of 1 m from source region.

^b Indented entries are radiologically significant short-lived decay products of parent radionuclide listed. Dose-rate conversion factors for decay products do not take into account branching fraction in decay of parent.

^c Entries for short-lived decay products Pb-212, Bi-212, and Tl-208 are listed under Th-232.

Table A.4-5. External dose-rate conversion factors for radionuclides uniformly distributed in infinite thickness of soil-equivalent material

Radionuclide ^a	Dose-rate factor (rem/y per $\mu\text{Ci}/\text{m}^3$)		
	No shielding ^b	45-cm shielding ^c	100-cm shielding ^c
Al-26	1.1×10^{-2}	3.2×10^{-4}	7.9×10^{-6}
Co-60	1.0×10^{-2}	2.5×10^{-4}	3.3×10^{-6}
Sn-121m	1.2×10^{-6}	---	---
Sn-126	9.2×10^{-5}	---	---
Sb-126m	5.8×10^{-3}	4.9×10^{-5}	1.8×10^{-7}
Sb-126	1.1×10^{-2}	9.7×10^{-5}	4.3×10^{-7}
I-129	8.1×10^{-6}	---	---
Cs-137	---	---	---
Ba-137m	2.3×10^{-3}	2.0×10^{-5}	6.6×10^{-8}
Eu-154	4.8×10^{-3}	9.0×10^{-5}	1.0×10^{-6}
Eu-155	1.1×10^{-4}	1.8×10^{-9}	---
Ra-226	---	---	---
Pb-214	8.4×10^{-4}	---	---
Bi-214	6.1×10^{-3}	1.7×10^{-4}	3.8×10^{-6}
Th-229	2.0×10^{-4}	2.4×10^{-8}	---
Ra-225	6.9×10^{-6}	---	---
Ac-225	4.0×10^{-5}	1.2×10^{-8}	---
Fr-221	9.6×10^{-5}	4.1×10^{-8}	---
Bi-213	4.8×10^{-4}	2.5×10^{-6}	7.5×10^{-9}
Tl-209	8.1×10^{-3}	2.2×10^{-4}	4.3×10^{-6}

See end of table for footnotes.

A-59
Table A.4-5. (continued)

WSRC-RP-94-218

Radionuclide ^a	Dose-rate factor (rem/y per $\mu\text{Ci}/\text{m}^3$)		
	No shielding ^b	45-cm shielding ^c	100-cm shielding ^c
Th-232	---	---	---
Ac-228	3.7×10^{-3}	6.1×10^{-5}	7.2×10^{-7}
Pb-212	4.4×10^{-4}	---	---
Bi-212	7.3×10^{-4}	1.4×10^{-5}	2.1×10^{-7}
Tl-208	1.4×10^{-2}	6.9×10^{-4}	3.0×10^{-5}
Pa-231	1.2×10^{-4}	1.6×10^{-7}	8.0×10^{-11}
Th-227	3.3×10^{-4}	3.6×10^{-7}	1.6×10^{-10}
Ra-223	3.8×10^{-4}	4.6×10^{-7}	2.9×10^{-10}
Pb-211	1.9×10^{-4}	1.7×10^{-6}	8.3×10^{-9}
Bi-211	1.6×10^{-4}	4.4×10^{-7}	3.4×10^{-10}
Tl-207	1.2×10^{-5}	1.2×10^{-7}	8.2×10^{-10}
U-232 ^d	---	---	---
U-235	4.5×10^{-4}	1.1×10^{-7}	6.5×10^{-12}
Th-231	2.3×10^{-5}	---	---
U-238	---	---	---
Th-234	1.5×10^{-5}	---	---
Pa-234m	5.6×10^{-5}	6.8×10^{-7}	5.2×10^{-9}
Pa-234	7.2×10^{-3}	1.1×10^{-4}	1.2×10^{-6}
Np-237	4.9×10^{-5}	---	---
Pa-233	6.4×10^{-4}	1.3×10^{-6}	7.9×10^{-10}
Am-241	2.7×10^{-5}	2.9×10^{-13}	---
Am-242m	1.1×10^{-6}	---	---
Am-242	3.1×10^{-5}	---	---
Np-238	2.1×10^{-3}	3.7×10^{-5}	3.1×10^{-7}

See end of table for footnotes.

A-60
Table A.4-5. (continued)

WSRC-RP-94-218

Radionuclide ^a	Dose-rate factor (rem/y per $\mu\text{Ci}/\text{m}^3$)		
	No shielding ^b	45-cm shielding ^c	100-cm shielding ^c
Am-243	8.9×10^{-5}	2.5×10^{-10}	---
Np-239	4.7×10^{-4}	3.2×10^{-7}	1.2×10^{-10}
Cm-243	3.6×10^{-4}	1.4×10^{-7}	5.8×10^{-11}
Cm-245	2.1×10^{-4}	1.5×10^{-8}	---
Cm-247	1.1×10^{-3}	3.6×10^{-6}	3.6×10^{-9}
Pu-243	5.0×10^{-5}	2.8×10^{-8}	---
Cf-249	1.2×10^{-3}	3.4×10^{-6}	3.0×10^{-9}
Cf-251	3.3×10^{-4}	8.8×10^{-8}	---

^a Indented entries are radiologically significant short-lived decay products of parent radionuclide listed. Dose-rate conversion factors for decay products do not take into account branching fraction in decay of parent.

^b Values from Eckerman and Ryman (1993) give EDE rates from external exposure per unit activity concentration in soil at distance of 1 m from source region.

^c Values give EDE rates from external exposure per unit activity concentration in soil at distance of 1 m from source region and are based on calculations for monoenergetic photon sources (Kocher and Sjoreen 1985) and energies and intensities of photons emitted in decay of radionuclides (Kocher 1981).

^d Entries for short-lived decay products Pb-212, Bi-212, and Tl-208 are listed under Th-232.

For the case of external exposure to waste shielded by engineered barriers at 100 years after disposal in the resident scenario, the total thickness of the concrete roof and layer of uncontaminated grout for the ILNT and ILT vaults thus is about 1.8 m. The thickness of shielding for these vaults is sufficient to reduce the external dose from the waste to minuscule levels for any possible concentrations of photon-emitting radionuclides (Kocher and Sjoreen 1985). Therefore, in order to evaluate the need for the concrete roof in limiting external dose at 100 years after disposal for the resident scenario, the dose analysis for the ILNT and ILT vaults at this time is based on the assumption that only the layer of uncontaminated grout is present to provide shielding. The nominal thickness of the grout is assumed to be 100 cm. This value is slightly higher than the planned thickness of the grout layer and is intended to take into account the somewhat greater shielding provided by the metal waste containers and waste forms in the ILNT and ILT vaults compared with the shielding provided by soil-equivalent material.

For the LAW vaults, the nominal thickness of the concrete roof at 100 years after disposal is assumed to be 45 cm. This value is slightly less than the planned thickness of the concrete roof and is intended to take into account the somewhat reduced shielding provided by the waste itself, compared with soil-equivalent material, due to the presence of void spaces in the vaults.

Thus, in Table A.4-5, the external dose-rate conversion factors for the resident scenario at 100 years after disposal are given in the column labeled "45-cm shielding" for the LAW vaults and the column labeled "100-cm shielding" for the ILNT and ILT vaults. Again, the assumed thickness of shielding for the ILNT and ILT vaults should provide considerable over-estimates of external dose, because the planned thickness of the concrete roof on top of the vaults is ignored.

For the case of external exposure to unshielded waste in the resident scenario, the external dose-rate conversion factors are given in the column in Table A.4-5 labeled "No shielding". These data apply to all disposal units. Although exposure to unshielded waste is expected to become credible only at times long after disposal, due to the expected lifetime of the engineered barriers above the waste, dose-rate factors for the case of no shielding are

provided for the shorter-lived radionuclides as well. Inclusion of these radionuclides permits an evaluation of the time period over which the engineered barriers must maintain their integrity and prevent access to unshielded waste in the agriculture and resident scenarios. Again, at any time after disposal, shielding provided by the walls of the home during indoor residence is taken into account in the dose analysis itself.

The external dose-rate conversion factors in Table A.4-4 and in the column labeled "No shielding" in Table A.4-5 were obtained from calculations of Eckerman and Ryman (1993). The external dose-rate conversion factors for the two thicknesses of shielding in Table A.4-5 were obtained from calculations of absorbed dose rates in air from monoenergetic photon sources in soil (Kocher and Sjoeren 1985), the spectrum of photons emitted in the decay of each radionuclide (Kocher 1981), and the assumption that absorbed doses in air can be converted to EDEs by multiplying by a factor of 0.8. The entries for any short-lived decay products of a longer-lived radionuclide do not take into account the branching fraction in the decay of the parent radionuclide; i.e., the values for each decay product assume exposure to the same unit activity concentration ($1 \mu\text{Ci}/\text{m}^3$).

On the basis of a direct comparison of results from Eckerman and Ryman (1993) and Kocher and Sjoeren (1985) for the case in Table A.4-5 of an infinitely thick source region with no shielding, the results from Kocher and Sjoeren for the two thicknesses of shielding in Table A.4-5 could be in error by as much as 25 to 30% in some cases. However, since the results from Kocher and Sjoeren appear to provide conservative overestimates of dose in almost all cases and the magnitude of the possible error is not large, these results reasonably can be used in this analysis. The calculations needed in this analysis for the different thicknesses of shielding between the source region and receptor location were not performed by Eckerman and Ryman.

A.4.5 Models and Parameter Values for Exposure Pathways

This section presents the models used to calculate doses to off-site individuals and inadvertent intruders for the various exposure pathways considered in this analysis involving use of contaminated groundwater or direct intrusion into disposal units. In each case, the

parameter values assumed in implementing the models also are presented. For each exposure pathway, the model results are presented in summary tables which give annual EDEs per unit concentration of radionuclides in water or in disposal units. For scenarios for direct intrusion into disposal units, the unit concentrations to which the dose estimates are normalized are the concentrations at the time exposures are assumed to occur, rather than the concentrations at the time of disposal.

A.4.5.1 Exposure Pathways for Off-Site Individuals

As discussed in Sect. 3.2.3.3 and A.4.3.1, direct consumption of drinking water from a source of contaminated groundwater is the only exposure pathway that needs to be considered in the dose analysis for off-site individuals, because the assumed limit on EDE of 4 mrem per year from the drinking water pathway only is expected to be more restrictive for any radionuclide than the limit on EDE of 25 mrem per year from all exposure pathways.

The annual EDE (rem/year) from direct ingestion of radionuclide i in drinking water (w) is given by

$$H_{iw} = C_{iw} U_w D_i \quad (\text{A.4-1})$$

where

- C_{iw} = concentration of radionuclide i in drinking water ($\mu\text{Ci/L}$),
- U_w = annual consumption of drinking water (L/year), and
- D_i = DCF for ingestion of radionuclide i ($\text{rem}/\mu\text{Ci}$).

In implementing the model, a daily consumption of contaminated drinking water of 2 L, i.e., an annual consumption of 730 L, is assumed.

The model for estimating dose from the drinking water pathway is summarized in Table A.4-6. The radionuclides listed in this table include those selected on the basis of a screening analysis for the groundwater pathway described in Sect. 4.1.1 and the long-lived decay products of U-234/U-238, Np-237, Pu-239, and Pu-241 that could occur in significant concentrations in groundwater at various times in the future. The annual dose per unit concentration of a radionuclide in water is obtained by multiplying the assumed annual consumption of drinking water by the ingestion DCF given in Table A.4-2.

A.4.5.2 Exposure Pathways for Inadvertent Intruders

As described in Sects. 3.2.4 and A.4.3.2, exposures of inadvertent intruders resulting from direct intrusion into disposal units are assumed to occur according to the agriculture, resident, or post-drilling scenarios. This section presents the models and parameter values used to estimate doses to inadvertent intruders for each of these scenarios.

Agriculture Scenario

In the agriculture scenario, exposures of inadvertent intruders are assumed to occur after an intruder exhumes waste from disposal units while excavating to build a foundation for a home on top of the disposal facility and some of the exhumed waste is mixed with native soil in a vegetable garden. The exposure pathways assumed for this scenario then include: 1) ingestion of vegetables grown in contaminated garden soil; 2) direct ingestion of contaminated soil in conjunction with vegetable intakes; 3) external exposure to contaminated soil while working in the garden and residing in the home on top of the disposal units; and 4) inhalation of suspended activity in particulate form and inhalation of isotopes of radon and their short-lived decay products while working in the garden and residing in the home. The model for each exposure pathway is described below. The radionuclides included in the dose analysis for the agriculture scenario were selected on the basis of a screening analysis described in Sect. 3.2.4.4. Long-lived decay products of U-234/U-238, U-235, and Np-237 that could occur in significant concentrations in disposal units at times far in the future also are included in the dose analysis.

Table A.4-6. Annual EDEs from drinking water pathway per unit concentration of radionuclides in water

Radionuclide^a	Annual EDEs (rem/y per $\mu\text{Ci/L}$)
H-3	4.6×10^{-2}
C-14	1.5
Al-26	9.5
Co-60	1.9×10^1
Ni-59	1.5×10^{-1}
Ni-63	3.9×10^{-1}
Se-79	6.1
Rb-87	3.5
Sr-90 + d	1.0×10^2
Zr-93 ^b	1.2
Nb-93m	3.9×10^{-1}
Tc-99	9.5×10^{-1}
Pd-107	1.0×10^{-1}
Cd-113m	1.1×10^2
Sn-121m	9.5×10^{-1}
Sn-126 + d	1.3×10^1
I-129	2.0×10^2
Cs-135	5.2
Cs-137	3.7×10^1
Sm-151	2.5×10^{-1}
Pb-210 + d	4.9×10^3
Ra-226 + d ^c	8.0×10^2
Th-229 + d	2.9×10^3
Th-230	3.9×10^2
Th-232 + d	3.5×10^3
Pa-231 + d	1.1×10^4

See end of table for footnotes.

A-66
Table A.4-6. (continued)

WSRC-RP-94-218

Radionuclide ^a	Annual EDEs (rem/y per $\mu\text{Ci/L}$)
U-232 + d	1.5×10^3
U-233	2.0×10^2
U-234	1.9×10^2
U-235	1.8×10^2
U-236	1.8×10^2
U-238 + d	1.8×10^2
Np-237	2.8×10^3
Pu-238	2.8×10^3
Pu-239	3.1×10^3
Pu-240	3.1×10^3
Pu-242	3.0×10^3
Pu-244	2.9×10^3
Am-241	3.3×10^3
Am-242m + d	3.1×10^3
Am-243	3.3×10^3
Cm-245	3.3×10^3
Cm-246	3.3×10^3
Cm-247	3.0×10^3
Cm-248	1.2×10^4
Cf-249	3.4×10^3
Cf-251	3.4×10^3

^a " + d" denotes short-lived decay products that are assumed to be in secular equilibrium with parent radionuclide; see Table A.4-1 for decay products and branching fractions.

^b Entry does not include possible contribution from Nb-93m decay product.

^c Entry does not include possible contribution from Pb-210 decay product.

Vegetable Pathway. The annual EDE (rem/year) from ingestion of radionuclide i in vegetables (v) is given by

$$H_v = C_v U_v D_i \quad (A.4-2)$$

where

C_v = concentration of radionuclide i in vegetables ($\mu\text{Ci/kg}$),

U_v = annual consumption of vegetables (kg fresh weight per year), and

D_i = DCF for ingestion of radionuclide i (rem/ μCi).

Radionuclides are assumed to be transferred to vegetables via root uptake from the contaminated garden soil, and the radionuclide concentrations in vegetables are given by

$$\begin{aligned} C_v &= B_v C_s / \rho_s \\ &= B_v f C_w / \rho_s \end{aligned} \quad (A.4-3)$$

where

B_v = plant-to-soil concentration ratio for radionuclide i ($\mu\text{Ci/kg}$ fresh weight in vegetation per $\mu\text{Ci/kg}$ dry weight in soil),

C_s = concentration of radionuclide i in soil in vegetable garden ($\mu\text{Ci/m}^3$),

ρ_s = bulk density of soil (kg/m^3),

C_w = concentration of radionuclide i in exhumed waste ($\mu\text{Ci/m}^3$), and

f = dilution factor for mixing of radionuclides in exhumed waste into soil in vegetable garden.

In implementing the model, the assumed plant-to-soil concentration ratios in vegetables are given in Table A.4-7. Since site-specific data generally are lacking, the adopted values for all elements are based entirely on published evaluations and compilations which are generic in nature. The adopted values for almost all elements were obtained from the evaluation of published data by Baes et al. (1984). Although selection of these concentration ratios for use at the SRS clearly is judgmental, the use of data from a single source at least ensures some degree of consistency among the adopted values for the different elements.

Baes et al. (1984) give concentration ratios for vegetative portions of food crops, which would apply to leafy vegetables, and for nonvegetative (reproductive) portions, which would apply to nonleafy vegetables. The values for nonvegetative portions of food crops were adopted for use in this analysis, because consumption of nonleafy vegetables is expected to be considerably greater than consumption of leafy vegetables (Baes et al. 1984; Hamby 1992). The reported concentration ratios on a dry-weight basis for nonleafy vegetation were converted to a fresh-weight basis by multiplying by a factor of 0.43, which represents the average conversion factor for all types of nonleafy vegetables (Baes et al. 1984).

The other parameter values assumed in the model for the vegetable pathway are as follows: a dilution factor for mixing of radionuclides in exhumed waste into native soil in the vegetable garden of 0.2 (Napier et al. 1984), a bulk density of soil of $1,400 \text{ kg/m}^3$ (Baes and Sharp 1983), and an annual fresh-weight consumption of contaminated vegetables of 90 kg. The assumed dilution factor for mixing of exhumed waste with native soil in a vegetable garden of 0.2 is based on a typical depth and area of an excavation for a home and the reasonable assumption that only a relatively small fraction of the soil in the vegetable garden could contain exhumed waste in order for the garden to be productive; this dilution factor is consistent with previous assumptions for the agriculture scenario (NRC 1981; Oztunali and Roles 1986). The assumed yearly consumption of vegetables of 90 kg is based on data obtained near the SRS (Hamby 1992), which indicate a total yearly consumption of all vegetables by an average adult of 180 kg, and the assumption that half of an intruder's total intake of vegetables is obtained from the home garden. An assumption that an intruder's entire intake of all vegetables would be obtained from the home garden is regarded as unreasonably conservative.

Table A4-7. Elemental plant-to-soil concentration ratios in vegetables^a

Element	B_v^b	Element	B_v^b
H	4.8 ^c	Cs	1.3×10^{-2}
C	5.6×10^{-1} ^d	Sm	1.7×10^{-3}
Al	2.8×10^{-4}	Eu	1.7×10^{-3}
Co	3.0×10^{-3}	Pb	3.9×10^{-3}
Ni	2.6×10^{-2}	Po	1.7×10^{-4}
Se	1.1×10^{-2}	Ra	6.5×10^{-4}
Rb	3.0×10^{-2}	Ac	1.5×10^{-4}
Sr	1.1×10^{-1}	Th	3.7×10^{-5}
Zr	2.2×10^{-4}	Pa	1.1×10^{-4}
Nb	2.2×10^{-3}	U	1.7×10^{-3}
Tc	6.5×10^{-1}	Np	4.3×10^{-3}
Pd	1.7×10^{-2}	Pu	1.9×10^{-3}
Cd	6.5×10^{-2}	Am	1.1×10^{-4}
Sn	2.6×10^{-3}	Cm	6.6×10^{-6}
Sb	1.3×10^{-2}	Cf	6.6×10^{-6}
I	2.2×10^{-2}		

^a $\mu\text{Ci/kg}$ fresh weight in vegetation per $\mu\text{Ci/kg}$ dry weight in soil.

^b Except as noted, values are based on concentration ratios reported on basis of dry weight of vegetation given in Fig. 2.2 of Baes et al. (1984) multiplied by a factor of 0.43 to convert to fresh weight of vegetation (Baes et al. 1984).

^c Value obtained from Table E-1 of NRC (1977).

^d Value based on measurement of Sheppard et al. (1991) for carbonate form in acidic soil with low organic matter content. Reported value for dry weight of vegetation is converted to fresh weight by multiplying by factor of 0.43 (Baes et al. 1984).

^e Value is assumed to be the same as value for Cm.

The model for estimating dose from the vegetable pathway is summarized in Table A.4-8. The annual dose per unit concentration of a radionuclide in exhumed waste from a disposal unit at the time intrusion occurs is based on the model and parameter values described above and the ingestion DCFs given in Table A.4-2.

Soil Ingestion Pathway. The annual EDE (rem/year) from direct ingestion of radionuclide i in contaminated soil (s) is given by

$$H_{is} = C_{is} U_i D_i \quad (\text{A.4-4})$$

where

C_{is} = concentration of radionuclide i in soil in vegetable garden ($\mu\text{Ci/kg}$),

U_i = annual consumption of contaminated soil (kg/year), and

D_i = DCF for ingestion of radionuclide i (rem/ μCi).

Ingestion of contaminated soil is assumed to occur primarily as a result of incomplete washing of vegetables from the garden before consumption. Since the SRS is a humid site with extensive vegetation, ingestion of contaminated soil from sources other than the garden should be relatively unimportant for an average adult. Radionuclide concentrations in soil in the vegetable garden are given by

$$C_{is} = f_i C_{iw} / \rho_s \quad (\text{A.4-5})$$

where

C_{iw} = concentration of radionuclide i in exhumed waste ($\mu\text{Ci/m}^3$),

f_i = dilution factor for mixing of radionuclides in exhumed waste into soil in vegetable garden, and

ρ_s = bulk density of soil (kg/m^3).

Table A.4-8. Annual EDEs from vegetable pathway per unit concentration of radionuclides in exhumed waste for agriculture scenario

Radionuclide ^a	Annual EDE (rem/y per $\mu\text{Ci}/\text{m}^3$)
H-3	3.9×10^{-6}
C-14	1.5×10^{-5}
Al-26	4.7×10^{-8}
Co-60	1.0×10^{-6}
Ni-59	6.7×10^{-8}
Ni-63	1.8×10^{-7}
Se-79	1.2×10^{-6}
Rb-87	1.9×10^{-6}
Sr-90	1.8×10^{-4}
Zr-93 ^b	2.4×10^{-8}
Nb-93m	1.5×10^{-8}
Tc-99	1.1×10^{-5}
Pd-107	3.1×10^{-8}
Cd-113m	1.3×10^{-4}
Sn-121m	4.4×10^{-8}
Sn-126 + d	7.8×10^{-7}
I-129	7.9×10^{-5}
Cs-135	1.2×10^{-6}
Cs-137	8.4×10^{-6}
Sm-151	7.5×10^{-9}
Eu-154	2.0×10^{-7}
Eu-155	2.9×10^{-8}
Pb-210 + d	2.6×10^{-4}
Ra-226 + d ^c	2.7×10^{-4}
Th-229 + d	4.5×10^{-6}
Th-230	2.5×10^{-7}
Th-232 + d	1.6×10^{-5}
Pa-231 + d	3.2×10^{-5}
U-232 + d	3.4×10^{-5}

See end of table for footnotes.

A-72
Table A.4-8. (continued)

WSRC-RP-94-218

Radionuclide ^a	Annual EDE (rem/y per $\mu\text{Ci/m}^3$)
U-233	5.9×10^{-6}
U-234	5.7×10^{-6}
U-235	5.5×10^{-6}
U-236	5.5×10^{-6}
U-238	5.0×10^{-6}
Np-237	2.2×10^{-4}
Pu-238	9.3×10^{-7}
Pu-239	1.1×10^{-6}
Pu-240	1.1×10^{-6}
Pu-241	2.1×10^{-8}
Pu-242	1.0×10^{-6}
Pu-244	9.8×10^{-7}
Am-241	6.4×10^{-6}
Am-242m	6.0×10^{-6}
Am-243	6.4×10^{-6}
Cm-243	2.5×10^{-7}
Cm-244	2.0×10^{-7}
Cm-245	3.8×10^{-7}
Cm-246	3.8×10^{-7}
Cm-247	3.5×10^{-7}
Cm-248	1.4×10^{-6}
Cf-249	3.9×10^{-7}
Cf-250	1.6×10^{-7}
Cf-251	3.9×10^{-7}

^a " + d" denotes short-lived decay products that are assumed to be in secular equilibrium with parent radionuclide; see Table A.4-1 for decay products and branching fractions.

^b Value assumes that Nb-93m is present in secular equilibrium.

^c Value assumes that Pb-210 is present in secular equilibrium.

In implementing the model, a dilution factor for mixing of radionuclides in exhumed waste into native soil in the vegetable garden of 0.2 and a soil bulk density of $1,400 \text{ kg/m}^3$ are assumed, as in the model for the vegetable pathway. A daily consumption of contaminated soil from the vegetable garden of 0.1 g, i.e., an annual consumption of 0.037 kg, also is assumed (U.S.EPA 1989b).

The model for estimating dose from the soil ingestion pathway is summarized in Table A.4-9. The annual dose per unit concentration of a radionuclide in exhumed waste from a disposal unit at the time intrusion occurs is based on the model and parameter values described above and the ingestion DCFs given in Table A.4-2.

External Exposure Pathways. For external exposure (e) to contaminated soil while working in the vegetable garden, the annual EDE (rem/year) from radionuclide i is given by

$$H_{ie} = C_u U_e D_{ie} \quad (\text{A.4-6})$$

where

C_u = concentration of radionuclide i in soil in vegetable garden ($\mu\text{Ci/m}^3$),

U_e = fraction of the year during which external exposure to contaminated soil in vegetable garden occurs, and

D_{ie} = dose-rate conversion factor for external exposure to radionuclide i in garden soil (rem/y per $\mu\text{Ci/m}^3$).

As in the models for the vegetable and soil ingestion pathways, the radionuclide concentrations in soil in the vegetable garden are given by

$$C_u = f_i C_w \quad (\text{A.4-7})$$

Table A.4-9. Annual EDEs from soil ingestion pathway per unit concentration of radionuclides in exhumed waste for agriculture scenario

Radionuclide ^a	Annual EDE (rem/y per $\mu\text{Ci}/\text{m}^3$)
H-3	3.3×10^{-10}
C-14	1.1×10^{-8}
Al-26	6.9×10^{-8}
Co-60	1.4×10^{-7}
Ni-59	1.1×10^{-9}
Ni-63	2.9×10^{-9}
Se-79	4.4×10^{-8}
Rb-87	2.5×10^{-8}
Sr-90 + d	7.4×10^{-7}
Zr-93 ^b	1.1×10^{-8}
Nb-93m	2.8×10^{-9}
Tc-99	6.9×10^{-9}
Pd-107	7.4×10^{-10}
Cd-113m	7.9×10^{-7}
Sn-121m	6.9×10^{-9}
Sn-126 + d	9.7×10^{-8}
I-129	1.5×10^{-6}
Cs-135	3.8×10^{-8}
Cs-137	2.6×10^{-7}
Sm-151	1.8×10^{-9}
Eu-154	4.8×10^{-8}
Eu-155	6.9×10^{-9}
Pb-210 + d	3.5×10^{-5}
Ra-226 + d ^c	4.1×10^{-5}
Th-229 + d	2.1×10^{-5}
Th-230	2.8×10^{-6}
Th-232 + d	2.5×10^{-5}
Pa-231 + d	1.4×10^{-4}
U-232 + d	1.1×10^{-5}

See end of table for footnote.

A-75
Table A.4-9. (continued)

WSRC-RP-94-218

Radionuclide ^a	Annual EDE (rem/y per $\mu\text{Ci}/\text{m}^3$)
U-233	1.4×10^{-6}
U-234	1.4×10^{-6}
U-235	1.3×10^{-6}
U-236	1.3×10^{-6}
U-238 + d	1.3×10^{-6}
Np-237	2.1×10^{-5}
Pu-238	2.0×10^{-5}
Pu-239	2.3×10^{-5}
Pu-240	2.3×10^{-5}
Pu-241	4.5×10^{-7}
Pu-242	2.2×10^{-5}
Pu-244	2.1×10^{-5}
Am-241	2.4×10^{-5}
Am-242m + d	2.3×10^{-5}
Am-243	2.4×10^{-5}
Cm-243	1.5×10^{-5}
Cm-244	1.2×10^{-5}
Cm-245	2.4×10^{-5}
Cm-246	2.4×10^{-5}
Cm-247	2.2×10^{-5}
Cm-248	8.5×10^{-5}
Cf-249	2.4×10^{-5}
Cf-250	1.0×10^{-5}
Cf-251	2.4×10^{-5}

^a " + d" denotes short-lived decay products that are assumed to be in secular equilibrium with parent radionuclide; see Table A.4-1 for decay products and branching fractions.

^b Value assumes that Nb-93m is present in secular equilibrium.

^c Value assumes that Pb-210 is present in secular equilibrium.

where

- C_i = concentration of radionuclide i in exhumed waste ($\mu\text{Ci}/\text{m}^3$), and
 f_e = dilution factor for mixing of radionuclides in exhumed waste into soil in vegetable garden.

In implementing the model, a dilution factor for mixing of radionuclides in exhumed waste into native soil in the vegetable garden of 0.2 is assumed, as in the models for the vegetable and soil ingestion pathways. The fraction of the year during which exposure while working in the garden occurs is assumed to be 0.01 (Oztunali et al. 1981); i.e., the assumed exposure time is about 100 h/year.

The model for estimating external dose while working in the garden is summarized in Table A.4-10. The annual dose per unit concentration of a radionuclide in exhumed waste from a disposal unit at the time intrusion occurs is based on the model and parameter values described above and the external dose-rate conversion factors given in Table A.4-4.

For external exposure during residence in a home on top of exposed disposal units, the annual EDE (rem/year) from radionuclide i is given by

$$H_{ie} = C_{ii} U_i D_{ii} S, \quad (\text{A.4-8})$$

where

- C_{ii} = concentration of radionuclide i in disposal unit ($\mu\text{Ci}/\text{m}^3$),
 U_i = fraction of the year during which external exposure while residing in the home occurs,
 D_{ii} = dose-rate conversion factor for external exposure to radionuclide i in disposal unit (rem/y per $\mu\text{Ci}/\text{m}^3$), and
 S = shielding factor for radionuclides during indoor residence.

Table A.4-10. Annual EDEs from external exposure in vegetable garden per unit concentration of radionuclides in exhumed waste for agriculture scenario

Radionuclide ^a	Annual EDE (rem/y per $\mu\text{Ci}/\text{m}^3$)
Al-26	1.8×10^{-5}
Co-60	1.7×10^{-5}
Sn-121m	2.4×10^{-9}
Sn-126 + d	1.3×10^{-5}
I-129	1.6×10^{-8}
Cs-137 + d	3.8×10^{-6}
Eu-154	8.2×10^{-6}
Eu-155	2.2×10^{-7}
Ra-226 + d	1.2×10^{-5}
Th-229 + d	1.8×10^{-6}
Th-232 + d	1.6×10^{-5}
Pa-231 + d	2.2×10^{-6}
U-232 + d	1.0×10^{-5}
U-235 + d	9.3×10^{-7}
U-238 + d	1.5×10^{-7}
Np-237 + d	1.3×10^{-6}
Am-241	5.4×10^{-8}
Am-242m + d	8.2×10^{-8}
Am-243 + d	1.1×10^{-6}
Cm-243	7.0×10^{-7}
Cm-245	4.2×10^{-7}
Cm-247 + d	2.1×10^{-6}
Cf-249	2.2×10^{-6}
Cf-251	6.4×10^{-7}

^a "+ d" denotes short-lived decay products that are assumed to be in secular equilibrium with parent radionuclide; see Table A.4-1 for decay products and branching fractions.

The shielding factor takes into account the reduction in external dose provided by the walls and floor of the home.

In implementing the model, the fraction of the year during which exposure in the home is assumed to occur is 0.5 (Oztunali et al. 1981); i.e., the assumed exposure time is about 4,000 h/year. A shielding factor during indoor residence of 0.7 is assumed for all radionuclides (NRC 1977).

The model for estimating external dose during indoor residence is summarized in Table A.4-11. The annual dose per unit concentration of a radionuclide in a disposal unit at the time intrusion occurs is based on the model and parameter values described above and the external dose-rate conversion factors for sources uniformly distributed in an infinite thickness of soil-equivalent material given in the column in Table A.4-5 labeled "No shielding".

Inhalation Pathways. While working in the vegetable garden or residing in the home, the annual EDE (rem/year) from inhalation of radionuclide *i* suspended into air (*a*) in particulate form is given by

$$H_{ia} = C_{ia} f_i U_i D_i \quad (A.4-9)$$

where

C_{ia} = concentration of radionuclide *i* in air ($\mu\text{Ci}/\text{m}^3$),

f_i = fraction of the year during which inhalation exposure occurs,

U_i = annual air intake (m^3/year), and

D_i = DCF for inhalation of radionuclide *i* ($\text{rem}/\mu\text{Ci}$).

Airborne concentrations of suspended radionuclides in particulate form are estimated using a mass-loading model (Anspaugh et al. 1975), which is based on observations of airborne concentrations of naturally occurring materials, such as uranium and thorium, relative to their

Table A.4-11. Annual EDEs from external exposure in home per unit concentration of radionuclides in disposal units for agriculture scenario

Radionuclide ^a	Annual EDE (rem/y per $\mu\text{Ci}/\text{m}^3$)
Al-26	3.9×10^{-3}
Co-60	3.5×10^{-3}
Sn-121m	4.2×10^{-7}
Sn-126 + d	2.6×10^{-3}
I-129	2.8×10^{-6}
Cs-137 + d	7.6×10^{-4}
Eu-154	1.7×10^{-3}
Eu-155	3.9×10^{-5}
Ra-226 + d	2.4×10^{-3}
Th-229 + d	3.5×10^{-4}
Th-232 + d	3.5×10^{-3}
Pa-231 + d	4.2×10^{-4}
U-232 + d	2.2×10^{-3}
U-235 + d	1.7×10^{-4}
U-238 + d	2.9×10^{-5}
Np-237 + d	2.4×10^{-4}
Am-241	9.5×10^{-6}
Am-242m + d	1.5×10^{-5}
Am-243 + d	2.0×10^{-4}
Cm-243	1.3×10^{-4}
Cm-245	7.4×10^{-5}
Cm-247 + d	4.0×10^{-4}
Cf-249	4.2×10^{-4}
Cf-251	1.2×10^{-4}

^a "+ d" denotes short-lived decay products that are assumed to be in secular equilibrium with parent radionuclide; see Table A.4-1 for decay products and branching fractions.

concentrations in surface soils. In this model, airborne concentrations of suspended radionuclides in particulate form are given by

$$C_{ia} = C_{is} L_s / \rho_s \quad (\text{A.4-10})$$

where

C_{is} = concentration of radionuclide i in surface soil ($\mu\text{Ci}/\text{m}^3$),

L_s = atmospheric mass loading of surface soil (kg/m^3), and

ρ_s = bulk density of soil (kg/m^3).

The model described above is applied to all radionuclides except Rn-222, Rn-220, and their short-lived decay products. The model for estimating inhalation doses from exposure to radon is described later in this section.

For inhalation exposure while working in the vegetable garden, the concentration of radionuclide i in soil again is given by

$$C_{is} = f_e C_{ie} \quad (\text{A.4-11})$$

where

C_{ie} = concentration of radionuclide i in exhumed waste ($\mu\text{Ci}/\text{m}^3$), and

f_e = dilution factor for mixing of radionuclides in exhumed waste into soil in vegetable garden.

In implementing the model, a dilution factor for mixing of radionuclides in exhumed waste into native soil in the garden of 0.2, a soil bulk density of $1,400 \text{ kg}/\text{m}^3$, and a fraction of the year during which exposure while working in the garden occurs of 0.01 (about 100 h/year) again are assumed, and the annual air intake is assumed to be $8,000 \text{ m}^3$ (NRC 1977). Finally, the atmospheric mass loading of contaminated soil while working in the garden is assumed to be $10^{-7} \text{ kg}/\text{m}^3$.

The assumed atmospheric mass loading of contaminated soil while working in the vegetable garden of 10^{-7} kg/m³ is a somewhat conservative approximation of the average background dust loading for nonurban locations in the U.S. of about 4×10^{-8} kg/m³ (Anspaugh et al. 1975) and, furthermore, is in good agreement with an average dust loading of 6×10^{-8} kg/m³ measured above two agricultural fields at the SRS (Shinn et al. 1982). The choice of an atmospheric mass loading for this exposure pathway is based on these data and the following considerations. Although some gardening activities (e.g., tilling and hoeing) presumably would increase atmospheric concentrations of suspended soil above background levels, it probably is unreasonable to assume that the average concentration during all gardening activities would be substantially above the average background level in the U.S. First, the average background level of suspended soil originating from the SRS should be substantially lower than the average level in the U.S. because of the high annual precipitation, extensive vegetation, and low average wind speed at the site. Second, at any location, airborne concentrations of suspended surface soil consist of material originating from a wide area, not just from the particular location where exposures occur. Finally, the model assumes that all suspended soil particles are respirable; but, particularly during more vigorous gardening activities that could result in above-average atmospheric mass loadings, some particles are likely to be too large to be respirable. Taking into account all of these factors, the choice of 10^{-7} kg/m³ to represent the average mass loading during gardening activities at the SRS seems reasonable.

The model for estimating inhalation dose while working in the vegetable garden is summarized in Table A.4-12. The annual dose per unit concentration of a radionuclide in exhumed waste from a disposal unit at the time intrusion occurs is based on the model and parameter values described above and the inhalation DCFs given in Table A.4-3. Again, the results for Rn-222 and Rn-220 are estimated using a different model described later in this section.

For inhalation exposure while residing in the home, the airborne concentration of radionuclide *i* is given by

$$C_{ia} = C_{ir}L_i/\rho_v \quad (A.4-12)$$

Table A.4-12. Annual EDEs from inhalation exposure in vegetable garden per unit concentration of radionuclides in exhumed waste for agriculture scenario

Radionuclide ^a	Annual EDE (rem/y per $\mu\text{Ci}/\text{m}^3$)	Radionuclide ^a	Annual EDE (rem/y per $\mu\text{Ci}/\text{m}^3$)
H-3	7.2×10^{-14}	Pa-231 + d	9.1×10^{-6}
C-14	2.7×10^{-12}	U-232 + d ^d	7.6×10^{-7}
Al-26	9.0×10^{-11}	Rn-220	2.1×10^{-5} ^e
Co-60	1.7×10^{-10}	U-233	1.5×10^{-7}
Ni-59	1.5×10^{-12}	U-234	1.5×10^{-7}
Ni-63	3.4×10^{-12}	U-235	1.4×10^{-7}
Se-79	1.0×10^{-11}	U-236	1.4×10^{-7}
Rb-87	3.8×10^{-12}	U-238	1.4×10^{-7}
Sr-90 + d	2.7×10^{-10}	Np-237	5.6×10^{-7}
Zr-93 ^b	4.0×10^{-10}	Pu-238	5.2×10^{-7}
Nb-93m	3.2×10^{-11}	Pu-239	5.8×10^{-7}
Tc-99	9.6×10^{-13}	Pu-240	5.8×10^{-7}
Pd-107	1.5×10^{-11}	Pu-241	1.1×10^{-8}
Cd-113m	1.8×10^{-9}	Pu-242	5.5×10^{-7}
Sn-121m	6.6×10^{-12}	Pu-244	5.5×10^{-7}
Sn-126 + d	9.9×10^{-11}	Am-241	5.9×10^{-7}
I-129	2.1×10^{-10}	Am-242m + d	5.9×10^{-7}
Cs-135	5.1×10^{-12}	Am-243	5.9×10^{-7}
Cs-137	3.6×10^{-11}	Cm-243	4.0×10^{-7}
Sm-151	3.3×10^{-11}	Cm-244	3.1×10^{-7}
Eu-154	3.0×10^{-10}	Cm-245	6.2×10^{-7}
Eu-155	4.5×10^{-11}	Cm-246	6.2×10^{-7}
Pb-210 + d	2.4×10^{-8}	Cm-247	5.6×10^{-7}
Ra-226 + d ^{c,d}	3.3×10^{-8}	Cm-248	2.2×10^{-6}
Rn-222	1.3×10^{-4} ^e	Cf-249	6.3×10^{-7}
Th-229	1.9×10^{-6}	Cf-250	2.5×10^{-7}
Th-230	3.0×10^{-7}	Cf-251	6.4×10^{-7}
Th-232 + d ^d	1.6×10^{-6}		
Rn-220	2.1×10^{-5} ^e		

^a + d^a denotes short-lived decay products that are assumed to be in secular equilibrium with parent radionuclide; see Table A.4-1 for decay products and branching fractions.

^b Value assumes that Nb-93m is present in secular equilibrium.

^c Value assumes that Pb-210 is present in secular equilibrium.

^d Dose from radon decay product is listed separately.

^e Dose is normalized to unit concentration of parent radionuclide.

where

C_{ii} = concentration of radionuclide i in disposal unit ($\mu\text{Ci}/\text{m}^3$),

L_a = atmospheric mass loading of surface soil (kg/m^3), and

ρ_s = bulk density of soil (kg/m^3).

In implementing the model, a fraction of the year during which exposure in the home occurs of 0.5 (i.e., about 4,000 h/year), a soil bulk density of $1,400 \text{ kg}/\text{m}^3$, and an annual air intake of $8,000 \text{ m}^3$ again are assumed. The atmospheric mass loading of contaminated soil at the location of the home on top of the disposal facility is assumed to be $10^{-8} \text{ kg}/\text{m}^3$, which is approximately one-fourth of the average background dust loading in the U.S. (Anspaugh et al. 1975). On the basis of the previous discussion of the atmospheric mass loading while working in the vegetable garden, it seems unreasonable to assume that the atmospheric mass loading of largely undisturbed surface soil at the SRS would be as high as the average dust loading in the U.S. The assumption that the atmospheric mass loading of contaminated soil at the disposal site is about one-fourth of the average background level in the U.S. is intended to take into account the abundant precipitation, extensive vegetation, and low average wind speed at the site, compared with average conditions in the U.S., as well as the presence of uncontaminated soil suspended from other locations and the possibility that some suspended soil particles may not be respirable. In addition, the model for inhalation exposure indoors does not take into account the possibility that indoor concentrations of suspended soil particles may be somewhat less than the concentrations outdoors, due to such factors as filtering of air entering the home through windows and doorways and enhanced deposition on indoor surfaces.

The model for estimating inhalation dose during indoor residence is summarized in Table A.4-13. The annual dose per unit concentration of a radionuclide in a disposal unit at the time intrusion occurs is based on the model and parameter values described above and the inhalation DCFs given in Table A.4-3. The results for Rn-222 and Rn-220 are estimated using the model described below.

Table A.4-13. Annual EDEs from inhalation exposure in home per unit concentration of radionuclides in disposal units for agriculture scenario

Radionuclide ^a	Annual EDE (rem/y per $\mu\text{Ci}/\text{m}^3$)	Radionuclide ^a	Annual EDE (rem/y per $\mu\text{Ci}/\text{m}^3$)
H-3	1.8×10^{-12}	Pa-231 + d	2.3×10^{-4}
C-14	6.0×10^{-11}	U-232 + d ^d	1.9×10^{-5}
Al-26	2.3×10^{-9}	Rn-220	1.0×10^{-2} ^e
Co-60	4.3×10^{-9}	U-233	3.7×10^{-6}
Ni-59	3.7×10^{-11}	U-234	3.7×10^{-6}
Ni-63	8.6×10^{-11}	U-235	3.4×10^{-6}
Se-79	2.5×10^{-10}	U-236	3.4×10^{-6}
Rb-87	9.4×10^{-11}	U-238	3.4×10^{-6}
Sr-90 + d	6.8×10^{-9}	Np-237	1.4×10^{-5}
Zr-93 ^b	1.0×10^{-8}	Pu-238	1.3×10^{-5}
Nb-93m	8.0×10^{-10}	Pu-239	1.5×10^{-5}
Tc-99	2.4×10^{-11}	Pu-240	1.5×10^{-5}
Pd-107	3.7×10^{-10}	Pu-241	2.9×10^{-7}
Cd-113m	4.6×10^{-8}	Pu-242	1.4×10^{-5}
Sn-121m	1.7×10^{-10}	Pu-244	1.4×10^{-5}
Sn-126 + d	2.5×10^{-9}	Am-241	1.5×10^{-5}
I-129	5.1×10^{-9}	Am-242m + d	1.5×10^{-5}
Cs-135	1.3×10^{-10}	Am-243	1.5×10^{-5}
Cs-137	9.2×10^{-10}	Cm-243	1.0×10^{-5}
Sm-151	8.3×10^{-10}	Cm-244	7.7×10^{-6}
Eu-154	7.4×10^{-9}	Cm-245	1.5×10^{-5}
Eu-155	1.1×10^{-9}	Cm-246	1.5×10^{-5}
Pb-210 + d	6.0×10^{-7}	Cm-247	1.4×10^{-5}
Ra-226 + d ^{c,d}	8.3×10^{-7}	Cm-248	5.4×10^{-5}
Rn-222	1.2×10^{-1} ^e	Cf-249	1.6×10^{-5}
Th-229	4.9×10^{-5}	Cf-250	6.3×10^{-6}
Th-230	7.4×10^{-6}	Cf-251	1.6×10^{-5}
Th-232 + d ^d	4.0×10^{-5}		
Rn-220	1.0×10^{-2} ^e		

^a "+ d" denotes short-lived decay products that are assumed to be in secular equilibrium with parent radionuclide; see Table A.4-1 for decay products and branching fractions.

^b Value assumes that Nb-93m is present in secular equilibrium.

^c Value assumes that Pb-210 is present in secular equilibrium.

^d Dose from radon decay product is listed separately.

^e Dose is normalized to unit concentration of parent radionuclide.

In this analysis, inhalation doses from Rn-222, Rn-220, and their short-lived decay products while working in the vegetable garden containing contaminated soil or while residing in the home on top of a disposal unit are estimated using a natural analog model. Specifically, estimated average doses to the general population from exposure to Rn-222 and Rn-220, both indoors and outdoors, which result from known average concentrations of their parent radionuclides Ra-226 and Th-232, respectively, in surface soil, are used to estimate doses from radon per unit concentration of its parent radionuclide in waste for the inhalation pathways of concern for the agriculture scenario. This approach has the advantage compared, for example, with using a mechanistic diffusion model to predict radon emanation rates to the atmosphere that the natural analog model is based on environmental measurements and it implicitly takes into account all factors that relate concentrations of radium or thorium in soil to average exposures to indoor radon (e.g., average residence time in basements and other living areas). The analysis based on the natural analog model proceeds as follows.

The NCRP (1987) has estimated that the average EDE from exposure to radon in the U.S. is about 0.2 rem per year. This dose estimate applies only to Rn-222 and its short-lived decay products in homes and, furthermore, assumes continuous residence indoors. The estimated dose from Rn-222 indoors results from an average concentration of the parent radionuclide Ra-226 in surface soil of 0.6 pCi/g (NCRP 1984) which, for an assumed bulk density of soil of 1.4 g/cm³ (Baes and Sharp 1983), corresponds to a concentration of 0.84 $\mu\text{Ci}/\text{m}^3$. Therefore, for continuous residence indoors, the EDE from exposure to Rn-222 and its short-lived decay products per unit concentration of Ra-226 in surface soil is estimated as:

Rn-222, continuous residence indoors -

$$(0.2 \text{ rem/y}) / (0.84 \mu\text{Ci}/\text{m}^3) = 0.24 \text{ rem/y per } \mu\text{Ci}/\text{m}^3.$$

The dose per unit concentration from Rn-222 during indoor residence derived above can be applied directly to the inhalation pathway during indoor residence in a home located on top of a disposal unit containing Ra-226. The only correction needed is to take into account the assumption for this pathway in the agriculture scenario that the fraction of the year during

which residence in the home at the disposal site occurs is 0.5. Thus, for inhalation exposure while residing in the home on a disposal unit in the agriculture scenario, the EDE from Rn-222 and its short-lived decay products per unit concentration of Ra-226 in the disposal unit is estimated as:

Rn-222, indoor residence in agriculture scenario -

$$(0.24 \text{ rem/y per } \mu\text{Ci/m}^3)(0.5) = 0.12 \text{ rem/y per } \mu\text{Ci/m}^3.$$

This dose estimate for Rn-222 is given in Table A.4-13.

The dose from Rn-222 per unit concentration of Ra-226 in soil while working in the vegetable garden is obtained as follows. The United Nations Scientific Committee on the Effects of Atomic Radiation (UNSCEAR 1988) has estimated that, for continuous exposure, the average EDE from exposure to Rn-222 outdoors would be 28% of the average dose from exposure to Rn-222 indoors. Therefore, for continuous residence outdoors, the EDE from exposure to Rn-222 and its short-lived decay products per unit concentration of Ra-226 in surface soil can be estimated from the previous result for continuous residence indoors as:

Rn-222, continuous residence outdoors -

$$(0.24 \text{ rem/y per } \mu\text{Ci/m}^3)(0.28) = 0.067 \text{ rem/y per } \mu\text{Ci/m}^3.$$

The dose per unit concentration from Rn-222 during outdoor residence derived above can be applied directly to the inhalation pathway while working in the vegetable garden containing Ra-226. Two corrections are needed in applying this result to the agriculture scenario. The first is the fraction of the year that an intruder spends working in the vegetable garden, which is assumed to be 0.01. The second is the dilution factor for mixing of radionuclides in exhumed waste from a disposal unit into soil in the garden, which is assumed to be 0.2. Thus, for inhalation exposure while working in the garden in the agriculture scenario, the EDE from Rn-222 and its short-lived decay products per unit concentration of Ra-226 in

exhumed waste is estimated as:

Rn-222, residence in vegetable garden in agriculture scenario -

$$(0.067 \text{ rem/y per } \mu\text{Ci/m}^3)(0.01)(0.2) = 1.3 \times 10^{-4} \text{ rem/y per } \mu\text{Ci/m}^3.$$

This dose estimate for Rn-222 is given in Table A.4-12. This estimate may be somewhat conservative because the natural analog model is based on a distribution of radium to depths well below the ground surface, whereas the radium in garden soil in the agriculture scenario is assumed to be confined to a layer of surface soil 15 cm thick.

The dose analysis for inhalation exposure to Rn-220 and its short-lived decay products during outdoor residence and while working in the garden is based on the data on average doses from Rn-222 both indoors and outdoors presented previously and the following information. First, for continuous residence, the average dose from indoor Rn-220 would be 14% of the average dose from indoor Rn-222, and the average dose from outdoor Rn-220 would be about 26% of the average dose from outdoor Rn-222 (UNSCEAR 1988). Second, the doses from Rn-220 result from an average concentration of Th-232 in surface soil of 1 pCi/g (NCRP 1984), which corresponds to a concentration of $1.4 \mu\text{Ci/m}^3$. Th-232 can be regarded as the parent radionuclide for Rn-220 because the intermediate decay products Ra-228, Ac-228, Th-228, and Ra-224 all are sufficiently short-lived (see Table A.4-1) that they should be in secular equilibrium with Th-232 at any time following loss of active institutional control at 100 years after disposal.

Using the data on doses indoors and outdoors from Rn-222 presented previously, the information on Rn-220 and Th-232 given above, and the assumptions for the indoor and outdoor residence times and dilution factor for mixing of waste in the vegetable garden for the agriculture scenario, the following dose estimates for Rn-220 are obtained. For inhalation during indoor residence, the EDE from exposure to Rn-220 and its short-lived decay products per unit concentration of Th-232 in a disposal unit is estimated as:

Rn-220, indoor residence in agriculture scenario -

$$(0.2 \text{ rem/y})(0.14)(0.5) / (1.4 \mu\text{Ci/m}^3) = 0.010 \text{ rem/y per } \mu\text{Ci/m}^3.$$

This dose estimate is given in Table A.4-13. For inhalation while working in the vegetable garden, the dose from exposure to Rn-220 per unit concentration of Th-232 in exhumed waste is estimated as:

Rn-220, residence in vegetable garden in agriculture scenario -

$$(0.2 \text{ rem/y})(0.28)(0.26)(0.01)(0.2) / (1.4 \mu\text{Ci/m}^3) = \\ 2.1 \times 10^{-5} \text{ rem/y per } \mu\text{Ci/m}^3.$$

This dose estimate is given in Table A.4-12. As described previously for Rn-222, this estimate may be somewhat conservative.

Decay of the long-lived isotopes U-235 and Pa-231 considered in the intruder dose analysis produces Rn-219. However, the 3.96-s half-life of this isotope (Kocher 1981) is too short for its production in surface soil to result in a significant inhalation exposure. Therefore, inhalation doses from Rn-219 and its short-lived decay products can be ignored in the dose analysis for the agriculture scenario.

All Pathways. For the agriculture scenario, the annual EDEs from all exposure pathways per unit concentration of radionuclides in disposal units at the time intrusion is assumed to occur are summarized in Table A.4-14. For each radionuclide the total dose is the sum of the doses from the vegetable, soil ingestion, external exposure, and inhalation pathways given in Tables A.4-8 through A.4-13.

Given the models and parameter values assumed in the dose analysis for the agriculture scenario, the most important exposure pathways depend on the particular radionuclide. For many of the fission and activation products, the vegetable pathway is by far the most important. However, for the photon-emitting radionuclides Co-60, Sn-126, and Cs-137, external exposure while residing in the home is the only important pathway. For Sm-151, the soil ingestion pathway is a minor contributor to the total dose. Finally, the inhalation pathways are never important for any fission and activation products. For Ra-226 and the actinide radionuclides, the vegetable and soil ingestion pathways and inhalation exposure while residing in the home usually are important contributors to the total dose, except the soil ingestion and

Table A.4-14. Annual EDEs per unit concentration of radionuclides in disposal units from all exposure pathways for agriculture scenario^a

Radionuclide ^a	Annual EDE (rem/y per $\mu\text{Ci}/\text{m}^3$)	Radionuclide ^a	Annual EDE (rem/y per $\mu\text{Ci}/\text{m}^3$)
H-3	3.9×10^{-6}	Th-232 + d ^d	3.6×10^{-3}
C-14	1.5×10^{-5}	Rn-220	1.0×10^{-2} ^e
Al-26	3.9×10^{-3}	Pa-231 + d	8.3×10^{-4}
Co-60	3.5×10^{-3}	U-232 + d ^d	2.3×10^{-3}
Ni-59	6.8×10^{-8}	Rn-220	1.0×10^{-2} ^e
Ni-63	1.8×10^{-7}	U-233	1.1×10^{-5}
Se-79	1.2×10^{-6}	U-234	1.1×10^{-5}
Rb-87	1.9×10^{-6}	U-235 + d	1.8×10^{-4}
Sr-90 + d	1.8×10^{-4}	U-236	1.0×10^{-5}
Zr-93 ^b	4.5×10^{-8}	U-238 + d	3.9×10^{-5}
Nb-93m	1.9×10^{-8}	Np-237 + d	5.0×10^{-4}
Tc-99	1.1×10^{-5}	Pu-238	3.4×10^{-5}
Pd-107	3.2×10^{-8}	Pu-239	4.0×10^{-5}
Cd-113m	1.3×10^{-4}	Pu-240	4.0×10^{-5}
Sn-121m	4.7×10^{-7}	Pu-241	7.7×10^{-7}
Sn-126 + d	2.6×10^{-3}	Pu-242	3.8×10^{-5}
I-129	8.3×10^{-5}	Pu-244	3.7×10^{-5}
Cs-135	1.2×10^{-6}	Am-241	5.6×10^{-5}
Cs-137 + d	7.7×10^{-4}	Am-242 + d	6.0×10^{-5}
Sm-151	1.0×10^{-8}	Cm-243	1.6×10^{-4}
Eu-154	1.7×10^{-3}	Cm-244	2.0×10^{-5}
Eu-155	4.0×10^{-5}	Cm-245	1.1×10^{-4}
Pb-210 + d	3.0×10^{-4}	Cm-246	4.0×10^{-5}
Ra-226 + d ^{c,d}	2.7×10^{-3}	Cm-247 + d	4.4×10^{-4}
Rn-222	1.2×10^{-1} ^e	Cm-248	1.4×10^{-4}
Th-229 + d	4.3×10^{-4}	Cf-249	4.6×10^{-4}
Th-230	1.1×10^{-5}	Cf-250	1.7×10^{-5}
		Cf-251	1.6×10^{-4}

^a "+ d" denotes short-lived decay products that are assumed to be in secular equilibrium with parent radionuclide; see Table A.4-1 for decay products and branching fractions.

^b Value assumes that Nb-93m is present in secular equilibrium.

^c Value assumes that Pb-210 is present in secular equilibrium.

^d Dose from radon decay product is listed separately.

^e Dose is normalized to unit concentration of parent radionuclide.

inhalation pathways are of lesser importance when external exposure while residing in the home is a significant contributor to the total dose. For isotopes of Th and Pu, which are assumed to have a low plant-to-soil concentration ratio, the soil ingestion pathway is more important than the vegetable pathway.

The models for the exposure pathways involving mixing of exhumed waste with native soil in a vegetable garden may be somewhat conservative for radionuclides that are highly mobile in surface soil, because the models assume that the concentration in soil during the first year after mixing is not reduced as a result of leaching and transport to deeper soil layers by infiltrating precipitation. Thus, for mobile radionuclides, the average concentration in surface soil during the first year after mixing, which is the appropriate concentration for calculating the maximum annual dose to an intruder, could be substantially less than the initial concentration after mixing, and the annual dose per unit concentration in exhumed waste could be correspondingly overestimated.

The radionuclides in Table A.4-14 for which leaching and transport from surface soil in a vegetable garden by infiltrating precipitation could reduce the annual dose per unit concentration in exhumed waste include H-3 and Tc-99. In each case, a leaching model described in Sect. 3.2.3.3 (Baes and Sharp 1983) could be used to estimate the average concentration in surface soil during the first year after mixing of exhumed waste with native soil in the garden.

For H-3, which is expected to be removed from the soil root zone (i.e., the first 30 cm of surface soil) at the same rate as infiltrating water, the leaching correction described above would reduce the annual dose per unit concentration in exhumed waste by about a factor of five. This correction is not applied to the dose estimate for H-3 in Table A.4-14, but it could be taken into account in the dose analysis if estimated doses from H-3 are a significant fraction of the performance objective for protection of inadvertent intruders.

For Tc-99, the assumption of a small but non-zero distribution coefficient (K_d) in surface soil, such as given in Sect. 3.2.3.3, would reduce the annual dose per unit concentration in exhumed waste by less than a factor of two. Thus, the leaching correction undoubtedly is considerably less than the uncertainty in the plant-to-soil concentration ratio (B_p), which is the most important parameter in determining the dose from Tc-99 in the agriculture scenario.

Furthermore, there is evidence that the usual assumption of a low distribution coefficient for Tc-99 may overestimate considerably the removal rate from the soil root zone for a substantial fraction of the activity initially mixed into surface soil (Vandecasteele et al. 1989). Therefore, application of a leaching correction may not be valid in this case.

Resident scenario

In the resident scenario, exposures of inadvertent intruders are assumed to occur after an intruder encounters an intact and impenetrable engineered barrier (e.g., a concrete roof) while excavating to build a foundation for a home at the disposal site. An intruder then is assumed to build a home immediately on top of the intact engineered barrier and receives an external exposure while residing in the home. Ingestion and inhalation exposures are precluded when the waste is assumed to be inaccessible during excavation. The radionuclides included in the dose analysis for the resident scenario were selected on the basis of a screening analysis described in Sect. 3.2.4.4.

External dose during indoor residence for the resident scenario is estimated using the model given in Eq. (A.4-8). In implementing the model, the fraction of the year for indoor residence is assumed to be 0.5 and the shielding factor during indoor residence is assumed to be 0.7, as in the agriculture scenario. The dose-rate conversion factor for each radionuclide is the external dose rate per unit concentration in disposal units taking into account the shielding provided by the material in the source region (i.e., the waste itself) and by an intact concrete roof and/or layer of uncontaminated grout above the waste.

As described in Sect. 3.2.4.1 and A.4.4, only two bounding cases need to be considered in evaluating potential doses for the resident scenario. The first is exposure to both shorter-lived and long-lived photon-emitting radionuclides at 100 years after disposal when all engineered barriers in disposal units are assumed to be intact. The second case is exposure only to long-lived photon-emitting radionuclides in unshielded waste at a time long after disposal when all engineered barriers have lost their physical integrity and weathered to soil-equivalent material. However, as described in Sect. A.4.4, shorter-lived radionuclides also are included in the dose analysis for exposure to unshielded waste in order to evaluate the time period over which the engineered barriers must maintain their integrity and prevent access to the waste.

The model for estimating external dose in the resident scenario is summarized in Table A.4-15, which gives the annual EDE per unit concentration of radionuclides in the disposal units at the time intrusion occurs for different assumed thicknesses of shielding above the waste (see Sect. A.4.4). The results are obtained from the assumed exposure time and shielding factor during indoor residence and the external dose-rate conversion factors for the radionuclides of concern given in Table A.4-5. The results for 45-cm and 100-cm shielding apply to the bounding case of intact engineered barriers described above. The results for no shielding apply to the bounding case of no engineered barriers above the waste and are the same as the dose estimates during indoor residence for the agriculture scenario given in Table A.4-11.

In Table A.4-15, the calculations for no shielding apply to all disposal units, the calculations for 45-cm shielding apply to the LAW vaults, and the calculations for 100-cm shielding apply to the ILNT and ILT vaults. For the case of 45-cm shielding, results are presented only for those radionuclides selected by the screening analysis for the LAW vaults (see Sect. 3.2.4.4). For 100-cm shielding, no entry is given for Am-241 because the dose per unit concentration is too low to be of concern for any possible concentrations of this radionuclide in waste.

Post-drilling scenario

In the post-drilling scenario, exposures of inadvertent intruders are assumed to occur after an intruder drills through a disposal unit, e.g., for the purpose of constructing a well for a domestic water supply. The entire amount of drilling waste is assumed to be mixed with native soil in a vegetable garden, and the exposure pathways assumed for this scenario then include: 1) ingestion of vegetables grown in contaminated garden soil; 2) direct ingestion of contaminated soil in conjunction with vegetable intakes; 3) external exposure to contaminated soil while working in the garden; and 4) inhalation of suspended activity in particulate form and inhalation of isotopes of radon and their short-lived decay products while working in the garden. The radionuclides included in the dose analysis for the post-drilling scenario were selected on the basis of a screening analysis described in Sect. 3.2.4.4.

Table A.4-15. Annual EDEs per unit concentration of radionuclides in disposal units for resident scenario

Radionuclide ^a	Annual EDE (rem/y per $\mu\text{Ci}/\text{m}^3$)		
	No shielding ^b	45-cm shielding ^c	100-cm shielding ^d
Al-26	3.9×10^{-3}	1.1×10^{-4}	2.8×10^{-6}
Co-60	---	8.8×10^{-5}	1.2×10^{-6}
Sn-121m	4.2×10^{-7}	---	---
Sn-126 + d	2.6×10^{-3}	2.2×10^{-5}	8.4×10^{-6}
I-129	2.8×10^{-6}	---	---
Cs-137 + d	7.6×10^{-4}	6.6×10^{-6}	2.2×10^{-8}
Eu-154	---	3.2×10^{-5}	3.5×10^{-7}
Eu-155	---	6.3×10^{-10}	---
Ra-226 + d	2.4×10^{-3}	6.0×10^{-5}	1.3×10^{-6}
Th-229 + d	3.5×10^{-4}	2.6×10^{-6}	3.5×10^{-8}
Th-232 + d	3.5×10^{-3}	1.1×10^{-4}	4.1×10^{-6}
Pa-231 + d	4.2×10^{-4}	1.1×10^{-6}	3.5×10^{-9}
U-232 + d	2.2×10^{-3}	9.2×10^{-5}	3.8×10^{-6}
U-235 + d	1.7×10^{-4}	3.9×10^{-8}	2.3×10^{-12}
U-238 + d	2.9×10^{-5}	3.0×10^{-7}	2.5×10^{-9}
Np-237 + d	2.4×10^{-4}	4.6×10^{-7}	2.8×10^{-10}
Am-241	9.5×10^{-6}	---	---
Am-242m + d	1.5×10^{-5}	6.2×10^{-8}	5.2×10^{-10}
Am-243 + d	2.0×10^{-4}	1.1×10^{-7}	4.2×10^{-11}
Cm-243	1.3×10^{-4}	4.9×10^{-8}	2.0×10^{-11}
Cm-245	7.4×10^{-5}	5.3×10^{-9}	---
Cm-247 + d	4.0×10^{-4}	1.3×10^{-6}	1.3×10^{-9}
Cf-249	4.2×10^{-4}	1.2×10^{-6}	1.1×10^{-9}
Cf-251	1.2×10^{-4}	3.1×10^{-8}	---

^a "+ d" denotes short-lived decay products that are assumed to be in secular equilibrium with parent radionuclide; see Table A.4-1 for decay products and branching fractions.

^b Results apply to all disposal units and at times long after disposal when engineered barriers above the waste are assumed to have lost their physical integrity and residence on unshielded waste becomes credible.

^c Results apply to LAW vaults at 100 years after facility closure when engineered barriers are assumed to be intact and residence on unshielded waste is precluded.

^d Results apply to ILNT and ILT vaults at 100 years after facility closure when engineered barriers are assumed to be intact and residence on unshielded waste is precluded.

The exposure pathways for the post-drilling scenario are the same as the corresponding pathways for the agriculture scenario described previously, but external and inhalation exposures during indoor residence do not occur in the post-drilling scenario since all of the exhumed waste is assumed to be mixed with native soil in the vegetable garden and the intruder's home is not located on top of exposed disposal units. Therefore, the models given by Eqs. (A.4-2) and (A.4-3) for the vegetable pathway, Eqs. (A.4-4) and (A.4-5) for the soil ingestion pathway, Eqs. (A.4-6) and (A.4-7) for external exposure while working in the garden, and Eqs. (A.4-9) through (A.4-11) for inhalation exposure to radionuclides in particulate form while working in the garden, as well as the natural analog model for estimating dose from exposure to radon while working in the garden, also apply to the post-drilling scenario.

In implementing the models for the different exposure pathways, most of the parameter values for the post-drilling scenario would be the same as the values assumed for the agriculture scenario. The one important exception is the dilution factor for mixing of radionuclides in exhumed waste with native soil in the vegetable garden, which is denoted by f_d . For all exposure pathways in the post-drilling scenario, the dose per unit concentration of a radionuclide in exhumed waste is directly proportional to this dilution factor.

In the post-drilling scenario, the volume of contaminated drilling waste is assumed to be 0.5 m^3 (Kennedy et al. 1983), and this material is assumed to be mixed to a depth of 15 cm in a vegetable garden of area about 200 m^2 . The assumed area of the garden reasonably could provide half of the entire yearly intake of all vegetables by an intruder, which is the value assumed in this analysis. Therefore, the volume of soil in the garden into which the drilling waste is mixed is about 30 m^3 , and the resulting dilution factor is about 0.02. The assumed dilution factor for the post-drilling scenario thus is a factor of ten less than the value 0.2 assumed for the agriculture scenario. Therefore, for any exposure pathway in the post-drilling scenario, the dose per unit concentration of a radionuclide in exhumed waste is a factor of ten less than the corresponding value for the same pathway in the agriculture scenario.

For the post-drilling scenario, the annual EDE from all exposure pathways per unit concentration of radionuclides in exhumed waste at the time intrusion occurs, as obtained from the models and parameter values described above, is summarized in Table A.4-16. The

**Table A4-16. Annual EDEs per unit concentration of radionuclides
in exhumed waste for post-drilling scenario^a**

Radionuclide ^b	Annual EDE (rem/y per $\mu\text{Ci}/\text{m}^3$)
H-3	3.9×10^{-7}
C-14	1.5×10^{-6}
Al-26	1.8×10^{-6}
Co-60	1.8×10^{-6}
Ni-59	6.8×10^{-9}
Ni-63	1.8×10^{-8}
Se-79	1.2×10^{-7}
Rb-87	1.9×10^{-7}
Sr-90 + d	1.8×10^{-5}
Zr-93 ^c	3.5×10^{-9}
Nb-93m	1.8×10^{-9}
Tc-99	1.1×10^{-6}
Pd-107	3.2×10^{-9}
Cd-113m	1.3×10^{-5}
Sn-121m	5.3×10^{-9}
Sn-126 + d	1.4×10^{-6}
I-129	8.1×10^{-6}
Cs-135	1.2×10^{-7}
Cs-137 + d	1.2×10^{-6}
Sm-151	9.3×10^{-10}
Eu-154	8.4×10^{-7}
Eu-155	2.6×10^{-8}
Pb-210 + d	3.0×10^{-5}
Ra-226 + d ^d	3.2×10^{-5}
Rn-222	$1.3 \times 10^{-5/}$
Th-229 + d	2.9×10^{-6}
Th-230	3.4×10^{-7}
Th-232 + d ^e	5.9×10^{-6}
Rn-220	2.1×10^{-6}
Pa-231 + d	1.8×10^{-5}
U-232 + d ^e	5.6×10^{-6}
Rn-220	2.1×10^{-6}

See end of table for footnotes.

A-96
Table A.4-16. (continued)

WSRC-RP-94-218

Radionuclide ^a	Annual EDE (rem/y per $\mu\text{Ci}/\text{m}^3$)
U-233	7.5×10^7
U-234	7.3×10^7
U-235 + d	7.9×10^7
U-236	6.9×10^7
U-238 + d	6.6×10^7
Np-237	2.4×10^5
Pu-238	2.1×10^4
Pu-239	2.5×10^4
Pu-240	2.5×10^4
Pu-241	4.8×10^4
Pu-242	2.4×10^4
Pu-244	2.3×10^4
Am-241	3.1×10^4
Am-242m + d	3.0×10^4
Am-243 + d	3.2×10^4
Cm-243	1.6×10^4
Cm-244	1.3×10^4
Cm-245	2.5×10^4
Cm-246	2.5×10^4
Cm-247 + d	2.5×10^4
Cm-248	8.9×10^4
Cf-249	2.7×10^4
Cf-250	1.0×10^4
Cf-251	2.6×10^4

^a Values are one-tenth the sum of doses for agriculture scenario in Tables A.4-8 through A.4-10 and A.4-12.

^b "+ d" denotes short-lived decay products that are assumed to be in secular equilibrium with parent radionuclide; see Table A.4-1 for decay products and branching fractions.

^c Value assumes that Nb-93m is present in secular equilibrium.

^d Value assumes that Pb-210 is present in secular equilibrium.

^e Dose from radon decay product is listed separately.

^f Dose is normalized to unit concentration of parent radionuclide.

dose per unit concentration from the vegetable, soil ingestion, external exposure, and inhalation pathways again is one-tenth of the corresponding values for the agriculture scenario in Tables A.4-8 through A.4-10 and A.4-12, respectively.

Since all of the exposure pathways for the post-drilling scenario involve mixing of exhumed waste into surface soil in a vegetable garden, the leaching correction for H-3 discussed previously with the agriculture scenario also could be applied in this case. However, for the reasons previously discussed, a leaching correction will be applied in the dose analysis for the post-drilling scenario only if the dose from H-3 is expected to be significant.

A.4.6 Summary

This appendix has presented the models and data bases used in estimating annual EDEs to 1) off-site individuals resulting from exposure to radionuclides in contaminated groundwater and 2) inadvertent intruders resulting from direct intrusion into the EAV. In each case, particular exposure scenarios and associated exposure pathways have been assumed. The scenarios and pathways chosen for analysis and the radionuclides selected for the dose analysis for each scenario were based on considerations discussed in Sect. 3.2.3 and 3.2.4. For each exposure pathway, simple models for estimating dose have been developed, and annual doses per unit concentration of radionuclides in groundwater or in disposal units have been estimated on the basis of assumed parameter values for the particular pathway models.

For each exposure scenario, the annual doses per unit concentration of a radionuclide for each exposure pathway have been combined to obtain the total dose per unit concentration from all pathways. The following tables give the total dose per unit concentration at the time intrusion occurs for the different exposure scenarios:

- Table A.4-6, exposure of off-site individuals to radionuclides in contaminated groundwater via the drinking water pathway;
- Table A.4-14, agriculture scenario for exposure of inadvertent intruders to radionuclides in disposal units;
- Table A.4-15, resident scenario for exposure of inadvertent intruders to photon-emitting radionuclides in disposal units; and

- Table A.4-16, post-drilling scenario for exposure of inadvertent intruders to radionuclides in disposal units.

The dose analyses for each exposure scenario and exposure pathway were based on certain model parameters, some of which are radionuclide- or element-specific and others of which are independent of radionuclide. The radionuclide- or element-specific parameter values are given in Tables A.4-2 through A.4-5 and A.4-7. The parameter values that are independent of radionuclide are summarized in Table A.4-17.

For the three scenarios involving direct intrusion into the EAV, the radionuclide concentrations in the disposal units to which the annual doses obtained in this analysis are normalized are the concentrations at the time intrusion is assumed to occur, rather than the concentrations at the time of disposal. That is, the dose analysis for these scenarios presented in this appendix does not include any assumptions about the time after disposal at which intrusion occurs, except in the case of the resident scenario where bounding calculations based on intrusion at 100 years after disposal or at times long after disposal were performed. In most cases, assumptions about the time intrusion occurs are applied when the results of the intruder dose analyses in this appendix are combined with the results of the PAs for the disposal facility, which yield predictions of the concentrations of radionuclides remaining in the disposal units as a function of time after disposal.

Table A.4-17. Summary of radionuclide-independent parameter values used in dose analyses for off-site individuals and inadvertent intruders

Parameter description	Symbol	Parameter value
Consumption of contaminated drinking water ^a	U_w	730 L/year
Consumption of contaminated vegetables ^b	U_v	90 kg (fresh weight) per year
Density of soil ^b	ρ_s	1,400 kg/m ³
Dilution factor for mixing of exhumed waste with native soil in vegetable garden	f_s	0.2 ^c 0.02 ^d
Consumption of contaminated soil ^b	U_s	0.037 kg/year
Exposure times - working in garden ^b	U_e	1% per year
residing in home ^c	U_h	50% per year
Shielding factor for external exposure during indoor residence ^e	S	0.7
Air intake (breathing rate) ^b	U_a	8,000 m ³ /year
Atmospheric mass loading of contaminated surface soil - working in garden ^b	L_a	10 ⁻⁷ kg/m ³
residing in home ^c		10 ⁻⁸ kg/m ³

^a Parameter applies to exposure of off-site individuals.

^b Parameter applies to agriculture and post-drilling scenarios for inadvertent intruders.

^c Parameter applies to agriculture scenario for inadvertent intruders.

^d Parameter applies to post-drilling scenario for inadvertent intruders.

^e Parameter applies to agriculture and resident scenarios for inadvertent intruders.

APPENDIX A REFERENCES

- ACRI. 1993. *PORFLOW: A Model for Fluid Flow, Heat and Mass Transport in Multifluid, Multiphase Fractured or Porous Media, Users Manual, Version 2.5*. Draft. Analytic and Computational Research, Inc., Los Angeles, Calif.
- Anspaugh, L. R., J. H. Shinn, P. L. Phelps, and N. C. Kennedy. 1975. Resuspension and Redistribution of Plutonium in Soils. *Health Physics*, 29:571.
- Baes, C. F. III, and R. D. Sharp. 1983. A Proposal for Estimation of Soil Leaching Constants for Use in Assessment Models. *Journal of Environmental Quality*, 12:17.
- Baes, C. F. III, R. D. Sharp, A. L. Sjoreen, and R. W. Shor. 1984. *A Review and Analysis of Parameters for Assessing Transport of Environmentally Released Radionuclides Through Agriculture*. ORNL-5786. Oak Ridge National Laboratory.
- Christiansen, E. J., and D. E. Gordon. 1983. *Technical Summary of Groundwater Quality Protection Program at Savannah River Plant*. DPST-83-829, Vol. 1.
E. I. Du Pont de Nemours & Co., Inc., Savannah River Laboratory, Aiken, S.C.
- CRC Press, Inc. 1981. *CRC Handbook of Chemistry and Physics*. Robert C. Weast and Melvin J. Astle, eds. Boca Raton, FL.
- de Marsily, G. 1986. *Quantitative Hydrogeology*. Academic Press, Inc., New York, NY.
- Dennehy, K. F., and P. B. McMahon. 1987. *Water Movement in the Unsaturated Zone at a Low-Level Radioactive-Waste Burial Site Near Barnwell, South Carolina*.
U. S. Geological Survey Open-File Report 87-46, p.66.
- Eckerman, K. F., and J. C. Ryman. 1993. *External Exposure to Radionuclides in Air, Water, and Soil*. Federal Guidance Report No. 12. EPA 402-R-93-081. Oak Ridge National Laboratory and U. S. Environmental Protection Agency.
- Freeze, R. A., and J. A. Cherry. 1979. *Groundwater*, Prentice-Hall, Inc., N.J.
- Geotrans. 1992. *Groundwater Flow Model for the General Separations Area, Savannah River Plant*. Draft Report. Geotrans, Inc., Sterling, Va.
- Hamby, D. M. 1992. Site-Specific Parameter Values for the Nuclear Regulatory Commission's Food Pathway Dose Model. *Health Physics*, 62:136.

- Hubbard, J. E., and M. Engelhardt. 1987. *Calculation of Groundwater Recharge at the Old SRP Burial Ground Using the CREAMS Model (1961-1986)*. July 31, 1987, Memorandum from J. E. Hubbard and M. Englehardt, Department of Earth Sciences, State University of New York, College at Brockport, N.Y.
- INTERA. 1986. *Validation of Unsaturated Flow Models Using Tank 24 Lysimeter Data*. INTERA Technologies report H01203R005, INTERA Technologies, Inc., Austin, Texas.
- Kennedy, W. E. Jr., B. A. Napier, and J. K. Soldat. 1983. Advanced Disposal Systems for Transuranic Waste: Preliminary Disposal Criteria for Plutonium-239 at Hanford. *Nuclear Chemical Waste Management*, 4:103.
- Kocher, D. C. 1981. *Radioactive Decay Data Tables*. DOE/TIC-11026. U. S. Department of Energy.
- Kocher, D. C., and A. L. Sjoreen. 1985. Dose-Rate Conversion Factors for External Exposure to Photon Emitters in Soil. *Health Physics*, 48:193.
- Napier, B. A., R. A. Peloquin, W. E. Kennedy, Jr., and S. M. Neuder. 1984. *Intruder Dose Pathway Analysis for the Onsite Disposal of Radioactive Waste: The ONSITE/MAXII Computer Program*. NUREG/CR-3620, PNL-4054. Pacific Northwest Laboratory.
- NCRP. 1984. *Exposures from the Uranium Series with Emphasis on Radon and Its Daughters*. NCRP Report No. 77. National Council on Radiation Protection and Measurements, Bethesda, MD.
- NCRP. 1987. *Exposure of the Population in the United States and Canada from Natural Background Radiation*. NCRP Report No. 94. National Council on Radiation Protection and Measurements, Bethesda, MD.
- NRC. 1977. *Regulatory Guide 1.109. Calculation of Annual Doses to Man from Routine Releases of Reactor Effluents for the Purpose of Evaluating Compliance with 10 CFR Part 50, Appendix I*. U. S. Nuclear Regulatory Commission, Washington, D.C.
- NRC. 1981. *Draft Environmental Impact Statement on 10 CFR Part 61 "Licensing Requirements for Land Disposal of Radioactive Waste"*. NUREG-0945, Vol. 1. U. S. Nuclear Regulatory Commission, Washington, D.C.

- Orebaugh, E. G., and R. M. Wallace. 1989. *Quantification of Hazards Associated with the Decay Storage/Disposal of Tritium Crucibles (U)*. WSRC-RP-89-1226.
- Oztunali, O. I., G. C. Re, P. M. Moskowitz, E. D. Picazo, and C. J. Pitt. 1981. *Data Base for Radioactive Waste Management*. NUREG/CR-1759, Vol. 3. Dames and Moore, Inc.
- Oztunali, O. I., and G. W. Roles. 1986. *Update of Part 61 Impacts Analysis Methodology*. NUREG/CR-4370. U. S. Nuclear Regulatory Commission and Envirosphere Company.
- Parizek, R. R., and R. W. Root. 1986. *Development of a Ground-Water Velocity Model for the Radioactive Waste Management Facility, Savannah River Plant, South Carolina*. College of Earth and Mineral Sciences, Pennsylvania State University, University Park, Penn.
- Sheppard, M. I., S. C. Sheppard, and B. D. Amiro. 1991. Mobility and Plant Uptake of Inorganic ^{14}C and ^{14}C -Labelled PCB in Soils of High and Low Retention. *Health Physics*, 61:481.
- Shinn, J. H., D. N. Homan, and D. D. Gay. 1982. Plutonium Aerosol Fluxes and Pulmonary Exposure Rates During Resuspension from Bare Soils Near a Chemical Separation Facility, p. 1131 in *Precipitation Scavenging, Dry Deposition, and Resuspension*. Vol. 2. Ed. by H. R. Pruppacher, R. G. Semonin, and W. G. N. Slinn, Elsevier Science Publishing Co., New York, N.Y.
- Thompson, D. G. 1991. RE: *Vault Closure Concept for Saltstone Vaults*. Internal Report OPS-DTZ-91-0002. Westinghouse Savannah River Co., Savannah River Site, Aiken, S.C.
- UNSCEAR. 1988. *Sources, Effects and Risks of Ionizing Radiation*. United Nations Scientific Committee on the Effects of Atomic Radiation, New York, N.Y.
- U.S.DOE. 1988a. Management of Low-Level Waste, Chapter III in *Radioactive Waste Management*. Order 5820.2A, U. S. Department of Energy.
- U.S.DOE. 1988b. *Internal Dose Conversion Factors for Calculation of Dose to the Public*. DOE/EH-0071. U. S. Department of Energy.
- U.S. EPA. 1989a. *User's Guide for AIRDOS-PC*. EPA/520/6-89-035. U. S. Environmental Protection Agency, Office of Radiation Programs, Las Vegas Facility, Las Vegas, Nev.

- U.S. EPA. 1989b. *Risk Assessment Guidance for Superfund. Volume I. Human Health Evaluation Manual (Part A)*. EPA/540/1-89/002. U. S. Environmental Protection Agency, Washington, D. C.
- Vandecasteele, C. M., J. P. Dehut, S. Van Laer, D. Deprins, and C. Myttenaere. 1989. Long-Term Availability of Tc Deposited on Soil after Accidental Releases. *Health Physics*, 57:247.

APPENDIX B
COMPUTER CODES

B.1. CODE SELECTION CRITERIA AND CONSIDERATIONS

Listed below are criteria that were considered in selecting computer codes for use in the RPA of the EAV at the Savannah River Plant. The first list, which follows directly, consists of absolute requirements for any code (1R = #1, Required); any code not meeting any one of these requirements was rejected.

1R. The theoretical framework of the selected computer code(s) should be based on appropriate fundamental principles of chemistry and physics (e.g., conservation of mass, momentum, and energy) and well established constitutive equations (e.g., Darcy's law, Fick's law, etc.).

2R. The selected code(s) should be verified (i.e., simulation results compared against known analytical solutions of the underlying equations) to demonstrate correctness of the source code. Such verification should be fully documented in a technical report made available, at a minimum, to SRS and the Peer Review Panel.

3R. The selected code should be documented in a technical report and contain descriptions of: 1) model theory, governing equations and assumptions, 2) computational techniques and algorithms, and 3) example applications.

4R. All simulation codes(s) selected for use in the PAs must be maintained under a software QA and management program that assures that modifications and updates are traceable, auditable and documented, and that all production versions have been verified and validated.

This second list contains criteria describing attributes of computer codes that, though desirable, may not be presently attainable (1S = #1, Suggested). Consideration was given to these criteria, and justification for using a code not meeting them is given in this appendix.

1S. The code(s) should allow site- and facility-specific applications; i.e., be capable of simulating the hydrologic, geologic and/or geochemical setting of the site, as well as specific design features of the facility over time.

2S. A contaminant transport code should be capable of: 1) tracking waste inventory over time, including radioactive daughter products, and 2) computing the contaminant fluxes at designated locations as a function of driving hydrologic processes and mass transport phenomena.

3S. The code(s) should be validated (e.g., simulation results compared with field data) for a system similar to that being modeled whenever possible. Benchmarking (i.e., code-to-code comparisons) is also useful in demonstrating code capabilities.

4S. The degree of complexity of the computer code(s) should be consistent with the quantity and quality of data, and the objectives of the computation. Screening calculations and sensitivity analyses should be used to simplify conceptual models, and ultimately direct code selection.

5S. Hardware requirements for the selected code should not be exotic (i.e., codes should run on readily accessible mainframe, mini, or personal computers (PC); convertibility is highly desirable).

6S. Proprietary codes should be used only if they provide a distinct advantage over public domain codes and only if the author(s)/custodian(s) allow inspection and verification of the source code. If a proprietary code is used, it must be made available by lease or purchase to WSRC-IWT.

7S. Consideration must be given to the ease of interfacing code output with other codes. For example, it is often desirable to use a groundwater code that simulates unsaturated and saturated flow, as well as mass transport, as coupling of output from each simulation type has already been accomplished.

8S. Familiarity with the code(s) should also be a consideration in selection, in light of time constraints that may be imposed for completion of a given Performance Assessment, and the need to revise the code if problems arise.

B.2 GEOCHEMICAL COMPUTER CODE

The composition of EAV pore fluids was estimated using the MINTEQ geochemical code.

I. Code Description - MINTEQ

Purpose and Scope: MINTEQ is a geochemical computer code used to predict and evaluate the equilibrium behavior of inorganic pollutants in a variety of geochemical environments. The code can model complex equilibrium relationships that exist among soluble species, insoluble solids, gases, and adsorbed species. The code can also be used to calculate the consequences of equilibrium mass transfer between aqueous and solid phases. However, the code does not have the capability to calculate reaction path models nor can it calculate reaction kinetics. MINTEQ is useful for calculating the source term concentrations and speciation of inorganic contaminants. In addition, MINTEQ contains algorithms that predict the sorption of contaminants on soils and sediments. The sorption algorithms include: activity K_d , Langmuir isotherm, Freundlich isotherm, ion exchange, and surface complexation models. The code incorporates a Newton-Raphson iteration scheme to solve the set of mass-action and mass-balance expressions.

Development History: The MINTEQ code was originally developed at Pacific Northwest Laboratory (Felmy et al. 1984a) by combining the mathematical structure of the MINEQL and the geochemical attributes of the WATEQ geochemical codes. MINTEQ was developed to solve geochemical equilibria problems by applying fundamental principles of

thermodynamics. Changes to the code since its creation have been confined to improving ease of input and the flexibility of the output. Additional thermodynamic data has also been added to the database.

Code Attributes: The code is written in FORTRAN 77 programming language and includes several input data files containing data necessary for the operation of the code, such as: thermodynamic data, component identification numbers, ion charge and size, and formula weights.

Computer Requirements: Many applications of MINTEQ can be performed effectively and efficiently on a PC with a 286 central processor unit (cpu). More complex calculations will be more efficiently processed on a PC with a 386 cpu or on a work station. MINTEQ can also be run on mainframe computer systems.

Restrictions: The MINTEQ code was developed by Pacific Northwest Laboratory for the U.S. NRC and the EPA; the code is public domain software. The code is documented in Felmy et al. (1984a), Brown and Allison (1987), and Peterson et al. (1987).

II. Code Selection Basis

General Critique: MINTEQ is one of several computer codes that has been developed to calculate equilibrium aqueous speciation and mineral mass transfer. Mechanistic adsorption models are included in the MINTEQ code, a major advantage over other geochemical codes such as EQ3/EQ6. The fundamental limitation of MINTEQ and other equilibrium based geochemical codes is that equilibrium conditions are often not obtained in low temperature systems. Furthermore, metastable conditions may persist for long periods of times in experimental systems, and experimentally observed concentrations may differ from those predicted by the code.

Code Verification: MINTEQ calculates the equilibrium speciation for an aqueous composition. Verification can be performed by using the MINTEQ output and hand calculations to evaluate equilibrium. In addition, the MINTEQ code was verified during its development by comparison calculations against WATEQ4 (Felmy et al. 1984a, b)

Code Benchmarking: The code has been benchmarked using the river water test case of Nordstrom et. al. (1979; see Peterson et al. 1987). In addition, the code was benchmarked against WATEQ4 during development (Krupka and Morrey 1985).

Code Validation: The MINTEQ code has been partially validated for aqueous systems containing Cu(II), Pu, and U (Krupka and Morrey 1985).

III. Theoretical Framework

Governing Equation and Assumptions: The MINTEQ code calculates equilibrium speciation of aqueous phases. Speciation is defined as the chemical form of an element in an aqueous solution. The code solves mass balance expressions for each component ion (e.g., Ca^{2+} , HCO_3^- , Na^+ , etc.) using mass action relationships and equilibrium constants relating each species (such as CO_3^{2-} , a species of the HCO_3^- component) to MINTEQ components. Equilibrium constants for species are provided in the THERMO.DAT data base for calculations at a reference temperature of 25°C and infinite dilution. For temperatures that differ from 25°C, equilibrium constants are calculated either by using the Van't Hoff equation and enthalpies of reaction included in the data base or from analytical expressions relating equilibrium constants to temperature (Smith 1988). The concentration dependence of equilibrium constants is derived from individual ion activity coefficients calculated from the modified Debye-Huckel equation (Trusdell and Jones 1974), the Davies equation (Trusdell and Jones 1974), or the B-dot equation (Smith 1988).

Initial Conditions: The algorithm used in MINTEQ requires estimated starting values for the activities of component species. If these activity estimates are too far from the true values, the algorithm may fail to converge.

Numerical Techniques: MINTEQ uses a Newton-Raphson iteration method to simultaneously solve the non-linear mass balance equations.

IV. Code Inputs and Outputs

Input Data Structure: To execute the MINTEQ computer code, an input data file is prepared for each problem. The data file consists of

- title or run identifier,
- analytical units and temperature,
- run-specific user options,
- component identification and concentrations, and
- component modifications (e.g., concentration of H^+ fixed by pH).

Output Options: The MINTEQ code outputs the following:

- Echo of the data file input
- progress of the Newton-Raphson iterations
- full speciation of the input water composition
- charge balance and ionic strength for the aqueous composition
- saturation state of the water with respect to minerals in the data base

The user can also specify that the thermodynamic data base be printed. Debugging printing options are supported.

B.3 VAULT DEGRADATION COMPUTER CODE

I. Code Description - Concrete Degradation and Steel Reinforcement Corrosion

Purpose and Scope: The code used to estimate concrete degradation and rebar corrosion is designed to model the important degradation processes that can affect the long-term performance of concrete barriers. The processes modeled include: 1) concrete attack by sulfate and magnesium, 2) concrete leaching (both concrete and geologically controlled), 3) carbonation, and 4) rebar corrosion.

Development History: The current model consists of analytical solutions for concrete degradation processes. These solutions were selected as the best available means of predicting long-term concrete barrier performance.

Code Attributes: The code is written in Mathematica programming language (Wolfram 1988) and consists of four separate modules. Three of the modules are used to estimate concrete degradation and one is used to predict corrosion of steel reinforcement.

Sulfate and magnesium attack on concrete is described by an empirical relationship determined by Atkinson and Hearne (1984). Leaching of concrete components is described by a shrinking core model, in the case of concrete-controlled leaching, and by diffusional mass transport for geologic-controlled leaching (Atkinson and Hearne 1984). Walton et al. (1990) derived a shrinking core model to describe concrete carbonation. Rebar corrosion is described by an empirical correlation to determine time to onset of corrosion from chloride attack (Clear 1976) and a one dimensional diffusion calculation for actual corrosion (Walton et al. 1990).

Computer Requirements: The code was developed on an Apple Macintosh™ IIcx and has also been run using a NEXT workstation. The code will run on any workstation, mainframe or PC that runs Mathematica. The degradation code will run on any system running the Mathematica software package. The Macintosh, Version 1.2.2, recommends a minimum of 4 megabytes of RAM.

Restrictions: The code has been developed in the Mathematica software package and is therefore restricted by the purchase of the software.

II. Code Selection Basis

General Critique: The code is a compilation of analytical solutions for important concrete degradation processes (Clear 1976; Atkinson and Hearne 1984; Walton et al. 1990) selected based on the work of Walton et al. (1990). These analytical solutions are considered to be the best available means of predicting concrete degradation. The equations that are used to represent the degradation processes are based on observed conditions (i.e., sulfate, magnesium, chloride and dissolved oxygen concentrations in groundwater, etc.). However, in some cases the conditions encountered in a PA are very different from the conditions on which the empirical relationships are based. Also, the observations that form the basis of the equation are for much shorter periods of time (tens of years) than is needed for PAs (thousands of years).

Code Verification: The Mathematica's version of the code has been verified against the results of Walton et al. 1990.

Code Benchmarking: The code is made up of analytical solutions, therefore the benchmarking process does not apply.

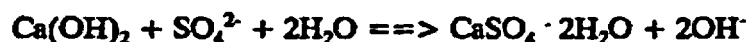
Code Validation: The code is made up of analytical solutions, therefore the validation process does not apply.

III. Theoretical Framework

Governing Equation and Assumptions:

Sulfate and Magnesium Attack. The equations that form the basis for the calculations are based on chemical reactions between concrete and rebar with chemical constituents from the waste and/or the geologic media surrounding the vault. Sulfate attack on concrete is the result of reactions of sulfate with hydrated tricalcium aluminate (C_3A) and portlandite [$Ca(OH)_2$] to form compounds of larger volume leading to expansion and disruption of the concrete. The reactions between sulfate and cement compounds can be written as

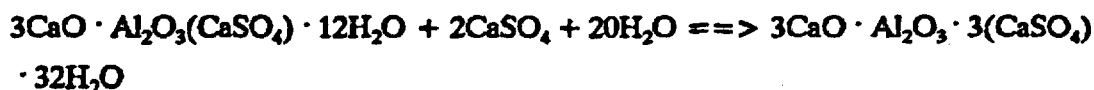
Gypsum:



Monosulphoaluminate:



Ettringite:



An example of a reaction between cement paste and magnesium sulfate is

Brucite:



The low solubility of $Mg(OH)_2$ causes the reaction to proceed to completion, making the attack more severe.

The depth of sulfate and magnesium attack is described by the equation

$$x = 0.55 C_s (Mg^{2+} + SO_4^{2-})t$$

where

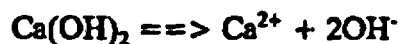
- x = depth of deterioration (cm),
- C_s = weight percent of C_3A in non-hydrated cement,
- Mg^{2+} = concentration of magnesium in the bulk solution (mol/L),
- SO_4^{2-} = concentration of sulfate in the bulk solution (mol/L), and
- t = time (years).

Assumptions: The rate of attack is proportional to sulfate and magnesium concentration in the solution and C_3A content of the cement.

Limitations: Correlations are only valid over the time/system parameters tested. Application outside this range is highly questionable.

The empirical correlation does not include the impacts of advective transport and/or the known importance of water to cement ratio (WCR) on durability. Application of the model is not clearly conservative.

Concrete-Controlled Leaching of Calcium Hydroxide. Cement components will be leached from concrete in environments in contact with water and have significant percolation rates. The alkalis are the first components to be leached followed by calcium hydroxide. The leaching of calcium hydroxide from the cement is described by



The equation that describes concrete controlled leaching is

$$x = [2D_i \{(C_i - C_{gw})/C_i\}t]^{1/2}$$

where

- x = depth of leaching (cm),
- D_i = intrinsic diffusion coefficient of Ca^{2+} in concrete solid (cm^2/s),
- C_i = concentration of Ca^{2+} in concrete pore water (mol/cm^3),
- C_{gw} = concentration of Ca^{2+} in the groundwater or soil moisture (mol/cm^3),
- C_s = bulk concentration of Ca^{2+} in the concrete solid (mol/cm^3), and
- t = time (s).

Assumptions: The rate of calcium removal from the exterior of the concrete is assumed to be rapid relative to the movement of calcium ions through the concrete. Therefore, diffusion controls the transport rate of the calcium.

Limitations: Diffusional mass transport is considered, but advection through and around the concrete is not considered.

D_i for the leached portion of the concrete will be substantially higher than D_i for intact concrete. Permeability of the concrete will increase as leaching proceeds leading to greater flow rates through the leached area. Diffusional control may no longer be valid under these conditions.

Geology-Controlled Leaching of Calcium Hydroxide. Geology-controlled leaching occurs as a result of the diffusion being controlled by the geologic material surrounding the concrete. The resulting equation is

$$x = 2 \phi [(C_i - C_{gw} / C_b) [(R_d D_E t) / \pi]^{1/2}$$

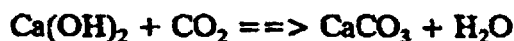
where

- x = depth of leaching (cm),
- ϕ = porosity of the geologic material (cm^3 voids/ cm^3 total),
- C_i = concentration of Ca^{2+} in concrete pore water (mol/cm^3),
- C_{gw} = concentration of Ca^{2+} in the groundwater or soil moisture (mol/cm^3),
- C_b = concentration of Ca^{2+} in the bulk concrete (solid+pore) (mol/cm^3),
- R_d = retardation factor for Ca^{2+} in the geologic material,
- D_E = effective dispersivity/diffusivity of Ca^{2+} in geologic material (cm^2/s), and
- t = time (s).

Assumptions: Diffusion into the surrounding geologic material controls leaching. Leaching is highest in low calcium concentration environments.

Limitations: Parameters for geologic material are needed (R_d , D_E , ϕ).

Concrete Carbonation. Carbonation is typically thought of as the reaction between calcium hydroxide and carbon dioxide as represented by



Carbonation can occur only as rapidly as dissolved carbonate can diffuse through the concrete. Carbonation rate is dependent on the moisture content of the concrete and the relative humidity of the ambient medium and the concentration of CO_2 in the ambient medium. If diffusion in the concrete is too slow, an equilibrium is reached where the diffusion of CO_2 and carbonation are stopped or severely reduced.

Carbonation rate is dependent on the moisture content of the concrete. As relative humidity changes from 0 to 100%, the rate of carbonation passes through a maximum.

Because the pH in concrete is high (>12), the carbonation reaction actually occurs as



The relationship between carbonation depth and groundwater concentration, portlandite in the concrete, and intrinsic diffusion coefficient of calcium is:

$$x = [2D_i (C_{gw}/C_s) t]^{1/2}$$

where

- x = depth of carbonation (cm),
- D_i = intrinsic diffusion coefficient of Ca^{2+} in concrete (cm^2/s),
- C_{gw} = concentration of total inorganic carbon in the groundwater (mol/cm^3),
- C_s = bulk concentration of $\text{Ca}(\text{OH})_2$ in the concrete solid (mol/cm^3), and
- t = time (s).

Assumptions: Concrete is saturated with water.

Limitations: The type of cement ultimately affects the depth of carbonation. This relationship becomes increasingly invalid as the relative humidity of the concrete decreases from 100% to 50%; below this level, the reaction rates decline rapidly resulting in a reduction in carbonation rate.

Reinforcement Corrosion/Chloride Attack. The alkaline environment of the concrete and the isolation it provides from external corrosive agents protects the steel reinforcement from corrosion by forming a protective oxide layer on the metal surface. The passive oxide layer may undergo attack by corrosive agents as the concrete deteriorates. Historically, aqueous chloride is the corrosive agent associated with the break up of the passive layer.

Reinforcement corrosion may also be associated with reduction of concrete alkalinity in the absence of elevated chloride levels. Carbonation and leaching can cause a decrease in the concrete pH with eventual loss of passivity.

Chloride attack is modeled in two stages (a) time to breakup of the passive layer and initiation of corrosion and (b) corrosion rate subsequent to breakup of the passive layer. An

empirical correlation for the time to passive layer breakup is

$$t_c = (129 x_c^{1.22}) / (WCR Cl^{0.42})$$

where

- t_c = time to onset of corrosion (years),
- x_c = thickness of concrete over the rebar (in.),
- WCR = water to cement ratio (by mass), and
- Cl = chloride ion concentration in groundwater (ppm).

Assumptions: The time to onset of corrosion is related to the water to cement ratio, depth of cement cover, and chloride concentration in groundwater.

Limitations: Applicability to conditions outside the observed chloride concentrations on which the equation is based is questionable.

The simplest method of estimating the corrosion rate subsequent to initiation of corrosion is a one dimensional diffusion calculation assuming limitation of the corrosion rate by oxygen diffusion. The percent of reinforcement remaining at any time is given by

$$\% \text{ remaining} = 100[(4 \cdot 9.4 \cdot s D_i C_{gw} t) / (\pi d^2 \text{ delta } x)]$$

where

- s = spacing between reinforcement bars (cm),
- D_i = intrinsic diffusion coefficient of O_2 in concrete (cm^2/s),
- C_{gw} = concentration of oxygen in the groundwater (mol/cm^3),
- delta x = depth of reinforcement below surface (cm), and
- t = time (s).

Assumptions: The corrosion rate is limited by oxygen diffusion.

Limitations: Applicable only if oxygen diffusion controls corrosion.

Initial Conditions: Not applicable.

Numerical Techniques: Not applicable.

IV. Code Inputs and Outputs

Input Data Structure: Input for the calculations is contained in the Mathematica file for degradation calculations. The values may be changed from within Mathematica and the file is evaluated as needed.

Output Options: Output can be in the form of numeric values, tables, two- or three-dimensional plots, and contour plots. Mathematica allows many forms of output to be displayed within the package and exported for use in other graphics packages.

B.4 SATURATED/UNSATURATED FLOW AND TRANSPORT CODE

I. General Code Description

Purpose and Scope. The PORFLOW computer code was selected and applied to predict the isolation performance of the EAVs in the vadose zone, to predict transport of radionuclides released to the underlying aquifer, and to predict contaminant transport in the aquifer. Specifically, the computer code was used to model water flow through the backfill, gravel-clay barrier, vault structure, and EAV waste forms. The code was then used to model the release of contaminants from the waste form, migration through the vault structure, surrounding soils and underlying formations. The simulation results generated by the

PORFLOW code were then post-processed to obtain predictions of

- water pathlines and travel times to the aquifer,
- contaminant plume distributions in the vadose zone,
- contaminant fluxes to the aquifer, and
- contaminant plume distributions in the aquifer's saturated zone.

These results are then used to characterize the isolation performance of the EAV.

Development History. The original version of the PORFLOW code (Runchal et al. 1985) was developed to analyze the isolation performance of deep geologic repositories. This early version was limited to saturated conditions and two-dimensional porous domains, and was extensively verified and benchmarked by Eyler and Budden (1984). The code was later extended to model variably saturated flow in three-dimensions and was therefore renamed PORFLO-3, Version 1.0 (Sagar and Runchal 1990). Version 1.0 of the three-dimensional computer code was independently verified and benchmarked by Magnuson et al. (1990) against FEMWATER, FLASH, TRACR3D, and MAGNUM-2D for some applications. The code has been used in practical applications at the Hanford Site to model various waste disposal problems (Smoot and Sagar 1990), at an experimental waste trench site in Las Cruces, NM to evaluate the solute transport simulation capabilities (Rockhold and Wurster 1991), and at the INEL to model a large organic vapor plume (Baca et al. 1988).

A newer version of PORFLO-3 (Version 2.3) was recently developed which has a number of enhancements and new options. For example, one of the new features of Version 2.3 is the capability to model multiphase flow. The commercial version of PORFLO-3 which was used to model the EAVs, suspect soil and NR waste performance in the vadose and saturated zones is PORFLOW, Version 2.5 (ACRI 1993). This later version has been verified and benchmarked to a greater degree than the previous one (ACRI 1994).

Code Attributes. The PORFLOW, Version 2.5, computer code is written in Fortran 77 programming language. Some of the unique attributes of this version are

- capability to model either single or multiphase flow,
- applicable to one-, two-, or three-dimensional geometries in Cartesian or cylindrical coordinate systems,
- alternate solver techniques (such as point successive over relaxation, Cholesky decomposition, Gauss elimination, and reduced system conjugate gradient) can be selected,
- multiple porosity representations can be used, and
- discrete features (such as fractures) can be represented by line or plate elements.

The computer program is relatively portable and can be run on PCs, workstations and main-frame computers.

Computer Requirements. Practical applications of the PORFLOW code to realistic multidimensional flow and transport problems require the availability of a high performance workstation or mainframe computer. The vault and vadose zone simulations presented in this report were performed on an IBM workstation. Complex simulation problems such as those performed for the EAVs often require double precision, and are cumbersome for PCs. For saturated flow, a PC with a 486 processor was sufficient to simulate the flow and mass transport regime.

Restrictions. Version 2.3 of PORFLO-3 was originally developed for the U.S. DOE and is therefore in the public domain. All versions of the PORFLO-3 code are copyright protected. Commercial versions of the code, PORFLOW, which include updates of the Version 2.3, are available from Analytic and Computational Research, Inc. (ACRI), Los Angeles, California.

II. Code Selection Basis

The code selection criteria put forth in Sect. B.1 of this appendix were used to select PORFLOW for use in the EAV RPA. The procedure followed was to identify several codes meeting requirements 1R - 4R, and subsequently evaluate those codes in terms of the remaining eight desirable criteria (1S - 8S). Table B.4.1 summarizes the results of this procedure. A more detailed explanation is given below.

General Critique. At present, there are relatively few general computer codes that have the capability to adequately simulate variably-saturated flow and transport in a multidimensional system. Such codes are scarce because the governing equations for flow in the unsaturated zone are highly nonlinear, and very difficult to solve. In addition to nonlinearity, this numerical difficulty is caused by such factors as:

- large contrasts in soil-hydraulic properties,
- high recharge rates and broad range of saturation conditions,
- contrasting thicknesses of soil strata, and
- advection dominated mass transport.

Advanced computational techniques (Celia et al. 1990 and Fletcher 1988) can overcome some of these difficulties; however, obtaining stable and accurate numerical solutions on a routine basis is still a modeling goal.

A number of computer codes with a demonstrated capability to model flow and transport were considered for application to the EAV study. The principal codes considered were: 1) PORFLOW (ACRI 1993); 2) FEMWATER/FEMWASTE (Yeh and Ward 1979; Yeh and Ward 1981; Yeh 1987); 3) FLASH (Baca and Magnuson 1992); 4) SUTRA (Voss 1984); 5) TRACR3D (Travis 1985); and 6) VAM3D-CG (Huyakorn and Panday 1990). All of these codes, with the possible exception of FEMWATER/FEMWASTE meet the first four requirements (1R-4R, see Table B.4.1). The availability of documentation of the most recent version of FEMWATER was in question, as was support by the primary developer of the code. Thus, this code was not considered further.

The remaining codes were evaluated with respect to their probability of satisfying the eight suggested criteria (1S - 8S, Sect. B-1). Reviews of available computer codes useful to PAs (Kozak et al. 1989, Case et al. 1989) were consulted to assess this probability. The results are summarized in Table B.4.1. From this table, the lack of familiarity with SUTRA, TRACR3D, and VAM3D-CG is the only distinguishing characteristic between these codes and FLASH and PORFLOW. Because of time constraints, this latter criteria was deemed important to code selection.

The PORFLOW computer code was ultimately selected over FLASH for these reasons:

- previous successful applications to modeling waste sites (Smoot and Sagar 1990);
- quality and completeness of code documentation (ACRI 1993; Sagar and Runchal 1990);
- favorable results of independent verification and benchmark testing of an earlier version (Magnuson et al. 1990);
- flexibility of the code, computational efficiency and ease of use;
- rigorous testing the source code has undergone using Fortran analyzers.

Applicability to EAVs. The hydrogeologic setting at the SRS is uniquely characterized by relatively high recharge rates, drainable soils, and a shallow vadose, or unsaturated, zone. In contrast, the vault and barrier components are typically low permeability. The PORFLOW computer code allows for consideration of heterogeneity and anisotropy, and employs various numerical techniques to enhance stability under the diverse conditions encountered. PORFLOW also has options for considering planar geologic features such as fractures, which is important to evaluating the possibility of vault failure during the time for which performance is being assessed.

Table B.4.1. Evaluation of identified alternative subsurface flow and transport codes

Selection Criteria (by number)*	Code Meets Criterion?					
	PORFLOW ^b	FEMWATER FEMWASTE ^c	FLASH ^d	SUTRA ^e	TRACR3D ^f	VAM3D-CG ^g
1R	yes	yes	yes	yes	yes	yes
2R	yes	yes	yes	yes	yes	yes
3R	yes	no	yes	yes	yes	yes
4R ^h	yes	yes	yes	yes	yes	yes
1S	yes	yes	yes	yes	yes	yes
2S	yes	no	yes	yes	yes	not known
3S	yes	not known	yes /	not known	yes	not known
4S	yes	yes	yes	yes	yes	yes
5S	yes	yes	yes	yes	yes	yes
6S	yes	yes	yes	not known	yes	not known
7S	yes	yes	yes	yes	yes	yes
8S	yes	no	yes	no	no	no

* Described in Appendix B-1.

^b ACRI 1993.

^c Yeh, G. T. 1987; Yeh, G. T. and D. S. Ward 1981.

^d Baca, R. G. and S. O. Magnuson 1992.

^e Voss, C. I. 1984

^f Travis, B. J. 1985.

^g Huyakorn, P. S. and S. Panday 1990.

^h Satisfying this criteria ensured by user.

Code Verification. Version 1.0 of the PORFLOW computer code has been verified by comparing the numerical solutions against known analytical solutions. In particular, the unsaturated flow component of the code has been verified against the Philip's (1957) analytical solutions for unsaturated flow in vertical and horizontal soil columns. In a like manner, the mass transport component has been verified against a number of analytical solutions for contaminant movement in steady-state flow fields. Results of the code verification are documented in Magnuson et al. (1990).

Version 2.5 of PORFLOW has been verified by ACRI (1994) using the same files compiled by Magnuson (1990).

Code Benchmarking. Version 1.0 of the PORFLOW code has been benchmarked by making code-to-code comparison for various flow and transport simulations. A number of hypothetical flow and transport situations were postulated and were simulated with PORFLOW and other independent computer codes. The hypothetical test problems were formulated to be representative of typical waste sites with realistic hydrogeologic settings. The PORFLOW code has been benchmark tested against such codes as TRACR3D (Travis 1985), FEMWATER (Yeh and Ward 1979), SUTRA (Voss 1984), and FLASH (Baca and Magnuson 1992). Results of the benchmark testing is documented in Magnuson et al. (1990).

Benchmarking of Version 2.5 was recently completed by ACRI (1994) and is in draft form at this writing.

Code Validation. At the present time, the PORFLOW code has not been validated by comparison to laboratory or field data. There is a definite need to perform such comparisons against experimental data collected at the SRS.

III. Theoretical Framework

Governing Equations and Assumptions. The governing equations solved in the PORFLOW code are based on the conservation principles of continuum mechanics. These equations describe fluid flow and mass transport processes in a heterogeneous and anisotropic

porous medium. The equations are well accepted mathematical representations and are found in such texts as Bear and Bachmat (1990), Freeze and Cherry (1979), and Huyakorn and Pinder (1983). The specific partial differential equation solved in PORFLOW for isothermal fluid flow around and through the EAVs is

$$S_e \frac{\partial H}{\partial t} = \frac{\partial}{\partial x_i} \left[K_{ij} \left(\frac{\partial H}{\partial x_j} - \delta_{ij} \right) \right] + m_v \quad (\text{B4.1})$$

where

S_e is the fluid storage term (i.e., specific storage or moisture capacity term),

H is the total or hydraulic head,

K_{ij} is the hydraulic conductivity tensor,

δ_{ij} is the buoyancy vector, and

m_v is the fluid source or sink term,

t is time, and

x_i is distance in the i th direction.

The quantity H is defined by:

$$H = h + z - z^* \quad (\text{B4.2})$$

where

h = pressure head,

z = elevation head, and

z^* = reference datum.

and the quantity S_e is defined by

$$S_e = S(\alpha_s + \theta_E \alpha_f) + \theta_E \frac{\partial S}{\partial H} \quad (\text{B4.3})$$

where

- S = the saturation level,
 α_s and α_f = the solid and fluid compressibilities normalized by the specific weight of the fluid, and
 θ_E = the effective porosity.

Some of the basic assumptions made in the above mathematical formulations are:

- fluid flow is laminar, slightly compressible, and single phase;
- fluid flow obeys Darcy's law for porous flow, where specific discharge is proportional to the hydraulic gradient;
- fluid viscosity is a function of temperature only;
- hydraulic properties of the porous continuum are volume averages; and
- osmotic effects are negligible.

In general, these assumptions are satisfied in the hydrogeologic environment of EAVs.

The specific partial differential equation solved in PORFLOW for contaminant transport from EAVs is

$$R_D \phi_D \frac{\partial C}{\partial t} + \frac{\partial}{\partial x_i} (V_i C) = \frac{\partial}{\partial x_i} \left[\Gamma_{ij}^C \frac{\partial C}{\partial x_j} \right] - \phi_D R_D \lambda C + S_C + \sum_p \phi_D R_D^p \sigma^p \lambda^p C \quad (\text{B4.4})$$

where

C = contaminant concentration,

V_i = fluid pore velocities,

R_D = retardation factor,

Γ_{ij}^C = hydrodynamic dispersivity tensor,

λ = decay rate,

S_e = mass source term,

σ^p = fraction of decay of the parent mass species which generates the current species, and the superscript p refers to the parent mass species.

The last term in equation B4.4 represents ingrowth of mass species. The quantity R_D is defined by:

$$R_D = \left[1 + \frac{(1-\theta_T) \rho_s k_d}{\phi_D} \right], \quad (B4.5)$$

where

ρ_s is bulk density,

θ_T is total porosity,

ϕ_D is water filled diffusive porosity, and

k_d is sorption coefficient,

and Γ_{ij}^C is defined by,

$$\Gamma_{ij}^C = \phi_D \tau_{ij} D_H + \phi_E D_{ij}, \quad (B4.6)$$

where

- ϕ_E is the effective pore space saturated with water,
- τ_{ij} is the tortuosity tensor,
- D_M is the molecular diffusion coefficient, and
- D_{ij} is the mechanical dispersion tensor.

All other coefficients are as previously defined.

Some of the key assumptions that limit the applicability of the above formulation are as follows:

- contaminant concentrations are low enough that the fluid flow is independent of mass transport, i.e., concentrations do not affect the density or viscosity of the fluid;
- diffusion of the contaminants through the fluid obeys Fick's first law, where mass flux is proportional to the concentration gradient with the constant of proportionality being the diffusion coefficient;
- mechanical dispersion is described by Scheidegger's equation, (Scheidegger 1961);
- adsorption (and desorption) of contaminants onto the porous medium is an equilibrium process described by a linear isotherm.

The model formulation is applicable to both unsaturated and saturated flow conditions.

Initial and Boundary Conditions. The PORFLOW code accommodates the specification of standard mathematical boundary conditions. These include: 1) Dirichlet, i.e., fixed head or concentration), 2) Neumann, i.e., specified flux, and 3) Robin, i.e., mixed, boundary conditions. Detailed information on boundary condition options is given in ACRI (1993).

Numerical Techniques. In the PORFLOW code, the governing equations for flow and transport are solved using a method referred to as the Nodal Point Integration, a variation of the finite volume or integrated finite difference technique (Runchal and Sagar 1992). In

this method, the difference approximations to the governing equations are derived on a staggered grid system. The state variables are computed at the grid nodes whereas the fluid velocities and fluxes are computed at the cell faces (located midway between adjacent grid nodes). Three discretization schemes, or basis functions to be integrated, are provided. The user may select which of the three schemes is to be used to maximize accuracy and stability.

The system of algebraic equations produced by the finite volume method are solved in the PORFLOW code using any one of five techniques

- Point successive over relaxation (Bear and Verruijt 1987),
- Alternating direction implicit (Peaceman and Rachford 1955),
- Cholesky decomposition (de Marsily 1986),
- Gauss elimination (Remson et al. 1971), or
- Reduced system conjugate gradient method (Hestenes and Stiefel 1952).

The nonlinearity of the governing equation for variably saturated flow is solved using a Picard iteration method.

IV. Code Inputs and Outputs

Input Data Structure. Input data files for the PORFLOW code are relatively easy to prepare and check. The code uses a free-form input which allows the user to document the input data deck. The input file uses a keyword approach to define primary input data groups. For typical flow and transport simulations, the data groups consist of

- Title card and comments,
- Finite difference grid specification, i.e., number of grid nodes in each direction,
- Lists of grid node coordinates,
- Zone definitions that specify the grid locations of distinct strata,
- Rock and hydraulic property specifications,
- Convergence and iteration parameters,

- Initial pressures and concentrations,
- Boundary values and/or fluxes,
- Mass properties including effective diffusion coefficients and K_d s,
- Source specifications, and
- Time step and output specifications.

Simulations of multidimensional flow and transport can be performed in either steady-state or time-dependent mode.

Output Options. Results from the PORFLOW simulation consist of total head, saturation, contaminant concentration, and Darcy velocities for each grid block in the computational grid. The user can select to print out any or all of the output variables. Each of these variables can be post-processed to produce graphical output.

Post-Processor Programs. A number of post-processor programs have been written by EG&G Idaho, Inc. which may be used to graph the simulation results. These post-processor programs are DISSPLA based routines that plot profiles, contours, streamlines and travel times, and time histories. These programs have been used extensively by EG&G Idaho on various projects. However, no formal documentation currently exists. Analytic and Computational Research, Inc. also distributes a PLOT88-based post-processor for use with the 486 PC versions of PORFLOW, documented by Runchal (1991).

Documentation of Users Instructions. The PORFLOW, Version 2.5, is documented in ACRI (1993). This report describes the mathematical theory and numerical techniques of this version, serves as a user's manual, and provides detailed information on the code organization, selection of computational grids and time steps, input structure and key-word definitions.

APPENDIX B REFERENCES

- ACRI. 1993. *PORFLOW: A Model for Fluid Flow, Heat and Mass Transport in Multifluid, Multiphase Fractured or Porous Media, Users Manual, Version 2.5*. Draft. Analytic and Computational Research, Inc., Los Angeles, Calif.
- ACRI. 1994. *Verification and Benchmarking of PORFLOW*. Analytic and Computational Research, Inc., draft (in review).
- Atkinson, A., and J.A. Hearne. 1984. *An Assessment of the Long-Term Durability of Concrete in Radioactive Waste Repositories*. AERE-R11465, Harwell, U.K.
- Baca, R. G., J. C. Walton, and A. S. Rood. 1988. Organic Contaminant Release from a Mixed Waste Disposal Site: Analysis of Vapor Transport through the Vadose Zone and Site Remediation. *Proceedings of Tenth Annual DOE Low-Level Waste Management Conference*. Denver, Colo.
- Baca, R. G. and S. O. Magnuson. 1992. *FLASH - Finite Element Computer Code for Variably Saturated Flow*. EGG-GEO-10274. EG&G Idaho, Inc., Idaho Falls, ID.
- Bear, J., and A. Verruijt. 1987. *Modeling Groundwater Flow and Pollution*. D. Reidel Publishing Co., Boston, Mass.
- Bear, J., and Y. Bachmat. 1990. *Introduction to Modeling of Transport Phenomena in Porous Media*. Kluwer Academic Publishers, Boston, Mass.
- Brown, D. S., and J. D. Allison. 1987. *MINTEQA1. An Equilibrium Metal Speciation Model: User's Manual*. EPA-600/3-87/012. U. S. Environmental Protection Agency, Athens, GA.
- Case, M. J., S. J. Maheras, M. D. Otis, and R. G. Baca. 1989. *A Review and Selection of Computer Codes for Establishing of the Performance Assessment Center*. DOE/LLW-83. EG&G Idaho, Inc.
- Celia, M. A., E. T. Bouloutas, and R. L. Zarba. 1990. A General Mass-Conservative Numerical Solution for the Unsaturated Flow Equation. *Water Resources Research*, 26(7):1483-1496.

- Clear, K.C. 1976. *Time to Corrosion of Reinforcing Steel in Concrete Slabs, Vol. 3. Performance After 830 Daily Salt Applications*. Federal Highway Administration Report No. FHWA-RD-76-70, NTIS PB-258 446.
- de Marsily, G. 1986. *Quantitative Hydrogeology*. Academic Press, Inc., New York, NY.
- Eyler, L. L., and M. J. Budden. 1984. *Verification and Benchmarking PORFLO: An Equivalent Porous Continuum Code for Repository Scale Analysis*. PNL-5044. Pacific Northwest Laboratory, Richland, Wash.
- Felmy, A. R., D. C. Girvin, and E. A. Jenne. 1984a. *MINTEQ: A Computer Program for Calculating Aqueous Geochemical Equilibria*. (NTIS PB84-157148) EPA-600/3-84-032. National Technical Information Service, Springfield, VA.
- Felmy A. R., S. M. Brown, Y. Onishi, S. B. Yabusaki, and R. S. Argo. 1984b. *MEXAMS--The Metals Exposure Analysis Modeling System*. EPA-600/3-84-031 (NTIS PB84-157155). U. S. Environmental Protection Agency, Athens, GA.
- Fletcher, C. A. J. 1988. *Computational Techniques for Fluid Dynamics*. Vols I & II, Springer-Verlag, New York, NY.
- Freeze, R. A. and J. A. Cherry. 1979. *Groundwater*. Prentice-Hall, Inc. Englewood Cliffs, NJ.
- Hestenes, M. R., and E. Stiefel. 1952. Methods of conjugate gradients for solving linear systems. *NBS J. Res.*, 49:409-436.
- Huyakorn, P. S., and G. F. Pinder. 1983. *Computational Methods in Subsurface Flow*. Academic Press, Inc., New York, NY.
- Huyakorn, P. S., and S. Panday. 1990. *VAM3D-CG - Variably Saturated Analysis Model in Three-dimensions with Preconditioned Conjugate Gradient Matrix Solvers, Documentation and User's Guide, Version 2.1*. HGL/89-02, Hydrogeologic, Inc., Herndon, VA.
- Kozak, M. W., M. S. Y. Chu, C. P. Harlan, and P. A. Mattingly. 1989. *Identification and Recommendation of Computer Codes for Low-Level Waste Performance Assessment*. Subtasks 3.0 and 4.1 of the Final Letter Report to the USNRC (August).

- Krupka, K. M., and J. R. Morrey. 1985. MINTEQ Geochemical Reaction Code: Status and Applications. *Proceedings of a Conference on the Application of Geochemical models to High-Level Nuclear Waste Repository Assessment*. G.K. Jacobs, and S. K. Whatley, Eds. NUREG/CP-0062. U.S. Nuclear Regulatory Commission, Washington, D.C.
- Magnuson, S. O., R. G. Baca, and A. J. Sondrup. 1990. *Independent Verification and Benchmark Testing of the PORFLO-3 Computer Code, Version 1.0*. EGG-BG-9175. EG&G Idaho, Inc., ID.
- Nordstrom, D. K., L. N. Plummer, T. M. L. Wigley, T. J. Wolery, J. W. Ball, E. A. Jenne, R. L. Basset, D. A. Crerar, T. M. Florence, B. Fritz, M. Morel, M. M. Reddy, G. Sposito, and J. Thraillkill. 1979. A Comparison of Computerized Chemical Models for Equilibrium Calculations in Aqueous Systems. *Chemical Modeling in Aqueous Systems*. E. A. Jenne, Ed. (ACS Symp. Series 93, American Chemical Society, Washington D.C.), pp. 857-892.
- Peaceman, D. W., and H. H. Rachford, Jr. 1955. The numerical solution of parabolic and elliptic differential equations. *J. Soc. of Industrial and Applied Mathematics*. 3:28-41.
- Peterson, S. R., C. J. Hostettler, W. J. Deutsch, and C. E. Cowan. 1987. MINTEQ User's Manual. (NUREG/CR-4808) PNL-6106. U.S. Nuclear Regulatory Commission, Washington, D.C.
- Philip, J. R. 1957. Numerical Solution of Equations of the Diffusion Type with Diffusivity Concentration-Dependent II. *Australian Journal of Physics*, 10(2):29-42.
- Remson, I., G. M. Hornberger, and R. F. Molz. 1971. *Numerical Methods in Subsurface Hydrology*. Wiley-Interscience, New York, NY.
- Rockhold, M. L., and S. K. Wurster. 1991. *Simulation of Unsaturated Flow and Solute Transport at the Las Cruces Trench Site Using the PORFLO-3 Computer Code*. PNL-7562. Pacific Northwest Laboratory, Richland, Wash.
- Runchal, A. K., B. Sagar, R. G. Baca, and N. W. Kline. 1985. *PORFLO - A Continuum Model for Fluid Flow, Heat Transfer, Mass Transport in Porous Media*. RHO-BW-CR-150P. Rockwell Hanford Operations, Richland, Wash.

- Runchal, A. K. 1991. *acrPLOT - A General Purpose Plotting Package, User's Manual - Version 8.00*. ACRI/014/Rev. A. Analytic and computational Research, Inc., Los Angeles, Calif.
- Sagar, B., and A. K. Runchal. 1990. *PORFLO-3: A Mathematical Model for Fluid Flow, Heat and Mass Transport in Variably Saturated Geologic Media, Theory and Numerical Methods, Version 1.0*. WHC-EP-0042. Westinghouse Hanford Operations, Richland, Wash.
- Scheidegger, A. E. 1961. General Theory of Dispersion in Porous Media. *J. Geophys. Res.* 66(10):3273-3278.
- Smith, R. W. 1988. Calculation of Equilibria at Elevated Temperatures Using the MINTEQ Geochemical Code. PNL-6700. Pacific Northwest Laboratory, Richland, Wash.
- Smoot, J. L., and B. Sagar. 1990. *Three-dimensional Contaminant Plume Dynamics in the Vadose Zone: Simulation of the 241-T-106 Single-Shell Tank Leak at Hanford*. PNL-7221. Pacific Northwest Laboratories, Richland, Wash.
- Travis, B. 1985. *TRACR3D: A Model of Flow and Transport in Porous Media*. LA-9667-MS. Los Alamos National Laboratory, Los Alamos, NM.
- Trusdell, A. H., and B. F. Jones. 1974. WATEQ, a Computer Program for Calculating Chemical Equilibria of Natural Waters." *J. Research U.S. Geol. Survey*, 2:233-348.
- Voss, C. I. 1984. *A Finite-Element Simulation Model for Saturated-Unsaturated, Fluid-Density-Dependent Ground-Water Flow and Energy Transport or Chemically-Reactive Single-Species Solute Transport*. U. S. Geological Survey, Reston, VA.
- Walton, J. C., L. E. Plansky, and R. W. Smith. 1990. *Models for Estimation of Service Life of Concrete Barriers in Low-Level Radioactive Waste Disposal*. Prepared for Division of Engineering Office of Nuclear Regulatory Research, U.S. Nuclear Regulatory Commission, Washington, DC 20555, NRC FIN A6858, NUREG/CR-5542, EGG-2597, RW,CC, 38 p.

- Wolfram, S. 1988. *Mathematica: A System for Doing Mathematics by Computer*. Addison-Wesley Publishing Company, Inc., USA, 749 p.
- Yeh, G. T., and D. S. Ward. 1979. *FEMWATER: A Finite-Element Model of Water Flow Through Saturated-Unsaturated Porous Media*. ORNL-5567. Oak Ridge National Laboratory, Oak Ridge, Tenn.
- Yeh, G. T., and D. S. Ward. 1981. *FEMWASTE: A Finite-Element Model of WASTE Transport Through Saturated-Unsaturated Porous Media*. ORNL-5601. Oak Ridge National Laboratory, Oak Ridge, Tenn.
- Yeh, G. T. 1987. *FEMWATER: a Finite-Element Model of WATER Flow Through Saturated-Unsaturated Porous Media - First Revision*. ORNL-5567/R1. Oak Ridge National Laboratory, Oak Ridge, Tenn.